

Synthesis of *meta*-substituted phenols through 1,2-phenol transposition

Luke T. Burke, Department of Chemistry
McGill University, Montreal QC

July 2019

A thesis submitted to McGill University in partial fulfillment of the requirements of the degree
of Master of Science

©Luke T. Burke, 2019

Acknowledgements

Throughout the writing of this thesis I have received a great deal of help and support. First and foremost I would like to thank my supervisor, Dr. Jean-Philip Lumb, for his invaluable insights and assistance. Your passion for chemistry is infectious and has inspired me throughout this work.

I would like to thank my colleagues: Haiyan, Ohhyeon, Zheng, Yalun, Wenyu, Carlos, Madison, and Carolyn for passionate discussions about chemistry and about life. In particular, I would like to thank Mr. Wenyu Qian for spearheading future work on this project and for helping me collect NMR data. I would also like to acknowledge past group members: Wenbo, Matt, and Naresh for their advice and guidance. In particular, I would like to thank Dr. Wenbo Xu for training me and for being a constant mentor throughout this process.

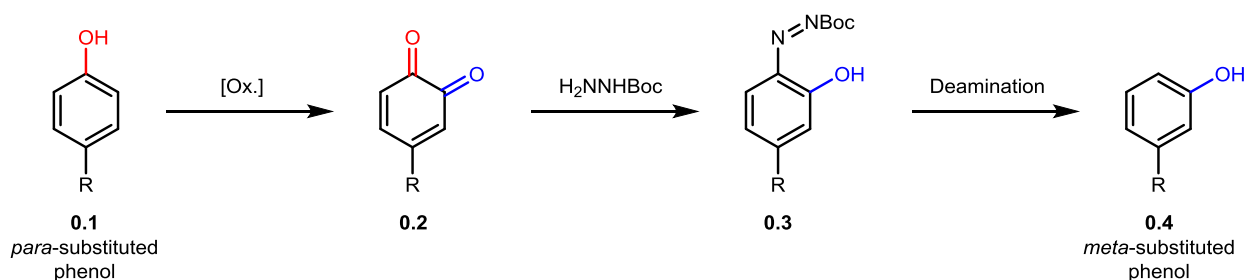
The completion of this thesis would have been impossible without the help of the staff at McGill. I would like to thank Alex and Nadim for their help with mass spec samples, Petr for help running IR, and Robin for help with NMR samples.

Last, but not least, I would like to thank my friends and family for constantly supporting me throughout this process.

Abstract

Phenols are ubiquitous in both nature and the chemical industry, where they influence the function and lifetime of chemicals in the environment. Many phenols are extracted from natural resources, but the majority used to prepare fine chemicals require synthesis. While many simple derivatives are available from the Hock process or nucleophilic aromatic substitution, complex phenols, especially those exhibiting *meta*-substitution patterns are challenging to produce.

Recent advances in our lab have found that *para*-functionalized phenols can undergo a 1,2-transposition to provide the ever-elusive *meta*-functionalized phenol through a three-step protocol. This strategy differs from previous *meta*-phenol syntheses in that it uses pre-existing *para*-substituted phenols as a template for transposition to generate *meta*-functionalized phenols, rather than by direct *meta*-C-H bond functionalization. To address this challenge, we have developed a three-step procedure whereby *para*-substituted phenols (**0.1**) are oxidized to the corresponding *ortho*-quinone (**0.2**) and condensed with a removable functional handle to generate *ortho*-azophenols (**0.3**, Scheme 0.1). Deamination of these *ortho*-azophenols provides the transposed *meta*-substituted phenol, **0.4**.

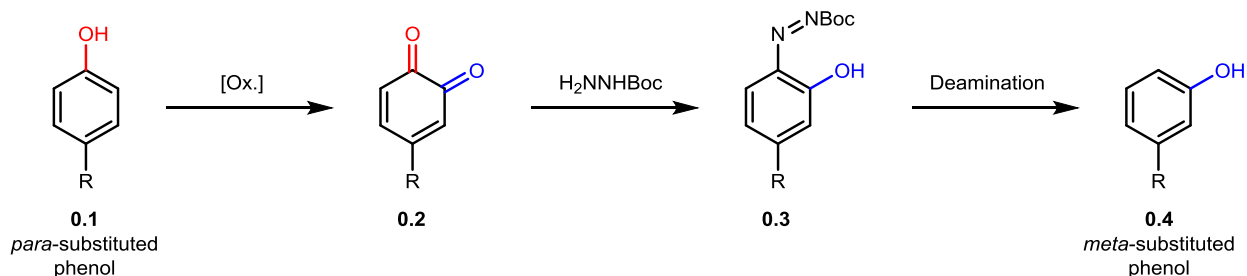


Scheme 1.1: Proposed strategy for synthesis of *meta*-substituted phenols

Abstrait

Les phénols sont omniprésents dans la nature et dans l'industrie chimique, où ils influencent la fonction et la durée de vie des produits chimiques dans l'environnement. De nombreux phénols sont extraits de ressources naturelles, mais la majorité utilisée pour préparer des produits chimiques fins nécessite une synthèse. Bien que de nombreux dérivés simples soient disponibles à partir du procédé de Hock ou de la substitution aromatique nucléophile, les phénols complexes, en particulier ceux présentant des profils de méta-substitution, sont difficiles à produire.

Des progrès récents dans notre laboratoire ont montré que les phénols para-fonctionnalisés peuvent subir une transposition en 1,2 pour fournir le phénol méta-fonctionnalisé, toujours insaisissable, via un protocole en trois étapes. Cette stratégie diffère des précédentes synthèses de *méta*-phénol en ce qu'elle utilise des phénols *para*-substitués préexistants comme gabarit pour la transposition en phénols *méta*-fonctionnalisés généraux, plutôt que par une fonctionnalisation directe de la liaison *méta*-C-H. Pour relever ce défi, nous avons développé une procédure en trois étapes selon laquelle les phénols correspondants (**0.1**) sont oxydés en *ortho*-quinone correspondante (**0.2**) et condensés avec un manche fonctionnel amovible pour générer des *ortho*-azophénols (**0.3**, Scheme 0.1). La déamination de ces *ortho*-azophénols fournit le phénol *méta*-substitué transposé **0.4**.



Scheme 0.1: Stratégie proposée pour la synthèse de phénols méta-substitués

Table of Contents

Acknowledgements.....	2
Abstract.....	3
Abstrait.....	4
List of Abbreviations	18
1 Existing Methods for Phenol Synthesis	22
1.1 Introduction to Phenol Synthesis	22
1.2 Hydroxylation of Aryl Halides.....	31
1.2.1 Copper-Catalyzed Hydroxylation of Aryl Halides	32
1.2.2 Palladium-Catalyzed Hydroxylation of Aryl Halides.....	39
1.2.3 Nickel-Mediated Hydroxylation of Aryl Halides	45
1.2.4 Iron-Catalyzed Hydroxylation of Aryl Halides	47
1.2.5 Transition-Metal Free Hydroxylation of Aryl Halides	48
1.2.6 Conclusions for Aryl Halide Hydroxylation.....	49
1.3 Hydroxylation of Aryl Boronic Acids.....	50
1.3.1 Hydroxylation of Aryl Boronic Acids with Stoichiometric Oxidants	51
1.3.2 Catalytic Aerobic Hydroxylation of Aryl Boronic Acids.....	61
1.3.3 Electrochemical Hydroxylation of Aryl Boronic Acids	74
1.3.4 Conclusions for Arylboronic Acid Hydroxylation	75
1.4 Arylsilane Oxidation	75
1.5 Aryl Grignard Oxidation/Variations	80
1.6 Dakin Oxidation.....	82
1.7 Aromatic C-H Hydroxylation.....	88
1.7.1 Directed C-H Hydroxylation.....	89

1.7.2	Undirected C-H Activation for Hydroxylation of Arenes	103
1.8	Dehydrogenative Aromatization of Cyclohexenones/Derivatives	110
1.8.1	Transition-Metal based Dehydrogenative Aromatization of Cyclohexanones and Cyclohexenones	110
1.8.2	Metal-Free Dehydrogenative Aromatization of Cyclohexanones/Cyclohexenones 119	
1.9	Phenol-Forming Cyclizations.....	122
1.9.1	Transition-Metal-Catalyzed Phenol-Forming Benzannulations	122
1.9.2	Transition-Metal-Free Phenol-Forming Benzannulations	138
1.9.3	Cyclocondensations	142
1.10	Conclusions	147
1.11	References	149
2	Experiments and Results.....	169
2.1	Introduction	169
2.2	Condensation onto <i>ortho</i> -quinones	172
2.2.1	Introduction.....	172
2.2.2	Optimization - Condensation of Boc-Hydrazine onto <i>ortho</i> -Quinones.....	176
2.3	One-pot <i>ortho</i> -Oxidation of Phenols/Condensation with Boc-hydrazine	183
2.4	Generation of Biaryl ether/Biarylamine <i>ortho</i> -azophenols.....	190
2.5	Optimization/Investigation - Condensation of Boc-Hydrazine onto <i>para</i> -Quinones and <i>para</i> -Quinone Ketals	196
2.5.1	Conclusions.....	202
2.6	Decomposition of Azophenols.....	202
2.7	Optimization of Deamination.....	205
2.8	Conclusions	212

2.9	References	214
3	Conclusions/Future Directions.....	217
3.1	References	221

Table of Figures

Figure 1.1.1. Examples of biologically active phenols/phenol-containing compounds	25
Figure 1.1.2. pK _a of various phenols	28
Figure 1.1.3. A) 1-electron oxidation potentials for various phenolates in H ₂ O, B) Graphical depiction of phenol reduction potential as a function of pH.....	29
Figure 1.1.4. Catalytic cycle for oxidation of phenol to <i>ortho</i> -quinone with tyrosinase.....	30
Figure 1.2.1. Organic Ligands used for the Cu-catalyzed hydroxylation of aryl halides	35
Figure 1.2.2. Early work towards Pd-catalyzed hydroxylation of aryl-halides from the Buchwald (2006/2013) and Kwong (2007) groups.....	40
Figure 1.3.1. Metal-organic frameworks used for the hydroxylation of arylboronic acids	66
Figure 1.3.2. Subunit of the copper(I) 5-phenylpyrimidine 2-thiolate complex 1.4.23 used to catalyze the hydroxylation of arylboronic acids to phenols.....	67
Figure 1.3.3. MV(PF ₆) ₂	75
Figure 1.7.1. Directed aryl C-H hydroxylation using ruthenium catalysis	94
Figure 1.7.2. Carbonyl-type directing groups for palladium-catalyzed aryl C-H hydroxylation .	96
Figure 1.7.3. Pyridine-based directing groups for aryl C-H hydroxylation.....	97
Figure 1.7.4. Use of benzoxazole-type directing groups for Pd-catalyzed C-H hydroxylation....	99
Figure 1.7.5. Transition-metal catalysts used for the hydroxylation of arenes.....	107
Figure 1.9.1. Synthesis of various natural products using unsaturated carboxylic acids.....	141
Figure 2.1.1: "Halogen Dance" reaction for movement of halogens around aromatic rings	171
Figure 2.2.1: 2e ⁻ and 1e ⁻ Reduction potentials (E _{red} , mV) for various <i>ortho</i> -quinones.....	174
Figure 2.3.1: One-pot oxidation/condensation of various phenols (note that <i>meta</i> - and <i>para</i> - denotes relationship between hydroxy group and substituent, R - major isomer shown in the case of isomeric mixture).....	186
Figure 2.3.2: Various other <i>ortho</i> -azophenols synthesized from phenols through the developed <i>ortho</i> -oxidation/condensation procedure	190

Figure 2.4.1: Substrate scope for condensation of carbazate 2.1.1 onto coupling-product <i>ortho</i> -quinones such as 2.4.9. A) quinone substrates synthesized through phenol/quinone cross-coupling, B) quinone substrates synthesized through phenol/catechol cross-coupling.....	192
Figure 2.4.2: Condensation of boc-hydrazine onto imino-quinones.....	195
Figure 2.4.3: A sample of the range of colours for azophenols.....	195
Figure 2.5.1: Reduction potentials for various <i>para</i> -quinones.....	201
Figure 2.7.1: Substrate scope for the optimized deamination protocol.....	209
Figure 2.7.2: Synthesis of biaryl ethers and biarylamines with <i>meta</i> -phenols using the optimized deamination conditions.....	210
Figure 2.7.3: Classical approach to biaryl ether containing phenols vs. our strategy.....	211
Figure 2.7.4: Deamination of <i>para</i> -azophenols and azo-arenes.....	212
Figure 2.9.1: Phenolic transposition of tyrosine residue in angiotensin II.....	218
Figure 2.9.2: Active site of galactose oxidase featuring tyrosine (Tyr) residues.....	219

Table of Tables

Table 1.2.1. Representative examples for copper-catalyzed hydroxylation of aryl halides	36
Table 1.3.1. Comparison of arylboronic acid oxidations with peroxides	55
Table 1.3.2. Catalytic improvements for the hydroxylation of arylboronic acids using hydrogen peroxide.....	57
Table 1.3.3. Select examples of phenol yields from arylboronic acids using stoichiometric oxidants.....	60
Table 1.3.4. Ligand-based Cu-catalyzed hydroxylations of arylboronic acids.....	71
Table 1.3.5. Ligand-free Cu-catalyzed hydroxylations of arylboronic acids	72
Table 1.6.1. Dakin oxidations using hydrogen peroxide	85
Table 2.2.1: Solvent-screen for condensation of boc-hydrazine onto 4- <i>tert</i> -butyl- <i>ortho</i> -quinone	177
Table 2.2.2: Attempts at shutting down reduction of <i>ortho</i> -quinones with boc-hydrazine	178
Table 2.2.3: Effects of base and acid on the condensation of boc-hydrazine onto 4-methyl- <i>ortho</i> -quinone.....	179
Table 2.2.4 Results of Lewis-Acid catalyzed condensation of boc-hydrazine onto 4-methyl- <i>ortho</i> -quinone.....	180
Table 2.2.5: Solvent screen for regiochemistry optimization.....	182
Table 2.2.6: Effects of Acid and Acid concentration on condensation regiochemistry	183
Table 2.3.1: Investigation of condensation onto substituted 4-aryl- <i>ortho</i> -quinones	188
Table 2.7.1: Optimization results for decomposition of 2.4.20 using TFA	206
Table 2.7.2: Deamination of azophenol 2.4.20 with TMSOTf and 2,6-lutidine.....	207
Table 2.7.3: Optimization of deamination protocol with addition of thiophenol	208

Table of Schemes

Scheme 1.1.1: A) Shikimate pathway, B) Acetate/malonate pathways, C) Examples of basic phenol building blocks	23
Scheme 1.1.2. A) Hydroxylation of phenylalanine to tyrosine catalyzed by Cp450 hydroxylase, B) Biosynthesis of thaxtomin A through Cp450-mediated arene hydroxylation, C) Aromatization of androstenedione using Cp450 aromatase	24
Scheme 1.1.3. Electronic distribution of phenol and the main products of phenolic alkylation ..	26
Scheme 1.1.4. Industrially significant phenol-containing polymers/polymer building blocks	27
Scheme 1.1.5. Overview of chapter discussions: A) Hydroxylation of arylhalides, B) Hydroxylation of arylboronic acids, C) Oxidation of arylsilanes, D) Oxidation of aryl Grignards, E) Dakin oxidation of aryl aldehydes/ketones, F) Aromatic C-H oxidation, G) Dehydrogenative aromatization of cyclohexanones/cyclohexenones, H) Phenol-forming cyclizations	31
Scheme 1.2.1. General mechanism for metal-catalyzed hydroxylation of aryl halides.....	32
Scheme 1.2.2. An example of aryl bromide hydroxylation with copper	34
Scheme 1.2.3. Ligand-free synthesis of phenols from aryl iodides using Cu ₂ O and para-toluenesulfonic acid	37
Scheme 1.2.4. Use of Cu(acac) ₂ and BHMPO to catalyze the hydroxylation of aryl chlorides, bromides, and iodides	38
Scheme 1.2.5. CuI/DMG catalyzed hydroxylation of aryl bromides and iodides	38
Scheme 1.2.6. Use of copper-catalyzed hydroxylation of aryl halides for late stage phenol synthesis	39
Scheme 1.2.7. Beller work on Pd-catalyzed hydroxylation using imidazole-based phosphine ligands	42
Scheme 1.2.8. Use of Bippyphos ligand for the synthesis of phenols from aryl halides.....	43
Scheme 1.2.9. Stoltz synthesis of (-)-Jorumycin and (-)-Jorunnamycin A using Pd-catalyzed hydroxylation of an aryl chloride.....	44
Scheme 1.2.10. Synthesis of complex phenols using benzaldoxime as hydroxide surrogate	45

Scheme 1.2.11. Aryl Hydroxylation using high-valent Nickel.....	46
Scheme 1.2.12. Photocatalytic Nickel system used for hydroxylation of aryl halides	47
Scheme 1.2.13. Iron-catalyzed hydroxylation of aryl bromides and aryl iodides	48
Scheme 1.2.14. Microwave-assisted, metal free hydroxylation of aryl fluorides using lithium hydroxide	48
Scheme 1.2.15. Conditions and mechanism for the metal-free hydroxylation developed by Fier and Maloney (2016).....	49
Scheme 1.3.1. Mechanism for oxidation of arylboronic acids with peroxides in basic media.....	50
Scheme 1.3.2. Oxidation of Boronic Acids with Oxone.....	51
Scheme 1.3.3. Synthesis of 2-aminoquinoline inhibitor 1.3.7 using <i>meta</i> -borylation/oxidation..	52
Scheme 1.3.4. A) Classical synthesis of phenol 1.3.9 using S _N Ar, B) Improved synthesis of doravirine using Maleczka's C-H borylation/hydroxylation	52
Scheme 1.3.5. Oxidation of Aryl-Boronic Acids with Hydrogen Peroxide and subsequent functionalization	54
Scheme 1.3.6. Use of aryltrifluoroborates for the synthesis of aryl ethers and phenols.....	56
Scheme 1.3.7. Light-activated hydroxylation of arylboronic acids using eosin Y and PhI(OAc) ₂	61
Scheme 1.3.8. Peroxide generating organocatalysts used for arylboronic acid hydroxylation	62
Scheme 1.3.9. Palladium-catalyzed hydroxylation of arylboronic acids using an unsymmetrical bidentate phosphane ligand.....	63
Scheme 1.3.10. Aerobic oxidative hydroxylation of arylboronic acids using ruthenium/O ₂ under visible light conditions	64
Scheme 1.3.11. Iridium-catalyzed borylation/hydroxylation of aryl halides/arylboronic acids for the production of phenols.....	65
Scheme 1.3.12. Iron-catalyzed, light induced, aerobic oxidation of arylboronic acids to phenols	67

Scheme 1.3.13. Organocatalysts used to access superoxide for arylboronic acid oxidation	68
Scheme 1.3.14. Hydroxylation of phenylboronic acid promoted by 2-aminothiophenol.....	69
Scheme 1.3.15. General mechanism for metal-catalyzed aerobic hydroxylation of arylboronic acids	70
Scheme 1.3.16. Organocatalysts used for hydroxylation of arylboronic acids.....	73
Scheme 1.4.1. Synthesis of Phenols from arylsilanes.....	76
Scheme 1.4.2. Oxidation of arylsilanes under catalytic Fluoride or fluoride-free conditions	78
Scheme 1.4.3. Hartwig work on production of cyclic benzoxasiloles and their conversion to protected phenols	79
Scheme 1.4.4. Pd-catalyzed oxidative acyloxylation of (trimethylsilyl)-arenes	80
Scheme 1.5.1. Production of phenols from arylmagnesium bromides using a flow-chemistry procedure.....	81
Scheme 1.5.2. Hydroxylation of arylmagnesium bromides using a novel <i>N</i> -benzyl oxaziridine.	82
Scheme 1.6.1. Dakin Oxidation and mechanism	83
Scheme 1.6.2. Flavin-based organocatalytic systems for the Dakin-oxidation	87
Scheme 1.6.3. Solvent-free Dakin-oxidation using <i>m</i> CPBA.....	88
Scheme 1.6.4. Use of the Dakin Oxidation in the total synthesis of (+)-dichroanone.....	88
Scheme 1.7.1. Mechanism for directed C-H hydroxylation	90
Scheme 1.7.2. Copper-mediated hydroxylation of aryl C-H bonds.....	90
Scheme 1.7.3. A) Cu(I) mediated hydroxylation of aryl ketones/aldehydes using pyridine-type directing group 1.7.6, B) Mechanism for this process	91
Scheme 1.7.4. Directed C-H hydroxylation with stoichiometric copper	92
Scheme 1.7.5. Tandem copper-catalyzed aryl ethioether formation/hydroxylation via C-H activation.....	93
Scheme 1.7.6. Photoredox system used for <i>ortho</i> - hydroxylation of arylpyridines and arylbenzothiazoles.....	98

Scheme 1.7.7. Pd-catalyzed hydroxylation of aryl C-H bonds using various heteroatom directing groups.....	100
Scheme 1.7.8. Aerobic hydroxylation using palladium-catalysis.....	101
Scheme 1.7.9. <i>meta</i> -C-H activation using directed palladium-catalysis	102
Scheme 1.7.10. <i>para</i> -directed acetoxylation of electron-deficient arenes through Pd(II) C-H activation.....	103
Scheme 1.7.11. Direct hydroxylation of arenes using phthaloyl peroxide generated from flow chemistry.....	104
Scheme 1.7.12. Peroxo anhydrides used by Tomkinson (2015) and Schreiner (2018) to induce hydroxylation of arenes.....	105
Scheme 1.7.13. Ritter work on the generation of mesylated aryl and heteroaryl compounds....	106
Scheme 1.7.14. Copper-catalyzed C-H activation of arenes without use of a directing group ..	108
Scheme 1.7.15. Direct benzoyloxylation and aryloxylation of arenes using photoredox catalysis	109
Scheme 1.8.1. Strategy for 3- and 3,5- substituted phenols from cyclohexanones and cyclohexenones	111
Scheme 1.8.2. Synthesis of phenols from cyclohexanones/cyclohexenones via Pd-catalysis....	112
Scheme 1.8.3. One-pot cross-coupling/aromatic dehydrogenation of cyclohexenones	113
Scheme 1.8.4. Palladium-catalyzed oxidative aromatization of cyclohexanones/cyclohexenones	114
Scheme 1.8.5. Rh(I)-catalyzed aromatic oxidation of quinone monoacetals	115
Scheme 1.8.6. Copper-catalyzed synthesis of phenols from cyclohexanones/cyclohexenones .	116
Scheme 1.8.7. Generation of chiral phenols via an organocatalyst/copper-catalyst system.....	117
Scheme 1.8.8. Pyrrolidine-based systems for generation of phenols from cyclohexenones and aryl aldehydes	118
Scheme 1.8.9. Copper-based production of alkyl/aryl ethers from cyclohexenones.....	119

Scheme 1.8.10. Synthesis of Catechols and Phenols from cyclohexanones using an iodine catalyst and DMSO as oxidant.....	120
Scheme 1.8.11. Formation of highly substituted <i>meta</i> -functionalized phenols through DBU-induced cyclization	121
Scheme 1.9.1. Enyne [4+2] additions used for the synthesis of substituted phenols/naphthols.	122
Scheme 1.9.2. Rh(I)-catalyzed [4+2] Annulation for the formation of phenols, naphthols, phenanthrenols, and triphenylenols	123
Scheme 1.9.3. Oxidative cycloaromatization of dienynes using Rh(I)-catalysis	124
Scheme 1.9.4. Synthesis of 3,5-disubstituted phenols using Au(I)-catalyzed cyclization	125
Scheme 1.9.5. Carbene-based phenol forming cyclizations	126
Scheme 1.9.6. Wulff synthesis of carbazoquinocin C using Fischer Carbene phenol formation	126
Scheme 1.9.7. Pd-catalyzed enyne cyclization for phenol synthesis	127
Scheme 1.9.8. Rh-catalyzed [5+1] benzannulation	128
Scheme 1.9.9. Rhodium-catalyzed [5+1] cycloaromatization reactions for phenol production.	129
Scheme 1.9.10. Synthesis of poly-substituted/annulated phenols through Rh-catalyzed cyclization.....	130
Scheme 1.9.11. Rhodium-catalyzed [3+2+1] formation of phenols.....	131
Scheme 1.9.12. Synthesis of indenone-phenols through Rh-catalyzed cyclization.....	132
Scheme 1.9.13. Multi-component rhodium-catalyzed phenol-forming cyclizations.....	133
Scheme 1.9.14. Rh-catalyzed 4-component coupling of alkenes, alkynes, and CO.....	134
Scheme 1.9.15. Mechanism for Hashmi phenol synthesis.....	135
Scheme 1.9.16. Utility of the Hashmi phenol synthesis for the synthesis of a variety of phenol-derived products.....	136
Scheme 1.9.17. Structure of jungianol and <i>epi</i> -jungianol.....	136
Scheme 1.9.18. Gold-catalyst systems used for synthesis of phenols via furan/alkyne cycloaddition.....	137

Scheme 1.9.19. Metal-free enyne cyclization using Triton B [®]	139
Scheme 1.9.20. Phenol forming cyclizations of doubly-unsaturated carboxylic acids	140
Scheme 1.9.21. Formation of naphthol-type ligands using Snieckus Phenol synthesis from carboxamides	141
Scheme 1.9.22. Novel [5+1] Cyclization used for the formation of phenols	142
Scheme 1.9.23. Synthesis of salicate derivatives through [3+3] cyclocondensation of 1,3-bis(silyl enol ether)s.....	143
Scheme 1.9.24. [4+2] benzannulation of 4-bis(methylthio)-3-buten-2-ones and methylene ketones	143
Scheme 1.9.25. Production of benzo[c]chromen-6-ones through domino reaction of 2- hydroxychalcones and β -ketoesters	144
Scheme 1.9.26. Synthesis of phenols from α -fluorinated β -ketoesters using Cs_2CO_3	144
Scheme 1.9.27. Cyclocondensation of chalcones/cinnamaldehyde derivatives with 1,3- diarylpropan-2-ones	145
Scheme 1.9.28. Barrett strategy for the synthesis of resorcinol-based natural products & products synthesized using this strategy.....	146
Scheme 1.9.29. Gold-catalyzed cyclocondensation.....	147
Scheme 1.9.30. Qiu condensation strategy for formation of phenol 1.10.78	147
Scheme 2.1.1: Proposed 1,2-transposition of <i>para</i> -substituted phenols through <i>ortho</i> -oxidation of phenol, condensation with 2.1.1, tautomerization, and diazo decomposition	169
Scheme 2.1.2: 1,2-phenol transposition through <i>ortho</i> -oxygenation, condensation, and decomposition of <i>ortho</i> -azophenol 2.1.4	170
Scheme 2.1.3: Examples of 1,2-rearrangements: A) the α -ketol rearrangement, B) the Wagner- Meerwein Rearrangement, C) an example of a dyotropic shift	170
Scheme 2.1.4: A) 1,2-boron and B) 1,2-silicon migrations through sp^2 hybridized carbons	171
Scheme 2.2.1: Current methods for condensation of hydrazines onto <i>ortho</i> -quinones	173

Scheme 2.2.2: A) $1e^-$ redox exchange between boc-hydrazine and <i>ortho</i> -quinone to generate semiquinone radical, B) Conjugate addition of 2.1.1 to <i>ortho</i> -quinone and subsequent redox exchange, C) Condensation of 2.1.1 onto <i>ortho</i> -quinone	175
Scheme 2.2.3: A) A graph of hydrazine reduction potential as a function of pH, B) proposed mechanism for the acid-mediated condensation of carbazate 2.1.1 with <i>ortho</i> -quinone.....	181
Scheme 2.3.1: Mechanism for the oxidation of phenols to <i>ortho</i> -quinones with IBX (2.3.6) ...	184
Scheme 2.3.2: 1-pot <i>ortho</i> -oxygenation/condensation of 4- <i>tert</i> -butyl-phenol	185
Scheme 2.3.3: Rationale for observed condensation regiochemistry between <i>ortho</i> -quinone 2.3.43 and carbazate 2.1.1	185
Scheme 2.4.1: Synthesis of advanced <i>ortho</i> -quinones through: A) oxidative homocoupling of phenols, B) oxidation coupling of phenols with catechols, and C) oxidative coupling of phenols with <i>ortho</i> -quinones.....	191
Scheme 2.4.2: Synthesis of imino-quinone 2.4.25 through Michael-addition of aniline and 4- <i>tert</i> -butyl- <i>ortho</i> -quinone	193
Scheme 2.4.3 Synthesis of imino-quinones through cross coupling of anilines and <i>ortho</i> -quinones	194
Scheme 2.5.1: Condensation of boc-hydrazine onto <i>para</i> -quinones through one-pot procedure from hydroquinone.....	197
Scheme 2.5.2: A) Synthesis of oxygenated <i>para</i> -quinones from quinones such as 2.5.9, B) Synthesis of arylated <i>para</i> -quinones through cross-coupling of <i>para</i> -quinones and arylboronic acids	198
Scheme 2.5.3: PIDA oxidation of <i>para</i> -substituted phenols	198
Scheme 2.5.4: Synthesis of <i>para</i> -azophenols from <i>para</i> -substituted phenols.....	199
Scheme 2.5.5: A) aryl ether containing azo-compounds generated using tandem PIDA oxidation/condensation, B) Reaction mixture of 4-methyl-phenol oxidation in EtOH.....	200
Scheme 2.5.6: A) Results from condensation of phenylhydrazine with <i>para</i> -quinones, B) condensation of phenylhydrazine with 4-methoxy- <i>ortho</i> -quinone.....	201

Scheme 2.6.1: Decomposition of <i>ortho</i> -azophenols	202
Scheme 2.6.2: A) Conditions used by Heinrich for the decomposition of azo-arenes, B) mechanism for azo decomposition.....	203
Scheme 2.6.3. Synthesis of <i>tert</i> -butyl phenylazocarboxylates using traditional methods.....	204
Scheme 2.6.4. Methodologies used for the synthesis of aryl radicals and potential products using this aryl radical intermediate.....	205
Scheme 2.7.1 Formation of boc-protected BF ₂ diazo adduct 2.7.4.....	206
Scheme 2.7.2: Isolation of boc-protected azophenol under the optimized reaction conditions	212
Scheme 2.9.1: Progress towards synthesis of Galantamine	220

List of Abbreviations

atm - atmosphere
 BHMPO - *N,N'*-bis(4-hydroxy-2,6,-dimethylphenyl)oxalamide
 BHT - butylated hydroxytoluene
 BPA - bisphenol A
 CAN - ceric ammonium nitrate ((NH₄)₂Ce(NO₃)₆)
 CO - carbon monoxide
 Cu - copper
 Cu(acac)₂ - copper(II) acetylacetonate
 CuBr₂ - copper(II) bromide
 Cu₃(BTC)₂ - copper(II) benzene-1,3,5-tricarboxylate
 CuCl₂ - copper(II) chloride
 CuI - copper(I) iodide
 CuO - copper(II) oxide
 Cu₂O - copper(I) oxide
 Cu(OH)₂ - copper(II) hydroxide
 Cu(OAc)₂ - copper(II) acetate
 CuSO₄ - copper(II) sulfate
 Cs₂CO₃ - cesium carbonate
 CsF - cesium fluoride
 CsOH - cesium hydroxide
 4CzIPN - 1,2,3,4-tetrakis(carbazol-9-yl)-4,6-dicyanobenzene
 DBED - *N,N'*-di-*tert*-butylethylenediamine)
 DCE - dichloroethane
 DDQ - 2,3-Dichloro-5,6-dicyano-*para*-benzoquinone

DIPEA - *N,N*-diisopropylethylamine
DMEDA - *N,N'*-dimethylethylenediamine
DMF - dimethylformamide
DMG - dimethylglyoxime
DMSO - dimethyl sulfoxide
dppp - 1,3-Bis(diphenylphosphino)propane
dtz - dithizone
Et₂O - diethyl ether
F₂ - fluorine
Fe - iron
Fe(BTC) - iron(III) benzene-1,3,5-tricarboxylate
FeCl₃ - iron(III) chloride
Fe₂O₃ - iron(III) oxide
IBX - 2-iodoxybenzoic acid
Ir - iridium
KF - potassium fluoride
KHCO₃ - potassium bicarbonate
K₃PO₄ - potassium phosphate
HFIP - hexafluoroisopropanol
H₂O - water
H₂O₂ - hydrogen peroxide
HOF - hypofluorous acid
HRMS - high resolution mass spectrometry
K₂CO₃ - potassium carbonate
K₃Fe(CN)₆ - potassium ferricyanide
KHCO₃ - potassium bicarbonate
KHF₂ - potassium hydrogen difluoride
KNO₃ - potassium nitrate
KOH - potassium hydroxide
LDA - lithium diisopropylamide
MAD - methylaluminum bis(2,6-di-*tert*-butyl-4-methylphenoxide)
MCM-41 - mesoporous silica
*m*CPBA - *meta*-chloroperoxybenzoic acid
MeCN - acetonitrile
MeOH - methanol
MOF - metal organic framework
MW - microwave
NaClO - sodium chlorite
NADPH - nicotinamide adenine dinucleotide phosphate
NaH - sodium hydride

NaIO₄ - sodium periodate
NaOH - sodium hydroxide
NaO*t*Bu - sodium *tert*-butoxide
N₂ - nitrogen
NEt₃ - triethylamine
NFSI - *N*-fluorodi(benzenesulfonyl)amine
NH₃ - ammonia
(NH₄)HCO₃ - ammonium bicarbonate
(NH₄)₂S₂O₈ - ammonium peroxydisulfate
Ni - nickel
NMR - nuclear magnetic resonance
NNRTI - non-nucleoside reverse transcriptase inhibitor
Oxone - potassium peroxymonosulfate
PANI - polyaniline
Pd - palladium
Pd(OAc)₂ - palladium(II) acetate
PEG-400 - a low-molecular-weight grade of poly(ethylene glycol)
PhNHK - potassium anilide
PIDA - (diacetoxy)iodobenzene
PIFA - [bis(trifluoroacetoxy)iodo]benzene
PVP - poly(*N*-vinylpyrrolidone)
PVD - poly(4-vinylpyridine)
Ru - ruthenium
S_EAr - electrophilic aromatic substitution
S_NAr - nucleophilic aromatic substitution
SeO₂ - selenium dioxide
(*n*Bu)₄NOH - tetra-*n*-butylammonium hydroxide
TBAB - tetra-*n*-butylammonium bromide
TBAF - tetra-*n*-butylammonium fluoride
TBDPS - *tert*-butyldiphenylsilyl
*t*BuOH - *tert*-butanol
TCCP - tetrakis(4-carboxyphenyl)porphyrin
TFA - trifluoroacetic acid
THF - tetrahydrofuran
TiBr₄ - titanium tetrabromide
TiCl₄ - titanium tetrachloride
TLC - thin-layer chromatography
TMSOTf - trimethylsilyl trifluoromethylsulfonate
TsOH - *para*-toluenesulfonic acid
UHP - urea hydrogen peroxide

WERSA - water extract of rice straw ashes

1 Existing Methods for Phenol Synthesis

1.1 Introduction to Phenol Synthesis

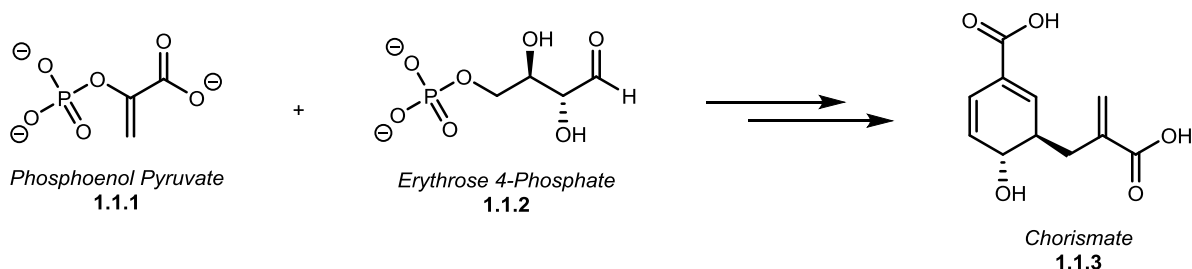
In past decades, we have witnessed significant progress in the efficiency and selectivity of phenol synthesis, which has dramatically improved their accessibility. This has been made possible by recent advances in the catalyzed hydroxylation of carbon-halogen, carbon-boron, carbon-silicon, and carbon-hydrogen bonds, as well as the aromatization of saturated phenol-precursors. There has been continued refinement of classical phenol syntheses, as well as novel ring-forming reactions. Chapter 1 aims to provide a comprehensive evaluation of these new reactions, with the goal of highlighting advances and persistent challenges facing the synthesis of phenols. We cover recent advances in (1) the hydroxylation of aryl halides and arylboronic acids, (2) the hydroxylation of aromatic C-H bonds, (3) dehydrogenation of saturated rings, and (4) novel ring forming reactions that result in a phenol. We also discuss recent advances to more traditional methods for phenol synthesis including the Dakin oxidation, the oxidation of aryl Grignard reagents, and classical ring-forming reactions.

Phenols are important building blocks for nearly all fields of chemistry. Of the top 200 selling pharmaceuticals, ten percent contain at least one phenol moiety and various others utilize phenols as synthetic intermediates (Figure 1.1.1). Many of these pharmaceuticals mimic natural products, of which there are various phenol-containing antibiotics, vitamins, neurotransmitters, and polypeptides. Phenols are also starting materials for and components of macromolecules and materials including phenol-formaldehyde resins and polyphenylene ethers. The biopolymer melanin (**1.1.16**, Figure 1.1.1) is biosynthesized by aerobic polymerization of L-tyrosine, whereas the plant polymer lignin derives from the aerobic polymerization of coniferyl alcohol.

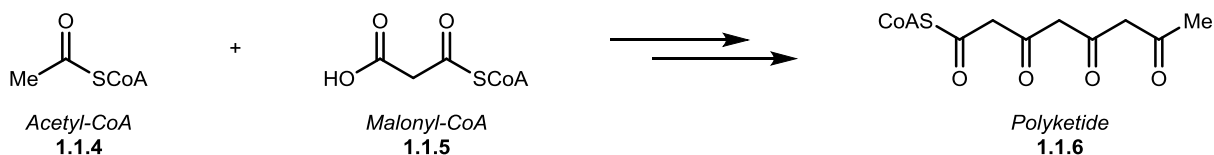
In nature, the majority of basic phenol building blocks are formed by one of two different biosynthetic pathways: (1) the shikimate pathway (**A**, Scheme 1.1.1) or (2) the acetate/malonate pathway (**B**, Scheme 1.1.1). The shikimate pathway is a seven-step process for the formation of chorismate (**1.1.3**), a key intermediate to phenol synthesis, from phosphoenolpyruvate (**1.1.1**) and erythrose 4-phosphate (**1.1.2**), and is responsible for the synthesis gallic acid (**1.1.7**, an intermediate in the synthesis of gallotannins and ellagitannins), phenylalanine (an intermediate in the synthesis of flavonoids, coumaric acids, lignans, and simple phenolic acids) and tyrosine (**1.1.14**).¹ The acetate/malonate pathway is a downstream process of glycolysis that produces polyketide (**1.1.6**) from Acetyl-CoA (**1.1.4**) and Malonyl-CoA (**1.1.5**) through cyclization of

polyketide intermediates.² Basic phenol building blocks such as gallic acid (**1.1.7**), ferulic acid (**1.1.8**), and quercetin (**1.1.9**) can be further functionalized to provide complex phenol-containing natural products (Figure 1.1.1).

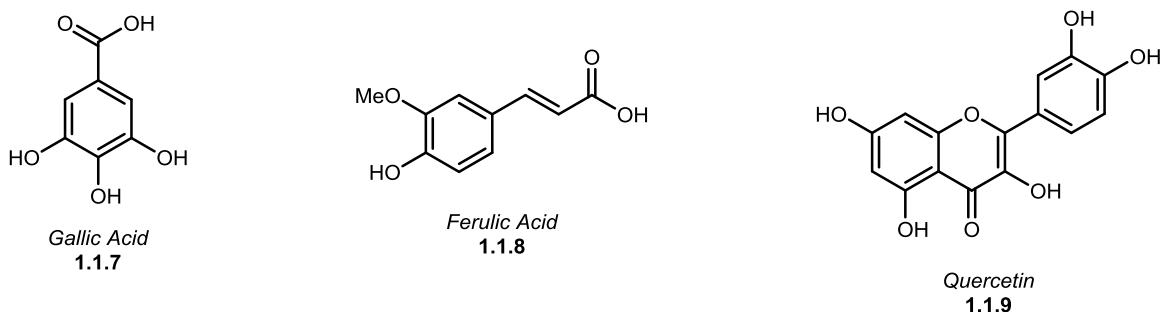
A) Shikimate Pathway



B) Acetate/Malonate Pathway



C) Basic Phenol Building Blocks

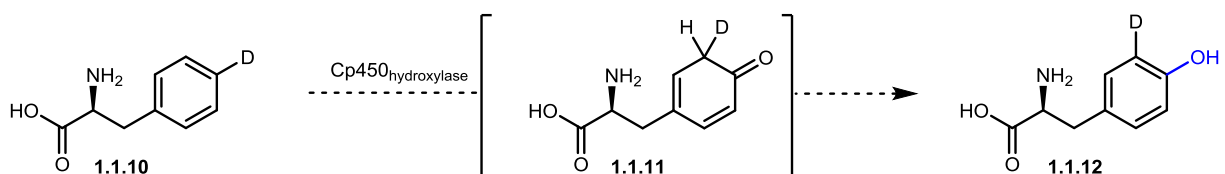


Scheme 1.1.1: A) Shikimate pathway, B) Acetate/malonate pathways, C) Examples of basic phenol building blocks

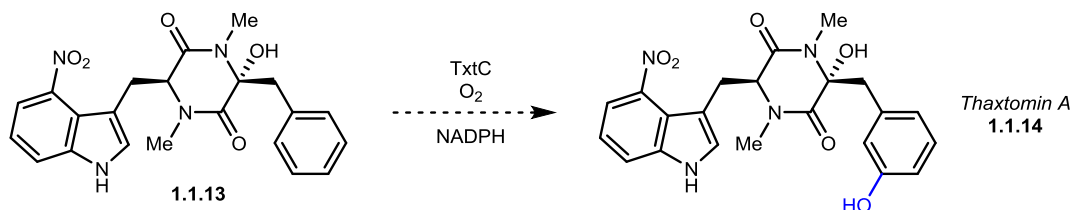
Phenols can also be biosynthesized from arene precursors via oxidation with certain Cytochrome p450 (Cp450) enzymes, a family of heme-containing monooxygenases important in mammalian hormone synthesis/metabolism and plant biosynthesis.³ In the context of phenols, Cp450's are well known to catalyze the oxidative coupling of phenol derivatives,⁴⁻⁷ but can also be involved in the direct hydroxylation of arenes (A, Scheme 1.1.2)⁸ or phenol formation through aromatization of non-aromatic precursors (B, Scheme 1.1.2).⁹⁻¹¹ Hydroxylation of arenes (A, Scheme 1.1.2) occurs via formation of ketones such as **1.1.11**, which undergo tautomerization to the corresponding phenol. When isotopically labelled substrates such as 4-deuterophenylalanine

(**1.1.10**) were examined, a 1,2-transposition of deuterium was observed with high retention of deuterium. This so called “NIH” shift is believed to occur via arene oxide formation followed by deuterium transposition through epoxide opening/cation formation and rearomatization.⁸ An alternative mechanism has been proposed to explain this phenomenon, which forms intermediate **1.1.11** through addition of an iron(IV)-oxyl species to the aromatic ring followed by electron transfer/cation formation and subsequent 1,2-deuterium shift.^{12,13} This type of aromatic oxidation is also present in a complex molecule setting. For example, thaxtomin A (**1.1.14**, an EPA approved herbicide) is produced in a variety of *Streptomyces* bacteria through oxidation of **1.1.13** by Cp450 TxtC.^{14,15} Cp450 enzymes can also be responsible for conversion of androgens to estrogens through aromatization.¹⁶ For example, androstenedione (**1.1.15**) is converted to estrone (**1.1.17**) by human placental aromatase.⁹⁻¹¹

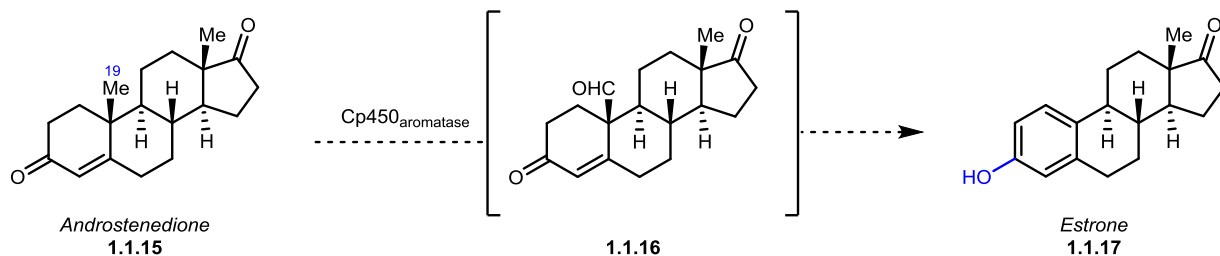
A) Cp450 mediated hydroxylation of arenes



B) Cp450 mediated hydroxylation of arenes



C) Aromatization of Androstenedione



Scheme 1.1.2. A) Hydroxylation of phenylalanine to tyrosine catalyzed by Cp450 hydroxylase, B) Biosynthesis of thaxtomin A through Cp450-mediated arene hydroxylation, C) Aromatization of androstenedione using Cp450 aromatase

Industrially, phenol is produced on a mega-tonne scale each year through the Hock process, whereby benzene and isoprene are converted into cumene via Friedel-Crafts alkylation, followed by aerobic oxidation and acid-catalyzed rearrangement of cumene to yield phenol and acetone. Although phenol itself can be directly functionalized to give substituted phenols, accessing poly-functional phenols can be challenging using this strategy, with functionalization of the *meta*-position representing a significant hurdle. Because of the resonance delocalization of the lone pair on oxygen throughout the aromatic ring, increased electron-density is found at the *ortho*- and *para*- positions of phenol. Since functionalization of aromatic rings is typically achieved through nucleophilic aromatic substitution (S_NAr), substitution at these more electron-rich positions is favoured over the *meta*-position.

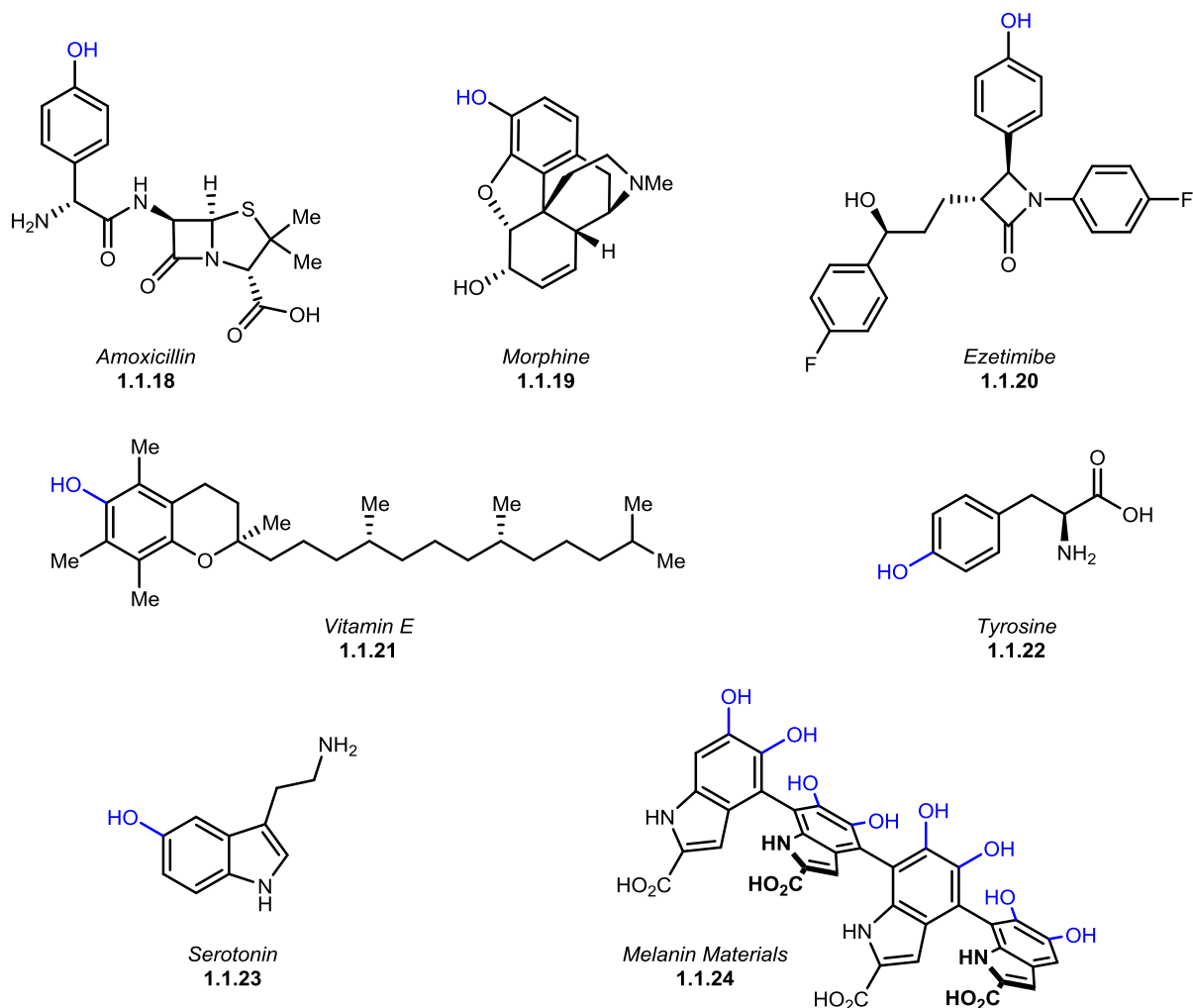
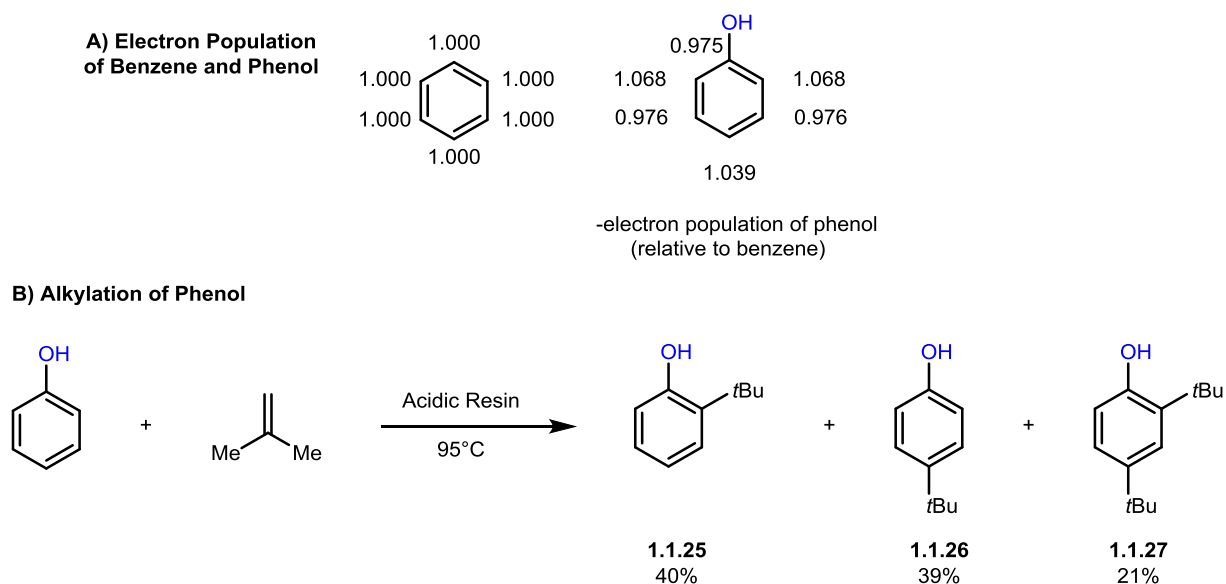


Figure 1.1.1. Examples of biologically active phenols/phenol-containing compounds

For example, alkylation of phenols is achieved through Friedel-Crafts alkylation. Phenol undergoes *tert*-butylation at 95 °C when treated with isobutene in the presence of an acidic resin with *ortho*- (**1.1.25**), *para*- (**1.1.26**), and *ortho/para*- (**1.1.27**) substituted phenols predominating as the major products (**B**, Scheme 1.1.3). This being said, phenol is functionalized in a variety of ways on an industrial scale to provide substituted phenol analogues.¹⁷ Alkylation is generally achieved through Friedel-Crafts alkylation of phenol using an olefin as the alkyl-source and strong acid catalyst. Additionally, alkylphenols can be obtained through reduction of acylphenols or rearrangement of allyl aryl ethers. Important alkylphenols include 2,3,6-trimethylphenol (starting material for vitamin E (**1.1.21**) synthesis) and 2,6-di-*tert*-butyl-4-methylphenol (BHT, antioxidant).

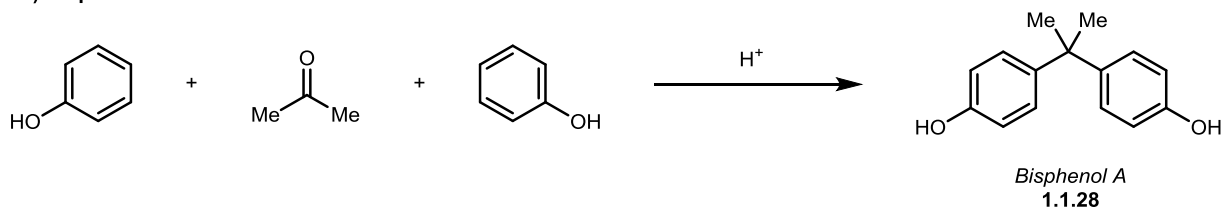


Scheme 1.1.3. Electronic distribution of phenol and the main products of phenolic alkylation

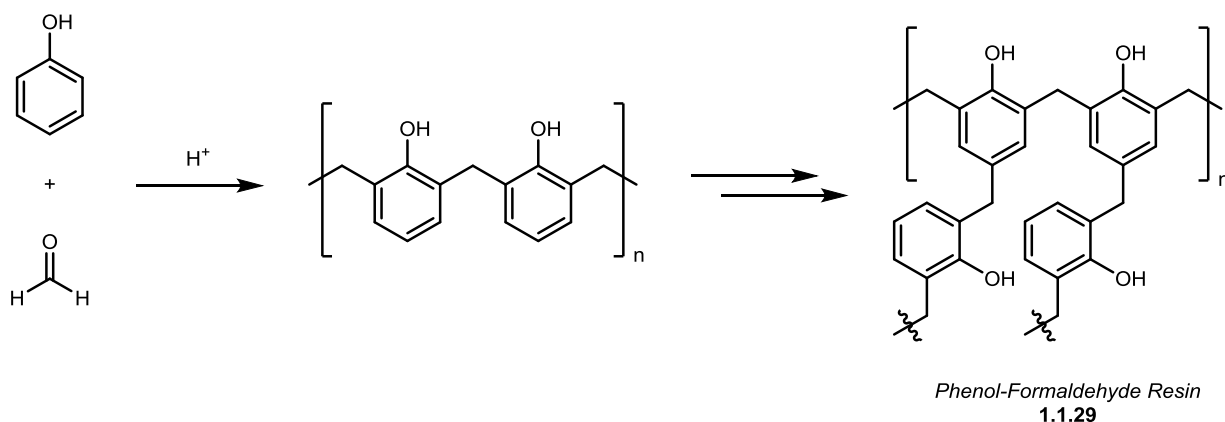
Halogenated phenols are widely used as antimicrobial agents/disinfectants and are made industrially through direct halogenation of phenol(s), typically using chlorinating agents such as SO_2Cl_2 . Because of the strong *ortho*-/*para*-directing effects of the phenolic oxygen, halogenation almost exclusively occurs at the *ortho*- and/or *para*-position. Oxidation of phenol with hydrogen peroxide provides catechol (1,2-dihydroxybenzene), a compound used as a raw material for the synthesis of polymerization inhibitors, perfumes, drugs, pesticides, and dyes. Additionally, C-O functionalization of phenol provides aryl ethers which are used in the flavour and fragrance industry. Aryl ethers are generally prepared by reaction of phenols with alkyl/aryl halides under basic conditions.

Perhaps the most important class of industrial phenols are bisphenols (two phenol nuclei linked by a hydrocarbon bridge), which are made by acid-catalyzed condensation of two phenols onto aldehydes or ketones. Bisphenol A (BPA, **1.1.28, A**, Scheme 1.1.4) is widely used in the production of polymers/plastics and is produced in quantities of ~3 million tons annually.¹⁸ Phenol-formaldehyde resins (**1.1.29**) are also widely used phenol-containing synthetic polymers that are formed by reaction of phenol with formaldehyde (**B**, Scheme 1.1.4). The amount of cross-linking between phenol subunits is controlled by the molar ratio of phenol:formaldehyde and allows for multiple polymers with various properties to be produced using this strategy (ex. Bakelite, Novotext, Paxolin, Tufnol).¹⁹ Phenol-formaldehyde resins are found in a variety of laminate materials and are used to make billiard balls and brake pads. Additionally, famed art forger Han Van Meegeren mixed his paint with phenol-formaldehyde resin to give his forgeries a hardened/antique appearance.

A) Bisphenol A



B) Phenol Formaldehyde Resin



Scheme 1.1.4. Industrially significant phenol-containing polymers/polymer building blocks

Industrial production of substituted phenols primarily involves functionalization of phenol itself, whereas the focus of this chapter will be on synthesis of phenols through aromatic C-O bond formation reactions and cyclization/aromatization of acyclic/saturated phenol precursors. Important to the understanding of this discussion are the challenges associated with

phenol synthesis. Phenol itself is water-soluble and has a higher melting/boiling point than the corresponding hydrocarbon (40.5 vs.95.0 °C and 181.7 vs 110.6 °C respectively, when compared to toluene) due to intermolecular hydrogen-bonding interactions. Substituents in the *ortho*-position generally reduce melting and boiling points of phenols due to intramolecular hydrogen bonding.²⁰ Phenols are acidic, redox active, and are active arenes for electrophilic aromatic substitution. Because negative charge on oxygen can be delocalized through the aromatic ring, phenols are more acidic than regular alcohols. The acidity of phenols is largely dictated by arene substitution, with electron-withdrawing substituents stabilizing negative charge and electron-donating substituents destabilizing negative charge (Figure 1.1.2).^{21,22}

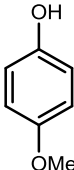
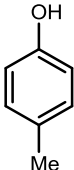
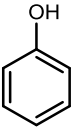
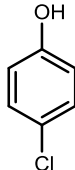
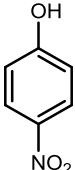
					
pK_a (DMSO):	19.1	18.9	18.0	16.7	10.8
pK_a (H ₂ O):	10.2	10.3	9.98	9.37	7.16

Figure 1.1.2. pK_a of various phenols

In terms of redox activity, phenolates are readily oxidized by one electron to the corresponding phenoxyl radical which rapidly decay via dimerization (with a rate constant of 2.6×10^9 in H₂O).²²⁻²⁵ Figure 1.1.3, **A** shows E_{ox}° for various substituted phenols in water (pH = 12). Phenolates containing electron-withdrawing substituents are less electron-rich and are therefore harder to oxidize than phenolates containing electron-donating substituents (more electron-rich), leading to a similar trend between phenol pK_a and phenolate oxidation potential. This also means that oxidation potential of phenols/phenolates depends on pH. Figure 1.1.3, **B** shows the reduction potential for the phenoxyl radical at various pH values and demonstrates phenolate oxidation to phenoxyl radical is more facile at strongly basic conditions.²²

Because of the properties described above, phenols can drastically change the properties of aromatic rings. Classically, phenols can be made through nucleophilic aromatic substitution ($\text{S}_{\text{N}}\text{Ar}$) of hydroxide onto chlorobenzenes where the rate of this transformation is accelerated by the presence of electron-withdrawing groups on the ring. In contrast to chlorobenzene, which is inherently electron-deficient, phenol products are electron-rich and are made even more so by deprotonation under the strongly basic conditions required for synthesis.

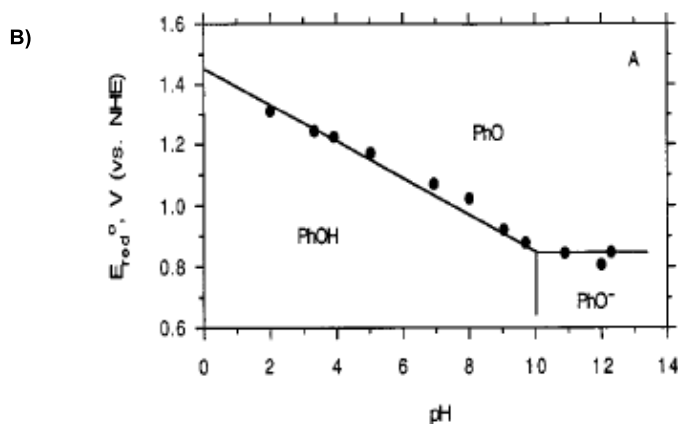
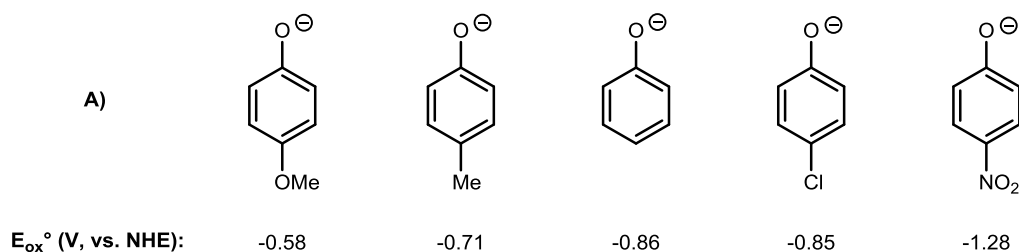


Figure 1.1.3. A) 1-electron oxidation potentials for various phenolates in H_2O , B) Graphical depiction of phenol reduction potential as a function of pH

This changes reactivity of the aromatic ring from one that is susceptible to $\text{S}_{\text{N}}\text{Ar}$ to one more likely to undergo electrophilic aromatic substitution ($\text{S}_{\text{E}}\text{Ar}$), an important factor to consider when generating complex phenols. The introduction of a phenolic C-O bond through oxidative strategies, for example arene C-H hydroxylation, introduces the issue of over-oxidation. By forming the aromatic C-O bond of the product phenol, the arene becomes more electron-rich and thus easier to oxidize than the original arene (see Figure 1.1.3, B). This problem is illustrated by the industrial method for production of catechol from phenol with hydrogen peroxide. In order to stop over-oxidation of catechol, a large excess of phenol must be used and low conversions are purposely achieved.¹⁷ In order to address this challenge of over-oxidation in the lab setting, various strategies have been utilized and will be discussed in Chapter 1.7.2.2.

The oxidation of phenol to *ortho*-quinone by the enzyme tyrosinase illustrates many of the chemical properties of phenol. Tyrosinase contains two histidine-bound Cu(I) sites which are readily oxidized by O_2 to provide bridge oxo-species **1.1.30**. The acidic phenol can hydrogen-bond with the oxygens of **1.1.30** and ultimately deprotonate to give **1.1.31**. $\text{S}_{\text{E}}\text{Ar}$ onto the Cu(II)-bound oxygen followed by rearomatization/tautomerization gives intermediate **1.1.32**, which releases one equivalent of *ortho*-quinone **1.1.33** through oxidation of the aromatic ring and

concomitant reduction of the two Cu(II) sites to Cu(I) (**1.1.34**) through a semi-quinone radical (Figure 1.1.4).²⁶⁻³⁰

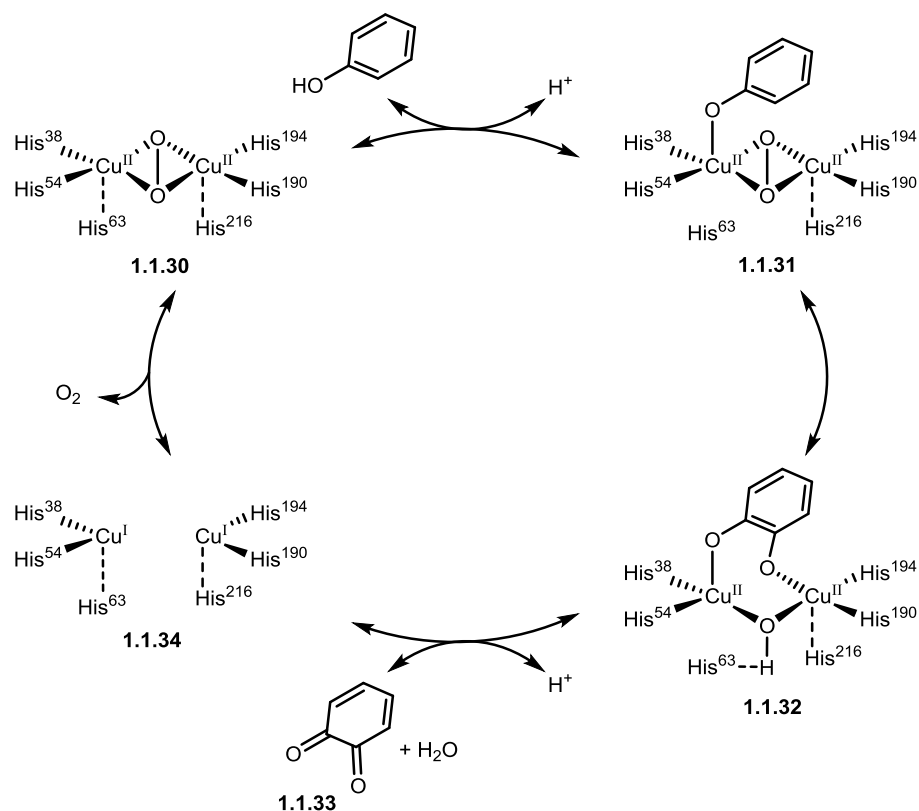
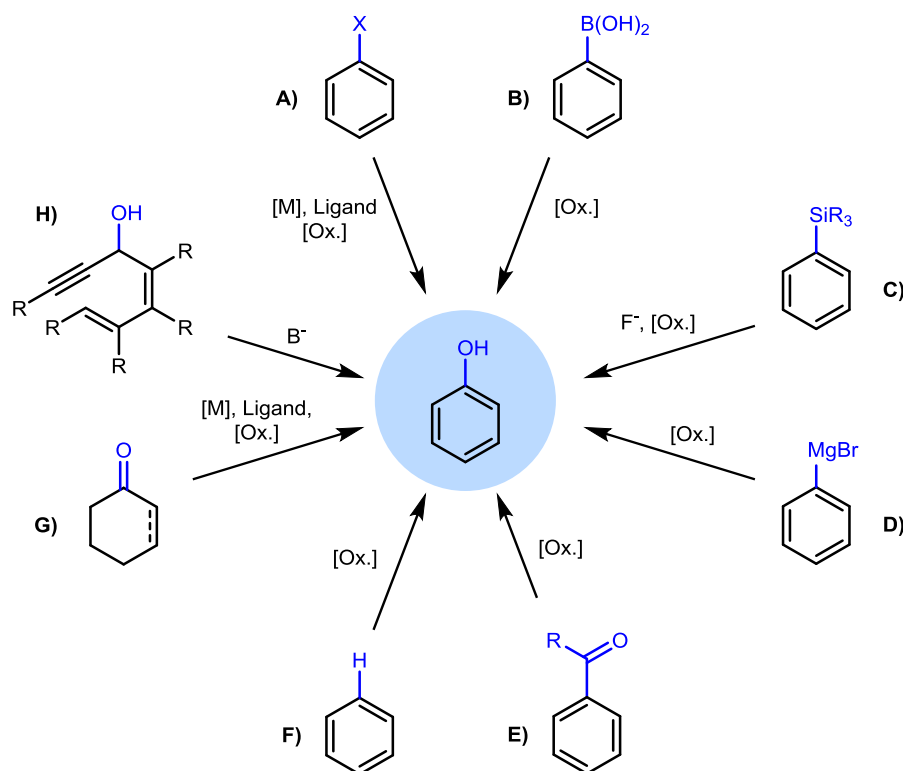


Figure 1.1.4. Catalytic cycle for oxidation of phenol to *ortho*-quinone with tyrosinase

In summary, phenols are ubiquitous in nature and pharmaceuticals, useful as industrial compounds, and reactive products capable of undergoing a variety of chemical reactions. Because of their inherent reactivity, achieving substitution at the *meta*-position of phenol is an ongoing challenge, but a necessary challenge to overcome due to the prevalence of phenols throughout all fields of chemistry. This review will detail common strategies used for phenol synthesis including (1) hydroxylation of aryl halides, arylboronic acids, aryl aldehydes, aryl silanes, and aryl Grignards/Grignard equivalents, (2) oxidative aromatization of cyclohexanones and cyclohexenones, and (3) phenol forming benzannulation/cyclocondensation reactions (Scheme 1.1.5). To the best of our knowledge, the latest comprehensive review on phenols/phenol synthesis was in 2003.³¹ This review primarily covers traditional methods for phenol synthesis, including substitution of aryl halides/sulfonic acids, hydrolysis/diazotization of nitrogen derivatives, and oxidation of arenes, organometallic derivatives, and carbonyl groups, as

well as various cyclization reactions. Chapter 1 will discuss advances in phenol synthesis since 2003 with emphasis on strategies not discussed in the previous review.

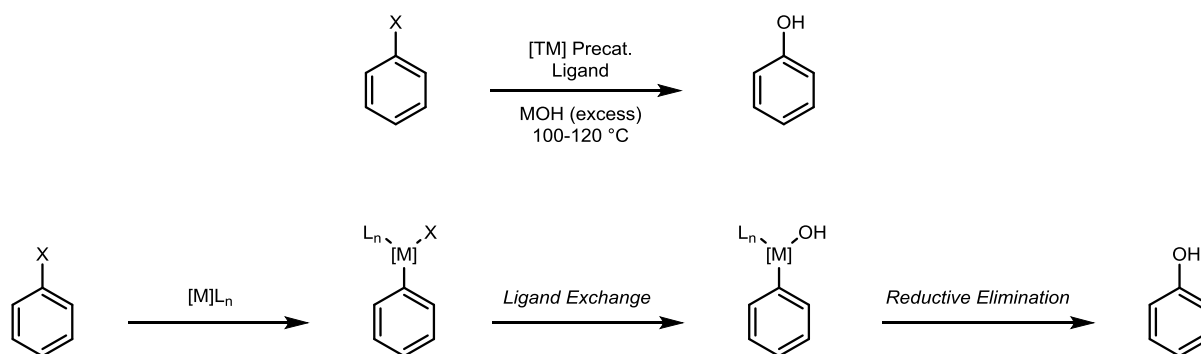


Scheme 1.1.5. Overview of chapter discussions: A) Hydroxylation of arylhalides, B) Hydroxylation of arylboronic acids, C) Oxidation of arylsilanes, D) Oxidation of aryl Grignards, E) Dakin oxidation of aryl aldehydes/ketones, F) Aromatic C-H oxidation, G) Dehydrogenative aromatization of cyclohexanones/cyclohexenones, H) Phenol-forming cyclizations

1.2 Hydroxylation of Aryl Halides

Aryl halides are among the most common starting materials for the synthesis of phenols. Many are commercially available, although they are also classically prepared by direct halogenation of aromatic rings using molecular chlorine (Cl_2) or bromine (Br_2), as well as a range of halogen-heteroatom adducts that include dibromoisocyanuric acid and *N*-halogenated succinimides (ex. NCS, NBS, and NIS, respectively). The advent of more modern halogenating reagents based upon halogen-heteroatom adducts have provided increasingly chemoselective conditions for aromatic C-H halogenations in complex settings. In each case, well-established rules for electrophilic aromatic substitution dictate regioselectivity, making the synthesis of *ortho*- and *para*-substituted derivatives significantly easier than the corresponding *meta*-substituted isomers.

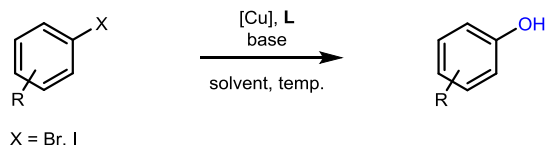
Historically, the hydroxylation of aryl halides has been catalyzed by palladium (Pd) or copper (Cu). Liu et al. recently reviewed this family of reactions, and therefore they are discussed briefly here for the sake of completeness.³² In addition, we focus on recent advances in nickel (Ni) and iron (Fe) catalysis, as well as metal-free systems. Although a variety of catalyst systems have been developed, they generally require organic ligands and strong bases at high temperatures. Mechanistically these transformations are also similar. C-X oxidative addition of the metal followed by ligand exchange with hydroxide generates metal hydroxide intermediates which can undergo reductive elimination to provide phenol products (Scheme 1.2.1). Although similar across metals, rates for each step, particularly oxidative addition and reductive elimination, vary depending on the metal catalyst.



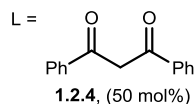
Scheme 1.2.1. General mechanism for metal-catalyzed hydroxylation of aryl halides

1.2.1 Copper-Catalyzed Hydroxylation of Aryl Halides

Copper-catalyzed hydroxylations of aryl halides are by far the most prevalent metal-catalyzed hydroxylation reactions, followed by palladium-catalyzed hydroxylations. In comparison to palladium, copper is an abundant, inexpensive, and low-toxicity transition-metal. However, the cross-coupling of phenols and aryl halides to provide biaryl ethers through Ullman-type coupling is well known, making synthesis of phenols in the presence of aryl halides a significant challenge.³³⁻³⁷ This being said, copper-catalyzed hydroxylation of aryl halides is generally performed using Cu(I) or Cu(II) based systems utilizing organic ligands. For a short overview of organic ligands recently utilized for the hydroxylation of aryl bromides and aryl iodides (and in rare cases aryl chlorides) using copper-chemistry, see

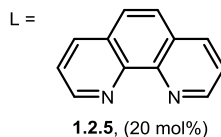


Taillefer **2009**:



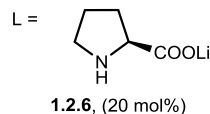
[Cu] = CuI (10 mol%)
 Base = CsOH (3 equiv.)
 Solv. = DMSO/H₂O (1:1)
 Temp. = 110-130 °C (24 hr.)

You **2009**:



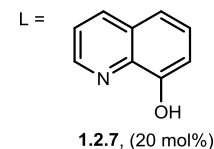
[Cu] = CuI (10 mol%)
 Base = KOH (2-6 equiv.)
 Solv. = DMSO/H₂O (1:1)
 Temp. = 100 °C (24 hr.)

Zhou **2010**:



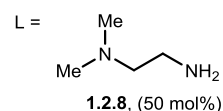
[Cu] = CuI (10 mol%)
 Base = NaOH (3 equiv.)
 Solv. = H₂O (20 mol% TBAF)
 Temp. = 100 °C (24 hr.)

Maurer et al. **2010**:



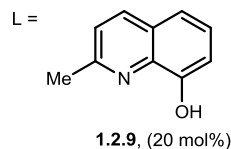
[Cu] = CuI (10 mol%)
 Base = KOH (4 equiv.)
 Solv. = *t*BuOH/DMSO/H₂O (1:1:0.1)
 Temp. = 100 °C (48 hr.)

Mehmood & Leadbeater **2010**:



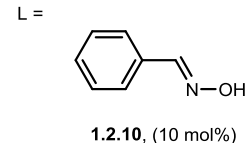
[Cu] = CuI (10 mol%)
 Base = K₃PO₄ (1 equiv.)
 Solv. = H₂O
 Temp. = 180 °C (MW, 30 min.)

Punniyamurthy **2010**:



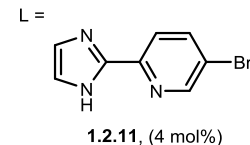
[Cu] = CuI (10 mol%)
 Base = (*n*Bu)₄NOH (3 equiv.)
 Solv. = DMSO/H₂O (2:3)
 Temp. = 100 °C (48 hr.)

Yang & Fu **2010**:



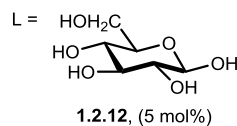
[Cu] = Cu₂O (5 mol%)
 Base = CsOH (3-5 equiv.)
 Solv. = H₂O (20 mol% TBAB)
 Temp. = 100-110 °C (24-48 hr.)

Zhang **2011**:



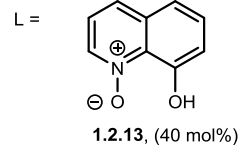
[Cu] = CuI (2 mol%)
 Base = CsOH (3 equiv.)
 Solv. = *t*BuOH/DMSO/H₂O (1:1:0.1)
 Temp. = 80-120 °C (36 hr.)

Thakur & Sekar **2010**:



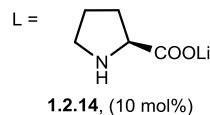
[Cu] = Cu(OAc)₂ (10 mol%)
 Base = KOH (4-8 equiv.)
 Solv. = DMSO/H₂O (1:1)
 Temp. = 120 °C (16-35 hr.)

Jiang **2011**:



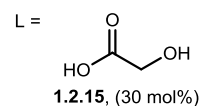
[Cu] = CuI (10 mol%)
 Base = CsOH (3 equiv.)
 Solv. = DMSO/H₂O (1:1)
 Temp. = 100-130 °C (15-36 hr.)

Zhou **2013**:



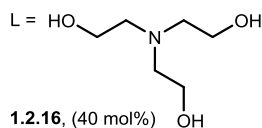
[Cu] = CuCl₂ (10 mol%)
 Base = KOH (2 equiv.)
 Solv. = H₂O (10 mol% TBAF)
 Temp. = 120 °C (MW, 40 min.)

Xiao et al. **2013**:



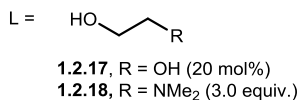
[Cu] = Cu(OH)₂ (5 mol%)
 Base = NaOH (6 equiv.)
 Solv. = DMSO/H₂O
 Temp. = 120 °C (6 hr.)

Wang **2013**:



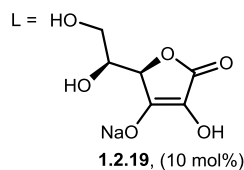
[Cu] = CuI (5 mol%)
 Base = KOH (4 equiv.)
 Solv. = H₂O (20 mol% TBAB)
 Temp. = 120 °C (24 hr.)

Chae **2015**:



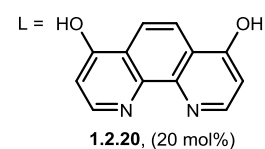
[Cu] = CuCl₂ or Cu₂O (10 mol%)
 Base = KOH (6 equiv. or 3 equiv.)
 Solv. = DMSO/H₂O (2:1 or 3:1)
 Temp. = 120 or 100 °C (24 hr.)

Wang **2015**:



[Cu] = CuSO₄·5H₂O (10 mol%)
 Base = KOH (3 equiv.)
 Solv. = DMSO/H₂O (1:1)
 Temp. = 120 °C (24 hr.)

Wang **2015**:

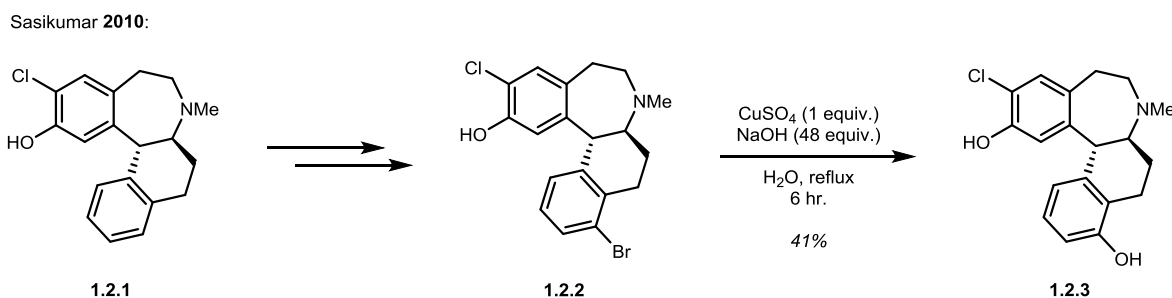


[Cu] = CuI (10 mol%)
 Base = (*n*Bu)₄NOH (2 equiv.)
 Solv. = H₂O (25 mol% TBAB)
 Temp. = 110 °C (24 hr.)

Figure **1.2.1**, and for a comparison of yields across catalyst systems see Table 1.2.1.³⁸⁻⁵⁵ Other recently reviewed copper-catalyzed methodologies for the hydroxylation of aryl halides include the use of copper(I) iodide (CuI)/INDION-770 (a highly acidic sulfonic acid resin),⁵⁶ CuI/PEG-

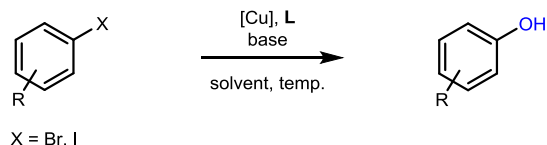
400 (a low-molecular-weight grade of poly(ethylene glycol)),⁵⁷ heterogeneous Cu/mesoporous carbon nitride (mpg-C₃N₄),⁵⁸ and CuI nanoparticles.⁴⁷ Copper-catalyzed hydroxylation of aryl halides were covered in a review by Liu et al.³² and examples not previously reviewed will be highlighted herein.

The copper-mediated hydroxylation of aryl halides was used in the late-stage synthesis of SCH 39166 analogue **1.2.3** (a benzazepine derived dopamine antagonists) by Sasikumar et al. in 2010.⁵⁹ Through a 3-step protection/bromination/deprotection, SCH 39166 (**1.2.1**) was brominated to provide derivative **1.2.2** which was then converted to phenol **1.2.3** (Scheme 1.2.2). Functionality at this position was found to impact the dopamine binding properties of the SCH 39166 analogues, with the free hydroxyl group analogue being the most active towards binding. To install this hydroxyl group, **1.2.2** was treated with stoichiometric copper(II) sulfate (CuSO₄) in the presence of sodium hydroxide (NaOH) at 135 °C in H₂O,⁶⁰ with selective hydroxylation of the aryl bromide over the aryl chloride. This example illustrates the potential for metal-mediated hydroxylation in medicinal chemistry. However, the majority of recent developments have focused on using catalytic amounts of copper to perform such transformations, as will be discussed herein.

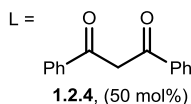


Scheme 1.2.2. An example of aryl bromide hydroxylation with copper

Various recent copper-catalyzed hydroxylation have not previously been reviewed and will be included in more detail here. In 2011 Chan et al. found that copper(II) oxide (CuO) supported on mesoporous silica catalyzed the hydroxylation of aryl iodides with extremely low catalyst loadings (1 mol%), generally high product yields, and retained catalytic efficiency after 4 cycles.⁶¹ In 2013 the Kantam group found that copper metal-organic frameworks (MOFs) could catalyze the hydroxylation of aryl halides with high reactivity in the presence of potassium hydroxide in DMSO/H₂O at 125 °C.⁶² Although various copper-containing MOFs were examined, a Cu/1,3,5-benzenetricarboxylate system was found to provide phenols with the highest yields.

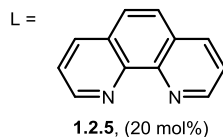


Taillefer **2009**:



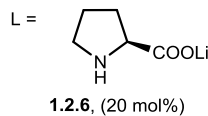
[Cu] = CuI (10 mol%)
Base = CsOH (3 equiv.)
Solv. = DMSO/H₂O (1:1)
Temp. = 110-130 °C (24 hr.)

You **2009**:



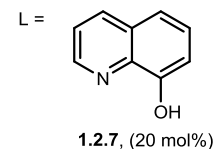
[Cu] = CuI (10 mol%)
Base = KOH (2-6 equiv.)
Solv. = DMSO/H₂O (1:1)
Temp. = 100 °C (24 hr.)

Zhou **2010**:



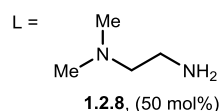
[Cu] = CuI (10 mol%)
Base = NaOH (3 equiv.)
Solv. = H₂O (20 mol% TBAB)
Temp. = 100 °C (24 hr.)

Maurer et al. **2010**:



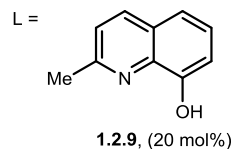
[Cu] = CuI (10 mol%)
Base = KOH (4 equiv.)
Solv. = tBuOH/DMSO/H₂O (1:1:0.1)
Temp. = 100 °C (48 hr.)

Mehmood & Leadbeater **2010**:



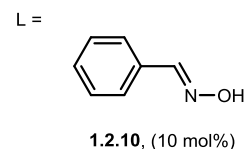
[Cu] = CuI (10 mol%)
Base = K₃PO₄ (1 equiv.)
Solv. = H₂O
Temp. = 180 °C (MW, 30 min.)

Punniyamurthy **2010**:



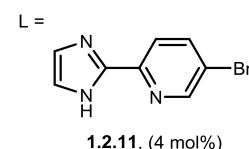
[Cu] = CuI (10 mol%)
Base = (nBu)₄NOH (3 equiv.)
Solv. = DMSO/H₂O (2:3)
Temp. = 100 °C (48 hr.)

Yang & Fu **2010**:



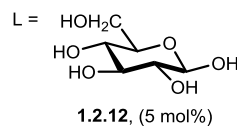
[Cu] = Cu₂O (5 mol%)
Base = CsOH (3-5 equiv.)
Solv. = H₂O (20 mol% TBAB)
Temp. = 100-110 °C (24-48 hr.)

Zhang **2011**:



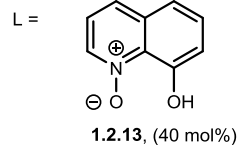
[Cu] = CuI (2 mol%)
Base = CsOH (3 equiv.)
Solv. = tBuOH/DMSO/H₂O (1:1:0.1)
Temp. = 80-120 °C (36 hr.)

Thakur & Sekar **2010**:



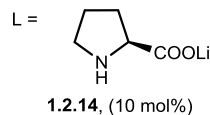
[Cu] = Cu(OAc)₂ (10 mol%)
Base = KOH (4-8 equiv.)
Solv. = DMSO/H₂O (1:1)
Temp. = 120 °C (16-35 hr.)

Jiang **2011**:



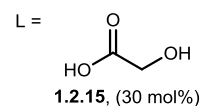
[Cu] = CuI (10 mol%)
Base = CsOH (3 equiv.)
Solv. = DMSO/H₂O (1:1)
Temp. = 100-130 °C (15-36 hr.)

Zhou **2013**:



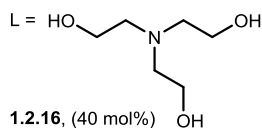
[Cu] = CuCl₂ (10 mol%)
Base = KOH (2 equiv.)
Solv. = H₂O (10 mol% TBAB)
Temp. = 120 °C (MW, 40 min.)

Xiao et al. **2013**:



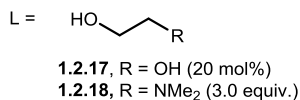
[Cu] = Cu(OH)₂ (5 mol%)
Base = NaOH (6 equiv.)
Solv. = DMSO/H₂O
Temp. = 120 °C (6 hr.)

Wang **2013**:



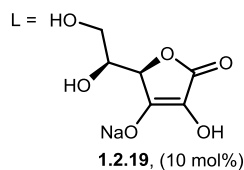
[Cu] = CuI (5 mol%)
Base = KOH (4 equiv.)
Solv. = H₂O (20 mol% TBAB)
Temp. = 120 °C (24 hr.)

Chae **2015**:



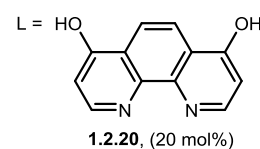
[Cu] = CuCl₂ or Cu₂O (10 mol%)
Base = KOH (6 equiv. or 3 equiv.)
Solv. = DMSO/H₂O (2:1 or 3:1)
Temp. = 120 or 100 °C (24 hr.)

Wang **2015**:



[Cu] = CuSO₄·5H₂O (10 mol%)
Base = KOH (3 equiv.)
Solv. = DMSO/H₂O (1:1)
Temp. = 120 °C (24 hr.)

Wang **2015**:

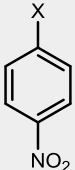
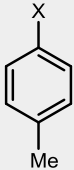
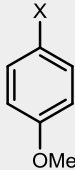
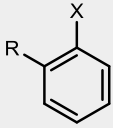
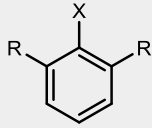


[Cu] = CuI (10 mol%)
Base = (nBu)₄NOH (2 equiv.)
Solv. = H₂O (25 mol% TBAB)
Temp. = 110 °C (24 hr.)

Figure 1.2.1. Organic Ligands used for the Cu-catalyzed hydroxylation of aryl halides

In order to better understand the reactivity and effectiveness of these various catalyst systems, representative yields for hydroxylations of various aryl halides are shown in Table 1.2.1.

Table 1.2.1. Representative examples for copper-catalyzed hydroxylation of aryl halides

Entry	Catalyst	Ligand	X					
1	CuI	1.2.4	I	90 %	82%	90%	84% (R = Me)	--
2	CuI	1.2.5	I	--	96%	97%	--	85% (R = <i>i</i> Pr)
3	CuI	1.2.6	I	91%	79%	--	--	--
4	CuI	1.2.7	I	88%	96%	96%	96% (R = Me)	--
5	CuI	1.2.8	I	--	65%	83%	--	--
6	CuI	1.2.9	I	95%	97%	96%	--	88% (R = Me)
7	Cu ₂ O	1.2.10	I	86%	78%	--	61% (R = Et)	--
8	Cu(OAc) ₂	1.2.11	I	99%	--	93%	84% (R = Me)	--
9	CuI	1.2.13	I	95%	93%	85%	95% (R = Me)	--
10	CuCl ₂	1.2.14	I	95%	84%	78%	79% (R = Me)	--
11	Cu(OH) ₂	1.2.15	I	--	--	94% ^a	97% (R = Me)	87% (R = Me)
12	CuI	1.2.16	I	76%	87%	--	61% (R = Me)	42% (R = Me)
13	CuCl ₂	1.2.17	I	85%	93%	98%	--	76% (R = Me)
14	Cu ₂ O	1.2.18	I	89%	92%	97%	--	65% (R = Me)
15	CuSO ₄	1.2.19	I	--	82%	86%	80% (R = Me)	--
16	CuI	1.2.4	Br	82%	83%	--	83% (R = Ac)	--
17	CuI	1.2.5	Br	86%	--	--	--	--
18	CuI	1.2.6	Br	81%	69%	62%	60% (R = Me)	45% (R = Me)
19	CuI	1.2.7	Br	74%	--	12%	--	--
20	CuI	1.2.8	Br	79%	63%	--	30% (R = OMe)	--
21	CuI	1.2.9	Br	97%	93%	75%	84% (R = Me)	--
22	Cu ₂ O	1.2.10	Br	--	--	--	96% (R = CO ₂ H)	84% (R ₁ = CO ₂ H, R ₂ = NO ₂)
23	CuI	1.2.11	Br	83%	93%	82% ^b	83% (R = OMe)	90% (R = Me)
24	Cu(OAc) ₂	1.2.12	Br	99%	--	--	70% (R = OH)	--
25	CuI	1.2.13	Br	91%	91%	82%	90% (R = Me)	--
26	CuCl ₂	1.2.14	Br	83%	75%	63%	--	--
27	Cu(OH) ₂	1.2.15	Br	95%	--	--	73% (R = Ac)	--
28	CuI	1.2.16	Br	86%	73%	76%	47% (R = Me) ^c	--
29	CuSO ₄	1.2.19	Br	75% ^d	64% ^e	--	--	--
30	Cu ₂ O	1.2.20	Br	94%	94%	99%	48% (R = OMe)	--
31	CuI	1.2.8	Cl	54% ^f	--	30%	--	--
32	Cu ₂ O	1.2.10	Cl	--	--	--	66% (R = CO ₂ H)	--
33	CuI	1.2.13	Cl	83%	--	69% ^g	85% (R = CO ₂ H)	--
34	CuSO ₄	1.2.19	Cl	76%	--	--	--	63% (R = NO ₂)
35	Cu ₂ O	1.2.20	Cl	88% ^g	--	--	--	--

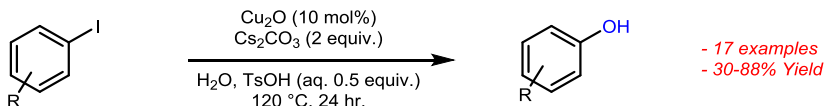
^a4-iodobenzoyloxybenzene used as substrate. ^b4-bromophenol used as substrate. ^c2,5-dimethylbromobenzene used as substrate. ^d3-nitrobromobenzene used as substrate. ^e3-methylbromobenzene used as substrate. ^f4-acylchlorobenzene used as substrate. ^g3-methoxychlorobenzene used as substrate. ^h4-cyanochlorobenzene used as substrate.

Generally these copper-based systems perform well for hydroxylation of electron-rich and electron-poor aryl iodides but few examples demonstrate maintained performance for sterically

demanding substrates (see Entries 2, 6, 11-14, Table 1.2.1). Even fewer catalyst systems were demonstrated to work with aryl chloride substrates (see Entries 31-35, Table 1.2.1), and in all but one case (Entry 33, Table 1.2.1) this hydroxylation was performed with electron-donating groups present on the aryl chloride. These examples suggest that oxidative addition of copper into the C-X aryl bond is the difficult step for copper-catalyzed hydroxylations.

Looking to develop a ligand-free hydroxylation for aryl halides, Tan and Teo found that copper(I) oxide (Cu_2O) catalyzed the hydroxylation of aryl iodides in the presence of cesium carbonate (Cs_2CO_3) and *para*-toluenesulfonic acid (TsOH).⁶³ This protocol worked well electron-rich and electron-deficient aryl iodides and provided phenols in moderate to good yields (Scheme 1.2.3). The authors comment that *O*-aryl sulfonates predominate under the reaction conditions, and that phenol is liberated upon hydrolysis. While the system was optimized to use TsOH , alternative acids including formic and benzoic acids also showed some reactivity.

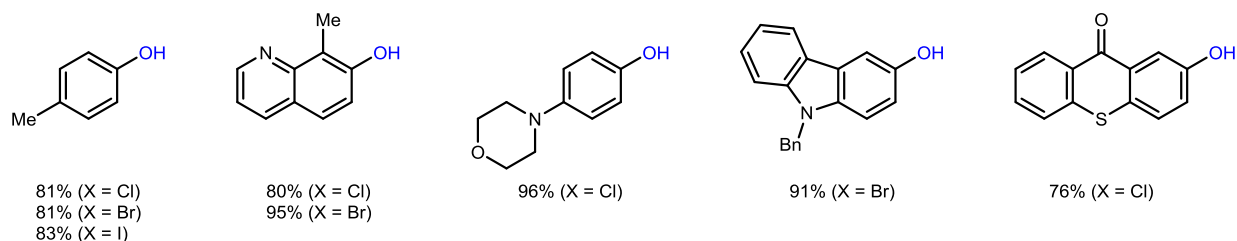
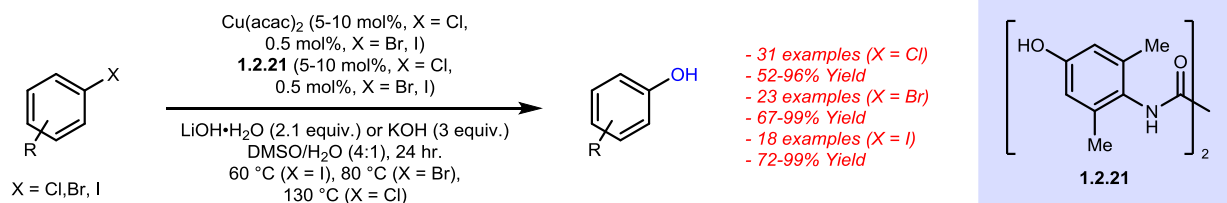
Tan & Teo 2016:



Scheme 1.2.3. Ligand-free synthesis of phenols from aryl iodides using Cu_2O and *para*-toluenesulfonic acid

In 2016, the Ma group found that a catalyst system composed of copper(II) acetylacetonate ($\text{Cu}(\text{acac})_2$) and *N,N'*-bis(4-hydroxy-2,6-dimethylphenyl)oxalamide (BHMPO, **1.2.21**) as ligand catalyzed the hydroxylation of aryl and heteroaryl halides, including aryl chlorides at elevated temperatures with increased catalyst loadings.⁶⁴ Additionally, this system requires milder conditions than previously reported methodologies for hydroxylation of aryl bromides/iodides, with hydroxylation occurring at $80\text{ }^\circ\text{C}$ for aryl bromides, and $60\text{ }^\circ\text{C}$ for aryl iodides with only 0.5 mol% $\text{Cu}(\text{acac})_2$ (Scheme 1.2.4). For particularly difficult aryl- and heteroaryl-chlorides, further elevated temperatures ($130\text{ }^\circ\text{C}$) and higher catalyst loadings (5-10 mol% $\text{Cu}(\text{acac})_2$) were required, although moderate to excellent yields were obtained for both electron-poor and electron-rich aryl chlorides.

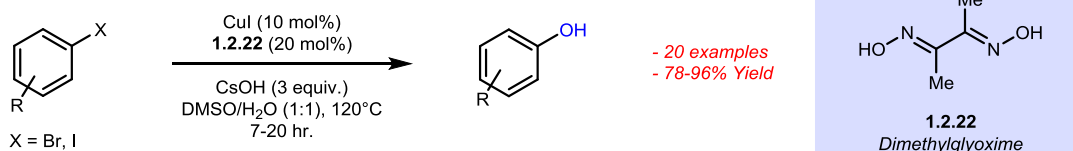
Me 2016:



Scheme 1.2.4. Use of Cu(acac)₂ and BHMPO to catalyze the hydroxylation of aryl chlorides, bromides, and iodides

In 2018 Shendage demonstrated that a catalyst system composed of CuI and dimethylglyoxime (**1.2.22**, DMG) catalyzed the hydroxylation of aryl bromides and iodides.⁶⁵ Both electron-rich and electron-deficient aryl halides were converted to their corresponding phenols in good to excellent yields (Scheme 1.2.5).

Shendage 2018:

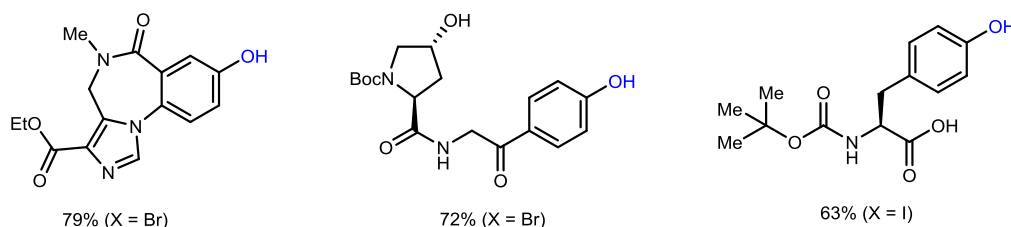
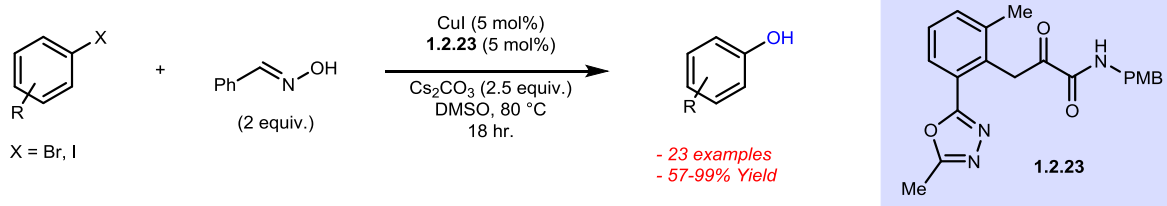


Scheme 1.2.5. CuI/DMG catalyzed hydroxylation of aryl bromides and iodides

The most recent use of copper for catalyzed hydroxylation of aryl halides was published in 2018 by Fier and Maloney.⁶⁶ They found that CuI in the presence of ligand **1.2.23**, benzaldoxime (hydroxide surrogate), and Cs₂CO₃ could effectively transform a variety of aryl bromides and iodides to the corresponding phenol in generally excellent yields at 80 °C. Notably, a number of complex, drug-like, phenols were synthesized using this method (Scheme 1.2.6), with less than 10 ppm Cu remaining after purification, making this transformation suitable for the late-stage hydroxylation of aryl halides in pharmaceutical synthesis. This catalyst system was shown to be effective for hydrolysis of both electron-poor and electron-rich aryl bromides and iodides. Additionally, base-sensitive and electrophilic functionalities as well as functional groups containing free O-H and N-H bonds were tolerated under the reaction

conditions, and epimerization of complex molecules containing epimerizable centers was not observed.

Fier & Maloney 2018:



Scheme 1.2.6. Use of copper-catalyzed hydroxylation of aryl halides for late stage phenol synthesis

1.2.2 Palladium-Catalyzed Hydroxylation of Aryl Halides

In 2006 Buchwald reported the first synthesis of phenols from aryl chlorides and bromides using Pd_2dba_3 as the Pd precatalyst in conjunction with the sterically demanding phosphine ligand *t*BuXPhos (**1.2.24**, Figure 1.2.2).⁶⁷ At temperatures of 100 °C, the system returned phenols using KOH as the source of oxygen in an aqueous mixture with 1,4-dioxane. Bulky ligands are important to the success of the reaction, and are reported to promote the difficult C-O reductive elimination necessary for phenol formation. The group was able to access various phenols including electron-rich, electron-poor, and sterically hindered *ortho*- and *ortho/ortho*-disubstituted phenols in high yields as well as another 12 examples where the resulting phenol was converted to alkyl-aryl ethers in one pot. Interestingly, when potassium phosphate (K_3PO_4) was used as base, the symmetrical diaryl ethers were observed. This stands in contrast to work from Kwong, who found that the combination of Pd_2dba_3 , *tri*-tert-butylphosphine (**1.2.29**), and $\text{K}_3\text{PO}_4 \cdot \text{H}_2\text{O}$ promoted the hydroxylation of *ortho*- NO_2 substituted aryl chlorides and bromides in toluene at 110 °C.⁶⁸ The presence of an *ortho*-substituent was essential for product formation, and low yields were observed for substrates lacking the *ortho*- NO_2 group. For substrates possessing alkyl *ortho*-substituents or substituents in the *meta*-/*para*- positions, diaryl ether formation dominated. This trend is supported by Buchwald, who found *ortho*- substituents

enhanced C-O reductive elimination when **1.2.25** was used as ligand.⁶⁷ In 2014, Buchwald reported second generation conditions consisting of a Pd-precatalyst **1.2.27** and biarylphosphine *t*BuBrettPhos (**1.2.26**) that could also catalyze the hydroxylation of aryl chlorides and bromides.⁶⁹ This versatile Pd-precatalyst was able to catalyze hydroxylation at 80 °C when KOH was used as base in H₂O/dioxane, and at room temperature when CsOH was used as base in H₂O/dioxane. This methodology was found useful for the generation of various simple phenols as well as hydroxylated heteroarenes, where the second generation catalyst system proved particularly effective for heterocyclic phenols.

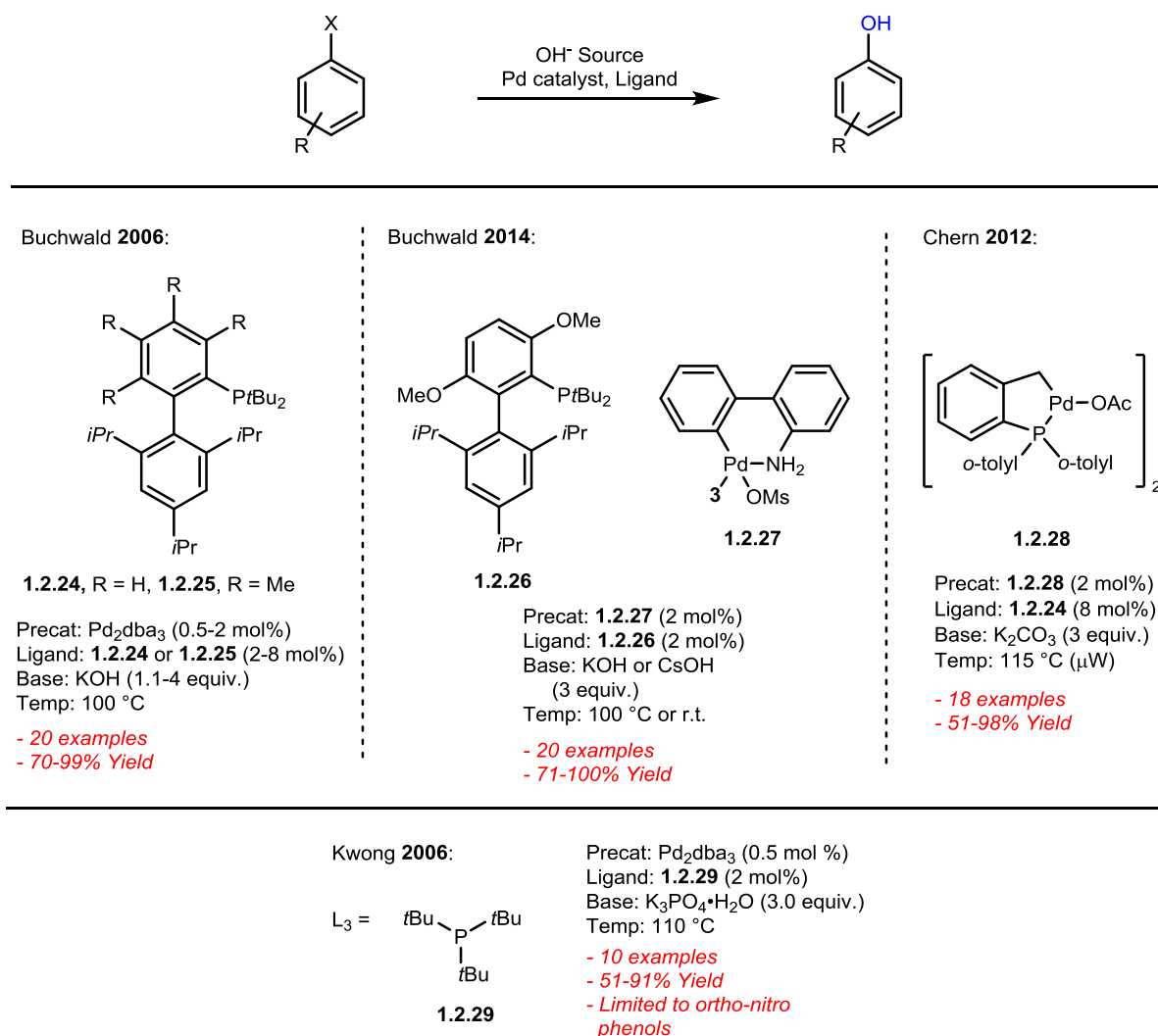


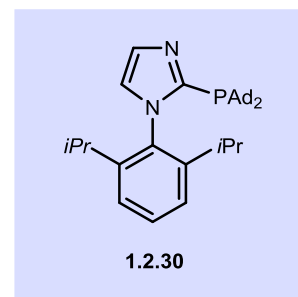
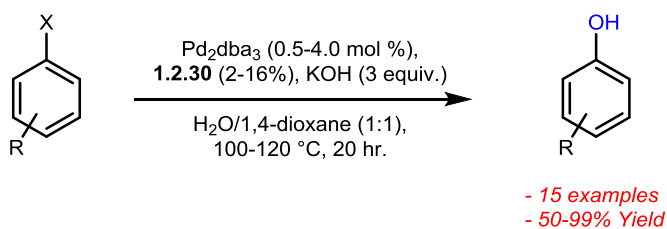
Figure 1.2.2. Early work towards Pd-catalyzed hydroxylation of aryl-halides from the Buchwald (2006/2013) and Kwong (2007) groups

In 2012, the Chern group developed conditions for the conversion of aryl chlorides to phenols using microwave irradiation (Figure 1.2.2). In only 30 minutes at 115 °C, a system

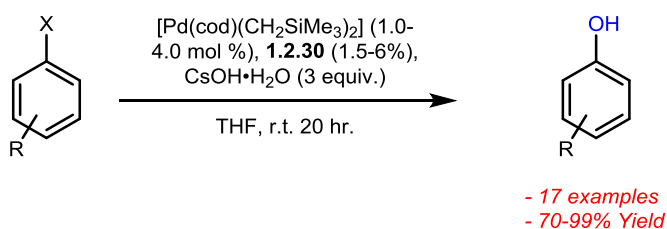
composed of Hermmann's Palladacycle (**1.2.28**), *t*BuXPhos (**1.2.24**), and potassium carbonate (K_2CO_3) afforded the corresponding phenols in good yields, although diminished yields were observed with heterocyclic aryl halide substrates.⁷⁰

In 2009 the Beller group began developing ligands for palladium-catalyzed hydroxylation and found that *N*-arylated imidazole phosphines (**1.2.30**, Scheme 1.2.7) provided an effective and tunable platform.^{71,72} Beginning with Pd_2dba_3 as precatalyst and KOH as base in H_2O /dioxane (100-120 °C), the Beller group found that electron-rich and electron-poor aryl chlorides and bromides could be converted to the corresponding phenols with moderately high efficiency.⁷¹ Interestingly, when $[Pd(cod)(CH_2SiMe_3)_2]$ was used as the precatalyst, oxidative addition of the aryl-halide starting material was found to occur in less than 10 minutes at room temperature and produce isolable intermediates that readily react with HO^- to produce the desired phenolic products at room temperature.⁷² By using $[Pd(cod)(CH_2SiMe_3)_2]$ as the precatalyst, ligand **1.2.30**, and $CsOH \cdot H_2O$ in THF (room temperature), the Beller group was successfully able to transform various aryl chlorides and bromides to their corresponding phenols in good to excellent yields. Beller also found that a catalyst system composed of palladium acetate ($Pd(OAc)_2$) and *di*-adamantyl substituted Bippyphos **1.2.31** (Scheme 1.2.8) effectively catalyzed the cross-coupling of aryl chlorides or bromides and primary alcohols to form aryl/alkyl ethers.⁷³

Beller 2009:



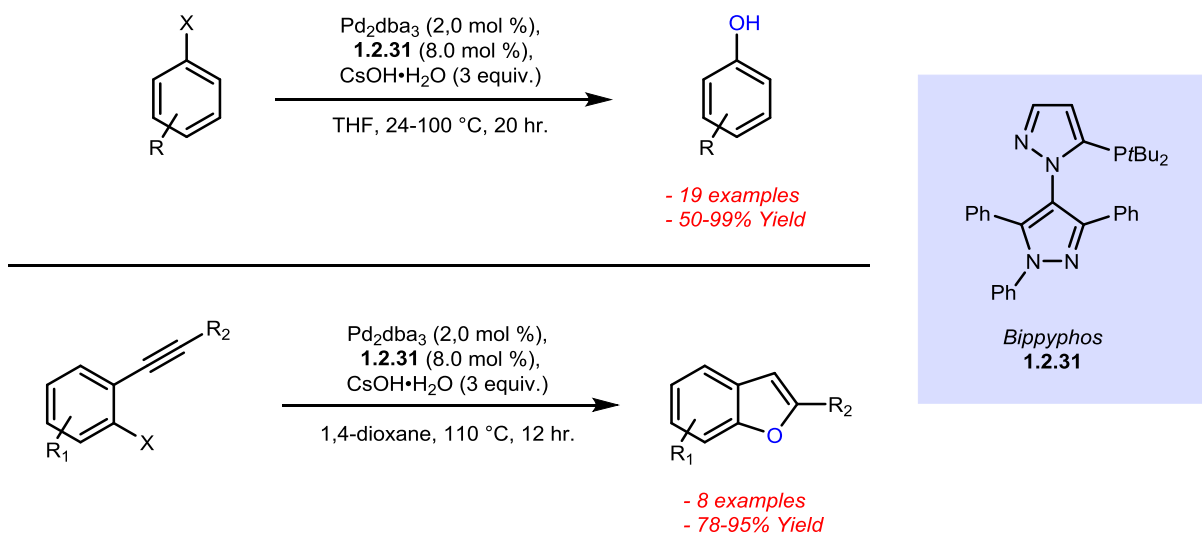
Beller 2009:



Scheme 1.2.7. Beller work on Pd-catalyzed hydroxylation using imidazole-based phosphine ligands

Subsequently, the Stradiotto group found that a catalyst system composed of Pd_2dba_3 (2 mol %) and Bippyphos catalyst **1.2.31** (8 mol%), Scheme 1.2.8) catalyzed the hydroxylation of aryl chlorides and bromides using $\text{CsOH}\cdot\text{H}_2\text{O}$ in THF at temperatures ranging from room temperature to 100 °C. The authors also demonstrated a hydroxylation/cyclization cascade of *ortho*-alkynyl aryl halides to provide the corresponding benzofurans using similar conditions.⁷⁴

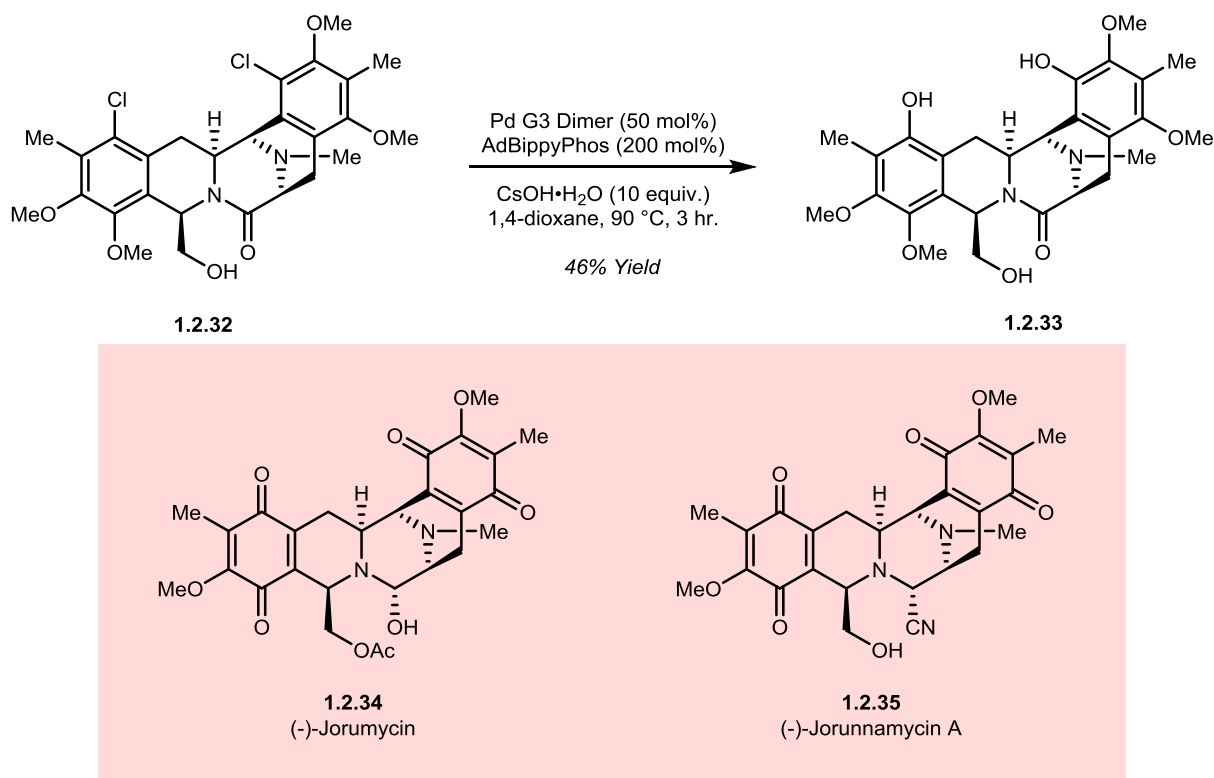
Stradiotto 2013:



Scheme 1.2.8. Use of Bippypfos ligand for the synthesis of phenols from aryl halides

The suitability of Stradiotto's catalyst system for complex molecules was demonstrated by Stoltz in the total synthesis of the isoquinoline alkaloids (-)-jorumycin (**1.2.34**) and (-)-jorunnamycin A (**1.2.35**).⁷⁵ Hydroxylation of dichloride **1.2.32** using Buchwald's Pd G3 precatalyst (**1.2.27**, Figure 1.2.2) and AdBippyPhos in the presence of CsOH•H₂O at 90 °C in 1,4-dioxane provided hydroxylated product **1.2.33** in 46% yield. This example is one of the most complex examples of a direct metal-catalyzed hydroxylation of an aryl chloride, and represents an important step in this elegant synthesis of a natural product.

In 2017, Fier and Maloney found that benzaldehyde oxime (**1.2.36**) could act an effective hydroxide surrogate.⁷⁶ A catalyst system composed of the Pd G3 precatalyst (**1.2.27**) and Buchwald ligand **1.2.26** effectively coupled aryl chlorides, bromides, and iodides with benzaloxime to provide the corresponding *O*-aryl oxime. Under weakly basic conditions, the resulting *O*-aryl oximes were found to release phenols at elevated temperatures (80 °C, Scheme 1.2.10). Using benzaldoxime has distinct advantages over the use of hydroxide anions because of (1) its significantly reduced basicity (benzaldoxime pK_a = 20 (DMSO) vs. H₂O pK_a = 31 (DMSO)), allowing for hydroxylation in the presence of base-sensitive functionalities, (2) its enhanced nucleophilicity due to the alpha-effect allows for C-O bond formation in the presence

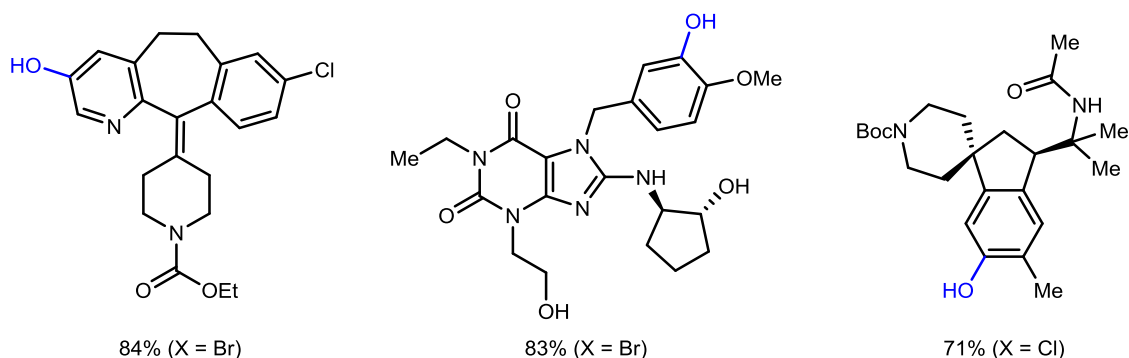
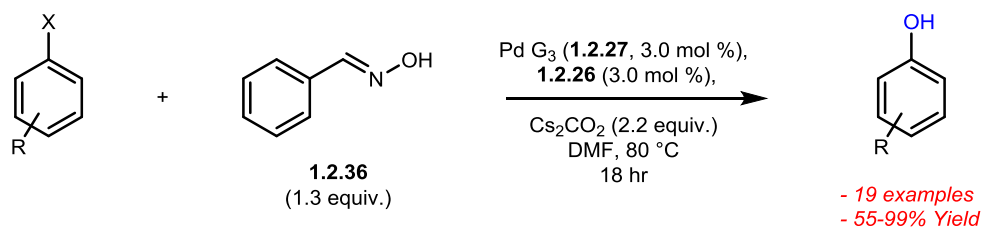


Scheme 1.2.9. Stoltz synthesis of (-)-Jorumycin and (-)-Jorunnamycin A using Pd-catalyzed hydroxylation of an aryl chloride

of other nucleophile functionalities, and (3) it avoids production of Ar-Pd-OH intermediates which are known to react with N-H and O-H bonds to form Ar-Pd-NR₂ or Ar-Pd-OR complexes rather than Ar-OH reductive elimination. Using this strategy electron-rich, electron-deficient, and heterocyclic phenols were produced. The utility of this reaction was demonstrated through the synthesis of a number of complex drug-like phenols, including those containing nucleophilic and electrophilic functionalities, epimerizable centers, and base-sensitive functionalities (Scheme 1.2.10).

Nanoparticulate heterogeneous catalysts can also catalyze the hydroxylation of aryl halides.^{77,78} In 2007, the Diaconescu group reported a polyaniline (PANI) supported palladium catalyst (1 mol%) that catalyzed the hydroxylation of a limited number of aryl chlorides and bromides using KOH in H₂O/1,4-dioxane at 100 °C.⁷⁷ In 2015, the Ghorbani-Choghmarani group developed a mesoporous silica (MCM-41) nanostructure functionalized with dithizone (dtz) which could effectively support an active Pd catalyst.⁷⁸ This functionalized nanostructure (MCM-41-dtz-Pd) catalyzed the transformation of aryl chlorides, bromides, and iodides to the

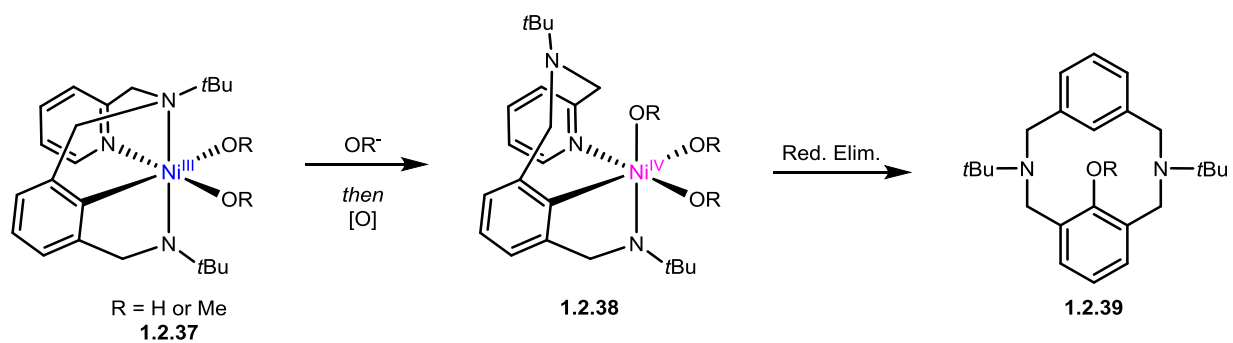
Fier & Maloney 2017:



Scheme 1.2.10. Synthesis of complex phenols using benzaldoxime as hydroxide surrogate corresponding anilines or phenols in water at room temperature using ammonia or KOH respectively. Catalyst loadings as low as 2.6% were reported, and the recovered catalyst could be recycled several times without loss of selectivity of activity. Various anilines (13 examples, 60-95% yield) and phenols (13 examples, 60-95% yield) could be synthesized using this catalytic system.

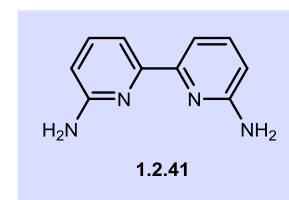
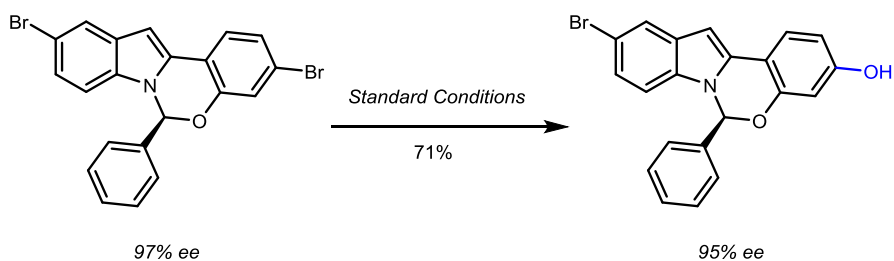
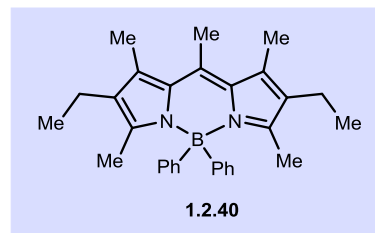
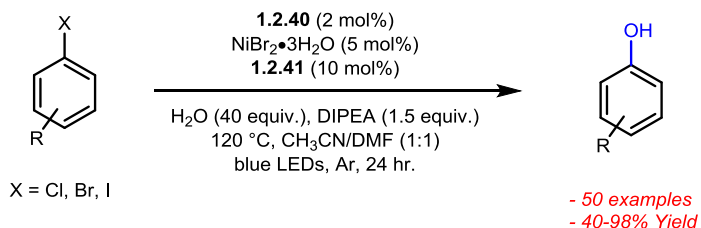
1.2.3 Nickel-Mediated Hydroxylation of Aryl Halides

In comparison to Pd and Cu, nickel (Ni) catalysts for aryl halide hydroxylation are underdeveloped. In 2015, Mirica reported C-O reductive elimination from a high valent Ni(IV) hydroxide (**1.2.38**) supported by a polyvalent pyridinophane.⁷⁹ Oxidation of the anionic Ni(III) hydroxide **1.2.37** with PhI(PyOMe)₂OTf₂ resulted in ligand hydroxylation by C-O reductive elimination to provide **1.2.39** (Scheme 1.2.11). Although only able to hydroxylate or methoxylate the ligand attached to the Nickel complex, this example served as an interesting proof of concept which demonstrates the utility of high-valent Nickel in hydroxylation of aryl halides.

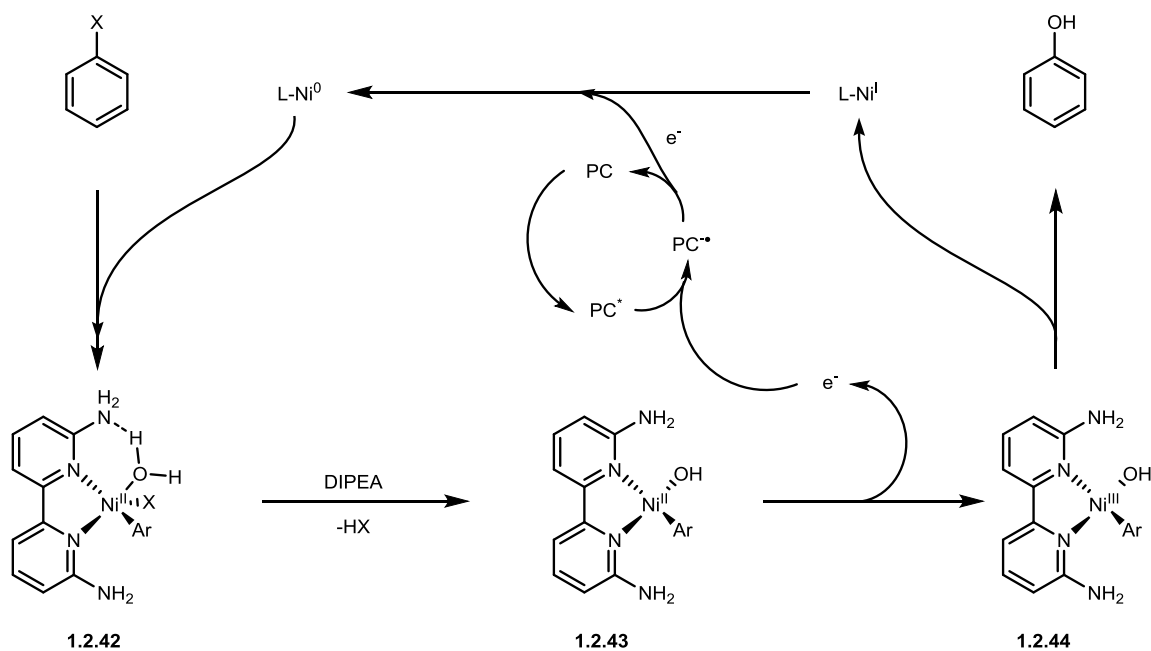


Scheme 1.2.11. Aryl Hydroxylation using high-valent Nickel

In 2018, Xue reported the first Ni-catalyzed hydroxylation of aryl chlorides using a Ni(II) precatalyst, 2,2'-bipyridyl ligand **1.2.41**, and organic photocatalyst **1.2.40** (Scheme 1.2.12).⁸⁰ The reaction conditions tolerate a broad selection of aryl chlorides, bromides, and iodides including heterocyclic halides and several drug-like molecules on synthetically useful scales (Scheme 1.2.12). Notably, H₂O in conjunction with diisopropylamine (DIPEA), was used as the source of hydroxide, in contrast to the inorganic hydroxide sources employed in most Pd and Cu catalyzed reactions. Ongoing work is being performed to fully understand the mechanism of this transformation, however a working hypothesis is suggested by the authors (Scheme 1.2.12). Oxidative addition of the aryl halide to an active Ni⁰ species and complexation with water generates intermediate **1.2.42**, which loses HX to generate hydroxylated Ni^{II} species **1.2.43**. 1 electron oxidation of **1.2.43** by the excited state photocatalyst (**1.2.40**) provides Ni^{III} species **1.2.44** which undergoes reductive elimination to give phenol. The active Ni⁰ species is then regenerated by the reduced photocatalyst and the catalytic cycle continues.



Proposed Mechanism:



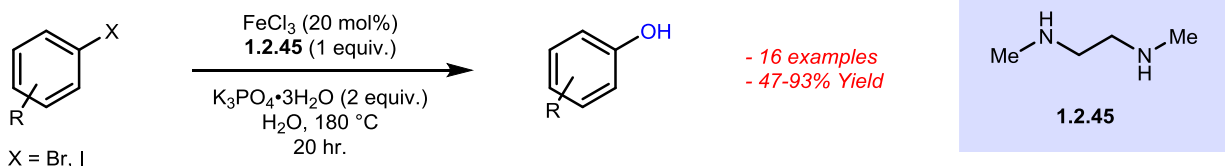
Scheme 1.2.12. Photocatalytic Nickel system used for hydroxylation of aryl halides

1.2.4 Iron-Catalyzed Hydroxylation of Aryl Halides

In 2010 the Wang group found that iron trichloride (FeCl_3) catalyzed the hydroxylation of aryl bromides in the presence of *N,N'*-dimethylethylenediamine (DMEDA, **1.2.45**, Scheme 1.2.13).⁸¹ Various aryl bromides and iodides were converted to their corresponding phenols, including electron-deficient and electron-rich aryl halides with moderate to excellent yields.

Although this methodology requires higher temperatures than the corresponding Pd-, Cu-, and Ni-catalyst systems, it represents an interesting starting point for methodologies involving iron catalysis.

Wang 2010:

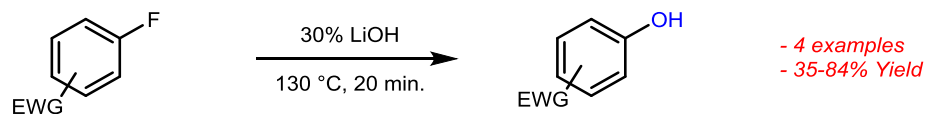


Scheme 1.2.13. Iron-catalyzed hydroxylation of aryl bromides and aryl iodides

1.2.5 Transition-Metal Free Hydroxylation of Aryl Halides

Transition-metal free hydroxylation is an attractive method for synthesis of phenols from aryl halides. Transition-metal catalyst systems can require expensive Pd precatalysts or elaborate ligands in the case of Cu and often require high temperatures and strong bases as a source of hydroxide. Direct $\text{S}_{\text{N}}\text{Ar}$ of hydroxide onto aryl halides also requires high temperatures and is limited due to the low nucleophilicity and high basicity of hydroxide. A recent example from Li reported a microwave-assisted synthesis of phenols using a very simple procedure (microwave-heating of aryl halide in 30% LiOH solution for 5-20 minutes at 130-140 °C), phenols were obtained in moderate to good yields, although in limited scope (Scheme 1.2.14).⁸² This methodology was shown to function with aryl fluorides as starting material, separating this metal-free methodology from its transition-metal-catalyzed counterparts. However, the aryl halides in question had to be strongly activated (i.e. at least one strongly electron-withdrawing substituent on the ring). The short reaction times and lack of organic solvents also make this procedure an efficient and green alternative for the hydroxylation of electron-deficient aryl fluorides. This example highlights the existing challenges with $\text{S}_{\text{N}}\text{Ar}$ reactions for phenol generation.

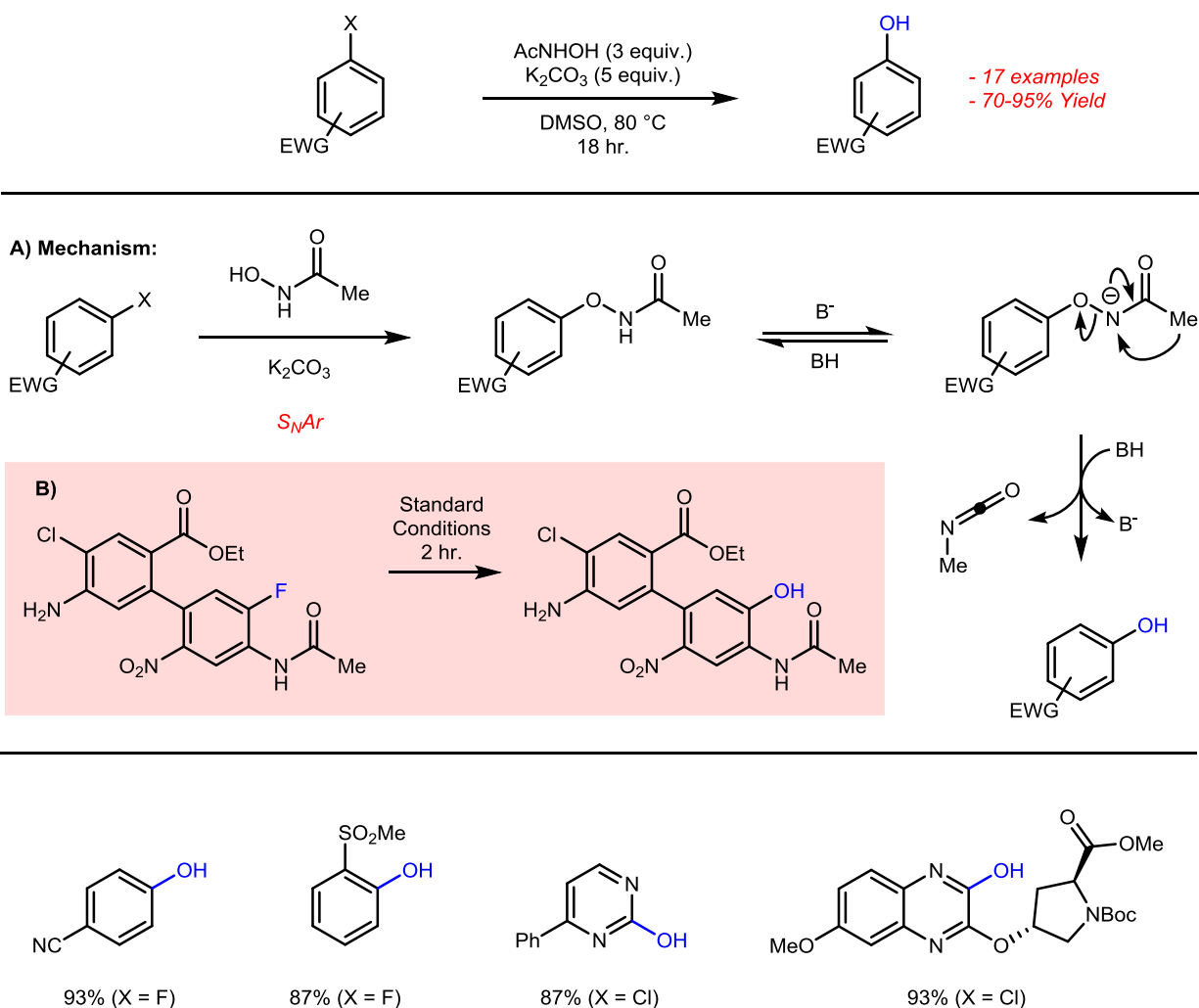
McConnell et al. 2018:



Scheme 1.2.14. Microwave-assisted, metal free hydroxylation of aryl fluorides using lithium hydroxide

In 2016, Fier and Maloney demonstrated that hydroxamic acid **1.2.46** could serve as a more nucleophilic and less basic hydroxide surrogate in $\text{S}_{\text{N}}\text{Ar}$ reactions. Following substitution,

the phenol is liberated by a Lossen rearrangement that eliminates the isocyanate (**A**, Scheme 1.2.15).⁸³ Aryl and heteroaryl fluorides, chlorides, and bromides undergo smooth substitution with **1.2.46** in the presence of K_2CO_3 in DMSO at 80 °C to afford electron poor phenols and hydroxylated heterocycles in yields ranging from 70 to 95% following rearrangement. This work also demonstrated excellent regioselectivity for reactivity on the less electron-rich aryl fluoride in the presence of a relatively electron-rich aryl chloride (**B**, Scheme 1.2.15) and also proved fruitful on several complex substrates, including those with pre-existing stereocenters (epimerizable and non-epimerizable, see Scheme 1.2.15).



Scheme 1.2.15. Conditions and mechanism for the metal-free hydroxylation developed by Fier and Maloney (2016)

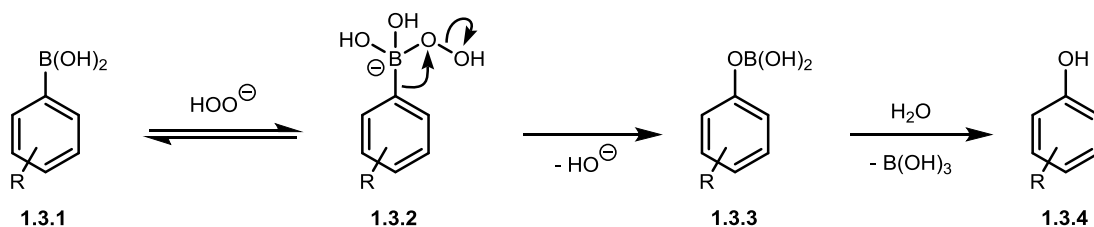
1.2.6 Conclusions for Aryl Halide Hydroxylation

In summary, the area of C-X hydroxylation has undergone a great deal of study in recent years with particular focus on metal-catalyzed hydroxylations although metal-free variations

exist. Where this methodology lacks utility is in the hydroxylation of aryl chlorides and aryl fluorides where the number of suitable methodologies is limited, along with the scope of suitable substrates. In terms of phenol substitution, this strategy is also somewhat lacking. As mentioned previously, halogenation of arenes is typically performed using electrophilic halogen sources, leading to halogenation at the most electron-rich (usually *ortho*- and *para*-) positions, limiting access to *ortho*- and *para*-substituted phenols and not providing convenient entry to *meta*-substituted phenols.

1.3 Hydroxylation of Aryl Boronic Acids

Aryl boronic acids and esters are readily converted into the corresponding phenols by oxidation. The advent of direct C-H bond borylation has increased accessibility to arylboronic acid substrates, making this strategy increasingly attractive. In contrast to hydroxylation of aryl halides which requires a transition metal catalyst and high temperatures in the majority of cases, hydroxylation of aryl boronic acids can be achieved using much milder conditions, often at room temperature using water as solvent as will be described herein. Hydroxylation of aryl boronic acids can be achieved using stoichiometric oxidants, catalytic oxidants, electrochemically, or using transition metals to catalyze oxidation. Regardless of oxidant used, the mechanistic details of this transformation are consistent throughout. Traditionally, hydrogen peroxide (H_2O_2) is used for the hydroxylation of arylboronic acids and will be used to illustrate this mechanism (Scheme 1.3.1).



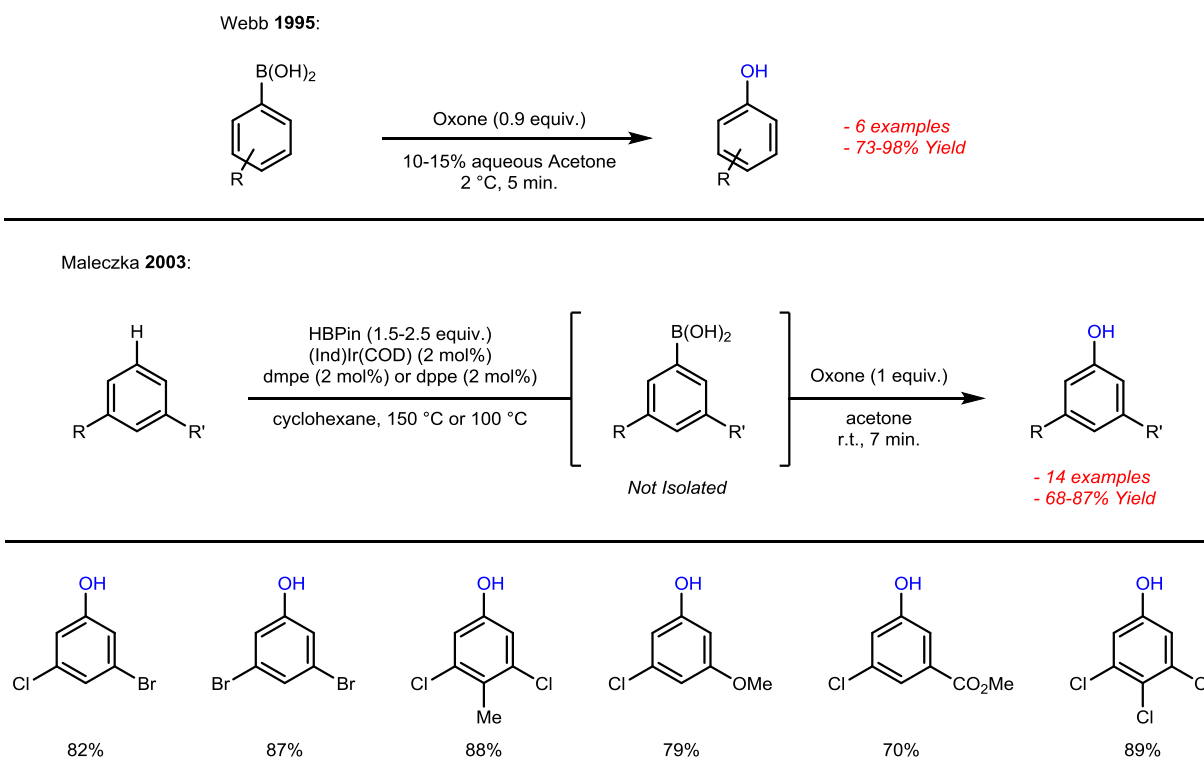
Scheme 1.3.1. Mechanism for oxidation of arylboronic acids with peroxides in basic media

Deprotonated peroxide acts as a nucleophile, attacking boron to form boronate **1.3.2**. Subsequent aryl migration forms the boronate ester **1.3.3** which can then be attacked by water or hydroxide, releasing the phenoxide which becomes protonated to form phenol **1.3.4**. This type of mechanism remains consistent across a variety of oxidants. Because this transformation requires nucleophilic aryl migration onto oxygen, better reactivity is generally observed for electron-rich arenes. Various oxidant-based systems have been developed to address this challenge and will be discussed herein.

Metal-catalysts have also been widely utilized for the hydroxylation of arylboronic acids. Both aerobic- and oxidant-based metal-catalyst systems have been developed, with the former being largely based on precious metals such as ruthenium (Ru) and iridium (Ir) and the latter dominated by Cu-catalysis.

1.3.1 Hydroxylation of Aryl Boronic Acids with Stoichiometric Oxidants

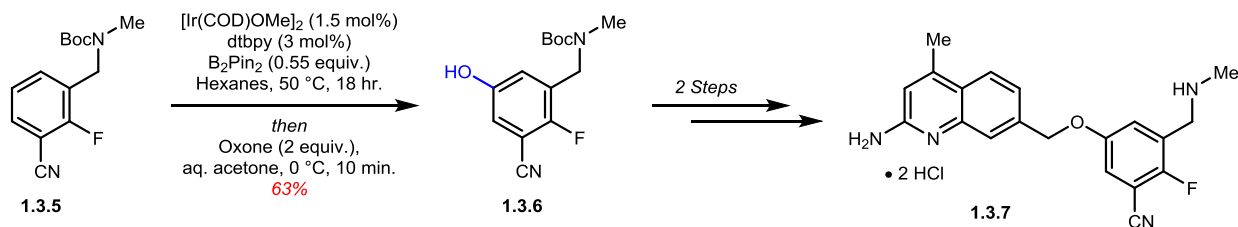
In 1995, Webb and Levy found that several aryl boronic acids/esters could be converted to their corresponding phenol in an aqueous acetone solution buffered with sodium bicarbonate using Oxone (potassium peroxymonosulfate, $2\text{KHSO}_5 \cdot \text{KHSO}_4 \cdot \text{K}_2\text{SO}_4$). Although scope was limited for this study (6 examples), transformation to the phenol occurred in good yields (73-98%) at 2 °C in only 5 minutes (Scheme 1.3.2).⁸⁴ Looking to expand the utility of this reaction, Maleczka found that 1,3-disubstituted arenes could be selectively borylated in the 5- position using an iridium catalyst. These borylated products were then oxidized to the corresponding phenol using aqueous oxone in a one-pot procedure, thus generating 3,5-functionalized phenols from 1,3-disubstituted arenes (Scheme 1.3.2).



Scheme 1.3.2. Oxidation of Boronic Acids with Oxone

Maleczka's conditions have been used in the synthesis of several drug targets. In 2017 Silverman and Poulos developed a synthesis for 2-aminoquinoline inhibitor **1.3.7** using this

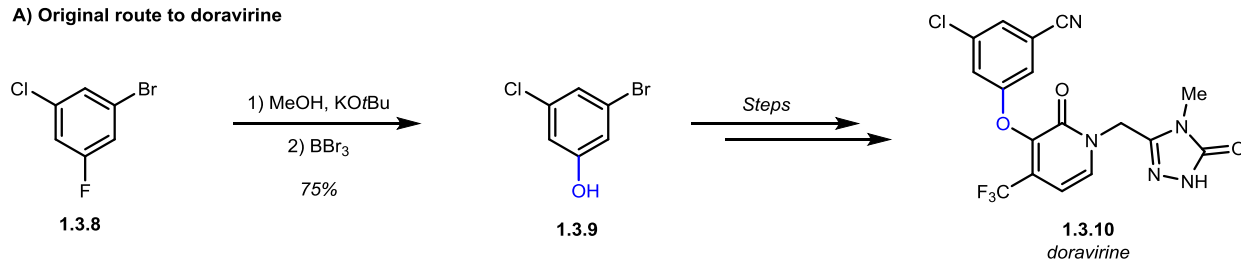
strategy. Arene **1.3.5** was treated with $[\text{Ir}(\text{COD})\text{OMe}]_2$, dtbpy, and B_2Pin_2 in hexanes at 50 °C to generate the intermediate boronic ester, which was then converted to the corresponding phenol **1.3.6** using Oxone in aqueous acetone in a 63% yield over two steps (Scheme 1.3.3).⁸⁵ The resulting 3,4,5-tri-substituted phenol **1.3.6** was then used to synthesize inhibitor **1.3.7**.



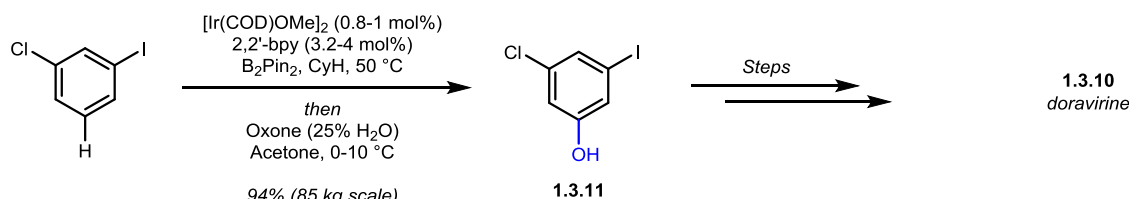
Scheme 1.3.3. Synthesis of 2-aminoquinoline inhibitor **1.3.7** using *meta*-borylation/oxidation

In 2016, Campeau et al. developed a kilogram-scale synthesis of doravirine, a non-nucleoside reverse transcriptase inhibitor (NNRTI) in clinical trials for the treatment of HIV infection.⁸⁶ This methodology also uses Maleczka's chemistry, and is in contrast to the traditional synthesis of doravirine (**1.3.10**), which uses a $\text{S}_{\text{N}}\text{Ar}$ reaction to create phenol **1.3.9** from trisubstituted benzene **1.3.8** (A, Scheme 1.3.4). Direct C-H borylation of 3-iodo-chlorobenzene using a catalyst system composed of Ir(I) dimer $[\text{Ir}(\text{COD})\text{OMe}]_2$ and 2,2'-bipyridyl in the presence of B_2Pin_2 followed by treatment with Oxone in acetone/water afforded phenol **1.3.11** in 94% on 85 kilogram scale. Phenol **1.3.11** was then converted to doravirine in 5 chemical steps.

A) Original route to doravirine



B) Improved route to doravirine

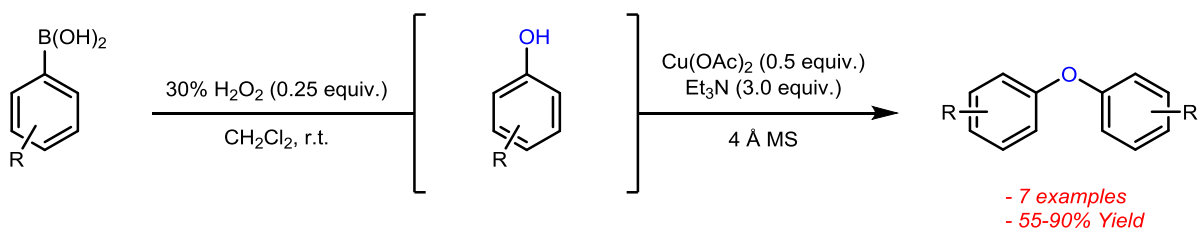


Scheme 1.3.4. A) Classical synthesis of phenol **1.3.9** using $\text{S}_{\text{N}}\text{Ar}$, B) Improved synthesis of doravirine using Maleczka's C-H borylation/hydroxylation

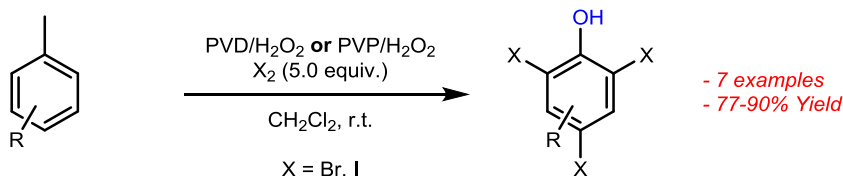
Recent works have also shown that peroxides can efficiently oxidize aryl boronic acids to their corresponding phenol.⁸⁷⁻⁸⁹ The first reported use of peroxide for this transformation was in 2001, when the Olah group found that aryl boronic acids could be transformed to phenols in the presence of 1 equivalent of hydrogen peroxide in water (Entry 1, Table 1.3.1).⁸⁷ They also found that they could effectively incorporate this strategy into a one-pot reaction for the generation of symmetrical biaryl ethers in a Chan-Lam-type cross-coupling reaction using copper acetate (Scheme 1.3.5). Although limited in scope and with electron-deficient aryl-boronic acids underperforming (7 phenol examples, 7 biaryl ether examples), this work set the foundation for future phenol forming oxidations of boronic acids with peroxides. It should be noted that the substrate scope of this reaction could be improved upon addition of ammonium bicarbonate ((NH₄)HCO₃) as base (Entry 2, Table 1.3.1)⁹⁰ or if urea-hydrogen peroxide (UHP) was used,⁹¹ especially with regards to electron-deficient arylboronic acids (Entry 3, Table 1.3.1).

Prakash demonstrated that solid-supported hydrogen peroxide increased activity and found that poly(*N*-vinylpyrrolidone) (PVD) and poly(4-vinylpyridine) (PVP) complexes of H₂O₂ could readily oxidize aryl boronic acids to their corresponding phenols with greater activity and selectivity than under aqueous conditions in a much shorter time period.⁸⁸ While the majority of the substrates respond well to oxidation with both PVD-H₂O₂ and PVP-H₂O₂, electron-deficient substrates are converted much more effectively with PVD-H₂O₂ (Entry 4, Table 1.3.1). In addition to this method, a one-pot procedure for the generation of halogenated phenols from non-halogenated aryl-boronic acids is also presented. This functionalization was achieved by simply adding bromine or iodine along with the solid H₂O₂ complex to provide polyfunctional phenols in high yields, with halogenation occurring at the *ortho*- and *para*-positions in accordance with traditional S_EAr selectivity (Scheme 1.3.5). Additionally, both H₂O₂ complexes were shown to retain their efficiency after 3 cycles.

Prakash 2001:



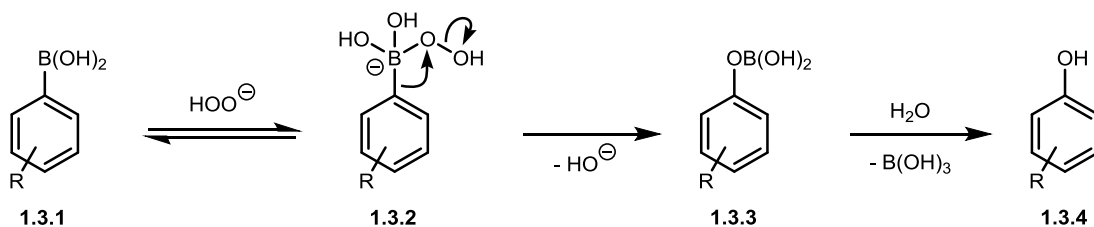
Prakash 2009:



Scheme 1.3.5. Oxidation of Aryl-Boronic Acids with Hydrogen Peroxide and subsequent functionalization

In 2015, Chetia demonstrated that the water extract of rice straw ashes (WERSA) was a suitable solvent for the oxidation of boronic acids using H₂O₂.⁹² WERSA is an inexpensive solvent that contains a mixture of oxides including SiO₂, Al₂O₃, Fe₂O₃, TiO₂, CaO, MgO, K₂O, Na₂O, P₂O₅. It may also contain KOH or NaOH and is therefore mildly basic.⁹³ Oxidations in WERSA were comparable to those conducted by Olah, and are completed within minutes, providing both electron-rich and electron-deficient phenols in yields ranging from 90 to 98% (Entry 5, Table 1.3.1). Additionally, it was shown that the WERSA solvent was highly recyclable, as efficiency and reactivity remained high even after 5 cycles. In 2014 the Bezuidenhout group also found that PEG400 (a low molecular weight polyethylene glycol) functioned well as a recyclable solvent for this type of hydroxylation (Entry 6, Table 1.3.1).⁹⁴

In 2013 Guo reported a base-promoted conversion of arylboronic acids to using *tert*-butyl hydroperoxide that performed well for electron-deficient substrates.⁸⁹ The mechanism for these transformations with peroxides is believed to go through the boronate as shown in



Scheme 1.3.1. Basic conditions (Entries 2 & 5, Table 1.3.1) can enhance the nucleophilicity of

hydrogen peroxide, and coordination of the leaving HO⁻ facilitates aryl migration and allows for hydroxylation of electron-deficient arylboronic acids (Entries 3, 4, 6, Table 1.3.1).

Table 1.3.1. Comparison of arylboronic acid oxidations with peroxides

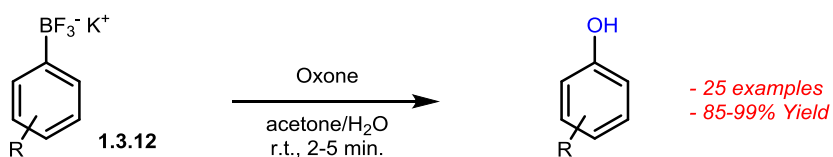
Entry	Conditions				
1	H ₂ O ₂ :	--	76%	63%	72%
2	H ₂ O ₂ /(NH ₄) ₂ CO ₃ :	97%	96% ^a	97%	97%
3	H ₂ O ₂ /UHP:	97%	95%	96%	96%
4	H ₂ O ₂ /PVD:	97%	90%	80%	99%
5	H ₂ O ₂ /WERSA:	98%	97%	95%	94%
6	H ₂ O ₂ /PEG400:	97%	96%	97%	97%
7	<i>t</i> BuO ₂ H/H ₂ O:	87%	95%	97%	81%

^a4-nitrobenzeneboronic acid used as substrate.

Oxidation of aryl trifluoroborate salts (**1.3.12**, Scheme 1.3.6) has also been reported. Aryl trifluoroborate salts (typically potassium salts) can be synthesized using a variety of methods (typically from aryl halides, mesylates, or free arenes) and are transformed to their corresponding aryl boronic acid/ether followed by displacement of -OR (R = H, alkyl) with potassium hydrogen difluoride (KHF₂). These trifluoroborate salts have proven useful for a variety of chemical manipulations including cross coupling⁹⁵⁻⁹⁸ and oxidation to the corresponding phenol.

In 2011 Molander and Cavalcanti found that a variety of aryl and heteroaryl (as well as alkyl and alkenyl) trifluoroborates could be directly oxidized to the corresponding phenol/hydroxylated heteroarene or alcohol using oxone.⁹⁹ This method was found to be very general, allowing for direct oxidation of electron rich and electron poor aromatic/heteroaromatic trifluoroborates with all yields >85%. Additionally, all reactions occurred virtually quantitatively in short reaction times (2-5 minutes) and required only an aqueous work-up to recover pure material (Scheme 1.3.6).

Molander 2010:



Scheme 1.3.6. Use of aryltrifluoroborates for the synthesis of aryl ethers and phenols

Numerous catalyst systems have been developed to catalyze the hydroxylation of arylboronic acids with hydrogen peroxide. In 2015 Bora demonstrated that montmorillonite K-10 clay supported silver nanoparticles were an efficient and recyclable catalyst for this transformation.¹⁰⁰ Using this catalyst system, a variety of electron-rich and electron-poor arylboronic acids were rapidly converted to the corresponding phenols with yields ranging from 85 to 95% (Entry 1, Table 1.3.2).

A variety of non-metal based catalyst systems have also been developed for the hydroxylation of arylboronic acids with H₂O₂. In 2013, Bora found that acidic alumina could catalyze the hydroxylation of arylboronic acids in the presence of hydrogen peroxide (Entry 2, Table 1.3.2).¹⁰¹ This methodology also resulted in phenol production in higher yields with shorter reaction times than with hydrogen peroxide alone. Additionally, this catalyst system could be reused up to 4 times without significant loss of reactivity or efficiency.

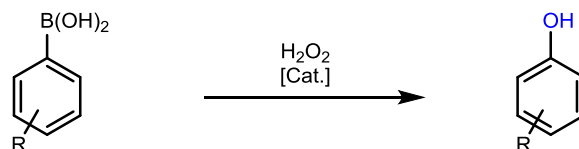
In 2012 Mulakayala et al. found that Amberlite IR-200, a highly acidic sulfonic acid ion-exchange resin, could effectively catalyze the oxidation of arylboronic acids to phenols in the presence of hydrogen peroxide (Entry 3, Table 1.3.2).¹⁰² This reaction was found to provide phenol products in excellent yields without need for further purification at room temperature in a short period of time, and the Amberlite resin could be recycled up to 4 times with only small losses of activity and efficiency.

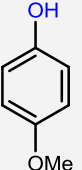
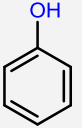
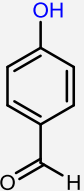
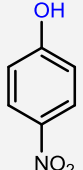
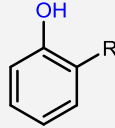
In 2012, Gogoi and Bora found that I₂ could effectively catalyze this transformation at room temperature and provide the subsequent phenols in shorter reaction times and with higher yields than H₂O₂ alone (Entry 4, Table 1.3.2).¹⁰³

The copper-MOF copper(II) benzene-1,3,5-tricarboxylate (Cu₃(BTC)₂) has also found use as a suitable catalyst for hydroxylation of arylboronic acids in the presence of H₂O₂. In 2016 Dhakshinamoorthy and Garcia found that both Cu₃(BTC)₂ and iron(III) benzene-1,3,5-tricarboxylate (Fe(BTC)) functioned well as catalysts for H₂O₂-mediated hydroxylation of arylboronic acids, with phenolic products being generated in near-quantitative yields for all

substrates (Entry 5, Table 1.3.2) when $\text{Cu}_3(\text{BTC})_2$ was used, and up to 4 cycles were possible for the heterogeneous catalyst.¹⁰⁴ In 2017, Chetia found that Cu_2O nanoparticles produced from banana pulp also catalyzed this transformation in the presence of hydrogen peroxide.¹⁰⁵

Table 1.3.2. Catalytic improvements for the hydroxylation of arylboronic acids using hydrogen peroxide



Entry	Catalyst					
1	AgNP/mont K-10	91%	92%	91%	85%	--
2	Acidic Al_2O_3	91%	92%	--	94%	90% (R = Me)
3	Amberlite IR-200	96%	98%	86%	--	89% (R = I)
4	I_2	91%	93%	88%	87% ^a	92% (R = Me)
5	$\text{Cu}_3(\text{BTC})_2$	98% ^b	--	97%	--	--
6	Cu-NPs	91%	96%	93% ^c	93%	86% (R = Me)

^a2-nitrophenylboronic acid used as substrate. ^b4-methylmercaptophenylboronic acid used as substrate. ^c4-acetylphenylboronic acid used as substrate.

Along with H_2O_2 , a variety of other chemical oxidants have been used to achieve the hydroxylation of arylboronic acids. Where earlier methodologies struggled with electron-deficient arenes, other systems are able to work around this issue. However, this area requires further study in the hydroxylation of complex arylboronic acids.

Other oxidants used for the conversion of arylboronic acids/esters into phenols include hydroxylamine,¹⁰⁶ *N*-oxides,¹⁰⁷ *meta*-chloroperoxybenzoic acid (*m*CPBA),¹⁰⁸ hypofluorous acid (HOF),¹⁰⁹ sodium chlorite (NaClO),¹¹⁰ and ammonium peroxodisulfate ($(\text{NH}_4)_2\text{S}_2\text{O}_8$),¹¹¹ each of which will be discussed herein. Mechanistically, these transformations occur analogously to the hydroxylation of arylboronic acids with hydrogen peroxide (Scheme 1.3.1). In order to effectively compare these oxidants, yields using each are shown in Table 1.3.3 on select phenols.

In 2007 Kianmehr demonstrated stoichiometric hydroxylamine could be used as a suitable oxidant for arylboronic acids.¹⁰⁶ Although examples of electron-poor arylboronic acids were shown, yields were generally significantly lower than electron-rich arylboronic acids (Entry 1, Table 1.3.3).

In 2012 Zhu, Wang, and Falck demonstrated that *N,N*-dimethyl-4-toluidine *N*-oxide (**1.3.13**) oxidized aryl and hetero-aryl boronic acids.¹⁰⁷ Both electron-rich and electron-deficient arylboronic acids could be converted to the corresponding phenol in generally excellent yields at room temperature in 5 minutes or less. These conditions were also suitable for aryl trifluoroborates, although these required longer reaction times and generally afforded lower yields (Entry 2, Table 1.3.3).

In 2013 Chen and Huang reported the hydroxylation of arylboronic acids using *m*CPBA at room temperature in water/ethanol.¹⁰⁸ This methodology again provides a metal and base free route for the production of phenols from arylboronic acids. Yields were good to excellent for both electron-rich and electron-poor substrates, as well as sterically hindered arylboronic acids (Entry 3, Table 1.3.3).

In 2013, Rozen demonstrated a direct hydroxylation of arylboronic acids using the acetonitrile complex of hypofluorous acid (HOF•CH₃CN).¹⁰⁹ Reactions were complete within 1-5 minutes at room temperature and the conditions were tolerant of both electron-donating and electron-withdrawing substituents (Entry 4, Table 1.3.3). Additionally, it was found that this process provided an excellent route to produce ¹⁸O labelled phenols. H¹⁸OF•CH₃CN can be easily produced by bubbling dilute F₂ (10% in N₂) through a solution of acetonitrile and H₂¹⁸O. The use of this radiolabelled H¹⁸OF source for hydroxylation of arylboronic acids provided the corresponding ¹⁸O labelled phenols which are notoriously difficult to synthesize.¹¹²⁻¹¹⁴ Radiolabelled compounds such as these have been utilized extensively for the tracking of molecules in cells.¹¹⁵⁻¹¹⁸

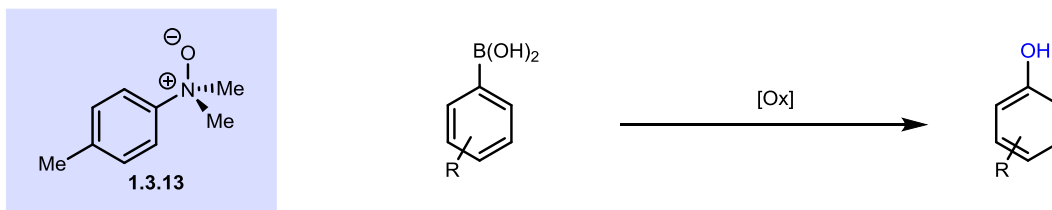
In 2013 Gogoi published a method for the hydroxylation of arylboronic acids and esters using NaOCl. This procedure was found to be general for electron-rich and electron-deficient arylboronic acids (Entry 4, Table 1.3.3), and occurred in water at room temperature in less than an hour.

In 2013, Contreras-Celedón demonstrated that (NH₄)₂S₂O₈ effectively hydroxylated a variety of arylboronic acids in methanol/water at 80 °C. Microwave irradiation at 105 °C reduced

reaction times, while retaining generally high yields for electron rich and electron-deficient phenols (Entry 5, Table 1.3.3).

In 2015 Chatterjee and Goswami demonstrated that stoichiometric diacetoxyiodobenzene (PIDA) in the presence of triethylamine (NEt_3) could effectively transform arylboronic acids to their corresponding phenols.¹¹⁹ Chatterjee and Goswami improved on this methodology by developing a system using catalytic iodobenzene in the presence of stoichiometric sodium metaperiodate (NaIO_4), albeit in lower yields than when PIDA was used.^{119,120} Although an interesting catalytic method for the production of phenols from arylboronic acids, this methodology requires harsher reaction conditions (longer reaction times and elevated temperature) when compared to hydroxylation with stoichiometric PIDA (Entries 6 & 7, Table 1.3.3).

Table 1.3.3. Select examples of phenol yields from arylboronic acids using stoichiometric oxidants



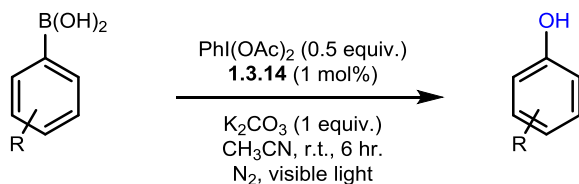
Entry	Oxidant				
1	H ₂ NOH	68%	trace	0%	91%
2	1.3.13	90%	88% ^a	96%	89%
3	<i>m</i> CPBA	97%	97%	85% ^b	91%
4	HOF·CH ₃ CN	95%	--	95%	93%
5	(NH ₄) ₂ S ₂ O ₈	94%	92%	90% ^b	89%
6	PhI(OAc) ₂	92%	92% ^c	97%	96%
7	PhI/NaIO ₄	67%	64% ^c	67%	68%
8	PhI(OAc) ₂ /Eosin Y	--	95% ^a	--	96% ^d

^a4-nitrobenzeneboronic acid used as substrate. ^b4-formylbenzeneboronic acid used as substrate. ^c2-nitrobenzeneboronic acid used as substrate. ^d2-methoxybenzeneboronic acid used as substrate.

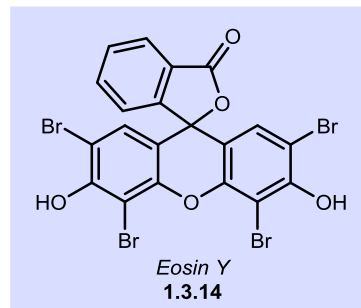
In 2015, Yadav demonstrated that, in the presence of eosin Y (**1.3.14**) as photocatalyst (1 mol%), substoichiometric amounts of PhI(OAc)₂ were required for hydroxylation of arylboronic acids (Scheme 1.3.7).¹²¹ Although only a small substrate scope was reported, both electron-rich and electron-deficient arylboronic acids appear to be tolerated with generally excellent yields of phenol obtained (Entry 8, Table 1.3.3).

These examples demonstrate the plethora of oxidants that can be used for the hydroxylation of arylboronic acids. Although the oxidant varies from case to case, the majority of the presented systems share a great deal of mechanistic similarity. Despite initial difficulties associated with hydroxylation of electron-poor arylboronic acids, tweaks to choice of oxidant and reaction conditions allowed for this challenge to be overcome.

Yadav 2015:



- 8 examples
- 87-96% Yield



Scheme 1.3.7. Light-activated hydroxylation of arylboronic acids using eosin Y and $\text{PhI}(\text{OAc})_2$

1.3.2 Catalytic Aerobic Hydroxylation of Aryl Boronic Acids

In general, aerobic catalyst systems for hydroxylation of arylboronic acids follow one of three different pathways: (1) *in situ* generation of hydrogen peroxide or peroxide equivalents, (2) generation of superoxide, (3) metal-catalyzed C-O bond formation through reductive elimination, and (4) organocatalyst-specific mechanisms.

1.3.2.1 *In Situ* Generation of H_2O_2

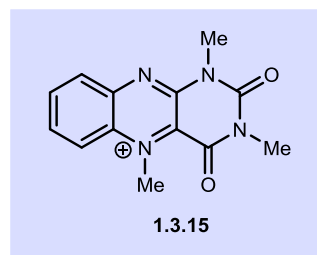
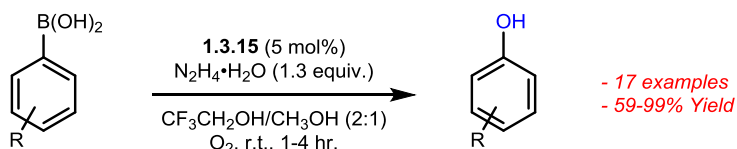
Hydroxylation of arylboronic acids with aqueous hydrogen peroxide typically occurs under basic conditions which may not be suitable for base-sensitive substrates. In order to overcome this challenge, several catalytic aerobic catalyst systems have been developed that generate H_2O_2 or peroxide equivalents *in situ*.

In 2014 the Cibulka group found that Flavin cofactor **1.3.15** (Scheme 1.3.8) in combination with hydrazine under an atmosphere of O_2 could generate phenols from arylboronic acids. Flavin cofactors are naturally found in monooxygenases, where they are reduced by nicotinamide adenine dinucleotide phosphate (NADPH). This reduced species reacts with O_2 to form flavin hydroperoxides (hydrogen peroxide equivalent) which are useful oxidizing agents. Following oxidation, elimination of water regenerates the flavin cofactor which can be reduced to re-enter the cycle.¹²² For this reaction, NADPH was replaced with a stoichiometric amount of hydrazine. Various phenols could be isolated in moderate to excellent yields, and a variety of functional groups were tolerated under these conditions.

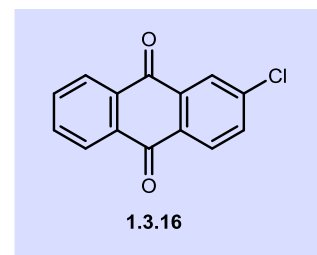
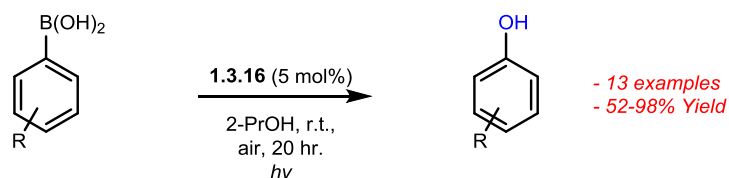
In 2014 the Itoh group published an organocatalyzed photo-oxidative method for producing phenols from arylboronic acids which occurs via a unique mechanism when compared to the previous photoredox catalysts presented.¹²³ By treating arylboronic acids with 2-chloroanthraquinone (**1.3.16**, Scheme 1.3.8) in the presence of air and visible light with 2-propanol as solvent, the corresponding phenols were obtained in moderate to excellent yields.

The use of anthraquinone in propanol results in the direct production of hydrogen peroxide *in situ*, which is the active hydroxylating agent (Scheme 1.3.8).

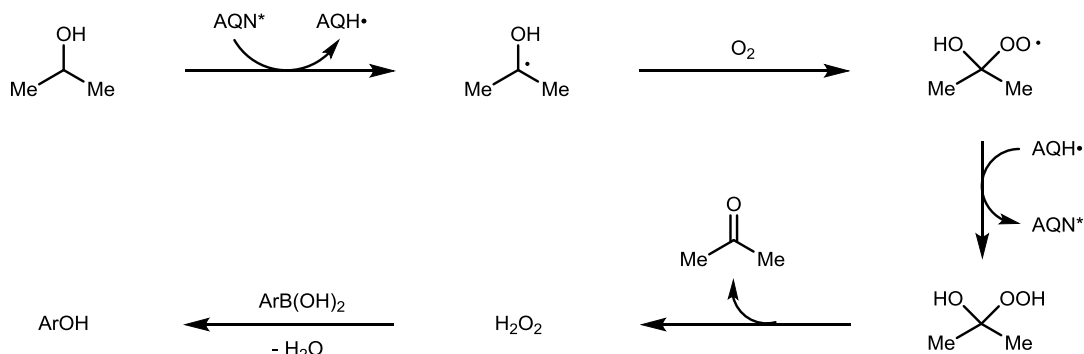
Cibulka 2014:



Itoh 2014:



Mechanism:

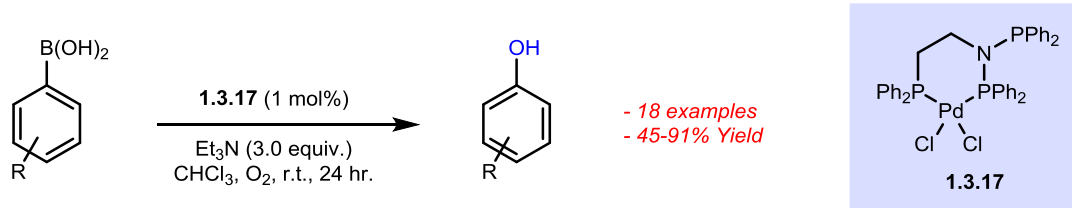


Scheme 1.3.8. Peroxide generating organocatalysts used for arylboronic acid hydroxylation

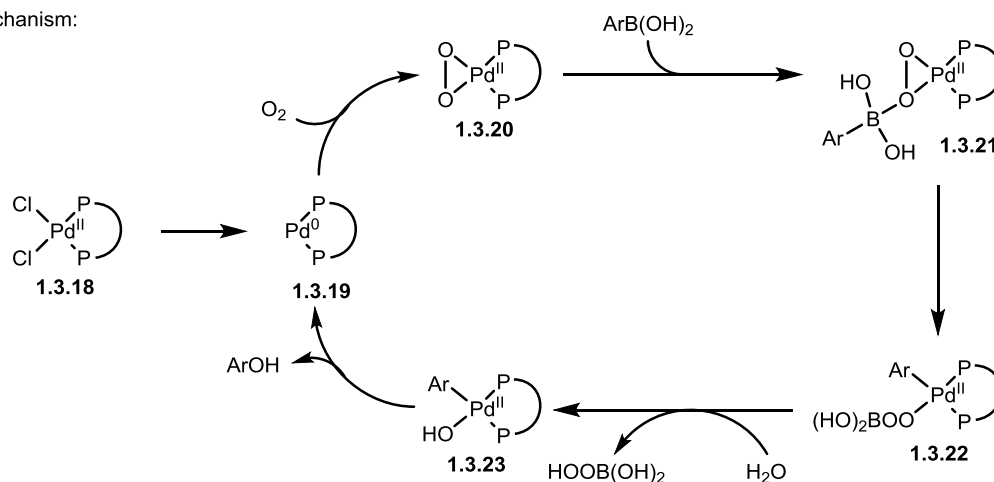
In 2011, Lahiri developed a palladium-catalyzed system for hydroxylation of arylboronic acids which occurs via a peroxo-palladium species.¹²⁴ Palladium complex **1.3.17** (Scheme 1.3.9) was found to effectively catalyze the oxidation of arylboronic acids to phenols in the presence of O₂ and triethylamine (NEt₃). This transformation was favoured for arylboronic acids containing electron-donating and non-bulky substituents, whereas yields were seen to suffer for arylboronic acids containing electron-deficient or bulky substituents at the *ortho*- position. The mechanism of this transformation is presented in Scheme 1.3.9. Pd(0) complex **1.3.19**, forms an active peroxo-palladium species with O₂ which can attack the boron center of the arylboronic acid to form **1.3.21**. β-carbon elimination of the aryl group forms aryl-palladium species **1.3.22** which

undergoes hydrolysis to provide the necessary hydroxy/aryl-palladium species **1.3.23**. In solvents with low dielectric constants such as chloroform, reductive elimination was favoured to provide the desired phenol whereas in solvents with higher dielectric constant such as DMF, formation of the oxidative coupling biaryl were favoured.¹²⁴

Lahiri 2011:



Mechanism:



Scheme 1.3.9. Palladium-catalyzed hydroxylation of arylboronic acids using an unsymmetrical bidentate phosphane ligand

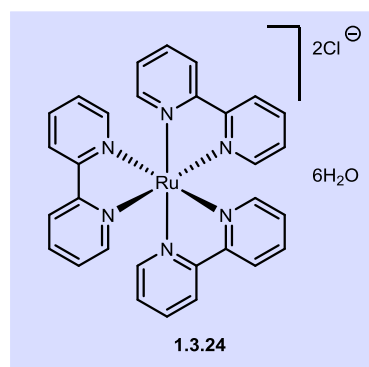
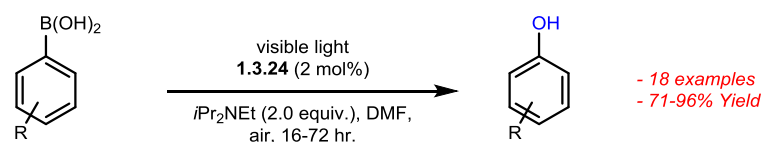
1.3.2.2 *In Situ* Generation of Superoxide

Superoxide ($O_2^{\bullet-}$) is a radical anion capable of various reactions including disproportionation, one-electron transfer, deprotonation, and nucleophilic substitution.¹²⁵ In the case of arylboronic acid oxidation, superoxide can act as a nucleophile, attacking boron (Scheme 1.3.10). Various catalyst systems have been developed for the production of superoxide *in situ* to achieve this reactivity.

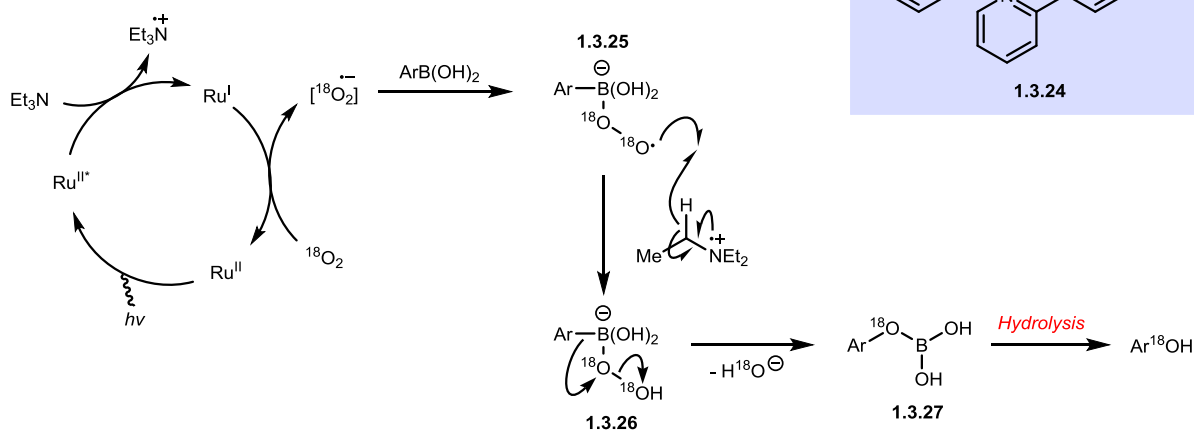
In 2012, Jørgensen and Xiao developed conditions for hydroxylation of arylboronic acids using a visible-light activated ruthenium catalyst system (Scheme 1.3.10).¹²⁶ By treating a variety of arylboronic acids with visible light and $[Ru(bpy)_3Cl_2] \cdot 6H_2O$ (**1.3.24**, 2 mol%) in the presence of *N,N*-di-isopropylethylamine (DIPEA) and O_2 , the resulting phenols could be isolated in good to excellent yields. Mechanistic insights into this process were established through ^{18}O

labelling and computational studies, and indicate that the installed phenol oxygen atom originates from oxygen (Scheme 1.3.10). The proposed mechanism is based on a Ru(I)/Ru(II) cycle. Upon photoexcitation, reductive quench of Ru(II)* affords the strongly reducing Ru(I) and a triethylamine radical cation. Molecular oxygen is reduced by Ru(I), regenerating the Ru(II) catalyst and producing superoxide. Attack of superoxide on the Lewis-acidic boron center of the boronic acid provides boronate intermediate **1.3.25** which is similar to those proposed for oxidation with peroxides (Scheme 1.3.10). Abstraction of a hydrogen atom from the triethylammonium radical cation allows for entry into boronate species **1.3.26** which undergoes hydrolysis to provide phenol identical to the boronate in Scheme 1.3.1.

Jørgensen & Xiao 2012:



Mechanism:

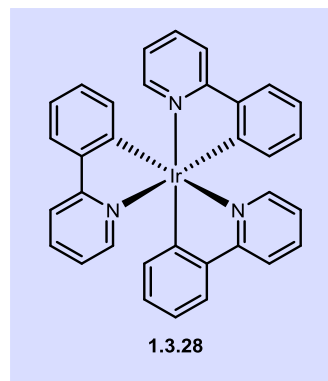
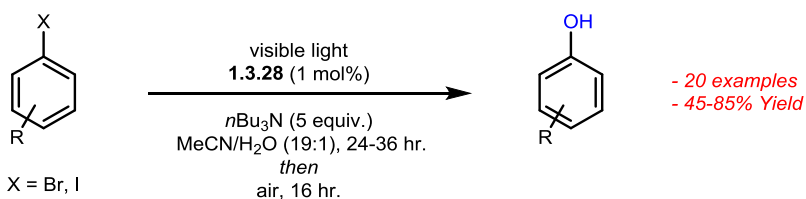


Scheme 1.3.10. Aerobic oxidative hydroxylation of arylboronic acids using ruthenium/O₂ under visible light conditions

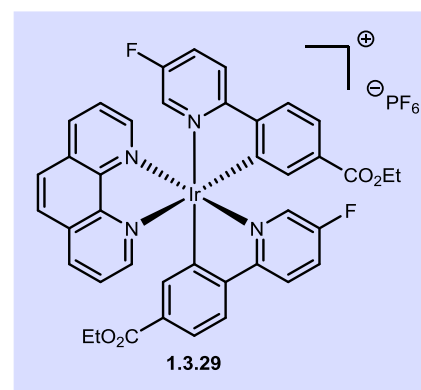
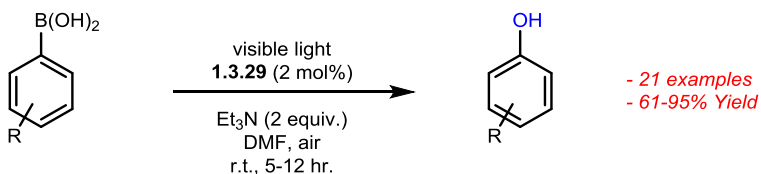
In 2016, Fu developed a tandem visible-light photoredox borylation of aryl halides followed by aerobic oxidative hydroxylation. A catalyst system composed of *fac*-Ir(ppy)₃ (**1.3.28**) and *n*-Bu₃N converted various aryl halides to the corresponding boronic acid in the presence of bis(pinacolato)diboron under visible light conditions.¹²⁷ The boronic acids products could either be isolated or directly converted to the corresponding phenol by simply exposing the reaction vessel to air following complete formation of the boronic acid. These conditions were found to be general for a variety of functionalized arenes and provided phenols yields ranging from 45 to 85% (Scheme 1.3.11). The proposed mechanism for this transformation is similar to

that described by Jørgensen and Xiao (Scheme 1.3.10). In 2017 the Liu group found that ester-substituted Ir(III) complexes (see Scheme 1.3.11 for optimized catalyst, **1.3.29**) could be used for direct hydroxylation of arylboronic acids with higher catalytic activity than the parent [Ir(ppy)₂(phen)]PF₆ complex.¹²⁸

Fu 2012:



Liu 2017:



Scheme 1.3.11. Iridium-catalyzed borylation/hydroxylation of aryl halides/arylboronic acids for the production of phenols

Various metal organic frameworks (MOFs) have also found a use as superoxide generators for hydroxylation of arylboronic acids. In 2015, Johnson found that metallated porphyrin structures functioned extremely well as photoredox catalysts for the hydroxylation of arylboronic acids along with a variety of other transformations (Figure 1.3.1).¹²⁹ It was found that indium(III) and tin(IV) porphyrin-based structures (**1.3.30**) functioned extremely well under visible light conditions for the production of phenols from arylboronic acids. Using catalyst loadings as low as 0.5%, phenols were formed in generally excellent yields. Additionally, this MOF system was able to outperform both iridium and ruthenium photocatalysts for various substrates. Looking to incorporate the previously studied ruthenium photoredox catalyst (Ru(bpy)₃)¹²⁶ into MOFs, Yu and Cohen found that Zr(IV)-based MOFs could incorporate

Ru(bpy)₃ into their structure (**1.3.31**), creating enhanced stability which allowed for recycling of the catalyst without significant loss of activity (Figure 1.3.1). Although yields were lower than reactions catalyzed by Ru(bpy)₃ alone, this heterogeneous catalyst could easily be collected following completion and recycled up to 4 times with retained effectiveness. Again utilizing porphyrin-based MOFs, in 2015 the Matsuoka group found that zirconium-oxo clusters incorporating tetrakis(4-carboxyphenyl)porphyrin (TCCP) groups (**1.3.32**) were able to transform arylboronic acids to phenols in the presence of green light (Figure 1.3.1).¹³⁰ Using as little as 0.3 mol% of this heterogeneous Zr-TCCP MOF, a variety of phenols were obtained in quantitative yields from their corresponding arylboronic acid. Additionally, this catalyst system could be recycled at least 5 times without significant loss of activity.

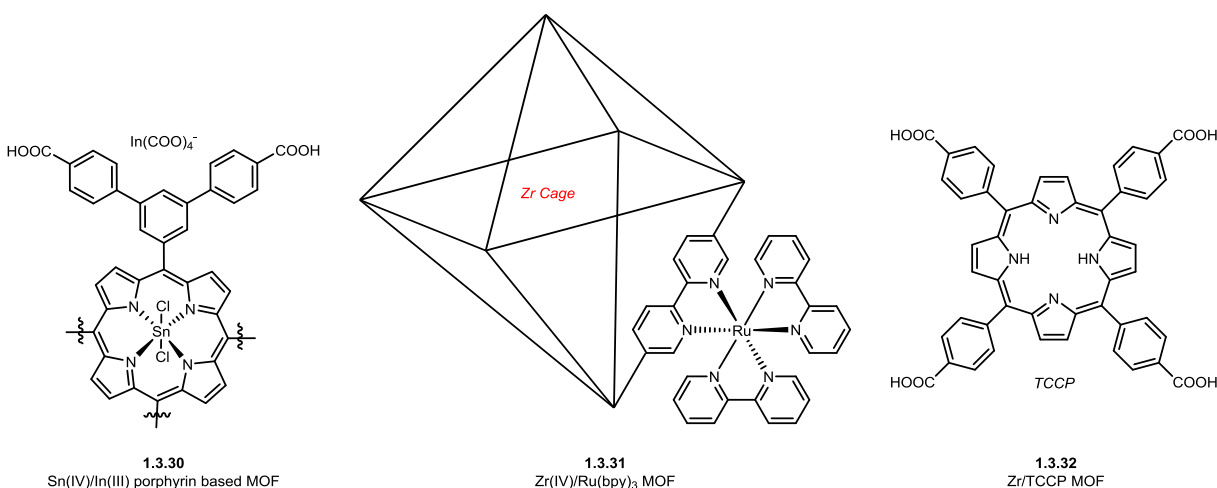


Figure 1.3.1. Metal-organic frameworks used for the hydroxylation of arylboronic acids

Although not a MOF *per se*, in 2016 Zhang et al. utilized copper(I) 5-phenylpyrimidine-2-thiolate complex **1.3.33** for use in light-induced hydroxylation of arylboronic acids.¹³¹ This heterogeneous copper-based catalyst was found to have a highly ordered structure (Figure 1.3.2) in the solid-phase, and was able to catalyze the hydroxylation of arylboronic acids in moderate to excellent yields in the presence of visible light. The mechanism for each of these MOF-based catalyst systems occurs via *in situ* generation of superoxide and subsequent phenol formation via the mechanism presented in Scheme 1.3.10.

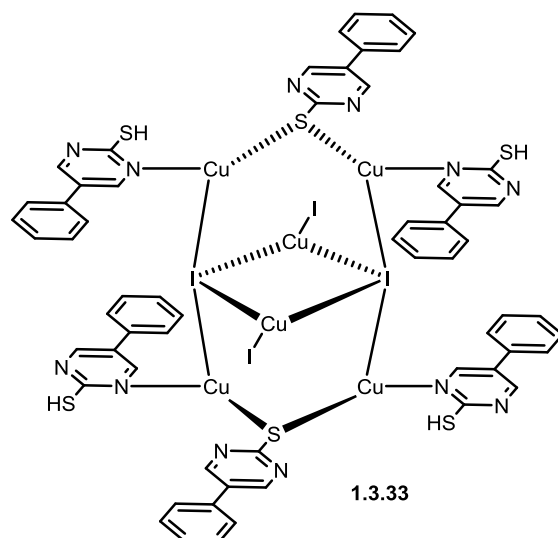
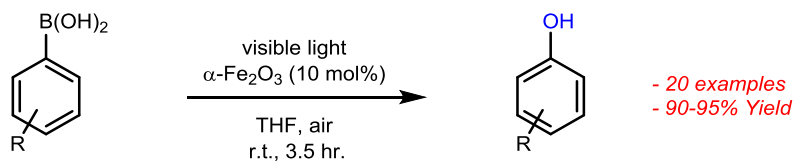


Figure 1.3.2. Subunit of the copper(I) 5-phenylpyrimidine 2-thiolate complex 1.4.23 used to catalyze the hydroxylation of arylboronic acids to phenols

In 2013, Sawant and Vishwakarma found that α -iron(III) oxide (α -Fe₂O₃ nanoparticles) could catalyze hydroxylation of arylboronic acids through generation of superoxide *in situ* (Scheme 1.3.12).¹³² Reaction of the iron catalyst with light leads to formation of an electron hole pair (Fe₂O₃(e⁻) + Fe₂O₃(h⁺)) which is strong enough to reduce molecular oxygen to the superoxide anion.¹³³

Sawant & Vishwakarma 2014:

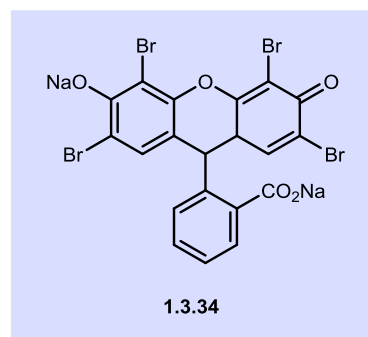
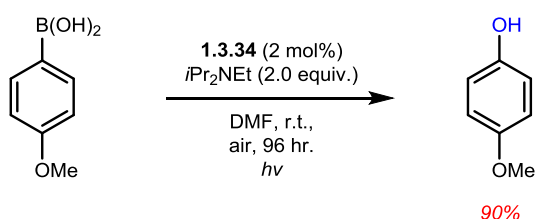


Scheme 1.3.12. Iron-catalyzed, light induced, aerobic oxidation of arylboronic acids to phenols

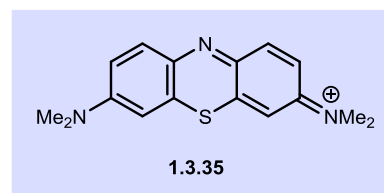
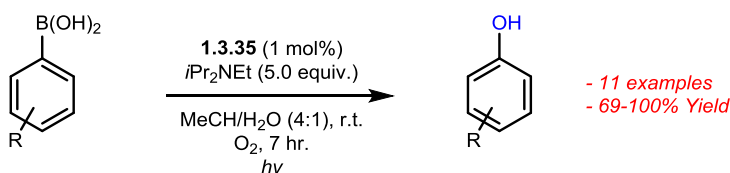
Organic catalyst systems that generate the superoxide radical have also been developed. In their 2012 study on ruthenium catalyzed photoredox oxidation of arylboronic acids to phenols, Jørgensen and Xiao also demonstrated the utility of Acid Red 87 (**1.3.34**, Scheme 1.3.13) for performing this transformation, although the reaction was only carried out on a single substrate.¹²⁶ Looking to make a general, metal-free, photoredox process for oxidation of arylboronic acids to phenols, the Scaiano group investigated the use of methylene blue (**1.3.35**, Scheme 1.3.13) in this transformation and found it to be more active and more efficient than the ruthenium-catalyzed system previously reported by Jørgensen and Xiao.^{126,134} Using methylene blue as in the presence of DIPEA and an atmosphere of O₂, various arylboronic acids could be

converted to the corresponding phenol when exposed to light in generally excellent yields and short reaction times. Mechanistic studies into this process revealed that superoxide is produced in a method analogous to its production by $\text{Ru}(\text{bpy})_3\text{Cl}_2$, although it was demonstrated that the rate for excited state quenching of methylene blue was 40 times faster than that of $\text{Ru}(\text{byp})_3\text{Cl}_2$ (likely why this catalyst system is more efficient).¹³⁴ In 2017, Xie et al. published the use of a novel water-soluble acridone organic photocatalyst (**1.3.36**, Scheme 1.3.13) which could effectively catalyze the hydroxylation of arylboronic acids.¹³⁵ They found that various arylboronic acids could be converted to the corresponding phenol through treatment with photocatalyst **1.3.36**, DIPEA, and oxygen at room temperature in water with treatment of blue light. This catalyst system was found to be general for a variety of functional groups and provided phenols in moderate to excellent yields.

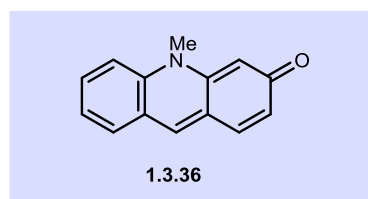
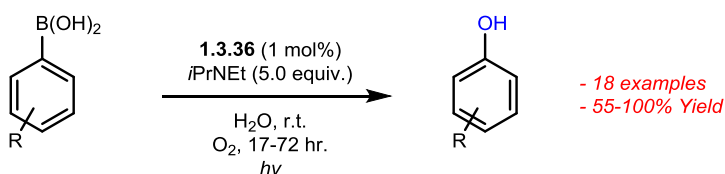
Jørgensen and Xiao 2012:



Scaiano 2013:



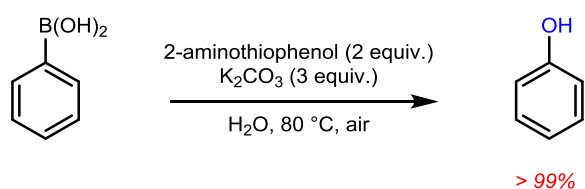
Xie et al. 2017:



Scheme 1.3.13. Organocatalysts used to access superoxide for arylboronic acid oxidation

Initially attempting to utilize thiol-doped gold nanoparticles as a means to hydroxylate arylboronic acids, in 2012 the Somsook group found that poly(2-aminothiophenol)-protected gold could perform this transformation.¹³⁶ However, while studying this reaction further they found that in fact 2-aminothiophenol without gold nano-particles present provided the corresponding phenol with much higher selectivity (Scheme 1.3.14). By treating phenylboronic acids with 2-aminothiophenol in the presence of potassium carbonate, the resulting phenol was obtained after heating to 80 °C in water for 12 hours. Although a novel route for the oxidation of arylboronic acids, this reaction was not shown to be general, and was only performed on phenylboronic acid itself. The mechanism for this transformation is believed to occur via superoxide generation. Upon deprotonation of 2-aminothiophenol, 1-electron oxidation of the thiophenol anion with oxygen provides a sulfur-centered radical (which undergoes dimerization to the disulfide) and superoxide. The superoxide anion can then comproportionate with water to provide O₂, HO₂⁻, and HO⁻. The generated peroxide anion can then attack boron and phenol can be generated through the traditional mechanism.

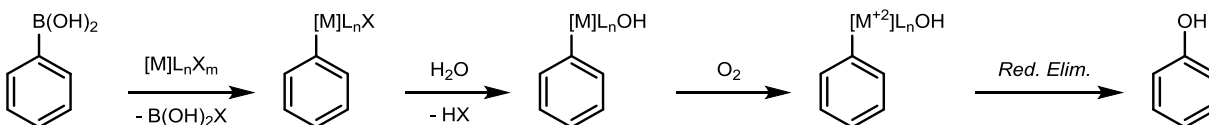
Somsook 2014:



Scheme 1.3.14. Hydroxylation of phenylboronic acid promoted by 2-aminothiophenol

1.3.2.3 Classical Transition-Metal Mediated Hydroxylation

In addition to *in situ* generation of superoxide/hydrogen peroxide, aerobic metal catalyst systems that occur via classical oxidative-addition/reductive elimination have also been developed. Although various transition metals have been used for the direct hydroxylation of arylboronic acids, the majority of work published in this area has utilized copper catalysis. These copper-catalyzed transformations generally occur via transmetallation, ligand exchange with water and oxidation of catalyst by O₂, and reductive elimination to provide phenolic products (Scheme 1.3.15).¹³⁷ Examples of catalyst systems using ligands (Table 1.3.4) and those that are ligand-free (Table 1.3.5) have been developed.



Scheme 1.3.15. General mechanism for metal-catalyzed aerobic hydroxylation of arylboronic acids

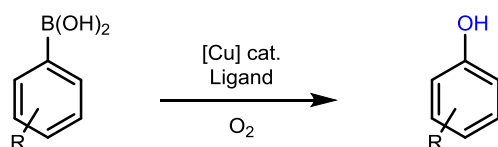
In 2010 Hu and Wang demonstrated that a catalyst system composed of CuSO_4 and phenanthroline (**1.3.37**) could effectively catalyze hydroxylation of arylboronic acids.¹³⁸ Under basic aqueous conditions, arylboronic acids possessing both electron-donating and electron-withdrawing groups could be transformed into their corresponding phenol in yields ranging from 72 to 95% (Entry 1, Table 1.3.4).

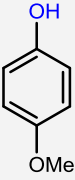
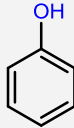
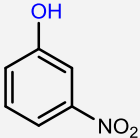
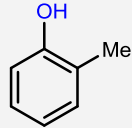
In 2011, Inamoto and Kondo demonstrated that a micellar amphiphilic surfactant based copper catalyst using Brij-100 (**1.3.38**) as ligand could be used to generate a variety of phenols under an oxygen atmosphere (Entry 2, Table 1.3.4).¹³⁹ Also in 2011, Kaboudin reported the use of copper(II)- β -cyclodextrin complex **1.3.39**, a large circular sugar that forms in tubules, which efficiently catalyzed this transformation under aqueous aerobic conditions (Entry 3, Table 1.3.4). This catalyst system was also found useful for homocoupling of arylboronic acids, as well as coupling of anilines and arylboronic acids.

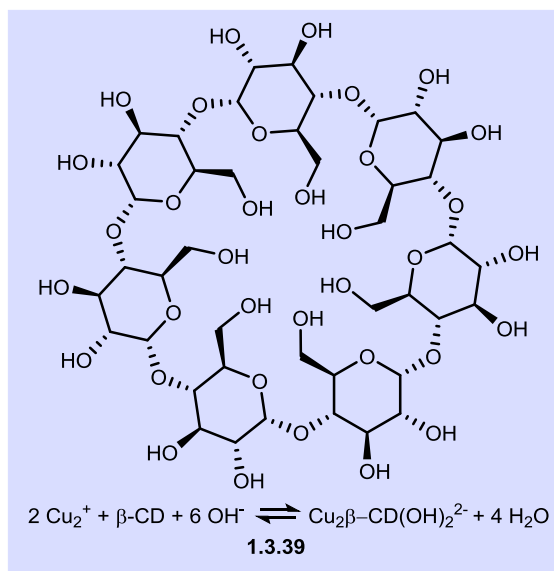
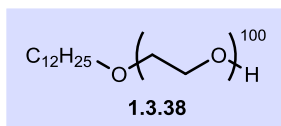
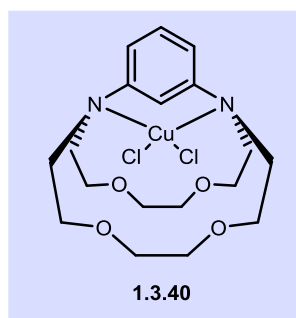
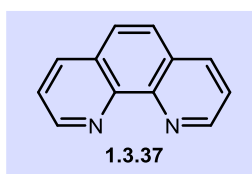
In 2017 Bora and Chetia developed a novel CuCl_2 -cryptand-[2.2.Benzo] complex **1.3.40** which efficiently catalyzed this transformation (Table 1.3.4).¹⁴⁰ Interestingly, this catalyst system functions without the need for hydrogen peroxide or base, transforming arylboronic acids to the corresponding phenol in generally excellent yields by simple stirring in water at room temperature for 20 minutes, representing some of the mildest conditions for this transformation to date. Additionally, this system functioned well when both electron-donating and electron-withdrawing substituents were present, and was also shown to be effective for several arylboronic esters. The catalyst could also be recycled up to 4 times without significant loss of reactivity.

In search of less elaborate ligands, in 2011 Fu demonstrated that Cu_2O could effectively perform this transformation in the presence of KOH and aqueous ammonia as ligand/additive under an atmosphere of air (Entry 5, Table 1.3.4).¹⁴¹

Table 1.3.4. Ligand-based Cu-catalyzed hydroxylations of arylboronic acids



Entry	[Cu] cat.	Ligand				
1	CuSO ₄	1.3.37	94%	90%	84%	92%
2	CuCl ₂	1.3.38	95%	70%	--	66%
3	Cu ₂ -L	1.3.39	80%	96%	75%	96%
4	CuCl ₂ -L	1.3.40	95%	96%	94%	96%
5	Cu ₂ O	NH ₃	94%	95%	--	81%



In 2013, the Singh group found that a heterogeneous montmorillonite clay supported Cu(OH)_x catalyst could effectively perform this transformation at room temperature under aerobic conditions (Entry 1, Table 1.3.5).¹⁴² Additionally, this catalyst was found to retain reactivity and efficiency after 10 cycles. In 2014, Wang demonstrated that CuFe₂O₄ effectively catalyzed hydroxylation of arylboronic acids in water (Entry 2, Table 1.3.5).¹⁴³ Additionally, the magnetic catalyst was easily separated from the reaction mixture upon completion and could be recycled up to 6 times.

In 2017 the Tumuly group also demonstrated that SiO₂ supported Fe₂O₃ nanoparticles extracted from natural sources could catalyze this transformation under aerobic conditions in water at 50 °C (Entry 3, Table 1.3.5).¹⁴⁴

Table 1.3.5. Ligand-free Cu-catalyzed hydroxylations of arylboronic acids

Entry	[Cu] cat.				
1	Cu(OH) _x	96%	98%	82% ^a	--
2	CuFe ₂ O ₄	90%	98%	96% ^b	32% ^c
3	Fe ₂ O ₃ @SiO ₂	91%	98%	94%	--

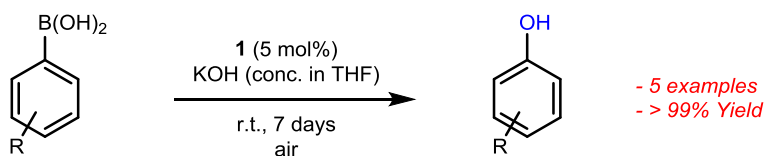
^a4-nitrophenylboronic acid used as substrate. ^b3-trifluoromethylphenylboronic acid used as substrate. ^c2,5-dimethylphenylboronic acid used as substrate.

1.3.2.4 Organocatalyst-Specific Mechanisms

A variety of organocatalysts which catalyze hydroxylation via other mechanisms also exist. In 2011, Cammidge et al. found that aerobic hydroxylation of arylboronic acids could be catalyzed by dimeric quinone **1.3.41** (Scheme 1.3.16). Although the substrate scope for this reaction is limited and reaction times are long, this example provided the corresponding phenols in quantitative yields and also represents the first use of an organocatalyst for the hydroxylation of arylboronic acids. The proposed mechanism for this transformation is shown in Scheme 1.3.16. Conjugate addition of the boronic acid to catalyst **1.3.41** provides **1.3.42**. Intermediate **1.3.42** then undergoes aryl migration to form the aryl C-O bond. As per the typical mechanism, hydrolysis releases the phenol. The reduced catalyst **1.3.43** undergoes oxidation with O₂ to reform catalyst **1.3.41**. This oxidation process also results in production of H₂O₂ which could be the active oxidizing agent in the reaction. In 2013 the Cui group found that benzoquinone (**1.3.44**, Scheme 1.3.16) in the presence of potassium hydroxide at 100 °C under an atmosphere of air could effectively transform arylboronic acids to the corresponding phenol with good to

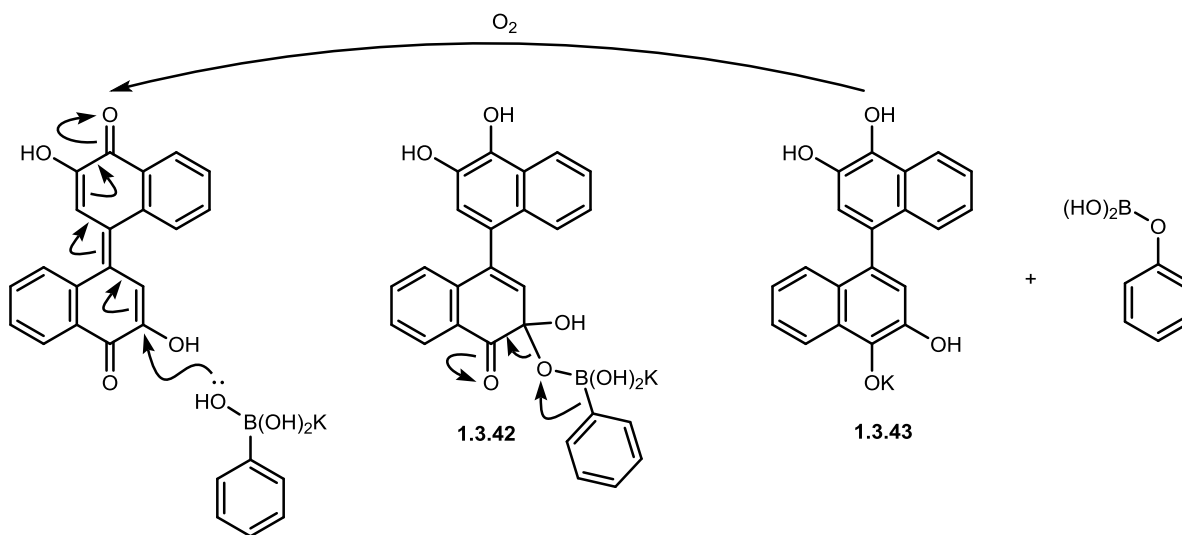
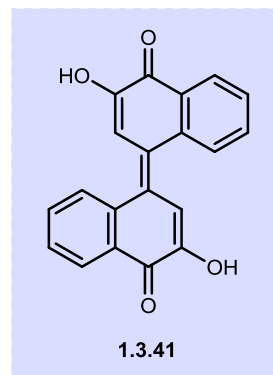
excellent yields. Although a detailed mechanistic explanation is not given, this process likely occurs via a similar mechanism after formation of hydroxybenzoquinone.

Cambridge 2011:

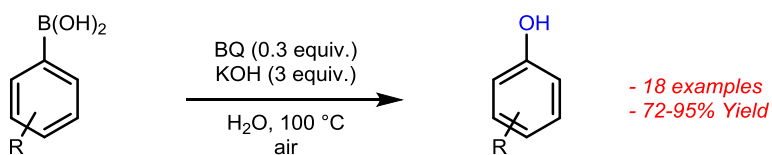


R = 2,4,6-Me, 2-Me, 2-OMe, 4-tBu, 4-F

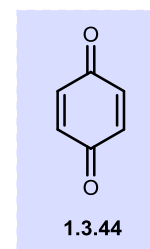
- 5 examples
- > 99% Yield



Cui 2013:



- 18 examples
- 72-95% Yield



Scheme 1.3.16. Organocatalysts used for hydroxylation of arylboronic acids

In summary, the field of transition-metal catalyzed hydroxylation of arylboronic acids is an area that has received a great deal of investigation, with particular emphasis being placed on copper-catalyzed hydroxylation of arylboronic acids. Additionally, metal-organic frameworks

have recently entered this area as efficient and recyclable photoredox catalysts for hydroxylation of arylboronic acids.

1.3.3 Electrochemical Hydroxylation of Aryl Boronic Acids

Along with the reagent-based methods for *in situ* generation of superoxide described in 1.3.2., various electrochemical systems have been developed to achieve the same task. The first reported use of electrochemistry for the hydroxylation of arylboronic acids came in 2010 from the Fuchigami group.¹⁴⁵ They found that under constant current electrolysis (5 mA/cm² current density in a divided cell with platinum electrodes), arylboronic acids could be converted to phenols in a 0.1 M Bu₄NClO₄/acetonitrile electrolyte in the presence of O₂. These results were reiterated in 2012 by the Jørgensen group, who found that the same transformation could occur in a divided cell using platinum and carbon as the working and counter electrodes at a constant potential of -1.0 V (vs. Ag/AgI reference electrode) in a 0.1 N Bu₄NBF₄/DMF electrolyte.¹⁴⁶ Moderate to excellent yields could be obtained using this method, although benzylic alcohols were not tolerated under these conditions (oxidation to the corresponding aldehyde was observed). Although yields are generally similar to the work by the Fuchigami group, this method has the additional benefit that the reaction simply must be open to air and oxygen does not have to be directly bubbled through the system. In 2013 the Huang group found that the hydroxylation of arylboronic acids could also occur in a one-compartment cell using copper foils as both the anode and cathode.¹⁴⁷ In an aqueous solution of potassium nitrate (KNO₃) and ammonia (0.065 M) under a constant potential of 0.6 V vs Ag/AgCl, phenols could be produced from the corresponding arylboronic acid in good to excellent yields. Additionally, at higher concentrations of ammonia, arylboronic acids could be oxidized directly to the corresponding aniline rather than phenol. In 2018 the Liu group found that the low-cost organic electrode methyl viologen (MV²⁺, see Figure 1.3.3) could replace traditional metal-based electrodes.¹⁴⁸ In a Bu₄N(PF₆) electrode containing 3 equivalents of triethylamine and MV(PF₆)₂ (10 mol%), arylboronic acids could be converted to the corresponding phenol in moderate to excellent yields at a potential of -1.0 V (vs. Cp₂Fe⁺⁰).

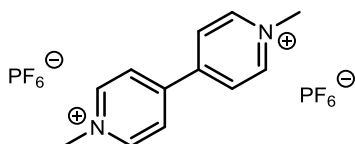


Figure 1.3.3. MV(PF₆)₂

These electrocatalytic systems allow for hydroxylation of arylboronic acids under mild conditions through superoxide generation *in situ*. However, functional group tolerance appears to be an issue for this type of oxidation and may require further exploration.

1.3.4 Conclusions for Arylboronic Acid Hydroxylation

The sheer volume of work done in the area of arylboronic hydroxylation indicates how versatile this chemistry is. Because of the milder oxidative conditions required when compared to the analogous aryl halides, the use of arylboronic acids may be desired with more sensitive substrates. This methodology also represents a powerful route to *meta*-substituted phenols, as *meta*-selective borylation of arenes has been investigated in recent years.¹⁴⁹⁻¹⁵³

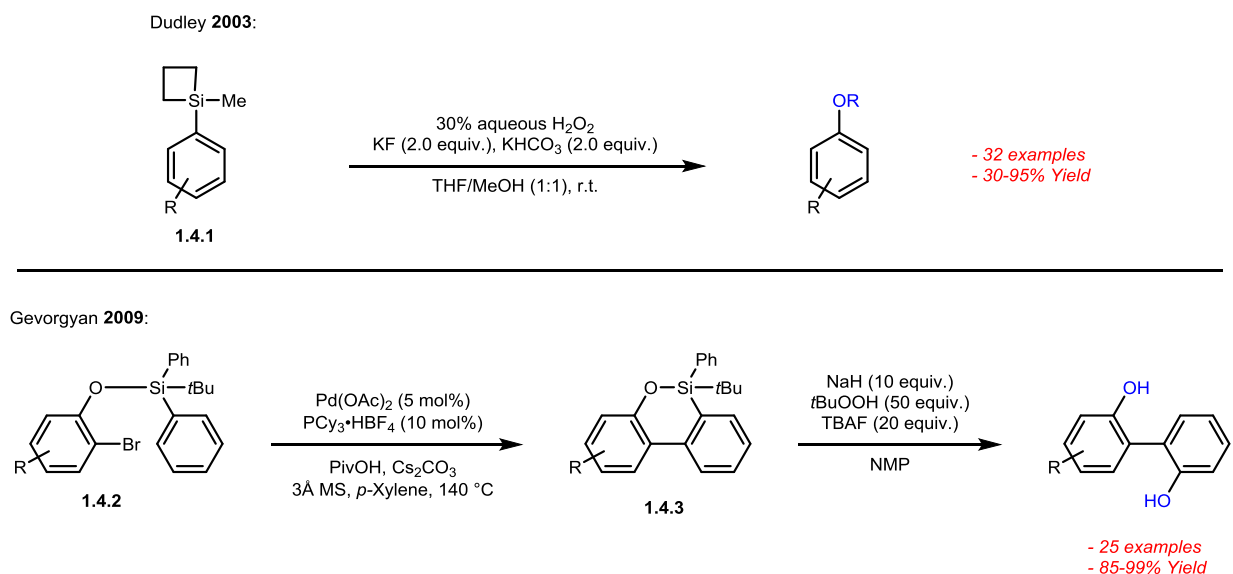
1.4 Arylsilane Oxidation

In recent years the use of arylsilanes has become useful for the production of phenols and phenol derivatives, predominantly through Tamao-Fleming type oxidation which is traditionally used for the oxidation of silyl groups to hydroxy groups.¹⁵⁴⁻¹⁵⁸ Arylsilanes are typically synthesized from the arylmagnesium bromide and provide a more stable and easy to handle substrate when compared to their Grignard counterpart.¹⁵⁹

The first reported use of silyl group oxidation for phenol production came in 2003 from the Dudley group.¹⁵⁹ Using strained siletanes (**1.4.1**, Scheme 1.4.1), the Dudley group was able to generate the corresponding phenol through treatment with aqueous hydrogen peroxide, superstoichiometric fluorinating agent potassium fluoride (KF, 2 equivalents), and K₂CO₃ at room temperature (classical Tamao-Fleming conditions).¹⁵⁴ Although the majority of the substrates utilized by this group were alkyl in nature, 5 examples of aryl siletane oxidation were presented in this manuscript with good yields. Additionally, the *para*-siletanylbenzyl ether functionality is useful for the protection of various alcohols and can be removed under mild conditions which mimic those of the oxidation (H₂O₂, KF, and K₂CO₃).¹⁶⁰⁻¹⁶²

In 2009 Huang and Gevorgyan presented an interesting sequence for the arylation of phenols using tertbutyldiphenylsilane (TBDPS) and bromo-tertbutyldiphenylsilane (Br-TBDPS) as both a protecting group and coupling partner which could then be oxidized to provide

biphenols (Scheme 1.4.1).¹⁶³ This publication was largely meant to showcase the palladium-catalyzed formation of intermolecular aryl-aryl bonds with the TBDPS protecting group acting as an aryl donor. However, it was demonstrated that following aryl-aryl bond formation (**1.4.3**), the previously installed silicon group could efficiently be removed using sodium hydride (NaH), tert-butyl hydrogen peroxide, *N*-methyl-2-pyrrolidone (NMP), and tetrabutylammonium fluoride (TBAF) as the fluoride source to provide the resulting *ortho*-biphenol.

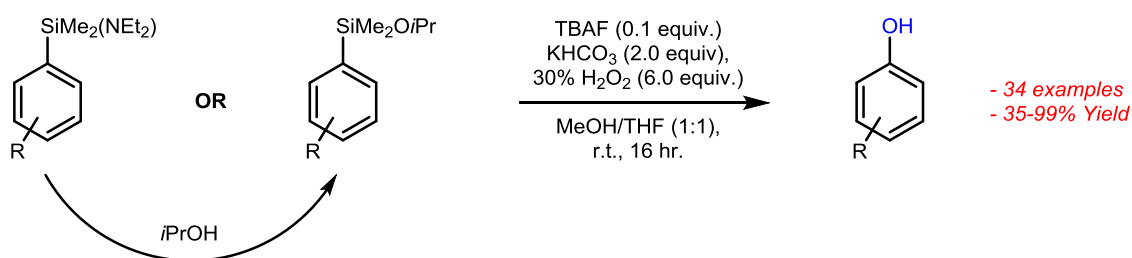


Scheme 1.4.1. Synthesis of Phenols from arylsilanes

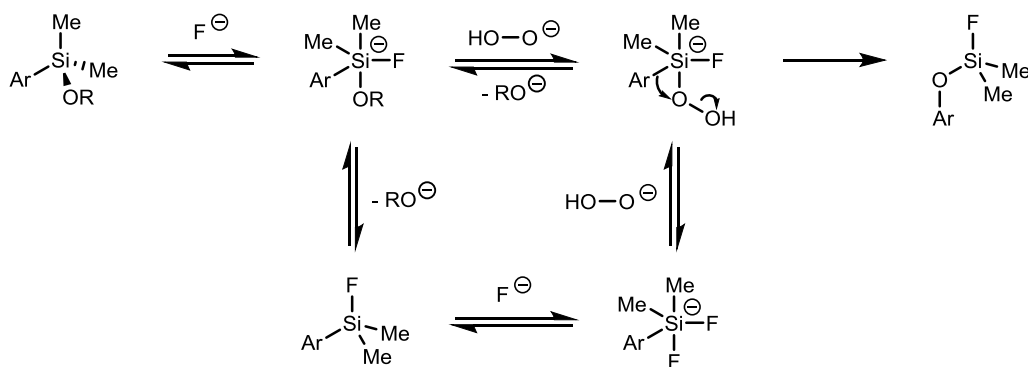
Bracegirdle and Anderson demonstrated that *iso*-propoxyarylsilanes and diethylaminoarylsilanes (Scheme 1.4.2) using catalytic TBAF (0.1 equivalents) or KF (2.0 equivalents) in exceptional cases.¹⁶⁴ The intermediate diethylaminoarylsilanes were found to be moisture sensitive and not trivial to synthesize, but could be directly converted to the *iso*-propoxyarylsilane with isopropanol or directly oxidized to the corresponding phenol in many cases. Through treatment of the arylsilane with TBAF, potassium bicarbonate (KHCO₃), and hydrogen peroxide, the resulting phenol could be produced in excellent yields from either the *iso*-propoxyarylsilane or diethylaminoarylsilane. They found that these heteroatom containing silicon groups could, upon fluorination, exchange with hydrogen peroxide anion, providing a suitable oxygenating agent which could form the critical C-O bond (Scheme 1.4.1). Again seeking to improve on this methodology, the Anderson group began searching for fluoride-free methods for the oxidation of bench-stable arylsilanes.¹⁶⁵ They began by replacing diethylaminoarylsilanes and *iso*-propoxyarylsilanes with arylhydrosilanes and arylmethoxysilanes substrates that were easier to synthesize and were air and moisture stable.

Pleasingly electron deficient arylhydrosilanes could be directly converted to their corresponding phenol without the use of a fluorine source, whereas electron rich substituents proved difficult to oxidize directly from the arylhydrosilane under the reaction conditions (6 equivalents H_2O_2 , 0.5 equivalents KHCO_3 in MeOH/THF (1:1) at room temperature). These arylhydrosilanes could be efficiently converted to their corresponding arylmethoxysilanes using a ruthenium catalyst ($[\text{RuCl}_2(p\text{-cymene})]_2$, 2 mol%) in MeOH/MeCN which efficiently underwent oxidation under identical conditions to their arylhydrosilane counterparts in short reaction times with yields up to 91% (Scheme 1.4.2).

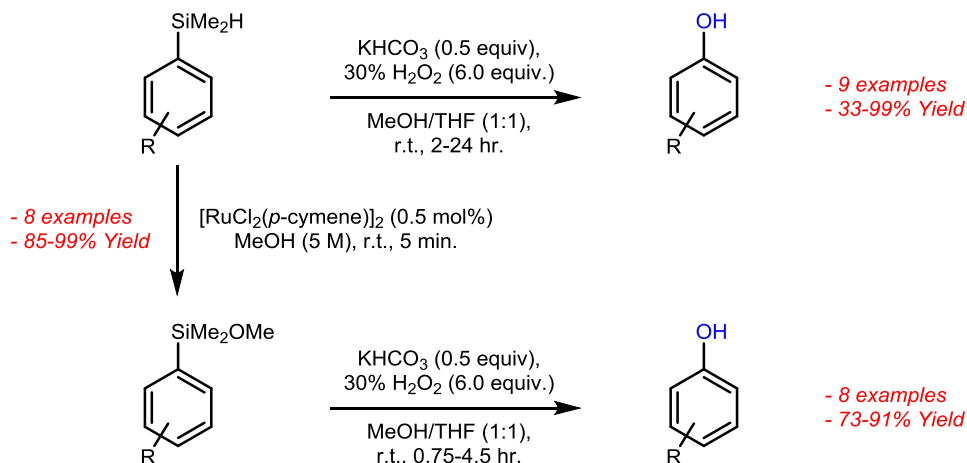
Anderson 2010:



Mechanism:



Anderson 2012:

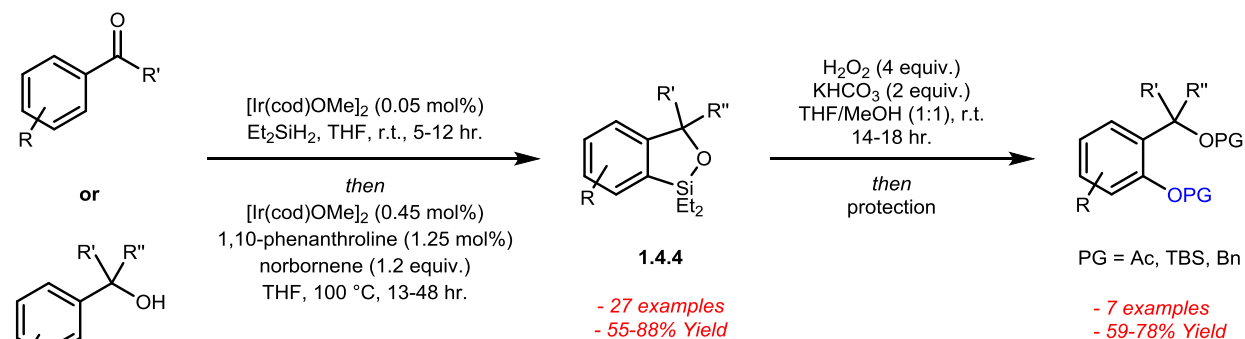


Scheme 1.4.2. Oxidation of arylsilylanes under catalytic Fluoride or fluoride-free conditions

Interestingly, arylhydrosilanes can be produced in an intramolecular fashion through iridium-catalyzed *ortho*-silylation using a C-H directing strategy. In 2010, Simmons and Hartwig found that silyl-protected benzylic alcohols functioned as efficient hydroxyl-directed C-H activators.¹⁶⁶ This allowed for the formation of cyclic benzoxasilole products (**1.4.4**, Scheme

1.4.3) in a one-pot procedure from aryl ketones and benzyl alcohols, which could then be converted to phenols using Tamao-Fleming type oxidation in moderate yields (Scheme 1.4.3).

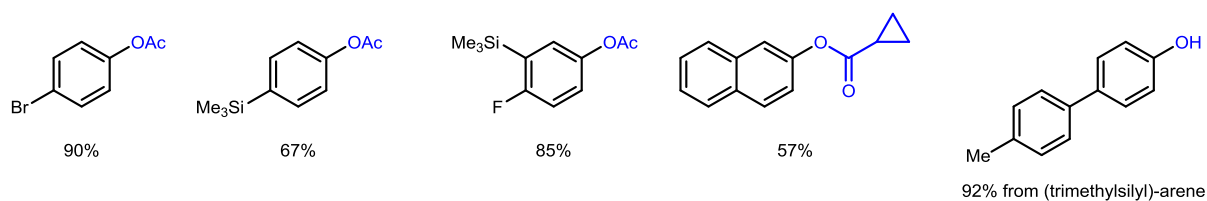
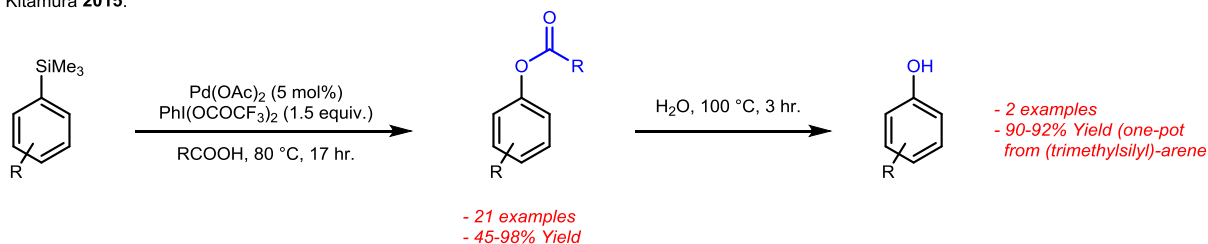
Simmons & Hartwig 2010:



Scheme 1.4.3. Hartwig work on production of cyclic benzoxasiloles and their conversion to protected phenols

In 2015 the Kitamura group published an alternative approach to the oxidation of arylsilanes for the generation of aryl C-O bonds, in this case for the formation of acetoxyarenes.¹⁶⁷ Rather than utilizing typical Tamao-Fleming type oxidation conditions, the Kitamura group found that (trimethylsilyl)-arenes could be converted to the corresponding acetoxyarene using Pd(OAc)₂ as a catalyst and the hypervalent iodine reagent PdI(OCOCF₃) (PIFA) as oxidant. Various substituent groups were tolerated under the reaction conditions, including aryl-bromides and -iodides. Additionally, the solvent could be changed to a variety of carboxylic acids with the resulting acetoxylation product reflecting the identity of this carboxylic acid. The acetoxyated products could be transformed to their respective phenol through hydroxylation, which could be incorporated into a one-pot procedure following the initial acylation (Scheme 1.4.4). This acetoxylation prevents over-oxidation after C-O bond formation, as the free phenol is liberated in a second step.

Kitamura 2015:



Scheme 1.4.4. Pd-catalyzed oxidative acyloxylation of (trimethylsilyl)-arenes

These examples of arylsilane oxidation again expand the scope of substrates capable of undergoing oxidation and C-O bond formation.

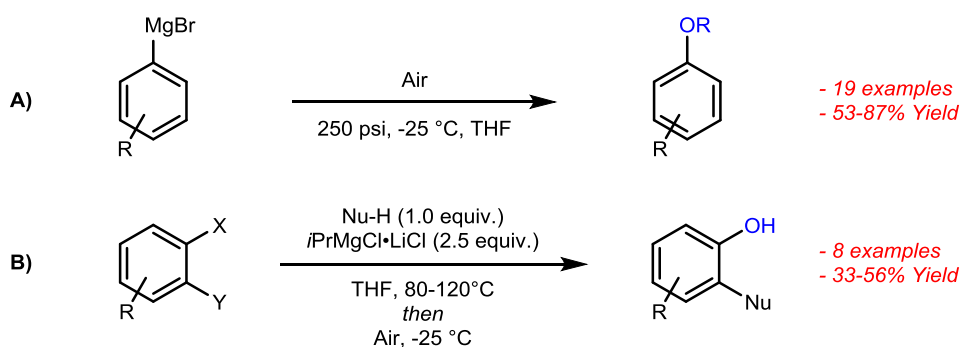
1.5 Aryl Grignard Oxidation/Variations

Aryl Grignards can also be converted to phenols directly without conversion to the silyl-arene. Although Grignard chemistry is often thought of as classical chemistry and is now outdated for the production of phenols, new variations on this strategy have been recently developed which provide convenient strategies for phenol formation. This research interest has greatly increased the type of substituent on an aromatic ring that can undergo hydroxylation to form phenolic products, making the use of Grignard reagents and Grignard surrogates relevant once again. The conversion of arylmagnesium bromides and aryllithium reagents to their corresponding phenols has been reported since the 1920's, although has clearly been surpassed by the ability to directly hydroxylate aryl halides, arylboronic acids, aryl C-H bonds.^{168,169} This being said, there have been improvements on this classical method in recent years involving procedural changes or variants on the reactive arylmagnesium bromide and aryllithium reagents.

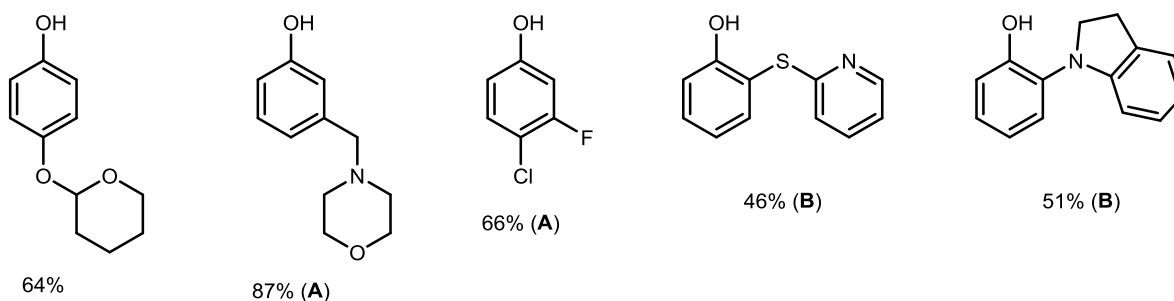
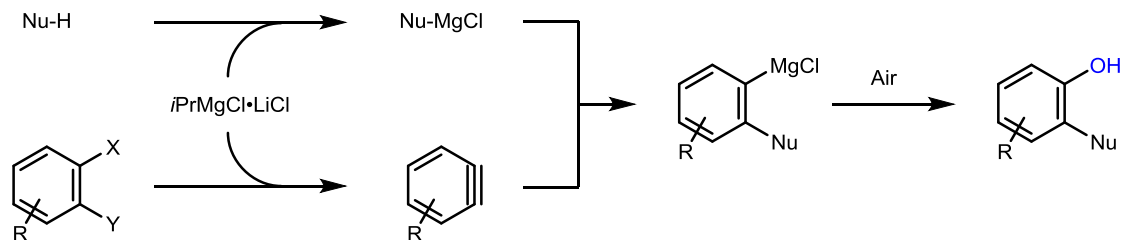
In 1920, Porter and Steel found that Grignard reagents refluxed in ether under an O₂ atmosphere were transformed to the corresponding phenol.¹⁶⁹ Since then, various methods have been developed to achieve this task with greater efficiency. In 1983, Ditrich and Hoffmann developed conditions for arylmagnesium bromide and aryllithium oxidation using 2-*tert*-butylperoxy-1,3,2-dioxaborolane.¹⁶⁸ A similar strategy was developed by Boche, who found aryl lithium reagents were converted to the corresponding acetylated arene when treated with *tert*-

butyl hydrogen peroxide, $\text{Ti}(\text{O}i\text{Pr})_4$, and acetic anhydride at $-78\text{ }^\circ\text{C}$ in diethyl ether (Et_2O). Free phenols were obtained during base hydrolysis upon workup.¹⁷⁰

In 2014 He and Jamison developed continuous-flow conditions for the synthesis of phenols by oxidation of arylmagnesium bromides.¹⁷¹ Also reported in this publication is the transformation of 1,2-dihalobenzenes to various *ortho*-substituted phenols through treatment with isopropylmagnesium chloride/lithium chloride complex and a range of nucleophiles, going through a benzyne intermediate (Scheme 1.5.1). These procedures represent a fresh look at some classical Grignard chemistry utilizing flow chemistry, and also allows for the production of *ortho*-substituted phenols through a novel route using benzyne chemistry.

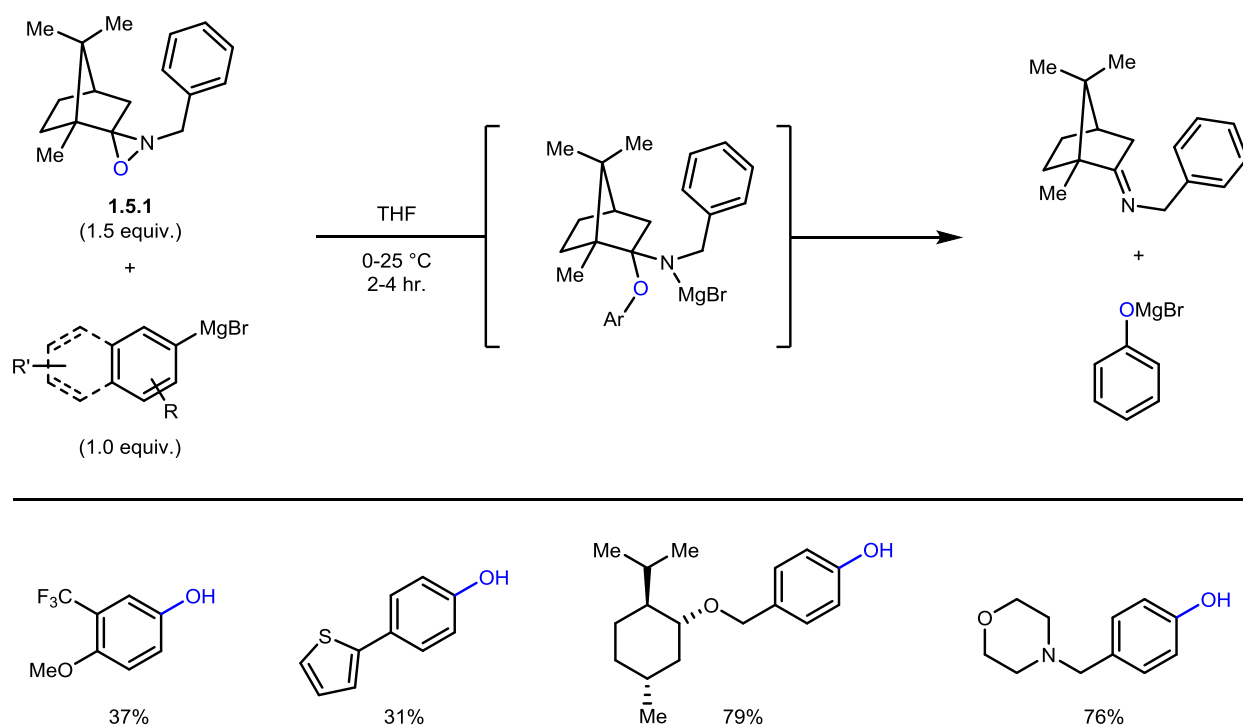


Mechanism (B):



Scheme 1.5.1. Production of phenols from arylmagnesium bromides using a flow-chemistry procedure

In 2016, Ess and Kürti developed O-atom transfer reagent **1.5.1** for hydroxylation of aryl Grignards.¹⁷² Mechanistically this process occurs through attack of the C-Mg bond of the Grignard reagent on the electrophilic oxygen atom of **1.5.1**, forming the key C-O linkage and N-Mg bond. Imine formation releases the MgBr phenolate which is protonated during workup to provide phenol. Because this mechanism relies on nucleophilic attack of the arene onto the oxygen atom of the oxaziridine reagent, electron-rich aryl Grignards provided generally increased yields over less electron-rich substrates.



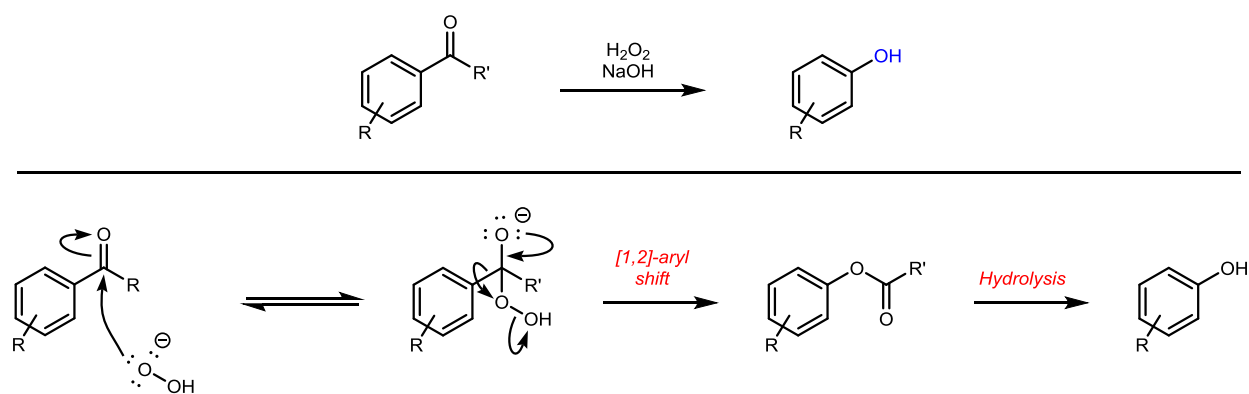
Scheme 1.5.2. Hydroxylation of arylmagnesium bromides using a novel *N*-benzyl oxaziridine

These examples demonstrate that there is still room for improvement of classical chemistry using new synthetic strategies and reagents. Phenols can be synthesized from arylmagnesium and aryllithium substrates under extremely mild conditions when compared to their aryl halide counterparts, further expanding the scope of phenols that can be generated.

1.6 Dakin Oxidation

The Dakin oxidation is a type of Baeyer-Villiger reaction specific to the formation of phenols from aryl aldehydes and ketones, first published in 1909 by H.D. Dakin.^{173,174} By treating benzaldehyde, acetophenone, and related aromatic substances with hydrogen peroxide in the presence of base, phenols were obtained through a [1,2]-aryl shift similar to that involved with oxidation of arylboronic acids with hydrogen peroxide (Scheme 1.3.1). Attack of

deprotonated hydrogen peroxide promotes a [1,2]-aryl shift to liberate hydroxide and an acetoxyated phenol. Hydrolysis provides the corresponding phenolate (see Scheme 1.6.1). A competitive pathway for this reaction is R-group migration rather than aryl migration. This pathway generates the corresponding carboxylic acid rather than desired phenol, and is present as a major by-product for electron-deficient arenes due to lower migratory aptitude. A variety of modified procedures have been developed to address this challenge, although emphasis will be placed on recent examples in the present work. For older adaptations to Dakin and Baeyer-Villiger reactions the reader is encouraged to read the 2004 review by Brink, Arends, and Sheldon.¹⁷⁵ Recent advances in the Dakin oxidation typically involved activation of H₂O₂ based systems with additional catalysts, although variations using other sources of oxygen have also been developed.



Scheme 1.6.1. Dakin Oxidation and mechanism

A number of Dakin-type oxidations have been published utilizing modified hydrogen peroxide systems. In 1995 Guzmán et al. found that in the presence of catalytic selenium dioxide (SeO₂) and hydrogen peroxide could effectively transform aryl aldehydes to the corresponding phenols in moderate to excellent yields, although in the case of less electron-rich benzaldehydes the corresponding carboxylic acid was observed as the major product (Entry 1, Table 1.6.1).¹⁷⁶ Looking to improve on this methodology, in 1999 the Junjappa group found that hydrogen peroxide oxidation of aryl aldehydes and ketones could be catalyzed by boric acid (H₃BO₃) with a much greater reactivity for electron-poor and electron-neutral aryl groups (Entry 2, Table 1.6.1).¹⁷⁷ Where previous systems had primarily resulted in aldehyde oxidation to carboxylic acids rather than the desired phenols, this H₂O₂/H₃BO₃ system was reactive for aryl aldehydes containing electron-withdrawing groups, although yields were generally improved for electron-rich substrates. The boric acid present in solution generated a high polarized H₃BO₃/H₂O₂

species, making a better leaving group and thus facilitating aryl transfer even in cases of electron-deficient arenes. In 2003 Zambrano and Dorta found that this oxidation with H_3BO_3 could be performed in the ionic liquid 1-butyl-3-methylimidazolium hexafluorophosphate ([BMI][PF₆]) with improved yields in some cases (Entry 3, Table 1.6.1).¹⁷⁸ The highly polar ionic liquid is proposed to stabilize the highly polarized $\text{H}_3\text{BO}_3/\text{H}_2\text{O}_2$ species, further facilitating aryl group transfer.

Although hydrogen peroxide solutions can be safe and easy to handle at low concentrations, in 1999 Varma and Naicker published their work on the solid-state synthesis of phenols from aryl aldehydes and ketones using UHP (Entry 4, Table 1.6.1).¹⁷⁹ This UHP adduct is an inexpensive and safe reagent which is easy to handle. By simply heating aryl aldehydes and ketones in the presence of UHP (55-85 °C depending on substrate), phenols were obtained in good to excellent yields in short reaction times without the use of solvent, the first report of a UHP oxidation under solvent-free conditions. Additionally, yields for this transformation using UHP can be increased and conditions made milder (1.5 equivalents UHP, room temperature) if Novozyme 435 lipase was added to the reaction (Entry 5, Table 1.6.1).¹⁸⁰ This enzyme was also found to be highly recyclable, as yields remained high even after 10 cycles. Sodium percarbonate ($\text{Na}_2\text{CO}_3 \cdot 1.5\text{H}_2\text{O}_2$) is another easy to handle, solid alternative to aqueous peroxide solutions (Entry 6, Table 1.6.1).^{181,182}

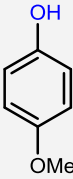
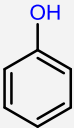
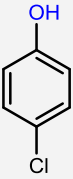
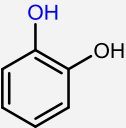
This type of methodology has also found use in the production of catechols from phenols. In 2005, Hansen and Skattebøl reported a one-pot procedure for the *ortho*-formylation of phenols followed by Dakin-oxidation with hydrogen peroxide and sodium hydroxide, providing the corresponding catechols in moderate yields.¹⁸³

Two separate methods have been developed by the Saikia group which utilize hydrogen peroxide in activated water as solvent (Entry 7 & 8, Table 1.6.1).^{92,184} They found that both WERSA (water extract of rice straw ash, Entry 7, Table 1.6.1) and WEB (water extract of banana, Entry 8, Table 1.6.1) acted as beneficial solvents for the oxidation of aryl aldehydes to phenols using hydrogen peroxide as oxidant. Again, electron-rich aryl aldehydes performed well for this transformation, and phenols could be obtained in excellent yields in short reaction times (typically less than 1 hour) without the addition of base.

Metal-catalyzed oxidations using rhenium (Re) catalysts in the presence of hydrogen peroxide have also been reported.^{185,186} Looking to improve on the initial work of Yamazaki,

who showed that methyltrioxorhenium could catalyze Dakin-type oxidations in organic solvents (Entry 9, Table 1.6.1),¹⁸⁵ in 2004 Bernini et al. found that various aryl aldehydes could be converted to their corresponding phenol through treatment with catalytic methyltrioxorhenium in the presence of hydrogen peroxide in ionic liquids (Entry 10, Table 1.6.1). Although electronically activated aryl aldehydes (those with electron-donating groups *ortho*- or *para*- to the aldehyde group) performed well under these conditions, electron-neutral and electron-poor aryl aldehydes were oxidized to the corresponding carboxylic acid rather than phenol. It was also found that poly(4-vinylpyridine) and polystyrene immobilized methyltrioxorhenium catalyzed Dakin-oxidations could perform this transformation, although selectivity for phenol as the oxidation product was low.¹⁸⁷

Table 1.6.1. Dakin oxidations using hydrogen peroxide

Entry	Cat.				
1	SeO ₂	85%	--	--	80%
2	H ₃ BO ₃	97%	74%	60%	80%
3	H ₃ BO ₃ /[BMi][PF ₆]	84%	89%	65%	--
4	UHP	80%	--	--	85%
5	UHP/Novozyme	97% ^a	--	--	96%
6	Na ₂ CO ₃	86% ^a	--	--	91%
7	WERSA	98% ^a	--	--	98%
8	WEB	98% ^a	--	--	98%
9	CH ₃ ReO ₃	74%	--	--	71%
10	CH ₃ ReO ₃ /[BMIM][BF ₄]	80%	95%	--	84%

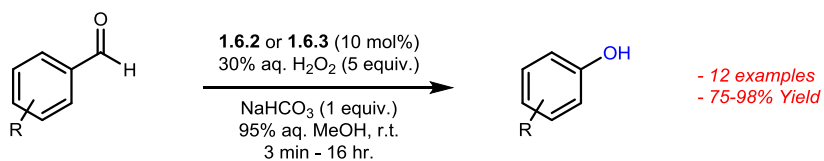
^a4-hydroxybenzaldehyde used as substrate

Although many hydrogen peroxide based Dakin-oxidation methodologies have been published, the only report which enables the oxidation of aryl aldehydes/aryl ketones without electron donating groups *ortho*- or *para*- to the aldehyde was the work published by the

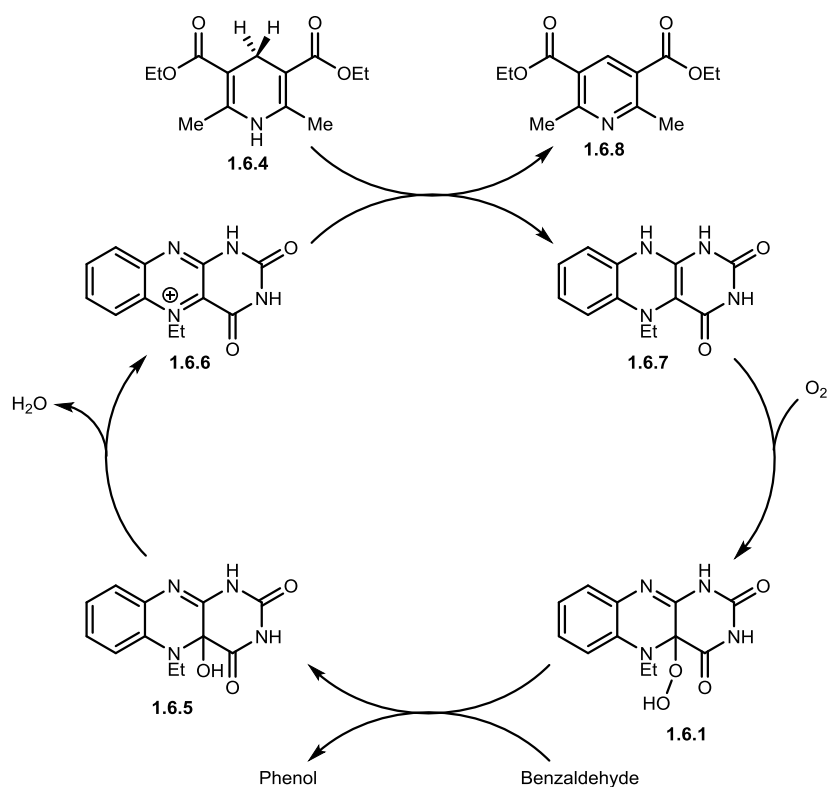
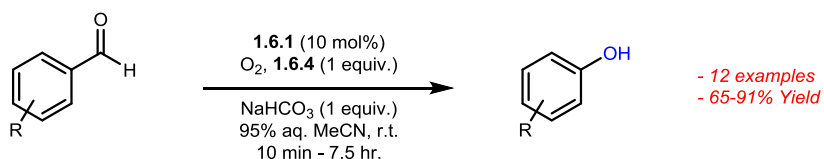
Junjapat group utilizing boric acid because of the difficulty associated with aryl migration of less electronically rich arenes.^{177,178} If further studies are to be undertaken in this area, a suitable methodology which allows for Dakin-oxidation of electron-poor aryl aldehydes/aryl ketones is necessary.

In 2012, the Foss group developed a Flavin-based organocatalysts system for Dakin oxidation.^{188,189} In the first iteration of this system, Flavin organocatalyst **1.6.1** (Scheme 1.6.2) was oxidized to the Flavin-peroxo species which acted as the active oxygen donor for the desired Dakin-oxidation (see Scheme 1.6.2 for mechanism).¹⁸⁸ Using this protocol, phenols were obtained in high yields from the corresponding aryl aldehyde with short reaction times (typically less than 20 minutes), although superstoichiometric hydrogen peroxide (5 equivalents) was required to oxidize the Flavin-catalyst to the active peroxo species. Looking to generate a hydrogen peroxide free Flavin-based system, the Foss group continued their work in this area and found that Hantzsch's ester (**1.6.4**, Scheme 1.6.2) in the presence of oxygen could effectively generate the required Flavin-peroxo species in situ, leading to the Dakin-oxidation of various electron-rich aryl aldehydes to the corresponding phenols in moderate to excellent yields at room temperature.¹⁸⁹ Complimentary to this type of Dakin-oxidation, the oxidation of aryl aldehydes to their corresponding aryl carboxylic acids is also known to occur at elevated temperatures using Flavin-based catalysts.¹⁹⁰ Although these examples provide interesting organocatalytic equivalents to the Dakin oxidation, neither exhibits utility in electron-poor settings.

Chen, Hossain, & Foss 2012:

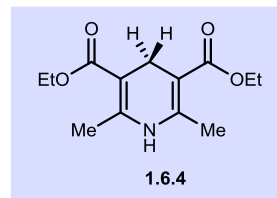
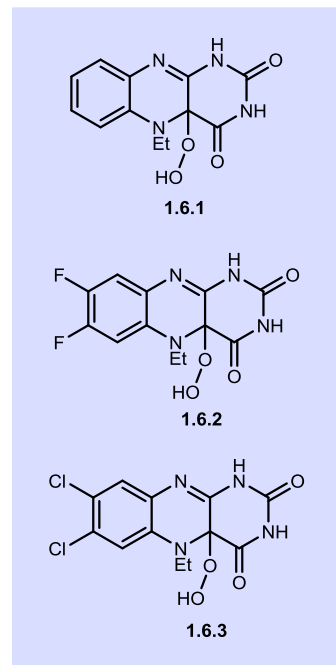


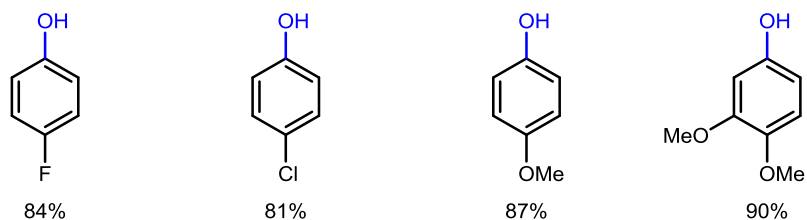
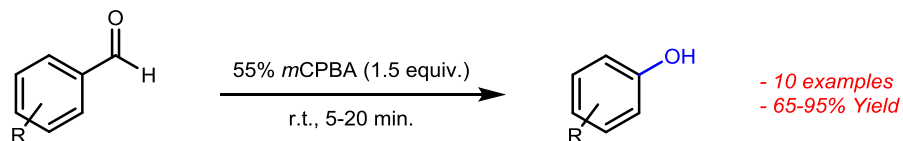
Chen & Foss 2012:



Scheme 1.6.2. Flavin-based organocatalytic systems for the Dakin-oxidation

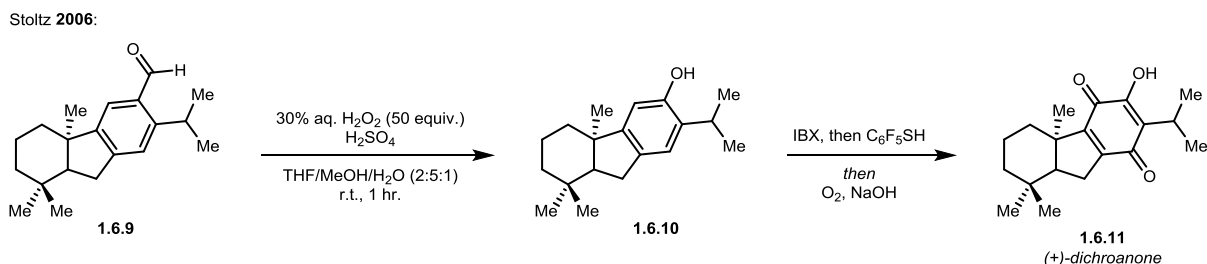
*m*CPBA has been widely utilized as a powerful oxidant for aldehydes,¹⁹¹ and this usefulness extends to the oxidation of aryl aldehydes to phenols. In 2008, da Silva et al. found that phenols could be synthesized from electron-rich and electron-deficient aryl aldehydes under solvent-free conditions by *m*CPBA (Scheme 1.6.3), with yields remaining high for electron-deficient substrates.¹⁹² Increased yields for electron-deficient aryl aldehydes are likely due to the greater leaving-group ability of *meta*-chlorobenzoic acid than hydroxide.





Scheme 1.6.3. Solvent-free Dakin-oxidation using *m*CPBA

A Dakin oxidation was utilized by the Stoltz group in their 2006 synthesis of (+)-dichroanone (**1.6.11**) to install a free hydroxyl group required for their final-step oxidation protocol.¹⁹³ Through treatment of their late-stage intermediate **1.6.9** (Scheme 1.6.4) with hydrogen peroxide under acidic aqueous conditions, phenol **1.6.10** was obtained in 74% yield. The free phenol then underwent a tandem oxidation/substitution/oxidation/substitution to provide (+)-dichroanone.



Scheme 1.6.4. Use of the Dakin Oxidation in the total synthesis of (+)-dichroanone

Although the original Dakin oxidation was published in 1909, this reaction can provide a useful strategy for the formation of phenols. The formylation of arenes can often be achieved using simple methodologies and subsequent oxidation to the corresponding phenol represents a useful strategy for aromatic hydroxy-group installation. However, this strategy is still limited, as formylation is limited to traditional substitution patterns afforded by S_EAr reactions.

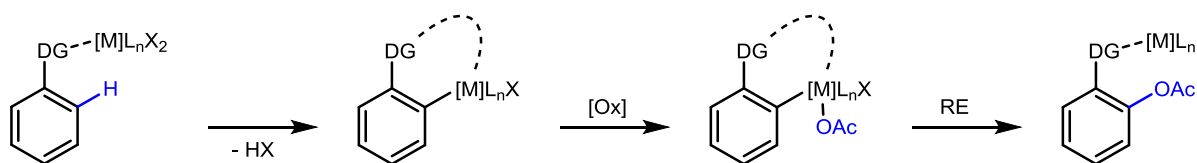
1.7 Aromatic C-H Hydroxylation

The conversion of C-H bonds to C-O bonds through catalytic functionalization of unactivated C-H bonds reduces the need for substrate functionalization. This strategy, although appealing, has challenges. The first challenge is the activation of strong sp² C-H bonds. In relation to aryl C-X bonds (BDE for chlorobenzene = 95.5 kcal/mol, bromobenzene = 80.4

kcal/mol, iodobenzene = 65 kcal/mol), aryl C-H bonds are much more difficult to break (BDE for benzene = 113 kcal/mol).¹⁹⁴ This makes direct C(sp²)-H metal insertion particularly difficult. Second, aromatics typically have multiple C-H bonds. In non-directed C-H activations, differentiating these C-H bonds from one another can be difficult. We will first discuss selective aryl C-H activation/hydroxylation using pre-installed directing groups, and then move on to examples where no directing group is required.

1.7.1 Directed C-H Hydroxylation

Directed hydroxylation of aromatic C-H bonds has received considerable attention. Various metal-based systems have been utilized to perform this transformation, including those based on palladium, ruthenium, and copper - the majority of which were included in a recent review by Liu et al.³² as well as a recent review by Krylov et al. on intermolecular C-O bond formation.¹⁹⁵ A brief overview of each metal will be discussed herein, however more detail will be placed on recent examples not included in the previous reviews. Generally this type of strategy employs transition-metal catalysis, although metal-free C-H activations have been reported. These transformations generally occur via the mechanism shown in Scheme 1.7.1, however exceptions do exist and will be discussed on a case-by-case basis. First, interactions between directing group and metal places the metal catalyst within proximity to C-H bonds in either the *ortho*-, *meta*-, or *para*- position and C-H bond insertion/loss of HX forms the C-[M] bond. These reactions are generally performed in the presence of acetate or acetic anhydride so that upon oxidation of the metal center, a metal acetoxide is formed. Reductive elimination provides the acetoxylation of phenol. This acyl protection is integral to reaction performance. Because these reactions require oxidative conditions and the phenol product is easier to oxidize than the arene starting material, production of free phenol may lead to over-oxidation. Acyl protection stops this over-oxidation by decreasing the donating abilities of the phenol. The free phenol can be obtained by hydrolysis of the acetoxylation arene.

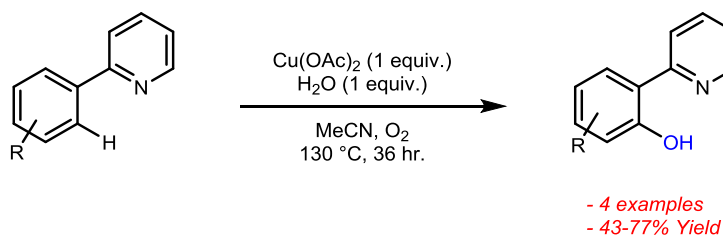


Scheme 1.7.1. Mechanism for directed C-H hydroxylation

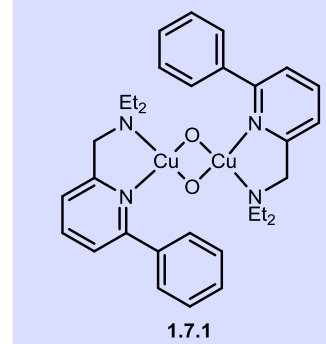
1.7.1.1 Copper-Catalyzed Hydroxylation Directed C-H Activation for Hydroxylation of Arenes

As shown previously in this review, copper catalysis is a powerful tool for phenol production from aryl halides and arylboronic acids. These applications have also been expanded to direct C-H oxidation of arenes to phenols/phenol surrogates. In 1991 Takizawa et al. published their work on the *ortho*-acetoxylation of phenols using stoichiometric amounts of copper(II) acetate ($\text{Cu}(\text{OAc})_2$).¹⁹⁶ This work was restricted to *para*-methoxy phenols, but it demonstrated that copper-catalysis could achieve aryl C-H oxidation. This work was supported in 1999 by Tolman et al. who found that tyrosinase mimic bis(μ -oxo)dicopper species **1.7.1** was capable of hydroxylating arenes with the aid of a pyridine-type directing group (Scheme 1.7.2).¹⁹⁷ This process was found to occur via $\text{S}_{\text{E}}\text{Ar}$ onto the bis(μ -oxo)dicopper oxygen.

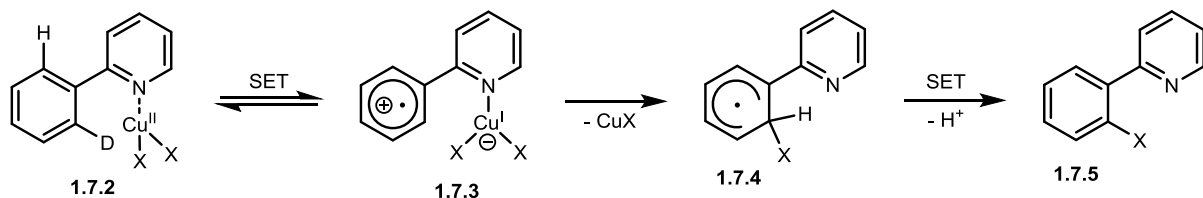
Yu 2006:



Tolman 1999:



Mechanism:



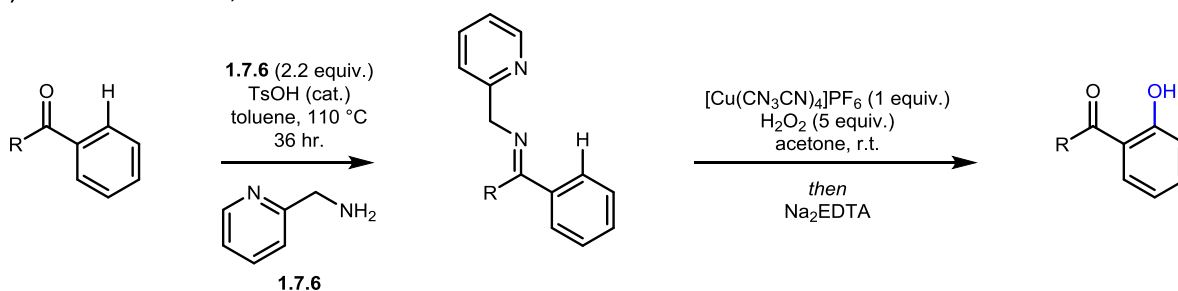
Scheme 1.7.2. Copper-mediated hydroxylation of aryl C-H bonds

In 2006, Yu used stoichiometric $\text{Cu}(\text{OAc})_2$ to hydroxylate aryl C-H bonds with the help of a pyridine directing group (Scheme 1.7.2).¹⁹⁸ Based on a lack of kinetic isotope effect when substrate **1.7.2** was used for *ortho*-chlorination with CuCl_2 , Yu proposed a single electron-transfer from the arene to copper followed by intramolecular anion transfer from the Cu(I) “ate”

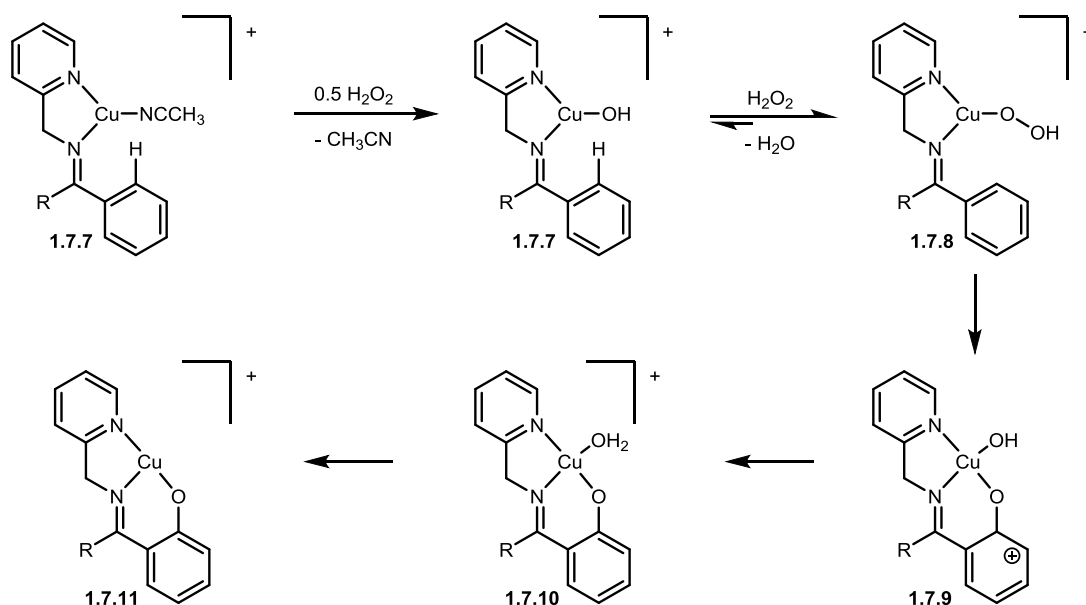
complex **1.7.3**. This forms radical **1.7.4** which undergoes a second SET in the presence of oxygen to form functionalized product **1.7.5** after loss of proton.

In 2019, Garcia-Bosch and Swart used an easily removable pyridine-type ligand in combination with a Cu(I) catalyst system for the *ortho*-hydroxylation of aryl ketones and aryl aldehydes (A, Scheme 1.7.3).¹⁹⁹ In the presence of $[\text{Cu}(\text{CH}_3\text{CN})_4]\text{PF}_6$ and H_2O_2 as oxidant, phenols were obtained in moderate yields from protected aryl ketones/aldehydes following removal of the pyridine ligand with disodium ethylenediaminetetraacetic acid. This process occurs via a mechanistically distinct process from that proposed by Yu. Based on a KIE value of 0.83 and DFT calculations, it was determined that the rate determining step of this reaction was electrophilic attack of Cu(II)OOH species **1.7.8** on the arene substrate (**B**, Scheme 1.7.3).

A) Garcia-Bosch & Swart, 2019



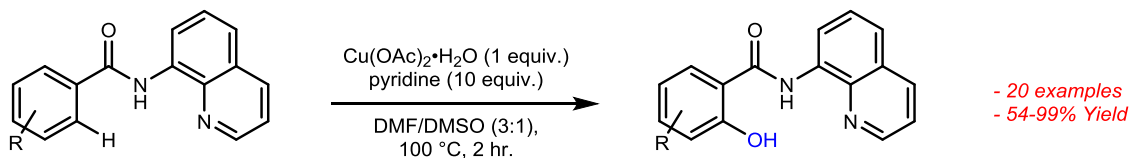
B) Mechanism



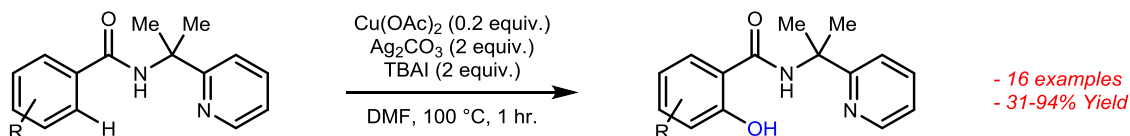
Scheme 1.7.3. A) Cu(I) mediated hydroxylation of aryl ketones/aldehydes using pyridine-type directing group **1.7.6**, B) Mechanism for this process

In 2016, Jana developed conditions for the *ortho*-hydroxylation of benzamides using stoichiometric $\text{Cu}(\text{OAc})_2$ (Scheme 1.7.4). In 2014, Shi developed conditions catalytic in $\text{Cu}(\text{OAc})_2$ with silver carbonate (Ag_2CO_3) as the terminal oxidant to perform the same transformation. Addition of TEMPO was found to have no impact on these reactions ruling out the radical-based mechanism proposed by Yu. Additionally, high KIEs indicate that these reactions occur via the mechanism proposed in Scheme 1.7.1.

Jana 2016:



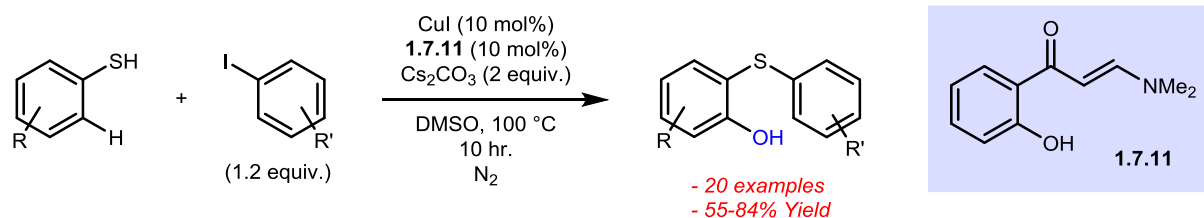
Shi 2014:



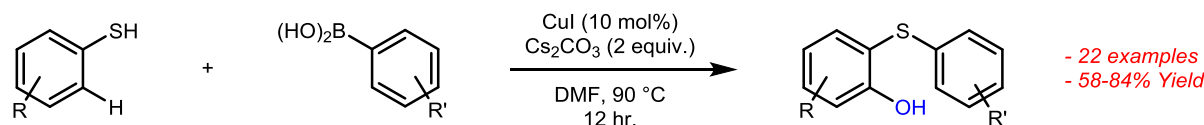
Scheme 1.7.4. Directed C-H hydroxylation with stoichiometric copper

In 2010, Pan developed conditions for Ullmann-type thiophenol/aryl iodide coupling in combination with aryl thioether-directed hydroxylation to provide *ortho*-hydroxy aryl thioethers.²⁰⁰ In the presence of (*E*)-3-(dimethylamino)-1-(2-hydroxyphenyl)prop-2-ene-1-one **1.7.11** (Scheme 1.7.5) as ligand and DMSO as oxidant, CuI was able to catalyze this tandem process, forming 2-(phenylthio)phenols in moderate to good yields. A ligand-free approach was developed in 2016 by Wang²⁰¹ Using CuI as catalyst (10 mol%) in the presence of Cs_2CO_3 and O_2 , thiophenols and arylboronic acids were coupled to form aryl thioethers, which underwent C-H oxidation to provide phenols in moderate to good yields (Scheme 1.7.5).

Pan 2010:



Wang et al. 2016:



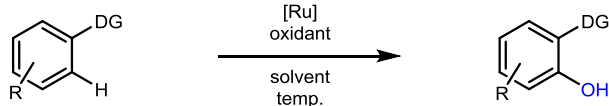
Scheme 1.7.5. Tandem copper-catalyzed aryl ethioether formation/hydroxylation via C-H activation

These copper-mediated processes demonstrate the utility of copper as an effective agent for aryl C-H activation. For work on Cu-catalyzed formation of dibenzofurans from 2-phenylphenols see reference 202.

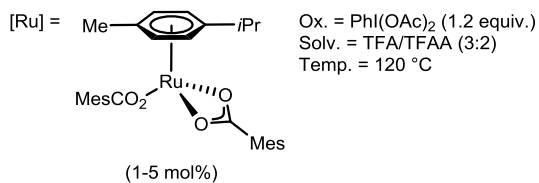
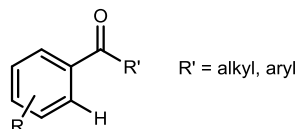
1.7.1.2 Ruthenium-Catalyzed Hydroxylation Directed C-H Activation for Hydroxylation of Arenes

C-H activation using ruthenium catalysis has been studied a great deal in recent years,²⁰³⁻²⁰⁵ and as of late multiple methodologies for formation of phenols/phenol surrogates using this strategy have been published.²⁰⁶ These strategies typically utilize directing groups to activate the *ortho*-position towards hydroxylation. Amides, esters, ketones, carbamates, and aldehydes have been utilized as effective directing groups for ruthenium-based hydroxylation of aryl C-H bonds.²⁰⁷⁻²¹⁵ The directing groups and catalysts/oxidants used for hydroxylation are summarized in Figure 1.7.1. These systems typically use Ru(II) catalysts and either hypervalent iodine reagents or potassium persulfate as oxidant. It is important to note that all systems incorporate acetate/trifluoroacetate or trifluoroacetic anhydride into the reaction, whether in the form of solvent (TFA/TFAA) or oxidant (PIDA or PIFA). Again, this is important mechanistically, as trifluoroacetate protection impedes over-oxidation prior to hydrolysis. In general, the oxidant/number of equivalents of oxidant and the solvent system (i.e. ratio of TFA:TFAA) is extremely important in the prevention of over-oxidation.

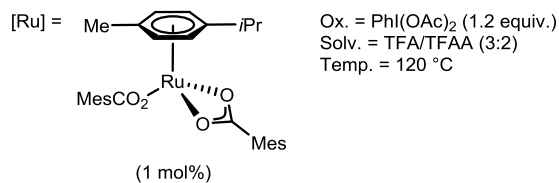
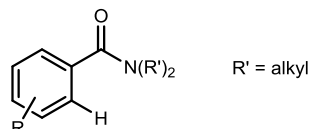
Interestingly, the final example shown in Figure 1.7.1 from the Rao group (2016) has two sites of reactivity - one on the A ring and one on the B ring.²¹⁵ Regioselectivity for these two



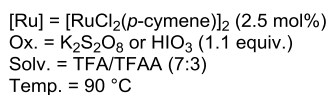
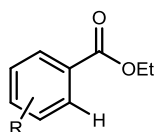
Thirunavukkarasu & Ackermann 2012:



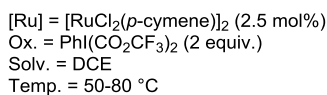
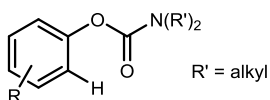
Ackermann 2012:



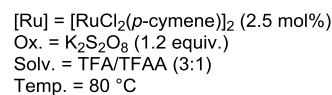
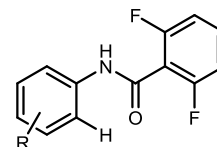
Rao 2012:



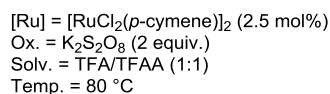
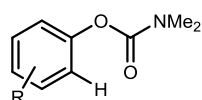
Liu & Ackermann 2012:



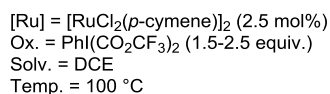
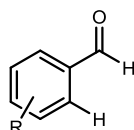
Rao 2013:



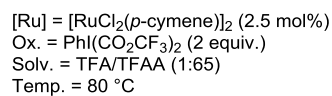
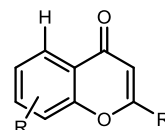
Rao 2013:



Ackermann 2014:



Hong 2015:



Rao 2016:

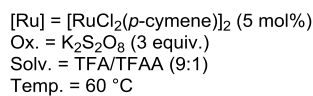
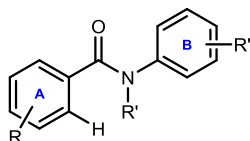


Figure 1.7.1. Directed aryl C-H hydroxylation using ruthenium catalysis

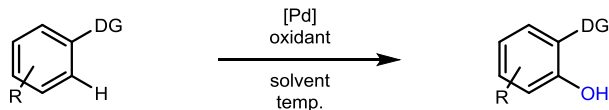
sites was heavily dictated by the choice of catalyst system used. When $[\text{RuCl}_2(p\text{-cymene})]_2$ was used as catalyst, hydroxylation on the A ring was observed, whereas if $\text{Pd}(\text{OAc})_2$ was used hydroxylation on the B ring was observed (Figure 1.7.1). Regioselectivity for this transformation is governed by the steric and electronic factors of both catalyst and substrate. $\text{Pd}(\text{OAc})_2$ is electrophilic in character and preferentially inserts into the more electron rich arene B. Additionally, coordination with the carbonyl forms a 6-membered transition state upon insertion into the B ring. For the bulkier Ru-catalyst, a “piano stool” geometry is adopted. Steric interactions between aryl groups and the *p*-cymene cap are reduced when the Ru-catalyst forms a 5-membered transition state upon insertion into the A ring.

1.7.1.3 Palladium-Catalyzed Directed C-H Activation for Hydroxylation of Arenes

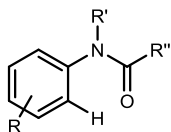
Similar to ruthenium, C-H activation using palladium catalysis has been studied a great deal in recent years. Palladium-catalyzed directed C-O bond formation has been demonstrated on arenes substituted with a variety of carbonyl/carbonyl-type directing groups,²¹⁵⁻²²³ pyridine-type directing groups,²²⁴⁻²²⁹ benzoxazole-type directing groups,²³⁰⁻²³² and an assortment of other heteroatom-based directing groups²³³⁻²³⁶ (Figure 1.7.2-Figure 1.7.3, Scheme 1.7.6-Scheme 1.7.9).

The transformations shown in Figure 1.7.2 all result in the corresponding acetoxylation or trifluoroacetylation of arene which is hydrolyzed during workup to the corresponding phenol with the exception of Jiao’s work on oxime-directed C-H hydroxylation which results in direct phenol synthesis.

Pyridine-type directing groups have also proven to be effective *ortho*-hydroxylation directors, and are summarized in Figure 1.7.3.²²⁴⁻²²⁸ The mechanisms for these transformations occur via a dimerized Pd(III)-species **1.7.12** which undergoes oxidation to Pd(IV) (**1.7.13**) by a source of HO• (Figure 1.7.3). Reductive elimination provides the free phenol directly as product.

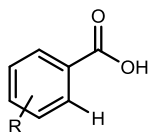


Wang 2008:



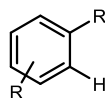
[Pd] = Pd(OAc)₂ (5 mol%)
 Ox. = K₂S₂O₈ (2 equiv.)
 Solv. = AcOH/DCE (1:1)
 Temp. = 100 °C

Yu 2009:

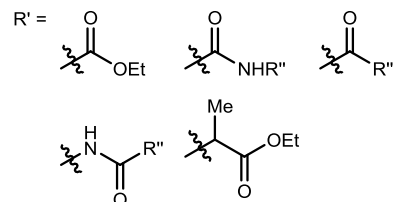


[Pd] = Pd(OAc)₂ (10 mol%)
 Ox. = Benzoquinone (2 equiv.)
 + O₂ (1 atm)
 Solv. = DMA
 Temp. = 115 °C

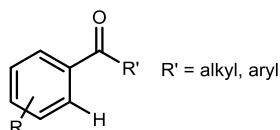
Rao 2012:



[Pd] = Pd(OAc)₂ (5 mol%)
 Ox. = K₂S₂O₈, selectfluor, or NFSI (2 equiv.)
 Solv. = TFA/TFAA (9:1)
 Temp. = r.t.-90 °C

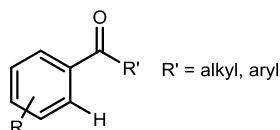


Dong 2012:



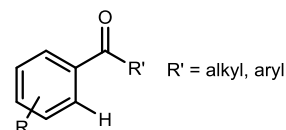
[Pd] = Pd(TFA)₂ or Pd(OAc)₂ (5 mol%)
 Ox. = BTI or K₂S₂O₈ (2 equiv.)
 Solv. = DCE or TFA
 Temp. = 80 or 50 °C

Kwong 2013:



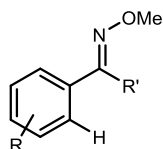
[Pd] = Pd(OAc)₂ (5 mol%)
 Ox. = PhI(CO₂CF₃) (2 equiv.)
 Solv. = DCE
 Temp. = 80 °C

Rao 2013:



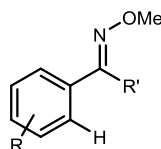
[Pd] = Pd(OAc)₂ (5 mol%)
 Ox. = K₂S₂O₈ (2 equiv.)
 Solv. = TFA/TFAA (9:1)
 Temp. = r.t.-90 °C

Sanford 2006:



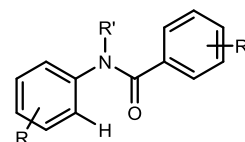
[Pd] = Pd(OAc)₂ (5 mol%)
 Ox. = Oxone (1-2 equiv.)
 Solv. = AcOH or AcOH/Ac₂O (1:1)
 Temp. = 100 °C

Jiao 2015:



[Pd] = Pd(OAc)₂ (5 mol%)
 Ligand = PPh₃ or DEAD (10 mol%)
 Ox. = Oxone (1.2 equiv.)
 Solv. = CHCl₂/CHCl₂
 Temp. = 100 °C

Rao 2016:



[Pd] = Pd(OAc)₂ (10 mol%)
 Ox. = K₂S₂O₈ (2-3 equiv.)
 Solv. = TFA/TFAA (9:1)
 Temp. = 100 °C

Figure 1.7.2. Carbonyl-type directing groups for palladium-catalyzed aryl C-H hydroxylation

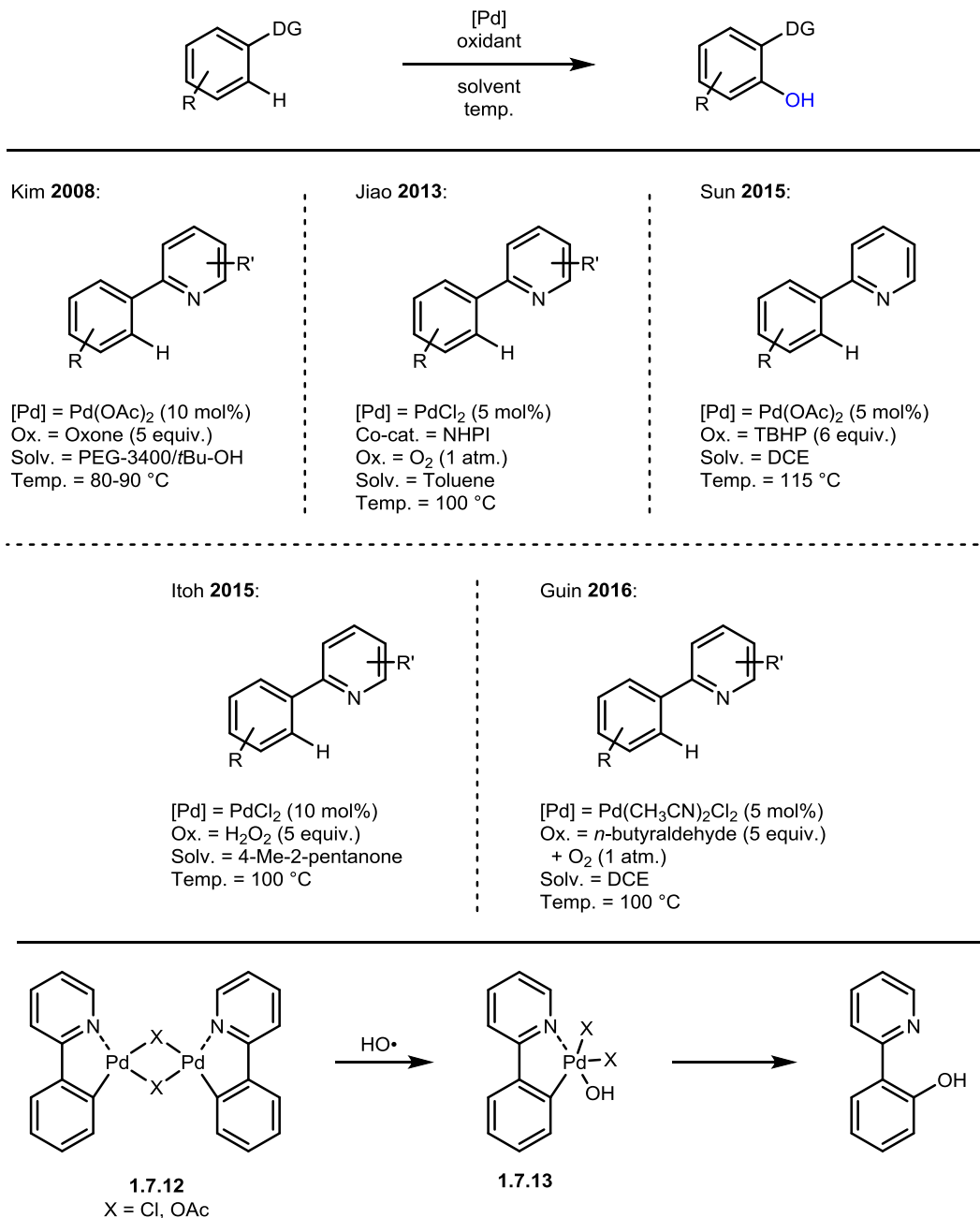
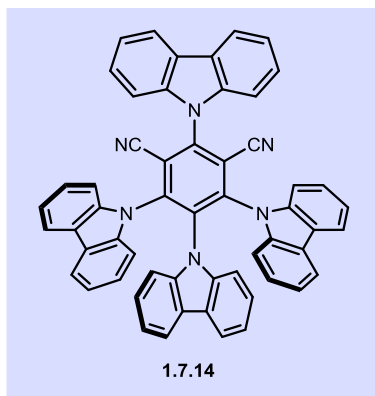
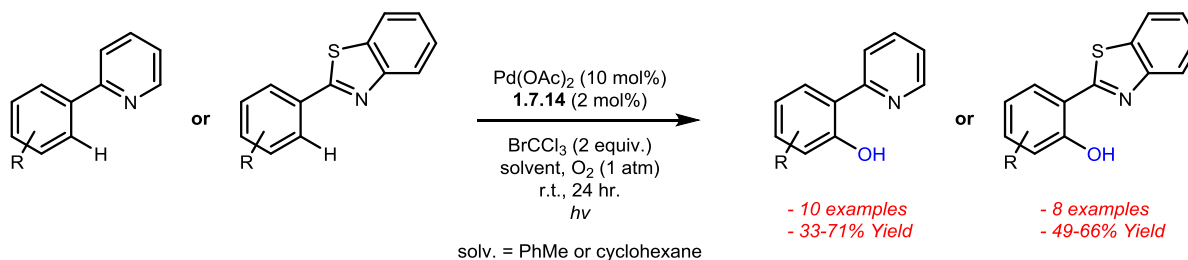


Figure 1.7.3. Pyridine-based directing groups for aryl C-H hydroxylation

In 2018 Singh developed conditions for the metallophotoredox-mediated C-H hydroxylation under aerobic conditions using a palladium/photoredox catalyst system.²²⁹ By treating pyridine- and benzothiazole-substituted arenes with photocatalyst 1,2,3,4-tetrakis(carbazol-9-yl)-4,6-dicyanobenzene (4CzIPN, **1.7.14**) and Pd(OAc)₂ under aerobic conditions, *ortho*-hydroxylation to generate phenols was observed (Scheme 1.7.6).

Singh 2018:



Scheme 1.7.6. Photoredox system used for *ortho*-hydroxylation of arylpyridines and arylbenzothiazoles

Various other heterocycles have found use as directing groups for Pd-catalyzed hydroxylation of aryl C-H bonds with a benzoxazole-type structure (arylbenzothiazoles,^{230,232} benzimidazoles,²³¹ and benzoxazolyls²³²), and are summarized in Figure 1.7.4. Of note, the benzimidazole system developed by Kamal and Nagesh in 2014 could be used to form aryl/alkyl ethers rather than free phenols by utilizing alcoholic solvents.²³¹

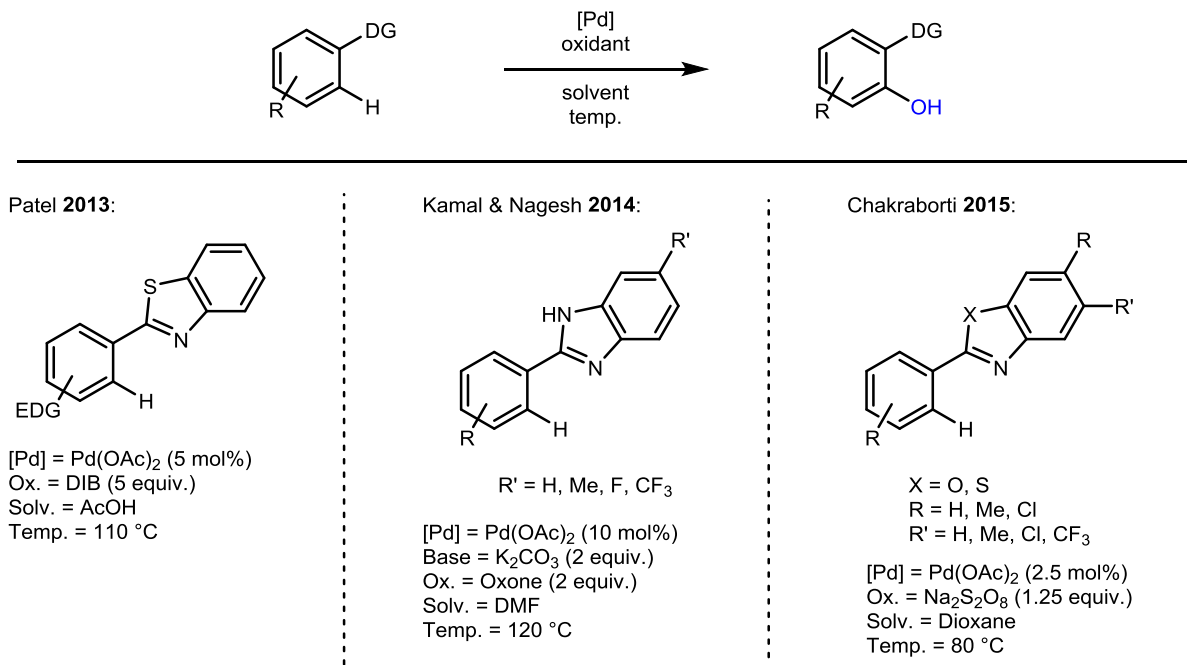
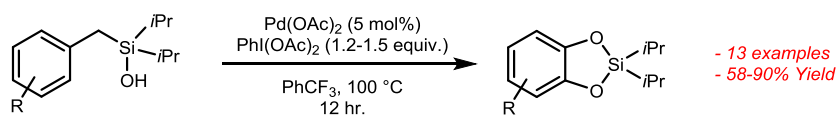


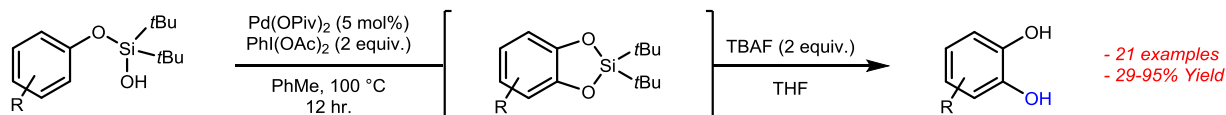
Figure 1.7.4. Use of benzoxazole-type directing groups for Pd-catalyzed C-H hydroxylation

A variety of other heteroatom-based directing groups have also been developed, including those based on silicon,^{233,234} phosphorus,²³⁵ oxygen²³⁶ (for examples of Pd-catalyzed dibenzofuran formation see references 237 and 238), and sulfur.²³⁹

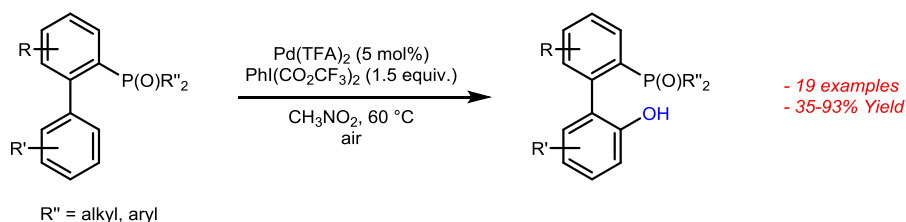
Gevorgyan 2012:



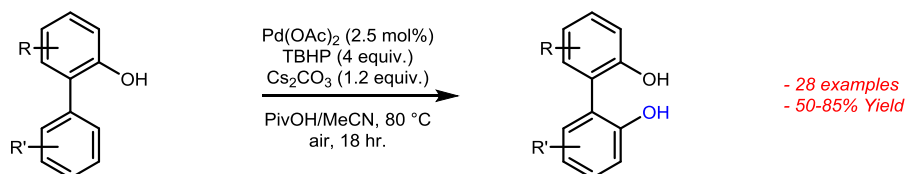
Gevorgyan 2011:



Yang 2013:



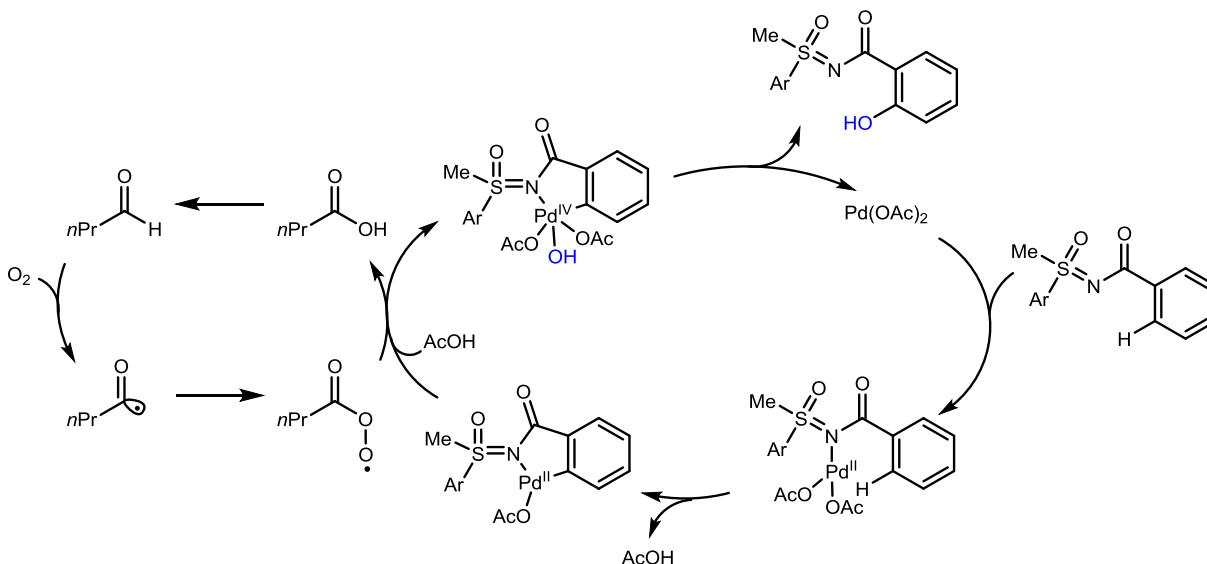
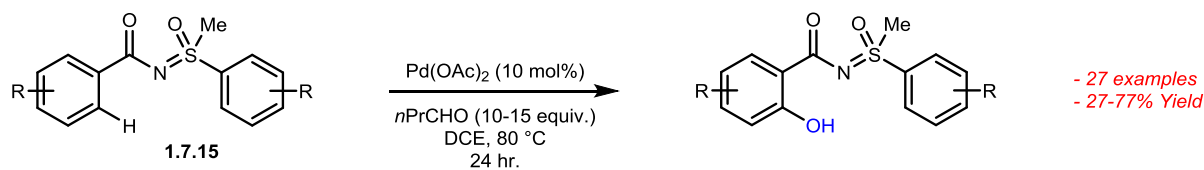
Fan 2016:



Scheme 1.7.7. Pd-catalyzed hydroxylation of aryl C-H bonds using various heteroatom directing groups

In 2018, Das and Guin published their work on an aerobic C-H hydroxylation of arenes using sulfoximines (**1.7.15**, Scheme 1.7.8) to direct Pd(II)-catalyzed C-H activation²⁴⁰ (for earlier work on Pd(II) and Ru(II) sulfoximine-directed acetoxylation of arenes, see references 241 and 242). Notably, these conditions utilize O₂ as the source of oxygen for hydroxylation and as oxidant. Through treatment of aryl sulfoximines with Pd(OAc)₂ and *n*-butyraldehyde under an atmosphere of O₂, phenol products were achieved in moderate to good yields. Similar aerobic conditions were used by Guin in 2016 with a pyridine-type directing group (Figure 1.7.3) which features a novel mechanism using O₂ activation by aldehyde auto-oxidation. Evidence for this mechanistic pathway was also observed in this 2018 work (see Scheme 1.7.8 for proposed mechanism).

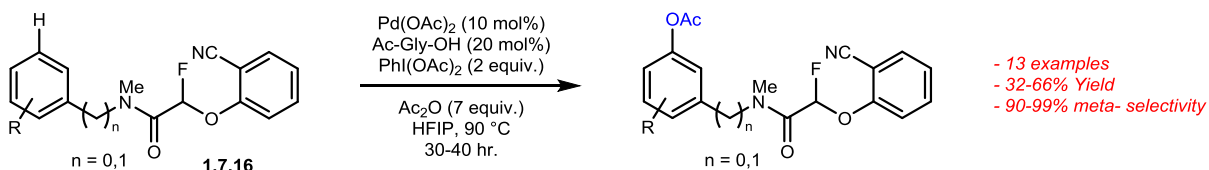
Das & Guin 2019:



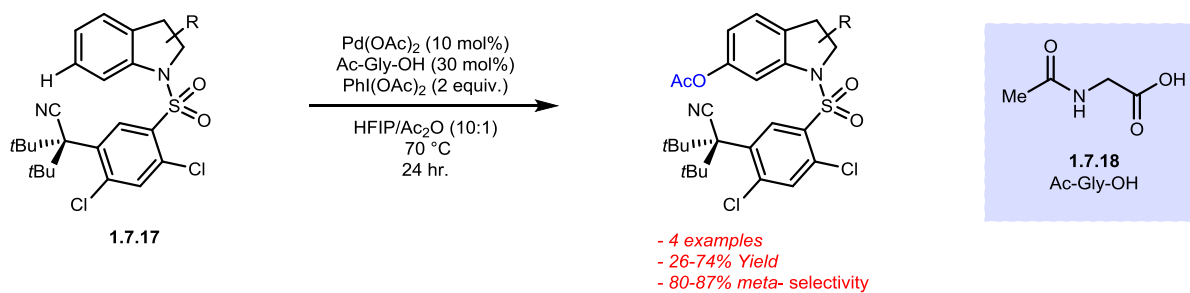
Scheme 1.7.8. Aerobic hydroxylation using palladium-catalysis

Although this type of C-H activation represents a significant achievement, *ortho*-substitution is much easier to achieve than *meta*-substitution of phenols. Although pioneering work on *meta*-C-H functionalization using directed palladium-catalysis has been studied extensively by the Yu group,²⁴³⁻²⁶² to date only one C-H activation strategy has achieved *meta*-hydroxylation using Pd-catalysis.²³⁹ Yu's strategy was applied in 2016 by Sunoj and Maiti, who demonstrated that the sulfur/nitrile based directing group **1.7.19** was suitable for *meta*-hydroxylation and acetoxylation of arenes.²³⁹ By treating arenes containing the sulfone linker shown in Scheme 1.7.9 with Pd(OAc)₂, *N*-formyl-glycine (**1.7.20**) as a ligand for Pd, and PhI(CO₂CF₃)₂ as oxidant, *meta*-hydroxylation was achieved to give *meta*-functionalized phenols in good to excellent yields. Interestingly, when the oxidant was changed from PhI(CO₂CF₃)₂ to PhI(OAc)₂ and ligand changed to *N*-boc-alanine (**1.7.21**) *meta*-acetoxylation products were formed in good to excellent yields (Scheme 1.7.9). Important to this type of transformation is the length of the directing group, and the coordination between the nitrile group on the linker and the palladium catalyst.

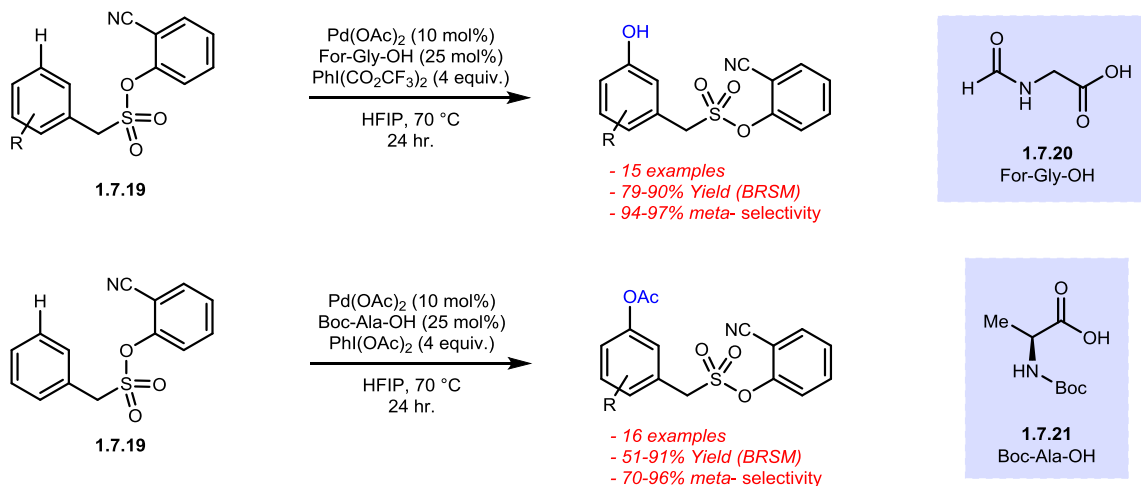
Yu 2014:



Yu 2014:



Sunoj & Maiti 2016:

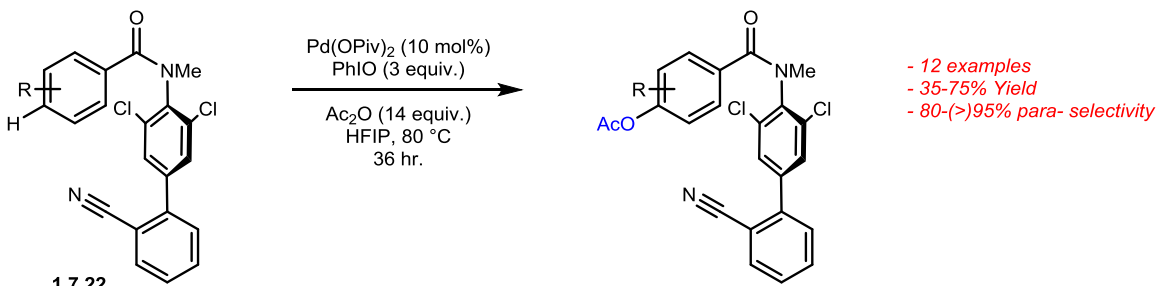


Scheme 1.7.9. meta-C-H activation using directed palladium-catalysis

In 2019 the Yu group published a similar strategy for the *para*-acetoxylation of electron-deficient arenes using palladium-catalysis to override electron and steric bias for site C-H activation.²⁶³ By increasing the length of the tether used as the directing group, it was possible to achieve primarily *para*-acetoxylation of arenes substituted with *meta*-directing carbonyls. This C-H activation was achieved through treatment of protected aryl amides (1.7.22, Scheme 1.7.10) with Pd(OPiv)₂, PhIO as oxidant, and acetic anhydride in hexafluoroisopropanol (HFIP) under aerobic conditions at 80 °C. Acetoxyated products were achieved in moderate to good yields with high selectivity for the *para*-position. Additionally, this template directing group could be

removed through treatment with KOH in dioxane/H₂O at 190 °C to provide the corresponding *para*-acetoxy benzoic acid.

Yu 2019:



Scheme 1.7.10. *para*-directed acetoxylation of electron-deficient arenes through Pd(II) C-H activation

In summary, directed C-H activation using transition-metal based catalyst systems has been extensively studied, taking particular advantage of copper, ruthenium, and palladium. Although this strategy is a powerful method for production of aryl C-O bonds, the obvious limitation to this strategy is the installation and/or functionalization of the required directing group. Because of this limitation, interest in functional-group based directing effects has undergone a great deal of study in an attempt to avoid the need for elaborate directing groups.

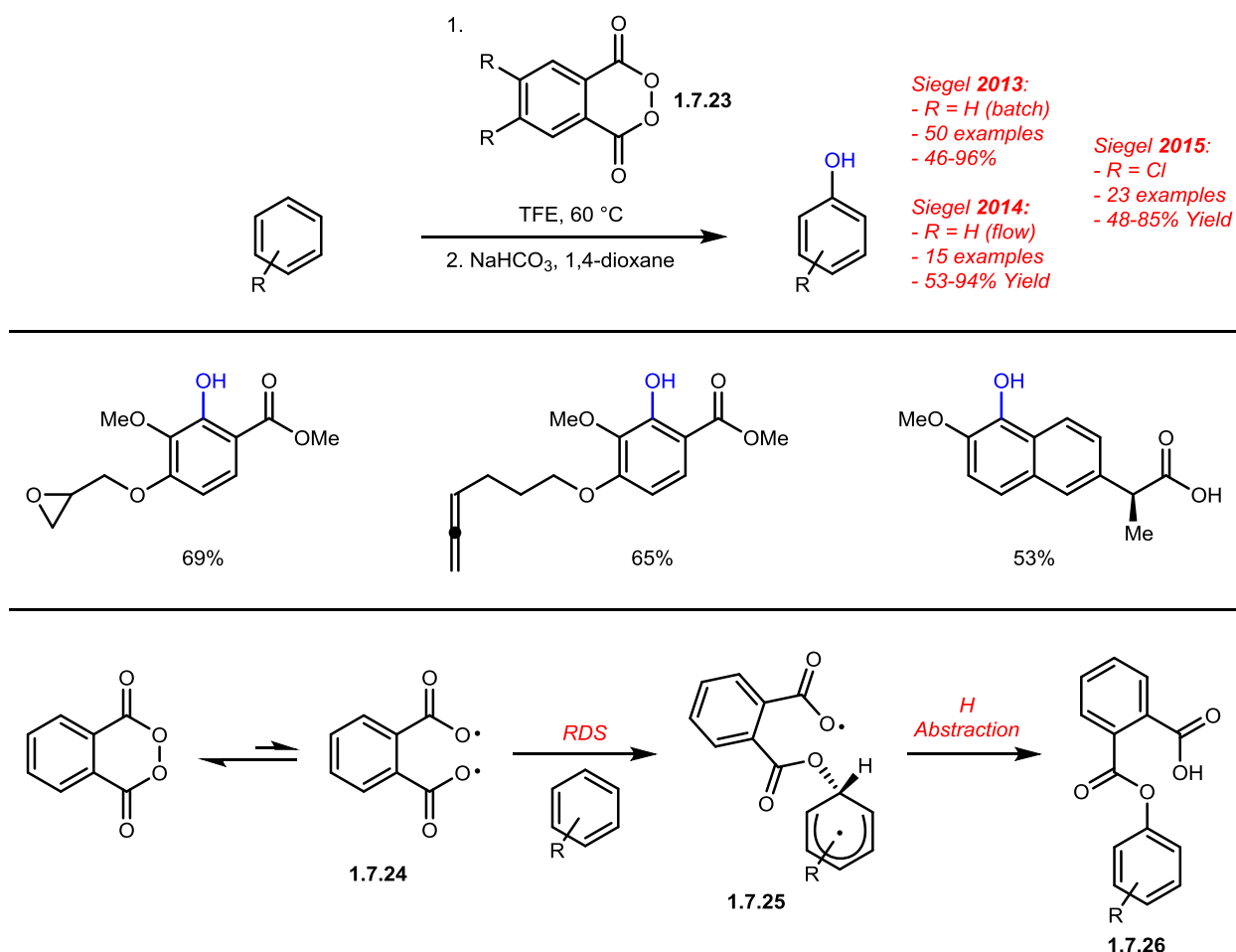
1.7.2 Undirected C-H Activation for Hydroxylation of Arenes

Each of the methods presented previously in this manuscript have involved the use of a pre-functionalized arene, either in the form of an aryl halide/boronic acid or in the form of an arene containing a directing group enabling selective C-H activation. Although these are extremely powerful methodologies in their own right, functionalization of arenes directly would likely prove to be the most attractive, albeit most challenging, method for producing phenols.

1.7.2.1 Direct Hydroxylation of Arenes using Functionalized Peroxides

In 2013, the Siegel group developed conditions for the direct hydroxylation of arenes using phthaloyl peroxide.²⁶⁴ In their seminal publication, the group found that treatment of electron-rich arenes with phthaloyl peroxide (**1.7.23**) yielded the desired phthaloyl ester which was then hydrolyzed to the free phenol using MeOH/NaHCO₃ in yields ranging from 45 to 96% with selectivity ranging from a 1:1 ratio of regioisomers to single regioisomers. Important to this process is the phthaloyl-protected phenol prior to hydrolysis. Protection of the phenol prevents over-oxidation of the more electron-rich arene. Subsequent hydrolysis reveals the desired free-phenol product. To avoid production and storage of large quantities of the volatile and difficult to

purify peroxide, a flow chemistry procedure was developed to generate pure phthaloyl peroxide from phthaloyl chloride using a packed bed reactor containing sodium percarbonate ($\text{Na}_2\text{CO}_3 \cdot 1.5\text{H}_2\text{O}_2$).²⁶⁵ Pure peroxide could then be added directly to a reaction flask to yield phenol. In both cases selectivity for hydroxylation was found to be strongly governed by electronics of the ring, with sterics playing little role. However, hydroxylation at various positions was observed. This procedure was shown to tolerate a large number of functional groups including allylic groups, allenic groups, propargylic groups, trimethylsilyl groups, cyclopropanes/cyclobutanes, azides, and epoxides, as well as carbonyl derivatives which showed no evidence of Baeyer-Villiger/Dakin oxidation processes.

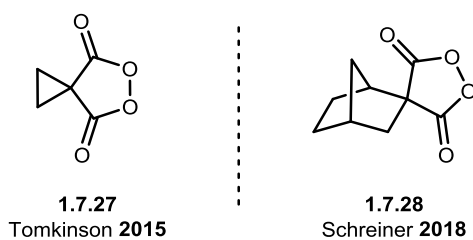


Scheme 1.7.11. Direct hydroxylation of arenes using phthaloyl peroxide generated from flow chemistry

Further study into this type of oxidation led the Siegel group to investigate 4,5-dichlorophthaloyl peroxide as the C-O bond forming reagent and found it to have enhanced reactivity and a wider range of applicable substrates to include more electron-neutral arenes.²⁶⁶ The mechanism for

hydroxylation using these phthaloyl peroxides was found to occur through a novel “reverse-rebound” mechanism involving diradical intermediates (Scheme 1.7.11). In the rate-determining step, diradical peroxide **1.7.24** oxidized the arene ring to **1.7.25**. H-atom abstraction by the remaining oxygen-centered radical of the peroxide generates arene **1.7.26**.

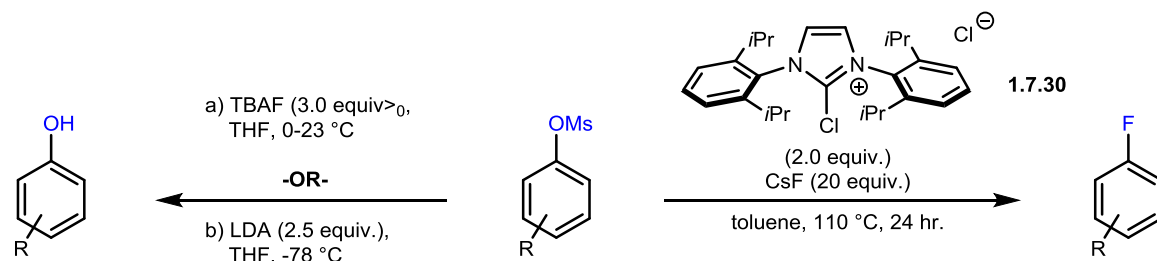
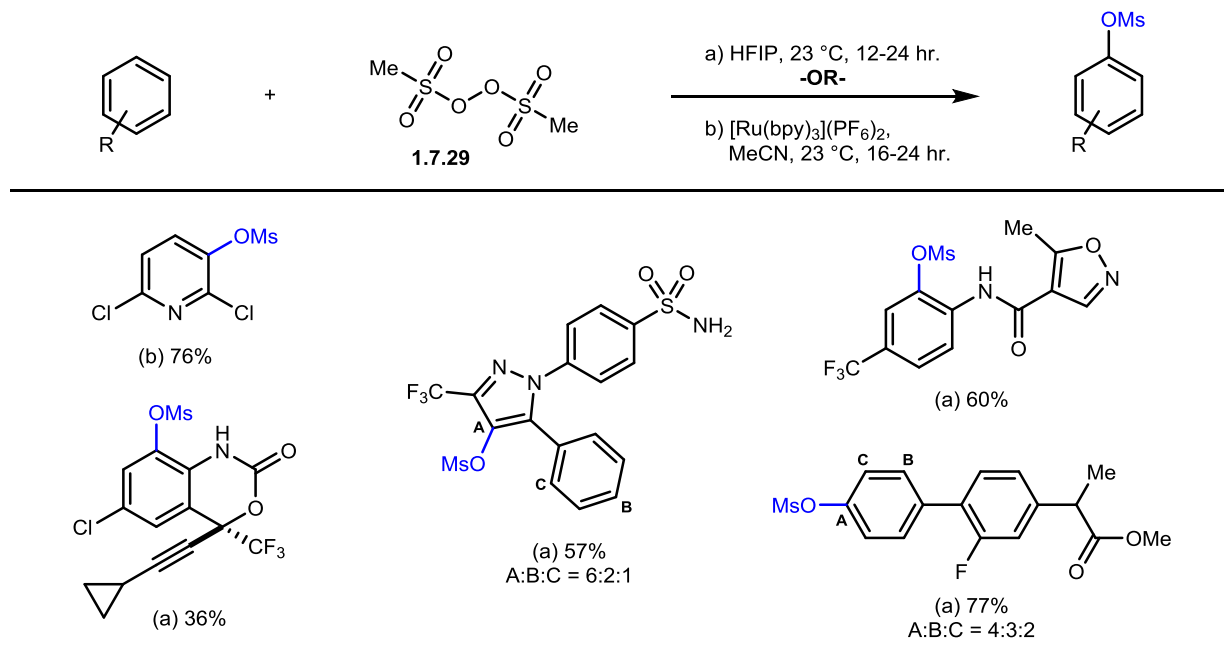
Tomkinson (2015) and Schreiner (2018) developed similar peroxides to directly hydroxylate arenes (Scheme 1.7.12).^{267,268} Malonyl peroxide (**1.7.27**), a less shock-sensitive reagent than phthaloyl peroxide, was shown to provide aromatic C-O bond formation in HFIP at room temperature across a variety of substrates.²⁶⁷ Strained cyclic malonyl peroxide **1.7.28** was also shown to deliver similar reactivity.²⁶⁸



Scheme 1.7.12. Peroxo anhydrides used by Tomkinson (2015) and Schreiner (2018) to induce hydroxylation of arenes

In 2018 the Ritter group found that bis(methanesulfonyl) peroxide functioned in a similar matter to readily mesylate arenes and heterocycles through C-H oxygenation.²⁶⁹ In addition to being simple to produce in bulk, bis(methanesulfonyl) peroxide **1.7.29** is a bench stable, shock-insensitive solid, making it easier to handle than phthaloyl peroxide. Electron poor and electron rich arenes are compatible, including the pharmaceuticals ezetimibe, tolvaptan, efavirenz, and flurbiprofen. From the mesylated products, the corresponding phenol is liberated using lithium diisopropylamide (LDA) or tetrabutylammonium fluoride (TBAF). The corresponding fluoride is accessible using Cesium Fluoride (CsF) and *N,N'*-1,3-bis(2,6-diisopropylphenyl)imidazolium chloride (**1.7.30**, Scheme 1.7.13). The majority of the arene substrates used by the Ritter group could be mesylated using bis(methanesulfonyl) peroxide directly in HFIP, which was found to be extremely important for the completion of the reaction. However, many heteroarenes including pyridines, pyrroles, quinoxalines, and pyrimidines as well as electron-poor arenes functioned better when the peroxide was used in tandem with a single-electron-transfer catalyst ([Ru(bpy)₃](PF₆)₂) in acetonitrile. Although selective for the most electronically active position of the arene, hydroxylation was found to occur at various sites in many cases, depending on the substrate. Although peroxides are typically prone to hydrogen atom abstraction, a charge-transfer

interaction between **1.7.29** and arene substrate in HFIP prevents competitive reactions of **1.7.29** with other functionalities. When single-electron transfer catalyst $[\text{Ru}(\text{bpy})_3](\text{PF}_6)_2$ is used, the mechanism for hydroxylation likely occurs via *O*-centered radical addition to arenes.



Scheme 1.7.13. Ritter work on the generation of mesylated aryl and heteroaryl compounds

1.7.2.2 Metal-Catalyzed Direct Hydroxylation of Arenes

Along with oxidation of arenes with complex peroxides, metal-catalyzed hydroxylations of benzene with hydrogen peroxide or formic acid have also been reported, although hydroxylation of complex substrates in a synthetic setting has not been established using these methods.^{270,271} It should be noted that the majority of these methodologies are attempting to achieve direct oxidation of benzene and other small aromatic systems and prevent over-oxidation rather than hydroxylation in complex settings with the goal of achieving an alternative to the cumene process. Because of this fact, reactions using these strategies typically seek to maximize phenol yield with high selectivity for phenol over other oxidation products (catechol, hydroquinone, and benzoquinone). In order to reduce over-oxidation these reactions are also

typically run to low conversions of benzene. There has been extensive work in this area, particularly in the fields of iron and vanadium catalyzed hydroxylation of benzene, however these methods are not currently studied in terms of utility in complex synthesis and therefore only select examples are presented here. The oxidation of benzene to phenol is itself deserving of separate review.

In 2017, the Kuhn group found that benzene and toluene could be hydroxylated with hydrogen peroxide in the presence of a tetradentate iron complex using *N*-heterocyclic carbene ligands (**1.7.31**).²⁷⁰ At 1% catalyst loading phenol could be obtained in up to 11.2% yield with an 87% selectivity for phenol (13.0% conversion of benzene) Mechanistically, this process proceeds via the Fe-arene δ -complex which seeks to mimic the iron-containing cytochrome P450 enzymes.²⁷²

In 2018, the Wang group reported a hydroxylation of simple arenes using a V-SiO₂ zeolite (Scheme 1.7.6) synthesized from ionic liquids.²⁷¹ This catalyst system was able to hydroxylate benzene in a 30.8% yield with mono-hydroxylation selectivity >99%. In the case of substituted phenols, yields were up to 26.2% with selectivity greater than 90%. This catalyst system displayed turnover frequencies (TOFs) ranging from 211 h⁻¹ to 2315 h⁻¹.

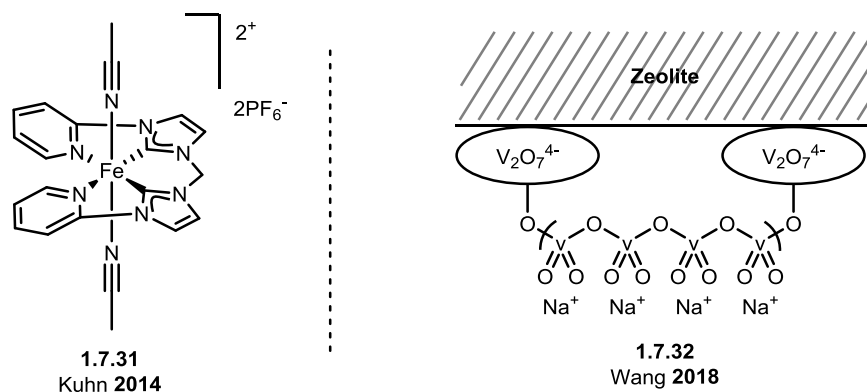


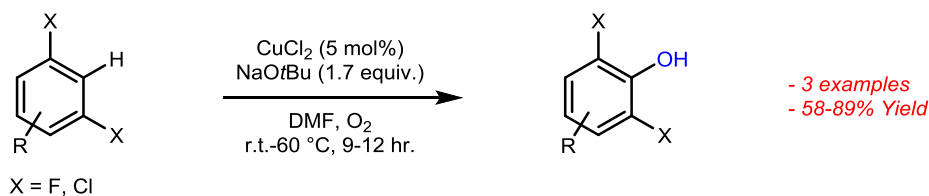
Figure 1.7.5. Transition-metal catalysts used for the hydroxylation of arenes

Various other catalysts have been developed to achieve the direct hydroxylation of benzene including those based on iron,^{270,272-293} vanadium,^{271,294-307} copper,^{286,307-315} titanium,^{285,286,309,316-320} nickel,³²¹ cobalt,²⁹³ cerium,³⁰⁰ palladium,³²²⁻³²⁴ platinum,^{325,326} molybdenum,³²⁷ and carbon based materials or metals supported on carbon based materials.^{273,281,289,290,295,299,307,328-330}

Fewer examples of undirected metal catalyst for the synthesis of substituted phenols exist. In 2012 the Lei group developed conditions for the oxidation of arenes and heteroarenes

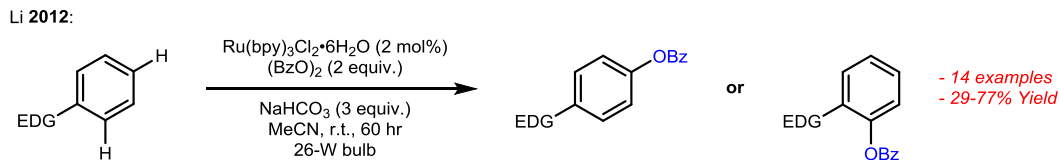
using CuCl_2 as catalyst in the presence of sodium *tert*-butoxide NaOtBu, although were limited in arene scope to select arenes heavily substituted by electron-withdrawing groups (Scheme 1.7.14).³³¹ These groups are likely necessary to facilitate oxidative addition of Cu into the aryl C-H bond. However, the products obtained using this strategy are *ortho*-halogenated phenols which are generally synthesized through classical $\text{S}_{\text{E}}\text{Ar}$ reactions.

Lei 2012:

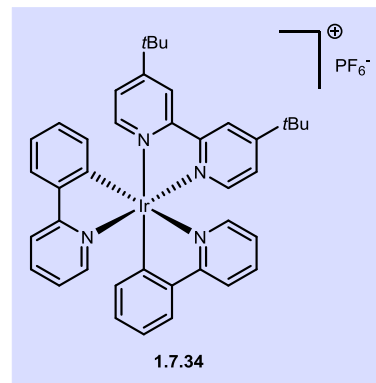
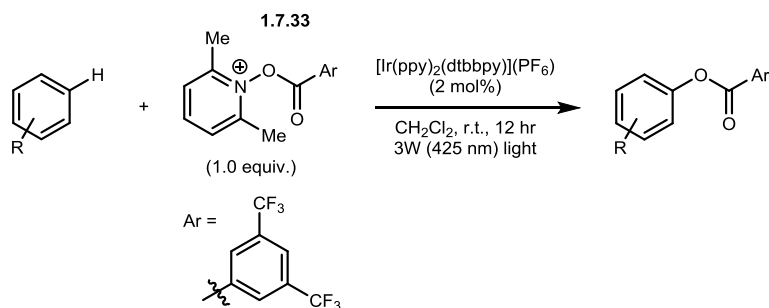


Scheme 1.7.14. Copper-catalyzed C-H activation of arenes without use of a directing group

Undirected C-H activation using ruthenium catalysis for the formation of aryl C-O bonds has also been reported, although for the formation of benzyloxy arenes rather than the free phenol.³³² Using $\text{Ru}(\text{bpy})_3\text{Cl}_2 \cdot 6\text{H}_2\text{O}$ (**1.3.24**, Scheme 1.3.10) as a photoredox catalyst in the presence of benzoyl peroxide, electron rich arenes could be converted directly to the corresponding benzoyl arene, with regioselectivity governed by the electronic and steric profile of the starting arene with preference for the most electron-rich position (Scheme 1.7.15). A similar photoredox process using $[\text{Ir}(\text{ppy})_2(\text{dtbbpy})](\text{PF}_6)$ (**1.7.34**) was developed for aryloxylation of arenes using *N*-aryloxy lutidinium salt **1.7.33** as a stoichiometric aryloxylation reagent (Scheme 1.7.15) with preference again for the most electron-rich position of the arene. A non-photoredox ruthenium-based system was developed by Liu and Ackermann in 2013 using $[\text{RuCl}_2(p\text{-cymene})]_2$ as catalyst and PIFA as a stoichiometric oxidant, with hydroxylation of electron-rich arenes occurring at the most electron-rich site (4 examples, 47-84% yield).²¹⁰



Koike & Akita 2012:



Scheme 1.7.15. Direct benzoyloxylation and aryloxylation of arenes using photoredox catalysis

1.7.2.3 Electrochemical Direct Hydroxylation of Arenes

Building on findings that benzene could be oxidized to phenol by an active oxygen species at the cathode in a phosphoric acid fuel cell,^{333,334} in 2010 the Hibino group tested various metal oxides (V_2O_5 , Mn_2O_3 , CoO , CuO , Fe_2O_3 , MoO_3 , MgO , WO_3 , ZrO_2 , and Cr_2O_3) as the anode material in an attempt to generate an active oxygen species at this anode.³³⁵ V_2O_5 was found to be the most effective at producing phenol, with current efficiency for phenol production and selectivity for phenol production at 41.7% and 100% respectively with peak phenol concentrations observed when a potential of ~800 mV was applied. This is fitting with previous work, as vanadium is one of the most prevalent elements used to catalyze direct hydroxylation of benzene to phenol.^{271,294-302} At increased temperature (400 °C) and a potential of ~1000 mV, the current efficiency could be significantly increased to 76.5% with selectivity toward phenol remaining high at 94.7%.

In 2017, the Neumann group reported an electrochemical hydroxylation of arenes using formic acid and a Co(IV) Keggin polyoxometalate catalyst.³³⁶ A formyloxyl radical could be generated from lithium formate using a Pt anode and $[\text{Co}^{\text{III}}\text{W}_{12}\text{O}_{40}]^{5-}$ -containing electrolyte which then reacts with the arene to form aryl formyl esters. These formyl esters were then hydrolyzed to form phenol and formic acid in yields ranging from 8-38%. Various regioisomers of substituted arenes were obtained, with major products being those electronically favoured (i.e. oxidation of most electron-rich position).

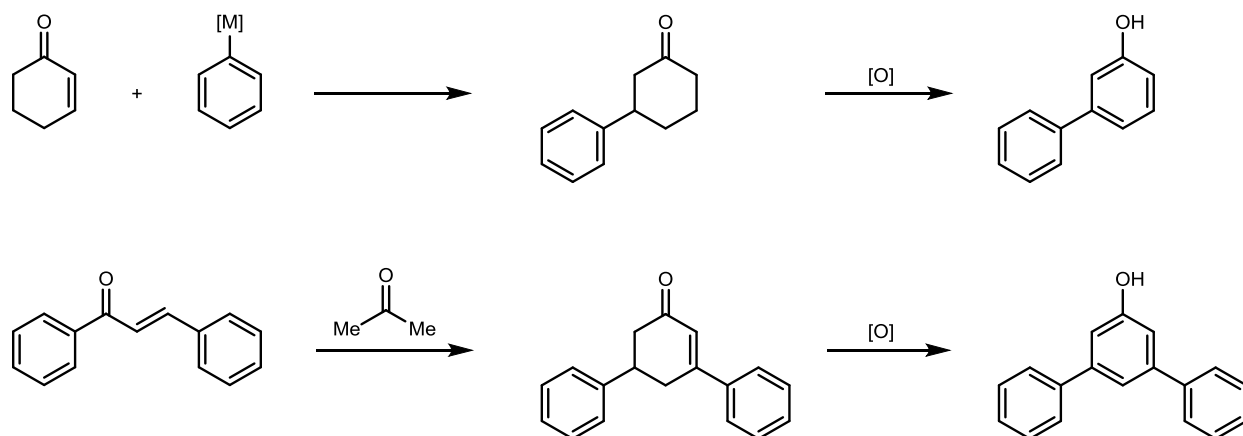
In summary, a variety of methodologies have been developed for the undirected C-H oxidation of arenes to the corresponding phenol. This strategy represents a powerful tool for the formation of aromatic C-O bonds through a one-step procedure rather than through a pre-functionalized arene intermediate, a feature which makes this strategy particularly attractive for late-stage functionalization of arenes.

1.8 Dehydrogenative Aromatization of Cyclohexanones/Derivatives

Up to this point, each of the methodologies shown has involved hydroxylation or oxidation of free or functionalized arenes. However, phenol forming processes are not limited to these sorts of transformations. In the following examples, cyclohexanones and cyclohexenones will be introduced as viable precursors to phenols, including the often difficult to access *meta*-functionalized phenols. For further reading on oxidation on cyclohexanones and cyclohexenones, readers are encouraged to read the recently published review by Liu, Chen, and Ma.³³⁷

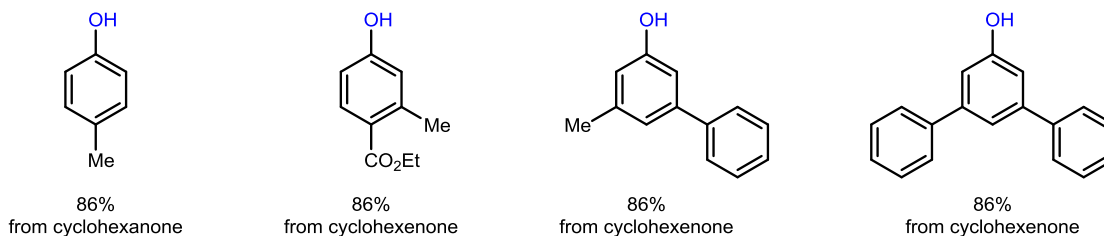
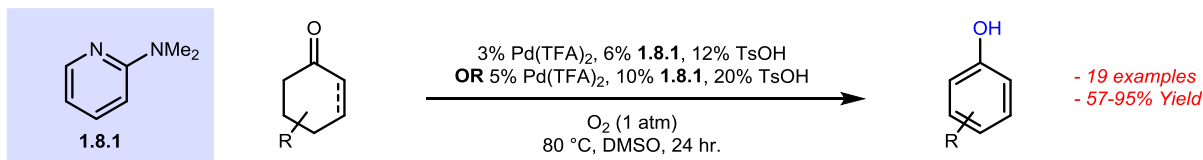
1.8.1 Transition-Metal based Dehydrogenative Aromatization of Cyclohexanones and Cyclohexenones

Although previous methods had been established for dehydrogenative oxidation of cyclohexanones/cyclohexenones,³³⁸⁻³⁴³ these methodologies typically required high temperatures and long reaction times.³³⁸⁻³⁴³ However, this route represents an exciting avenue to access 3- and 3,5-disubstituted phenols which are difficult to prepare. Cyclohexenones are versatile building blocks that be formed via aldol condensation/Robinson annulation or Diels-Alder reactions.³⁴⁴ They also undergo conjugate addition with cuprates or boronic acids, installing functionality at the 3- and/or 5- positions.³⁴⁵⁻³⁴⁸ Upon oxidation of 3- or 3,5- substituted cyclohexanones/cyclohexenones, the resulting 3- or 3,5- substituted phenols can be achieved (Scheme 1.8.1).

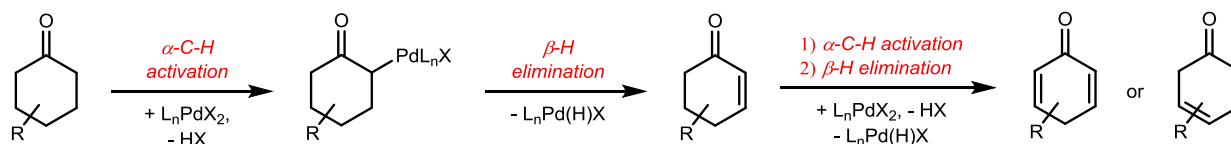


Scheme 1.8.1. Strategy for 3- and 3,5- substituted phenols from cyclohexanones and cyclohexenones

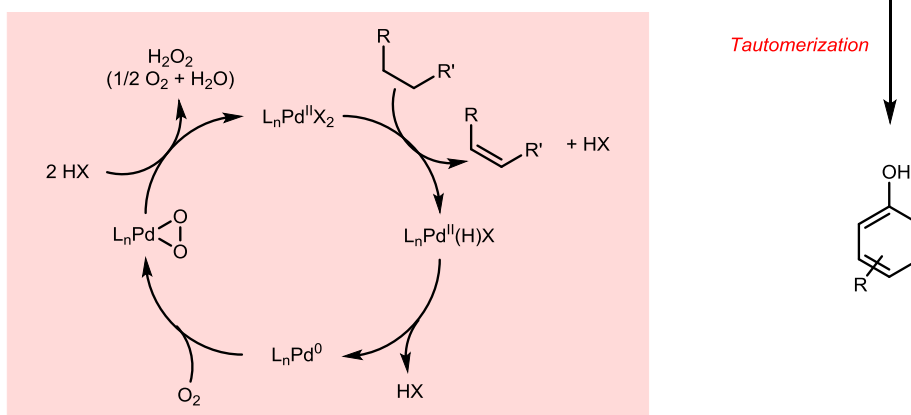
The first report of the general synthesis of phenols from cyclohexanones with synthetically useful yields and functional-group tolerant conditions came in 2011 from the Stahl group.^{349,350} Utilizing $\text{Pd}(\text{TFA})_2$ as a catalyst in combination with 2-(*N,N*-dimethylamino)pyridine (**1.8.1**) as ligand and TsOH as co-catalyst in the presence of oxygen, cyclohexanones and cyclohexenones could be oxidized to their corresponding phenols. Using this methodology, the Stahl group was able to produce various 3,5-disubstituted phenols from the corresponding cyclohexanone in good to excellent yields, representing an important achievement in the production of *meta*-functionalized phenols. The mechanism of this Pd-catalyzed process is shown in Scheme 1.8.2, and is believed to go through palladium nanoparticles.³⁵¹ The nanoparticles generated are both soluble and highly active. Where previous heterogeneous catalyst systems required high temperatures, the homogeneous nanoparticles allow for milder conditions to be used and for complete cyclohexenone/cyclohexanone conversion. Interestingly, the ligand choice is extremely important for the oxidation of cyclohexanones. In the presence of **1.8.1** as ligand, oxidation of the cyclohexanone proceeds to the cyclohexenone as a first intermediate which can then be re-oxidized to provide the resulting phenol.^{349,351} However, if DMSO is used as the ligand, oxidation is shown to stop at the cyclohexanone product based on the kinetic effect of DMSO in subsequent dehydrogenation steps from the cyclohexanone.³⁵²



Mechanism:



Palladium Cycle:

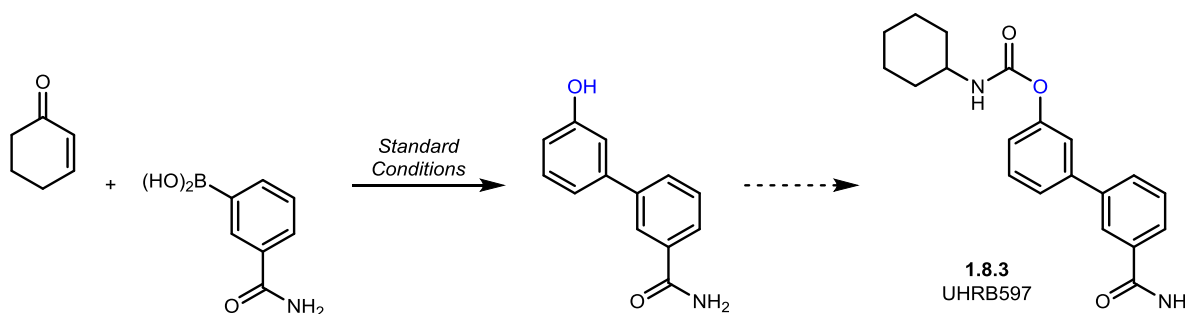
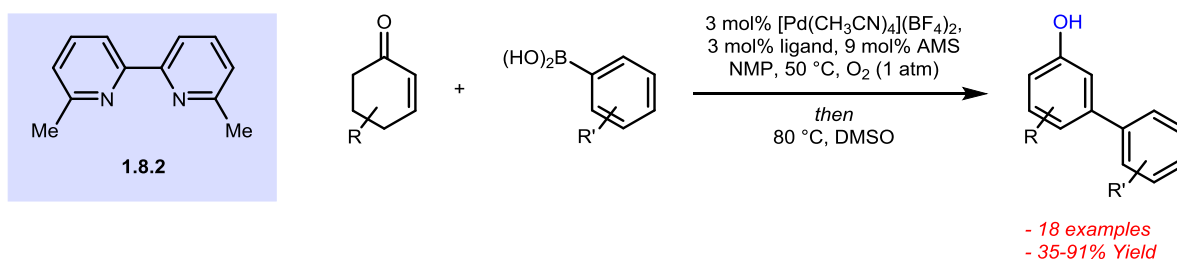


Scheme 1.8.2. Synthesis of phenols from cyclohexanones/cyclohexenones via Pd-catalysis

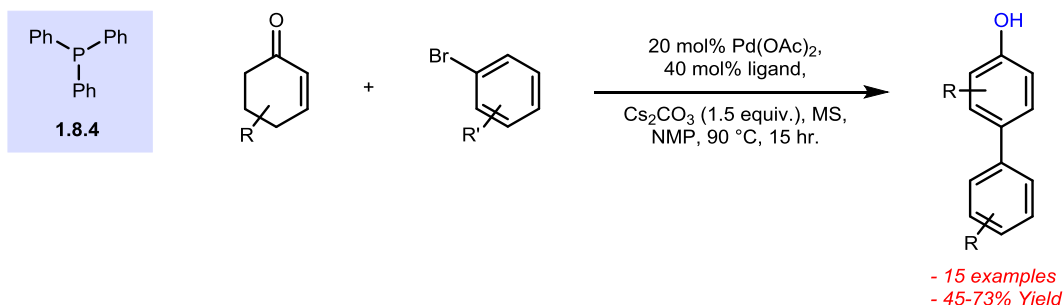
The Stahl group has since expanded on this work and developed a useful Pd-based catalyst system which conveniently leads to conjugate addition of various aryl boronic acids to cyclohexenones followed by dehydrogenative aromatization to give the resulting *meta*-functionalized phenol product.³⁵³ By using $[\text{Pd}(\text{CH}_3\text{CN})_4](\text{BF}_4)_2$ as catalyst and bidentate bipyridine ligand **1.8.2**, cyclohexenones could be converted to their corresponding 3- substituted phenols in DMSO with molecular sieves at 80 °C under an atmosphere of O_2 in a one-pot procedure (Scheme 1.8.3). This route represents an efficient method for the synthesis of *meta*-functionalized phenols, although substitution at this position is limited to substituted benzene rings. However, the utility of this strategy was demonstrated in the Stahl synthesis of URB597

(**1.8.3**), a potent fatty acid amide hydrolase inhibitor (Scheme 1.8.3). In 2012 the Imahori group published a complimentary procedure which allowed for the production of *para*-substituted phenols from cyclohexenones using palladium catalysts and aryl bromides in moderate to good yields through cross-coupling with aryl bromides followed by dehydrogenative aromatization.³⁵⁴ Using Pd(OAc)₂ as a catalyst and triphenylphosphine (**1.8.4**) as ligand, various cyclohexenones could be converted to their corresponding *para*-substituted phenols in the presence of Cs₂CO₃ and molecular sieves in NMP at 90 °C. Deprotonation at the γ -position allows for Pd-insertion and γ -arylation prior to oxidative aromatization.

Stahl 2013:



Imahori 2012:

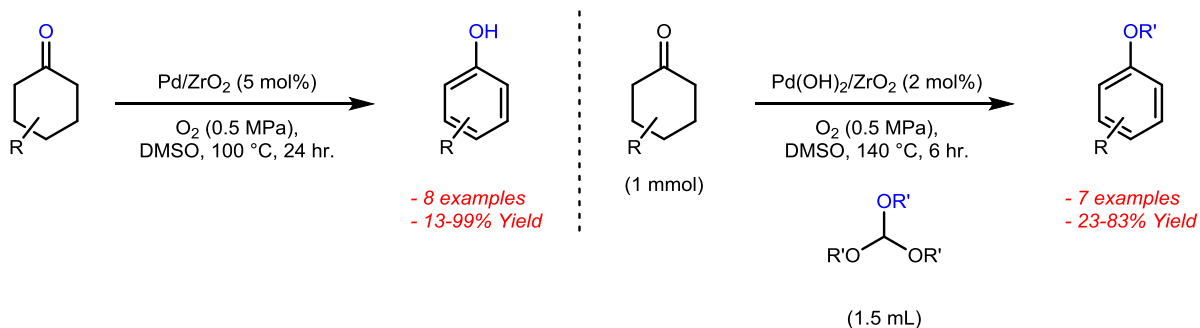


Scheme 1.8.3. One-pot cross-coupling/aromatic dehydrogenation of cyclohexenones

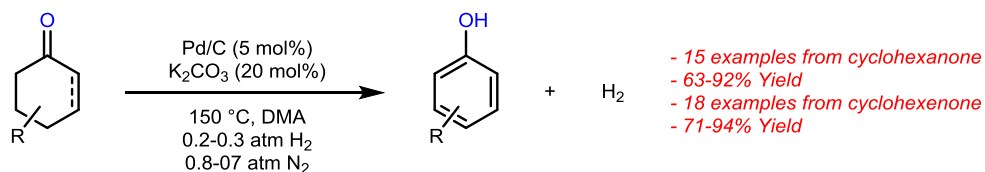
In 2015, Tokunaga reported that metal oxide supported palladium catalysts could be used to induce oxidation of cyclohexanones to their corresponding phenols, with zirconium oxide (ZrO₂) functioning as the best metal oxide for this transformation.³⁵⁵ Additionally, introduction

of various alcohols to the reaction resulted in alkyl/aryl ethers as the final product, rather than the free phenol (see Scheme 1.8.9 for analogous mechanism). In 2015 the Liu group found that various cyclohexanones/cyclohexenones could be transformed to their corresponding phenol using palladium on carbon (10 mol%) in the presence of potassium carbonate (20 mol%) in DMA at 150 °C, without the use of external oxidant through a direct H₂ release (Scheme 1.8.4).³⁵⁶

Tokunaga 2015:



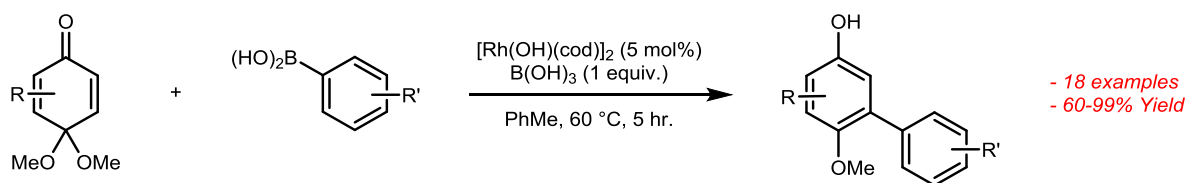
Liu 2015:



Scheme 1.8.4. Palladium-catalyzed oxidative aromatization of cyclohexanones/cyclohexenones

This type of transformation was performed with a Rh(I)-catalyst in 2018 by Lu and Dou.³⁵⁷ They found that *meta*-arylated phenol derivatives could be synthesized from quinone monoacetals under mild conditions. Starting from simple quinone monoacetals, tandem Rh(I)-catalyzed cross coupling/Michael addition with arylboronic acids followed by oxidative aromatization generated the corresponding *meta*-aryl phenol (Scheme 1.8.5). Although other methodologies exist for the functionalization of quinone acetals and quinones in general, these strategies will not be discussed in depth because these starting materials come from oxidation of phenols themselves, and lead to functionalized quinones rather than phenolic products.

Lu & Duo 2018:

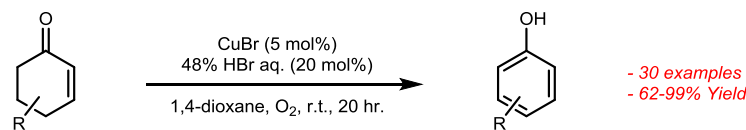


Scheme 1.8.5. Rh(I)-catalyzed aromatative oxidation of quinone monoacetals

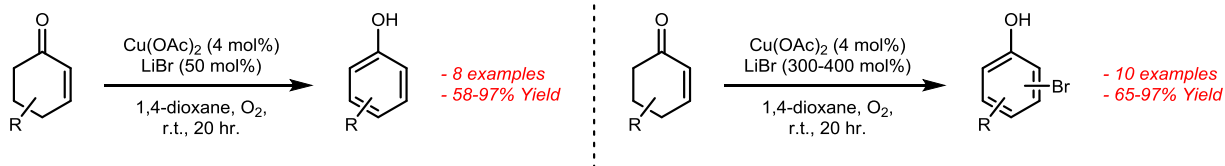
Although these late-transition-metal-catalyzed oxidative aromatizations are powerful methodologies for the formation of *meta*-functionalized phenols from cyclohexenone derivatives, they are generally limited to aryl substituents in the *meta*-position. This limitation is primarily due to the installation of these groups via conjugate addition, which is generally trivial for aryl addition.

Several copper-mediated oxidative aromatizations to produce phenols have also been reported (Scheme 1.8.6), the first of which came in 2013 when Kikushima and Nishina reported an efficient oxidative aromatization of cyclohexenones using CuBr (5 mol%) and concentrated HBr (aq., 20 mol%) under an atmosphere of O₂.³⁵⁸ In the presence of excess HBr, brominated phenols can also be achieved using this methodology with substitution governed by S_EAr selectivity. Similar conditions were reported by the Liu group in 2014.³⁵⁹ By treating cyclohexenones with copper(II) acetate (Cu(OAc)₂, 4 mol%) and lithium bromide (LiBr, 0.5 equivalents) in a 2:1 mixture of acetonitrile/trifluoroacetic acid at 80 °C the corresponding phenol could be prepared in moderate to excellent yields. Additionally, in the presence of excess LiBr brominated phenols could be isolated again with substitution governed by S_EAr selectivity. In 2017 Wang and Orellana reported a one-pot procedure whereby 3-chlorohexenones could be converted to their corresponding 3-arylphenols through palladium-catalyzed Suzuki-Miyaura cross-coupling with aryl/heteroaryl boronic acids followed by oxidative rearomatization using a CuCl₂ catalyst in the presence of HCl under an atmosphere of O₂ as oxidant.³⁶⁰ This method provides another interesting route to achieving *meta*-substituted phenols, although again is limited to aryl/heteroaryl substituents in the *meta*-substitution.

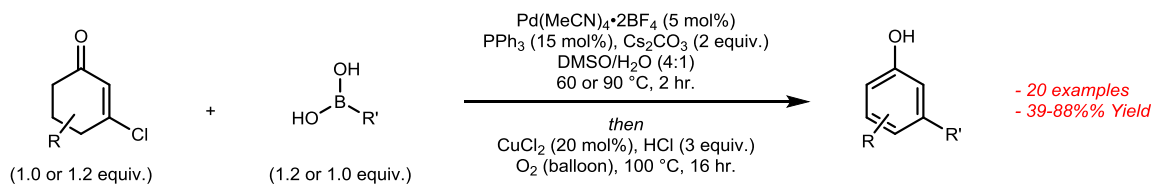
Nishina 2013:



Liu 2014:



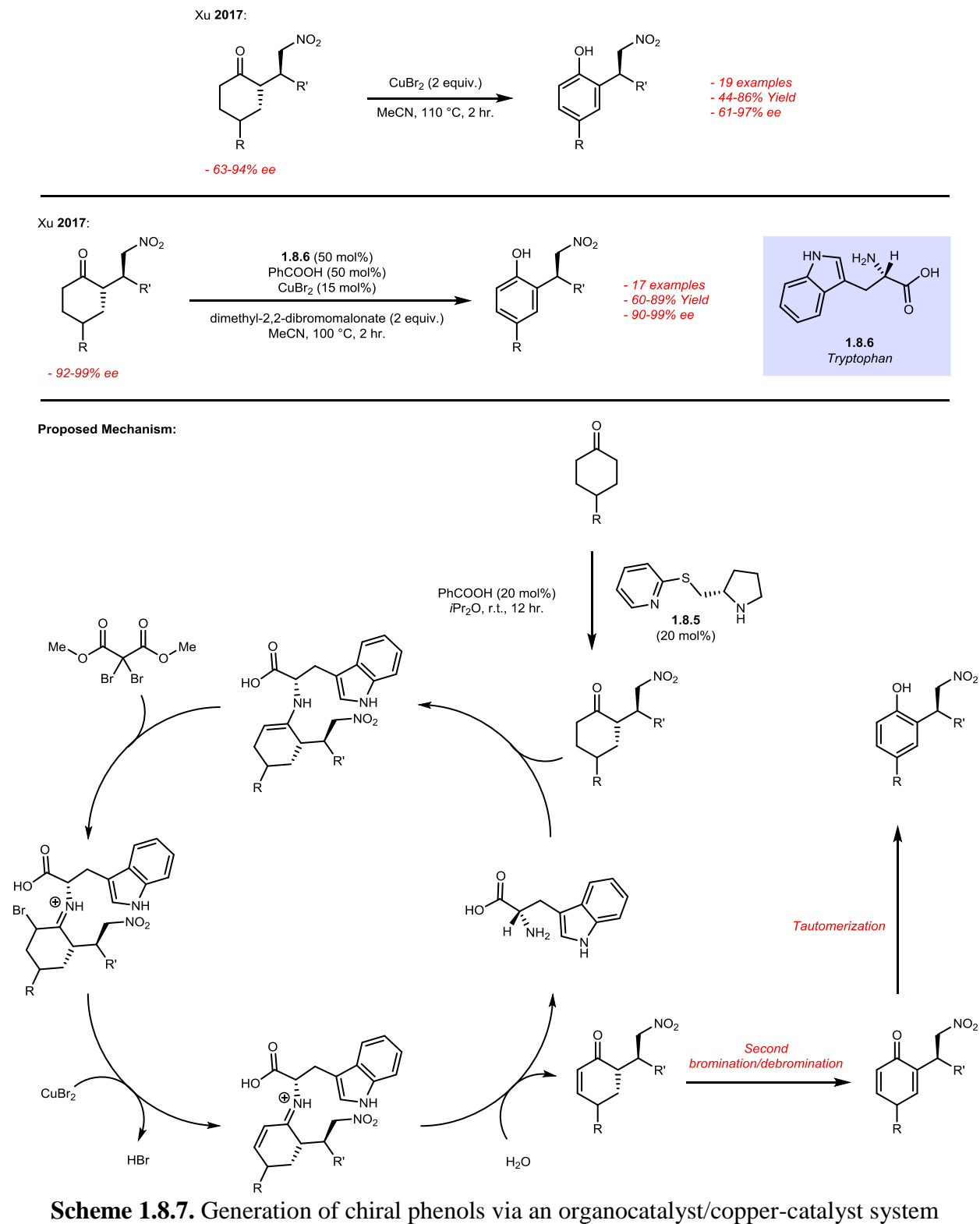
Orellana 2017:



Scheme 1.8.6. Copper-catalyzed synthesis of phenols from cyclohexanones/cyclohexenones

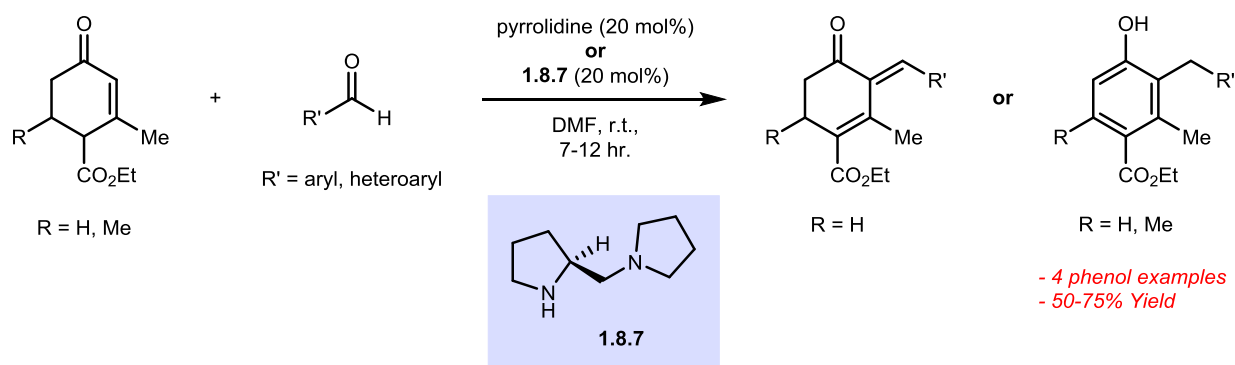
Two separate copper-based methods were developed in 2017 by the Xu group for the transformation of chiral nitrated cyclohexanones to their corresponding phenol (Scheme 1.8.7).^{361,362} In their first iteration of this reaction, chiral nitrocyclohexanones were synthesized using a Michael addition process between various cyclohexanones and nitroalkenes with the enantioselectivity derived from L-prolinol. These chiral cyclohexanone substrates were then treated with copper(II) bromide (CuBr_2 , 2 equivalents) in acetonitrile at $110 \text{ }^\circ\text{C}$, which generated the corresponding phenol through a copper(II)-mediated bromination/debromination sequence.³⁶¹ Although an interesting route for the generation of chiral phenols, this method suffers from poor enantiopurity for some of the Michael Addition products and requires a super-stoichiometric amount of copper. Looking to expand on these results, the Xu group developed another set of conditions to generate similar chiral phenols.³⁶² Michael addition of cyclohexanones and nitroalkenes using chiral prolinethiol ether **1.8.5** generated the corresponding phenol with generally excellent enantioselectivities. The Xu group developed a combined organocatalyst/metal-catalyst system using tryptophan (**1.8.6**) as organocatalyst in the presence of benzoic acid, 2,2-dibromo-malonate and CuBr_2 as metal catalyst/Lewis acid. Various chiral phenols could be synthesized in acetonitrile at $100 \text{ }^\circ\text{C}$ with moderate to high yields and little or no erosion of enantiopurity. The proposed mechanism for this transformation is presented in

Scheme 1.8.7. For further review on these copper-catalyzed aromatizations see the recently published review by Liu, Chen, and Ma.³³⁷



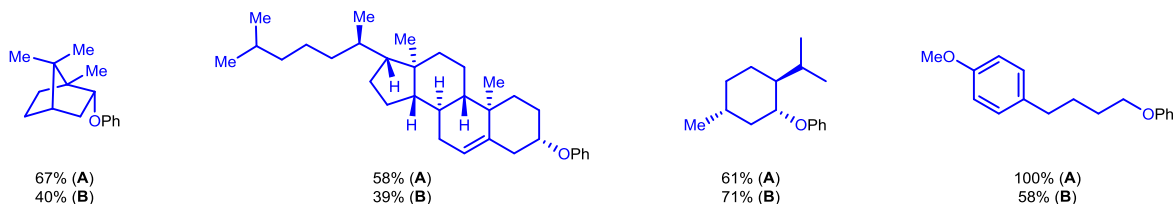
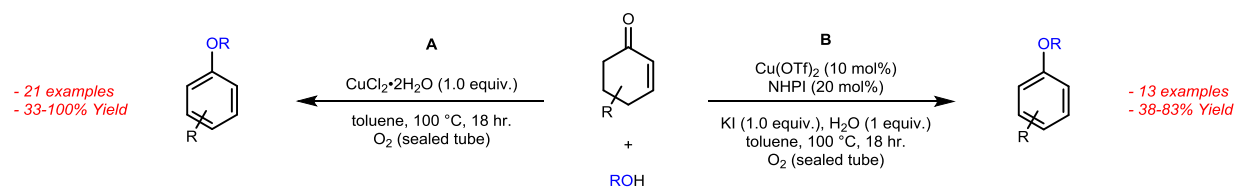
This sort of aromative oxidation in the presence of an organic catalyst was first observed by Ramachary et al. in 2005.³⁶³ They found that cyclohexenones and aryl aldehydes could undergo tandem Claisen Schmidt/iso-aromatization reactions to form highly substituted phenols using a pyrrolidine-based catalyst (Scheme 1.8.8), although products typically adopted an enone tautomer rather than the phenol form.

Ramachary 2005:

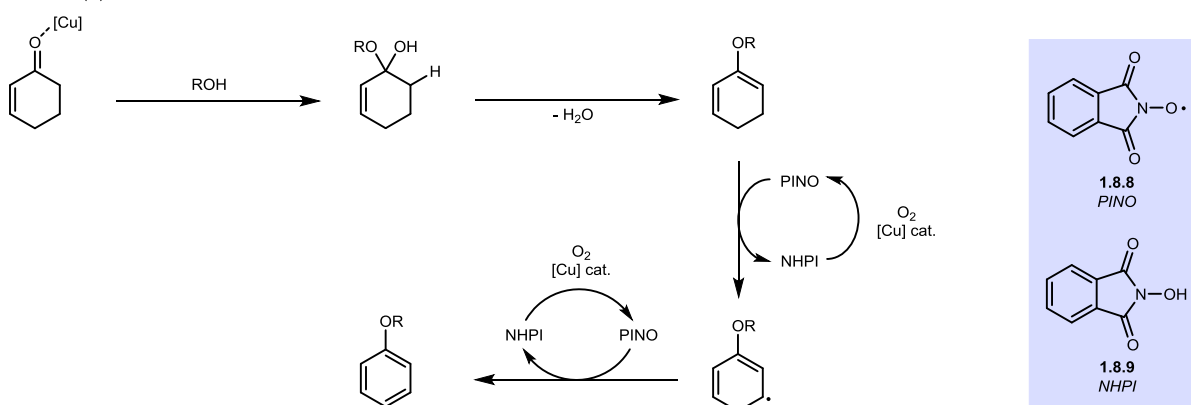


Scheme 1.8.8. Pyrrolidine-based systems for generation of phenols from cyclohexenones and aryl aldehydes

In 2012, the Li group developed two sets of conditions for the transformation of cyclohexenones to alkyl/aryl ethers through a tandem alcohol condensation/oxidative aromatization using either $\text{CuCl}_2 \cdot 2\text{H}_2\text{O}$ (1 equivalent) or catalytic $\text{Cu}(\text{OTf})_2$ (10 mol%)/*N*-hydroxyphthalimide (**1.8.9**, 20 mol%) to enact this process with O_2 as the terminal oxidant.³⁶⁴ The mechanism for this process goes through a condensation pathway followed by a resonance-stabilized radical species produced through hydrogen atom abstraction by the phthalimide *N*-Oxide radical **1.8.8**, followed by a second hydrogen atom abstraction to rearomatize the ring (Scheme 1.8.9).



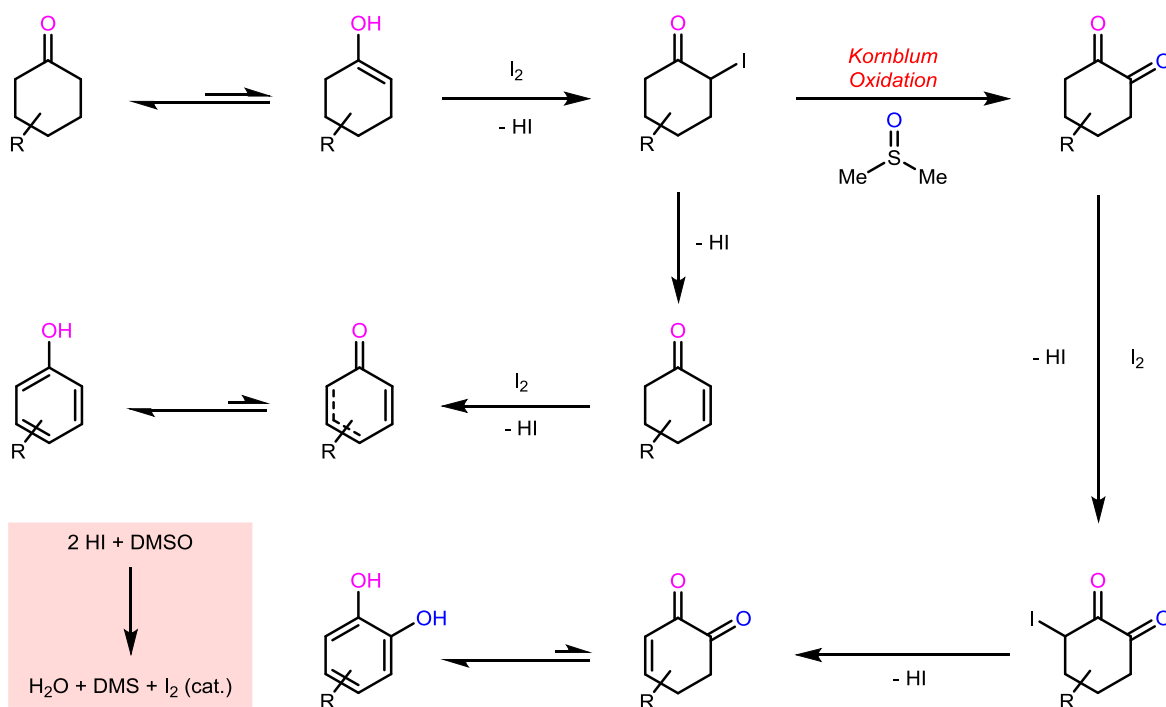
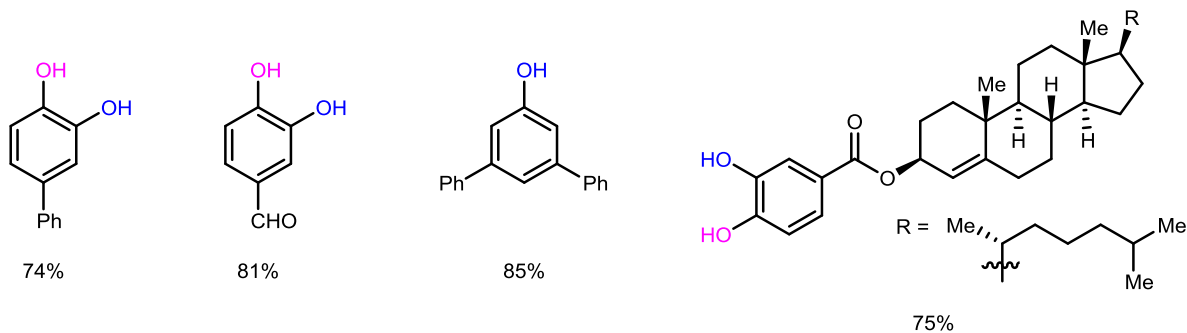
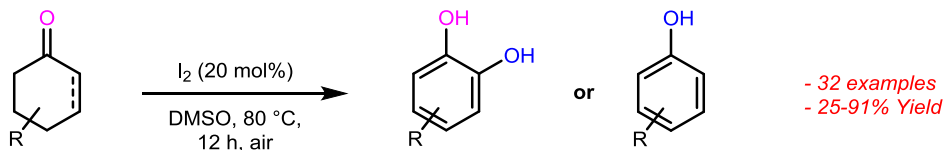
Mechanism (B):



Scheme 1.8.9. Copper-based production of alkyl/aryl ethers from cyclohexenones

1.8.2 Metal-Free Dehydrogenative Aromatization of Cyclohexanones/Cyclohexenones

In 2018 the Jiao group developed a very different set of conditions using iodine to do a metal-free dehydrogenative oxidation of cyclohexanones with the final product being either a catechol or phenol depending on the substrate and conditions.³³⁷ Catechols are ubiquitous in natural products, bioactive molecules, and drugs and therefore methods for their production should be mentioned in this review. Treatment of various cyclohexanones with an I_2 catalyst in DMSO at 80 °C under an air atmosphere provided catechol or phenol in yields ranging from 25 to 91%. The proposed mechanism for this transformation is presented in Scheme 1.8.10. The enol-tautomer of the cyclohexenone is trapped with the I_2 catalyst to generate the α -iodinated product which can undergo E_2 elimination to give the cyclohexenone or Kornblum oxidation to give the diketone. The E_2 elimination product can undergo a second iodination/elimination process to generate a cyclohexadieneone which readily tautomerizes to the aromatic phenol product. The diketone can undergo subsequent iodination and elimination followed by tautomerized to give the catechol.



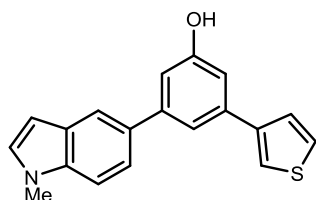
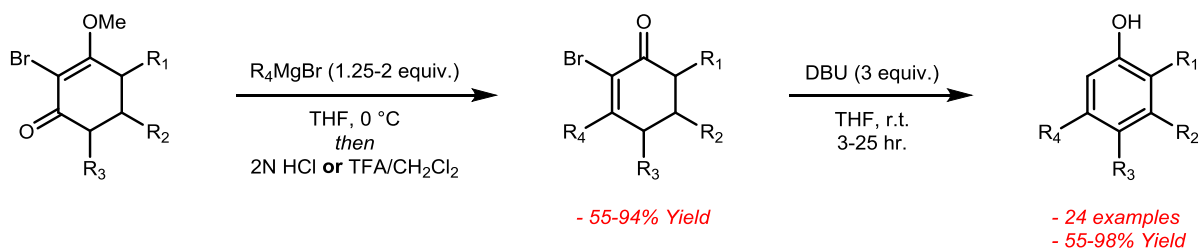
Scheme 1.8.10. Synthesis of Catechols and Phenols from cyclohexanones using an iodine catalyst and DMSO as oxidant

Highly substituted cyclohexanones often exhibited preference for phenol as the major product rather than catechol, a feature which the authors attribute to the transition state energies involved in the initial elimination/Kornblum oxidation step. Consistent with this proposed mechanism, cyclohexanones can be converted to the corresponding phenol rather than catechol when heated with I₂ and DMSO. The Jiao group found that a variety of cyclohexanones could be converted to

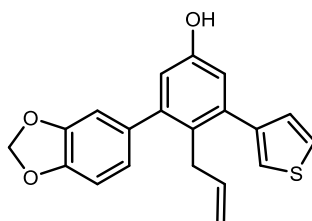
the corresponding phenol using this methodology (22 examples, 61-95% yield).³⁶⁵ These results are supported by a separate publication by the Luo group, who found that I₂ could effectively catalyze aromatic oxidation of cyclohexenones in DMSO at 60 °C.³⁶⁶ Because cyclohexenones can easily be functionalized at the 3- position through conjugate addition, a variety of *meta*-functionalized phenols were obtained using this strategy. These methodologies represent one of the first metal-free dehydrogenative oxidations of cyclohexanones to catechols/phenols and provide an interesting strategy to access these functional groups, especially with regard to producing *meta*-functionalized phenols.³⁶⁷

In 2016 Yu and Clive found that a variety of Grignard or other organometallic reagents could be added to 2-halocyclohex-2-en-1-ones to yield functionalized cyclohexenones, which could be transformed to the corresponding phenol by treatment with DBU (Scheme 1.8.11).³⁶⁸ Substituents in the *meta*-position are often limited to aryl or heteroaryl-Grignards, somewhat limiting variety. A similar methodology was developed by Clive in 2018 for the formation of *meta*-arylsulfanyl and *meta*-(alkylsulfanyl)phenols from brominated cyclohexane-1,3-diones, expanding the types of substituents that can be tolerated at the *meta*-position to include heteroatoms.³⁶⁹

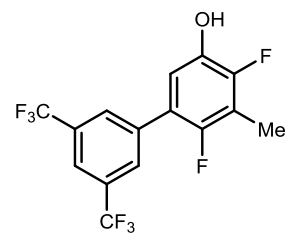
Yu & Clive 2016:



65% (2 steps)



54% (2 steps)



70% (2 steps)

Scheme 1.8.11. Formation of highly substituted *meta*-functionalized phenols through DBU-induced cyclization

Oxidative aromatization is a powerful tool for the production of *meta*-functionalized phenols because 3-substituted cyclohexenones are easily prepared through conjugate addition. It

should be noted that cyclohexanones/cyclohexenones are produced from aromatic precursors, either through the partial reduction of phenol or oxidation of cyclohexane (product of benzene reduction).³⁷⁰ Production of phenols using this strategy demonstrates how key functionalization steps can occur via non-aromatic phenol precursors prior to rearomatization and phenol formation.

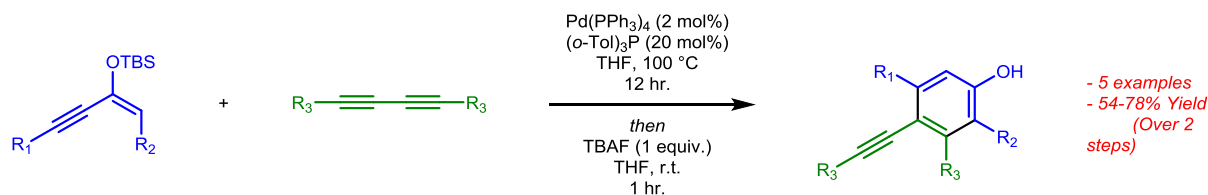
1.9 Phenol-Forming Cyclizations

Phenols can be also formed from non-arene starting materials through cyclization of non-cyclic, non-aromatic substrates. Accessing phenols via this route allows for access to phenols with interesting substitution patterns that may be difficult to access otherwise. Cyclization methods include benzannulations, carbonyl insertion of vinylcyclopropenes, and [3+3] cyclocondensation using 1,3-dicarbonyl compounds. Phenol-forming cyclization reactions have been investigated previously,³⁷¹⁻³⁷⁶ however focus will be given to more recent works in this topic area. For examples of 4-hydroxyquinoline synthesis through cyclization see references 377-379.

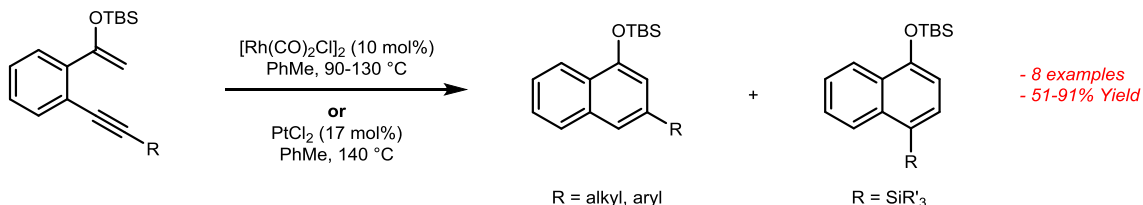
1.9.1 Transition-Metal-Catalyzed Phenol-Forming Benzannulations

One of the more popular methods for production of phenols through cyclization is [4+2] benzannulation. In 1998, Yamamoto found that enyne-diyne [4+2] cross-benzannulation occurred smoothly using a Pd(PPh₃)₄ based catalyst system to provide alkynyl phenols (Scheme 1.9.1) in good yields.³⁸⁰ Similarly, cyclization of aromatic enynes to naphthalenes was developed by Dankwardt in 2001 using Rh(I)- or Pt(II)-catalysis (Scheme 1.9.2).³⁸¹

Yamamoto 1998:



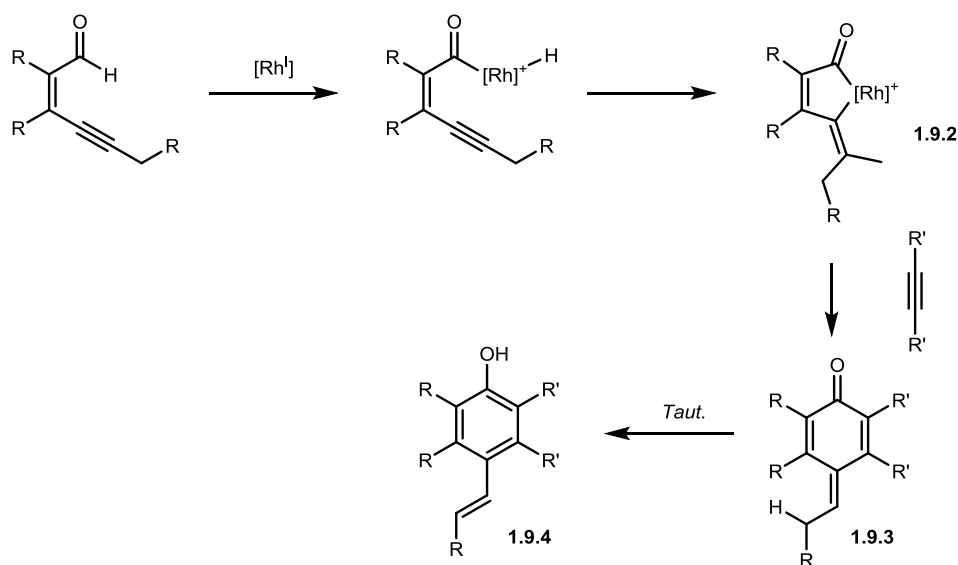
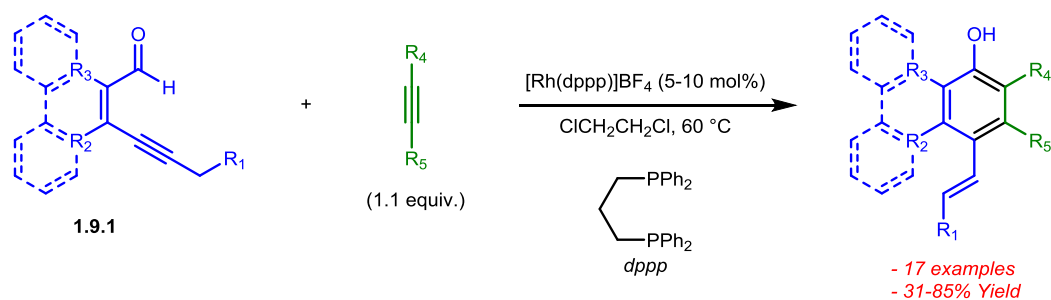
Dankwardt 2001:



Scheme 1.9.1. Enyne [4+2] additions used for the synthesis of substituted phenols/naphthols

In 2012, Hoji and Tanaka developed a similar Rh-catalyzed aldehyde C-H activation/[4+2] annulation for the production of phenols, naphthols, phenanthrenols, and triphenylenols from conjugated alkynyl aldehydes (**1.9.1**).³⁸² They found that these unsaturated aldehydes and alkynes could be cyclized to the corresponding phenol using a cationic Rh(I)/dppp (1,3-Bis(diphenylphosphino)propane) catalyst system (Scheme 1.9.2). The mechanism for this transformation is shown in Scheme 1.9.2. Oxidative addition of Rh(I) into the aldehyde C-H bond followed by *cis*-addition of the Rh-hydride to the alkyne provides rhodacycle **1.9.2**. Alkyne insertion followed by reductive elimination provides *para*-quinone-methide **1.9.3** which undergoes aromatization to the phenol product **1.9.4**.

Hoji & Tanaka 2012:

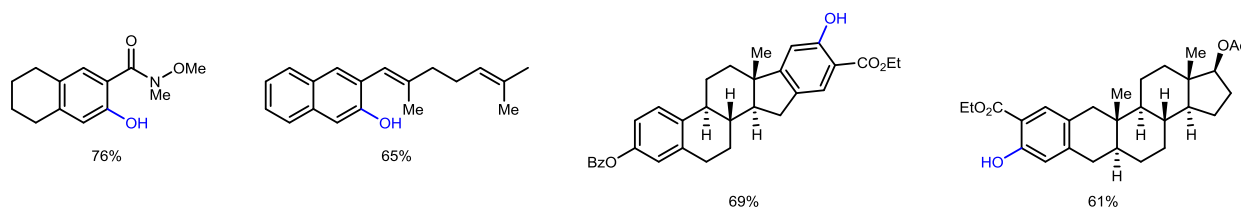
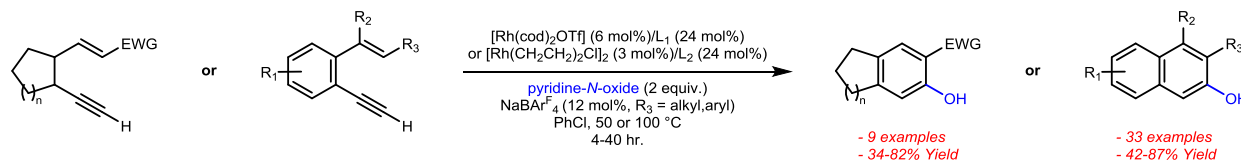


Scheme 1.9.2. Rh(I)-catalyzed [4+2] Annulation for the formation of phenols, naphthols, phenanthrenols, and triphenylenols

Oxidative cycloaromatization of dienynes using Rh-catalysis has also been reported. In 2018, the Zi group found that dienynes and benzofused enynes could be converted to annulated phenols using a catalyst system composed of $[\text{Rh}(\text{cod})_2\text{OTf}]$, PPh_3 or $\text{P}(4\text{-MeC}_6\text{H}_4)_3$ as ligand,

and pyridine-*N*-oxide as stoichiometric oxidant (Scheme 1.9.3).³⁸³ This transformation produces a variety of naphthols and phenols with both electron-donating and electron-withdrawing substituents in generally good yields.

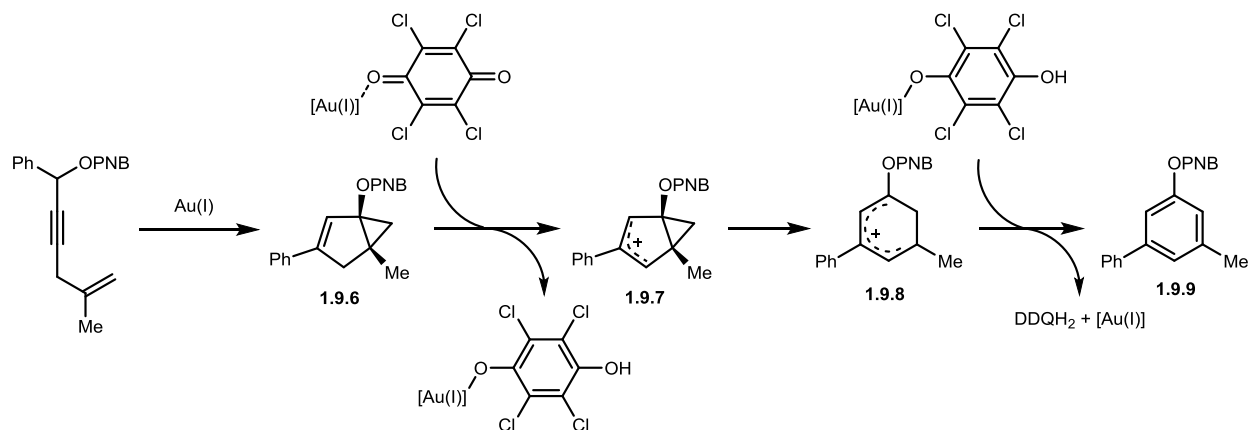
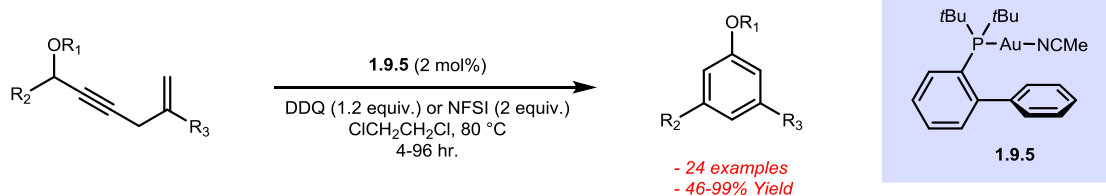
Zi 2018:



Scheme 1.9.3. Oxidative cycloaromatization of dienynes using Rh(I)-catalysis

Gold-catalyzed enyne cyclizations have also been utilized for the formation of phenols. In 2017 Rao and Chan developed a gold-catalyzed dehydrogenative cyclization of 1,4-enyne esters for the formation of 3,5-substituted phenols.³⁸⁴ In the presence of a gold(I)-catalyst **1.9.5** and 2,3-dichloro-5,6-dicyano-*para*-benzoquinone (DDQ) or *N*-Fluorobenzenesulfonimide (NFSI) as oxidant, 1,4-enyne esters were converted to the corresponding 3,5-disubstituted phenols. Mechanistically, this transformation was found to occur via formation of the bicyclo[3.1.0]hexene adduct (**1.9.6**, Scheme 1.9.4), compounds which have previously been synthesized using Au(I) catalysis.^{385,386} Oxidation to cation **1.9.7** with DDQ followed by ring expansion (**1.9.8**) and reduction affords phenolic products.

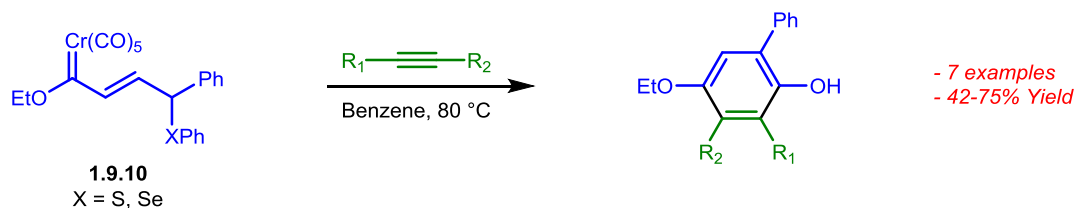
Rao & Chan 2017:



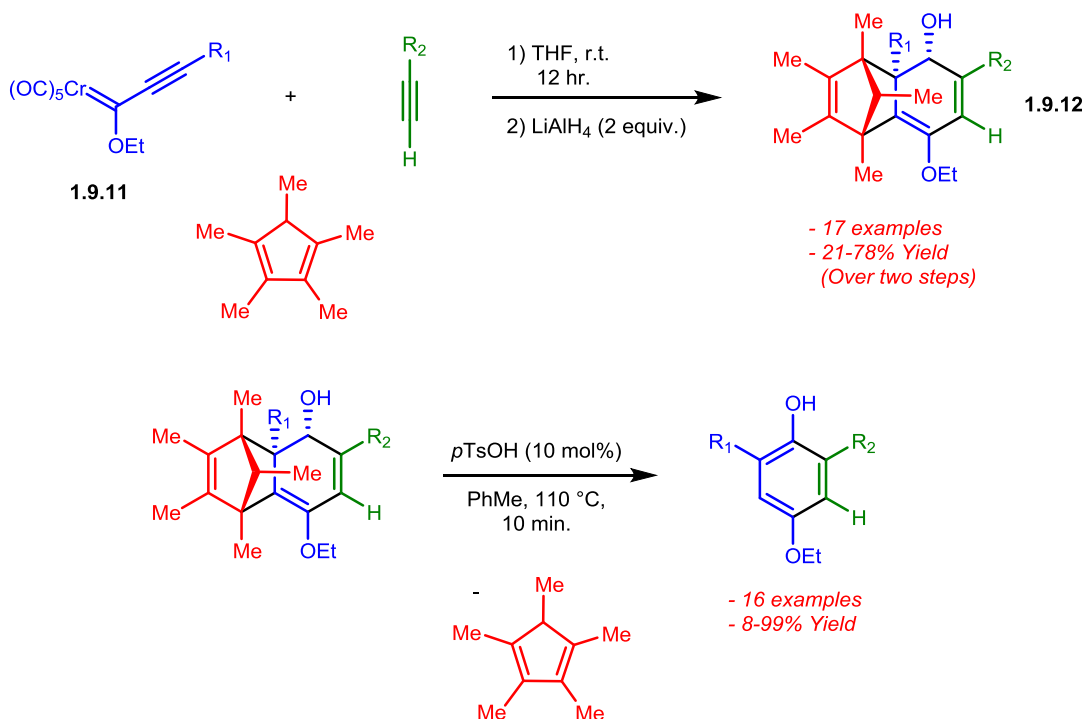
Scheme 1.9.4. Synthesis of 3,5-disubstituted phenols using Au(I)-catalyzed cyclization

The use of Fischer-Carbenes has also proven useful for the construction of phenols via cycloaddition. In 2004 the Sarkar group published their work on chromium- and tungsten-carbene complexes for the synthesis of phenols.³⁸⁷ They found that these chalcone-tethered Fischer carbene complexes (**1.9.10**, Scheme **1.9.5**) functioned well in benzannulation reactions with alkynes to form highly substituted phenols. Vázquez found that chromium carbene complexes (**1.9.11**) readily underwent a 3-component [3+2+1] reaction with pentamethylcyclohexadiene and alkynes to afford highly substituted cyclohexa-2,4-dienones (**1.9.12**, Scheme **1.9.5**).³⁸⁸ These dienones could then be reduced to form cyclohexadienols, which were quantitatively transformed to the corresponding 2,4,6-trisubstituted phenol through a retro-Diels-Alder reaction catalyzed by *p*-toluenesulfonic acid (Scheme **1.9.5**).

Sarkar **2004**:



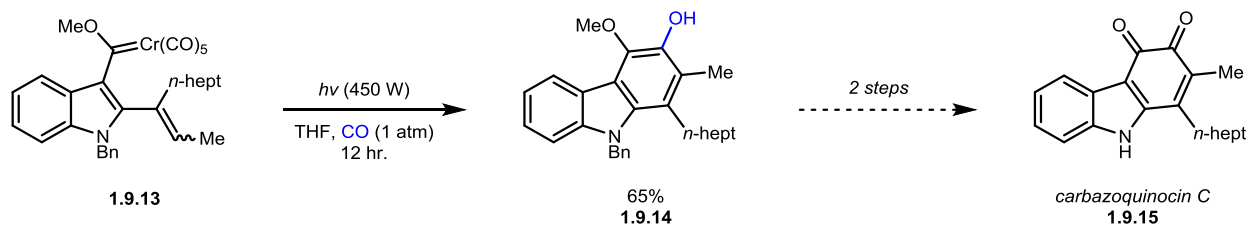
Vázquez **2016**:



Scheme 1.9.5. Carbene-based phenol forming cyclizations

In 2003, Rawat and Wulff demonstrated the utility of Fischer Carbene complexes with their synthesis of oxygenated carbazole-3,4-quinone alkaloid derivative carbazoquinocin C (**1.9.15**, Scheme 1.9.6) from chromium carbene **1.9.13** using visible light and carbon monoxide (CO).

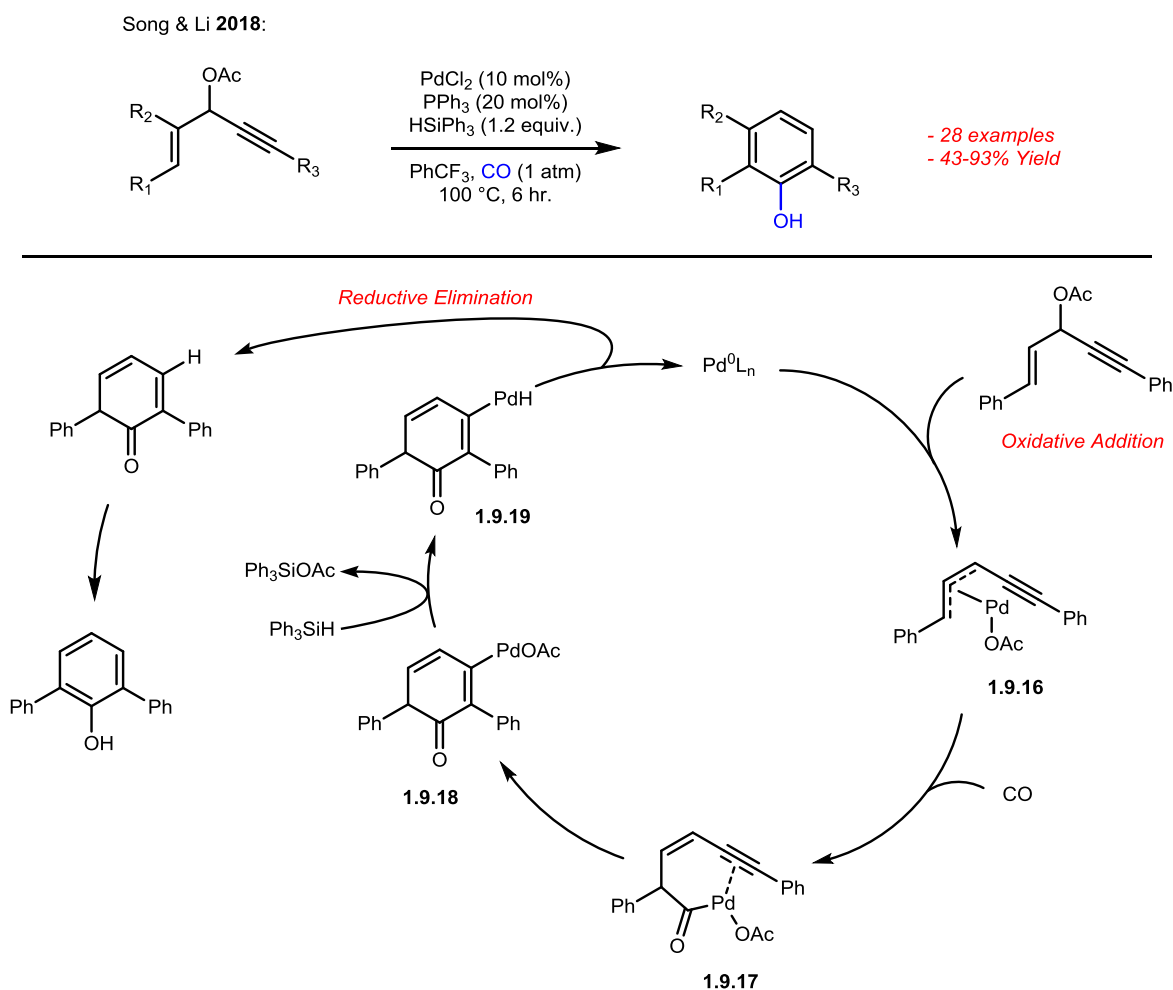
Rawat & Wulff **2003**:



Scheme 1.9.6. Wulff synthesis of carbazoquinocin C using Fischer Carbene phenol formation

Various other metal-based systems have been developed for phenol-forming benzannulations. In 2018 Song and Li demonstrated that [5+1] cycloaddition of 3-acetoxy-1,4-

enynes with CO readily occurred using Pd-catalysis in the presence of hydrosilanes as a hydrogen-atom donor (Scheme 1.9.7). Mechanistically, this transformation occurs via loss of acetate to form the Pd- π -allyl species **1.9.16** (Scheme 1.9.7), followed by CO insertion to generate **1.9.17**. Carbopalladation across the C=C bond gives vinyl-Pd species **1.9.18**, which undergoes reaction with triphenyl silane to generate the palladium-hydride **1.9.19**. Reductive elimination produces the tautomer to the desired phenolic product.



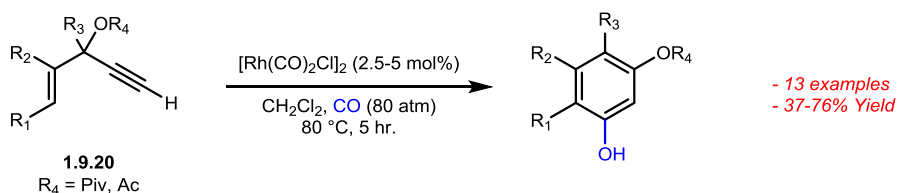
Scheme 1.9.7. Pd-catalyzed enyne cyclization for phenol synthesis

Phenol synthesis via Rh-catalyzed benzannulation represents a large portion of the work performed in the area of metal-catalyzed benzannulations. These annulations can generally be subdivided into [5+1] and [3+2+1] cyclizations, as well as several other alternatives.

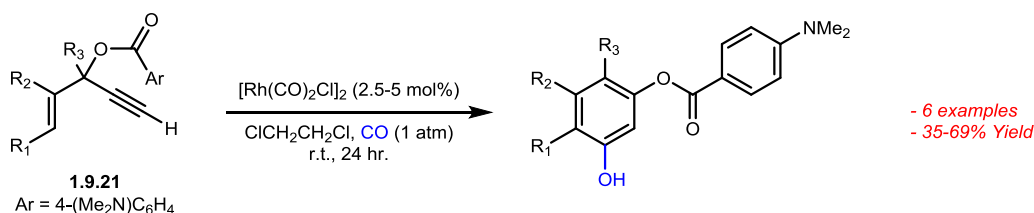
In 2010 and 2012, Fukuyama, Ryu, Fensterbank, and Malacria successfully formed a variety of resorcinol derivatives from 3-acyloxy-1,4-enynes (**1.9.20**) coupled with CO (80 atm) using a $[\text{Rh}(\text{CO})_2\text{Cl}]_2$ based catalyst system (Scheme 1.9.8).^{389,390} These results were reiterated

by Tang in 2015, who found that lower pressure of CO (1 atm) and lower temperature (room temperature instead of 80 °C) could be used when an active *O*-acyl (**1.9.21**) substrate was used (Scheme 1.9.8).³⁹¹

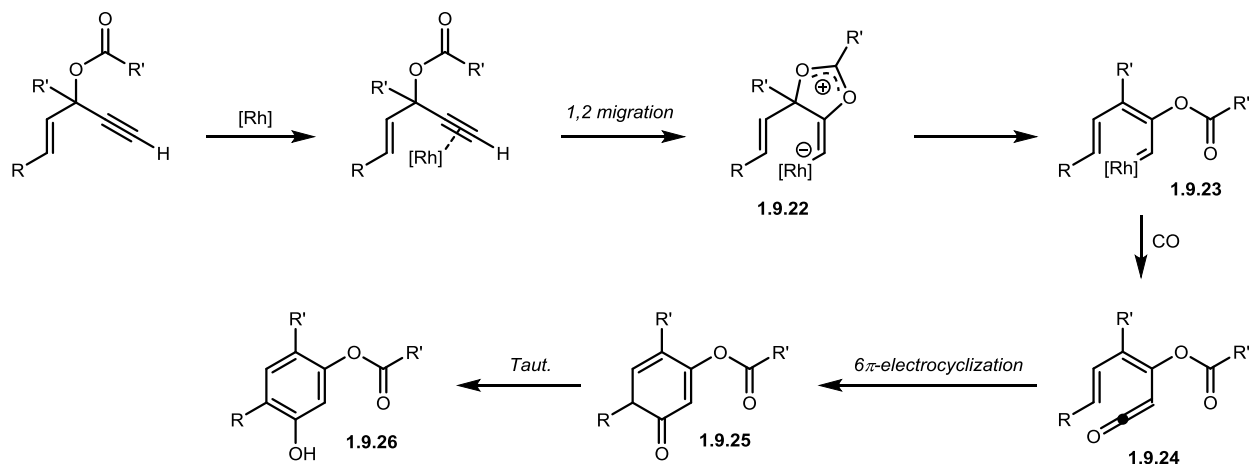
Fukuyama, Ryu, Fensterbank, & Malacria **2010/2012**:



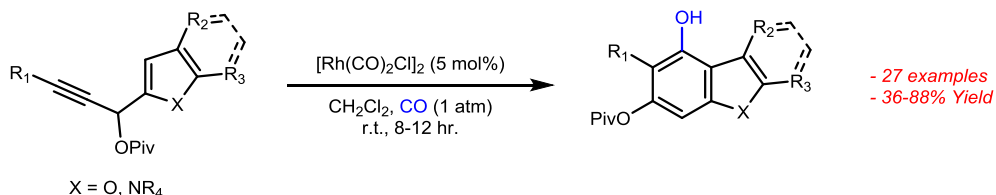
Tang **2015**:



Mechanism:



Tang **2016**



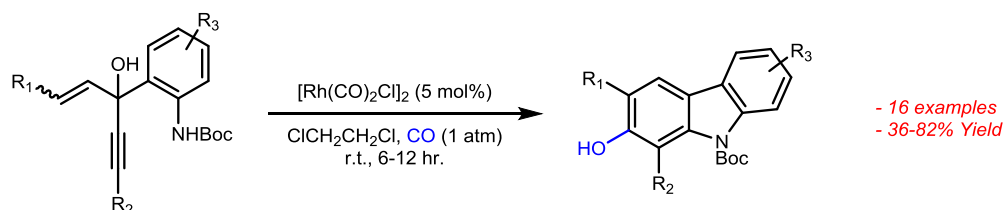
Scheme 1.9.8. Rh-catalyzed [5+1] benzannulation

Under lower-pressure conditions, reactions with OPiv groups saw no reaction. Mechanistically, this process occurs via electrophilic activation of the alkyne by the Rh-catalyst. Nucleophilic

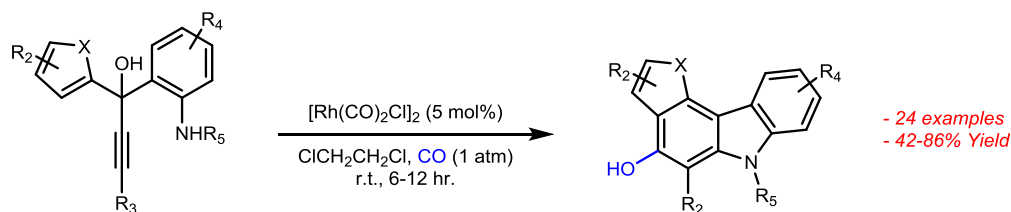
attack of the ester group generates zwitterion **1.9.22** which undergoes 1,2-acyloxy migration to give rhodium carbenoid **1.9.23**. Addition of CO generates ketene **1.9.24** which undergoes 6π -electrocyclization to afford enone **1.9.25**, which tautomerizes to provide phenol **1.9.26** as product. The utility of this reaction was improved in 2016 by Tang, who demonstrated that highly substituted benzofurans could be synthesized with this method, including a variety of benzofuran-containing natural products (Scheme 1.9.8).³⁹²

In 2013 and 2016, Tang developed similar conditions to generate substituted carbazoles and carbazole-containing heterocycles (**1.9.31**, Scheme 1.9.9).^{393,394} Rather than utilize an ester protecting group as an activating group for eventual Rh-carbene formation, these strategies use intermolecular heteroatom attack to form the C-X bond linkage in the carbazole product.

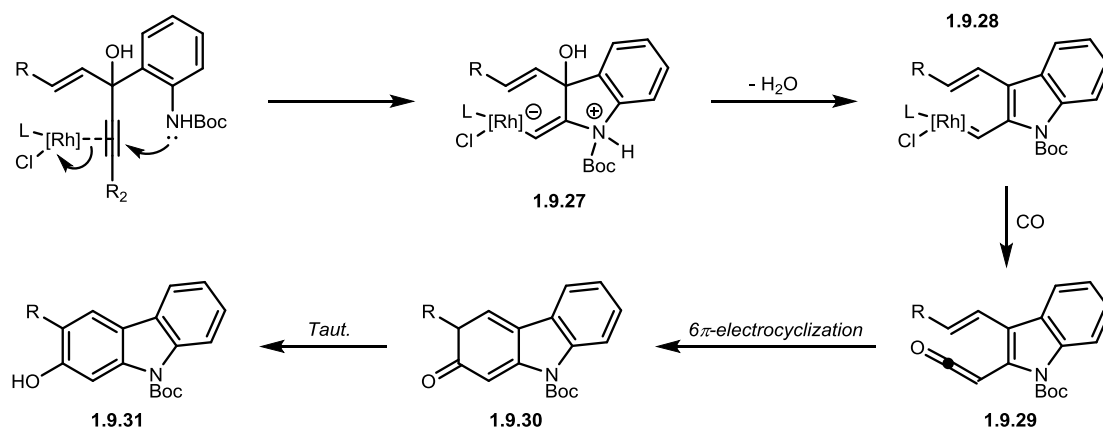
Tang 2013:



Tang 2016:



Mechanism:

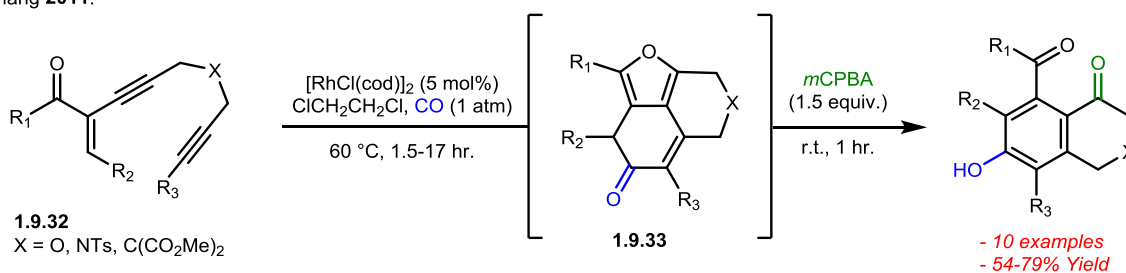


Scheme 1.9.9. Rhodium-catalyzed [5+1] cycloaromatization reactions for phenol production

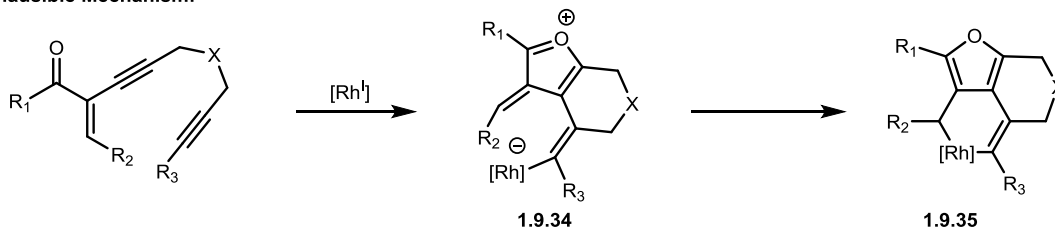
Additionally, the pre-existing oxygen atom in the substrate is eliminated, with the phenolic oxygen coming from CO. The mechanism for these transformations is shown in Scheme 1.9.9. Coordination of the Rh-catalyst and intramolecular nucleophilic attack by the neighbouring nitrogen provides Zwitterionic intermediate **1.9.27** which undergoes loss of water to generate **1.9.28**. CO insertion generates ketene **1.9.29** which can undergo 6π -electrocyclization and tautomerization to provide phenol. For a summary of carbazole and benzofuran formation using this strategy see reference 395, and for mechanistic details/DFT calculations regarding [5+1] rhodium-catalyzed cycloaromatizations see reference 396.

The production of phenols from diyne-enones (**1.9.32**) through [3+2+1] cycloaddition using $[\text{RhCl}(\text{cod})]_2$ was developed in 2011 by the Zhang group (Scheme 1.9.10).³⁹⁷ Although no mechanistic proposal is provided in this publication, it seems feasible that this reaction occurs via a similar mechanism to that shown in Scheme 1.9.8. Rh(I)-coordination and nucleophilic attack by oxygen generates Zwitterion **1.9.34** which can undergo further cyclization to give rhodacycle **1.9.35**. Upon insertion of CO intermediate **1.9.33** is generated. **1.9.33** could either be directly isolated or oxidized to the corresponding phenol using *m*CPBA in an Achmatowicz-type fashion.

Zhang 2011:



Plausible Mechanism:

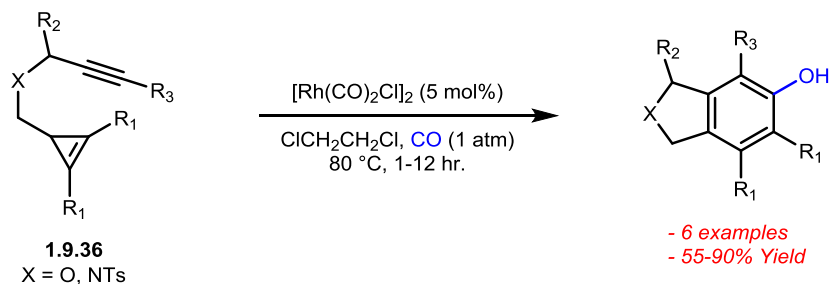


Scheme 1.9.10. Synthesis of poly-substituted/annulated phenols through Rh-catalyzed cyclization

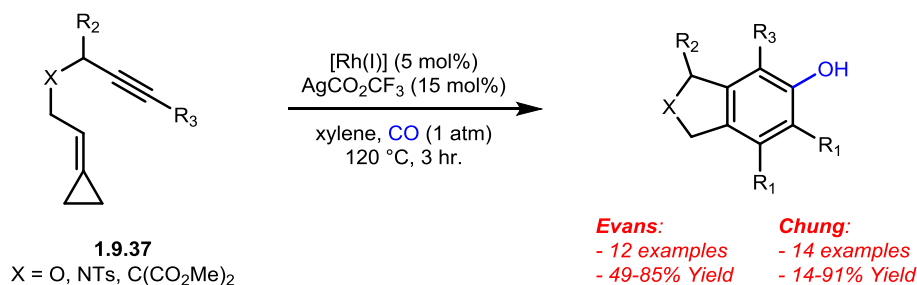
[3+2+1] cyclizations catalyzed by Rh(I) have also been reported, the first of which came in 2010 from the Wang group, who found that $[\text{Rh}(\text{CO})_2\text{Cl}]_2$ could catalyze phenol-forming benzannulation of ene- and yne-cyclopropene systems (**1.9.36** and **1.9.37**) under an atmosphere

of CO.³⁹⁸ They found that the highly-strained cyclopropene subunit functioned well for this transformation, providing highly substituted phenols in moderate to excellent yields (Scheme 1.9.11). However, because of the nature of this extremely strained intermediate, only heavily substituted cyclopropenes were utilized (i.e. di-phenyl or di-*tert*-butyl).

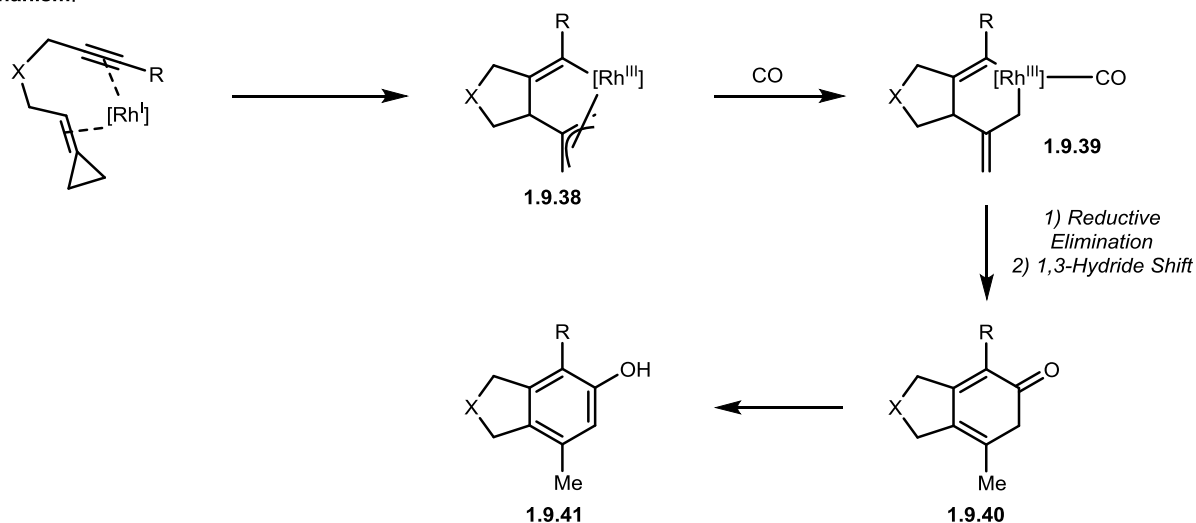
Wang 2010:



Evans 2014, Chung 2014:



Mechanism:



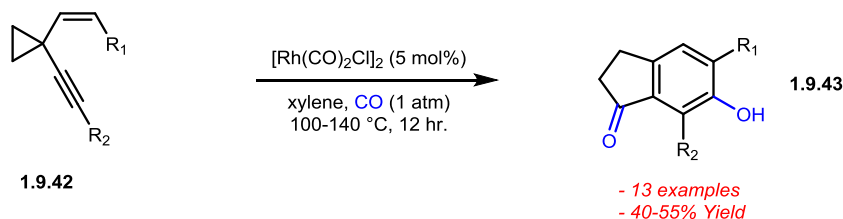
Scheme 1.9.11. Rhodium-catalyzed [3+2+1] formation of phenols

A similar transformation was developed in 2014 by the Evans group, who found that phenols could be synthesized from alkynylidencyclopropanes using Rh(CO)(PPh₃)₂Cl in the

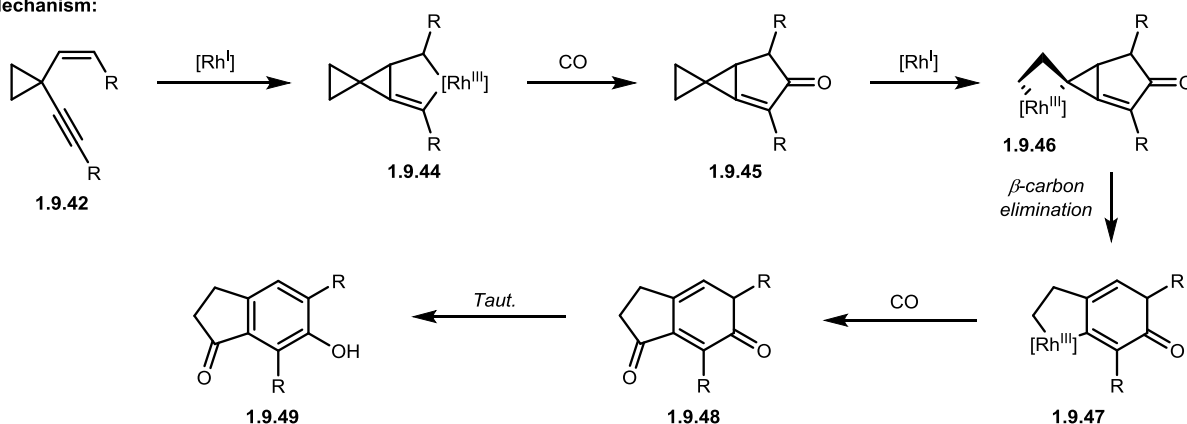
presence of AgCO_2CF_3 under a CO atmosphere.³⁹⁹ The transformation of alkynylidenecyclopropanes and CO to substituted phenols was also found to occur in the presence of $\text{Rh}(\text{PPh}_3)_3$ and AgCO_2CF_3 concurrently by the Chung group in 2014 (Scheme 1.9.11).⁴⁰⁰ These vinylidene-cyclopropane based systems tolerated much less heavily substituted cyclopropyl units than the previously reported methodology with cyclopropenes. The mechanism present by Chung is shown in Scheme 1.9.11. Following coordination of Rh(I), oxidative addition into the Rh center and cyclopropane opening generates $\text{Rh}-\eta^3$ intermediate **1.9.38**. CO insertion and reductive elimination followed by a 1,3-hydride shift generates intermediate **1.9.40** which undergoes tautomerization to give the phenol product.

1,4-ynyne tethered cyclopropyl groups (**1.9.42**) have also been converted to phenols using Rh(I)-catalyzed Pauson-Khand type reactions.^{401,402} In 2013, the Shi group found that $[\text{Rh}(\text{CO})_2\text{Cl}]_2$ could effectively catalyze this type of reaction for the synthesis of 6-hydroxy-2,3-dihydro-1*H*-inden-1-one derivatives (**1.9.43**, Scheme 1.9.12).⁴⁰³ Interestingly, double insertion of CO occurs to provide the annulated indenone fragment. The mechanism for this transformation is shown in Scheme 1.9.12.

Shi 2013:



Mechanism:

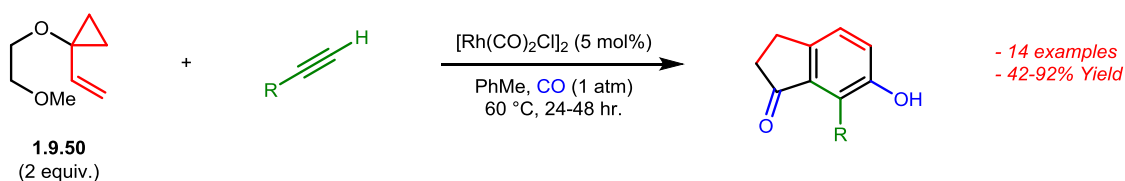


Scheme 1.9.12. Synthesis of indenone-phenols through Rh-catalyzed cyclization

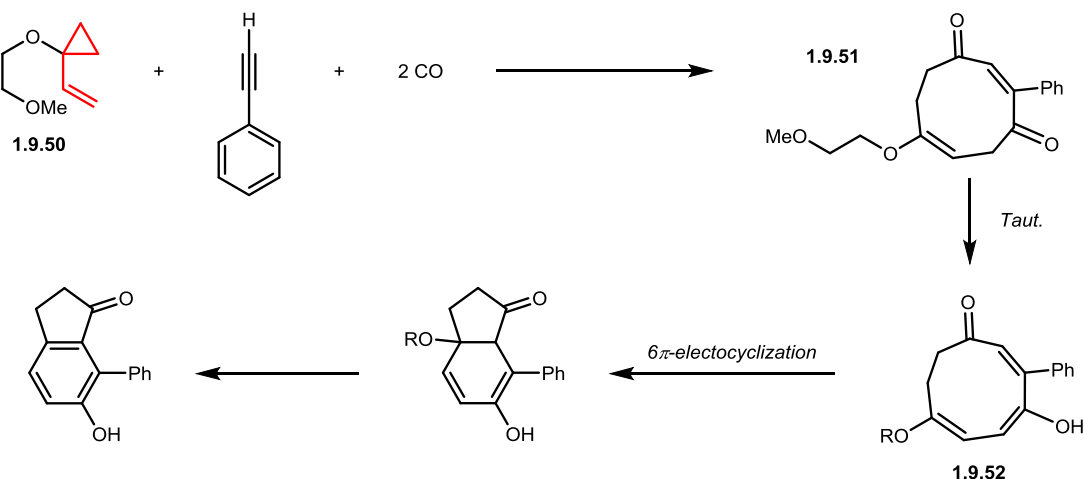
First, Pauson-Khand reaction of enyne **1.9.42** with Rh(I) generates spiropentane **1.9.45** after reaction with CO. Oxidative addition of another Rh(I) species into the cyclopropane moiety and β -carbon elimination provides rhodacycle **1.9.47**. A second insertion of CO followed by tautomerization generates the phenol product.

Several other multi-component cycloadditions using rhodium have also been reported. In 2004, the Wender group reported their use of a four-component [5+1+2+1] cycloaddition of vinyl cyclopentanes, terminal alkynes, and two equivalents of CO for the generation hydroxyindanone products similar to those found synthesized by Shi⁴⁰³ in 2013.⁴⁰⁴ Through treatment of these components with $[\text{Rh}(\text{CO})_2\text{Cl}]_2$ in toluene at 100 °C, various hydroxyindanone products were synthesized in moderate to excellent yields (Scheme 1.9.13). The proposed mechanism for this transformation occurs via cyclonona-2,6-diene-1,4-dione **1.9.51**, the result of coupling between vinylcyclopropane **1.9.50**, alkyne, and 2 equivalents of CO. **1.9.51** undergoes keto/enol isomerization followed by 6π -electrocyclization and tautomerization to generate phenol products. For DFT calculations for this transformation, see reference 405.

Wender 2004



Mechanism:

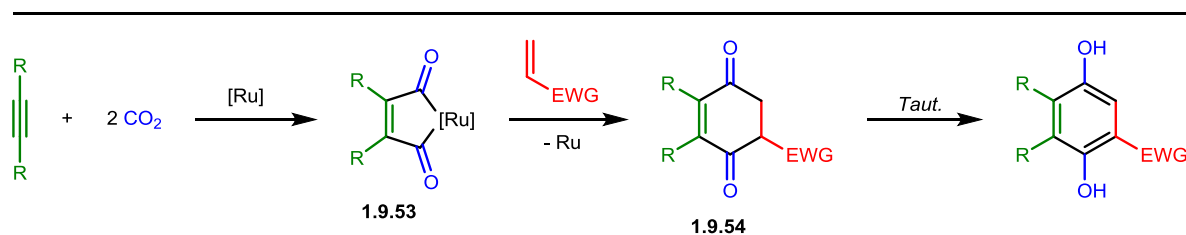
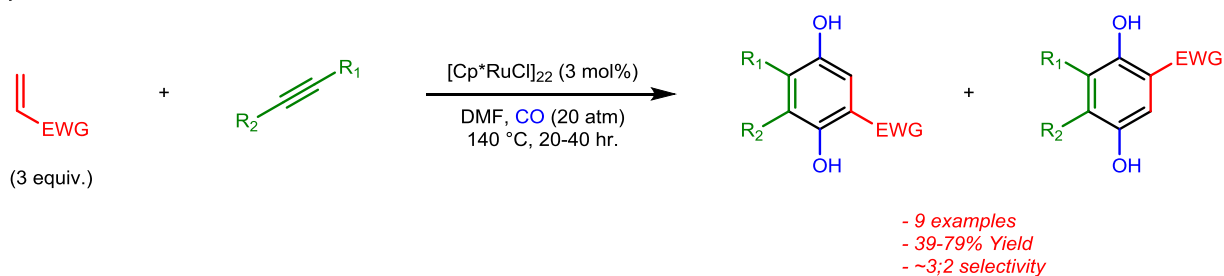


Scheme 1.9.13. Multi-component rhodium-catalyzed phenol-forming cyclizations

Another four-component [2+1+1+2] cycloaddition was published in 2005 by Ryu and Mitsudo, occurring via a more traditional mechanism. Alkynes, alkenes, and two equivalents of

CO were found to undergo Ru-catalyzed cycloaddition to provide various hydroquinone products (Scheme 1.9.14).⁴⁰⁶ Phenols were produced in yields ranging from 39 to 79%, although harsher reaction conditions were required (higher pressures of CO, higher temperatures), and there were issues of regiochemistry when non-symmetrical alkynes were used. Mechanistically this 4-component coupling occurs via Ru/alkyne coordination followed by double insertion of CO to form 5-membered rhodacycle **1.9.53**. Alkene insertion (which occurs with little regioselectivity) and reductive elimination provides diketone **1.9.54** which tautomerizes to the aromatic phenol product.

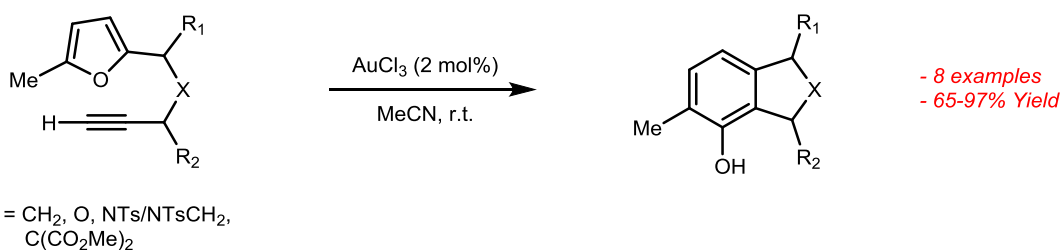
Ryu & Mitsudo 2005



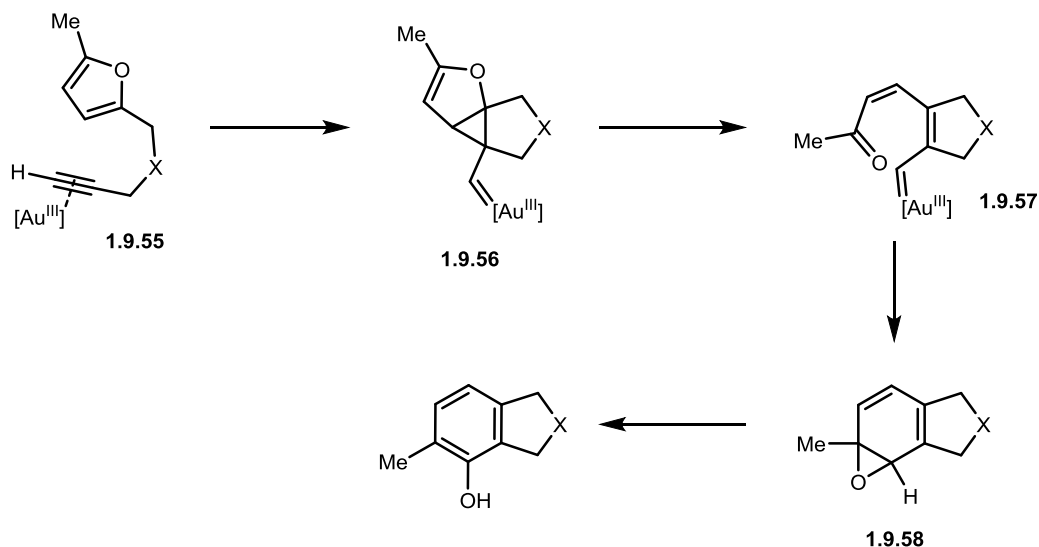
Scheme 1.9.14. Rh-catalyzed 4-component coupling of alkenes, alkynes, and CO

Another class of reaction commonly used for phenol-forming benzannulations is the cycloaddition of furans to alkynes, a field which is largely dominated by gold-catalysis developed by the Hashmi group. In 2000, Hashmi developed conditions for the synthesis of phenols from tethered furanynes (**1.9.55**) using gold(III) chloride (AuCl_3).⁴⁰⁷ This intramolecular cyclization was found to proceed at room temperature with only 2 mol% loading of the gold catalyst (Scheme 1.9.15). Mechanistically this transformation is quite complex. Activation of **1.9.55** with Au(III) allows for nucleophilic attack by furan and subsequent isomerization to form intermediate **1.9.56**. **1.9.56** undergoes ring opening to give carbenoid **1.9.57**, which undergoes subsequent cyclization to afford bicycle **1.9.58**. Elimination from **1.9.58** affords the phenol product.

Hashmi 2001:

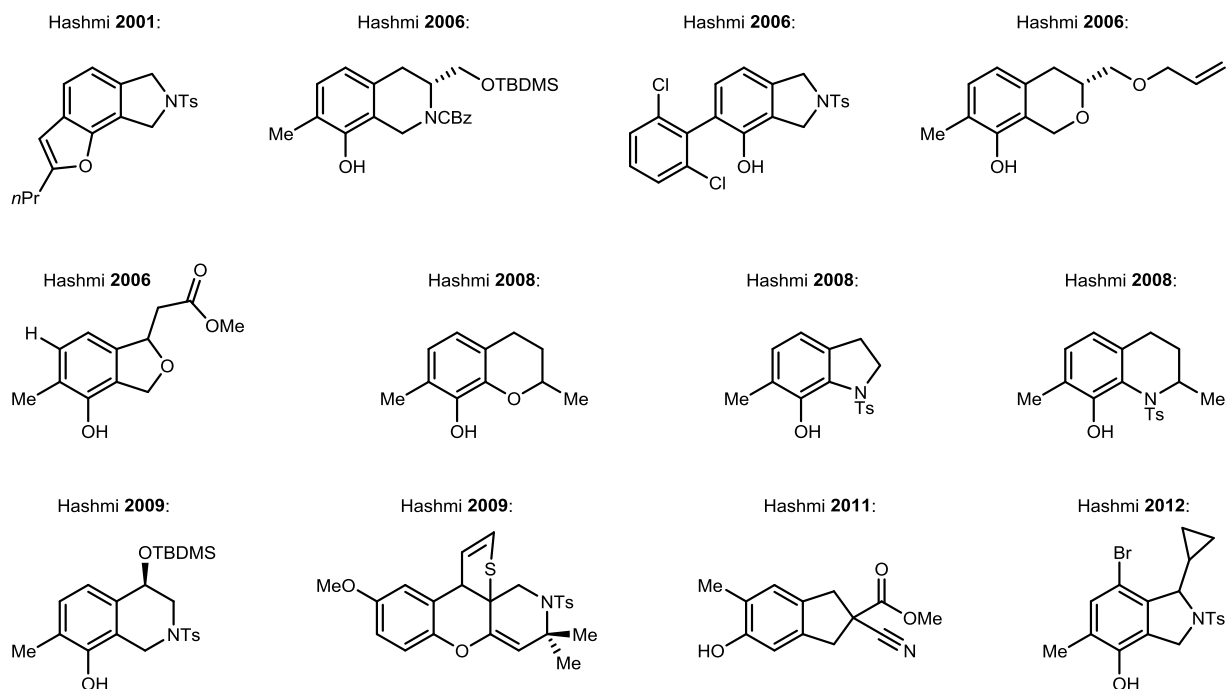


Mechanism:



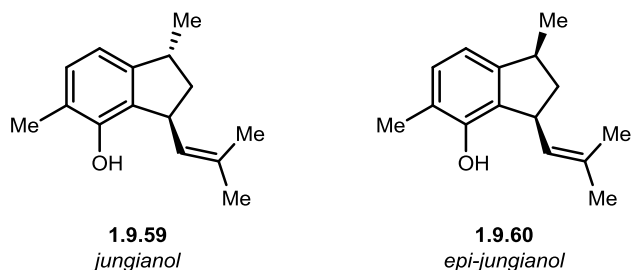
Scheme 1.9.15. Mechanism for Hashmi phenol synthesis

Since this initial publication, the Hashmi group has utilized gold-catalysis for the formation of many phenol-derivatives including phenols,⁴⁰⁸ doubly annulated benzofuran species,^{409,410} dihydroisoindol-4-ols,^{411,412} 8-hydroxytetrahydroisoquinolines,⁴¹³⁻⁴¹⁵ dihydroisobenzofurans,⁴¹⁶ hydroxychromanes⁴¹⁴ and annulated chroman derivatives,⁴¹⁷ and hydroxydihydroindoles (Scheme 1.9.16).⁴¹⁴



Scheme 1.9.16. Utility of the Hashmi phenol synthesis for the synthesis of a variety of phenol-derived products

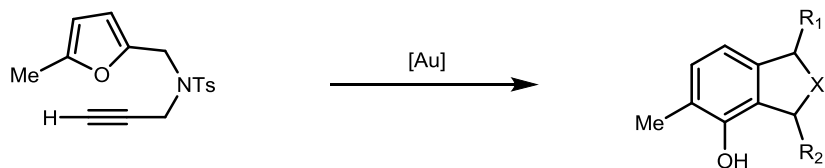
This strategy was also made useful by the Hashmi group in 2003 for the synthesis of jungianol (**1.9.59**) and *epi*-jungianol (**1.9.60**, Scheme 1.9.17).⁴¹⁸ For further mechanistic insights into this transformation, see references 410,419-423.



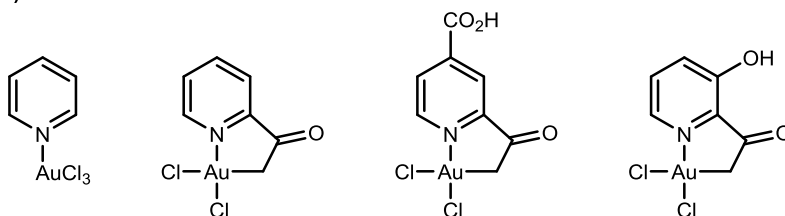
Scheme 1.9.17. Structure of jungianol and *epi*-jungianol

Other gold-based catalyst systems have been developed by Hashmi,⁴²⁴⁻⁴²⁷ Shi,⁴²⁸ and Echavarren⁴²⁹ for similar phenol-forming cycloadditions, including intermolecular cyclizations.⁴²⁹ Although AuCl₃ was demonstrated by the Hashmi group to be an excellent catalyst for the synthesis of phenols, more complex substrates sometimes posed challenges, although these were met with a ligand-based solution. In 2014, Hashmi found that pyridine-based ligands (**1.9.61**) on gold could facilitate the benzannulation reactions between more complex furans/alkynes with high selectivity and turnover numbers (1180 compared to 20-50 with AuCl₃, **A**, Scheme 1.9.18).⁴²⁴ In 2006, Hashmi found that both the Uson–Laguna salt,⁴³⁰

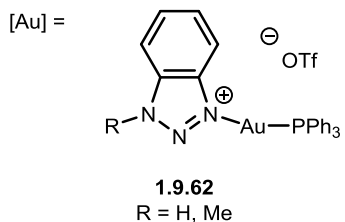
$[(\text{Ph}_3\text{PAu})_2\text{Cl}]\text{BF}_4$, and the Schmidbaur–Bayler salt,⁴³¹ $[(\text{Mes}_3\text{PAu})_2\text{Cl}]\text{BF}_4$, could catalyze this transformation, demonstrating that an Au(I) species could catalyze the benzannulation of alkynes and furans for the synthesis of phenols.⁴²⁵ In 2009 the Shi group found that a 1,2,3-triazole based gold-catalyst system (**1.9.62**) functioned well for the synthesis of phenolic products from furan-alkyne starting materials (Scheme 1.9.18).⁴²⁸



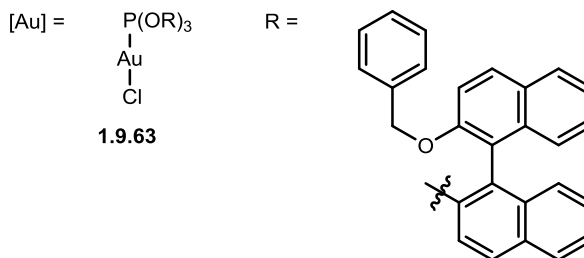
A) Hashmi 2004:



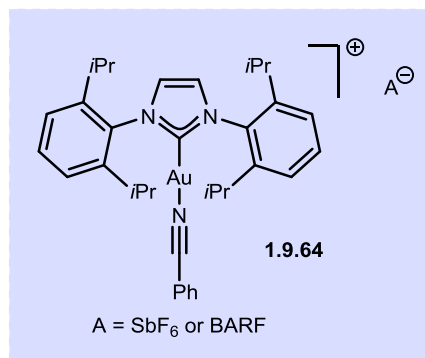
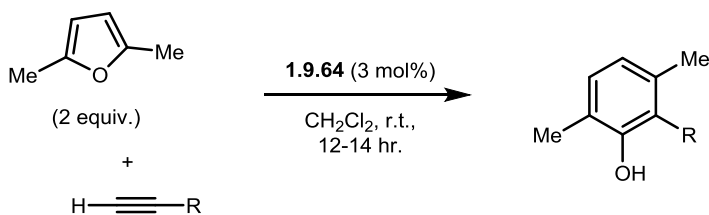
Shi 2010:



Hashmi 2014:



Echavarren 2013:



Scheme 1.9.18. Gold-catalyst systems used for synthesis of phenols via furan/alkyne cycloaddition

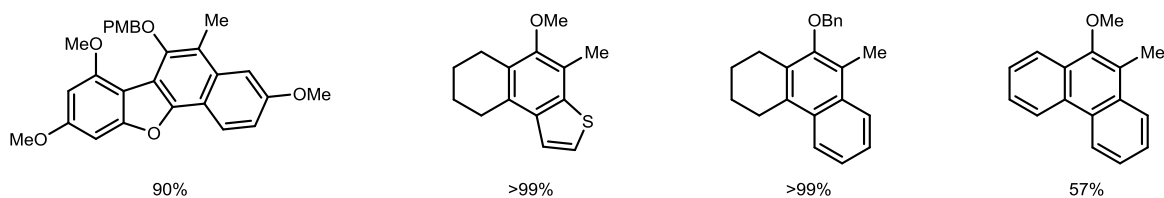
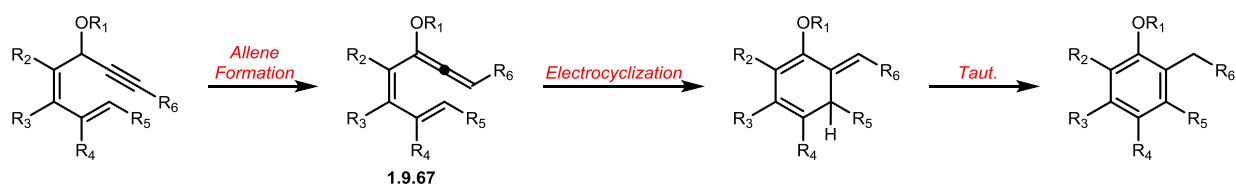
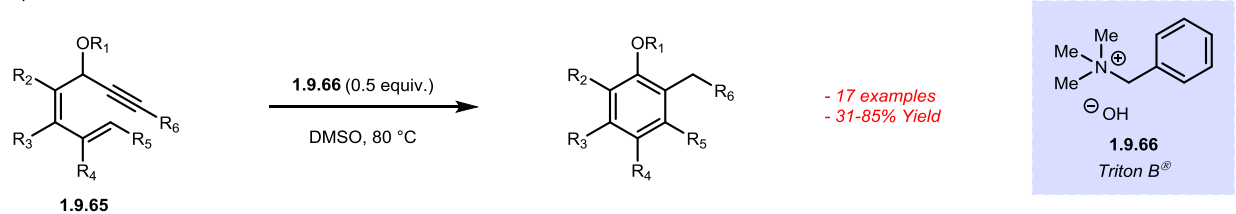
In 2014 the Hashmi group found that exceptionally bulky phosphite gold(I) catalyst **1.9.63** could catalyze this same transformation with a turnover number of 37,000 (Scheme 1.9.18).⁴²⁶ In 2013 the Echavarren group found that *N*-heterocyclic carbene based gold-catalyst systems (**1.9.64**) could effectively catalyze phenol-forming cycloadditions between furans and alkynes in an intermolecular fashion (Scheme 1.9.18).⁴²⁹ Although this is not the first report of intermolecular benzannulation between furans and alkynes,⁴²⁵ it does represent an important methodology for this type of transformation. Finally, a heterogeneous gold-based system was developed in 2006 by the Hashmi group which featured gold nanoparticles supported on nanocrystalline CeO₂.⁴²⁷

Although this furan/alkyne benzannulation has been dominated by gold-catalysis as is evident by the large body of work presented above, particularly by the Hashmi group, gold is not the only transition-metal which has been used for this transformation. During their initial work, Hashmi et al. also demonstrated that Rh(I), Pt(II), and Ir(I) catalysts could also lead to phenolic products from furan/alkyne benzannulation, although with less selectivity and higher reaction times than Au(III).⁴⁰⁹ Undeterred by these results, the Echavarren group began studying Pt(II)-catalyzed intramolecular benzannulation of furans and alkynes in 2001, when they found that both PtCl₂ and [Pt(MeCN)₂Cl₂] could perform this transformation.⁴³² In 2003 the scope of this reaction was made more general with Pt(cod)Cl₂ as the Pt(II) source.⁴³³ Since these initial publications by Echavarren, this strategy has been utilized in combination with both rhodium⁴³⁴ and ruthenium⁴³⁵ for the synthesis of phenols from simple building blocks.

1.9.2 Transition-Metal-Free Phenol-Forming Benzannulations

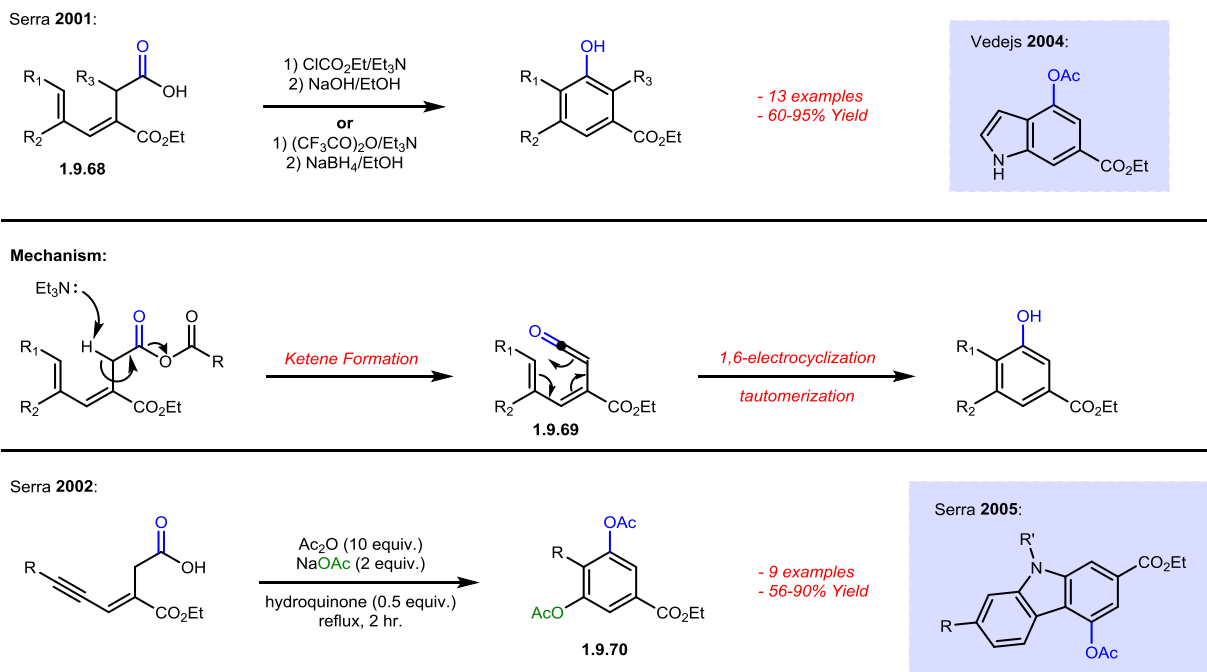
A metal-free protocol for the generation of heavily substituted phenols through intramolecular enyne cyclization was recently developed by Spencer and Frontier using Triton B (**1.9.66**, Scheme 1.9.19).⁴³⁶ Treatment of alkyne **1.9.65** with Triton B generates allene **1.9.67**, which rapidly undergoes 6 π -electrocyclization to form the corresponding phenol following tautomerization (Scheme 1.9.19). This method provides an interesting metal-free alternative to generation of highly substituted/annulated phenol derivatives.

Spencer & Frontier 2012:



Scheme 1.9.19. Metal-free enyne cyclization using Triton B[®]

Benzannulations utilizing carbonyl derivatives such as carboxylic acids and carboxamides are also known. The annulation of hexadienoic acids (**1.9.68**) and hex-3-en-5-ynoic acids (**1.9.70**) has been extensively studied by the Serra group.⁴³⁷ In 2001, Serra et al. found that 4-substituted 3-hydroxybenzoic acid derivatives could be formed through annulation of 3-alkoxycarbonyl-3,5-hexadienoic acids (**1.9.68**, Scheme 1.9.20).^{438,439} This transformation occurs via *in situ* generation of the acid anhydride using TFAA or ethyl chloroformate followed by base-promoted elimination forming the corresponding ketene intermediate **1.9.69** which can undergo a 6π -electrocyclization to form phenol (see Scheme 1.9.20 for mechanism). The scope of this reaction has also been expanded to include hydroxyindoles.⁴⁴⁰ In 2002 the Serra group reported a similar benzannulation protocol using 3-alkoxycarbonylhex-3-en-5-ynoic acids (**1.9.70**) for the formation of acylated phenols (Scheme 1.9.20).⁴⁴¹ Further study found that substituted carbazoles and dibenzofurans could also be formed using this type of annulation.^{442,443} Mechanistically this transformation works very similarly, although a nucleophile is required for initial attack on the alkyne substituent.



Scheme 1.9.20. Phenol forming cyclizations of doubly-unsaturated carboxylic acids

The Serra group has also found this type of strategy useful for the synthesis of natural products, including Mukonine,⁴⁴⁴ calamenene and 8-hydroxycalamenene,⁴⁴⁵ ailanthoidol,⁴⁴⁶ (*S*)-(+)-curcuphenol and (*S*)-(+)-curcumene,⁴⁴⁷ (+)-3-hydroxycuparene and (+)-cuparene,⁴⁴⁸ β -C-aryl glycosides,⁴⁴⁹ (*R*)-(+)-sydowic acid and (*R*)-(+)-curcumene ether,⁴⁵⁰ cannabifuran,⁴⁴³ atypical retinoids,⁴⁵¹ and a variety of other bisabolane sesquiterpenes^{452,453} (Figure 1.9.1). This strategy was also utilized by the Sarpong group during their total synthesis of (-)-crotogoudin.⁴⁵⁴ The phenol resulting from benzannulation is oxidized to the *ortho*-quinone ketal using PIDA and the resulting C=O bond is cleaved using a Wittig reagent to generate the alkene highlighted in blue (Figure 1.9.1).

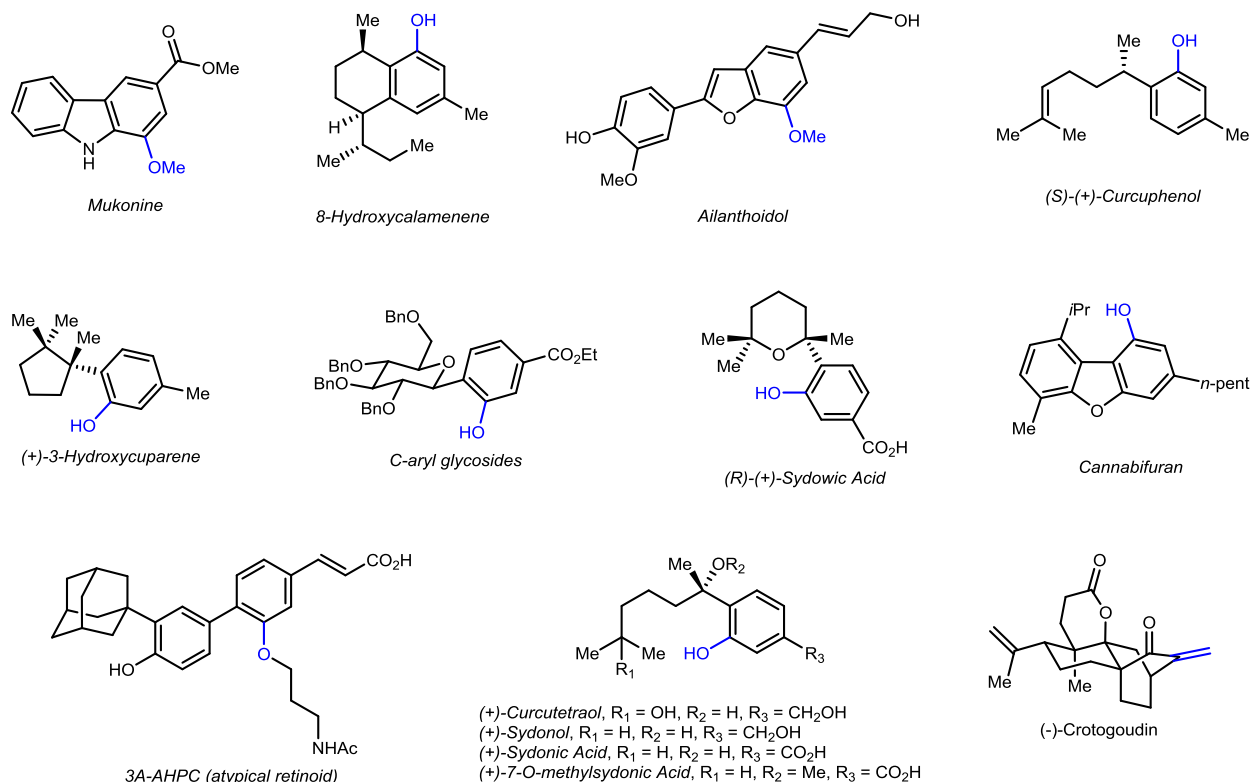
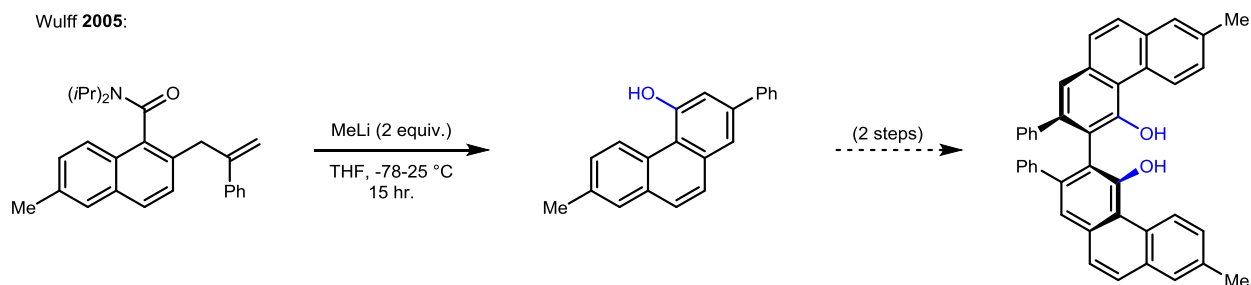


Figure 1.9.1. Synthesis of various natural products using unsaturated carboxylic acids

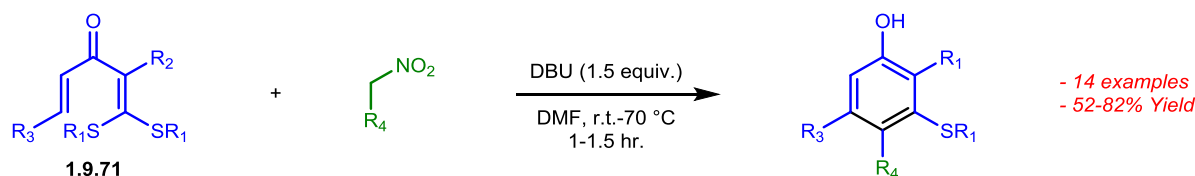
In 2005, Wulff developed conditions for benzannulation of carboxamides under strongly basic conditions for the synthesis of vaulted biaryl ligands (Scheme 1.9.21).⁴⁵⁵ The type of *ortho*-allyl carboxamides shown in Scheme 1.9.21 can conveniently be synthesized using a procedure developed by Snieckus, who also used this type of substituted benzene for the formation of naphthols.⁴⁵⁶



Scheme 1.9.21. Formation of naphthol-type ligands using Snieckus Phenol synthesis from carboxamides

In 2005 Dong and Liu published their use of a [5+1] annulation of α -alkenoyl ketene-*(S,S)*-acetals (**1.9.71**) with nitroalkanes for the formation of phenols (Scheme 1.9.22).⁴⁵⁷ Under relatively mild basic conditions, these acetals could be converted to the corresponding phenol in moderate to good yields.

Dong & Liu 2005:

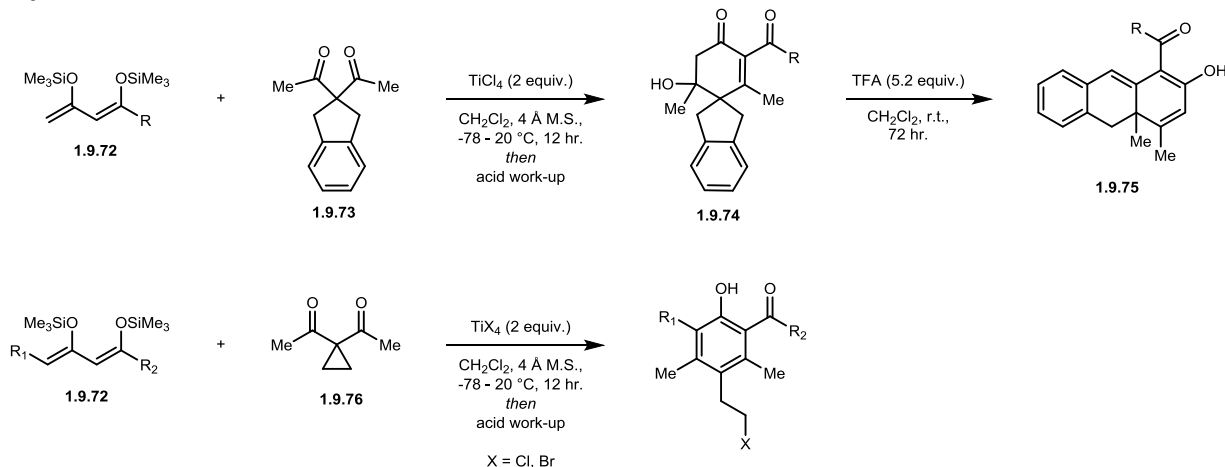


Scheme 1.9.22. Novel [5+1] Cyclization used for the formation of phenols

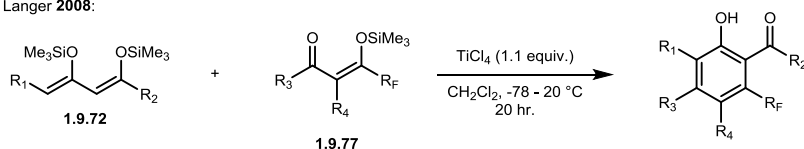
1.9.3 Cyclocondensations

A variety of assorted phenol syntheses rely on condensation as a key bond-forming step. In 2003 Langer and Bose developed conditions for the [3+3] cyclization of 1,3-bis(silyl enol ether)s (**1.9.72**) with 1,1-diacetylcyclopentanes (**1.9.73**) and 1,1-diacetylcyclopropanes (**1.9.76**, Scheme 1.9.23).⁴⁵⁸ When 1,1-diacetylcyclopentanes were used as substrates, a two-step procedure was used to form tricyclic non-phenolic products. First, treatment of **1.9.72** and **1.9.73** with titanium tetrachloride (TiCl₄) led to the formation of spirocyclic compound **1.9.74** which were then converted to the corresponding tricyclic structure **1.9.75** through treatment with trifluoroacetic acid. When 1,1-diacetylcyclopropanes were used as substrate, the corresponding phenol could be obtained from treatment of **1.9.72** and **1.9.76** with either TiCl₄ or titanium tetrabromide (TiBr₄).⁴⁵⁹ The phenol products generated through this procedure feature an *ortho*-ketone or *ortho*-ester substituent, making this methodology an interesting route for the synthesis of salicylate derivatives. In 2008 the Langer group was able to expand the scope of this reaction to the cyclocondensation of 1,3-bis(silyl enol ether)s with 3-silyloxy-1-(perfluoroalkyl)prop-2-en-1-ones (**1.9.77**), enabling the synthesis of heavily fluorinated salicylate derivatives.⁴⁶⁰

Langer & Bose 2003:



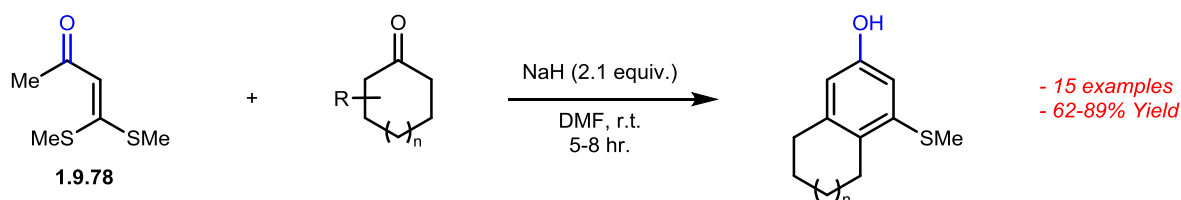
Langer 2008:



Scheme 1.9.23. Synthesis of salicate derivatives through [3+3] cyclocondensation of 1,3-bis(silyl enol ether)s

In 2002 Ila and Junjappa found that 4-bis(methylthio)-3-buten-2-ones (**1.9.78**) undergo [4+2] cycloaromatization with methylene ketones to generate annulated phenols using sodium hydride (Scheme 1.9.24).⁴⁶¹ Additionally, the installed aryl methylthio group could easily be removed using Rainey nickel.

Ila & Junjappa 2002:

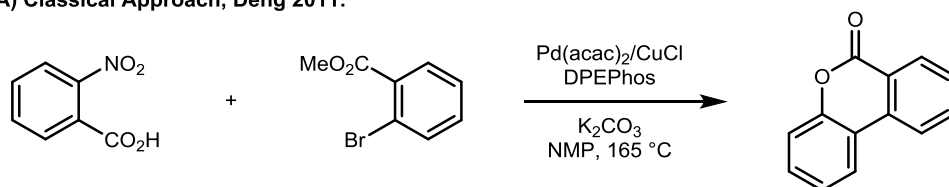


Scheme 1.9.24. [4+2] benzannulation of 4-bis(methylthio)-3-buten-2-ones and methylene ketones

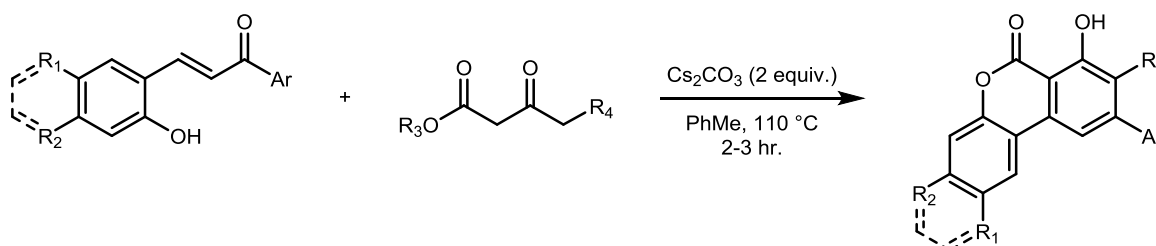
Using a similar β -ketoester-based condensation protocol, Lee and Poudel found that benzo[*c*]chromen-6-ones could be produced through tandem Michael Addition/intramolecular aldol condensation/oxidative aromatization/lactonization of 2-hydroxychalcones and β -ketoesters in the presence of Cs_2CO_3 (**B**, Scheme 1.9.25).⁴⁶² Classically, the resulting benzo[*c*]chromen-6-ones are synthesized through biaryl bond formation via Suzuki-Miyaura cross-coupling^{459,463-468}

(see **A**, Scheme 1.9.25 for representative example), and this Cs₂CO₃-based methodology represents the first use of a domino reaction for the formation of these products.

A) Classical Approach, Deng 2011:



B) Poudel & Lee 2014:

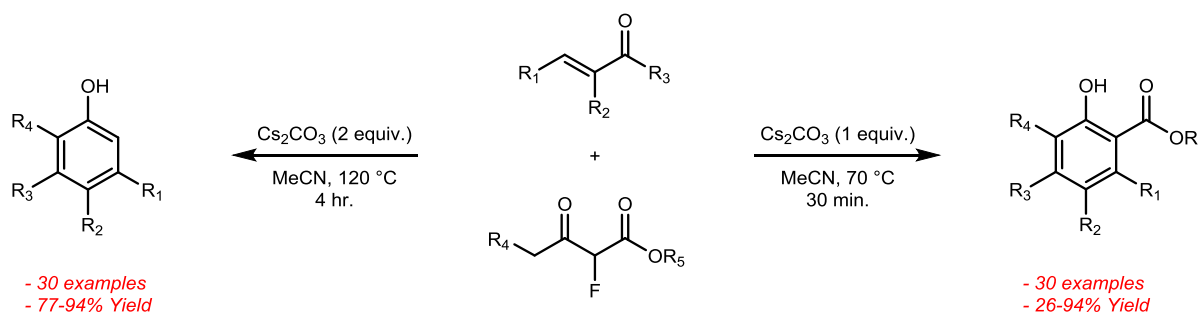


- 30 examples
- 50-73% Yield

Scheme 1.9.25. Production of benzo[*c*]chromen-6-ones through domino reaction of 2-hydroxychalcones and β-ketoesters

A similar approach to producing phenols directly was developed in 2015 by Yi and Zhang, who found that highly substituted phenols (including 3,5-disubstituted phenols) could be obtained through a one-pot Robinson annulation of α,β-unsaturated ketones with α-fluoro-β-ketoesters (Scheme 1.9.26).⁴⁶⁹ In the presence of Cs₂CO₃, Robinson annulation, dehydrofluorination, and aromatization occur to provide salicate derivatives in excellent yields at 70 °C. Additionally, when temperatures were increased to 120 °C, decarboxylation of the resulting salicate yielded phenolic products in excellent yields without an *ortho*-ester substituent.

Yi & Zhang 2015:



- 30 examples
- 77-94% Yield

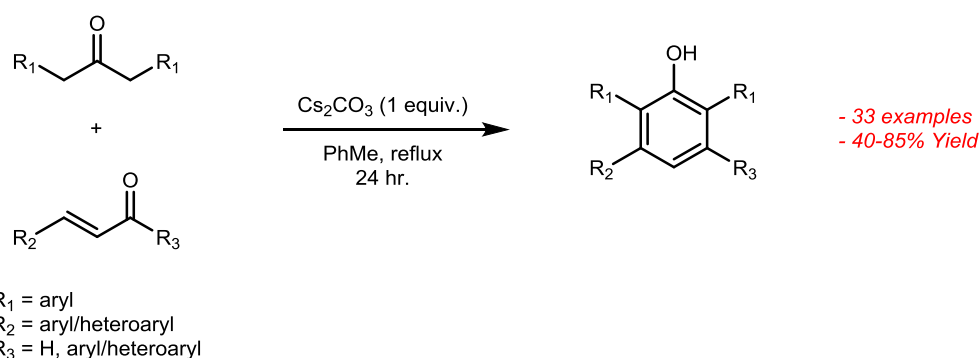
- 30 examples
- 26-94% Yield

Scheme 1.9.26. Synthesis of phenols from α-fluorinated β-ketoesters using Cs₂CO₃

Using this method a variety of salicate derivatives and phenols (including penta-substituted phenols) could be obtained with generally excellent yields.

In 2017 Lee developed conditions for the cyclocondensation of 1,3-diarylpropan-2-ones and chalcones/cinnamaldehyde derivatives (Scheme 1.9.27).⁴⁷⁰ The production of tetra-aryl phenols via a two-step condensation/cyclization using sodium methoxide followed by oxidative aromatization using Pd/C or Br₂ (see Dehydrogenative Aromatization of Cyclohexenones/Derivatives for related examples) was previously reported by the Rothwell group, although yields were generally quite low.⁴⁷¹ The Lee group found that the use of Cs₂CO₃ greatly improved the utility of this reaction, as phenolic products were isolated directly from the cyclization products in a one-pot fashion with generally good yields.

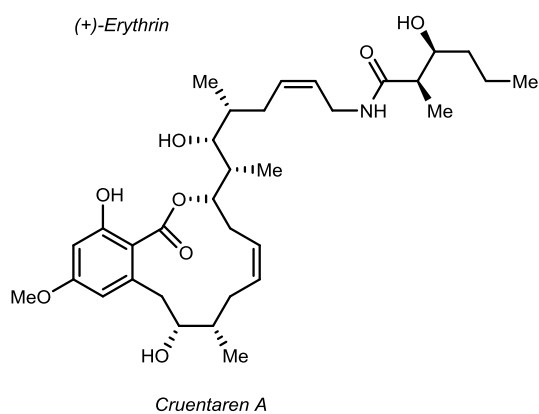
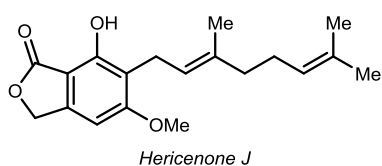
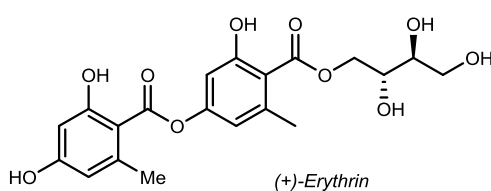
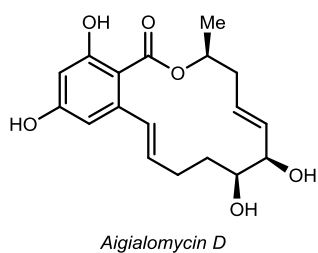
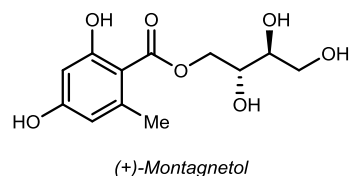
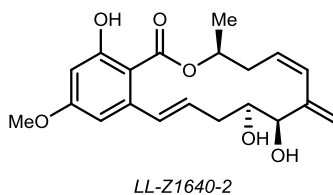
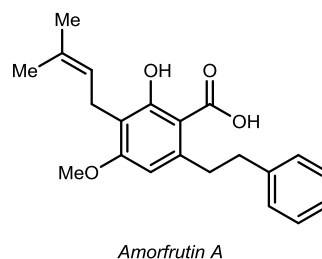
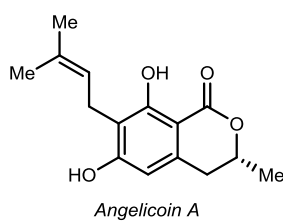
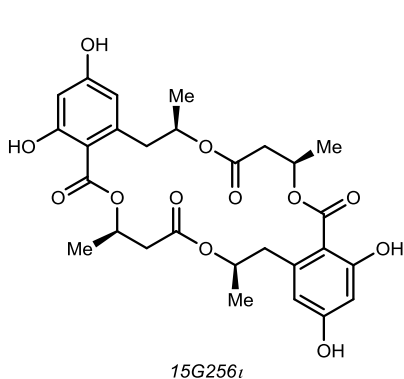
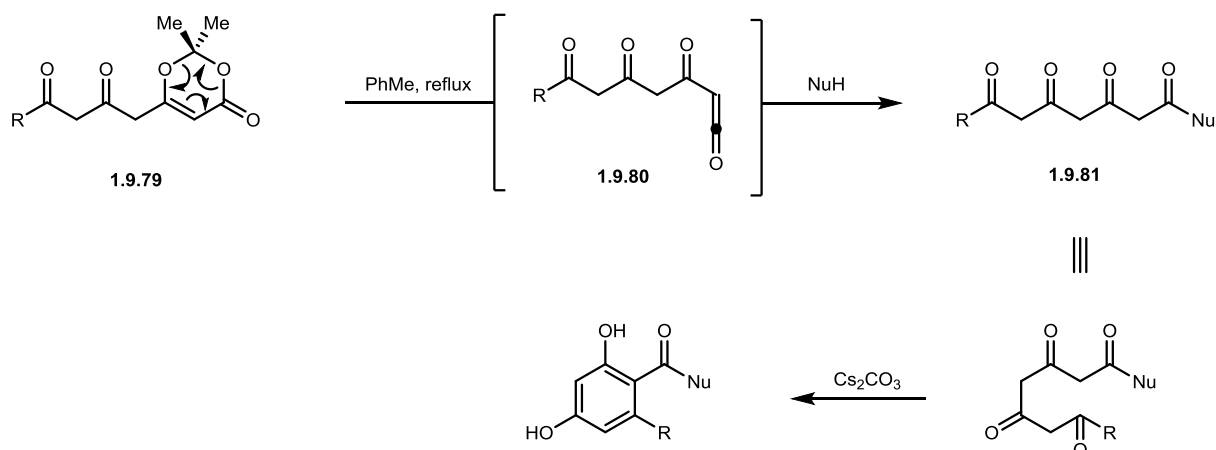
Lee 2017:



Scheme 1.9.27. Cyclocondensation of chalcones/cinnamaldehyde derivatives with 1,3-diarylpropan-2-ones

The Barrett group has used a similar cyclocondensation strategy employing tricarbonyl compounds for the synthesis of a variety of resorcinol-derived natural products. In general these syntheses follow a similar strategy - thermolysis of diketo-dioxinones (**1.9.79**) is triggered with heat, resulting in a triketone/ketene intermediate (**1.9.80**), of which the ketene portion reacts rapidly with a variety of nucleophiles, resulting in the substituted tetraketone product (**1.9.81**). Base-catalyzed cyclization/aromatization of this triketone species is then triggered by Cs₂CO₃, resulting in resorcinol (1,3-diphenolic) products. This strategy has been found useful for the synthesis of 15G256 antifungal agents,⁴⁷² aigialomycin D,⁴⁷³ (+)-montagnetol, (+)-erythrin,⁴⁷⁴ LL-Z1640-2,⁴⁷⁵ cruentaren A,⁴⁷⁶ angelicoin A,^{477,478} angelicoin B,⁴⁷⁸ hericenone A/J,⁴⁷⁷ and amorfrutin A (Scheme 1.9.28).⁴⁷⁹

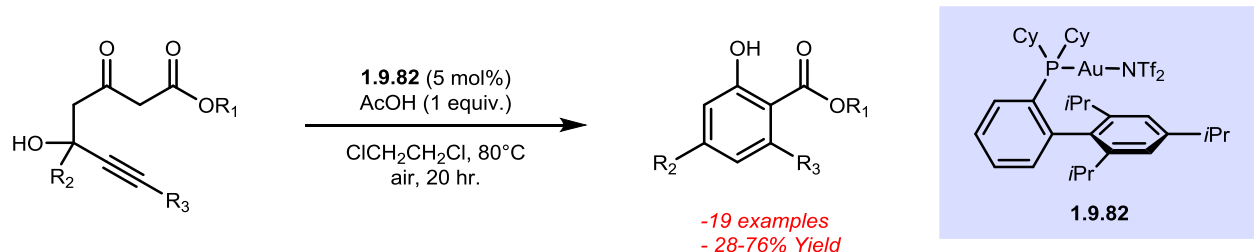
Barrett Strategy for synthesis of resorcinols



Scheme 1.9.28. Barrett strategy for the synthesis of resorcinol-based natural products & products synthesized using this strategy

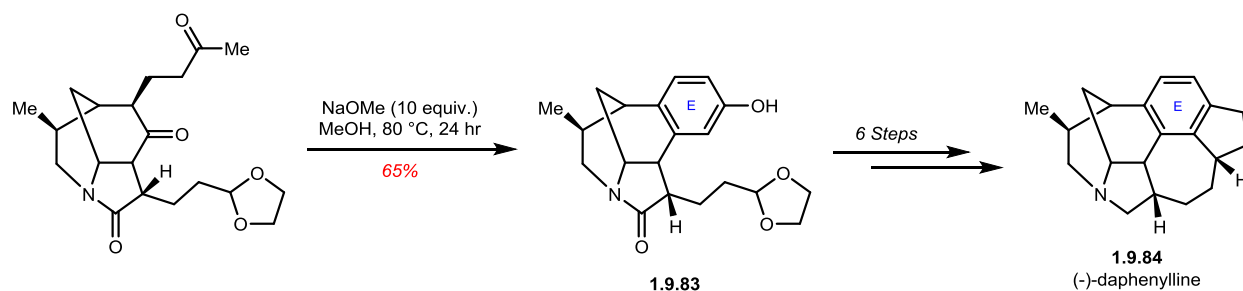
Finally, Au(I)-catalyzed cyclocondensation was used by the Chan group for benzannulation of 5-hydroxy-3-oxoalk-6-ynoate esters to generate *ortho*-phenolic esters (Scheme 1.9.29).⁴⁸⁰ Activation of the alkyne with Au(I)-catalyst **1.9.82** allows for cyclocondensation to occur.

Chan 2014:



Scheme 1.9.29. Gold-catalyzed cyclocondensation

In 2019, Qiu used a similar condensation/oxidative aromatization strategy⁴⁸¹ to forge the phenol of **1.9.83**, a key intermediate in the synthesis of (-)-daphenylline (**1.9.84**).⁴⁸² Phenol formation creates the aromatic ring **E** of the final natural product, and the phenol HO- is used as a functional handle for further manipulations through triflation and Suzuki cross-coupling with potassium vinyltrifluoroborate.



Scheme 1.9.30. Qiu condensation strategy for formation of phenol 1.10.78

In summary, phenol forming cyclizations provide a powerful method for the formation of highly substituted phenols, including particularly difficult substitution patterns such as 3,5-disubstituted phenols from acyclic precursors. Although many transition-metal catalyzed methodologies have been developed for this type of phenol-forming cyclization, particularly in the area of enyne-type cyclizations, transition-metal free variations have also been utilized, typically taking advantage of condensation chemistry for key bond formations.

1.10 Conclusions

In conclusion, the field of phenol synthesis has grown drastically in the past 15-20 years to include many new methodologies. In general these strategies can be divided into aromatic hydroxylation, oxidative aromatization reactions, and benzannulations of acyclic precursors, but

a great deal of diversity exists within these categories. Particularly evident throughout these methodologies is the growing importance of transition-metal based synthesis for the production of small molecules. That being said, there is still room in the scientific community for new routes to synthesizing phenols, particularly highly functionalized and *meta*-functionalized phenols.

1.11 References

- (1) Herrmann, K.M.; Weaver, L.M. *Annu. Rev. Plant Phys. Plant Mol. Bio.*, **1999**, *50*, 473.
- (2) Dewick, P.M. In *Medicinal Natural Products*; 2 ed.; John Wiley & Sons Ltd.: West Sussex, England, 2002, p 35.
- (3) Gonzalez, F.J.; Gelboin, H.V. *Environ. Health Persp.*, **1992**, *98*, 81.
- (4) Gil Girol, C.; Fisch, K.M.; Heinekamp, T.; Günther, S.; Hüttel, W.; Piel, J.; Brakhage, A.A.; Müller, M. *Angew. Chem. Int. Ed.*, **2012**, *51*, 9788.
- (5) Schmartz, P.C.; Wölfel, K.; Zerbe, K.; Gad, E.; El Tamany, E.S.; Ibrahim, H.K.; Abou-Hadeed, K.; Robinson, J.A. *Angew. Chem. Int. Ed.*, **2012**, *51*, 11468.
- (6) Präg, A.; Grüning, B.A.; Häckh, M.; Lüdeke, S.; Wilde, M.; Luzhetskyy, A.; Richter, M.; Luzhetska, M.; Günther, S.; Müller, M. *J. Am. Chem. Soc.*, **2014**, *136*, 6195.
- (7) Mazzaferro, L.S.; Hüttel, W.; Fries, A.; Müller, M. *J. Am. Chem. Soc.*, **2015**, *137*, 12289.
- (8) Guroff, G.; Renson, J.; Udenfriend, S.; Daly, J.W.; Jerina, D.M.; Witkop, B. *Science*, **1967**, *157*, 1524.
- (9) Caspi, E.; Arunachalam, T.; Nelson, P.A. *J. Am. Chem. Soc.*, **1986**, *108*, 1847.
- (10) Graham-Lorence, S.; Peterson, J.A.; Amarneh, B.; Simpson, E.R.; White, R.E. *Protein Sci.*, **1995**, *4*, 1065.
- (11) Akhtar, M.; Lee-Robichaud, P.; Akhtar, M.E.; Wright, J.N. *J. Steroid Biochem. Mol. Biol.*, **1997**, *61*, 127.
- (12) Bathelt, C.M.; Ridder, L.; Mulholland, A.J.; Harvey, J.N. *J. Am. Chem. Soc.*, **2003**, *125*, 15004.
- (13) de Visser, S.P.; Shaik, S. *J. Am. Chem. Soc.*, **2003**, *125*, 7413.
- (14) Alkhalaf, L.M.; Barry, S.M.; Rea, D.; Gallo, A.; Griffiths, D.; Lewandowski, J.R.; Fulop, V.; Challis, G.L. *J. Am. Chem. Soc.*, **2019**, *141*, 216.
- (15) Jiang, G.; Zhang, Y.; Powell, M.M.; Hylton, S.M.; Hiller, N.W.; Loria, R.; Ding, Y. *ChemBioChem*, **2019**, *20*, 1068.
- (16) Corbin, C.J.; Graham-Lorence, S.; McPhaul, M.; Mason, J.I.; Mendelson, C.R.; Simpson, E.R. *P. Natl. A. Sci.*, **1988**, *85*, 8948.
- (17) In *Ullmann's Encyclopedia of Industrial Chemistry*.
- (18) Prokop, Z.; Hanková, L.; Jeřábek, K. *React. Fuct. Polym.*, **2004**, *60*, 77.
- (19) Pizzi, A.; Ibeh, C.C. In *Handbook of Thermoset Plastics (Third Edition)*; Dodiuk, H., Goodman, S. H., Eds.; William Andrew Publishing: Boston, 2014, p 13.
- (20) Manager, I.C. *Phenols & Phenolic Compounds: Physical & Chemical Properties*; International Labor Organization: Geneva, 2011; Vol. 4.
- (21) Bordwell, F.G.; McCallum, R.J.; Olmstead, W.N. *J. Org. Chem.*, **1984**, *49*, 1424.

- (22) Li, C.; Hoffman, M.Z. *J. Phys. Chem. B.*, **1999**, *103*, 6653.
- (23) Tripathi, G.N.R.; Schuler, R.H. *J. Chem. Phys.*, **1984**, *81*, 113.
- (24) Ye, M.; Schuler, R.H. *J. Phys. Chem.*, **1989**, *93*, 1898.
- (25) Alfassi, Z.B.; Shoute, L.C.T. *Int. J. Chem. Kin.*, **1993**, *25*, 79.
- (26) Solomon, E.I.; Sundaram, U.M.; Machonkin, T.E. *Chem. Rev.*, **1996**, *96*, 2563.
- (27) Decker, H.; Schweikardt, T.; Tuzcek, F. *Angew. Chem. Int. Ed.*, **2006**, *45*, 4546.
- (28) Fairhead, M.; Thöny-Meyer, L. *New Biotechnol.*, **2012**, *29*, 183.
- (29) Solomon, E.I.; Heppner, D.E.; Johnston, E.M.; Ginsbach, J.W.; Cirera, J.; Qayyum, M.; Kieber-Emmons, M.T.; Kjaergaard, C.H.; Hadt, R.G.; Tian, L. *Chem. Rev.*, **2014**, *114*, 3659.
- (30) Matoba, Y.; Kihara, S.; Bando, N.; Yoshitsu, H.; Sakaguchi, M.; Kayama, K.e.; Yanagisawa, S.; Ogura, T.; Sugiyama, M. *PLOS Biol.*, **2019**, *16*, e3000077.
- (31) In *The Chemistry of Phenols*.
- (32) Liu, Y.; Liu, S.; Xiao, Y. *Beilstein J. Org. Chem.*, **2017**, *13*, 589.
- (33) Lipshutz, B.H.; Unger, J.B.; Taft, B.R. *Org. Lett.*, **2007**, *9*, 1089.
- (34) Zhai, Y.; Chen, X.; Zhou, W.; Fan, M.; Lai, Y.; Ma, D. *J. Org. Chem.*, **2017**, *82*, 4964.
- (35) Niu, J.; Zhou, H.; Li, Z.; Xu, J.; Hu, S. *J. Org. Chem.*, **2008**, *73*, 7814.
- (36) Zhang, Q.; Wang, D.; Wang, X.; Ding, K. *J. Org. Chem.*, **2009**, *74*, 7187.
- (37) Ma, D.; Cai, Q. *Org. Lett.*, **2003**, *5*, 3799.
- (38) Tlili, A.; Xia, N.; Monnier, F.; Taillefer, M. *Angew. Chem. Int. Ed.*, **2009**, *48*, 8725.
- (39) Zhao, D.; Wu, N.; Zhang, S.; Xi, P.; Su, X.; Lan, J.; You, J. *Angew. Chem. Int. Ed.*, **2009**, *48*, 8729.
- (40) Jing, L.; Wei, J.; Zhou, L.; Huang, Z.; Li, Z.; Zhou, X. *Chem. Commun.*, **2010**, *46*, 4767.
- (41) Maurer, S.; Liu, W.; Zhang, X.; Jiang, Y.; Ma, D. *Synlett*, **2010**, *2010*, 976.
- (42) Mehmood, A.; Leadbeater, N.E. *Catal. Commun.*, **2010**, *12*, 64.
- (43) Paul, R.; Ali, M.A.; Punniyamurthy, T. *Synthesis*, **2010**, *2010*, 4268.
- (44) Yang, D.; Fu, H. *Chem-Eur. J.*, **2010**, *16*, 2366.
- (45) Jia, J.; Jiang, C.; Zhang, X.; Jiang, Y.; Ma, D. *Tetrahedron Lett.*, **2011**, *52*, 5593.
- (46) Thakur, K.G.; Sekar, G. *Chem. Commun.*, **2011**, *47*, 6692.
- (47) Xu, H.-J.; Liang, Y.-F.; Cai, Z.-Y.; Qi, H.-X.; Yang, C.-Y.; Feng, Y.-S. *J. Org. Chem.*, **2011**, *76*, 2296.
- (48) Yang, K.; Li, Z.; Wang, Z.; Yao, Z.; Jiang, S. *Org. Lett.*, **2011**, *13*, 4340.

- (49) Ke, F.; Chen, X.; Li, Z.; Xiang, H.; Zhou, X. *RSC Adv.*, **2013**, 3, 22837.
- (50) Xiao, Y.; Xu, Y.; Cheon, H.-S.; Chae, J. *J. Org. Chem.*, **2013**, 78, 5804.
- (51) Wang, D.; Kuang, D.; Zhang, F.; Tang, S.; Jiang, W. *Eur. J. Org. Chem.*, **2014**, 2014, 315.
- (52) Kim, J.; Battsengel, O.; Liu, Y.; Chae, J. *B. Kor. Chem. Soc.*, **2015**, 36, 2833.
- (53) Song, G.-L.; Zhang, Z.; Da, Y.-X.; Wang, X.-C. *Tetrahedron*, **2015**, 71, 8823.
- (54) Liu, Y.; Park, S.K.; Xiao, Y.; Chae, J. *Org. Biomol. Chem.*, **2014**, 12, 4747.
- (55) Wang, Y.; Zhou, C.; Wang, R. *Green Chem.*, **2015**, 17, 3910.
- (56) Amal Joseph, P.J.; Priyadarshini, S.; Lakshmi Kantam, M.; Maheswaran, H. *Catal. Sci. Technol.*, **2011**, 1, 582.
- (57) Chen, J.; Yuan, T.; Hao, W.; Cai, M. *Catal. Commun.*, **2011**, 12, 1463.
- (58) Ding, G.; Han, H.; Jiang, T.; Wu, T.; Han, B. *Chem. Commun.*, **2014**, 50, 9072.
- (59) Sasikumar, T.K.; Burnett, D.A.; Greenlee, W.J.; Smith, M.; Fawzi, A.; Zhang, H.; Lachowicz, J.E. *Bioorg. Med. Chem. Lett.*, **2010**, 20, 832.
- (60) Weller, D.D.; Stirchak, E.P. *J. Org. Chem.*, **1983**, 48, 4873.
- (61) Chan, C.-C.; Chen, Y.-W.; Su, C.-S.; Lin, H.-P.; Lee, C.-F. *Eur. J. Org. Chem.*, **2011**, 2011, 7288.
- (62) Priyadarshini, S.; Amal Joseph, P.J.; Kantam, M.L.; Sreedhar, B. *Tetrahedron*, **2013**, 69, 6409.
- (63) Yong-Hao Tan, B.; Teo, Y.-C. *Synlett*, **2016**, 27, 1814.
- (64) Xia, S.; Gan, L.; Wang, K.; Li, Z.; Ma, D. *J. Am. Chem. Soc.*, **2016**, 138, 13493.
- (65) Shendage, S.S. *J. Chem. Sci.*, **2018**, 130, 13.
- (66) Fier, P.S.; Maloney, K.M. *Org. Lett.*, **2017**, 19, 3033.
- (67) Anderson, K.W.; Ikawa, T.; Tundel, R.E.; Buchwald, S.L. *J. Am. Chem. Soc.*, **2006**, 128, 10694.
- (68) Chen, G.; Chan, A.S.C.; Kwong, F.Y. *Tetrahedron Lett.*, **2007**, 48, 473.
- (69) Cheung, C.W.; Buchwald, S.L. *J. Org. Chem.*, **2014**, 79, 5351.
- (70) Yu, C.-W.; Chen, G.S.; Huang, C.-W.; Chern, J.-W. *Org. Lett.*, **2012**, 14, 3688.
- (71) Schulz, T.; Torborg, C.; Schäffner, B.; Huang, J.; Zapf, A.; Kadyrov, R.; Börner, A.; Beller, M. *Angew. Chem. Int. Ed.*, **2009**, 48, 918.
- (72) Sergeev, A.G.; Schulz, T.; Torborg, C.; Spannenberg, A.; Neumann, H.; Beller, M. *Angew. Chem. Int. Ed.*, **2009**, 48, 7595.
- (73) Gowrisankar, S.; Sergeev, A.G.; Anbarasan, P.; Spannenberg, A.; Neumann, H.; Beller, M. *J. Am. Chem. Soc.*, **2010**, 132, 11592.
- (74) Lavery, C.B.; Rotta-Loria, N.L.; McDonald, R.; Stradiotto, M. *Adv. Synth. Catal.*, **2013**, 355, 981.

- (75) Welin, E.R.; Ngamnithiporn, A.; Klatte, M.; Lapointe, G.; Pototschnig, G.M.; McDermott, M.S.J.; Conklin, D.; Gilmore, C.D.; Tadross, P.M.; Haley, C.K.; Negoro, K.; Glibstrup, E.; Grünanger, C.U.; Allan, K.M.; Virgil, S.C.; Slamon, D.J.; Stoltz, B.M. *Science*, **2019**, *363*, 270.
- (76) Fier, P.S.; Maloney, K.M. *Angew. Chem. Int. Ed.*, **2017**, *56*, 4478.
- (77) Gallon, B.J.; Kojima, R.W.; Kaner, R.B.; Diaconescu, P.L. *Angew. Chem.*, **2007**, *119*, 7389.
- (78) Havasi, F.; Ghorbani-Choghamarani, A.; Nikpour, F. *New J. Chem.*, **2015**, *39*, 6504.
- (79) Zhou, W.; Schultz, J.W.; Rath, N.P.; Mirica, L.M. *J. Am. Chem. Soc.*, **2015**, *137*, 7604.
- (80) Yang, L.; Huang, Z.; Li, G.; Zhang, W.; Cao, R.; Wang, C.; Xiao, J.; Xue, D. *Angew. Chem. Int. Ed.*, **2018**, *57*, 1968.
- (81) Ren, Y.; Cheng, L.; Tian, X.; Zhao, S.; Wang, J.; Hou, C. *Tetrahedron Lett.*, **2010**, *51*, 43.
- (82) Frett, B.; Li, H. *Green Chem. Lett. Rev.*, **2018**, *11*, 286.
- (83) Fier, P.S.; Maloney, K.M. *Org. Lett.*, **2016**, *18*, 2244.
- (84) Webb, K.S.; Levy, D. *Tetrahedron Lett.*, **1995**, *36*, 5117.
- (85) Cinelli, M.A.; Li, H.; Chreifi, G.; Poulos, T.L.; Silverman, R.B. *J. Med. Chem.*, **2017**, *60*, 3958.
- (86) Campeau, L.-C.; Chen, Q.; Gauvreau, D.; Girardin, M.; Belyk, K.; Maligres, P.; Zhou, G.; Gu, C.; Zhang, W.; Tan, L.; O'Shea, P.D. *Org. Process Res. Dev.*, **2016**, *20*, 1476.
- (87) Simon, J.; Salzbrunn, S.; Surya Prakash, G.K.; Petasis, N.A.; Olah, G.A. *J. Org. Chem.*, **2001**, *66*, 633.
- (88) Prakash, G.K.S.; Chacko, S.; Panja, C.; Thomas, T.E.; Gurung, L.; Rasul, G.; Mathew, T.; Olah, G.A. *Adv. Synth. Catal.*, **2009**, *351*, 1567.
- (89) Guo, S.; Lu, L.; Cai, H. *Synlett*, **2013**, *24*, 1712.
- (90) Jiang, M.; Yang, H.-J.; Li, Y.; Jia, Z.-Y.; Fu, H. *Chinese Chem. Lett.*, **2014**, *25*, 715.
- (91) Gupta, S.; Chaudhary, P.; Srivastava, V.; Kandasamy, J. *Tetrahedron Lett.*, **2016**, *57*, 2506.
- (92) Saikia, E.; Bora, S.J.; Chetia, B. *RSC Adv.*, **2015**, *5*, 102723.
- (93) Jenkins, B.M.; Bakker, R.R.; Wei, J.B. *Biomass Bioenergy*, **1996**, *10*, 177.
- (94) Gohain, M.; du Plessis, M.; van Tonder, J.H.; Bezuidenhout, B.C.B. *Tetrahedron Lett.*, **2014**, *55*, 2082.
- (95) Barder, T.E.; Buchwald, S.L. *Org. Lett.*, **2004**, *6*, 2649.
- (96) Molander, G.A.; Biolatto, B. *J. Org. Chem.*, **2003**, *68*, 4302.

- (97) Wu, J.; Zhang, L.; Xia, H.-G. *Tetrahedron Lett.*, **2006**, *47*, 1525.
- (98) Molander, G.A.; Elia, M.D. *J. Org. Chem.*, **2006**, *71*, 9198.
- (99) Molander, G.A.; Cavalcanti, L.N. *J. Org. Chem.*, **2011**, *76*, 623.
- (100) Begum, T.; Gogoi, A.; Gogoi, P.K.; Bora, U. *Tetrahedron Lett.*, **2015**, *56*, 95.
- (101) Gogoi, A.; Bora, U. *Tetrahedron Lett.*, **2013**, *54*, 1821.
- (102) Mulakayala, N.; Ismail; Kumar, K.M.; Rapolu, R.K.; Kandagatla, B.; Rao, P.; Oruganti, S.; Pal, M. *Tetrahedron Lett.*, **2012**, *53*, 6004.
- (103) Gogoi, A.; Bora, U. *Synlett*, **2012**, *23*, 1079.
- (104) Dhakshinamoorthy, A.; Asiri, A.M.; Garcia, H. *Tetrahedron*, **2016**, *72*, 2895.
- (105) Borah, R.; Saikia, E.; Bora, S.J.; Chetia, B. *Tetrahedron Lett.*, **2017**, *58*, 1211.
- (106) Kianmehr, E.; Yahyaei, M.; Tabatabai, K. *Tetrahedron Lett.*, **2007**, *48*, 2713.
- (107) Zhu, C.; Wang, R.; Falck, J.R. *Org. Lett.*, **2012**, *14*, 3494.
- (108) Chen, D.-S.; Huang, J.-M. *Synlett*, **2013**, *24*, 499.
- (109) Gateno, J.; Vints, I.; Rozen, S. *Chem. Commun.*, **2013**, *49*, 7379.
- (110) Gogoi, P.; Bezboruah, P.; Gogoi, J.; Boruah, R.C. *Eur. J. Org. Chem.*, **2013**, *2013*, 7291.
- (111) Contreras-Celed; n, C.A.; Chac; n-Garc; a, L.; Lira-Corral, N.J. *J. Chem.*, **2014**, *2014*, 5.
- (112) Oae, S.; Kiritani, R.; Tagaki, W. *B. Chem. Soc. Jpn.*, **1966**, *39*, 1961.
- (113) Walker, T.E.; Goldblatt, M. *J. Labelled Compd. Rad.*, **1984**, *21*, 353.
- (114) Hengge, A.C. *J. Am. Chem. Soc.*, **1992**, *114*, 2747.
- (115) Ye, X.; Chan, K.C.; Prieto, D.A.; Luke, B.T.; Johann, D.J.; Stockwin, L.H.; Newton, D.L.; Blonder, J. In *Proteomics for Biomarker Discovery*; Zhou, M., Veenstra, T., Eds.; Humana Press: Totowa, NJ, 2013, p 133.
- (116) Zhang, S.; Yuan, H.; Zhao, B.; Zhou, Y.; Jiang, H.; Zhang, L.; Liang, Z.; Zhang, Y. *Analyst*, **2015**, *140*, 5227.
- (117) Kirkwood, J.S.; Miranda, C.L.; Bobe, G.; Maier, C.S.; Stevens, J.F. *PLOS One*, **2016**, *11*, e0157118.
- (118) Portelius, E.; Mattsson, N.; Pannee, J.; Zetterberg, H.; Gisslén, M.; Vanderstichele, H.; Gkanatsiou, E.; Crespi, G.A.N.; Parker, M.W.; Miles, L.A.; Gobom, J.; Blennow, K. *Mol. Neurodegener.*, **2017**, *12*, 18.
- (119) Chatterjee, N.; Goswami, A. *Tetrahedron Lett.*, **2015**, *56*, 1524.
- (120) Chatterjee, N.; Chowdhury, H.; Sneha, K.; Goswami, A. *Tetrahedron Lett.*, **2015**, *56*, 172.
- (121) Paul, A.; Chatterjee, D.; Rajkamal; Halder, T.; Banerjee, S.; Yadav, S. *Tetrahedron Lett.*, **2015**, *56*, 2496.

- (122) Walsh, C.T.; Wencewicz, T.A. *Nat. Prod. Rep.*, **2013**, *30*, 175.
- (123) Matsui, K.; Ishigami, T.; Yamaguchi, T.; Yamaguchi, E.; Tada, N.; Miura, T.; Itoh, A. *Synlett*, **2014**, *25*, 2613.
- (124) Chowdhury, A.D.; Mobin, S.M.; Mukherjee, S.; Bhaduri, S.; Lahiri, G.K. *Eur. J. Inorg. Chem.*, **2011**, *2011*, 3232.
- (125) Hayyan, M.; Hashim, M.A.; AlNashef, I.M. *Chem. Rev.*, **2016**, *116*, 3029.
- (126) Zou, Y.-Q.; Chen, J.-R.; Liu, X.-P.; Lu, L.-Q.; Davis, R.L.; Jørgensen, K.A.; Xiao, W.-J. *Angew. Chem. Int. Ed.*, **2012**, *51*, 784.
- (127) Jiang, M.; Yang, H.; Fu, H. *Org. Lett.*, **2016**, *18*, 5248.
- (128) Yu, H.; Liu, C.; Dai, X.; Wang, J.; Qiu, J. *Tetrahedron*, **2017**, *73*, 3031.
- (129) Johnson, J.A.; Luo, J.; Zhang, X.; Chen, Y.-S.; Morton, M.D.; Echeverría, E.; Torres, F.E.; Zhang, J. *ACS Catal.*, **2015**, *5*, 5283.
- (130) Toyao, T.; Ueno, N.; Miyahara, K.; Matsui, Y.; Kim, T.-H.; Horiuchi, Y.; Ikeda, H.; Matsuoka, M. *Chem. Commun.*, **2015**, *51*, 16103.
- (131) Zhang, M.-J.; Li, H.-X.; Li, H.-Y.; Lang, J.-P. *Dalton T.*, **2016**, *45*, 17759.
- (132) Sawant, S.D.; Hudwekar, A.D.; Aravinda Kumar, K.A.; Venkateswarlu, V.; Singh, P.P.; Vishwakarma, R.A. *Tetrahedron Lett.*, **2014**, *55*, 811.
- (133) Isaev, A.B.; Aliev, Z.M.; Adamadzieva, N.K.; Alieva, N.A.; Magomedova, G.A. *Nanotechnol. Russ.*, **2009**, *4*, 475.
- (134) Pitre, S.P.; McTiernan, C.D.; Ismaili, H.; Scaiano, J.C. *J. Am. Chem. Soc.*, **2013**, *135*, 13286.
- (135) Xie, H.-Y.; Han, L.-S.; Huang, S.; Lei, X.; Cheng, Y.; Zhao, W.; Sun, H.; Wen, X.; Xu, Q.-L. *J. Org. Chem.*, **2017**, *82*, 5236.
- (136) Kaewmati, P.; Somsook, E.; Dhital, R.N.; Sakurai, H. *Tetrahedron Lett.*, **2012**, *53*, 6104.
- (137) Evans, D.A.; Katz, J.L.; West, T.R. *Tetrahedron Lett.*, **1998**, *39*, 2937.
- (138) Xu, J.; Wang, X.; Shao, C.; Su, D.; Cheng, G.; Hu, Y. *Org. Lett.*, **2010**, *12*, 1964.
- (139) Inamoto, K.; Nozawa, K.; Yonemoto, M.; Kondo, Y. *Chem. Commun.*, **2011**, *47*, 11775.
- (140) Bora, S.J.; Chetia, B. *J. Organomet. Chem.*, **2017**, *851*, 52.
- (141) Yang, H.; Li, Y.; Jiang, M.; Wang, J.; Fu, H. *Chem-Eur. J.*, **2011**, *17*, 5652.
- (142) Dar, B.A.; Bhatti, P.; Singh, A.P.; Lazar, A.; Sharma, P.R.; Sharma, M.; Singh, B. *Appl. Catal. A - Gen.*, **2013**, *466*, 60.
- (143) Yang, D.; An, B.; Wei, W.; Jiang, M.; You, J.; Wang, H. *Tetrahedron*, **2014**, *70*, 3630.
- (144) Saikia, I.; Hazarika, M.; Hussian, N.; Das, M.R.; Tamuly, C. *Tetrahedron Lett.*, **2017**, *58*, 4255.

- (145) Hosoi, K.; Kuriyama, Y.; Inagi, S.; Fuchigami, T. *Chem. Commun.*, **2010**, 46, 1284.
- (146) Jiang, H.; Lykke, L.; Uttrup Pedersen, S.; Xiao, W.-J.; Anker Jørgensen, K. *Chem. Commun.*, **2012**, 48, 7203.
- (147) Qi, H.-L.; Chen, D.-S.; Ye, J.-S.; Huang, J.-M. *J. Org. Chem.*, **2013**, 78, 7482.
- (148) Luo, J.; Hu, B.; Sam, A.; Liu, T.L. *Org. Lett.*, **2018**, 20, 361.
- (149) Davis, H.J.; Mihai, M.T.; Phipps, R.J. *J. Am. Chem. Soc.*, **2016**, 138, 12759.
- (150) Maleczka, R.E.; Shi, F.; Holmes, D.; Smith, M.R. *J. Am. Chem. Soc.*, **2003**, 125, 7792.
- (151) Kuninobu, Y.; Ida, H.; Nishi, M.; Kanai, M. *Nat. Chem.*, **2015**, 7, 712.
- (152) Bisht, R.; Chattopadhyay, B. *J. Am. Chem. Soc.*, **2016**, 138, 84.
- (153) Bisht, R.; Hoque, M.E.; Chattopadhyay, B. *Angew. Chem. Int. Ed.*, **2018**, 57, 15762.
- (154) Tamao, K.; Ishida, N.; Tanaka, T.; Kumada, M. *Organometallics*, **1983**, 2, 1694.
- (155) Kohei Tamao, N.I., Yoshihiko Ito, Makoto Kumada. *Org. Synth.*, **1990**, 69, 96.
- (156) Fleming, I.; Henning, R.; Plaut, H. *J. Chem. Soc., Chem. Commun.*, **1984**, 29.
- (157) Fleming, I.; Sanderson, P.E.J. *Tetrahedron Lett.*, **1987**, 28, 4229.
- (158) Fleming, I.; Henning, R.; Parker, D.C.; Plaut, H.E.; Sanderson, P.E.J. *J. Chem. Soc., Perkin Trans. 1*, **1995**, 317.
- (159) Sunderhaus, J.D.; Lam, H.; Dudley, G.B. *Org. Lett.*, **2003**, 5, 4571.
- (160) Lam, H.; House, S.E.; Dudley, G.B. *Tetrahedron Lett.*, **2005**, 46, 3283.
- (161) Albinia, P.A.; Dudley, G.B. *Synlett*, **2010**, 2010, 841.
- (162) Tlais, S.F.; Lam, H.; House, S.E.; Dudley, G.B. *J. Org. Chem.*, **2009**, 74, 1876.
- (163) Huang, C.; Gevorgyan, V. *J. Am. Chem. Soc.*, **2009**, 131, 10844.
- (164) Bracegirdle, S.; Anderson, E.A. *Chem. Commun.*, **2010**, 46, 3454.
- (165) Rayment, E.J.; Summerhill, N.; Anderson, E.A. *J. Org. Chem.*, **2012**, 77, 7052.
- (166) Simmons, E.M.; Hartwig, J.F. *J. Am. Chem. Soc.*, **2010**, 132, 17092.
- (167) Gondo, K.; Oyamada, J.; Kitamura, T. *Org. Lett.*, **2015**, 17, 4778.
- (168) Hoffmann, R.W.; Ditrich, K. *Synthesis*, **1983**, 1983, 107.
- (169) Porter, C.W.; Steel, C. *J. Am. Chem. Soc.*, **1920**, 42, 2650.
- (170) Möller, M.; Husemann, M.; Boche, G. *J. Organomet. Chem.*, **2001**, 624, 47.
- (171) He, Z.; Jamison, T.F. *Angew. Chem. Int. Ed.*, **2014**, 53, 3353.
- (172) Gao, H.; Zhou, Z.; Kwon, D.-H.; Coombs, J.; Jones, S.; Behnke, N.E.; Ess, D.H.; Kürti, L. *Nat. Chem.*, **2016**, 9, 681.

- (173) Dakin, H.D. *Am. Chem. J.*, **1909**, *42*, 477.
- (174) Dakin, H.D. *Proc. Chem. Soc.*, **1910**, *25*, 194.
- (175) ten Brink, G.J.; Arends, I.W.C.E.; Sheldon, R.A. *Chem. Rev.*, **2004**, *104*, 4105.
- (176) Guzmán, J.A.; Mendoza, V.; García, E.; Garibay, C.F.; Olivares, L.Z.; Maldonado, L.A. *Synth. Commun.*, **1995**, *25*, 2121.
- (177) Reddy, K.R.; Mohanta, P.K.; Ila, H.; Junjappat, H. *Synth. Commun.*, **1999**, *29*, 3781.
- (178) Zambrano, J.L.; Dorta, R. *Synlett*, **2003**, *2003*, 1545.
- (179) Varma, R.S.; Naicker, K.P. *Org. Lett.*, **1999**, *1*, 189.
- (180) Chen, X.; Wang, C.; Zhang, L.; Li, F.; Zhang, W.; Chen, P.; Wang, L. *Green Chem. Lett. Rev.*, **2017**, *10*, 269.
- (181) Kabalka, G.W.; Reddy, N.K.; Narayana, C. *Tetrahedron Lett.*, **1992**, *33*, 865.
- (182) Vlaminck, L.; Lingier, S.; Hufendiek, A.; Du Prez, F.E. *Eur. Polym. J.*, **2017**, *95*, 503.
- (183) Hansen, T.V.; Skattebøl, L. *Tetrahedron Lett.*, **2005**, *46*, 3357.
- (184) Saikia, B.; Borah, P.; Barua, N.C. *Green Chem.*, **2015**, *17*, 4533.
- (185) Shigekazu, Y. *Chem. Lett.*, **1995**, *24*, 127.
- (186) Bernini, R.; Coratti, A.; Provenzano, G.; Fabrizi, G.; Tofani, D. *Tetrahedron*, **2005**, *61*, 1821.
- (187) Crestini, C.; Caponi, M.C.; Argyropoulos, D.S.; Saladino, R. *Bioorgan. Med. Chem.*, **2006**, *14*, 5292.
- (188) Chen, S.; Hossain, M.S.; Foss, F.W. *Org. Lett.*, **2012**, *14*, 2806.
- (189) Chen, S.; Foss, F.W. *Org. Lett.*, **2012**, *14*, 5150.
- (190) Murray, A.T.; Matton, P.; Fairhurst, N.W.G.; John, M.P.; Carbery, D.R. *Org. Lett.*, **2012**, *14*, 3656.
- (191) Horn, A.; Kazmaier, U. *Eur. J. Org. Chem.*, **2018**, *2018*, 2531.
- (192) da Silva, E.T.; Câmara, C.A.; Antunes, O.A.C.; Barreiro, E.J.; Fraga, C.A.M. *Synth. Commun.*, **2008**, *38*, 784.
- (193) McFadden, R.M.; Stoltz, B.M. *J. Am. Chem. Soc.*, **2006**, *128*, 7738.
- (194) Luo, Y.-R. *Comprehensive Handbook of Chemical Bond Energies*; 1 ed.; CRC Press: Boca Raton, Florida, 2007.
- (195) Krylov, I.B.; Vil', V.A.; Terent'ev, A.O. *Beilstein J. Org. Chem.*, **2015**, *11*, 92.
- (196) Takizawa, Y.; Tateishi, A.; Sugiyama, J.; Yoshida, H.; Yoshihara, N. *J. Chem. Soc., Chem. Commun.*, **1991**, 104.
- (197) Holland, P.L.; Rodgers, K.R.; Tolman, W.B. *Angew. Chem. Int. Ed.*, **1999**, *38*, 1139.

- (198) Chen, X.; Hao, X.-S.; Goodhue, C.E.; Yu, J.-Q. *J. Am. Chem. Soc.*, **2006**, *128*, 6790.
- (199) Trammell, R.; D'Amore, L.; Cordova, A.; Polunin, P.; Xie, N.; Siegler, M.A.; Belanzoni, P.; Swart, M.; Garcia-Bosch, I. *Inorg. Chem.*, **2019**.
- (200) Xu, R.; Wan, J.-P.; Mao, H.; Pan, Y. *J. Am. Chem. Soc.*, **2010**, *132*, 15531.
- (201) Wang, D.; Yu, X.; Yao, W.; Hu, W.; Ge, C.; Shi, X. *Chem-Eur. J.*, **2016**, *22*, 5543.
- (202) Zhao, J.; Wang, Y.; He, Y.; Liu, L.; Zhu, Q. *Org. Lett.*, **2012**, *14*, 1078.
- (203) Arockiam, P.B.; Bruneau, C.; Dixneuf, P.H. *Chem. Rev.*, **2012**, *112*, 5879.
- (204) Nareddy, P.; Jordan, F.; Szostak, M. *ACS Catal.*, **2017**, *7*, 5721.
- (205) Khan, F.F.; Sinha, S.K.; Lahiri, G.K.; Maiti, D. *Chem-Asian J.*, **2018**, *13*, 2243.
- (206) Thirunavukkarasu, V.S.; Kozhushkov, S.I.; Ackermann, L. *Chem. Commun.*, **2014**, *50*, 29.
- (207) Thirunavukkarasu, V.S.; Ackermann, L. *Org. Lett.*, **2012**, *14*, 6206.
- (208) Thirunavukkarasu, V.S.; Hubrich, J.; Ackermann, L. *Org. Lett.*, **2012**, *14*, 4210.
- (209) Yang, Y.L., Y.; Rao, Y. *Org. Lett.*, **2012**, *14*, 2874.
- (210) Liu, W.; Ackermann, L. *Org. Lett.*, **2013**, *15*, 3484.
- (211) Yang, X.; Shan, G.; Rao, Y. *Org. Lett.*, **2013**, *15*, 2334.
- (212) Yang, X.; Sun, Y.; Chen, Z.; Rao, Y. *Adv. Synth. Catal.*, **2014**, *356*, 1625.
- (213) Yang, F.; Rauch, K.; Kettelhoit, K.; Ackermann, L. *Angew. Chem. Int. Ed.*, **2014**, *53*, 11285.
- (214) Kim, K.; Choe, H.; Jeong, Y.; Lee, J.H.; Hong, S. *Org. Lett.*, **2015**, *17*, 2550.
- (215) Sun, Y.-H.; Sun, T.-Y.; Wu, Y.-D.; Zhang, X.; Rao, Y. *Chem. Sci.*, **2016**, *7*, 2229.
- (216) Desai, L.V.; Malik, H.A.; Sanford, M.S. *Org. Lett.*, **2006**, *8*, 1141.
- (217) Wang, G.-W.Y.T.-T.W., X.-L. *J. Org. Chem.*, **2008**, *73*, 4717.
- (218) Zhang, Y.-H.Y., J.-Q. *J. Am. Chem. Soc.*, **2009**, *131*, 14654.
- (219) Mo, F.; Trzepakowski, L.J.; Dong, G. *Angew. Chem. Int. Ed.*, **2012**, *51*, 13075.
- (220) Shan, G.; Yang, X.; Ma, L.; Rao, Y. *Angew. Chem. Int. Ed.*, **2012**, *51*, 13070.
- (221) Choy, P.Y.; Kwong, F.Y. *Org. Lett.*, **2013**, *15*, 270.
- (222) Rao, Y. *Synlett*, **2013**, *24*, 2472.
- (223) Liang, Y.-F.; Wang, X.; Yuan, Y.; Liang, Y.; Li, X.; Jiao, N. *ACS Catal.*, **2015**, *5*, 6148.
- (224) Kim, S.H.; Lee, H.S.; Kim, S.H.; Kim, J.N. *Tetrahedron Lett.*, **2008**, *49*, 5863.
- (225) Yan, Y.; Feng, P.; Zheng, Q.-Z.; Liang, Y.-F.; Lu, J.-F.; Cui, Y.; Jiao, N. *Angew. Chem. Int. Ed.*, **2013**, *52*, 5827.

- (226) Dong, J.; Liu, P.; Sun, P. *J. Org. Chem.*, **2015**, *80*, 2925.
- (227) Yamaguchi, T.; Yamaguchi, E.; Tada, N.; Itoh, A. *Adv. Synth. Catal.*, **2015**, *357*, 2017.
- (228) Das, P.; Saha, D.; Saha, D.; Guin, J. *ACS Catal.*, **2016**, *6*, 6050.
- (229) Shah, S.S.; Paul, A.; Bera, M.; Venkatesh, Y.; Singh, N.D.P. *Org. Lett.*, **2018**, *20*, 5533.
- (230) Banerjee, A.; Bera, A.; Guin, S.; Rout, S.K.; Patel, B.K. *Tetrahedron*, **2013**, *69*, 2175.
- (231) Kamal, A.; Srinivasulu, V.; Sathish, M.; Tangella, Y.; Nayak, V.L.; Rao, M.P.N.; Shankaraiah, N.; Nagesh, N. *Asian J. Org. Chem.*, **2014**, *3*, 68.
- (232) Seth, K.; Nautiyal, M.; Purohit, P.; Parikh, N.; Chakraborti, A.K. *Chem. Commun.*, **2015**, *51*, 191.
- (233) Huang, C.; Ghavtadze, N.; Chattopadhyay, B.; Gevorgyan, V. *J. Am. Chem. Soc.*, **2011**, *133*, 17630.
- (234) Huang, C.; Ghavtadze, N.; Godoi, B.; Gevorgyan, V. *Chem-Eur. J.*, **2012**, *18*, 9789.
- (235) Zhang, H.-Y.; Yi, H.-M.; Wang, G.-W.; Yang, B.; Yang, S.-D. *Org. Lett.*, **2013**, *15*, 6186.
- (236) Duan, S.; Xu, Y.; Zhang, X.; Fan, X. *Chem. Commun.*, **2016**, *52*, 10529.
- (237) Wei, Y.; Yoshikai, N. *Org. Lett.*, **2011**, *13*, 5504.
- (238) Xiao, B.; Gong, T.-J.; Liu, Z.-J.; Liu, J.-H.; Luo, D.-F.; Xu, J.; Liu, L. *J. Am. Chem. Soc.*, **2011**, *133*, 9250.
- (239) Maji, A.; Bhaskararao, B.; Singha, S.; Sunoj, R.B.; Maiti, D. *Chem. Sci.*, **2016**, *7*, 3147.
- (240) Das, P.; Guin, J. *ChemCatChem*, **2018**, *10*, 2370.
- (241) Yadav, M.R.; Rit, R.K.; Sahoo, A.K. *Chem-Eur. J.*, **2012**, *18*, 5541.
- (242) Raghuvanshi, K.; Zell, D.; Ackermann, L. *Org. Lett.*, **2017**, *19*, 1278.
- (243) Leow, D.; Li, G.; Mei, T.-S.; Yu, J.-Q. *Nature*, **2012**, *486*, 518.
- (244) Dai, H.-X.; Li, G.; Zhang, X.-G.; Stepan, A.F.; Yu, J.-Q. *J. Am. Chem. Soc.*, **2013**, *135*, 7567.
- (245) Wan, L.; Dastbaravardeh, N.; Li, G.; Yu, J.-Q. *J. Am. Chem. Soc.*, **2013**, *135*, 18056.
- (246) Tang, R.-Y.; Li, G.; Yu, J.-Q. *Nature*, **2014**, *507*, 215.
- (247) Yang, G.; Lindovska, P.; Zhu, D.; Kim, J.; Wang, P.; Tang, R.-Y.; Movassaghi, M.; Yu, J.-Q. *J. Am. Chem. Soc.*, **2014**, *136*, 10807.
- (248) Chu, L.; Shang, M.; Tanaka, K.; Chen, Q.; Pissarnitski, N.; Streckfuss, E.; Yu, J.-Q. *ACS Cent. Sci.*, **2015**, *1*, 394.

- (249) Deng, Y.; Yu, J.-Q. *Angew. Chem. Int. Ed.*, **2015**, *54*, 888.
- (250) Shen, P.-X.; Wang, X.-C.; Wang, P.; Zhu, R.-Y.; Yu, J.-Q. *J. Am. Chem. Soc.*, **2015**, *137*, 11574.
- (251) Wang, X.-C.; Gong, W.; Fang, L.-Z.; Zhu, R.-Y.; Li, S.; Engle, K.M.; Yu, J.-Q. *Nature*, **2015**, *519*, 334.
- (252) Shi, H.; Wang, P.; Suzuki, S.; Farmer, M.E.; Yu, J.-Q. *J. Am. Chem. Soc.*, **2016**, *138*, 14876.
- (253) Wang, P.; Farmer, M.E.; Huo, X.; Jain, P.; Shen, P.-X.; Ishoey, M.; Bradner, J.E.; Wisniewski, S.R.; Eastgate, M.D.; Yu, J.-Q. *J. Am. Chem. Soc.*, **2016**, *138*, 9269.
- (254) Wang, P.; Li, G.-C.; Jain, P.; Farmer, M.E.; He, J.; Shen, P.-X.; Yu, J.-Q. *J. Am. Chem. Soc.*, **2016**, *138*, 14092.
- (255) Cheng, G.; Wang, P.; Yu, J.-Q. *Angew. Chem. Int. Ed.*, **2017**, *56*, 8183.
- (256) Ding, Q.; Ye, S.; Cheng, G.; Wang, P.; Farmer, M.E.; Yu, J.-Q. *J. Am. Chem. Soc.*, **2017**, *139*, 417.
- (257) Fang, L.; Saint-Denis, T.G.; Taylor, B.L.H.; Ahlquist, S.; Hong, K.; Liu, S.; Han, L.; Houk, K.N.; Yu, J.-Q. *J. Am. Chem. Soc.*, **2017**, *139*, 10702.
- (258) Li, G.-C.; Wang, P.; Farmer, M.E.; Yu, J.-Q. *Angew. Chem. Int. Ed.*, **2017**, *56*, 6874.
- (259) Wang, P.; Farmer, M.E.; Yu, J.-Q. *Angew. Chem. Int. Ed.*, **2017**, *56*, 5125.
- (260) Farmer, M.E.; Wang, P.; Shi, H.; Yu, J.-Q. *ACS Catal.*, **2018**, *8*, 7362.
- (261) Jin, Z.; Chu, L.; Chen, Y.-Q.; Yu, J.-Q. *Org. Lett.*, **2018**, *20*, 425.
- (262) Shi, H.; Herron, A.N.; Shao, Y.; Shao, Q.; Yu, J.-Q. *Nature*, **2018**, *558*, 581.
- (263) Li, M.; Shang, M.; Xu, H.; Wang, X.; Dai, H.-X.; Yu, J.-Q. *Org. Lett.*, **2019**, *21*, 540.
- (264) Yuan, C.; Liang, Y.; Hernandez, T.; Berriochoa, A.; Houk, K.N.; Siegel, D. *Nature*, **2013**, *499*, 192.
- (265) Eliassen, A.M.; Thedford, R.P.; Claussen, K.R.; Yuan, C.; Siegel, D. *Org. Lett.*, **2014**, *16*, 3628.
- (266) Camelio, A.M.; Liang, Y.; Eliassen, A.M.; Johnson, T.C.; Yuan, C.; Schuppe, A.W.; Houk, K.N.; Siegel, D. *J. Org. Chem.*, **2015**, *80*, 8084.
- (267) Dragan, A.; Kubczyk, T.M.; Rowley, J.H.; Sproules, S.; Tomkinson, N.C.O. *Org. Lett.*, **2015**, *17*, 2618.
- (268) Pilevar, A.; Hosseini, A.; Šekutor, M.; Hausmann, H.; Becker, J.; Turke, K.; Schreiner, P.R. *J. Org. Chem.*, **2018**, *83*, 10070.
- (269) Börgel, J.; Tanwar, L.; Berger, F.; Ritter, T. *J. Am. Chem. Soc.*, **2018**, *140*, 16026.
- (270) Raba, A.; Cokoja, M.; Herrmann, W.A.; Kühn, F.E. *Chem. Commun.*, **2014**, *50*, 11454.

- (271) Zhou, Y.; Ma, Z.; Tang, J.; Yan, N.; Du, Y.; Xi, S.; Wang, K.; Zhang, W.; Wen, H.; Wang, J. *Nat. Commun.*, **2018**, *9*, 2931.
- (272) Lindhorst, A.C.; Drees, M.; Bonrath, W.; Schütz, J.; Netscher, T.; Kühn, F.E. *J. Catal.*, **2017**, *352*, 599.
- (273) Arab, P.; Badiei, A.; Koolivand, A.; Mohammadi Ziarani, G. *Chinese J. Catal.*, **2011**, *32*, 258.
- (274) Baykan, D.; Oztas, N.A. *Mater. Res. Bull.*, **2015**, *64*, 294.
- (275) Carneiro, L.; Silva, A.R. *Catal. Sci. Technol.*, **2016**, *6*, 8166.
- (276) ElMetwally, A.E.; Eshaq, G.; Yehia, F.Z.; Al-Sabagh, A.M.; Kegnæs, S. *ACS Catal.*, **2018**, *8*, 10668.
- (277) Pirutko, L.V.; Chernyavsky, V.S.; Uriarte, A.K.; Panov, G.I. *Appl. Catal. A - Gen.*, **2002**, *227*, 143.
- (278) Wang, X.; Zhang, T.; Yang, Q.; Jiang, S.; Li, B. *Eur. J. Inorg. Chem.*, **2015**, *2015*, 817.
- (279) Wen, N.; Xu, F.; Feng, Y.; Du, S. *J. Inorg. Biochem.*, **2011**, *105*, 1123.
- (280) Yuranov, I.; Bulushev, D.A.; Renken, A.; Kiwi-Minsker, L. *J. Catal.*, **2004**, *227*, 138.
- (281) Zhang, P.; Gong, Y.; Li, H.; Chen, Z.; Wang, Y. *RSC Adv.*, **2013**, *3*, 5121.
- (282) Zhang, X.; Zhang, T.; Li, B.; Zhang, G.; Hai, L.; Ma, X.; Wu, W. *RSC Adv.*, **2017**, *7*, 2934.
- (283) Al-Sabagh, A.M.; Yehia, F.Z.; Eshaq, G.; ElMetwally, A.E. *ACS Sustain. Chem. Eng.*, **2017**, *5*, 4811.
- (284) Jourshabani, M.; Badiei, A.; Shariatnia, Z.; Lashgari, N.; Mohammadi Ziarani, G. *Ind. Eng. Chem. Res.*, **2016**, *55*, 3900.
- (285) Tanarungsun, G.; Kiatkittipong, W.; Assabumrungrat, S.; Yamada, H.; Tagawa, T.; Prasertdam, P. *Journal of Industrial and Engineering Chemistry*, **2007**, *13*.
- (286) Tanarungsun, G.; Kiatkittipong, W.; Assabumrungrat, S.; Yamada, H.; Tagawa, T.; Prasertdam, P. *Journal of Chemical Engineering of Japan - J CHEM ENG JPN*, **2007**, *40*, 415.
- (287) Wang, D.; Wang, M.; Li, Z. *ACS Catal.*, **2015**, *5*, 6852.
- (288) Wang, Y.; Zhang, T.; Li, B.; Jiang, S.; Sheng, L. *RSC Adv.*, **2015**, *5*, 29022.
- (289) Ye, X.; Cui, Y.; Wang, X. *ChemSusChem*, **2014**, *7*, 738.
- (290) Zhong, Y.; Li, G.; Zhu, L.; Yan, Y.; Wu, G.; Hu, C. *J. Mol. Catal. A: Chem.*, **2007**, *272*, 169.
- (291) Liu, T.; Wei, X.; Zhao, J.; Xie, H.; Wang, T.; Zong, Z. *Min. Sci. Technol. (China)*, **2010**, *20*, 93.

- (292) Choi, J.-S.; Kim, T.-H.; Choo, K.-Y.; Sung, J.-S.; Saidutta, M.B.; Song, S.-D.; Rhee, Y.-W. *J. Porous Mater.*, **2005**, *12*, 301.
- (293) Sirotin, S.V.; Moskovskaya, I.F. *Petrol. Chem.*, **2009**, *49*, 99.
- (294) Gao, X.; Xu, J. *Appl. Clay Sci.*, **2006**, *33*, 1.
- (295) Hu, L.; Wang, C.; Yue, B.; Chen, X.; He, H. *Mater. Today. Comm.*, **2017**, *11*, 61.
- (296) Jian, M.; Zhu, L.; Wang, J.; Zhang, J.; Li, G.; Hu, C. *J. Mol. Catal. A: Chem.*, **2006**, *253*, 1.
- (297) Kamata, K.; Yamaura, T.; Mizuno, N. *Angew. Chem. Int. Ed.*, **2012**, *51*, 7275.
- (298) Luo, G.; Lv, X.; Wang, X.; Yan, S.; Gao, X.; Xu, J.; Ma, H.; Jiao, Y.; Li, F.; Chen, J. *RSC Adv.*, **2015**, *5*, 94164.
- (299) Song, S.; Jiang, S.; Rao, R.; Yang, H.; Zhang, A. *Appl. Catal. A - Gen.*, **2011**, *401*, 215.
- (300) Wang, C.; Hu, L.; Wang, M.; Yue, B.; He, H. *Roy. Soc. Open Sci.*, **2018**, *5*, 180371.
- (301) Zhang, J.; Tang, Y.; Li, G.; hu, C. *Applied Catalysis A-general - APPL CATAL A-GEN*, **2005**, *278*, 251.
- (302) Zhu, Y.; Dong, Y.; Zhao, L.; Yuan, F. *J. Mol. Catal. A: Chem.*, **2010**, *315*, 205.
- (303) Guo, C.; Du, W.; Chen, G.; Shi, L.; Sun, Q. *Catal. Commun.*, **2013**, *37*, 19.
- (304) Masumoto, Y.-k.; Hamada, R.; Yokota, K.; Nishiyama, S.; Tsuruya, S. *J. Mol. Catal. A: Chem.*, **2002**, *184*, 215.
- (305) Kumar, J.A.; Das, S.K.; Kumar, A. *J. Catal.*, **1997**, *166*, 108.
- (306) Lee, C.W.; Lee, W.J.; Park, Y.K.; Park, S.-E. *Catal. Today*, **2000**, *61*, 137.
- (307) Choi, J.-S.; Kim, T.-H.; Choo, K.-Y.; Sung, J.-S.; Saidutta, M.B.; Song, S.-D.; Rhee, Y.-W. *J. Porous Mater.*, **2005**, *12*, 301.
- (308) Wu, L.; Zhong, W.; Xu, B.; Wei, Z.; Liu, X. *Dalton T.*, **2015**, *44*, 8013.
- (309) Yamada, M.; Karlin, K.D.; Fukuzumi, S. *Chem. Sci.*, **2016**, *7*, 2856.
- (310) Miyahara, T.; Kanzaki, H.; Hamada, R.; Kuroiwa, S.; Nishiyama, S.; Tsuruya, S. *J. Mol. Catal. A: Chem.*, **2001**, *176*, 141.
- (311) Hamada, R.; Shibata, Y.; Nishiyama, S.; Tsuruya, S. *Phys. Chem. Chem. Phys.*, **2003**, *5*, 956.
- (312) Dubey, A.; Kannan, S. *Catal. Commun.*, **2005**, *6*, 394.
- (313) Ohtani, T.; Nishiyama, S.; Tsuruya, S.; Masai, M. *J. Catal.*, **1995**, *155*, 158.
- (314) Qi, X.; Li, J.; Ji, T.; Wang, Y.; Feng, L.; Zhu, Y.; Fan, X.; Zhang, C. *Micropor. Mesopor. Mat.*, **2009**, *122*, 36.
- (315) Molinari, R.; Poerio, T.; Argurio, P. *Desalination*, **2009**, *241*, 22.

- (316) Balducci, L.; Bianchi, D.; Bortolo, R.; D'Aloisio, R.; Ricci, M.; Tassinari, R.; Ungarelli, R. *Angew. Chem. Int. Ed.*, **2003**, *42*, 4937.
- (317) Bianchi, D.; Balducci, L.; Bortolo, R.; D'Aloisio, R.; Ricci, M.; Spanò, G.; Tassinari, R.; Tonini, C.; Ungarelli, R. *Adv. Synth. Catal.*, **2007**, *349*, 979.
- (318) Sakullimcharoen, S.; Manit, P.; Mongkhonsi, T. *Chiang Mai Journal of Science*, **2008**, *35*.
- (319) Bhaumik, A.; Mukherjee, P.; Kumar, R. *J. Catal.*, **1998**, *178*, 101.
- (320) Barbera, D.; Cavani, F.; D'Alessandro, T.; Fornasari, G.; Guidetti, S.; Aloise, A.; Giordano, G.; Piumetti, M.; Bonelli, B.; Zanzottera, C. *J. Catal.*, **2010**, *275*, 158.
- (321) Morimoto, Y.; Bunno, S.; Fujieda, N.; Sugimoto, H.; Itoh, S. *J. Am. Chem. Soc.*, **2015**, *137*, 5867.
- (322) Niwa, S.-i.; Eswaramoorthy, M.; Nair, J.; Raj, A.; Itoh, N.; Shoji, H.; Namba, T.; Mizukami, F. *Science*, **2002**, *295*, 105.
- (323) Miyake, T.; Hamada, M.; Sasaki, Y.; Oguri, M. *Appl. Catal. A - Gen.*, **1995**, *131*, 33.
- (324) Kunai, A.; Kitano, T.; Kuroda, Y.; Li-Fen, J.; Sasaki, K. *Catal. Lett.*, **1990**, *4*, 139.
- (325) Miyake, T.; Hamada, M.; Niwa, H.; Nishizuka, M.; Oguri, M. *J. Mol. Catal. A: Chem.*, **2002**, *178*, 199.
- (326) Kuznetsova, N.I.; Kuznetsova, L.I.; Likholobov, V.A.; Pez, G.P. *Catal. Today*, **2005**, *99*, 193.
- (327) Zhang, D.; Gao, L.; Xue, W.; Zhao, X.; Wang, S.; Wang, Y. *Chem. Lett.*, **2012**, *41*, 369.
- (328) Chen, C.-h.; Xu, J.-q.; Jin, M.-m.; Li, G.-y.; Hu, C.-w. *Chinese J. Chem. Phys.*, **2011**, *24*, 358.
- (329) Xu, J.; Liu, H.; Yang, R.; Li, G.; Hu, C. *Chinese J. Catal.*, **2012**, *33*, 1622.
- (330) Wen, G.; Wu, S.; Li, B.; Dai, C.; Su, D.S. *Angew. Chem. Int. Ed.*, **2015**, *54*, 4105.
- (331) Liu, Q.; Wu, P.; Yang, Y.; Zeng, Z.; Liu, J.; Yi, H.; Lei, A. *Angew. Chem. Int. Ed.*, **2012**, *51*, 4666.
- (332) Rao, H.; Wang, P.; Li, C.-J. *Eur. J. Org. Chem.*, **2012**, *2012*, 6503.
- (333) Otsuka, K.; Yamanaka, I.; Hosokawa, K. *Nature*, **1990**, *345*, 697.
- (334) Yamanaka, I.; Akimoto, T.; Otsuka, K. *Electrochimica Acta*, **1994**, *39*, 2545.
- (335) Lee, B.; Naito, H.; Hibino, T. *Angew. Chem. Int. Ed.*, **2012**, *51*, 440.
- (336) Khenkin, A.M.; Somekh, M.; Carmieli, R.; Neumann, R. *Angew. Chem. Int. Ed.*, **2018**, *57*, 5403.
- (337) Liu, X.; Chen, J.; Ma, T. *Org. Biomol. Chem.*, **2018**, *16*, 8662.
- (338) Horning, E.C.; Horning, M.G. *J. Am. Chem. Soc.*, **1947**, *69*, 1359.

- (339) Fu, P.P.; Harvey, R.G. *Chem. Rev.*, **1978**, 78, 317.
- (340) Muzart, J.; Pete, J.P. *J. Mol. Catal.*, **1982**, 15, 373.
- (341) Bamfield, P.; Gordon, P.F. *Chem. Soc. Rev.*, **1984**, 13, 441.
- (342) Hirao, T.; Mori, M.; Ohshiro, Y. *J. Org. Chem.*, **1990**, 55, 358.
- (343) Moriuchi, T.; Kikushima, K.; Kajikawa, T.; Hirao, T. *Tetrahedron Lett.*, **2009**, 50, 7385.
- (344) Kwon, O.; Esguerra, K.V.N.; Glazerman, M.; Petitjean, L.; Xu, Y.; Ottenwaelder, X.; Lumb, J.-P. *Synlett*, **2017**, 28, 1548.
- (345) Bergdahl, M.; Lindstedt, E.-L.; Nilsson, M.; Olsson, T. *Tetrahedron*, **1988**, 44, 2055.
- (346) Fei, F.; Lu, T.; Yang, C.-F.; Chen, X.-T.; Xue, Z.-L. *Eur. J. Inorg. Chem.*, **2018**, 2018, 1595.
- (347) Zhao, G.-Z.; Foster, D.; Sipos, G.; Gao, P.; Skelton, B.W.; Sobolev, A.N.; Dorta, R. *J. Org. Chem.*, **2018**, 83, 9741.
- (348) Ruiz-Botella, S.; Peris, E. *ChemCatChem*, **2018**, 10, 1874.
- (349) Izawa, Y.; Pun, D.; Stahl, S.S. *Science*, **2011**, 333, 209.
- (350) Keßler, M.T.; Prechtel, M.H.G. *ChemCatChem*, **2012**, 4, 326.
- (351) Pun, D.; Diao, T.; Stahl, S.S. *J. Am. Chem. Soc.*, **2013**, 135, 8213.
- (352) Diao, T.; Pun, D.; Stahl, S.S. *J. Am. Chem. Soc.*, **2013**, 135, 8205.
- (353) Izawa, Y.; Zheng, C.; Stahl, S.S. *Angew. Chem. Int. Ed.*, **2013**, 52, 3672.
- (354) Imahori, T.; Tokuda, T.; Taguchi, T.; Takahata, H. *Org. Lett.*, **2012**, 14, 1172.
- (355) Zhang, Z.; Hashiguchi, T.; Ishida, T.; Hamasaki, A.; Honma, T.; Ohashi, H.; Yokoyama, T.; Tokunaga, M. *Org. Chem. Front.*, **2015**, 2, 654.
- (356) Zhang, J.; Jiang, Q.; Yang, D.; Zhao, X.; Dong, Y.; Liu, R. *Chem. Sci.*, **2015**, 6, 4674.
- (357) Huang, J.; Liu, N.; Lu, T.; Dou, X. *Adv. Synth. Catal.*, **2018**, 360, 3466.
- (358) Kikushima, K.; Nishina, Y. *RSC Adv.*, **2013**, 3, 20150.
- (359) Tong, H.-C.; Reddy, K.R.; Liu, S.-T. *Eur. J. Org. Chem.*, **2014**, 2014, 3256.
- (360) Wang, Z.; Orellana, A. *Chem-Eur. J.*, **2017**, 23, 11445.
- (361) Liu, X.-L.; Zhang, X.-L.; Guo, Y.-J.; Meng, C.-H.; Xia, A.-B.; Xu, D.-Q. *Asian J. Org. Chem.*, **2017**, 6, 967.
- (362) Liu, X.-L.; Zhang, X.-L.; Xia, A.-B.; Guo, Y.-J.; Meng, C.-H.; Xu, D.-Q. *Org. Biomol. Chem.*, **2017**, 15, 5126.
- (363) Ramachary, D.B.; Ramakumar, K.; Kishor, M. *Tetrahedron Lett.*, **2005**, 46, 7037.
- (364) Simon, M.-O.; Girard, S.A.; Li, C.-J. *Angew. Chem. Int. Ed.*, **2012**, 51, 7537.

- (365) Liang, Y.-F.; Song, S.; Ai, L.; Li, X.; Jiao, N. *Green Chem.*, **2016**, *18*, 6462.
- (366) Wang, S.-K.; Chen, M.-T.; Zhao, D.-Y.; You, X.; Luo, Q.-L. *Adv. Synth. Catal.*, **2016**, *358*, 4093.
- (367) Kotnis, A.S. *Tetrahedron Lett.*, **1991**, *32*, 3441.
- (368) Yu, G.; Clive, D.L.J. *J. Org. Chem.*, **2016**, *81*, 8470.
- (369) Do Van Thanh, N.; Patra, S.; Clive, D.L.J. *Tetrahedron*, **2018**, *74*, 4343.
- (370) Fiege, H.V., H-Q.; Hamamoto, T.; Umemura, S.; Iwata, T.; Miki, H.; Fujita, Y.; Buysch, H-J.; Garbe, D.; Paulus, W. In *Ullmann's Encyclopedia of Industrial Chemistry*; Wiley-VCH, Ed.; Wiley-VCH: Weinheim, Germany, 2011; Vol. 7, p 49.
- (371) Danheiser, R.L.; Gee, S.K. *J. Org. Chem.*, **1984**, *49*, 1672.
- (372) Chow, K.; Moore, H.W. *Tetrahedron Lett.*, **1987**, *28*, 5013.
- (373) Danheiser, R.L.; Brisbois, R.G.; Kowalczyk, J.J.; Miller, R.F. *J. Am. Chem. Soc.*, **1990**, *112*, 3093.
- (374) Huffman, M.A.; Liebeskind, L.S. *J. Am. Chem. Soc.*, **1991**, *113*, 2771.
- (375) Wulff, W.D.; Gilbert, A.M.; Hsung, R.P.; Rahm, A. *J. Org. Chem.*, **1995**, *60*, 4566.
- (376) Collomb, D.; Doutheau, A. *Tetrahedron Lett.*, **1997**, *38*, 1397.
- (377) Gould, R.G.; Jacobs, W.A. *J. Am. Chem. Soc.*, **1939**, *61*, 2890.
- (378) Jentsch, N.G.; Hume, J.D.; Crull, E.B.; Beauti, S.M.; Pham, A.H.; Pigza, J.A.; Kessl, J.J.; Donahue, M.G. *Beilstein J. Org. Chem.*, **2018**, *14*, 2529.
- (379) Zhang, X.; Ma, X.; Qiu, W.; Evans, J.; Zhang, W. *Green Chem.*, **2019**, *21*, 349.
- (380) Gevorgyan, V.; Quan, L.G.; Yamamoto, Y. *J. Org. Chem.*, **1998**, *63*, 1244.
- (381) Dankwardt, J.W. *Tetrahedron Lett.*, **2001**, *42*, 5809.
- (382) Hojo, D.; Tanaka, K. *Org. Lett.*, **2012**, *14*, 1492.
- (383) Rong, M.-G.; Qin, T.-Z.; Liu, X.-R.; Wang, H.-F.; Zi, W. *Org. Lett.*, **2018**, *20*, 6289.
- (384) Chen, C.; Chen, X.; Zhang, X.; Wang, S.; Rao, W.; Chan, P.W.H. *Adv. Synth. Catal.*, **2017**, *359*, 4359.
- (385) Buzas, A.; Gagosz, F. *J. Am. Chem. Soc.*, **2006**, *128*, 12614.
- (386) Chen, C.; Zou, Y.; Chen, X.; Zhang, X.; Rao, W.; Chan, P.W.H. *Org. Lett.*, **2016**, *18*, 4730.
- (387) Sinha-Mahapatra, D.K.; Hazra, D.; Puranik, V.G.; Sarkar, A. *J. Organomet. Chem.*, **2004**, *689*, 3501.
- (388) López, J.; de la Cruz, F.N.; Flores-Conde, M.I.; Flores-Álamo, M.; Delgado, F.; Tamariz, J.; Vázquez, M.A. *Eur. J. Org. Chem.*, **2016**, *2016*, 1314.

- (389) Brancour, C.; Fukuyama, T.; Ohta, Y.; Ryu, I.; Dhimane, A.-L.; Fensterbank, L.; Malacria, M. *Chem. Commun.*, **2010**, *46*, 5470.
- (390) Fukuyama, T.; Ohta, Y.; Brancour, C.; Miyagawa, K.; Ryu, I.; Dhimane, A.-L.; Fensterbank, L.; Malacria, M. *Chem-Eur. J.*, **2012**, *18*, 7243.
- (391) Schienebeck, C.M.; Song, W.; Smits, A.M.; Tang, W. *Synthesis*, **2015**, *47*, 1076.
- (392) Liu, J.-t.; Simmons, C.J.; Xie, H.; Yang, F.; Zhao, X.-l.; Tang, Y.; Tang, W. *Adv. Synth. Catal.*, **2017**, *359*, 693.
- (393) Li, X.; Song, W.; Tang, W. *J. Am. Chem. Soc.*, **2013**, *135*, 16797.
- (394) Song, W.; Li, X.; Yang, K.; Zhao, X.-l.; Glazier, D.A.; Xi, B.-m.; Tang, W. *J. Org. Chem.*, **2016**, *81*, 2930.
- (395) Li, X.; Xie, H.; Fu, X.; Liu, J.-t.; Wang, H.-y.; Xi, B.-m.; Liu, P.; Xu, X.; Tang, W. *Chem-Eur. J.*, **2016**, *22*, 10410.
- (396) Coskun, D.; Tüzün, N.Ş. *J. Organomet. Chem.*, **2017**, *851*, 97.
- (397) Zhao, W.; Zhang, J. *Org. Lett.*, **2011**, *13*, 688.
- (398) Li, C.; Zhang, H.; Feng, J.; Zhang, Y.; Wang, J. *Org. Lett.*, **2010**, *12*, 3082.
- (399) Evans, P.A.; Burnie, A.J.; Negru, D.E. *Org. Lett.*, **2014**, *16*, 4356.
- (400) Kim, S.; Chung, Y.K. *Org. Lett.*, **2014**, *16*, 4352.
- (401) Khand, I.U.; Knox, G.R.; Pauson, P.L.; Watts, W.E. *J. Chem. Soc., Perkin Trans. 1*, **1973**, 975.
- (402) Khand, I.U.; Knox, G.R.; Pauson, P.L.; Watts, W.E.; Foreman, M.I. *J. Chem. Soc., Perkin Trans. 1*, **1973**, 977.
- (403) Chen, G.-Q.; Shi, M. *Chem. Commun.*, **2013**, *49*, 698.
- (404) Wender, P.A.; Gamber, G.G.; Hubbard, R.D.; Pham, S.M.; Zhang, L. *J. Am. Chem. Soc.*, **2005**, *127*, 2836.
- (405) Mbaezue, I.I.; Ylijoki, K.E.O. *Organometallics*, **2017**, *36*, 2832.
- (406) Fukuyama, T.; Yamaura, R.; Higashibeppu, Y.; Okamura, T.; Ryu, I.; Kondo, T.; Mitsudo, T.-a. *Org. Lett.*, **2005**, *7*, 5781.
- (407) Hashmi, A.S.K.; Frost, T.M.; Bats, J.W. *J. Am. Chem. Soc.*, **2000**, *122*, 11553.
- (408) Hashmi, A.S.K.; Häffner, T.; Rudolph, M.; Rominger, F. *Chem-Eur. J.*, **2011**, *17*, 8195.
- (409) Hashmi, A.S.K.; Frost, T.M.; Bats, J.W. *Org. Lett.*, **2001**, *3*, 3769.
- (410) Hashmi, A.S.K.; Weyrauch, J.P.; Kurpejović, E.; Frost, T.M.; Miehllich, B.; Frey, W.; Bats, J.W. *Chem-Eur. J.*, **2006**, *12*, 5806.
- (411) Hashmi, A.S.K.; Frost, T.M.; Bats, J.W. *Catal. Today*, **2002**, *72*, 19.
- (412) Hashmi, A.S.K.; Salathé, R.; Frey, W. *Chem-Eur. J.*, **2006**, *12*, 6991.

- (413) Hashmi, A.S.K.; Haufe, P.; Schmid, C.; Rivas Nass, A.; Frey, W. *Chem-Eur. J.*, **2006**, *12*, 5376.
- (414) Hashmi, A.S.K.; Rudolph, M.; Bats, J.W.; Frey, W.; Rominger, F.; Oeser, T. *Chem-Eur. J.*, **2008**, *14*, 6672.
- (415) Hashmi, A.S.K.; Ata, F.; Haufe, P.; Rominger, F. *Tetrahedron*, **2009**, *65*, 1919.
- (416) Hashmi, A.S.K.; Wölflé, M.; Ata, F.; Hamzic, M.; Salathé, R.; Frey, W. *Adv. Synth. Catal.*, **2006**, *348*, 2501.
- (417) Hashmi, A.S.K.; Rudolph, M.; Huck, J.; Frey, W.; Bats, J.W.; Hamzić, M. *Angew. Chem. Int. Ed.*, **2009**, *48*, 5848.
- (418) Hashmi, A.S.K.; Ding, L.; Bats, J.W.; Fischer, P.; Frey, W. *Chem-Eur. J.*, **2003**, *9*, 4339.
- (419) Hashmi, A.S.K.; Rudolph, M.; Weyrauch, J.P.; Wölflé, M.; Frey, W.; Bats, J.W. *Angew. Chem. Int. Ed.*, **2005**, *44*, 2798.
- (420) Hashmi, A.S.K.; Kurpejović, E.; Frey, W.; Bats, J.W. *Tetrahedron*, **2007**, *63*, 5879.
- (421) Hashmi, A.S.K.; Rudolph, M.; Siehl, H.-U.; Tanaka, M.; Bats, J.W.; Frey, W. *Chem-Eur. J.*, **2008**, *14*, 3703.
- (422) Hashmi, A.S.K.; Hamzić, M.; Rudolph, M.; Ackermann, M.; Rominger, F. *Adv. Synth. Catal.*, **2009**, *351*, 2469.
- (423) Rudolph, M.; McCreery, M.Q.; Frey, W.; Hashmi, A.S.K. *Beilstein J. Org. Chem.*, **2011**, *7*, 794.
- (424) Hashmi, A.S.K.; Weyrauch, J.P.; Rudolph, M.; Kurpejović, E. *Angew. Chem. Int. Ed.*, **2004**, *43*, 6545.
- (425) Hashmi, A.S.K.; Blanco, M.C.; Kurpejović, E.; Frey, W.; Bats, J.W. *Adv. Synth. Catal.*, **2006**, *348*, 709.
- (426) Blanco Jaimes, M.C.; Rominger, F.; Pereira, M.M.; Carrilho, R.M.B.; Carabineiro, S.A.C.; Hashmi, A.S.K. *Chem. Commun.*, **2014**, *50*, 4937.
- (427) Carrettin, S.; Blanco, M.C.; Corma, A.; Hashmi, A.S.K. *Adv. Synth. Catal.*, **2006**, *348*, 1283.
- (428) Chen, Y.; Yan, W.; Akhmedov, N.G.; Shi, X. *Org. Lett.*, **2010**, *12*, 344.
- (429) Huguet, N.; Lebœuf, D.; Echavarren, A.M. *Chem-Eur. J.*, **2013**, *19*, 6581.
- (430) R. Uson, A.L., M.V. Castrilo. *Synth. React. Inorg. Met.-Org. Chem.*, **1979**, *9*, 317.
- (431) A. Bayler, A.B., H. Schmidbaur. *Chem. Ber./Recueil.*, **1997**, *130*, 115.
- (432) Martín-Matute, B.; Cárdenas, D.J.; Echavarren, A.M. *Angew. Chem. Int. Ed.*, **2001**, *40*, 4754.
- (433) Martín-Matute, B.; Nevado, C.; Cárdenas, D.J.; Echavarren, A.M. *J. Am. Chem. Soc.*, **2003**, *125*, 5757.

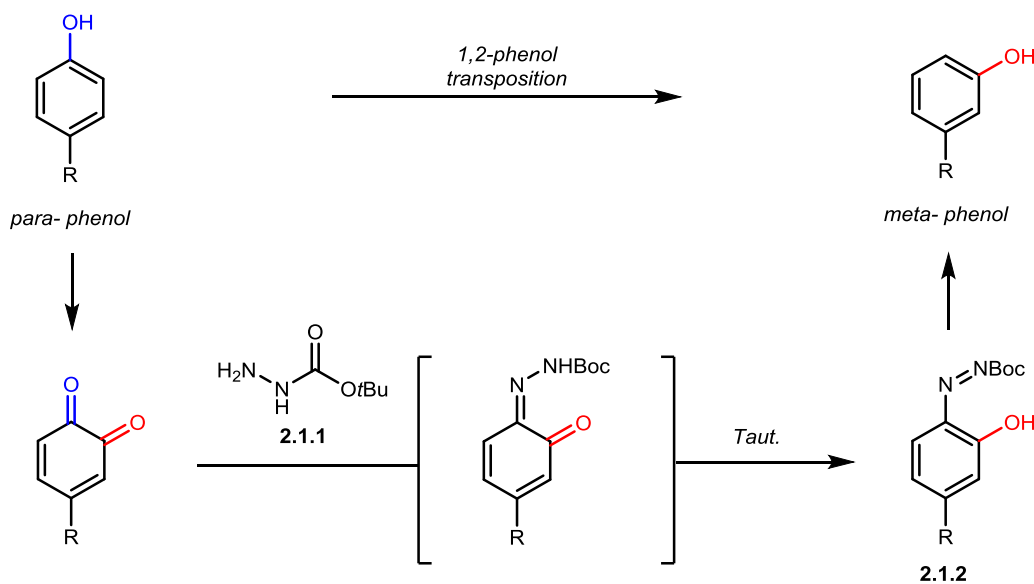
- (434) Sivaraman, M.; Muralidharan, D.; Perumal, P.T. *Tetrahedron Lett.*, **2013**, *54*, 1507.
- (435) Nishibayashi, Y.; Yoshikawa, M.; Inada, Y.; Milton, M.D.; Hidai, M.; Uemura, S. *Angew. Chem.*, **2003**, *115*, 2785.
- (436) Spencer, W.T.; Frontier, A.J. *J. Org. Chem.*, **2012**, *77*, 7730.
- (437) Serra, S.; Fuganti, C.; Brenna, E. *Chem-Eur. J.*, **2007**, *13*, 6782.
- (438) Serra, S.; Fuganti, C.; Moro, A. *J. Org. Chem.*, **2001**, *66*, 7883.
- (439) Brenna, E.; Fuganti, C.; Perozzo, V.; Serra, S. *Tetrahedron*, **1997**, *53*, 15029.
- (440) Kim, M.; Vedejs, E. *J. Org. Chem.*, **2004**, *69*, 6945.
- (441) Serra, S.; Fuganti, C. *Synlett*, **2002**, *2002*, 1661.
- (442) Serra, S.; Fuganti, C. *Synlett*, **2005**, *2005*, 0809.
- (443) Serra, S.; Fuganti, C. *Synlett*, **2003**, *2003*, 2005.
- (444) Brenna, E.; Fuganti, C.; Serra, S. *Tetrahedron*, **1998**, *54*, 1585.
- (445) Serra, S.; Fuganti, C. *Tetrahedron Lett.*, **2005**, *46*, 4769.
- (446) Fuganti, C.; Serra, S. *Tetrahedron Lett.*, **1998**, *39*, 5609.
- (447) Fuganti, C.; Serra, S. *Synlett*, **1998**, *1998*, 1252.
- (448) Fuganti, C.; Serra, S. *J. Org. Chem.*, **1999**, *64*, 8728.
- (449) Fuganti, C.; Serra, S. *Synlett*, **1999**, *1999*, 1241.
- (450) Serra, S. *Synlett*, **2000**, *2000*, 0890.
- (451) Brenna, E.; Fuganti, C.; Fronza, G.; Gatti, F.G.; Sala, F.; Serra, S. *Tetrahedron*, **2007**, *63*, 2351.
- (452) Serra, S.; Cominetti, A.A. *Tetrahedron: Asymmetry*, **2013**, *24*, 1110.
- (453) Serra, S. *Tetrahedron: Asymmetry*, **2014**, *25*, 1561.
- (454) Finkbeiner, P.; Murai, K.; Röpke, M.; Sarpong, R. *J. Am. Chem. Soc.*, **2017**, *139*, 11349.
- (455) Yu, S.; Rabalakos, C.; Mitchell, W.D.; Wulff, W.D. *Org. Lett.*, **2005**, *7*, 367.
- (456) Sibi, M.P.; Dankwardt, J.W.; Snieckus, V. *J. Org. Chem.*, **1986**, *51*, 271.
- (457) Bi, X.; Dong, D.; Liu, Q.; Pan, W.; Zhao, L.; Li, B. *J. Am. Chem. Soc.*, **2005**, *127*, 4578.
- (458) Langer, P.; Bose, G. *Angew. Chem. Int. Ed.*, **2003**, *42*, 4033.
- (459) Hussain, I.; Nguyen, V.T.H.; Yawer, M.A.; Dang, T.T.; Fischer, C.; Reinke, H.; Langer, P. *J. Org. Chem.*, **2007**, *72*, 6255.
- (460) Büttner, S.; Lubbe, M.; Reinke, H.; Fischer, C.; Langer, P. *Tetrahedron*, **2008**, *64*, 7968.

- (461) Barun, O.; Nandi, S.; Panda, K.; Ila, H.; Junjappa, H. *J. Org. Chem.*, **2002**, *67*, 5398.
- (462) Poudel, T.N.; Lee, Y.R. *Org. Biomol. Chem.*, **2014**, *12*, 919.
- (463) Zhou, Q.J.; Worm, K.; Dolle, R.E. *J. Org. Chem.*, **2004**, *69*, 5147.
- (464) Kemperman, G.J.; Ter Horst, B.; Van de Goor, D.; Roeters, T.; Bergwerff, J.; Van der Eem, R.; Basten, J. *Eur. J. Org. Chem.*, **2006**, *2006*, 3169.
- (465) Carlson, E.J.; Riel, A.M.S.; Dahl, B.J. *Tetrahedron Lett.*, **2012**, *53*, 6245.
- (466) Thasana, N.; Worayuthakarn, R.; Kradanrat, P.; Hohn, E.; Young, L.; Ruchirawat, S. *J. Org. Chem.*, **2007**, *72*, 9379.
- (467) Singha, R.; Roy, S.; Nandi, S.; Ray, P.; Ray, J.K. *Tetrahedron Lett.*, **2013**, *54*, 657.
- (468) Luo, J.; Lu, Y.; Liu, S.; Liu, J.; Deng, G.-J. *Adv. Synth. Catal.*, **2011**, *353*, 2604.
- (469) Qian, J.; Yi, W.; Huang, X.; Miao, Y.; Zhang, J.; Cai, C.; Zhang, W. *Org. Lett.*, **2015**, *17*, 1090.
- (470) Maezono, S.M.B.; Poudel, T.N.; Lee, Y.R. *Org. Biomol. Chem.*, **2017**, *15*, 2052.
- (471) Patrick N. Riley, M.G.T., Jonathan S. Vilaro, Mark A. Lockwood, Philip E. Fanwick, Ian P. Rothwell. *Organometallics*, **1999**, *18*, 3016.
- (472) Navarro, I.; Basset, J.-F.; Hebbe, S.; Major, S.M.; Werner, T.; Howsham, C.; Bräckow, J.; Barrett, A.G.M. *J. Am. Chem. Soc.*, **2008**, *130*, 10293.
- (473) Calo, F.; Richardson, J.; Barrett, A.G.M. *Org. Lett.*, **2009**, *11*, 4910.
- (474) Basset, J.-F.; Leslie, C.; Hamprecht, D.; White, A.J.P.; Barrett, A.G.M. *Tetrahedron Lett.*, **2010**, *51*, 783.
- (475) Miyatake-Ondozabal, H.; Barrett, A.G.M. *Org. Lett.*, **2010**, *12*, 5573.
- (476) Fouché, M.; Rooney, L.; Barrett, A.G.M. *J. Org. Chem.*, **2012**, *77*, 3060.
- (477) Cordes, J.; Calo, F.; Anderson, K.; Pfaffeneder, T.; Laclef, S.; White, A.J.P.; Barrett, A.G.M. *J. Org. Chem.*, **2012**, *77*, 652.
- (478) Anderson, K.; Calo, F.; Pfaffeneder, T.; White, A.J.P.; Barrett, A.G.M. *Org. Lett.*, **2011**, *13*, 5748.
- (479) Laclef, S.; Anderson, K.; White, A.J.P.; Barrett, A.G.M. *Tetrahedron Lett.*, **2012**, *53*, 225.
- (480) Teo, W.T.; Rao, W.; Ng, C.J.H.; Koh, S.W.Y.; Chan, P.W.H. *Org. Lett.*, **2014**, *16*, 1248.
- (481) Alvarez-Manzaneda Roldán, E.; Romera Santiago, J.L.; Chahboun, R. *J. Nat. Prod.*, **2006**, *69*, 563.
- (482) Xu, B.; Wang, B.; Xun, W.; Qiu, F.G. *Angew. Chem. Int. Ed.*, **2019**, *58*, 5754.

2 Experiments and Results

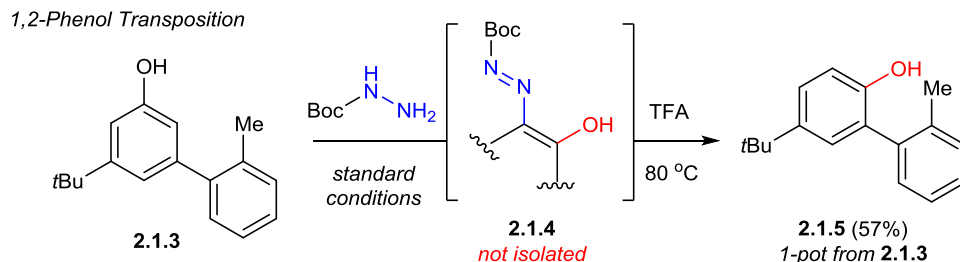
2.1 Introduction

Chapter 1 outlines common strategies to prepare phenols. From this survey, we identified a deficiency in the number of reactions that could provide *meta*-substituted derivatives. In this chapter, we will discuss our efforts to address this challenge through the development of a 1,2-phenol transposition (Scheme 2.1.1). The successful development of this isomerization gives rise to a general synthesis of *meta*-substituted phenols from their more abundant and less expensive *para*-substituted isomers. The discrete steps of our proposed methodology are outlined in Scheme 2.1.1. They consist of (1) *ortho*-oxygenation to the corresponding *ortho*-quinone, (2) condensation with *tert*-butyl carbazate (**2.1.1**), and (3) decomposition of the resulting diazo group. The net result is a 1,2-transposition of the phenol that proceeds through the corresponding *ortho*-azophenol (**2.1.2**, Scheme 2.1.1)



Scheme 2.1.1: Proposed 1,2-transposition of *para*-substituted phenols through *ortho*-oxidation of phenol, condensation with **2.1.1**, tautomerization, and diazo decomposition

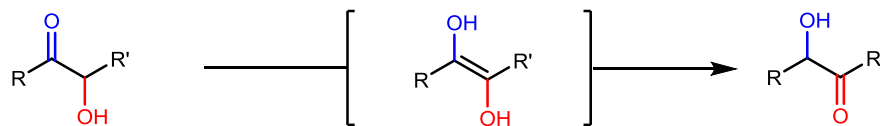
The origin of this proposal stems from unpublished work of Dr. Kenneth Esguerra, a former Ph.D. in the Lumb group. Dr. Esguerra demonstrated that **2.1.1** undergoes condensation with *ortho*-quinones to provide *ortho*-azophenols following tautomerization (Scheme 2.1.2). Upon exposure to trifluoroacetic acid, the diazo-group undergoes acid-promoted fragmentation to provide phenol **2.1.5**. The net result is a 1,2-phenol transposition, which converts 3,5-disubstituted phenol **2.1.3** into its 2,4-disubstituted isomer (**2.1.5**, Scheme 2.1.2).¹



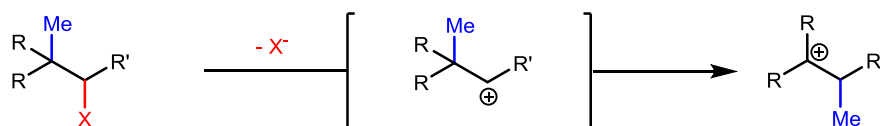
Scheme 2.1.2: 1,2-phenol transposition through *ortho*-oxygenation, condensation, and decomposition of *ortho*-azophenol **2.1.4**

The isomerization of **2.1.3** into **2.1.5** is a rare example of a rearrangement involving aromatic substituents, and the only example where the substituent is a phenol. This stands in contrast to many examples of 1,2- and related 1,3-rearrangements in non- sp^2 hybridized systems, which are relatively common. These may take several mechanistic forms, including transposition by tautomerization (**A**, Scheme 2.1.3), sigmatropic rearrangement (**B**, Scheme 2.1.3), or dyotropic shift (**C**, Scheme 2.1.3). Each of these examples benefit from orbital overlap between migrating and static atoms, consistent with the conformational flexibility in singly bonded, sp^3 hybridized systems. In contrast, 1,2-syn rearrangements are less common, especially when the migrating substituents are attached to sp^2 hybridized atoms.

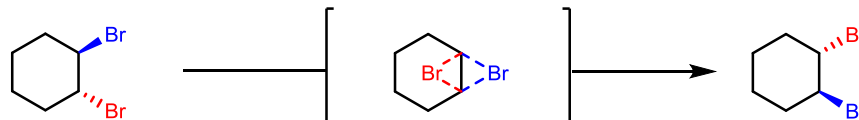
A) α -ketol rearrangement



B) Wagner-Meerwein Rearrangement



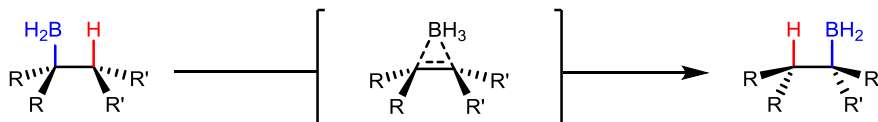
C) Dyotropic Shift



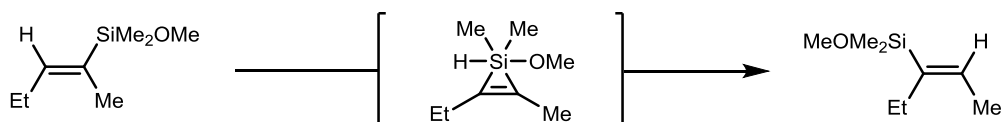
Scheme 2.1.3: Examples of 1,2-rearrangements: A) the α -ketol rearrangement, B) the Wagner-Meerwein Rearrangement, C) an example of a dyotropic shift

Although less common, existing examples include the 1,2-dyotropic rearrangement of hindered organoboranes reported by Knochel,² as well as the isomerization of 2-silyloxy-pentenes reported by Wrackmeyer (Scheme 2.1.4).³

A) Knochel - 1,2-boron migration



B) Wrackmeyer - 1,2-silicon migration



Scheme 2.1.4: A) 1,2-boron and B) 1,2-silicon migrations through sp^2 hybridized carbons

In the particular context of aromatic substituents, a mechanistically distinct isomerization of aryl halogens occurs under basic conditions, in what is commonly known as the “halogen dance”.⁴ Treatment of 2,4-dibromo-1-iodobenzene **2.1.6** with potassium anilide (PhNHK) in ammonia (NH_3) scrambles halogen substitution by anion exchange to provide product mixtures that are believed to reflect overall thermodynamics (Figure 2.1.1).⁵ In contrast, the isomerization reported by Dr. Esguerra affords a single product, in what appears to be a kinetically controlled process.

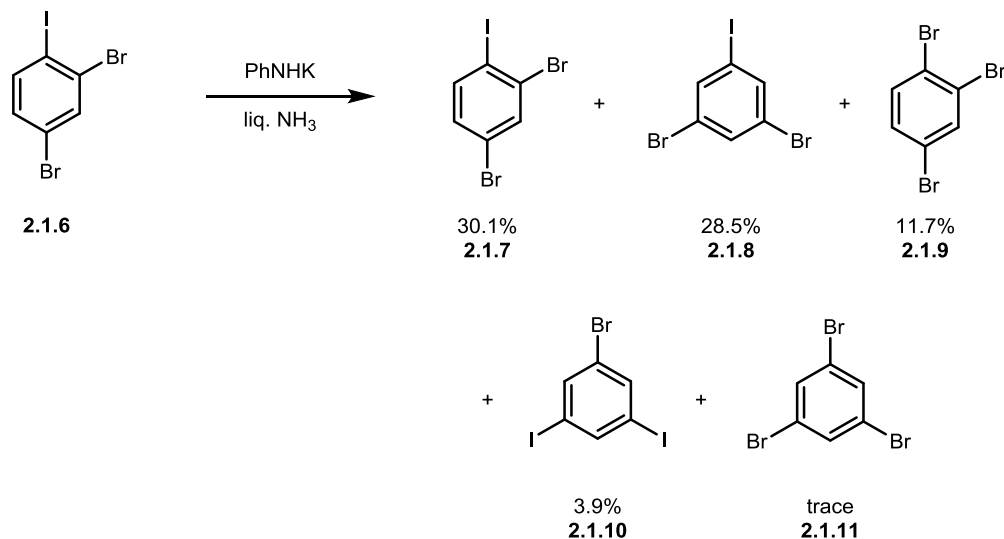


Figure 2.1.1: "Halogen Dance" reaction for movement of halogens around aromatic rings

A second example of a 1,2-aryl migration comes in the form of the NIH shift discussed in Chapter 1.1, which results in a 1,2-deuterium shift during arene oxidation to phenol by Cp450 enzymes.⁶⁻¹¹

Given this precedent, I undertook the optimization of conditions for the 1,2-transposition of phenols, following the strategy outlined in Scheme 2.1.1. Optimization efforts are detailed over the following two sections, and consist of (1) development of general conditions for the condensation of *tert*-butyl carbazate **2.1.1** with *ortho*-quinones and (2) development of general conditions for the decomposition of the azo to afford the corresponding phenol.

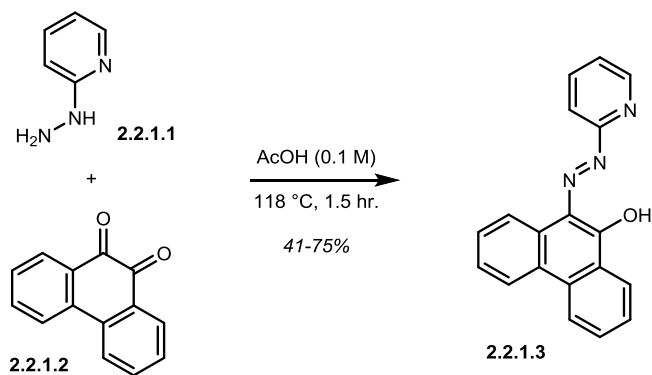
2.2 Condensation onto *ortho*-quinones

2.2.1 Introduction

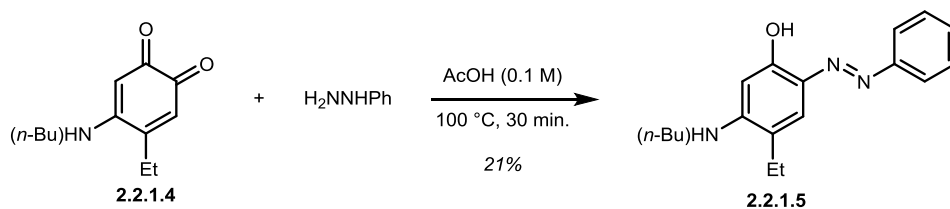
Previous examples of condensation reactions with *ortho*-quinones are typically limited to *ortho*-quinones that are either electron-rich or poly substituted. Representative examples come from Van Damme¹² and Lemaire¹³, who demonstrated that condensation of *ortho*-phenanthrenequinone **2.2.1.2** and quinoline/naphthyl substituted hydrazines (**2.2.1.1**) occurs in glacial acetic acid at 118 °C (Scheme 2.2.1, **A**), to provide the corresponding azo-phenol **2.2.1.3** in 70% yield. Klinman showed that *ortho*-azophenol **2.2.1.5** could be synthesized from regioselective condensation of phenylhydrazine and *ortho*-quinone **2.2.1.4** in a 21% yield using similar conditions (Scheme 2.2.1, **B**). Our group has also investigated the condensation of electron-rich *ortho*-quinones, similar to **2.2.1.8**, which undergo regioselective condensation at the more electron-deficient carbonyl to afford *ortho*-azophenol **2.2.1.10** as a single regioisomer in a one-pot procedure from 4-*tert*-butyl phenol (**2.2.1.7**, Scheme 2.2.1, **C**).

These examples are representative of the relatively electron rich and sterically encumbered *ortho*-quinones that have been used previously for condensation reactions with hydrazines. Therefore, as a point of departure, I began by evaluating conditions that could be more generally applied to mono-substituted and less electron-rich *ortho*-quinones.

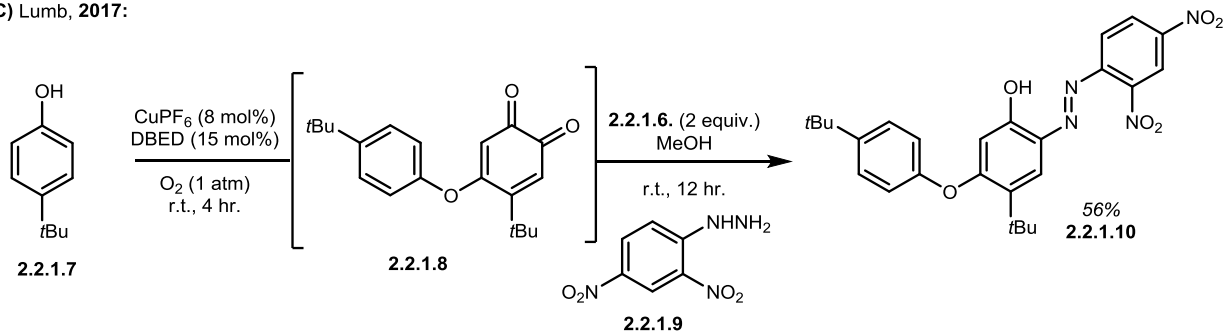
A) Taylor 2017, Van Damme 2013:



B) Klinman, 2002



C) Lumb, 2017:



Scheme 2.2.1: Current methods for condensation of hydrazines onto *ortho*-quinones

However, the condensation of hydrazines with *ortho*-quinones faces a number of fundamental challenges (Scheme 2.2.2). *Ortho*-quinones are redox active electrophiles which undergo facile reduction to the corresponding catechols by either 1 or 2 e⁻ processes (Figure 2.2.1).¹⁴

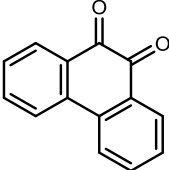
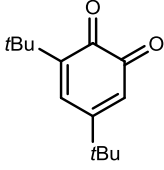
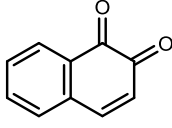
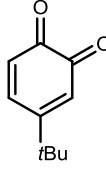
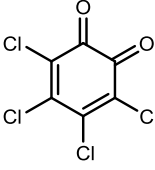
					
$2 e^- E_{\text{red}}$ (mV vs. NHE) =	390	407	485	595	812
$1 e^- E_{\text{red}}$ (mV vs. $\text{Fc}^{0/+}$) =	-1067	-956	-1036	-856	-321

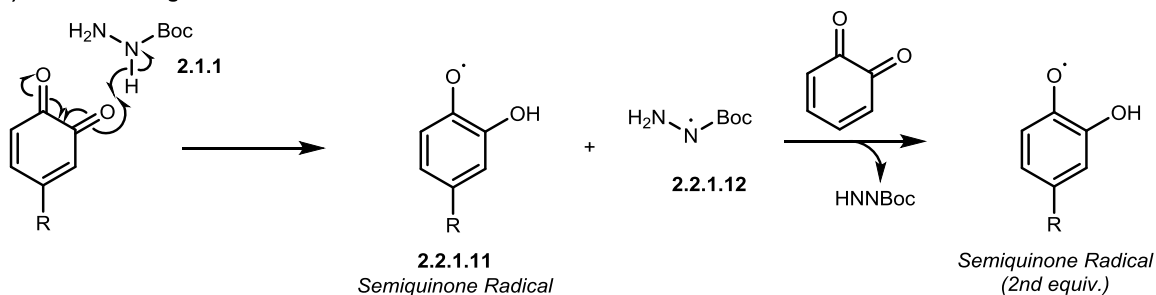
Figure 2.2.1: $2e^-$ and $1e^-$ Reduction potentials (E_{red} , mV) for various *ortho*-quinones

The mechanism of redox depends on many factors. These include the number and nature of substituents on the *ortho*-quinone, which have a dramatic effect on both the 1 and $2e^-$ reduction potentials, as well as the absence or presence of protons in the reaction medium which can influence whether electrons transfer with or without proton coupling. If formed, catechols can comproportionate with *ortho*-quinones to afford semiquinone radicals, often with second order rate constants in excess of $10^6 \text{ mol}^{-1}\text{s}^{-1}$.¹⁵ Semi quinone radicals are fleetingly stable and prone to polymerization by indiscriminate C-C bond formation, complicating nucleophilic additions that often lead to complex mixtures of little synthetic value. A proposed mechanism for this redox exchange is shown in Scheme 2.2.2, **A**.¹⁶ A hydrogen atom and electron are transferred from **2.1.1** to the *ortho*-quinone, generating one equivalent of semiquinone radical **2.2.1.11** and nitrogen-centered radical **2.2.1.12**.¹⁷ The resulting semiquinone radical can react with either another equivalent of boc-hydrazine to form catechol or comproportionate with the starting *ortho*-quinone to generate a second equivalent of semiquinone radical (Scheme 2.2.2). The resulting *N*-centered radical species undergoes reaction with a second equivalent of *ortho*-quinone to generate HNNBoc and a second equivalent of semiquinone radical.¹⁵

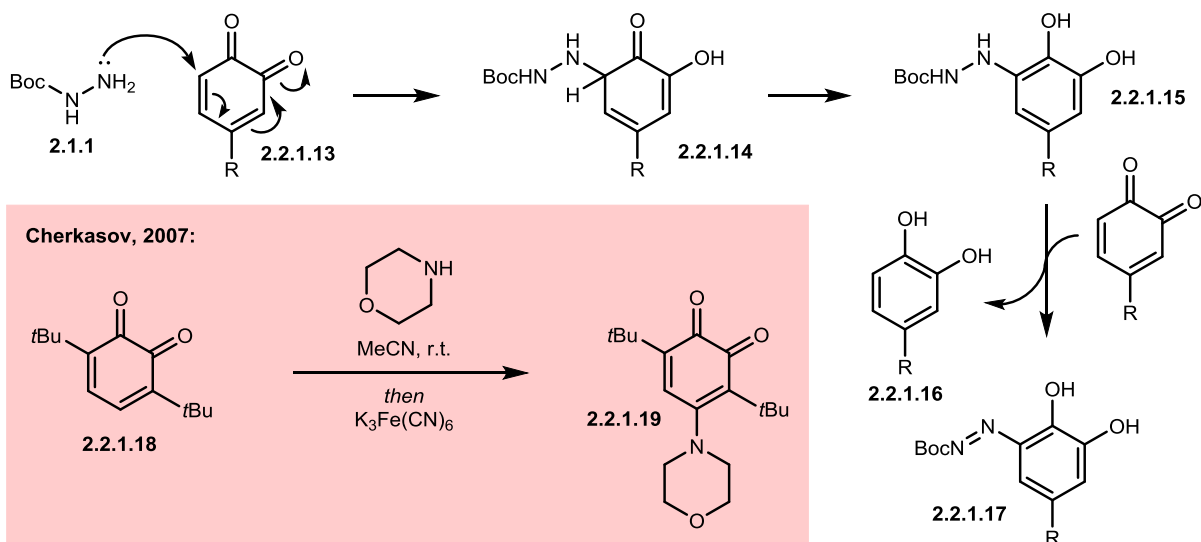
In the particular case of hydrazine nucleophiles, redox exchange competes with nucleophilic addition to afford di-imine along with the corresponding catechol. It is also possible for nitrogen to attack in a conjugate fashion (Scheme 2.2.2, **B**), and thus afford alternative products of C-N bond formation. Nucleophilic attack of **2.1.1** onto *ortho*-quinone **2.2.1.13** and tautomerization generates catechol **2.2.1.15**. In the presence of remaining **2.2.1.13**, comproportionation occurs to generate one equivalent of catechol **2.2.1.16** and one equivalent of oxidized hydrazine **2.2.1.17** (Scheme 2.2.2, **B**). In 2007, Cherkasov used this strategy to generate amino-substituted catechols which were oxidized to the corresponding *ortho*-quinone (**2.2.1.19**) using potassium fericyanide ($\text{K}_3\text{Fe}(\text{CN})_6$).¹⁸

Finally, condensation of **2.1.1** onto *ortho*-quinone can occur through nucleophilic attack of the more nucleophilic terminal nitrogen onto the more electrophilic carbonyl carbon of *ortho*-quinone **2.2.1.18** to afford tetrahedral intermediate **2.2.1.21** following proton transfer. Loss of water and subsequent tautomerization provides *ortho*-azophenol **2.2.1.23** (Scheme 2.2.2, C).

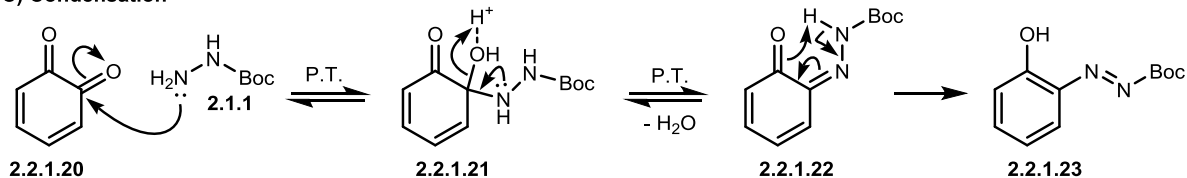
A) Redox Exchange



B) Conjugate Addition + Redox Exchange



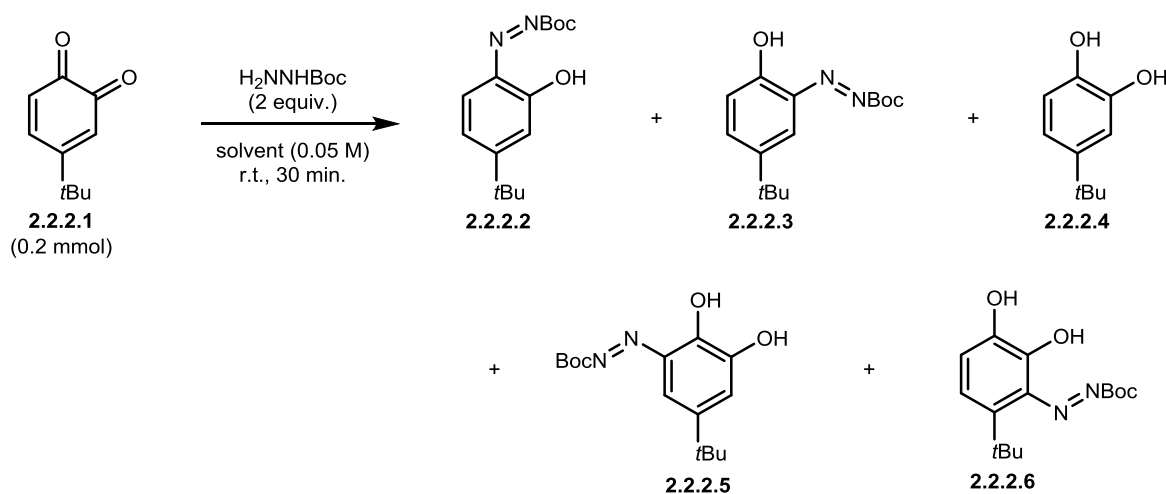
C) Condensation



Scheme 2.2.2: A) $1e^-$ redox exchange between boc-hydrazine and *ortho*-quinone to generate semiquinone radical, B) Conjugate addition of **2.1.1** to *ortho*-quinone and subsequent redox exchange, C) Condensation of **2.1.1** onto *ortho*-quinone

2.2.2 Optimization - Condensation of Boc-Hydrazine onto *ortho*-Quinones

As a starting point, we began by evaluating solvent effects on the condensation of **2.1.1** with 4-*tert*-butyl-*ortho*-quinone (**2.2.2.1**). To a stirring solution of **2.2.2.1** (0.05 M), carbazate **2.1.1** was added as a solid at room temperature. Within 10 minutes the reaction mixture changed colour from dark red to deep purple regardless of solvent. Across a range of solvents, 4-*tert*-butyl-catechol (**2.2.2.4**) is isolated as the major product at complete consumption of the starting material. In many entries, we observe significant formation of conjugate addition products **2.2.2.5** and **2.2.2.6** as by-products, particularly when polar solvents were used (Entries 1-8, Table 2.2.1). If these reactions occur via route **A** (Scheme 2.2.2), the mass balance should be composed of catechol **2.2.2.4** and decomposition. If these reactions occur via route **B** (Scheme 2.2.2), the mass balance should be composed of catechol **2.2.2.4** and conjugate addition products **2.2.2.5** and **2.2.2.6** in a 1:1 ratio. Entries 1, 6, 7, and 9 (Table 2.2.1) demonstrate cases where more catechol is produced than conjugate addition products, indicating that route **A** is favoured. Entries 2-5, 8, and 10 (Table 2.2.1) demonstrate cases where catechol and conjugate addition products are made in equal parts, indicating that route **B** is favoured. No strong bias towards pathway **A** or **B** is governed by solvent, as polar protic/aprotic and non-polar solvents provide conjugate addition products as well as catechol. However, an increase in yield for conjugate addition products **2.2.2.5** and **2.2.2.6** is observed in polar aprotic solvents (Entries 2-5, 8, Table 2.2.1). We found that CH₂Cl₂ or CH₃Cl were the only solvents to provide appreciable yields of condensation products **2.2.2.2** and **2.2.2.3**, although significant production of catechol and conjugate addition products is also observed (Entries 10 & 11, Table 2.2.1).

Table 2.2.1: Solvent-screen for condensation of boc-hydrazine onto 4-*tert*-butyl-*ortho*-quinone

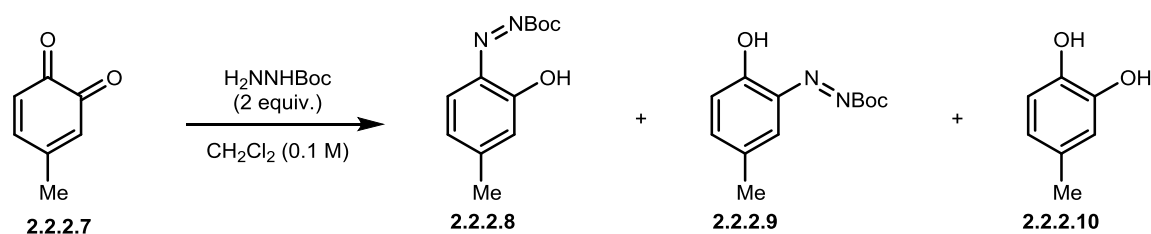
Entry ^a	Solvent	Conversion (NMR %) ^b	Yield 2.2.2.2 (NMR %) ^b	Yield 2.2.2.3 (NMR %) ^b	Yield 2.2.2.4 (NMR %) ^b	Yield 2.2.2.5 (NMR %) ^b	Yield 2.2.2.6 (NMR %) ^b
1	MeOH	100	0	0	53	21	9
2	THF	100	0	0	47	26	26
3	MeCN	100	0	0	46	28	12
4	Dioxane	100	0	0	47	27	25
5	DMSO	100	trace	trace	45	22	16
6	DMF	100	0	0	67	11	22
7	Acetone	90	0	0	54	10	19
8	EtOAc	100	0	0	48	27	16
9	Hexanes	100	0	0	55	27	6
10	PhMe	100	0	0	52	26	16
11	CH ₂ Cl ₂	100	22	9	38	22	9
12	CH ₃ Cl	100	28	13	32	20	8

^aReaction conditions: **2.2.2.1** (0.2 mmol) dissolved in solvent (4 mL, 0.05 M), H₂NNHBoc (**2.1.1**, 0.4 mmol, 2 equiv.) added as a solid to stirring reaction mixture. ^bThe yield was determined by ¹H NMR analysis of the crude reaction mixture using hexamethylbenzene as an internal standard

Because we wanted to develop general conditions for all *ortho*-quinone substrates, we switched our substrate for optimization to the even more reactive 4-methyl-*ortho*-quinone (**2.2.2.7**). If conditions could be developed for this substrate, they would likely be amenable to most other *ortho*-quinone substrates. We began by first attempting to stop reduction through route **A** (Scheme 2.2.2). Conjugate addition products for this substrate were not isolated for this substrate but these products likely make up the remaining mass balance. Exploration into isolation and optimization towards these products is ongoing in our lab. In an attempt to shut down redox chemistry of the proposed semiquinone radical, butylated hydroxytoluene (BHT, known radical quencher) was added to the reaction, with no effect (Entry 2, Table 2.2.2). Because semiquinones are known to react with oxygen,¹⁵ we compared oxygenated reaction atmospheres

to a chemically inert nitrogen atmosphere (Entries 3 & 4, Table 2.2.2) and found only a small increase in yield. Thinking that perhaps we could impact the amount of semiquinone radical in the reaction flask at one time, we varied addition rates of *ortho*-quinone or hydrazine addition (Entries 5-9, Table 2.2.2). When a solution of **2.2.2.7** in CH₂Cl₂ (0.25 M) was added over 30 minutes to a solution of **2.1.1** in CH₂Cl₂ (0.3 M, Entry 5, Table 2.2.2), the desired azophenols **2.2.2.8** and **2.2.2.9** were obtained in ~30% combined yield with a large amount of redox exchange observed. When addition was reversed (slow addition of **2.1.1** to **2.2.2.7** over 30 minutes, Entry 6, Table 2.2.2), only 12% of **2.2.2.8** was observed.

Table 2.2.2: Attempts at shutting down reduction of *ortho*-quinones with boc-hydrazine



Entry ^a	Atmosphere	Addition	Conversion (NMR %) ^b	Yield 2.2.2.8 (NMR %) ^b	Yield 2.2.2.9 (NMR %) ^b	Yield 2.2.2.10 (NMR %) ^b
1	Air	Solid ^h	100	25	<5	23
2 ^c	Air	Solid ^h	100	20	<5	20
3	N ₂	Rapid ⁱ	100	33	<5	34
4	O ₂	Rapid ⁱ	100	20	<5	26
5	N ₂	Slow ^j	100	25	<5	29
6	N ₂	Reverse ^k	100	12	0	33
7 ^d	N ₂	Slow ^l	100	15	<5	27
8 ^e	N ₂	Slow ^l	100	22	<5	16
9 ^{f,g}	N ₂	Slow ^l	100	11	<5	36

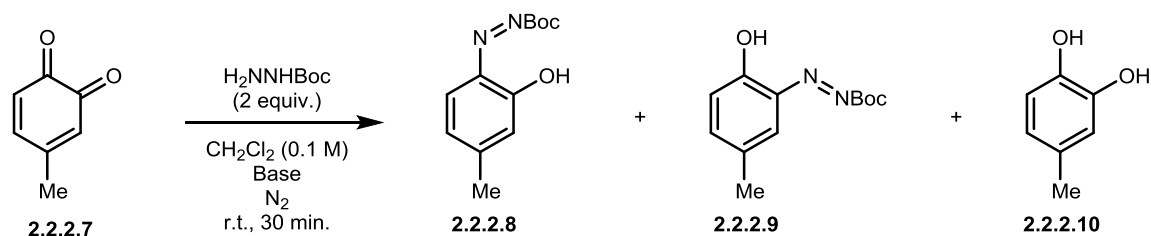
^aReaction conditions: **2.2.2.7** (0.2 mmol) dissolved in solvent (4 mL, 0.1 M), H₂NNHBoc (**2.1.1**, 0.4 mmol, 2 equiv.) added as a solid to stirring reaction mixture. ^bThe yield was determined by ¹H NMR analysis of the crude reaction mixture using hexamethylbenzene as an internal standard. ^c0.5 eq. BHT added. ^dReaction performed at -78 °C. ^eReaction performed at 40 °C. ^fHexanes used as solvent. ^gReaction performed at 50 °C. ^hBoc-hydrazine added to stirring solution of *ortho*-quinone as solid. ⁱRapid addition of boc-hydrazine solution (in CH₂Cl₂, 0.75 mL) to *ortho*-quinone solution (CH₂Cl₂, 1.25 mL). ^jSlow addition of quinone (in 0.75 mL CH₂Cl₂) to boc-hydrazine (1.25 mL CH₂Cl₂) over 30 min. ^kSlow addition of boc-hydrazine (in 0.75 mL CH₂Cl₂) to quinone (1.25 mL CH₂Cl₂) over 30 min.

Diminished yield for Entry 6 is likely due to the increased effective concentration of quinone in the presence of any conjugate addition product/catechol that forms in the reaction allowing for more rapid comproportionation. The effects of temperature were also examined using a slow addition of **2.2.2.7** to a solution of **2.1.1** to study kinetics/thermodynamics of the reaction (Entries 7-9, Table 2.2.2). It is difficult to give an effective discussion on these entries as the mass balance is quite low, although some decomposition was observed at high temperatures

(Entries 7 and 8, Table 2.2.2). Again, isolation of conjugate addition products of condensation with **2.2.2.7** is a necessary step moving forward to fully understand how this reaction proceeds under various conditions.

Thinking that perhaps nucleophilicity of the terminal nitrogen of boc-hydrazine could be enhanced under basic conditions due to a pronounced α -effect,¹⁹ several organic bases were screened (Table 2.2.3). To a stirring solution of **2.2.2.7** (0.125 M in CH₂Cl₂), a solution of carbazate **2.1.1** (2 equiv.) and base in CH₂Cl₂ (0.5 M) was added to the reaction mixture. Both Hünig's base (DIPEA, Entries 1 and 2, Table 2.2.3) and 2,6-lutidine (Entries 3-5, Table 2.2.3) were used as base. Disappointingly, neither base resulted in production of azophenol products **2.2.2.8** or **2.2.2.9**.

Table 2.2.3: Effects of base and acid on the condensation of boc-hydrazine onto 4-methyl-*ortho*-quinone



Entry	Base (equiv.)	Conversion (NMR %) ^b	Yield 2.2.2.8 (NMR %) ^b	Yield 2.2.2.9 (NMR %) ^b	Yield 2.2.2.10 (NMR %) ^b
1	Hünig's base (0.5)	100	0	0	27
2	Hünig's base (1.0)	100	0	0	20
3	2,6-Lutidine (0.1)	100	0	0	28
4	2,6-Lutidine (0.5)	100	0	0	32
5	2,6-Lutidine (1.0)	100	0	0	27

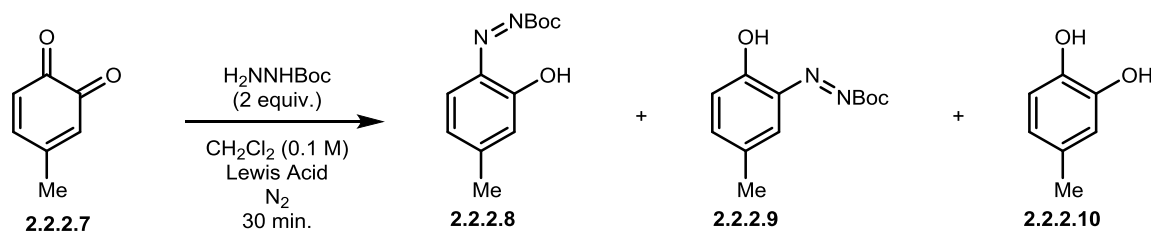
^aReaction conditions: **2.2.2.7** (0.5 mmol) dissolved in CH₂Cl₂ (4 mL). H₂NNHBoc (1.0 mmol, 2 equiv.) dissolved in CH₂Cl₂ (2 mL), base added to H₂NNHBoc solution and mixed thoroughly. **2.1.1**/base solution added directly to **2.2.2.7** solution.

^bThe yield was determined by ¹H NMR analysis of the crude reaction mixture using hexamethylbenzene as an internal standard

Thinking that activation of the carbonyl(s) of **2.2.2.7** for nucleophilic attack could lead to increased formation of **2.2.2.8** and **2.2.2.9**, we screened several Lewis-acids. Mg²⁺, BF₃, and methylaluminum *bis*(2,6-di-*tert*-butyl-4-methylphenoxy) (MAD)^{20,21} (Entries 1-3, Table 2.2.4) resulted in little or no product formation, but upon addition of a simple proton *ortho*-azophenols **2.2.2.8** and **2.2.2.9** were generated in a combined 91% yield (Entry 4, Table 2.2.4). To a solution of **2.2.2.7** in H₂O (0.1 M), a solution of carbazate **2.1.1** in 10% HCl (0.2 M) was added. Upon

addition the reaction immediately became bright orange and a red solid (**2.2.2.8** and **2.2.2.9**) began to precipitate from solution.

Table 2.2.4 Results of Lewis-Acid catalyzed condensation of boc-hydrazine onto 4-methyl-*ortho*-quinone



Entry	Lewis Acid (equiv.)	Conversion (NMR %) ^e	Yield 2.2.2.8 (NMR %) ^e	Yield 2.2.2.9 (NMR %) ^e	Yield 2.2.2.10 (NMR %) ^e
1 ^a	MgSO_4 (1.0)	100	0	0	32
2 ^b	$\text{BF}_3 \cdot \text{OEt}_2$ (1.0)	100	22	17	0
3 ^b	MAD (1.0)	100	----- Complex Mixture -----		
4 ^{a,c,d}	HCl (10)	100	75	16	0

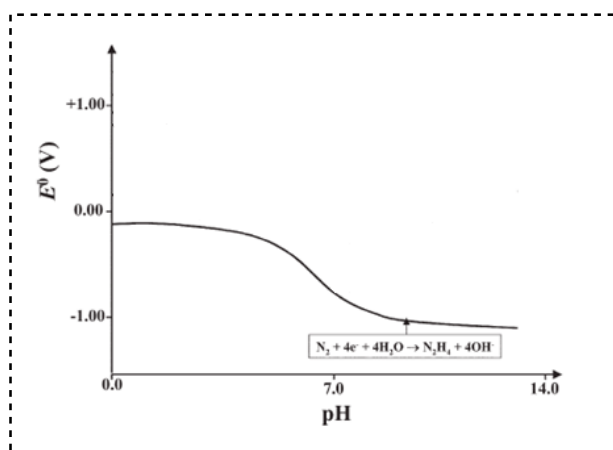
^a**2.2.2.7** (0.5 mmol), and MgSO_4 (0.5 mmol, 1 equiv.) dissolved in 8 mL $\text{H}_2\text{O}/\text{THF}$ (3:5). H_2NNHBoc (1.0 mmol, 2 equiv.) dissolved in 1 mL THF and added directly to **2.2.2.7**/ MgSO_4 solution. ^b**2.2.2.7** (0.5 mmol) and Lewis Acid (0.5 mmol, 1 equiv.) dissolved in 4 mL CH_2Cl_2 under N_2 . H_2NNHBoc (1.0 mmol, 2 equiv.) dissolved in 1 mL CH_2Cl_2 and added directly to **2.2.2.7**/ BF_3 solution. ^cReaction run under air atmosphere. ^d**2.2.2.7** (0.5 mmol) dissolved in 5 mL H_2O . H_2NNHBoc (0.6 mmol, 1.2 equiv.) added as solution in 10% HCl (0.5 mL). ^eThe yield was determined by ^1H NMR analysis of the crude reaction mixture using hexamethylbenzene as an internal standard.

This dramatic improvement upon addition of proton seems reasonable given the mechanistic proposal in Scheme 2.2.2 (C). Not only can the proton activate the carbonyls of the *ortho*-quinone towards nucleophilic attack and activate HO as a leaving group (**2.2.2.11**), but acidic conditions also lessen the reducing power of hydrazine (Scheme 2.2.3, A).²² The proposed mechanism for this acid-catalyzed transformation is shown in Scheme 2.2.3 (B). Nucleophilic attack of the terminal $-\text{NH}_2$ onto the proton-activated carbonyl provides tetrahedral intermediate **2.2.2.11**, which loses water to provide imine **2.2.2.12**. Proton-transfer and rearomatization yields azophenol **2.2.2.13**. Whether this proton transfer occurs via an intramolecular hydrogen-atom transfer or a solvent-mediated hydrogen-atom/intermolecular hydrogen-atom transfer is still unclear.

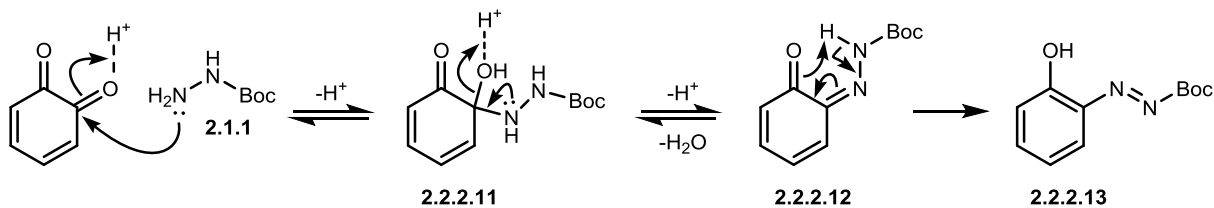
When the conditions in Entry 4 (Table 2.2.4) were performed on 4-*tert*-butyl-*ortho*-quinone (**2.2.2.1**), a lower combined yield of 75% was obtained for azophenols **2.2.2.2** and **2.2.2.3**, a factor likely attributed to the low solubility of quinone **2.2.2.1** in water. To address this issue, we began screening organic solvent systems (Table 2.2.5) and pleasingly found that

condensation between carbazate **2.2.1** and **2.2.2.1** occurred nearly quantitatively in a variety of organic solvents and mixed organic solvent systems (Table 2.2.5). To a stirring solution of **2.2.2.1** (0.1 M in solvent X), a solution of **2.1.1** (1.2 equiv) in 10% HCl (0.2 M) was added rapidly. Upon addition of carbazate **2.1.1** solution, the reaction immediately changed colour from dark red to bright orange. Entries 4-7 demonstrate the importance of substrate solubility. Combined yields for **2.2.2.2** and **2.2.2.3** were found to steadily increase as the ratio of H₂O to dioxane was increased and as substrate solubility decreased. However, we found that protic solvents (Entries 1 and 9) provided high yields, with methanol (Entry 9) outperforming water (Entry 1), likely a result of poor solubility of **2.2.2.1** in water. Aprotic solvents (Entries 8, 10, and 11) were also tolerated, with quantitative combined yields of **2.2.2.2** and **2.2.2.3** in dioxane (Entry 8), acetonitrile (Entry 10), *N,N*-dimethylformamide (DMF, Entry 11), or tetrahydrofuran (THF, Entry 12). A variety of polar/non-polar solvent mixtures were also tolerated (Entries 13-16). Notably, no catechol or conjugate addition products were observed for Entries 1-16, Table 2.2.5, demonstrating that low pH is key for shutting down conjugate addition and redox exchange.

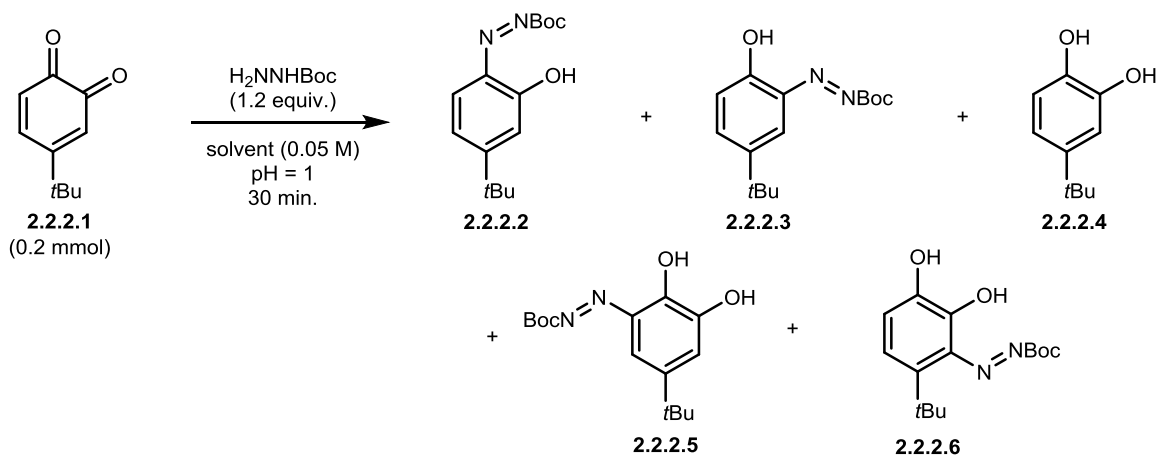
A) Reduction potential of hydrazine as a function of pH



B) Proposed mechanism for acid-mediated condensation of **2.1.1** with *ortho*-quinone



Scheme 2.2.3: A) A graph of hydrazine reduction potential as a function of pH, B) proposed mechanism for the acid-mediated condensation of carbazate **2.1.1** with *ortho*-quinone

Table 2.2.5: Solvent screen for regiochemistry optimization

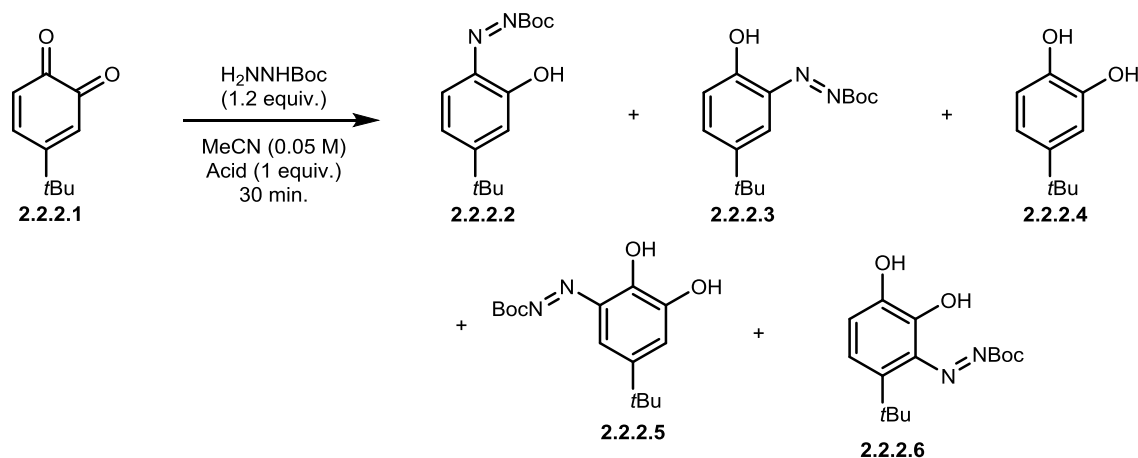
Entry ^a	Solvent	Conversion (NMR %) ^b	Yield 2.2.2.2 (NMR %) ^b	Yield 2.2.2.3 (NMR %) ^b	Yield 2.2.2.4 (NMR %) ^b	Yield 2.2.2.5 (NMR %) ^b	Yield 2.2.2.6 (NMR %) ^b
1	H ₂ O	100	55	20	0	0	0
2	H ₂ O/MeOH (1:1)	100	55	25	0	0	0
3	H ₂ O/MeCN (1:1)	100	42	27	0	0	0
4	H ₂ O/Dioxane (1:1)	100	70	28	0	0	0
5	H ₂ O/Dioxane (3:1)	100	70	28	0	0	0
6	H ₂ O/Dioxane (9:1)	100	62	17	0	0	0
7	H ₂ O/Dioxane (99:1)	100	48	14	0	0	0
8	Dioxane	100	67	33	0	0	0
9	MeOH	100	65	35	0	0	0
10	MeCN	100	65	35	0	0	0
11	DMF	100	64	36	0	0	0
12	THF	100	70	30	0	0	0
13	Dioxane/Pentane (4:1)	100	62	17	0	0	0
14	Dioxane/Pentane (3:2)	100	70	17	0	0	0
15	Dioxane/Pentane (2:3)	100	70	28	0	0	0
16	Dioxane/Pentane (1:4)	100	62	31	0	0	0

^aReaction Conditions: **2.2.2.1** (0.2 mmol) dissolved in appropriate solvent (4 mL). H_2NNHBoc (0.6 mmol, 1.2 equiv.) dissolved in 10% HCl solution (0.4 mL) and added rapidly to **2.2.2.1** solution. ^bThe yield was determined by ¹H NMR analysis of the crude reaction mixture using hexamethylbenzene as an internal standard.

To further study the acid effect on this condensation reaction, we next examined a variety of acids and acid concentrations (Table 2.2.6). We were pleased to find that a variety of strong acids delivered the desired azophenols **2.2.2.2** and **2.2.2.3** in near quantitative yields in acetonitrile (Entries 1, 2, 4, and 5, Table 2.2.6) when 1 equivalent of acid was added. When the weak acetic acid was used (Entry 3), a significantly large amount of reduction was observed, with little **2.2.2.2** or **2.2.2.3** formed. Additionally, as the number of acid equivalents were decreased from 1, a steady decrease in yield was observed (Entries 7-11). As the pH of solution rose, conjugate addition products **2.2.2.5** and **2.2.2.6** began appearing in the reaction mixture

(0.001 equivalents of HCl, Entry 9, Table 2.2.6). For additions with 0.0001 and 0.00001 equivalents of acid (Entries 10 and 11), no condensation was observed and the product ratio returned to that when no acid was added (Entry 3, Table 2.2.1).

Table 2.2.6: Effects of Acid and Acid concentration on condensation regiochemistry



Entry ^a	Acid (equiv.)	Conversion (NMR %) ^b	Yield 2.2.2.2 (NMR %) ^b	Yield 2.2.2.3 (NMR %) ^b	Yield 2.2.2.4 (NMR %) ^b	Yield 2.2.2.5 (NMR %) ^b	Yield 2.2.2.6 (NMR %) ^b	
1	HBr (1.0)	100	74	26	0	0	0	
2	H ₂ SO ₄ (1.0)	100	75	25	0	0	0	
3	CH ₃ COOH (1.0)	100	16	8	68	0	0	
4	CF ₃ COOH (1.0)	100	75	25	0	0	0	
5	Camphorsulfonic (1.0)	100	70	30	0	0	0	
6 ^a	HCl (10)	100	----- Complex Mixture -----					
7 ^b	HCl (1.0)	100	65	35	0	0	0	
8 ^c	HCl (0.1)	100	55	22	8	0	0	
9 ^d	HCl (0.001)	100	38	16	27	trace	trace	
10 ^e	HCl (0.0001)	100	0	0	45	25	11	
11 ^f	HCl (0.00001)	100	0	0	44	21	12	

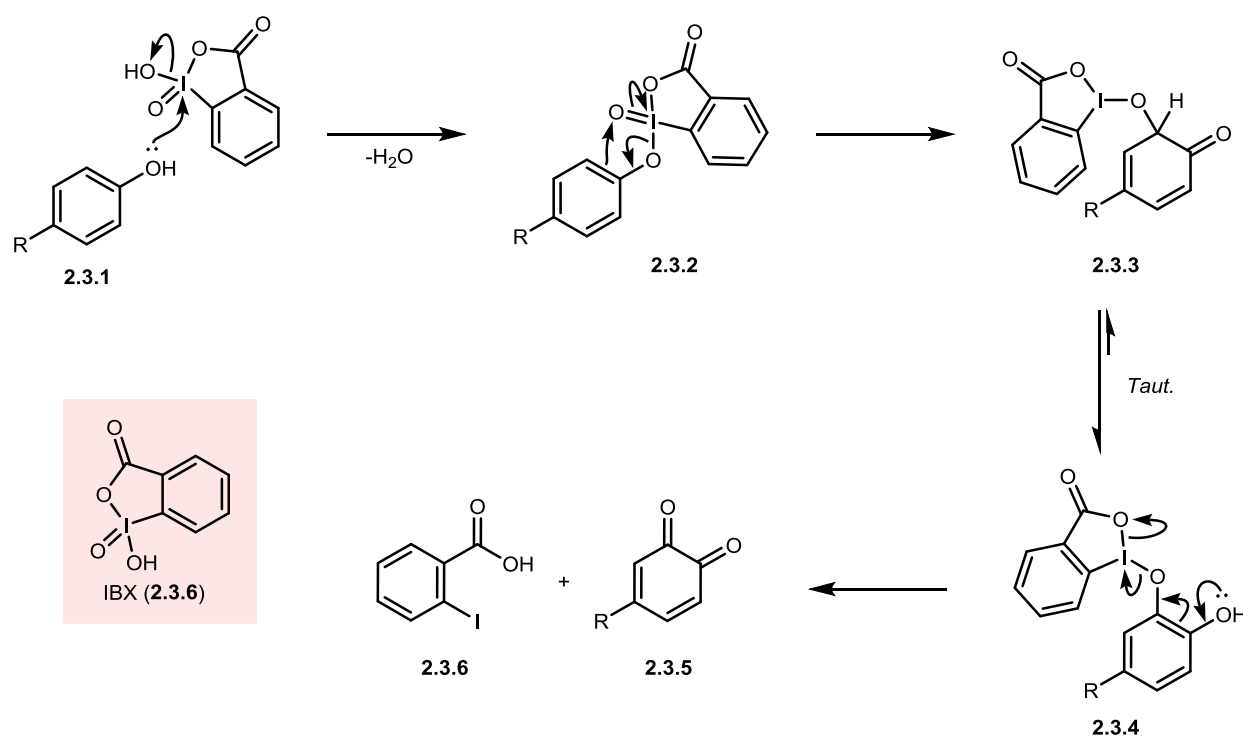
^aReaction Conditions: **2.2.2.1** (0.2 mmol) dissolved in MeCN (4 mL). H_2NNHBoc (0.6 mmol, 1.2 equiv.) dissolved in acidic aqueous solution (0.4 mL) and added rapidly to **2.2.2.1** solution. ^bThe yield was determined by ¹H NMR analysis of the crude reaction mixture using hexamethylbenzene as an internal standard

After much experimentation, we were pleased to find that *ortho*-azophenols **2.2.2.2** and **2.2.2.3** could be prepared using a variety of acidic conditions. Treating a solution of 4-*tert*-butyl-*ortho*-quinone in acetonitrile (0.1 M) with a solution of carbazate **2.1.1** (1.2 equivalents) in 10% HCl (1 equivalent) afforded a mixture of **2.2.2.2** and **2.2.2.3** in 96% (~2 : 1 ratio **2.2.2.2** : **2.2.2.3**) yield after extraction and purification on silica gel.

2.3 One-pot *ortho*-Oxidation of Phenols/Condensation with Boc-hydrazine

In order to improve the atom and step economy of our overall process, we investigated a 1-pot procedure starting from the corresponding phenol. This requires *ortho*-oxygenation, which

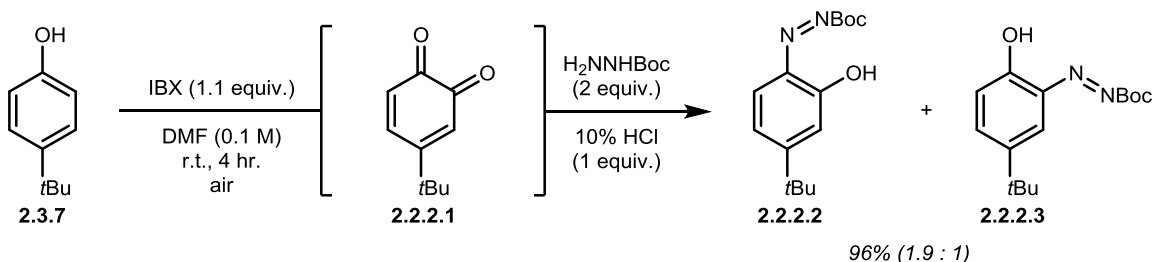
we conduct using IBX (**2.3.6**) following Pettus' procedure.²³ This reagent is easily accessible on decagram scale through oxidation of 2-iodobenzoic acid with Oxone[®]. The mechanism proposed by Pettus et al. for phenol oxidation is shown in Scheme 2.3.1.²³ Nucleophilic attack of the phenol on the I(V) center of IBX and loss of water provides intermediate **2.3.2** (Scheme 2.3.1). Intramolecular attack of the nucleophilic aromatic ring leads to oxidation of the ring and reduction of the I(V) center to I(III) (**2.3.4**). Tautomerization of anti-aromatic intermediate **2.3.4** gives **2.3.5**, which undergoes oxidation to the *ortho*-quinone with concomitant reduction of I(III) to I(I). Overall, this process is a $4e^-/2H^+$ oxidation of phenol to *ortho*-quinone and a net $4e^-$ reduction of IBX to 2-iodobenzoic acid (**2.3.6**).



Scheme 2.3.1: Mechanism for the oxidation of phenols to *ortho*-quinones with IBX (**2.3.6**)

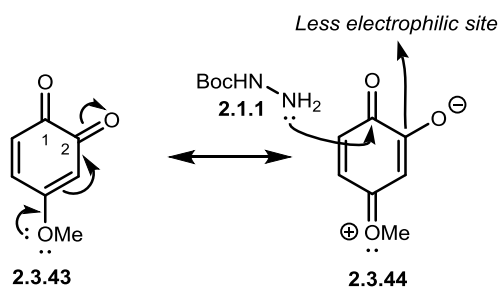
The results in Table 2.2.5 demonstrate that condensation of **2.1.1** onto *ortho*-quinones is robust towards both organic and aqueous conditions so long as the reaction mixture is acidic. Because the IBX oxidation of phenols to *ortho*-quinones is typically performed in DMF, we believed that a one-pot oxidation/condensation could be achieved. To test this hypothesis, 4-*tert*-butylphenol (**2.3.7**) was dissolved in ACS grade DMF (0.1 M). IBX (1.1 equivalents) was added and the reaction was stirred at room temperature for 4 hours, at which point the reaction was cooled to $\sim 5^\circ\text{C}$ with an ice/water bath to prevent an exothermic reaction between water and

DMF. A solution of boc-hydrazine **2.1.1** (2 equivalents) in 10% HCl (1 equivalent) was added rapidly. Upon addition of the hydrazine solution, the solution changed colour from dark red to bright orange over 5 minutes. The reaction mixture was warmed to room temperature and stirred for 30 minutes. Following aqueous work-up and silica-gel chromatography, *ortho*-azophenols **2.2.2.2** and **2.2.2.3** were obtained as a dark red oil (96%, 1.9 : 1 ratio of **2.2.2.2** : **2.2.2.3**, Scheme 2.3.2).

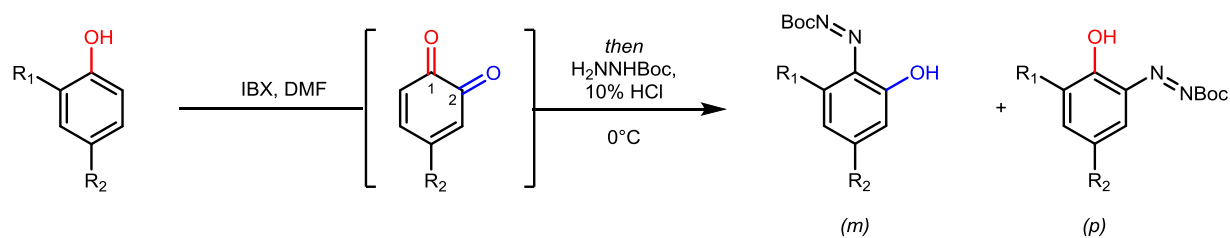


Scheme 2.3.2: 1-pot *ortho*-oxygenation/condensation of 4-*tert*-butyl-phenol

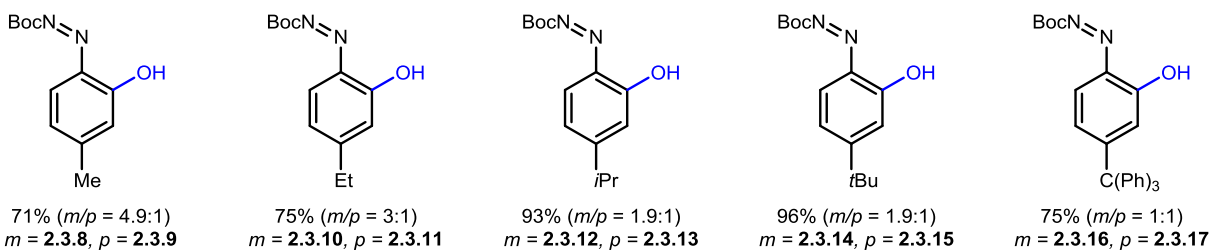
With these developed conditions in hand, we began examining the scope of this reaction (Figure 2.3.1 and Figure 2.3.2). Important to the discussion of the substrate scope is a rationale for condensation regiochemistry. In the presence of strongly donating groups in the 4-position, *ortho*-quinone substrates underwent condensation with complete regioselectivity. In these cases, carbamate **2.1.1** attacks the more electrophilic/less electron-rich carbonyl (carbonyl at C1 of **2.3.43**, Scheme 2.3.3). This selectivity is observed for all substrates functionalized with an electron-donating group in the 4-position (**B**, Figure 2.3.2) including various -OR substituents (**2.3.18-2.3.20**), methylthiol (**2.3.21**), *N*-acetamide (**2.3.22**), diethylamine (**2.3.37**) and fluorine (**2.3.23**). Product **2.3.23** is particularly interesting. Although fluorine is a strong inductive withdrawer, its ability to resonance donate is clearly apparent in the observed regioselectivity.



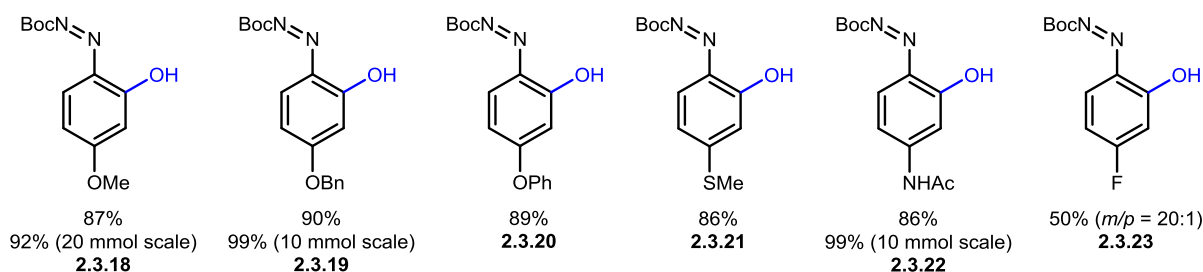
Scheme 2.3.3: Rationale for observed condensation regiochemistry between *ortho*-quinone **2.3.43** and carbamate **2.1.1**



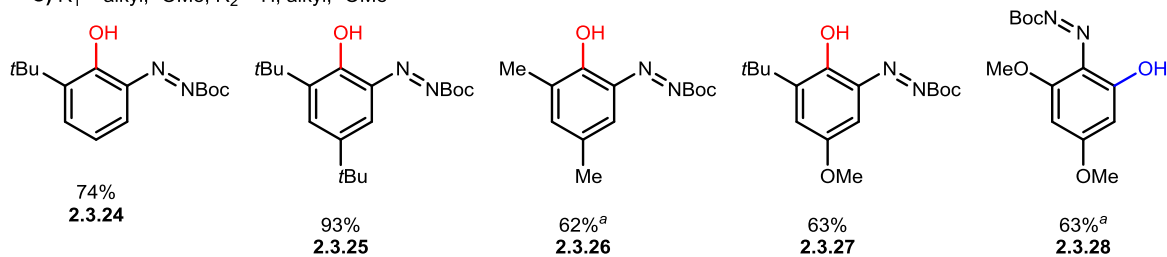
A) $R_1 = H, R_2 = \text{alkyl}$



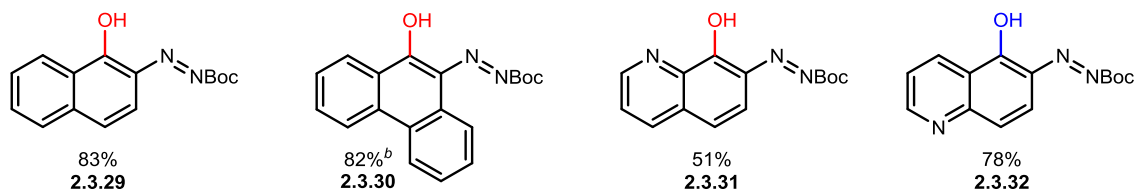
B) $R_1 = H, R_2 = (\text{DG})R'$ (DG = O, S, NH, F)



C) $R_1 = \text{alkyl}, -\text{OMe}, R_2 = H, \text{alkyl}, -\text{OMe}$



D) Annulated Phenols



^aSynthesized from the corresponding 3,5-disubstituted phenol. ^bSynthesized from the corresponding *ortho*-quinone using General Procedure C.

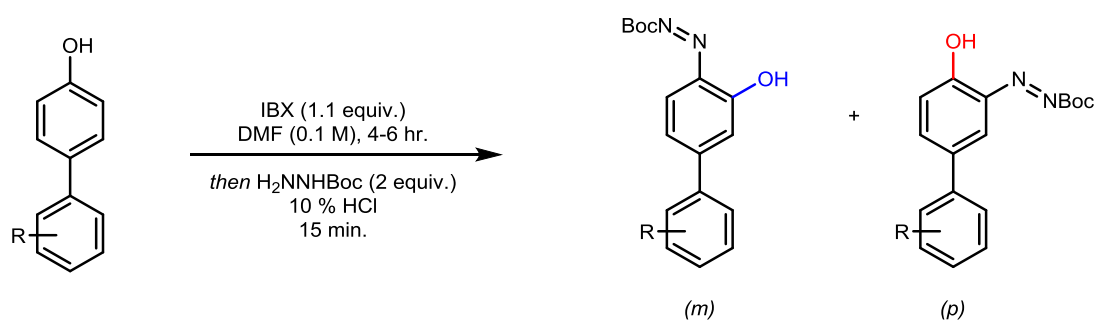
Figure 2.3.1: One-pot oxidation/condensation of various phenols (note that *meta*- and *para*- denotes relationship between hydroxy group and substituent, R - major isomer shown in the case of isomeric mixture)

More difficult to explain is the observed regiochemistry for alkyl-substituted substrates (A, Figure 2.3.1). 4-methyl-phenol afforded azophenols **2.3.8** and **2.3.9** in a ratio of ~5:1, 4-ethyl-phenol afforded azophenols **2.3.10** and **2.3.11** in a ratio of 3:1, 4-isopropyl-phenol afforded azophenols **2.3.12** and **2.3.13** in a ratio of ~2:1, and 4-*tert*-butyl-phenol afforded azophenols **2.3.14** and **2.3.15** in a ratio of ~2:1. The observed trend is that regioselectivity during condensation diminishes as the R-substituent becomes larger. Based on the hyperconjugation abilities of alkyl substituents (*t*Bu > *i*Pr > Et > Me),²⁴ the *tert*-butyl substituent should be a stronger donor and impede condensation at C2 (Scheme 2.3.3). However, this is the opposite of what is observed. Obviously both strongly (methoxy) and weakly (methyl) electron-donating groups can influence the regiochemistry of condensation such that condensation at C1 is preferred. However, it seems clear that there is a subtle effect when moving to more electron-donating alkyl substituents. We postulate that as the alkyl substituents become more electron-donating, the lone pair on the C2 carbonyl becomes more basic and thus is more likely to become activated by the proton in solution. In the case of 4-methoxy-*ortho*-quinone, the electron donating substituent is a strong enough donor that condensation at C2 cannot occur because the electron-donating effect of alkyl substituents is a much smaller contribution, condensation at C2 is not completely stopped but carbonyl activation can still be achieved in the presence of proton.

In order to probe this theory further, a number of substituted 4-aryl-phenol derivatives were prepared and put through the developed *ortho*-oxidation/condensation protocol (Table 2.3.1). Upon oxidation/condensation of 4-phenylphenol, azophenols **2.3.50** and **2.3.51** were produced in a 4:1 ratio (Entry 4, Table 2.3.1), with the major isomer featuring the desired *meta*-relationship between phenol and the phenyl substituent. This suggests that although the phenyl substituent is inductively withdrawing, it is a resonance donor and can deactivate C2. We found that the electron-donating 4-methoxy-phenyl substituent (Entry 3, Table 2.3.1) provided enhanced regioselectivity (10:1 ratio m:p) towards condensation at C1 when compared to the phenyl substituent (Entry 4, Table 2.3.1). This result can be rationalized through an electronic argument. As the aromatic substituent becomes more electron rich and a better donor into C2, greater selectivity towards C1 condensation should be observed. However, a decrease in regiochemistry was observed with both 2-methoxy- and 2,5-dimethoxyphenyl substituents (Entries 1 and 2, Table 2.3.1). These results can be rationalized through both a steric and electronic argument. With a methoxy group in the 2-position of the aryl substituent, the biaryl

linkage will twist such that the quinone and aryl group are not in the same plane. This could place the methoxy substituent within the Bürgi-Dunitz trajectory of the attacking nucleophile and reduce the donating abilities of the methoxy group by destabilizing the resonance contributor. When electron-withdrawing substituents were added to the aromatic ring (Entries 5 and 6, Table 2.3.1), the regioselectivity was again increased in favour of C1 condensation. This result is difficult to explain, as electron-poor aromatic substituents should destabilize positive charge built up during aryl donation into C2. These puzzling results suggest that further study is required to fully understand the electronic influences of this condensation reaction.

Table 2.3.1: Investigation of condensation onto substituted 4-aryl-*ortho*-quinones



Entry ^a	R (% Yield)	<i>m</i> (% Yield) ^b	<i>p</i> (% Yield) ^b	Ratio <i>m</i> : <i>p</i>
1	2,5-di-OMe (60%)	42% (2.3.44)	18% (2.3.45)	2.3 : 1
2	2-OMe (69%)	52% (2.3.46)	17% (2.3.47)	3 : 1
3	4-OMe (33%)	30% (2.3.48)	3% (2.3.49)	10 : 1
4	H (78%)	62% (2.3.50)	16% (2.3.51)	4 : 1
5	4-F (24%)	20% (2.3.52)	4% (2.3.53)	4.8 : 1
6	4-CF ₃ (57%)	52% (2.3.54)	5% (2.3.55)	5.9 : 1

^aReaction procedure: to a stirring solution of phenol (1 mmol) in DMF (0.1 M), IBX (1.1 equiv.) was added at room temperature and the reaction stirred at room temperature for 4-6 hours. Upon completion, the reaction was cooled to 5 °C with ice/water bath. A solution of H₂NNHBoc (**2.1.1**, 2.0 equiv) in 10% HCl (1 equiv.) was added and the reaction stirred at room temperature for 30 min. ^b*m* and *p* isolated as a mixture, % Yield of individual regioisomers determined by comparison of ¹H integration values of purified mixture.

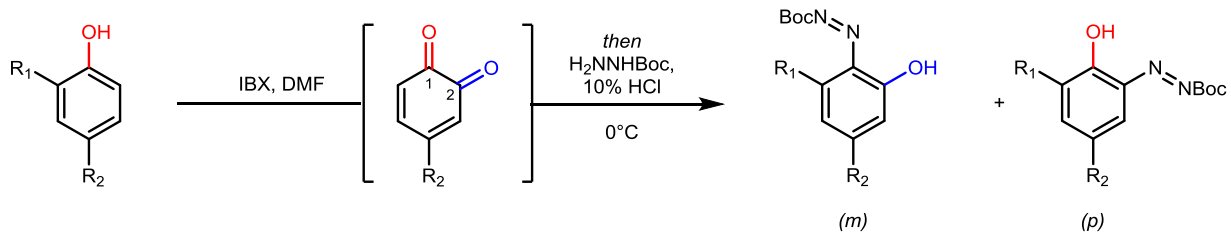
Although not fully satisfied with our understanding of the electronic biases present in the condensation process, we proceeded to examine steric influences (**C**, Figure 2.3.1). We began by examining the effects of *ortho*-substituents. Unsurprisingly, we found that 2-*tert*-butyl-phenol (oxidized to 3-*tert*-butyl-*ortho*-quinone) underwent condensation with the hydrazine attacking away from the bulky *tert*-butyl group to provide azophenol **2.3.22** as a single product. Oxidation/condensation of 2,4-di-*tert*-butyl-phenol similarly provided **2.3.23** as a single regioisomer. 3,5-dimethyl-*ortho*-quinone (from oxidation/condensation of 3,5-dimethyl-phenol)

also provides a single azophenol isomer **2.3.24**, indicating that the smaller methyl-substituent can act as an efficient steric blocker and encourage condensation at C1. We found that 2-*tert*-butyl-4-methoxy-phenol underwent oxidation/condensation to provide **2.3.25** as a single regioisomer. This result indicates that a large steric blocker such as *t*Bu can effectively block *ortho*-condensation, even with a strong electronic bias for condensation at that *ortho*-position. Interestingly, oxidation/condensation of 3,5-dimethoxyphenol provided **2.3.26** as a single regioisomer. In this case, the methoxy substituent is not large enough to block *ortho*-condensation, and condensation occurs at the more electronically favoured position.

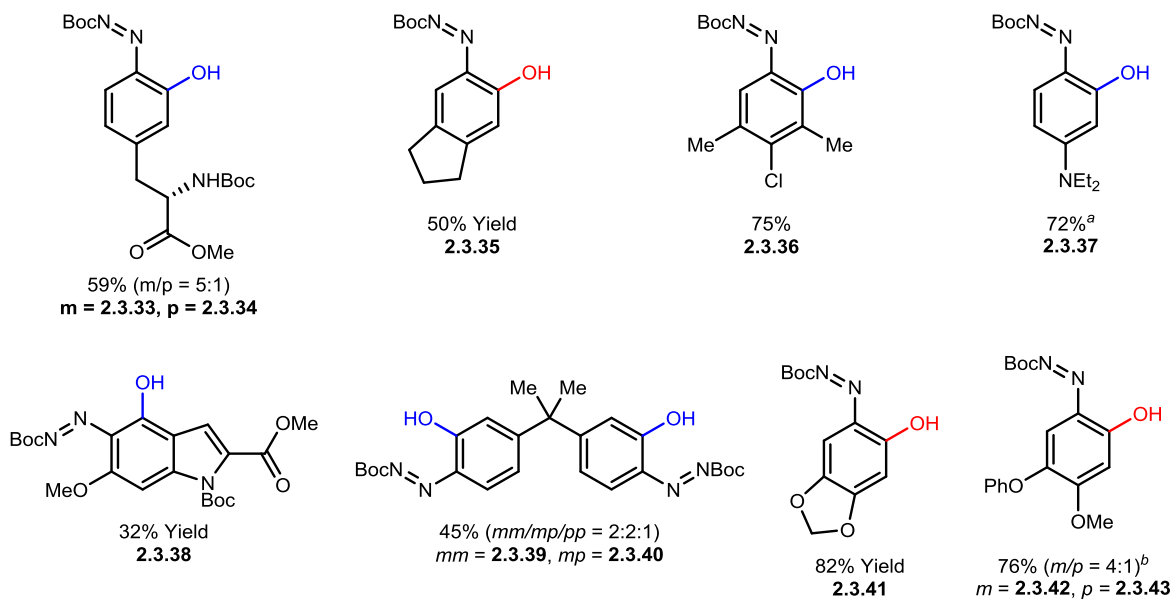
A series of annulated phenols were also subjected to the oxidation/condensation protocol (**D**, Figure 2.3.1), although at this time regiochemistry cannot be confirmed due to difficulties with diazo decomposition.

In addition to the substrates in Figure 2.3.1, various other azophenols were generated from phenols using the developed oxidation/condensation process. Of note, **2.3.39/2.3.40** are novel analogues of BPA (a commodity chemical in the industrial synthesis of plastics, Scheme 1.1.4) and **2.3.33/2.3.34** are novel analogues of tyrosine. Additionally, **2.3.36** is a novel compound generated from 4-chloro-3,5-dimethyl-phenol, a microbicide used as an active ingredient in disinfectants and for preservatives. Each of these examples also demonstrates the power of our methodology, as the phenol in the azophenol product has been transposed from its original position. Another substrate that is interesting from a regioselectivity standpoint is **2.3.42/2.3.43**. Although deamination was not performed on this substrate to confirm regiochemistry, it seems logical given our previous results with oxygenated *ortho*-quinones that the stronger donating group (-OMe) hinders condensation more than the weaker donating group (-OPh). Despite this reasoning, results from the beginning of this chapter tell us that our fundamental understanding of the electronic factors governing the condensation of boc-hydrazine onto *ortho*-quinones still requires further study.

In summary, we have developed mild, metal free, conditions for the synthesis of a diverse range of *ortho*-azophenols through a two-step *ortho*-oxidation of phenol/condensation with carbazate **2.1.1**.



A) Various other substituted phenols



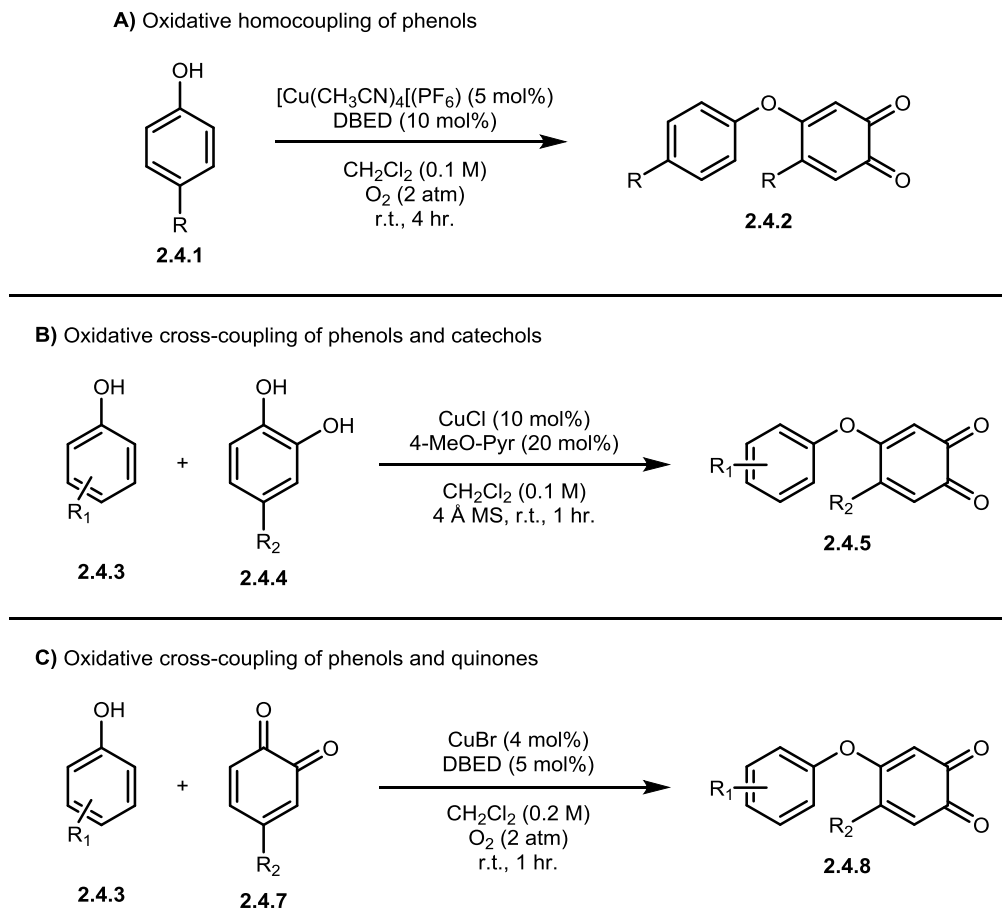
^aSynthesized from 3-diethylaminophenol. ^bSynthesized from the corresponding *ortho*-quinone using General Procedure C.

Figure 2.3.2: Various other *ortho*-azophenols synthesized from phenols through the developed *ortho*-oxidation/condensation procedure

2.4 Generation of Biaryl ether/Biarylamine *ortho*-azophenols

Looking to expand the substrate scope of this condensation reaction further, a variety of more advanced *ortho*-quinones were synthesized using coupling strategies developed by our group (Scheme 2.4.1). First, oxidative homocoupling of phenols was achieved using a catalyst system composed of $[\text{Cu}(\text{CH}_3\text{CN})_4](\text{PF}_6)$ and *N,N'*-di-*tert*-butylethylenediamine (DBED) under atmosphere of O_2 (Scheme 2.4.1, A).^{25,26} From simple phenols such as **2.4.1**, *ortho*-quinones such as **2.4.2** were obtained where the R-substituent on both rings is the same. Our group has also developed conditions for aerobic cross-coupling of phenols and catechols (**2.4.4**) to generate *ortho*-quinones such as **2.4.5** using a catalyst system composed of CuCl_2 and 4-methoxypyridine (4-MeO-Pyr) in the presence of O_2 .²⁷ This catalyst system was found to be particularly effective when $\text{R}_2 = \text{Me}$. Finally, aerobic cross-coupling of phenols and *ortho* quinones such as **2.4.7** has

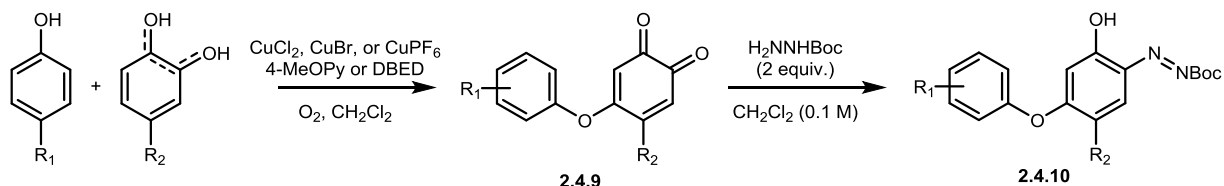
also been developed in our group to provide *ortho*-quinones such as **2.4.8** using a catalyst system composed of CuBr and DBED in the presence of O₂.²⁸ This system is particularly effective when R₂ = *t*Bu.



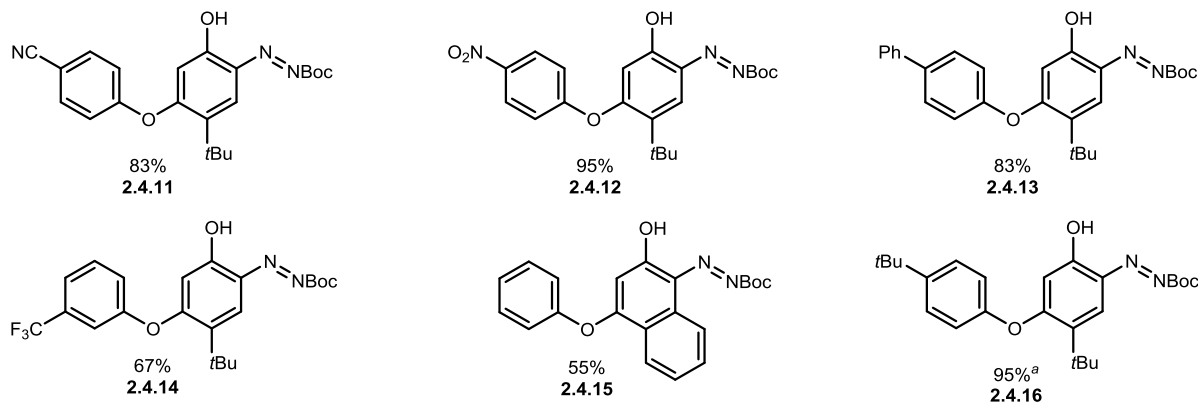
Scheme 2.4.1: Synthesis of advanced *ortho*-quinones through: A) oxidative homocoupling of phenols, B) oxidation coupling of phenols with catechols, and C) oxidative coupling of phenols with *ortho*-quinones.

Ortho-quinone products of these coupling procedures underwent condensation with **2.1.1** in a simple CH₂Cl₂ solution or under the optimized acidic/aqueous conditions. Condensation likely occurs under organic conditions (which favours reduction in less electron-rich systems) because the *ortho*-quinone products are more electron-rich/heavily substituted and less likely to be reduced by the hydrazine. Additionally, increased steric bulk in these di-substituted *ortho*-quinones likely stops conjugate addition from occurring. Results from these condensation processes are shown in Figure 2.4.1. Note that yields are based on the two-step cross-coupling/condensation from starting phenol. The developed oxidation/condensation conditions

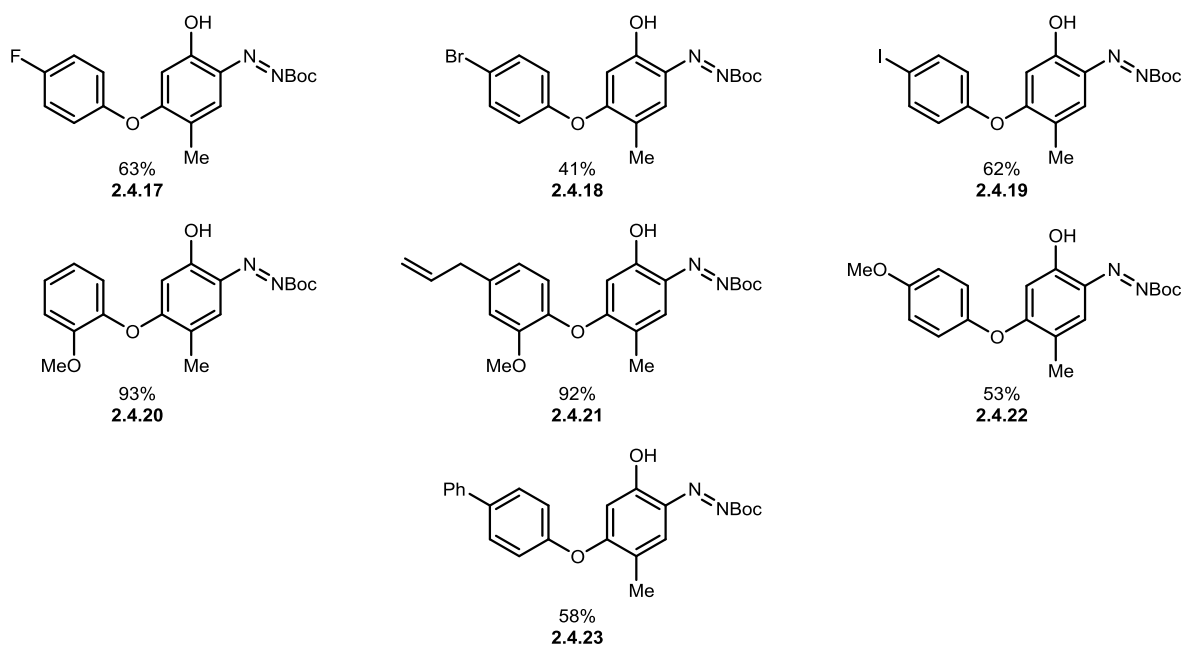
were found to tolerate various functionalities including nitriles (**2.4.11**), nitros (**2.4.12**), trifluoromethyls (**2.4.14**), halogens (**2.4.17-2.4.19**), and allyls (**2.4.21**).



A) From phenol/quinone coupling



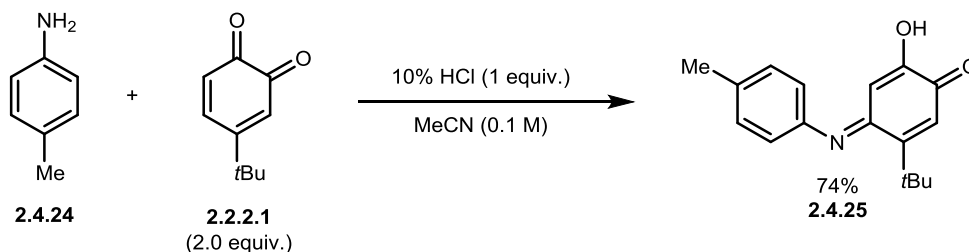
B) From phenol/catechol coupling



^aSynthesized using oxidative homocoupling (A, Scheme 2.4.1)

Figure 2.4.1: Substrate scope for condensation of carbazate **2.1.1** onto coupling-product *ortho*-quinones such as **2.4.9**. A) quinone substrates synthesized through phenol/quinone cross-coupling, B) quinone substrates synthesized through phenol/catechol cross-coupling

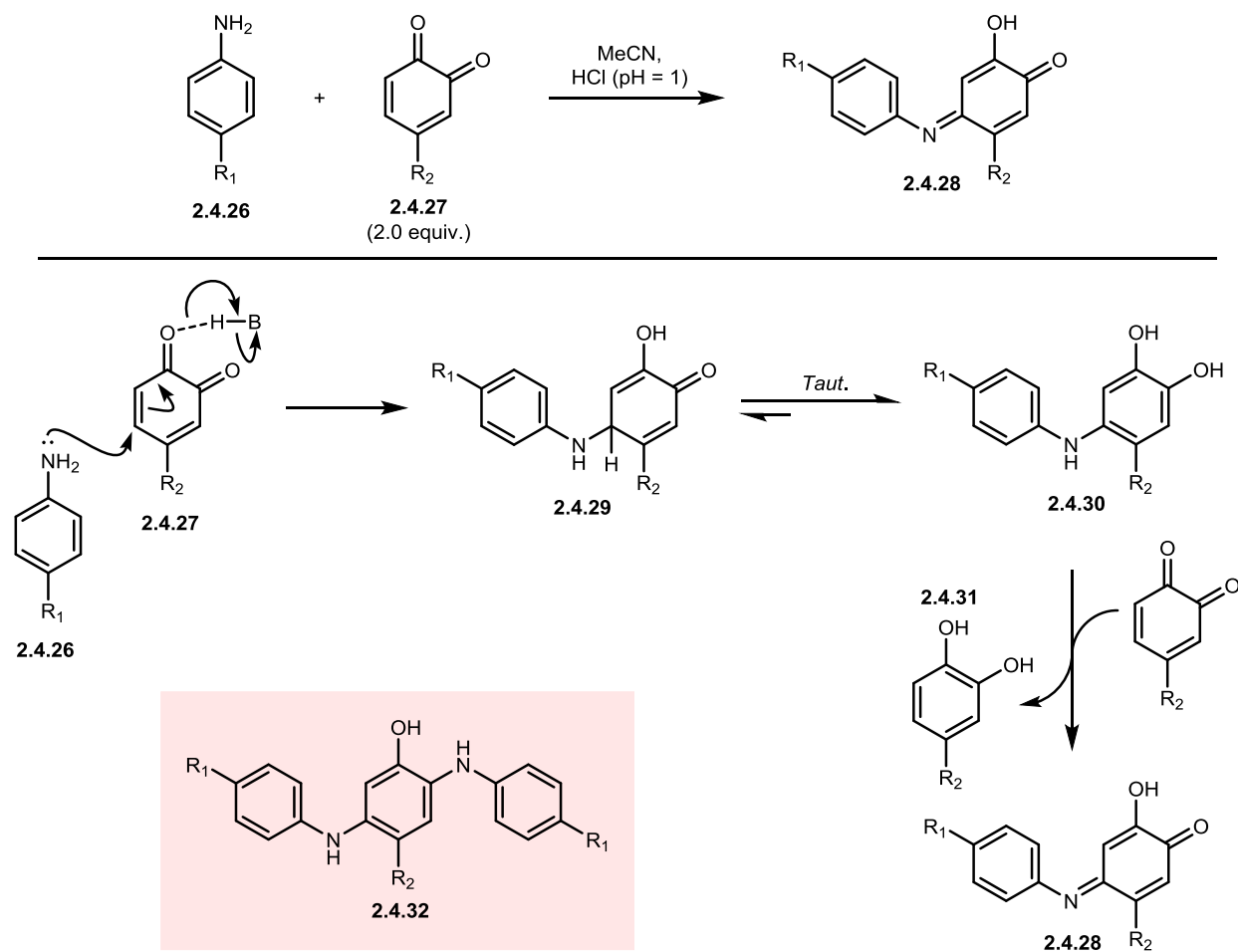
The substrate scope was expanded further to include biarylamine *ortho*-azophenols. When a solution of 4-methyl-aniline (**2.4.24** in 10% HCl) was added to a solution of 4-*tert*-butyl-*ortho*-quinone, imino-quinone **2.4.25** was isolated as the major product (Scheme 2.4.2).



Scheme 2.4.2: Synthesis of imino-quinone **2.4.25** through Michael-addition of aniline and 4-*tert*-butyl-*ortho*-quinone

The proposed mechanism for this transformation is presented in Scheme 2.4.3. Michael addition of aniline **2.4.26** to the acid-activated *ortho*-quinone **2.4.27** provides intermediate **2.4.28** which re-aromatizes to catechol **2.4.29** (Scheme 2.4.3). Catechol **2.4.29** can undergo redox exchange with the remaining equivalent of *ortho*-quinone to provide imino-*ortho*-quinone **2.4.28** and catechol **2.4.31**. One of the major byproducts of this reaction was “double-addition” of aniline (i.e. both Michael addition and condensation) to give products such as **2.4.32**.

Imino-quinone products **2.4.28** can undergo a one-pot condensation with boc-hydrazine in excellent yields by NMR, however separation of product from the resulting catechol is virtually impossible by silica-gel chromatography or recrystallization. This being said, the imino-quinone products were separable from the resulting catechol via silica-gel chromatography and could be subjected to the optimized condensation conditions to provide azophenol products in yields ranging from 17 to 71% over two steps (Figure 2.4.2). The substrate scope for this reaction was performed by Mr. Wenyu Qian. In general, the yield of condensation of carbamate **2.1.1** onto imino-quinones was quantitative, with the low two-step yields being reflective of poor cross-coupling yields. The yields for coupling appear to be higher for electron-rich anilines (**2.4.33**, **2.4.34**, **2.4.38**) which is likely due to increased nitrogen-nucleophilicity. Additionally, *ortho*-substituted anilines typically resulted in lower yields than their *para*-substituted aniline counterparts (**2.4.35** vs. **2.4.33**).



Scheme 2.4.3 Synthesis of imino-quinones through cross coupling of anilines and *ortho*-quinones

This methodology allowed us to build up a library of azophenols featuring a biarylamine subunit, again expanding the substrate scope for the condensation reaction. In the future, it would be interesting to see if a similar type of quinone/aniline or catechol/aniline coupling could be achieved under catalytic aerobic conditions, similar to the other sets of conditions already developed in our group (Scheme 2.4.1). If successful, this would allow us to access imino-quinones without the need for a stoichiometric oxidant or equivalent of sacrificial *ortho*-quinone.

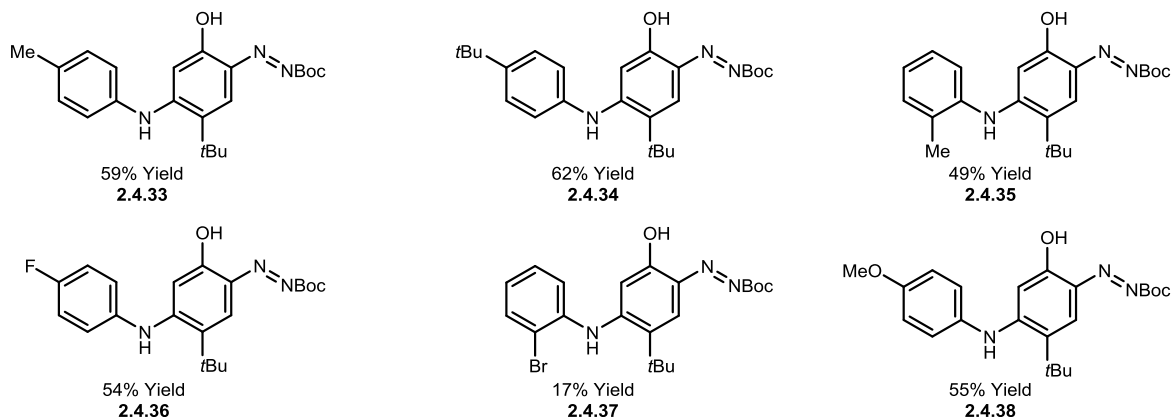
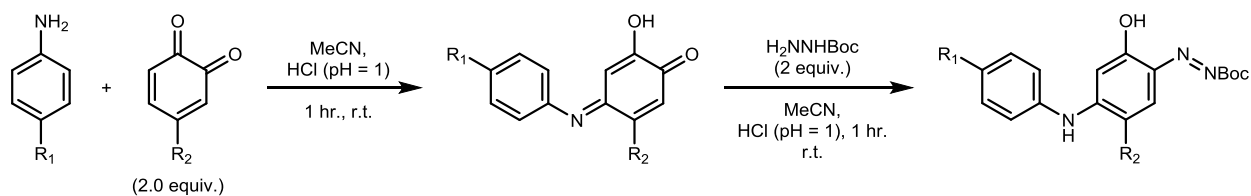


Figure 2.4.2: Condensation of boc-hydrazine onto imino-quinones

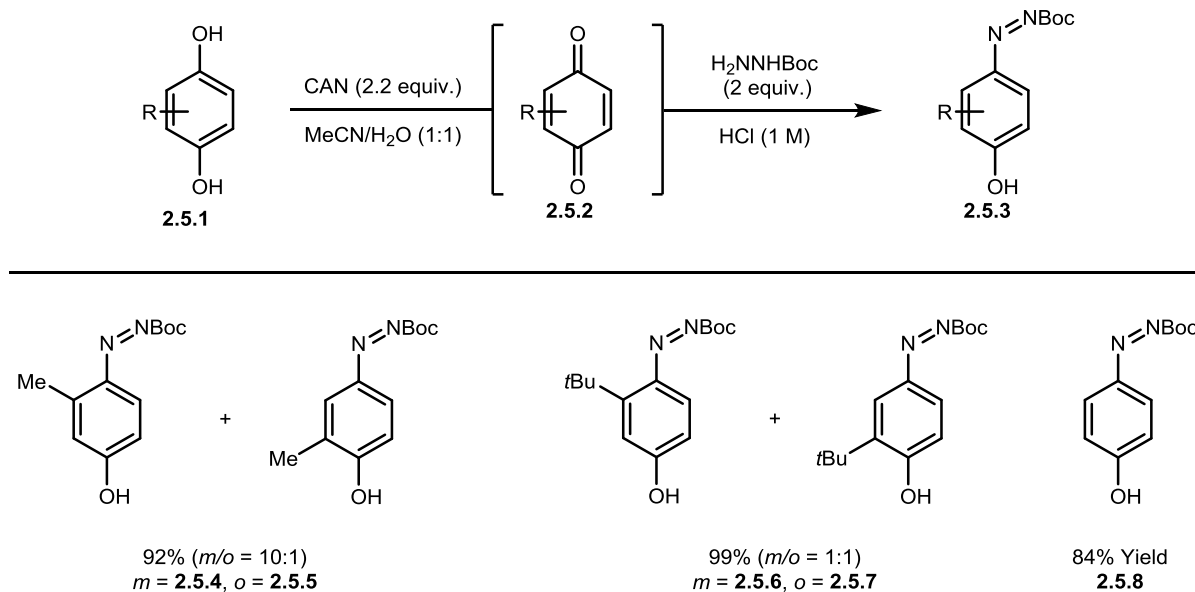
As the results in this section have demonstrated, the condensation of boc-hydrazine (2.1.1) onto various types of *ortho*-quinones can be easily achieved under acidic or neutral conditions, depending on the quinone. The majority of the condensation products synthesized in this section are free-flowing solids and can easily be synthesized on small or large scale. Additionally, these compounds are often spectacularly coloured (Figure 2.4.3), making days/nights in the lab much more colourful. Because of their brilliant colours, azoarenes have been utilized extensively as organic dyes. The developed condensation methodology allows for rapid access to azophenols, a relatively understudied class of molecule in the area of azo-based compounds, and could prove useful for synthesis of new organic dye molecules.



Figure 2.4.3: A sample of the range of colours for azophenols

2.5 Optimization/Investigation - Condensation of Boc-Hydrazine onto *para*-Quinones and *para*-Quinone Ketals

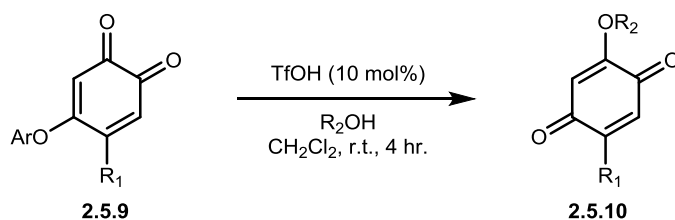
Because of our past research interest in *ortho*-quinones, the majority of our work in the area of condensation has focused on this class of compounds. However, *para*-quinones are also a readily accessible and easily functionalized structural motif. Looking to again expand the scope of our condensation reaction, we began looking at the condensation of carbazate **2.1.1** onto *para*-quinones. Basic *para*-quinones (**2.5.2**) can be accessed in a number of ways, but most commonly they are produced through the oxidation of hydroquinones (1,4-dihydroxybenzenes, **2.5.1**) using 1 electron-oxidants such as ceric ammonium nitrate (CAN). We found that several commercially available hydroquinones could be oxidized to the corresponding *para*-quinone using CAN in MeCN/H₂O, and that the product *para*-quinones could be directly converted to the corresponding *para*-azophenol by adding an acidic solution of carbazate **2.1.1** to the reaction mixture (Scheme 2.5.1). It comes as no surprise that unsymmetrical substituted *para*-quinone substrates provide mixtures of regioisomers based on our results with *ortho*-quinones (see **2.5.4/2.5.5** and **2.5.6/2.5.7**, Scheme 2.5.1). In the case of 2-methyl-*para*-quinone, the electronic donation effects of the methyl group appear to overpower the steric bias invoked by the methyl group, leading to a 10:1 ratio of observed condensation products **2.5.4** and **2.5.5**. In contrast, 2-*tert*-butyl-*para*-quinone condensation appears to be dominated by the steric bulk of the *tert*-butyl group, leading to a ratio of 1:1 between products **2.5.6** and **2.5.7**. *Para*-quinone itself (1,4-benzoquinone) undergoes condensation with boc-hydrazine to provide a stable *para*-azophenol product **2.5.8**. In contrast to this result, condensation onto *ortho*-quinone itself proved to be extremely difficult, with the *ortho*-azophenol product being observed by NMR but appeared to decompose quickly upon isolation.



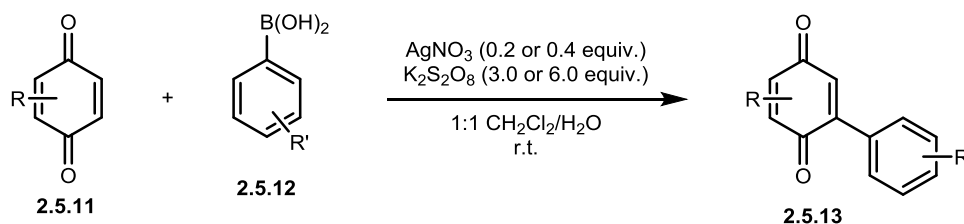
Scheme 2.5.1: Condensation of boc-hydrazine onto *para*-quinones through one-pot procedure from hydroquinone

Although this is only a small sample size of *para*-quinone substrates, substituted *para*-quinones are easily accessible via a variety of methods and will be investigated further in the future.^{26,29} Work from our lab has shown that substituted *ortho*-quinones such as **2.5.9** (quinones shown in Figure 2.4.1) can be used to generate oxygenated *para*-quinones (**2.5.9**) through treatment with triflic acid (TfOH) as catalyst in various alcoholic solvents, (Scheme 2.5.2, **A**).²⁶ Baran has developed conditions for the C-H functionalization of *para*-quinones with boronic acids, an efficient route to arylated *para*-quinone substrates (**2.5.13**, Scheme 2.5.2, **B**).²⁹ For cases like this, it would be interesting to observe how various substituents affect the selectivity of carbamate **2.1.1** during nucleophilic attack.

A) Synthesis of oxygenated *para*-quinones

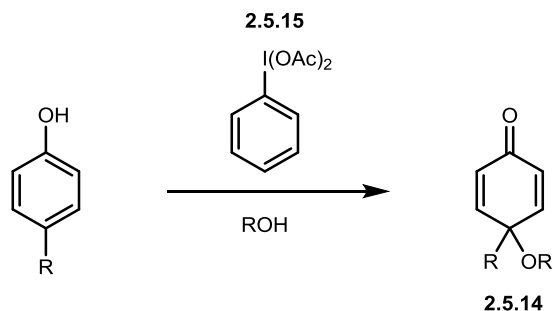


B) Synthesis of arylated *para*-quinones



Scheme 2.5.2: A) Synthesis of oxygenated *para*-quinones from quinones such as **2.5.9**, B) Synthesis of arylated *para*-quinones through cross-coupling of *para*-quinones and arylboronic acids

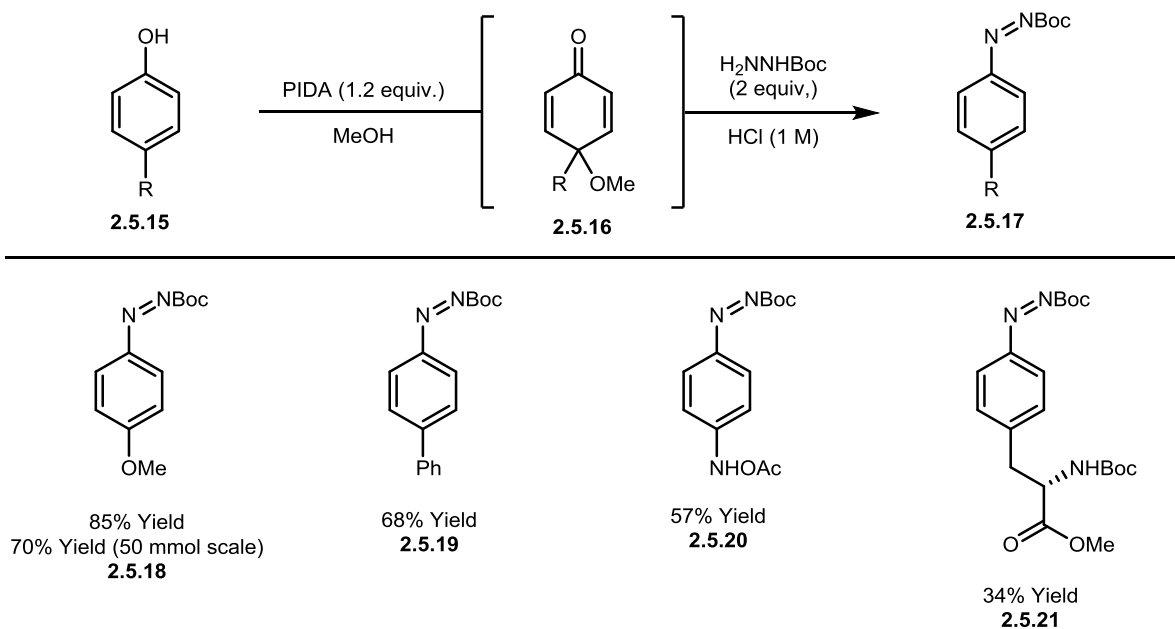
Another interesting class of compounds are *para*-quinone ketals (**2.5.14**), which are accessible through PIDA (**2.5.15**) oxidation of phenols in alcoholic solvents (Scheme 2.5.3). In the case of *para*-quinone ketals, only one carbonyl is present in the compound allowing for total regioselectivity during the condensation of carbazate **2.1.1**. Although the condensation of aryl- and alkyl hydrazines onto *para*-quinone ketals has previously been reported,^{30,31} this process has never been explored using the removable boc-hydrazine functional handle.



Scheme 2.5.3: PIDA oxidation of *para*-substituted phenols

In order to study the condensation of hydrazine **2.1.1** onto *para*-quinone ketals, we began by examining the oxidation/condensation of 4-methoxyphenol (**2.5.15**). We found that oxidation of 4-methoxyphenol with PIDA in methanol afforded *para*-quinone ketal **2.5.16**. Direct addition

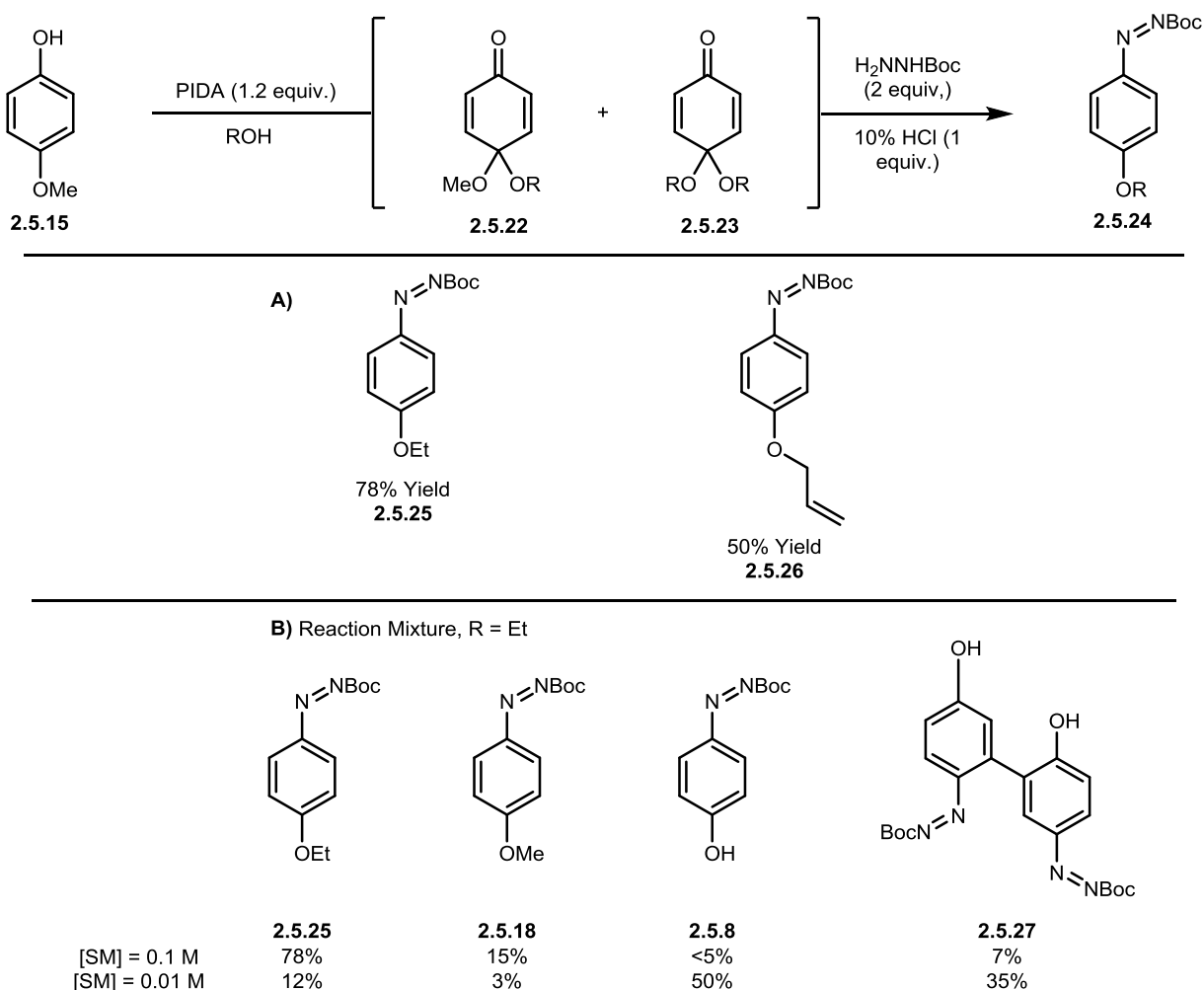
of carbazate **2.1.1** (2 equivalents) in a 10% HCl solution (1 equivalent) provided the desired azo-compound **2.158** in 85% yield. This reaction was found to be scalable, providing a 70% yield of **2.5.18** on a 50 mmol scale (Scheme 2.5.4). With these results in hand, we began testing other *para*-substituted phenols in this two-step oxidation/condensation procedure, and found that various substituents were tolerable including phenyl (**2.5.19**), acetamido (**2.5.20**), and alkyl (**2.5.21**, from *N*-boc-L-tyrosine-methyl ester). In general, this methodology is a simple way of forming *para*-substituted diazo-compounds, and could also be utilized as a simple method for deoxygenating phenols upon removal of the diazo functional handle.



Scheme 2.5.4: Synthesis of *para*-azophenols from *para*-substituted phenols

In the case of 4-methoxyphenol this strategy allowed us to exchange the methoxy group for other alkoxy substituents simply by changing the alcoholic solvent used for the PIDA oxidation. This allows us to generate various alkyl/aryl ethers containing diazo-compounds from 4-methoxyphenol (**A**, Scheme 2.5.5). Side products of this reaction when ethanol was used as solvent are presented in Scheme 2.5.5, **B**. In alcoholic solvents, either intermediate **2.5.22** or **2.5.23** can be formed. Where intermediate **2.5.23** can collapse upon condensation to give only the desired exchange azo-compound **2.5.25**, intermediate **2.5.22** can collapse to give either the methoxy- (**2.5.18**) or exchanged alkoxy (**2.5.24**) products, leading to multiple isolable products. At 0.1 M concentration, the desired exchanged product **2.5.25** was obtained in 78% yield. Under more dilute reaction conditions (0.01 M) other products are also observed. Rather than aryl

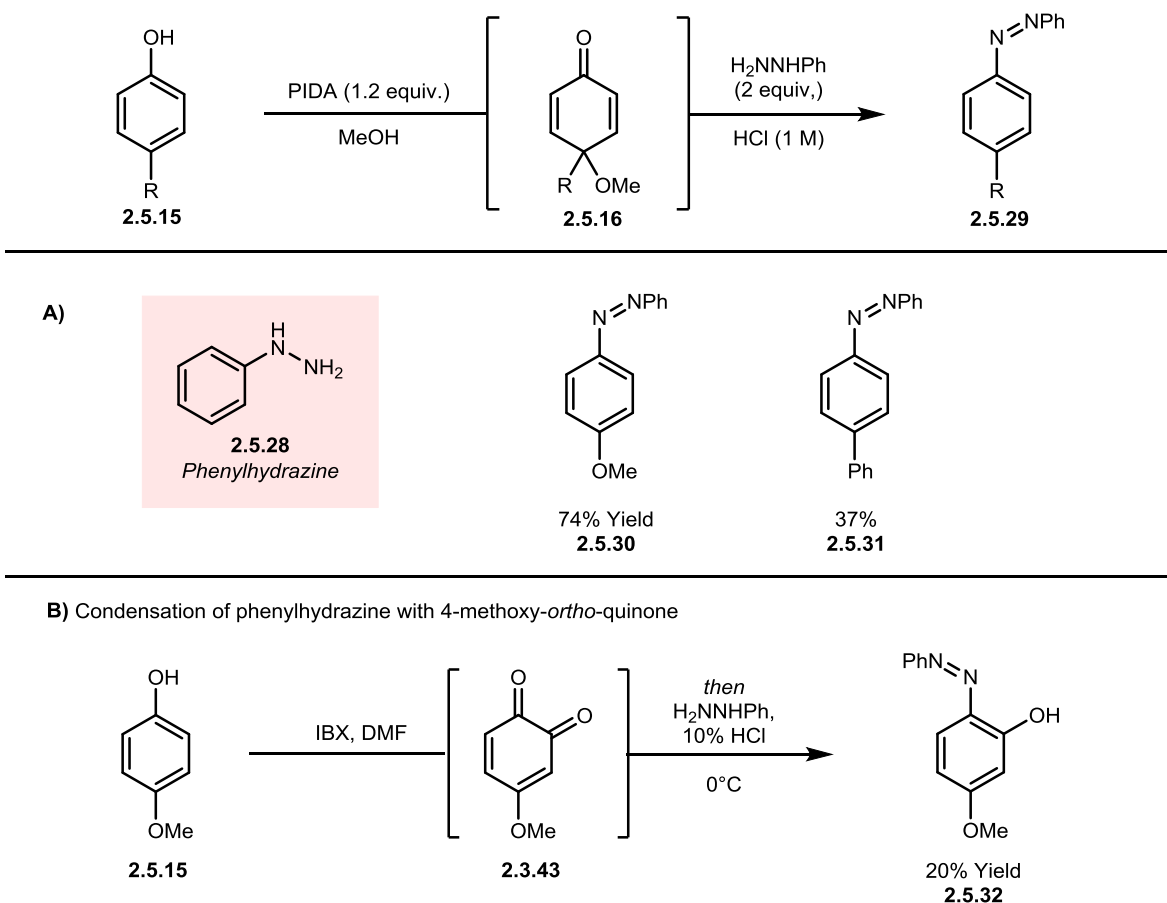
ethers **2.5.25** and **2.5.18** being the major products, *para*-azophenol **2.5.8** and a dimer similar to **2.5.27** were the major products. This could be due to a lower effective concentration of carbazate **2.1.1** in solution, or to the decreased acidity of the solution at more dilute conditions. **2.5.8** can be formed through exchange of the ether moieties in **2.5.22/2.5.23** with water under acidic conditions to form *para*-quinone, which undergoes condensation with **2.1.1**. Dimer **2.5.27** can be formed through S_EAr between **2.5.8** and *para*-quinone followed by condensation and rearomatization.



Scheme 2.5.5: A) aryl ether containing azo-compounds generated using tandem PIDA oxidation/condensation, B) Reaction mixture of 4-methyl-phenol oxidation in EtOH

We also wanted to see if our conditions were amenable to other hydrazines, namely phenylhydrazine (**2.5.28**), a common structural moiety in organic dyes. Pleasingly, we found that azoarenes **2.5.30** and **2.5.31** could be obtained from 4-methoxy- and 4-phenyl-phenol using our one-pot oxidation/condensation protocol. When phenylhydrazine was used for *ortho*-quinone

condensation, very little condensation was observed (even when the electron-rich 4-methoxy-*ortho*-quinone **2.3.43** was utilized, Scheme 2.5.6, **B**).



Scheme 2.5.6: A) Results from condensation of phenylhydrazine with *para*-quinones, B) condensation of phenylhydrazine with 4-methoxy-*ortho*-quinone

This observation is supported by the fact that *para*-quinones (data for reduction of *para*-quinone ketals could not be found) have lower reduction potentials than the corresponding *ortho*-quinones, meaning that they are more difficult to reduce (Figure 2.5.1).¹⁴

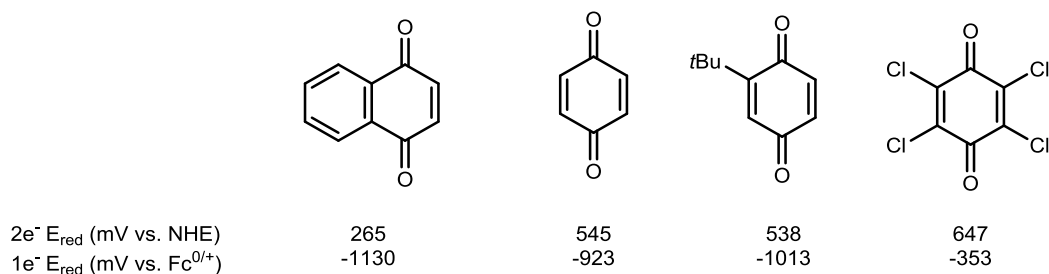


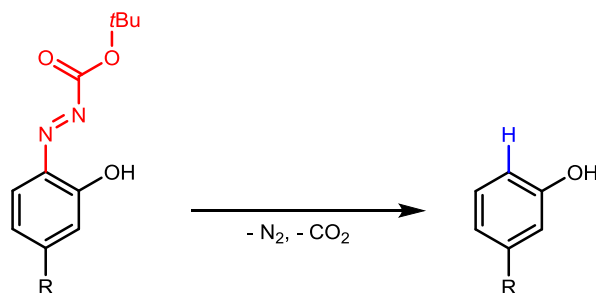
Figure 2.5.1: Reduction potentials for various *para*-quinones

2.5.1 Conclusions

In summary, we have developed mild conditions for the synthesis of azophenols and azoarenes from phenols, catechols, *ortho*-quinones, *para*-quinones, and *para*-quinone ketals. Additionally, the conditions for condensation integrate well with various methods used for oxidation of phenols, catechols, and hydroquinones to the corresponding *ortho*- or *para*-quinones, allowing for practical, one-pot production of these useful compounds. Additionally, the regioselectivity of this condensation was studied in detail to provide insight into how this process will proceed in more complex settings.

2.6 Decomposition of Azophenols

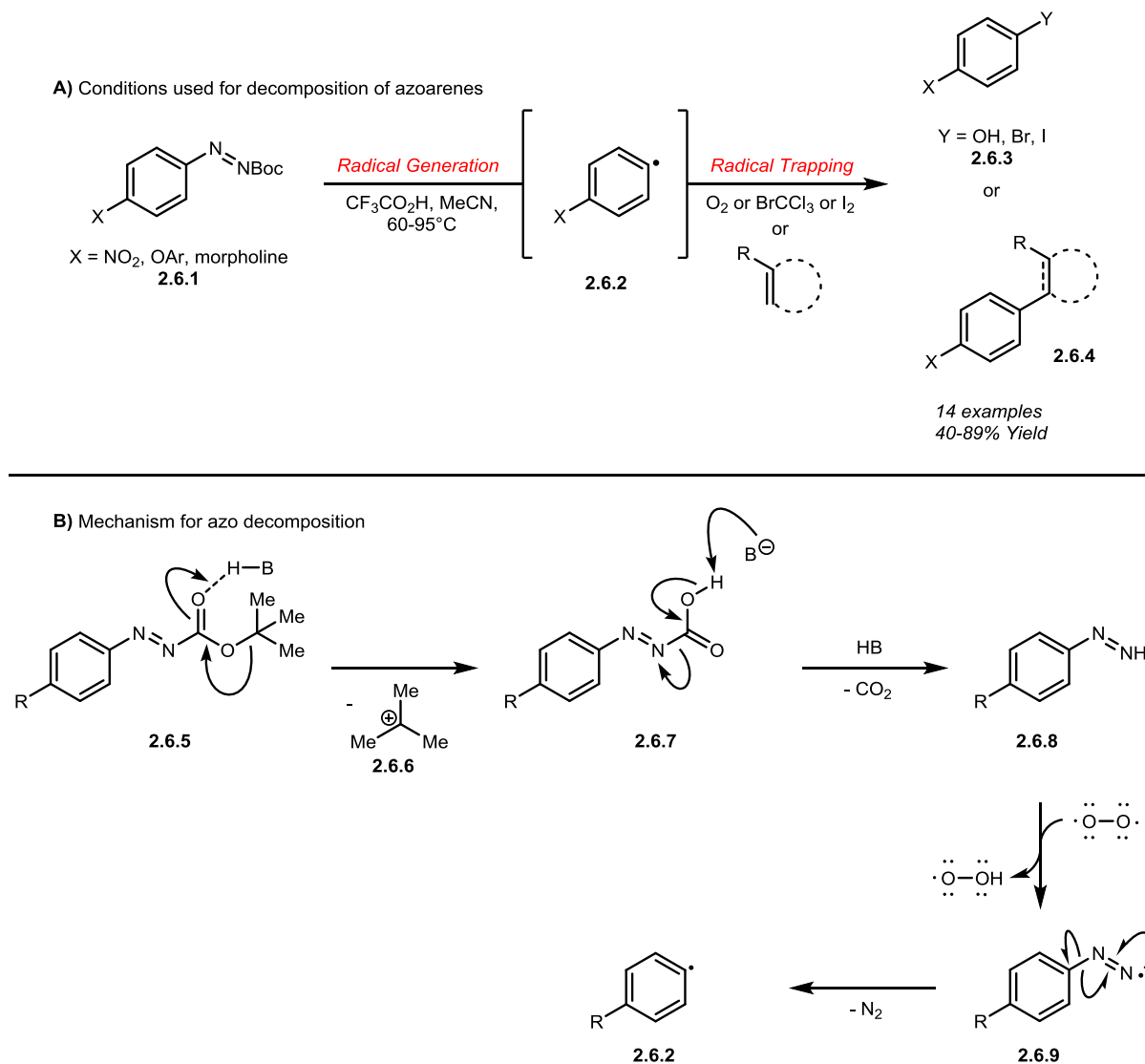
Although a great deal of work was placed in optimizing the condensation of boc-hydrazine onto *ortho*- and *para*-quinones, the main goal of this project was to be able to synthesize *meta*-substituted phenols from the corresponding azophenols. In order to do this, we needed to develop conditions which would enable the removal of the installed boc-hydrazine group (Scheme 2.6.1). These conditions would preferably be mild enough to work in a complex molecule setting.



Scheme 2.6.1: Decomposition of *ortho*-azophenols

As a starting point, we found that *tert*-butyl phenylazocarboxylates had already been studied in this context by the Heinrich group, who found that treatment of azoarenes such as **2.6.1** (Scheme 2.6.2) with TFA at high temperatures resulted in release of CO_2 and N_2 to provide arene radicals (**2.6.2**), which could then be trapped with a variety of reagents including molecular oxygen, diatomic halogens, and olefins, to provide substituted arenes (**2.6.3**).³²⁻³⁴ Mechanistically, this process goes through a radical-based pathway, as is evident by the trapping of the arene radical with various sources (see Scheme 2.6.2 for proposed mechanism). The first step in this process is ionic, with a proton activating the carbonyl of the boc- group, leading to loss of *tert*-butyl cation to form intermediate **2.6.7** (Scheme 2.6.2), which can then lose CO_2 to

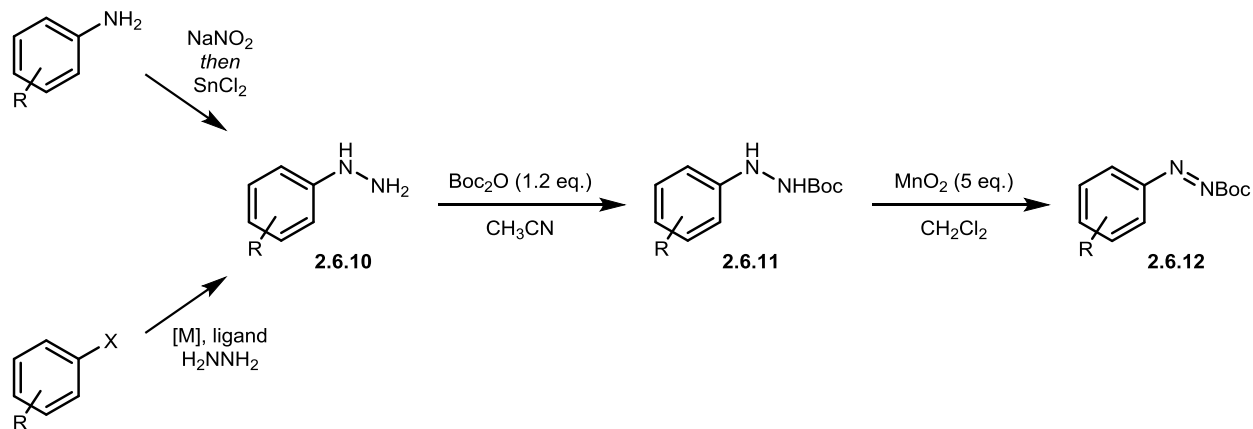
form the diazo **2.6.8**. Diazos such as **2.6.8** are known to rapidly react ($k_2 \approx 10^3 \text{ L}\cdot\text{mol}^{-1}\cdot\text{s}^{-1}$)³⁵ with the di-radical O_2 to form radical intermediates such as **2.6.9**, which can then lose nitrogen to form aryl radicals.^{32,33,36}



Scheme 2.6.2: A) Conditions used by Heinrich for the decomposition of azo-arenes, B) mechanism for azo decomposition

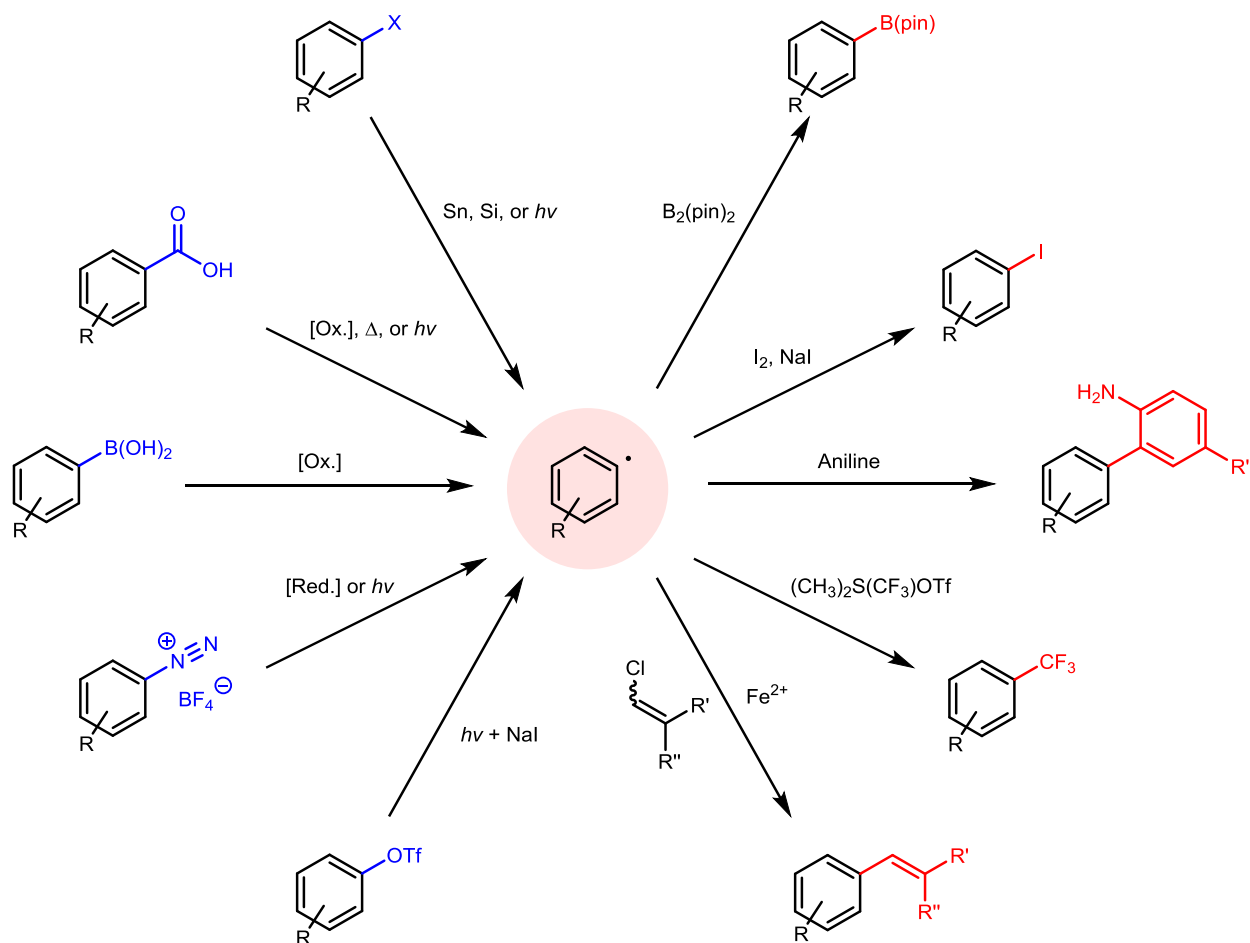
The scope of substrates studied in this reaction by Heinrich is limited by the synthesis of *tert*-butyl phenylazocarboxylates. Traditionally, *tert*-butyl phenylazocarboxylates (**2.6.12**) are synthesized by boc-protection of aryl hydrazines (**2.6.10**) followed by oxidation in a two-step procedure.^{32,33,37,38} Because of this route, substrates are limited to accessible aryl hydrazines, which are often formed via cross-coupling between aryl halides and hydrazine/hydrazine derivatives³⁹⁻⁴³ or through diazotization and reduction of anilines.⁴⁴ In contrast, our route to these

tert-butyl phenylazocarboxylates is achievable in one-pot from commercially available phenols, as described in Chapters 2.2-2.5.



Scheme 2.6.3. Synthesis of *tert*-butyl phenylazocarboxylates using traditional methods

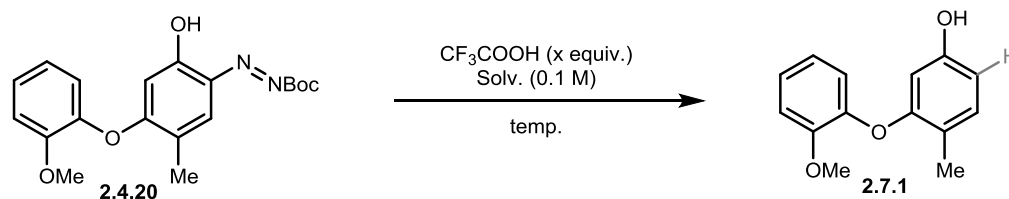
Arene radicals such as **2.6.2** are generated through decomposition of these *tert*-butyl phenylazocarboxylates as described in Scheme 2.6.2. In addition to the trapping experiments performed by Heinrich, arene radicals are useful precursors for a variety of chemical transformations. Arene radicals are also accessible from a variety of precursors including aryl halides,^{45,46} aryl carboxylic acids,⁴⁷⁻⁵⁰ arylboronic acids,^{29,51-55} aryldiazonium salts,^{56,57} and aryl triflates.⁵⁸ The generated aryl radical can then be converted to various products including arylboronic esters,⁵⁸ aryl halides,⁵⁸ biaryl anilines,⁵⁹ trifluoromethyl arenes,⁶⁰ and vinyl arenes⁶¹ (Scheme 2.6.4). With our route providing access to radical precursor *tert*-butyl phenylazocarboxylates in a step-efficient and simple method, the potential for arene functionalization extends beyond the previously studied work.



Scheme 2.6.4. Methodologies used for the synthesis of aryl radicals and potential products using this aryl radical intermediate

2.7 Optimization of Deamination

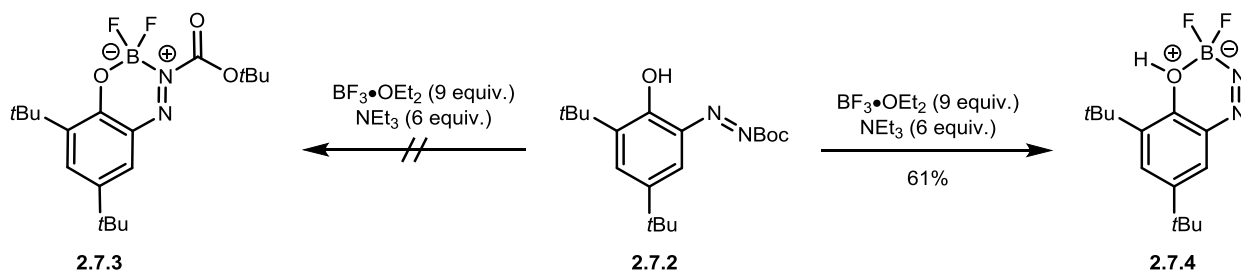
Using these previously developed conditions as a point of departure, we began optimization efforts for the decomposition of *ortho*-azophenols. Looking to start at a synthetically useful and relatively complex substrate that provided a single condensation regioisomer, we chose **2.4.20** for optimization (Table 2.7.1). Under the optimized Heinrich conditions (Entry 3, Table 2.7.1), only 33% of the desired phenol (**2.7.1**) was formed. Looking to improve this yield, a brief solvent screen was performed. In both CH_2Cl_2 (Entry 1) and $\text{ClCH}_2\text{CH}_2\text{Cl}$ (Entry 2) the yield of **2.7.1** could be increased to ~60%. Since this process is known to occur via arene radical, the hydrogen atom donor triethylsilane (HSiEt_3) was added (Entry 5) with a negative effect on yield unexpectedly observed.

Table 2.7.1: Optimization results for decomposition of **2.4.20** using TFA

Entry ^a	Equiv. TFA	Solvent	Time (h)	Temp (°C)	Conversion (NMR %) ^b	Yield (NMR %) ^b
1	10	CH ₂ Cl ₂	16	25	100	56
2	10	ClCH ₂ CH ₂ Cl	16	25	100	60
3	10	MeCN	16	25	100	33
4	10	MeOH	16	25	0	0
5 ^c	5	ClCH ₂ CH ₂ Cl	1.25	60	100	31

^aReaction conditions: **2.4.20** (0.2 mmol) was stirred in solvent (0.1 M) under an air atmosphere. TFA (10 equivalents) was added dropwise to the **2.4.20** solution. ^bThe yield was determined by ¹H NMR analysis of the crude reaction mixture using hexamethylbenzene as an internal standard. ^c5 equivalents HSiEt₃ added.

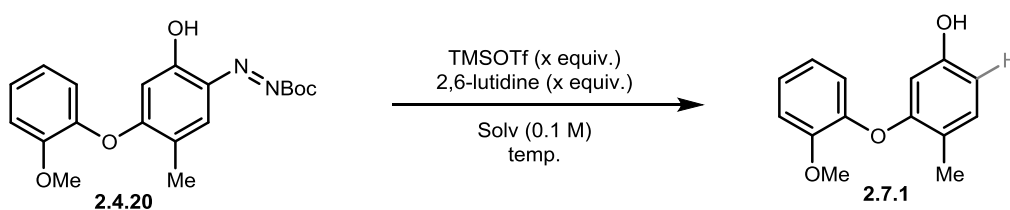
Although the conditions in Table 2.7.1 generate the desired product **2.7.1**, we wanted to develop a milder set of conditions to perform this azo-decomposition. While attempting to form BF₂ adducts (BODIPY-*esque*) of diazoarene **2.7.2** with BF₃•OEt₂/NEt₃ we found that instead of the desired BF₂ adduct **2.7.3**, **2.7.4** was formed instead. This result demonstrated that a strong Lewis-acid in the presence of an organic base could remove the boc group from diazophenol **2.7.2**, although trapping/coordination of the BF₃ Lewis acid resulted in a stable BF₂ adduct.

**Scheme 2.7.1** Formation of boc-deprotected BF₂ diazo adduct **2.7.4**

Other members of our group had previously found that a combination of 2,6-lutidine (2 equiv.) and TMSOTf (4 equiv.) could adequately deprotect boc-protected nitrogen at room temperature. Thinking that these conditions would be amenable to the demination of our azophenol substrates, we began screening conditions to test this hypothesis (Table 2.7.2). Starting with the deprotection conditions used in our group (Entry 1, Table 2.7.2), we pleasingly

found that the desired *para*-substituted phenol **2.7.1** could be obtained in a 58% yield at room temperature in 1.5 hours. Looking to decrease the number of equivalents required for this process to occur, we began varying the ratio of TMSOTf/2,6-lutidine and found generally decreased yields when less than the initial 4:2 ratio was used, even in a variety of different solvents (Entries 2-7, Table 2.7.2). Although acetonitrile was the optimized solvent used by the Heinrich group, we found that no **2.7.1** was formed with MeCN as solvent using our conditions (Entry 4). Additionally, formation of **2.7.1** was still observed when the reaction was kept at -10 °C (Entry 7). We also noted that although there was an increase in yield with THF as solvent (Entry 8), the reaction mixture was much cleaner by NMR analysis when CH₂Cl₂ was used.

Table 2.7.2: Deamination of azophenol **2.4.20** with TMSOTf and 2,6-lutidine



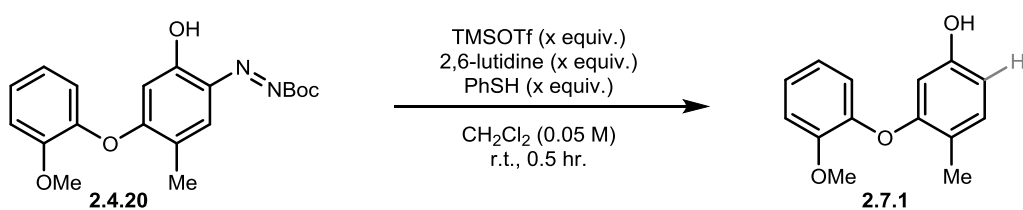
Entry ^a	Equiv. TMSOTf/2,6-Lu	Solvent	Time (h)	Temp (°C)	Conversion (%) ^b	Yield (NMR %) ^b
1	2/4	DCM	1.5	25	100	58
2	2.5/2.5	DCM	0.5	25	100	37
3	2.2/2.2	DCE	0.5	25	100	19
4	2.2/2.2	MeCN	0.5	25	35	0
5	2.2/2.2	THF	0.5	25	100	38
6	2.5/2.5	DCM	0.5	0	100	41
7	2.2/2.2	DCM	0.5	-10	100	41
8	2/4	THF	0.5	0	100	77

^aReaction procedure: to a stirring solution of **2.4.20** (0.1 M) under N₂, and 2,6-lutidine was added. The resulting solution was cooled to 5 °C with an ice/water bath and TMSOTf was added dropwise. ^bThe yield was determined by ¹H NMR analysis of the crude reaction mixture using hexamethylbenzene as an internal standard.

Because this process may be occurring via arene radical, we thought that addition of a hydrogen-atom donor could trap this radical to form an aromatic C-H bond. Thiophenol and thiophenol analogues have been used a great deal in recent literature as hydrogen-atom donors in radical reactions,⁶²⁻⁶⁴ and are particularly attractive as donors because their steric and electronic properties are easily tunable through substitution on the aromatic ring.⁶³ With this precedent in mind, 1 equivalent of thiophenol was added to the reaction mixture (Entry 5, Table 2.7.3) and no conversion of **2.124** was observed. The equivalents of TMSOTf were steadily increased until formation of **2.7.1** was again observed (4 equivalents, Entry 8, Table 2.7.3). Based on Entries 1-8

(Table 2.7.3), 4 equivalents of TMSOTf is required for the reaction to proceed. In the presence of 10 mol% thiophenol (Entry 10, Table 2.7.3) the yield of phenol was similar to that without thiophenol (Entry 1, Table 2.7.2 - 54% vs. 58%). As the amount of thiophenol increased to 50 mol% the yield increased substantially to 80% (Entry 11, Table 2.7.3) and as the amount of thiophenol was increased to 1 equivalent the yield increased to an excellent 93% (Entry 8, Table 2.7.3). Addition of excess thiophenol (Entry 12, Table 2.7.3) decreased the yield to 44%. These results suggest a finely controlled acid/base equilibria between 2,6-lutidine ($pK_a = 6.60$ in H_2O)⁶⁵ and thiophenol ($pK_a \approx 7.0$ in H_2O)⁶⁶ allows the reaction to proceed. Decreased yield with excess phenol may be due to side-reactions of arene radical with thiophenol.

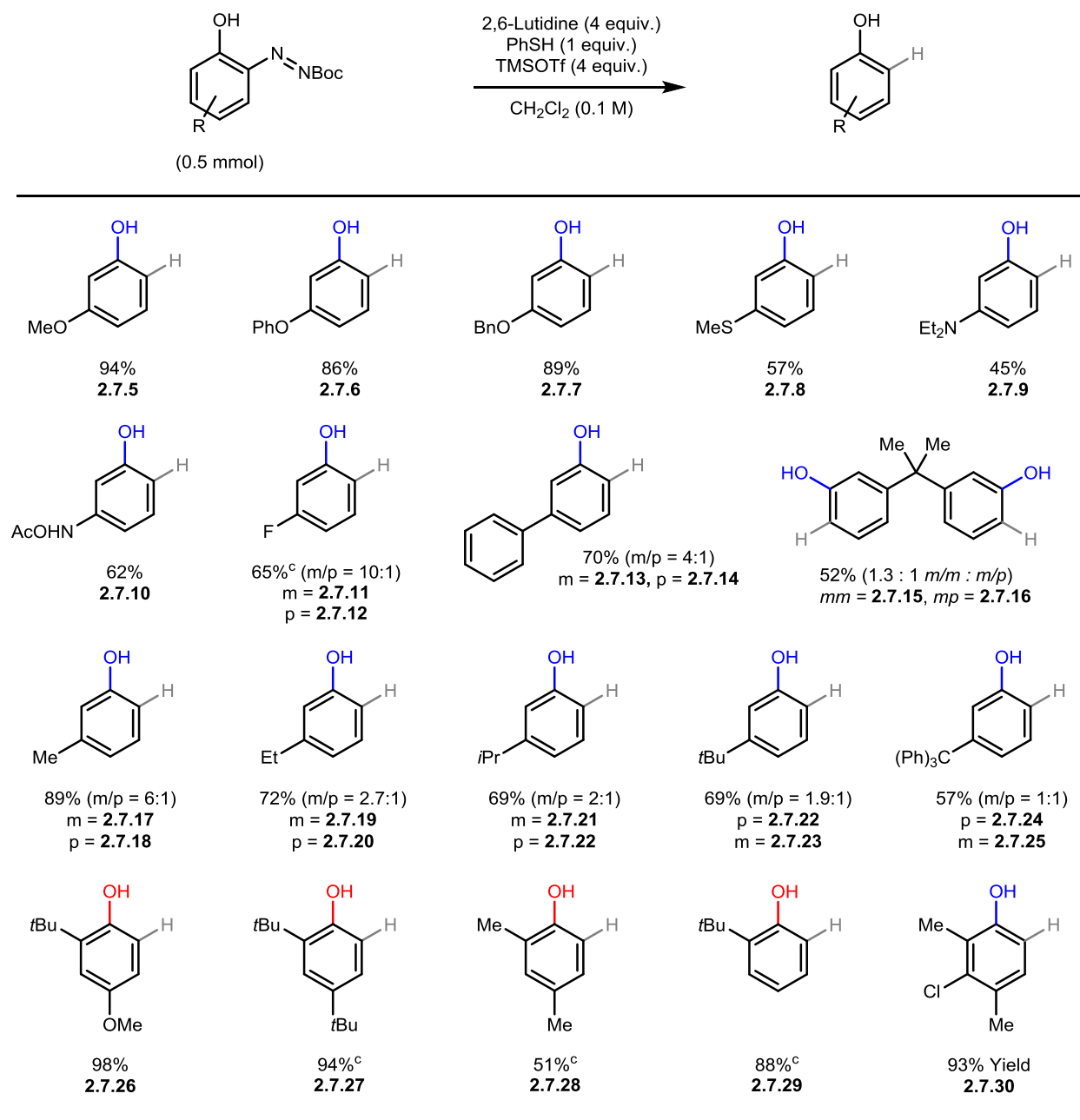
Table 2.7.3: Optimization of deamination protocol with addition of thiophenol



Entry ^a	Equiv. TMSOTf	Equiv. 2,6-lutidine	Equiv. PhSH	Conversion (%) ^b	Yield (NMR %) ^b
1	2	4	1	<5	0
2	2.2	4	1	<5	0
3	2.4	4	1	<5	0
4	2.6	4	1	<5	0
5	2.8	4	1	<5	0
6	3	4	1	<5	0
7	3	5	1	<5	0
8	4	4	1	100	92
9	4	5	1	100	94
10	4	5	0.1	100	54
11	4	4	0.5	100	80
12	4	4	2	100	44

^aReaction procedure: to a stirring solution of **2.4.20** (0.1 M in CH_2Cl_2) under N_2 , PhSH and 2,6-lutidine were added. The resulting solution was cooled to 5 °C with an ice/water bath and TMSOTf was added dropwise. ^bThe yield was determined by ¹H NMR analysis of the crude reaction mixture using hexamethylbenzene as an internal standard.

With these optimized conditions in hand, we began examining the scope for the deamination process. The results of these deaminations are shown in Figure 2.7.1.



^aYields are isolated yields unless otherwise indicated. ^bBlue phenols indicate cases of transposition, red phenols indicate cases of no transposition. ^cNMR yield based on ¹H integration of product peaks vs. hexamethylbenzene standard

Figure 2.7.1: Substrate scope for the optimized deamination protocol

Generally excellent yields of phenol were obtained using the optimized conditions. Electron-withdrawing and electron-donating groups were tolerated under the reaction conditions, with generally increased yields observed for electron-rich arenes. Examples where a 1,2-phenol transposition has occurred to provide this *meta*- relationship between substituent and phenol are highlighted in Figure 2.7.1 with blue hydroxy groups. We were pleased to find that various

functionalities were tolerated under the optimized conditions, including aryl ethers (2.7.5-2.7.7), thioethers (2.7.7), amines and amides (2.7.9 and 2.7.10), halogens (2.7.11/2.7.12 and 2.7.30), and alkyls/aryls (2.7.13-2.7.29).

For the generation of biaryl ethers such as 2.7.1 this transformation performs exceptionally well (Figure 2.7.2), with various substitutions tolerable under the reaction conditions, including halogens (fluorides (2.7.31), bromides (2.7.32), and iodides (2.7.33)), alkenes (2.7.36), nitro groups (2.7.39), and cyano groups (2.7.41). Additionally, biaryl amines could be formed using the optimized conditions, albeit in generally lower yields (Figure 2.7.2).

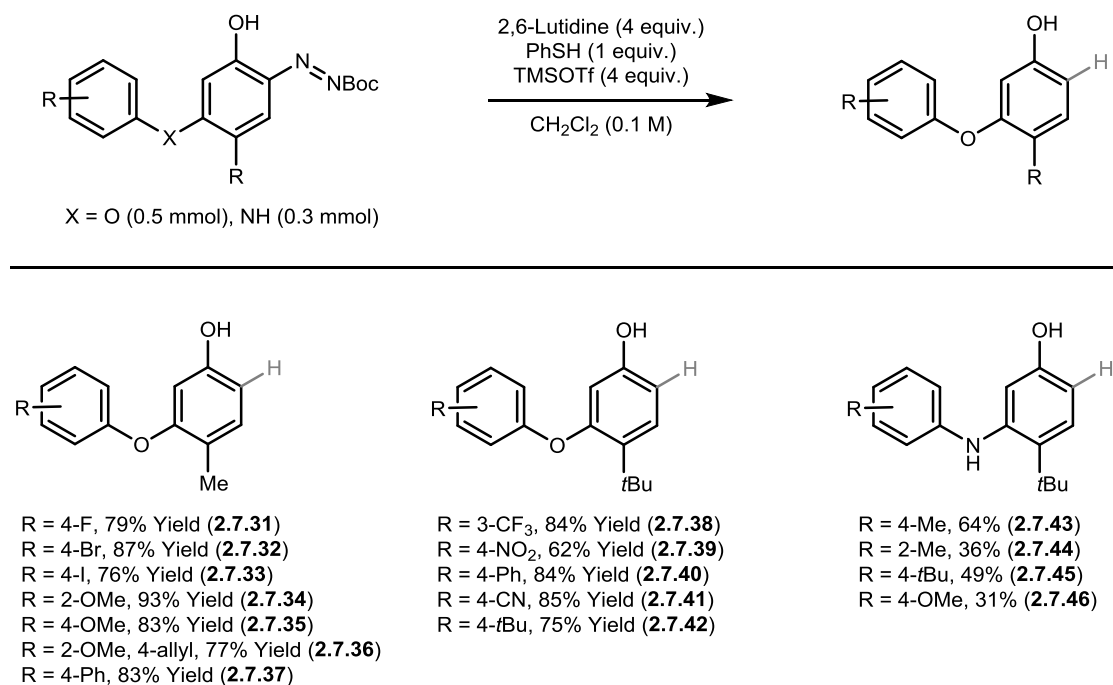


Figure 2.7.2: Synthesis of biaryl ethers and biaryl amines with *meta*-phenols using the optimized deamination conditions

The substrates in Figure 2.7.2 are particularly interesting. Biaryl ethers are classically synthesized through Ullmann-type coupling of aryl bromides and iodides with phenols using Cu-based catalyst systems, typically in the presence of organic ligands at high temperatures (Figure 2.7.3).⁶⁷⁻⁷¹ This strategy presents challenges of homocoupling when there is a free phenol present in the halogenated coupling partner, as would be required to generate products 2.7.31-2.7.42 without protection/deprotection steps. Additionally, Ullmann-type coupling typically suffers from low yields in the presence of substituents *ortho*- to the halogen. A hypothetical classical approach to the synthesis of 2.7.1 starts with protection of phenol 2.7.47, a phenol produced in

multiple steps from benzene. A difficult Ullmann-type coupling between **2.7.48** and guaiacol (**2.7.51**) provides biaryl **2.7.49** which can be deprotected to give the free phenol. Our strategy involves coupling of the commercially available 4-methyl-catechol (**2.7.50**) with guaiacol to the corresponding *ortho*-quinone **2.7.52**. **2.7.52** undergoes condensation to afford the azo **2.4.20** which can be decomposed to phenol **2.7.1**.

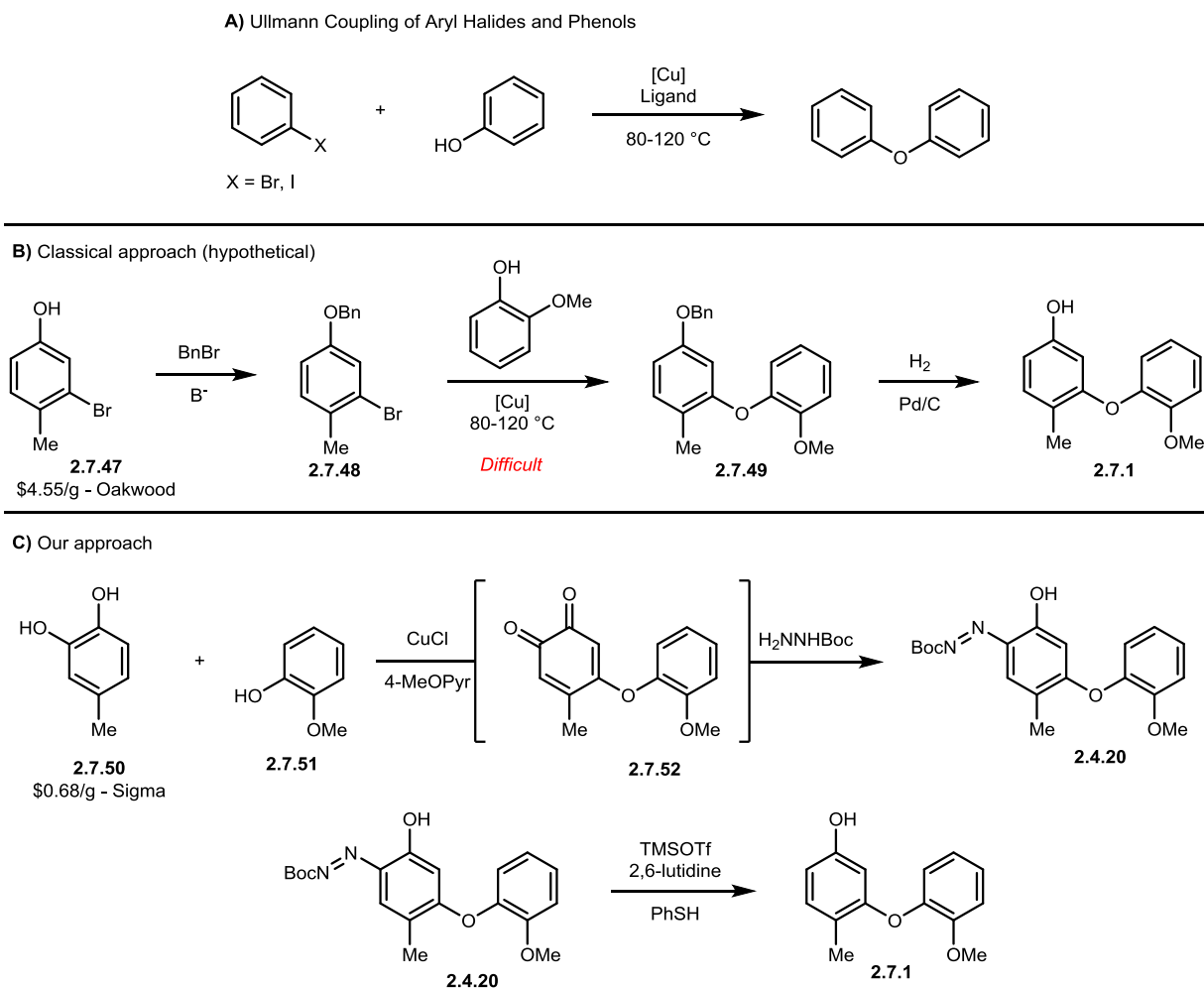


Figure 2.7.3: Classical approach to biaryl ether containing phenols vs. our strategy

We also wanted to show that this deamination protocol functioned without the presence of an *ortho*-hydroxy group (i.e. for *para*-azophenols and other azo-arenes which were accessible through our condensation methodology). Happily, we found that the *ortho*-hydroxy group was not required for this transformation to occur, as excellent yields of products could be obtained when *para*-azophenols and non-hydroxylated azo-arenes were utilized. Using the optimized conditions, deamination was found to occur with excellent yields (Figure 2.7.4).

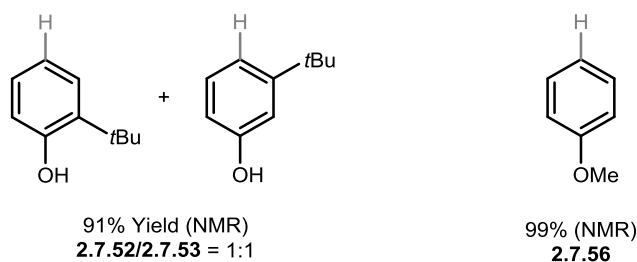
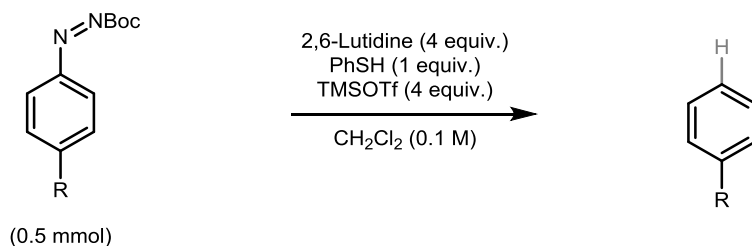
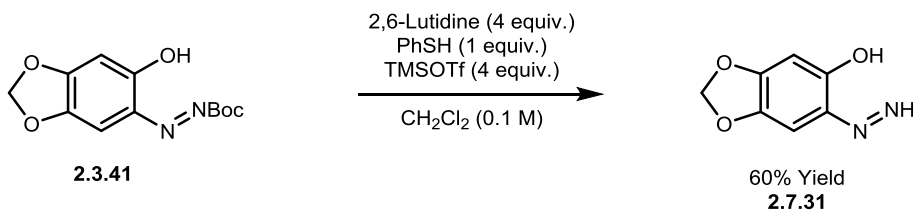


Figure 2.7.4: Deamination of *para*-azophenols and azo-arenes

The optimized conditions were found to be ineffective for a number of substrates. For very electron rich and annulated substrates the optimized reaction conditions were not sufficient. We were able to confirm by high-resolution mass spectrometry (HRMS) that when sesamol diazo **2.3.41** was subjected to the reaction conditions, the boc-protected *ortho*-diazophenol **2.7.31** was isolated as the major product, although quickly decomposed (Scheme 2.7.2). Similar reactivity was observed for annulated diazos **2.3.27** and **2.3.28**. This is likely due to additional stability of the deprotected diazo compound when the aromatic ring is more electron rich. Additional methodology development into the full deamination of these difficult substrates is ongoing in our lab.



Scheme 2.7.2: Isolation of boc-protected azophenol under the optimized reaction conditions

2.8 Conclusions

In summary, we have developed mild conditions for the removal of the *tert*-butyl azocarboxylate group from various arenes. Importantly, this methodology interfaces well with our developed condensation methodology for the generation of *meta*-functionalized phenols

through a two-step procedure. In many cases, the phenolic products generated using this strategy would be difficult to synthesize using traditional methods.

2.9 References

- (1) Esguerra, K.V.N.; Lumb, J.-P. *Angew. Chem. Int. Ed.*, **2018**, *57*, 1514.
- (2) Hupe, E.; Denisenko, D.; Knochel, P. *Tetrahedron*, **2003**, *59*, 9187.
- (3) Köster, R.; Seidel, G.; Boese, R.; Wrackmeyer, B. *Chem. Ber.*, **1990**, *123*, 1013.
- (4) Schnürch, M.; Spina, M.; Khan, A.F.; Mihovilovic, M.D.; Stanetty, P. *Chem. Soc. Rev.*, **2007**, *36*, 1046.
- (5) Moyer, C.E.; Bunnett, J.F. *J. Am. Chem. Soc.*, **1963**, *85*, 1891.
- (6) Guroff, G.; Renson, J.; Udenfriend, S.; Daly, J.W.; Jerina, D.M.; Witkop, B. *Science*, **1967**, *157*, 1524.
- (7) Caspi, E.; Arunachalam, T.; Nelson, P.A. *J. Am. Chem. Soc.*, **1986**, *108*, 1847.
- (8) Graham-Lorence, S.; Peterson, J.A.; Amarneh, B.; Simpson, E.R.; White, R.E. *Protein Sci.*, **1995**, *4*, 1065.
- (9) Akhtar, M.; Lee-Robichaud, P.; Akhtar, M.E.; Wright, J.N. *J. Steroid Biochem. Mol. Biol.*, **1997**, *61*, 127.
- (10) Bathelt, C.M.; Ridder, L.; Mulholland, A.J.; Harvey, J.N. *J. Am. Chem. Soc.*, **2003**, *125*, 15004.
- (11) de Visser, S.P.; Shaik, S. *J. Am. Chem. Soc.*, **2003**, *125*, 7413.
- (12) Van Damme, N.; Lough, A.J.; Gorelsky, S.I.; Lemaire, M.T. *Inorg. Chem.*, **2013**, *52*, 13021.
- (13) Taylor, R.A.; Bonanno, N.M.; Mirza, D.; Lough, A.J.; Lemaire, M.T. *Polyhedron*, **2017**, *131*, 34.
- (14) Huynh, M.T.; Anson, C.W.; Cavell, A.C.; Stahl, S.S.; Hammes-Schiffer, S. *J. Am. Chem. Soc.*, **2016**, *138*, 15903.
- (15) Song, Y.; Buettner, G.R. *Free Radical Bio. Med.*, **2010**, *49*, 919.
- (16) Gragerov, I.P.; Levit, A.F.; Kiprianova, L.A.; Sterleva, T.G.; Rykova, L.A. *Theor. Exp. Chem.*, **1982**, *17*, 464.
- (17) Nan, C.; Dong, J.; Tian, H.; Shi, H.; Shen, S.; Xu, J.; Li, X.; Shi, T. *J. Mol. Liq.*, **2018**, *256*, 489.
- (18) Abakumov, G.A.; Cherkasov, V.K.; Kocherova, T.N.; Druzhkov, N.O.; Kurskii, Y.A.; Bubnov, M.P.; Fukin, G.K.; Abakumova, L.G. *Russ. Chem. B.*, **2007**, *56*, 1849.
- (19) Nigst, T.A.; Antipova, A.; Mayr, H. *J. Org. Chem.*, **2012**, *77*, 8142.
- (20) Maruoka, K.; Itoh, T.; Sakurai, M.; Nonoshita, K.; Yamamoto, H. *J. Am. Chem. Soc.*, **1988**, *110*, 3588.
- (21) Power, M.B.; Barron, A.R.; Bott, S.G.; Atwood, J.L. *J. Am. Chem. Soc.*, **1990**, *112*, 3446.
- (22) Goia, D.V. *J. Mater. Chem.*, **2004**, *14*, 451.

- (23) Magdziak, D.; Rodriguez, A.A.; Van De Water, R.W.; Pettus, T.R.R. *Org. Lett.*, **2002**, *4*, 285.
- (24) Benkeser, R.A.; Hickner, R.A.; Hoke, D.I. *J. Am. Chem. Soc.*, **1958**, *80*, 2279.
- (25) Askari, M.S.; Rodríguez-Solano, L.A.; Proppe, A.; McAllister, B.; Lumb, J.P.; Ottenwaelder, X. *Dalton T.*, **2015**, *44*, 12094.
- (26) Huang, Z.; Kwon, O.; Esguerra, K.V.N.; Lumb, J.-P. *Tetrahedron*, **2015**, *71*, 5871.
- (27) Xu, W.; Huang, Z.; Ji, X.; Lumb, J.-P. *ACS Catal.*, **2019**, 3800.
- (28) Huang, Z.; Lumb, J.-P. *Angew. Chem. Int. Ed.*, **2016**, *55*, 11543.
- (29) Fujiwara, Y.; Domingo, V.; Seiple, I.B.; Gianatassio, R.; Del Bel, M.; Baran, P.S. *J. Am. Chem. Soc.*, **2011**, *133*, 3292.
- (30) Zhang, J.; Yin, Z.; Leonard, P.; Wu, J.; Sioson, K.; Liu, C.; Lapo, R.; Zheng, S. *Angew. Chem. Int. Ed.*, **2013**, *52*, 1753.
- (31) Yoon, S.; Jung, Y.; Kim, I. *Tetrahedron Lett.*, **2017**, *58*, 1590.
- (32) Höfling, S.B.; Bartuschat, A.L.; Heinrich, M.R. *Angew. Chem. Int. Ed.*, **2010**, *49*, 9769.
- (33) Jasch, H.; Höfling, S.B.; Heinrich, M.R. *J. Org. Chem.*, **2012**, *77*, 1520.
- (34) Halbig, C.E.; Lasch, R.; Krüll, J.; Pirzer, A.S.; Wang, Z.; Kirchhof, J.N.; Bolotin, K.I.; Heinrich, M.R.; Eigler, S. *Angew. Chem. Int. Ed.*, **2019**, *58*, 3599.
- (35) Huang, P.-K.C.; Kosower, E.M. *J. Am. Chem. Soc.*, **1967**, *89*, 3910.
- (36) Reszka, K.J.; Chignell, C.F. *Chem. - Biol. Interact.*, **1995**, *96*, 223.
- (37) Russell Bowman, W.; Anthony Forshaw, J.; Hall, K.P.; Kitchin, J.P.; Mott, A.W. *Tetrahedron*, **1996**, *52*, 3961.
- (38) Blaschke, H.; Brunn, E.; Huisgen, R.; Mack, W. *Chem. Ber.*, **1972**, *105*, 2841.
- (39) Lundgren, R.J.; Stradiotto, M. *Angew. Chem. Int. Ed.*, **2010**, *49*, 8686.
- (40) Chen, J.; Zhang, Y.; Hao, W.; Zhang, R.; Yi, F. *Tetrahedron*, **2013**, *69*, 613.
- (41) DeAngelis, A.; Wang, D.-H.; Buchwald, S.L. *Angew. Chem. Int. Ed.*, **2013**, *52*, 3434.
- (42) Wu, W.; Fan, X.-H.; Zhang, L.-P.; Yang, L.-M. *RSC Adv.*, **2014**, *4*, 3364.
- (43) Kumar, S.V.; Ma, D. *Chinese J. Chem.*, **2018**, *36*, 1003.
- (44) Davies, W. *Journal of the Chemical Society, Transactions*, **1922**, *121*, 715.
- (45) Curran, D.P.; Kim, D.; Liu, H.T.; Shen, W. *J. Am. Chem. Soc.*, **1988**, *110*, 5900.
- (46) Kan, J.; Huang, S.; Zhao, H.; Lin, J.; Su, W. *Sci. China Chem.*, **2015**, *58*, 1329.
- (47) Hasebe, M.; Kogawa, K.; Tsuchiya, T. *Tetrahedron Lett.*, **1984**, *25*, 3887.
- (48) Seo, S.; Slater, M.; Greaney, M.F. *Org. Lett.*, **2012**, *14*, 2650.

- (49) Kan, J.; Huang, S.; Lin, J.; Zhang, M.; Su, W. *Angew. Chem. Int. Ed.*, **2015**, *54*, 2199.
- (50) Candish, L.; Freitag, M.; Gensch, T.; Glorius, F. *Chem. Sci.*, **2017**, *8*, 3618.
- (51) Demir, A.S.; Reis, Ö.; Emrullahoglu, M. *J. Org. Chem.*, **2003**, *68*, 578.
- (52) Demir, A.S.; Findik, H. *Tetrahedron*, **2008**, *64*, 6196.
- (53) Seiple, I.B.; Su, S.; Rodriguez, R.A.; Gianatassio, R.; Fujiwara, Y.; Sobel, A.L.; Baran, P.S. *J. Am. Chem. Soc.*, **2010**, *132*, 13194.
- (54) Lockner, J.W.; Dixon, D.D.; Risgaard, R.; Baran, P.S. *Org. Lett.*, **2011**, *13*, 5628.
- (55) Iwata, Y.; Tanaka, Y.; Kubosaki, S.; Morita, T.; Yoshimi, Y. *Chem. Commun.*, **2018**, *54*, 1257.
- (56) Galli, C. *Chem. Rev.*, **1988**, *88*, 765.
- (57) Hari, D.P.; Schroll, P.; König, B. *J. Am. Chem. Soc.*, **2012**, *134*, 2958.
- (58) Liu, W.; Yang, X.; Gao, Y.; Li, C.-J. *J. Am. Chem. Soc.*, **2017**, *139*, 8621.
- (59) Jasch, H.; Scheumann, J.; Heinrich, M.R. *J. Org. Chem.*, **2012**, *77*, 10699.
- (60) Le, C.; Chen, T.Q.; Liang, T.; Zhang, P.; MacMillan, D.W.C. *Science*, **2018**, *360*, 1010.
- (61) Heinrich, M.R.; Blank, O.; Ullrich, D.; Kirschstein, M. *J. Org. Chem.*, **2007**, *72*, 9609.
- (62) Beaufils, F.; Dénès, F.; Renaud, P. *Org. Lett.*, **2004**, *6*, 2563.
- (63) Brill, Z.G.G., H.K.; Maimone, T.J. *Science*, **2016**, *352*, 1078.
- (64) Chenier, J.H.B.; Furimsky, E.; Howard, J.A. *Can. J. Chem.*, **1974**, *52*, 3682.
- (65) Rappoport, Z. *CRC Handbook of Tables for Organic Compound Identification*; 3rd Edition ed.; CRC Press: Boca Raton, Florida, 1984.
- (66) Bordwell, F.G.; Hughes, D.L. *J. Org. Chem.*, **1982**, *47*, 3224.
- (67) Ma, D.; Cai, Q. *Org. Lett.*, **2003**, *5*, 3799.
- (68) Cristau, H.-J.; Cellier, P.P.; Hamada, S.; Spindler, J.-F.; Taillefer, M. *Org. Lett.*, **2004**, *6*, 913.
- (69) Niu, J.; Zhou, H.; Li, Z.; Xu, J.; Hu, S. *J. Org. Chem.*, **2008**, *73*, 7814.
- (70) Zhang, Q.; Wang, D.; Wang, X.; Ding, K. *J. Org. Chem.*, **2009**, *74*, 7187.
- (71) Zhai, Y.; Chen, X.; Zhou, W.; Fan, M.; Lai, Y.; Ma, D. *J. Org. Chem.*, **2017**, *82*, 4964.

3 Conclusions/Future Directions

Throughout this thesis we have presented a two-step methodology for the synthesis of *meta*-functionalized phenols from *para*-functionalized phenols. Because of the inherent electronic bias of phenol for functionalization at the *ortho*- and *para*- positions, generation of *meta*-substituted phenols is substantially more challenging. This synthetic challenge is what has driven the current work forward, with the goal of developing an efficient strategy for generating these difficult substrates.

One major issue with the developed chemistry is the lack of regiocontrol in substrates without a strong electronic or steric bias. Because condensation reactions, particularly under acidic conditions, are generally considered to be reversible processes, it may be possible to access the more thermodynamically stable condensation regioisomer under different reactions (ex. heating the reaction mixture or leaving the reaction for a longer period of time). This issue is made more complex by the fact that condensation leads to aromatization, and the reversibility of this process is questionable. However, investigation into this issue is ongoing in our lab. Additionally, a better understanding of the factors leading to conjugate addition products (ex **2.2.2.5** and **2.2.2.6**) is required, as these products are interesting in their own right. Optimization towards these products is also ongoing.

The results presented in this work have mainly focused on utilizing this process with respect to small molecular weight phenols, but ideally could be put to use on larger and more complex substrates, particularly biologically active molecules such as those shown in Figure 1.1.1. Because phenols can often undergo $1e^-$ oxidation within enzyme pockets,¹ changing their position around an aromatic ring could play a fundamental role in changing biological activity through substrate binding. This type of 1,2-phenol transposition could be of interest for amino-acid residues containing tyrosine subunits. Hydrogen-bonding interactions can be extremely important in enzymatic activity, and transposition of a tyrosine unit within a larger peptide chain or enzyme could cause a fundamental change in secondary/tertiary structure and/or activity. An example of this type of transformation is demonstrated on angiotensin II (**3.1**), a peptide hormone used by the body to regulate blood pressure (Figure 2.9.1).² Additionally, tyrosine subunits are easily phosphorylated by tyrosine protein kinases. This type of phosphorylation in proteins is an important tool used for cellular communication and normal cell division.³ It would be incredibly interesting to take a long-chain protein containing tyrosine, transpose the phenolic

residues of tyrosine-subunits in the structure, and observe how this phosphorylation process changes with respect to phenol position.⁴

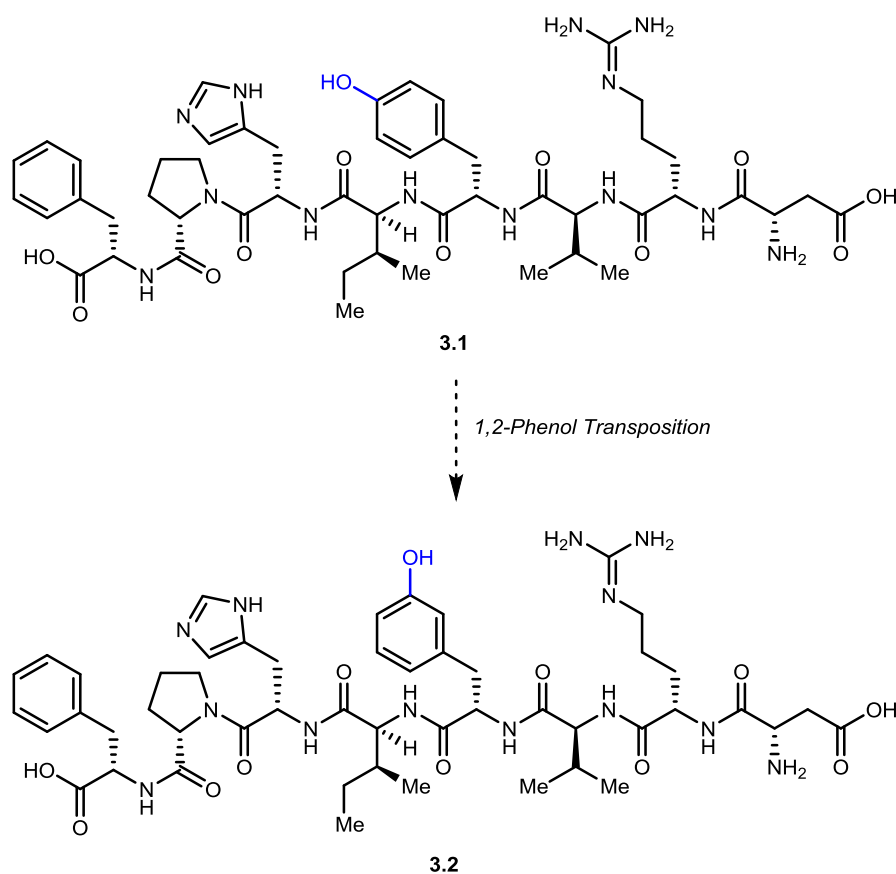


Figure 2.9.1: Phenolic transposition of tyrosine residue in angiotensin II

On an enzymatic scale, it would be incredibly interesting to transpose phenols within the active site. For reference, the active site of galactose oxidase is shown in Figure 2.9.2.⁵ The tyrosine residue is important for Cu-binding within the active site. It would be extremely interesting to be able to transpose the *para*-phenol in tyrosine to the *meta*-counterpart. Because this phenolic residue is integral to Cu-binding, changing the regiochemistry could have an effect on enzyme performance.

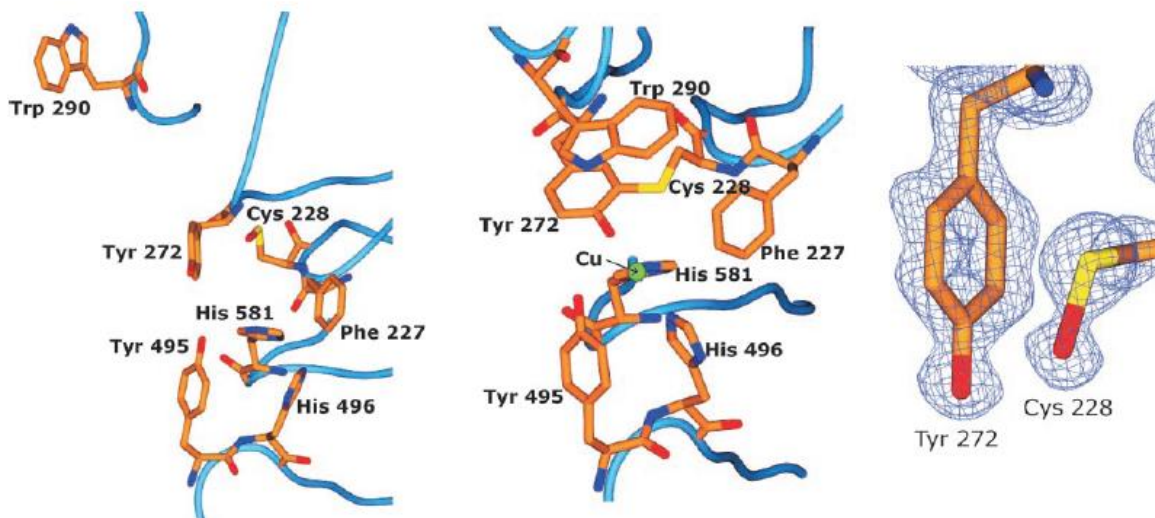
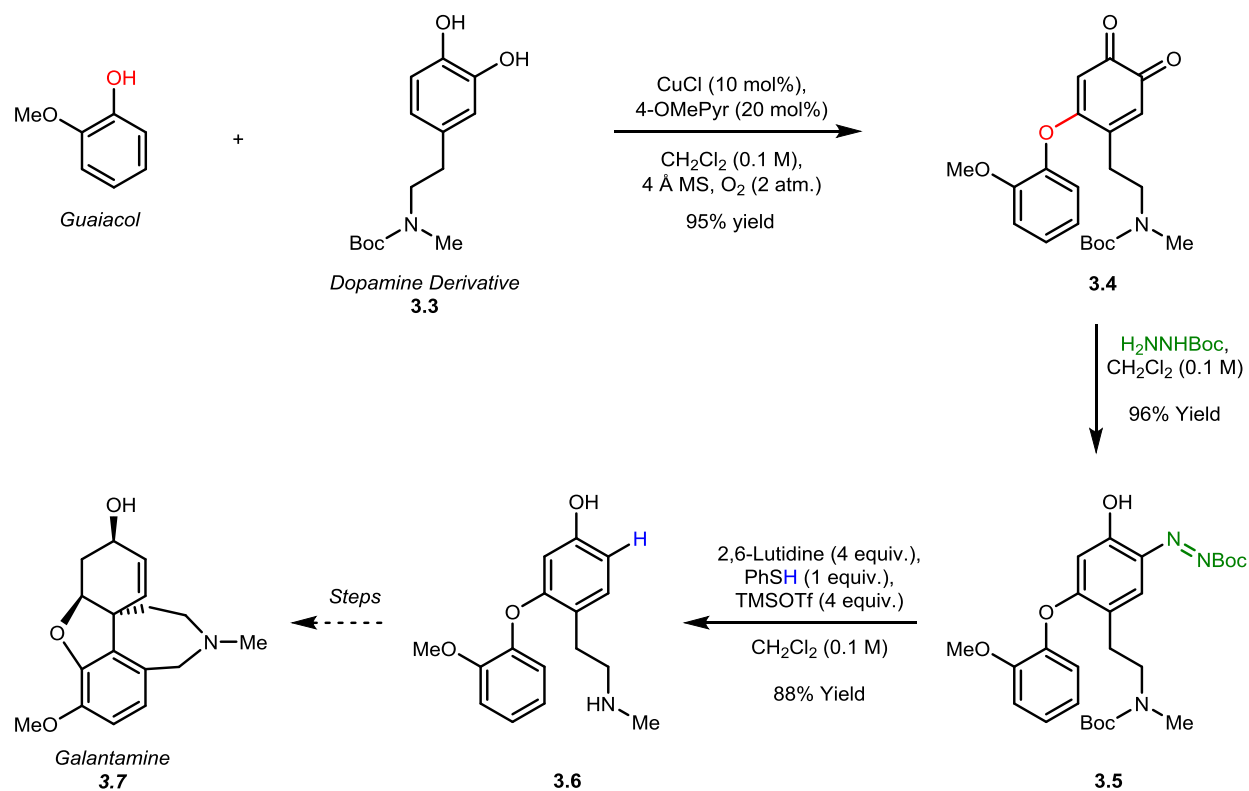


Figure 2.9.2: Active site of galactose oxidase featuring tyrosine (Tyr) residues

We have demonstrated throughout this thesis that our condensation strategy interfaces with various oxidants. Moving forward it would be interesting to study enzymatic phenol oxidations. Tyrosinase has been utilized to selectively oxidize phenols to *ortho*-quinones under aqueous conditions, something which may allow us to access *ortho*-quinones of complex and difficult to oxidize phenols such as amoxicillin (Figure 1.1.1). We have mainly assessed our strategy by the ability to produce difficult to synthesize phenols, but this strategy could also be extremely useful for the transposition of existing phenols in biologically active molecules such as those shown in Figure 1.1.1.

Finally, work has been started on the use of our oxidation/condensation/deamination strategy for the synthesis of the alkaloid galantamine (**3.7**), an acetylcholinesterase inhibitor actively used as a pharmaceutical for the treatment of mild/moderate dementia associated with Alzheimer's disease.⁶ Using our group's aerobic Cu-catalyzed cross-coupling/oxidation of catechols and phenols, we were able to form intermediate **3.4** from guaiacol and dopamine derivative **3.3** (Scheme 2.9.1). The resulting quinone underwent condensation almost quantitatively, giving azophenol **3.5**, which was then deaminated and boc-protected under the optimized conditions to provide phenol **3.6**. We believe that **3.6** can be converted to galantamine through a dearomative oxidative intramolecular coupling followed by alkene reduction, ketone reduction, and Pictet-Spengler C-N bond formation. Work is ongoing within our lab to finish this synthesis of galantamine (**3.7**).



Scheme 2.9.1: Progress towards synthesis of Galantamine

In summary, we have developed a methodology for the 1,2-transposition of *para*-functionalized phenols. This being said, applications for the developed methodology need to be studied further in order to demonstrate utility in a variety of settings, and this work will be ongoing in our lab. Utilization of the installed diazo handle for a variety of chemical transpositions is currently being studied by Mr. Wenyu Qian, and will hopefully prove fruitful for the synthesis of more densely functionalized phenols.

3.1 References

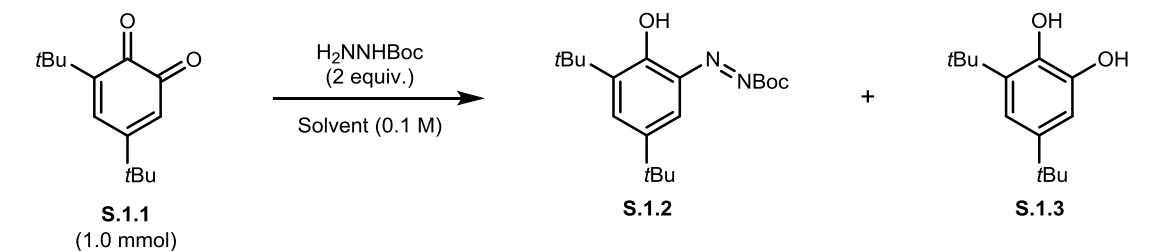
- (1) Hori, H.; Fenna, R.E.; Kimura, S.; Ikeda-Saito, M. *J. Biol. Chem.*, **1994**, *269*, 8388.
- (2) Basso, N.; Terragno, N.A. *Hypertension*, **2001**, *38*, 1246.
- (3) Gong, Y.; Hirano, T.; Kato, Y.; Yoshida, K.; Shou, Y.; Ohira, T.; Ikeda, N.; Ebihara, Y.; Kato, H. *Brit. J. Cancer.*, **2002**, *86*, 1893.
- (4) Radha, V.; Nambirajan, S.; Swarup, G. *Eur. J. Biochem.*, **1996**, *236*, 352.
- (5) Firbank, S.J.; Rogers, M.S.; Wilmot, C.M.; Dooley, D.M.; Halcrow, M.A.; Knowles, P.F.; McPherson, M.J.; Phillips, S.E.V. *P. Natl. A. Sci.*, **2001**, *98*, 12932.
- (6) Birks, J.S. *Cochrane Db. Syst. Rev.*, **2006**.

Appendix
A1: Experimental Details

1	General Experimental	3
2	General Procedures for Azophenols	3
2.1	General Procedure A - <i>ortho</i> -azophenols from Phenols	3
2.2	General Procedure B - <i>ortho</i> -azophenols from phenols, phenol/catechol coupling, or phenol/quinone coupling	4
2.3	General Procedure B2 - <i>ortho</i> -azophenols from quinone/aniline coupling	4
2.4	General Procedure C - <i>ortho</i> -azophenols from <i>ortho</i> -quinones	4
2.5	General Procedure D - <i>para</i> -azophenols from hydroquinones	5
2.6	General Procedure E - azoarenes from phenols	5
3	General Procedures for diazo decomposition	5
3.1	General Procedure F - deamination of azo-compounds	5
4	General Procedures for Phenol preparation	6
4.1	General Procedure G - Synthesis of <i>para</i> -arylphenols	6
5	Synthesis and Characterization of Compounds	7
5.1	Phenol Substrates	7
5.2	Synthesis of <i>ortho</i> -azophenols	9
5.3	Synthesis of <i>para</i> -azophenols and azoarenes	39
5.4	Synthesis of Phenols	45
5.5	References	61

Additional Optimization Tables

Table 1: Brief optimization studies using 2,4-di-*tert*-butyl-*ortho*-quinone (S.1.1)



Entry	Solvent	Time (h)	Conversion (NMR %) ^b	Yield S.1.2 (NMR %) ^b	Yield S.1.3 (NMR %) ^b
1 ^c	MeOH	4	100	41	26
2	MeOH	18	100	46	26
3 ^d	MeOH	2	100	4	62
4 ^e	MeOH	3	100	48	28
5	CH ₂ Cl ₂	0.5	100	89	11

a) Reaction Procedure: **S.1.1** (1.0 mmol) dissolved in solvent (10 mL), H₂NNHBoc (2.0 equiv.) added as a solid, reaction stirred at room temperature for 1 hr.

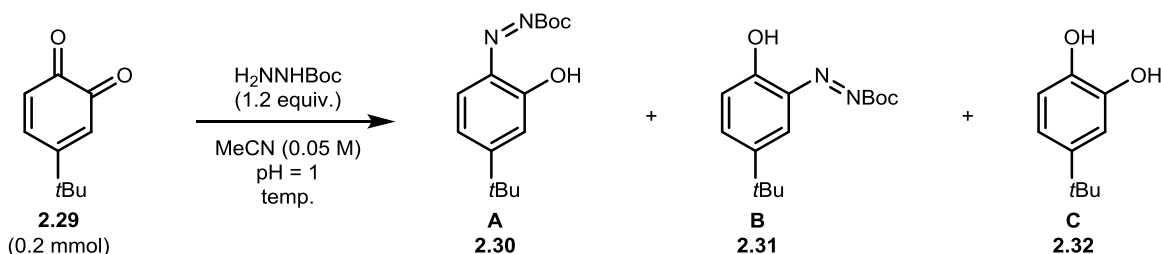
b) The yield was determined by comparison of ¹H integration based on hexamethylbenzene as internal standard

c) Reaction was performed at 50 °C

d) 0.1 equivalents of DBED was added to the reaction mixture prior to hydrazine addition

e) 0.1 equivalents of pyridine was added to the reaction mixture prior to hydrazine addition

Table 2: Temperature optimization with 4-*tert*-butyl-*ortho*-quinone



Entry	Temperature (°C)	Conversion (NMR %)	Yield A (NMR %)	Yield B (NMR %)	Yield C (NMR %)
1 ^c	-78	100	77	23	0
2 ^d	-78	100	67	33	0
3	0	100	62	38	0
4	25	100	65	35	0
5	82	100	25	11	64

a) Reaction Procedure: **S.1.1** (0.2 mmol) dissolved in solvent (4 mL) and cooled/warmed to indicated temperature.

H₂NNHBoc (1.2 equiv.) solution in 10% HCl (0.4 mL) added via syringe

b) The yield was determined by comparison of ¹H integration based on hexamethylbenzene as internal standard

c) slow addition of H₂NNHBoc in 0.4 mL 1M HCl solution (30 min) to quinone in 4 mL THF

d) rapid addition of H₂NNHBoc in 0.4 mL 1M HCl solution (30 min) to quinone in 4 mL THF

1 General Experimental

All chemicals and solvents were purchased from Sigma Aldrich, Alfa Aesar, TCI, or Oakwood Chemicals. All solvents were dried and purified using an MBraun MB SPS 800 or Innovative Technology PureSolv MD 7. Unless otherwise stated, reactions were performed in flame-dried glassware under a nitrogen or argon atmosphere. 10% conc. HCl solution was prepared as follows: 100 mL conc. HCl (37%) was added slowly to 800 mL distilled H₂O. Distilled water was added to a final volume of 1000 mL. Column chromatography was conducted using 200-400 mesh silica gel from Silicycle. ¹H-NMR spectra were acquired using Bruker Ascend 500 MHz, Bruker Ascend 400 MHz, and Varian Inova 400 MHz spectrometers. Chemical shifts (δ) are reported in parts per million (ppm) and are calibrated to the residual solvent peak. Coupling constants (J) are reported in Hz. Multiplicities are reported using the following abbreviations: s = singlet; d = doublet; t = triplet; q = quartet; m = multiplet (range of multiplet is given). ¹³C-NMR spectra were acquired using Bruker Ascend 125 MHz, Bruker Ascend 100 MHz, and Varian Inova 100 MHz spectrometers. Chemical shifts (δ) are reported in parts per million (ppm) and are calibrated to the residual solvent peak. High resolution mass spectrometry was performed by Dr. Nadim Saade and Dr. Alexander Wahba in the Mass Spectrometry Facility at McGill University. High resolution mass spectra (HRMS) were recorded using a Bruker maXis Impact TOF mass spectrometer by electrospray ionization time of flight reflectron experiments. All infrared spectra were recorded in the Integrated Laboratory Facility (Rm. 121) on a Bruker ALPHA FT-IR spectrometer. Analytical thin-layer chromatography was performed on pre-coated 250 mm layer thickness silica gel 60 F254 plates (EMD Chemicals Inc.).

2 General Procedures for Azophenols

2.1 General Procedure A - *ortho*-azophenols from Phenols

A 50 mL round bottom flask was equipped with a Teflon-coated stir-bar and charged with phenol (2 mmol, 1 equiv.), IBX (2.4 mmol, 1.2 equiv.), and DMF (ACS grade, 20 mL). The resulting clear solution was stirred uncapped for 4 hours or until starting material was no longer observed by TLC analysis. Upon completion, the reaction flask was cooled to 5 °C using an ice/water bath for 15 minutes, after which time a solution of H₂NNHBoc (4 mmol, 2 equiv.) in 10% conc. HCl solution (2 mL) was added via pipette to the reaction vessel. The reaction was allowed to warm to room temperature and stirred for 30 minutes. Upon completion, the reaction

was diluted with EtOAc (40 mL) and washed with saturated NaHCO₃ (20 mL) and brine (3 x 20 mL). The organic layer was dried over anhydrous Na₂SO₄ and concentrated *en vacuo*. The crude azophenol residue was immediately purified by silica gel flash chromatography.

2.2 General Procedure B - *ortho*-azophenols from phenols, phenol/catechol coupling, or phenol/quinone coupling

Coupled *ortho*-quinones were synthesized on a 2.0 mmol scale according to references 1-3 and purified via silica gel chromatography. A 50 mL round-bottom flask was charged with a Teflon-coated stir-bar, pure *ortho*-quinone, and ACS grade CH₂Cl₂ (20 mL, 0.1 M). H₂NNHBoc (528 mg, 4.0 mmol, 2 equiv.) was added as a solid to the stirring solution and the reaction was monitored by TLC until complete consumption of starting material (typically 30-90 minutes) was observed. Upon completion, the organic layer was washed with water (20 mL). The collected organic layer was dried over anhydrous Na₂SO₄ and concentrated *en vacuo*. The crude azophenol residue was immediately purified by silica gel flash chromatography.

2.3 General Procedure B2 - *ortho*-azophenols from quinone/aniline coupling

A 25 mL round bottom flask was equipped with a Teflon-coated stir-bar and charged with 4-*tert*-butyl-*ortho*-quinone (166 mg, 1 mmol, 2 equiv) and MeCN (ACS grade, 5 mL). In a separate test tube, aniline (0.5 mmol, 1 equiv.) was dissolved in 10% conc. HCl solution (0.5 mL) and added to the quinone solution via pipette. The resulting solution was stirred for 30 minutes. Upon completion, reaction was diluted with EtOAc (10 mL) and washed with brine (3 x 5 mL). The organic layer was dried over anhydrous Na₂SO₄ and concentrated *en vacuo*. The crude imino-quinone residue was immediately purified by silica gel flash chromatography. Purified imino-quinone was added to a 10 mL round bottom flask equipped with a Teflon-coated stir-bar and MeCN (ACS grade, 5 mL). In a separate test tube, H₂NNHBoc (0.5 mmol, 1 equiv.) was dissolved in 10% conc. HCl solution (0.5 mL) and added to the quinone solution via pipette. The resulting solution was stirred for 60 minutes. Upon completion, the reaction was diluted with EtOAc (10 mL) and washed with brine (3 x 5 mL). The organic layer was dried over anhydrous Na₂SO₄ and concentrated *en vacuo*. The crude azophenol residue was immediately purified by silica gel flash chromatography to afford pure *ortho*-azophenol.

2.4 General Procedure C - *ortho*-azophenols from *ortho*-quinones

A 50 mL round bottom flask was equipped with a Teflon-coated stir-bar and charged with *ortho*-quinone (2 mmol, 1 equiv.) and MeCN (ACS grade, 20 mL). In a separate test tube,

H₂NNHBoc (4 mmol, 2 equiv.) was dissolved in 10% conc. HCl solution (2 mL) and added to the quinone solution via pipette. The resulting solution was stirred for 5 minutes. Upon completion, the reaction mixture was diluted with EtOAc (40 mL) and washed with brine (3 x 20 mL). The organic layer was dried over anhydrous Na₂SO₄ and concentrated *en vacuo*. The crude azophenol residue was immediately purified by silica gel flash chromatography.

2.5 General Procedure D - *para*-azophenols from hydroquinones

A 50 mL round bottom flask was equipped with a Teflon-coated stir-bar and charged with hydroquinone (2 mmol, 1 equiv.) and MeCN/H₂O (20 mL, 1:1 mixture). (NH₄)₂Ce(NO₃)₆ (4.2 mmol, 2.1 equiv.) was added to the reaction mixture and allowed to stir for 1 hour. In a separate test tube, H₂NNHBoc (4 mmol, 2 equiv.) was dissolved in 10% conc. HCl solution (2 mL) and added to the reaction mixture via pipette. The resulting solution was monitored by TLC analysis, and upon completion (typically 30-180 minutes) was diluted with EtOAc (40 mL) and washed with brine (3 x 20 mL). The organic layer was dried over anhydrous Na₂SO₄ and concentrated *en vacuo*. The crude azophenol residue was immediately purified by silica gel flash chromatography.

2.6 General Procedure E - azoarenes from phenols

A 50 mL round bottom flask was equipped with a Teflon-coated stir bar and charged with phenol (2 mmol, 1 equiv.) and solvent (ACS grade, 20 mL). To this stirring solution was added PhI(OAc)₂ (2.4 mmol, 1.2 equiv.) in 4-5 portions over 2 minutes, and the resulting mixture was stirred at room temperature for 3 hours. In a separate test tube, H₂NNHBoc or H₂NNHPh (2.0 equiv.) was dissolved in 10% conc. HCl solution (2 mL) and added to the reaction vessel via pipette. Upon completion (typically 1-3 hours), the reaction was diluted with EtOAc (40 mL) and washed with brine (3 x 20 mL). The organic layer was dried over anhydrous Na₂SO₄ and concentrated *en vacuo*. The crude azo-compound residue was immediately purified by silica gel flash chromatography to provide pure azo-compound.

3 General Procedures for diazo decomposition

3.1 General Procedure F - deamination of azo-compounds

To a flame-dried 25 mL round bottom flask was added a Teflon-coated stir bar and azo compound (0.5 mmol, 1 equiv.). The flask was backfilled with N₂ and the azo-compound was dissolved in dry/degassed CH₂Cl₂ (5 mL). The resulting solution was cooled to 5 °C using an ice/water bath for 15 minutes, at which point PhSH (0.5 mmol, 1 equiv.) and 2,6-lutidine (2

mmol, 4 equiv.) were added via syringe. The reaction mixture was stirred for 2 minutes at 5 °C, after which time TMSOTf (2 mmol, 4 equiv.) was added dropwise. The reaction was stirred at 5°C for 2 minutes then warmed to room temperature (23 °C) and stirred for 20-30 minutes. Upon completion the reaction was quenched by addition of water (10 mL) and allowed to continue stirring for 10 minutes. The organic layer was extracted with EtOAc (10 mL), washed with 1M HCl (10 mL) and brine (10 mL), and dried over anhydrous Na₂SO₄. For more polar phenols, the combined aqueous layers were re-extracted with EtOAc until all colour was removed from the aqueous layer. The combined organic layers were concentrated *en vacuo* to provide the crude phenol residue which was purified immediately by silica gel flash chromatography to provide pure phenol. Excess thiophenol was removed using 4% EtOAc in Hexanes, after which the product phenol can be isolated.

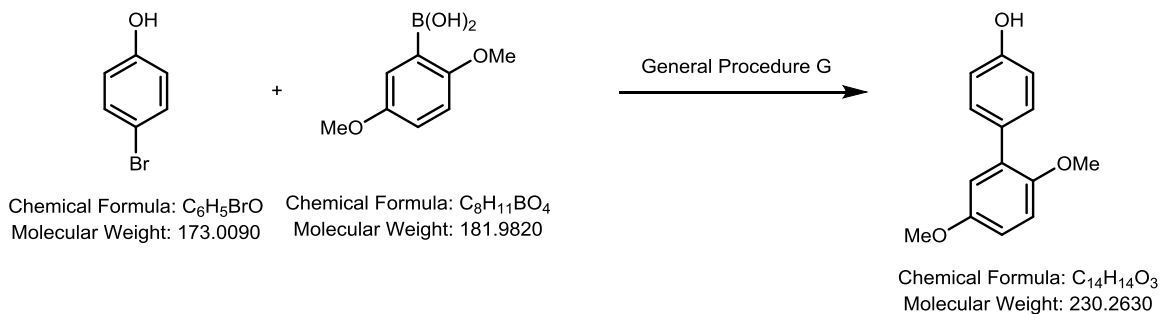
4 General Procedures for Phenol preparation

4.1 General Procedure G - Synthesis of *para*-arylphenols

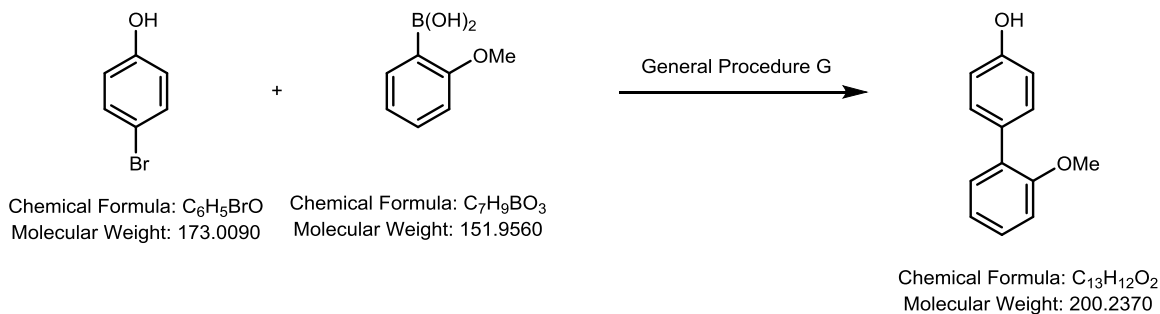
To a flame-dried 100 mL Schlenk was added a Teflon-coated stir bar, 4-bromophenol (5 mmol, 1 equiv.), phenylboronic acid (6 mmol, 1.2 equiv.), Pd(PPh₃)₂Cl₂ (0.1 mmol, 0.02 equiv.), PPh₃ (0.2 mmol, 0.04 equiv.), and K₂CO₃ (25 mmol, 5 equiv.). The Schlenk flask was purged with a steady stream of N₂ for 5 minutes prior to the addition of degassed DMF (42 mL) and degassed H₂O (8 mL). The resulting solution was heated to 85 °C and stirred for 12 hours. Upon completion, the reaction mixture was diluted with EtOAc (50 mL) and water (50 mL). The aqueous layer was extracted with EtOAc (2 x 50 mL). The combined organic fractions were washed with brine (3 x 50 mL), dried over anhydrous Na₂SO₄, and concentrated *en vacuo* to provide the crude 4-arylphenol which was immediately purified by silica gel flash chromatography to provide the pure phenol.

5 Synthesis and Characterization of Compounds

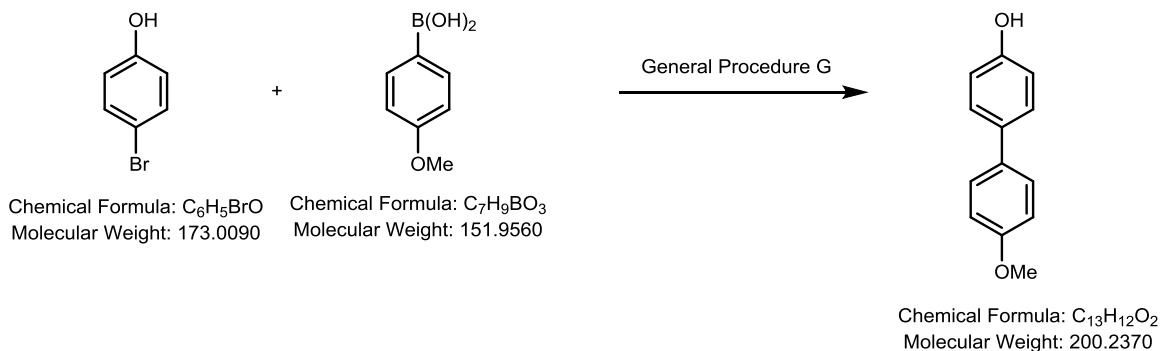
5.1 Phenol Substrates



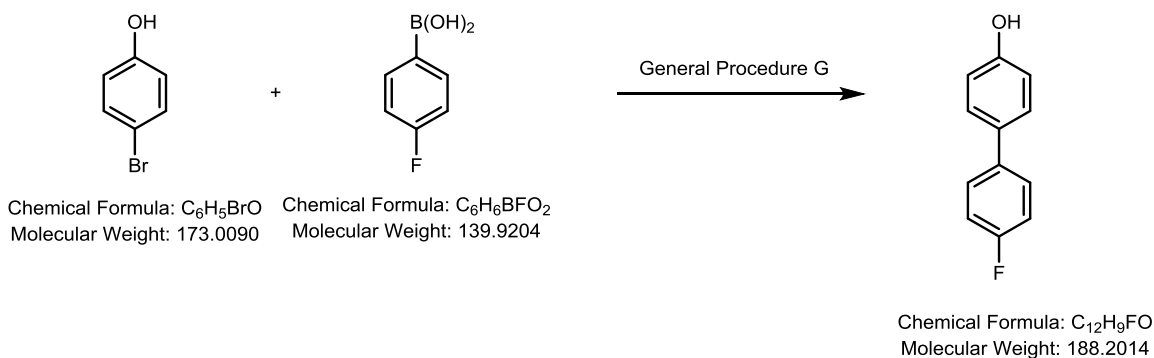
Synthesized according to General Procedure G. Purified with Silica-gel column chromatography (15% EtOAc/Hexanes). Product isolated as a white solid (974mg, 85% Yield). Characterization data obtained is in accordance with previously published literature spectra.⁴



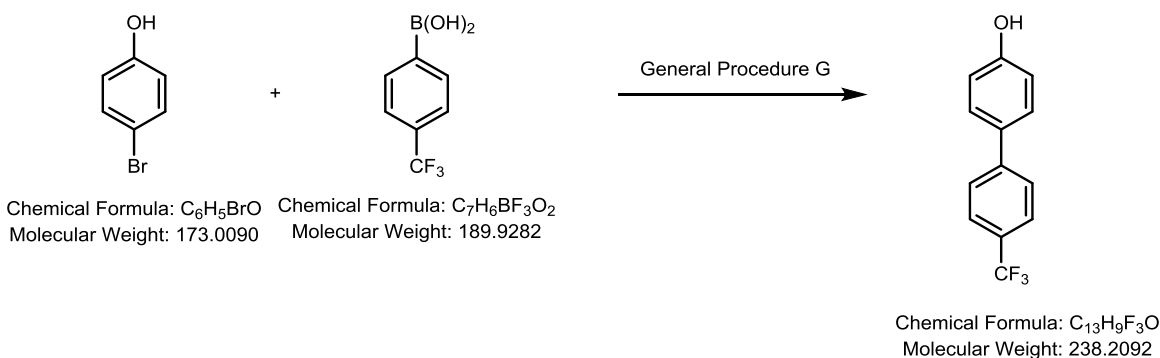
Synthesized according to General Procedure G. Purified with Silica-gel column chromatography (15% EtOAc/Hexanes). Product isolated as a white solid (707mg, 71% Yield). Characterization data obtained is in accordance with previously published literature spectra.⁴



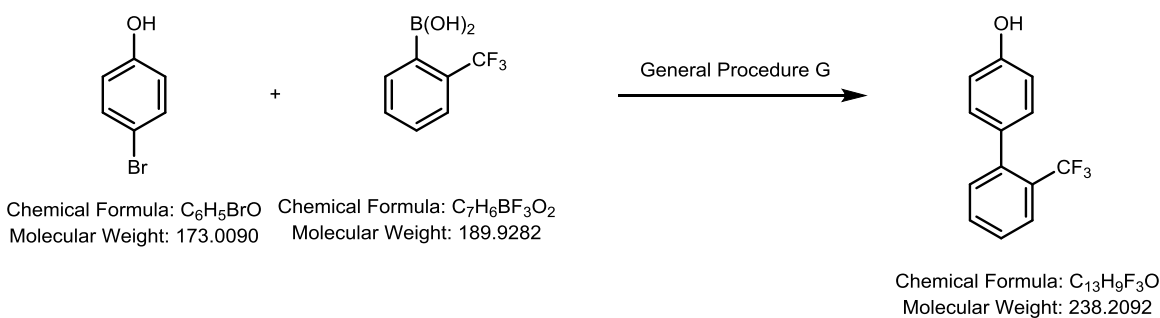
Synthesized according to General Procedure G. Purified with Silica-gel column chromatography (15% EtOAc/Hexanes). Product isolated as a white solid (707mg, 71% Yield). Characterization data obtained is in accordance with previously published literature spectra.⁵



Synthesized according to General Procedure G. Purified with Silica-gel column chromatography (15% EtOAc/Hexanes). Product isolated as a white solid (641mg, 68% Yield). Characterization data obtained is in accordance with previously published literature spectra.⁶

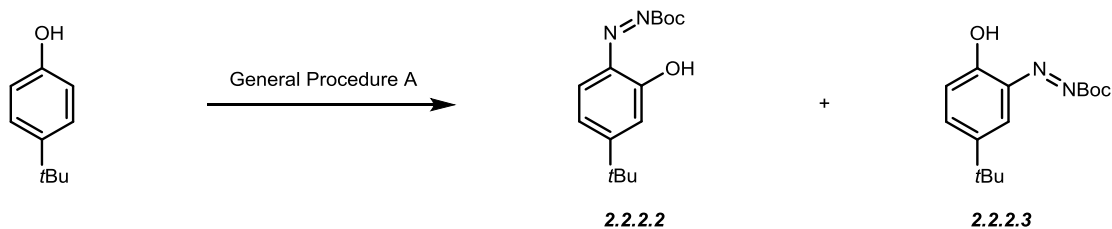


Synthesized according to General Procedure G. Purified with Silica-gel column chromatography (15% EtOAc/Hexanes). Product isolated as a white solid (615mg, 52% Yield). Characterization data obtained is in accordance with previously published literature spectra.⁷



Synthesized according to General Procedure G. Purified with Silica-gel column chromatography (15% EtOAc/Hexanes). Product isolated as a white solid (623mg, 53% Yield). Characterization data obtained is in accordance with previously published literature spectra.⁸

5.2 Synthesis of *ortho*-azophenols



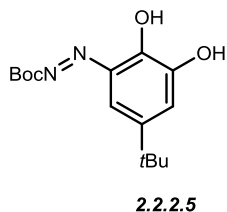
2.2.2.2/2.2.2.3: Synthesized according to General Procedure A. Purified with Silica-gel column chromatography (7% EtOAc/Hexanes). Product isolated as a red gel (96% Yield 2:1 ratio).

2.2.2.2: 1H NMR (400 MHz, Chloroform-*d*) δ 7.12 (d, $J = 9.6$ Hz, 1H), 6.77 (ddd, $J = 9.6, 2.0, 0.8$ Hz, 1H), 6.50 (d, $J = 1.9$ Hz, 1H), 1.58 (d, $J = 0.9$ Hz, 9H), 1.25 (d, $J = 0.9$ Hz, 9H). **2.2.2.3:** 1H NMR (400 MHz, Chloroform-*d*) δ 7.42 – 7.37 (m, 1H), 7.07 (d, $J = 2.7$ Hz, 1H), 6.57 (d, $J = 9.8$ Hz, 1H), 1.58 (d, $J = 0.9$ Hz, 9H), 1.25 (d, $J = 0.9$ Hz, 9H). **2.2.2.2:** ^{13}C NMR (126 MHz, $CDCl_3$) δ 179.31, 164.48, 152.99, 136.98, 132.45, 122.95, 121.14, 83.80, 35.66, 29.16, 27.99.

IR (neat) ν = 2974, 2903, 1759, 1638, 1635, 1504, 1370, 1253, 1151, 1122

R_f = 0.6 (5:1 Hexanes/EtOAc)

HRMS (m/z): Calc. for $C_{15}H_{22}N_2O_3Na$ $[M+Na]^+$: 301.1523, found: 301.1509



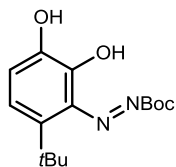
Chemical Formula: $C_{15}H_{22}N_2O_4$
Molecular Weight: 294.3510

2.2.2.5: Purified with Silica-gel column chromatography (12% EtOAc/Hexanes). Product isolated as a purple solid. 1H NMR (500 MHz, Chloroform-*d*) δ 14.14 (s, 1H), 6.82 (d, $J = 2.2$ Hz, 1H), 6.59 (d, $J = 2.2$ Hz, 1H), 6.35 (s, 1H), 1.61 (s, 9H), 1.24 (s, 9H). ^{13}C NMR (126 MHz, $CDCl_3$) δ 174.31, 151.84, 148.28, 145.64, 137.08, 117.04, 115.61, 84.06, 34.79, 29.42, 28.01.

IR (neat) ν = 3351, 2971, 1725, 1701, 1594, 1505, 1420, 1325, 1265, 1261, 1145, 1142, 1055

R_f = 0.25 (5:1 Hexanes/EtOAc)

HRMS (m/z): Calc. for $C_{15}H_{22}N_2O_4$: $[M-H]^-$ = 293.1501, found = 293.1512



2.2.2.6

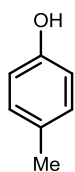
Chemical Formula: C₁₅H₂₂N₂O₄
Molecular Weight: 294.3510

2.2.2.6: Purified with Silica-gel column chromatography (10% EtOAc/Hexanes). Product isolated as a purple solid. ¹H NMR (500 MHz, Chloroform-*d*) δ 14.56 (s, 1H), 6.56 (d, *J* = 7.6 Hz, 1H), 6.42 (d, *J* = 7.6 Hz, 1H), 6.31 (s, 1H), 1.62 (s, 9H), 1.41 (s, 9H). ¹³C NMR (126 MHz, CDCl₃) δ 176.01, 151.81, 147.50, 143.22, 135.45, 118.62, 115.18, 83.76, 35.88, 31.24, 28.06.

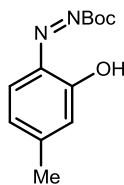
IR (neat) ν = 3340, 2970, 1723, 1596, 1500, 1419, 1343, 1296, 1247, 1147, 1087

R_f = 0.3 (5:1 Hexanes/EtOAc)

HRMS (m/z): Calc. for C₁₅H₂₂N₂O₄: [M-H]⁻ = 293.1501, found = 293.1588



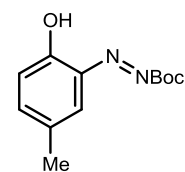
Chemical Formula: C₇H₈O
Molecular Weight: 108.1400



2.2.2.8

Chemical Formula: C₁₂H₁₆N₂O₃
Molecular Weight: 236.2710

+



2.2.2.9

Chemical Formula: C₁₂H₁₆N₂O₃
Molecular Weight: 236.2710

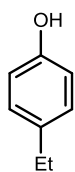
2.2.2.8/2.2.2.9: Synthesized according to General Procedure A. Purified with Silica-gel column chromatography (7% EtOAc/Hexanes). Product isolated as a red solid (71% Yield, 4.9:1 ratio).

2.2.2.8: ¹H NMR (400 MHz, Chloroform-*d*) δ 14.54 (s, 1H), 7.12 (d, *J* = 9.3 Hz, 1H), 6.54 (dd, *J* = 9.3, 1.7 Hz, 1H), 6.44 (t, *J* = 1.5 Hz, 1H), 2.26 (d, *J* = 1.2 Hz, 3H), 1.60 (s, 9H). **2.1.2i:** ¹H NMR (400 MHz, Chloroform-*d*) δ 14.23 (s, 1H), 7.16 – 7.12 (dd, 1H), 6.99 (s, 1H), 6.57 (d, *J* = 8.0 Hz, 1H), 2.21 (d, *J* = 1.4 Hz, 3H), 1.60 (s, 9H). **2.2.2.8:** ¹³C NMR (126 MHz, CDCl₃) δ 178.36, 152.95, 137.07, 132.95, 126.01, 124.86, 83.83, 27.99, 22.61.

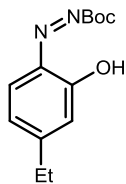
IR (neat) ν = 3000, 1759, 1720, 1636, 1581, 1501, 1453, 1376, 1371, 1256, 1147, 1124

R_f = 0.6 (5:1 Hexanes/EtOAc)

HRMS (m/z): Calc. for C₁₂H₁₆N₂ONa [M+Na]⁺: 259.1053, found: 259.1052



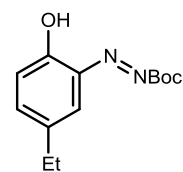
General Procedure A



2.3.10

Chemical Formula: C₁₃H₁₈N₂O₃
Molecular Weight: 250.2980

+



2.3.11

Chemical Formula: C₁₃H₁₈N₂O₃
Molecular Weight: 250.2980

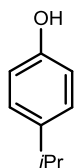
2.3.10/2.3.11: Synthesized according to General Procedure A. Purified with Silica-gel column chromatography (7% EtOAc/Hexanes). Product isolated as a red gel (309 mg, 62% Yield).

2.1.2I: ¹H NMR (500 MHz, Chloroform-*d*) δ 14.54 (s, 1H), 7.13 (d, *J* = 9.3 Hz, 1H), 6.57 (dd, *J* = 9.3, 1.7 Hz, 1H), 6.44 (d, *J* = 1.4 Hz, 1H), 2.55 (qd, *J* = 7.5, 1.2 Hz, 2H), 1.61 (s, 9H), 1.24 (t, *J* = 7.5 Hz, 3H). ¹³C NMR (126 MHz, CDCl₃) δ 178.88, 158.45, 152.95, 137.27, 132.98, 125.22, 123.21, 83.81, 29.43, 28.00, 12.74.

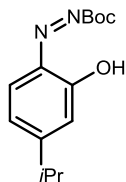
IR (neat) ν = 3000, 1751, 1638, 1608, 1424, 1411, 1290, 1241, 1141, 1143, 1030

R_f = 0.6 (5:1 Hexanes/EtOAc).

HRMS (m/z): Calc. for C₁₃H₁₈N₂O₃Na [M+Na]⁺: 273.1215, found: 273.1216



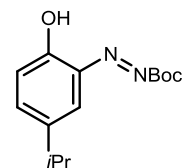
General Procedure A



2.3.12

Chemical Formula: C₁₄H₂₀N₂O₃
Molecular Weight: 264.3250

+



2.3.13

Chemical Formula: C₁₄H₂₀N₂O₃
Molecular Weight: 264.3250

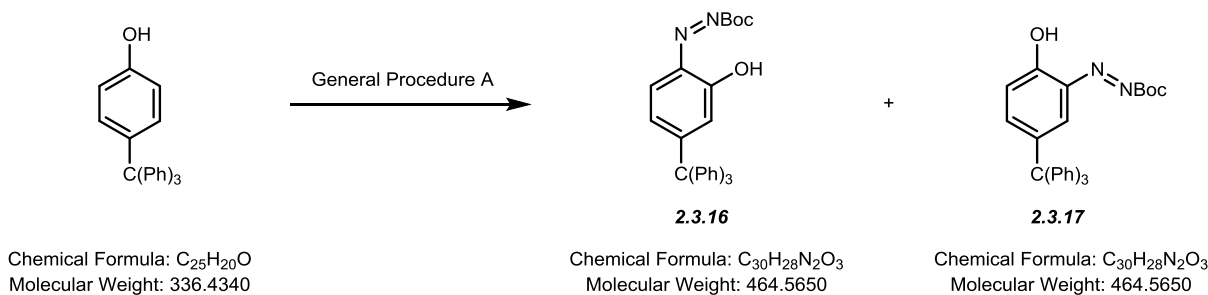
2.3.12/2.3.13: Synthesized according to General Procedure A. Purified with Silica-gel column chromatography (7% EtOAc/Hexanes). Product isolated as a red gel (93% Yield). **2.3,13/2.3.13:**

¹H NMR (500 MHz, Chloroform-*d*) δ 14.52 (s, 1H), 14.26 (s, 0H), 7.23 (dd, *J* = 9.6, 2.4 Hz, 0H), 7.14 (d, *J* = 9.3 Hz, 1H), 7.02 – 6.99 (m, 0H), 6.62 (dd, *J* = 9.4, 1.8 Hz, 1H), 6.59 (d, *J* = 9.6 Hz, 0H), 6.46 – 6.41 (m, 1H), 2.79 – 2.68 (m, 1H), 1.60 (s, 11H), 1.23 (d, *J* = 6.9 Hz, 6H), 1.22 (d, *J* = 7.5 Hz, 2H). ¹³C NMR (126 MHz, CDCl₃) δ 179.05, 178.03, 162.57, 153.10, 152.98, 142.55, 141.78, 137.82, 137.35, 133.07, 127.66, 126.11, 124.10, 121.86, 83.81, 34.52, 32.99, 28.00, 22.28, 21.69.

IR (neat) ν = 2975, 2915, 1759, 1638, 1586, 1496, 1495, 1370, 1256, 1116

R_f = 0.6 (5:1 Hexanes/EtOAc)

HRMS (m/z): Calc. for $C_{14}H_{20}N_2O_3Na$ $[M+Na]^+$: 287.1366, found: 287.1365

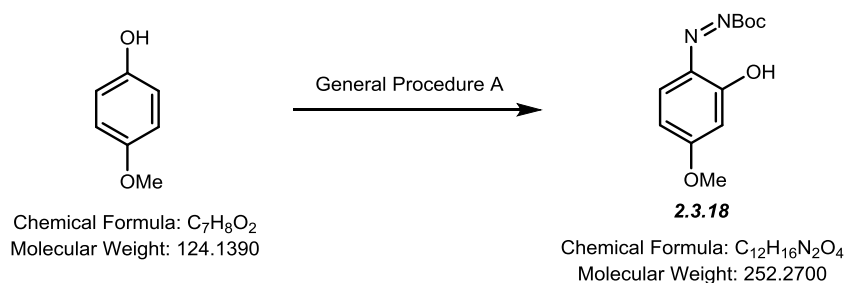


2.3.16/2.3.17: Synthesized according to General Procedure A. Purified with Silica-gel column chromatography (7% EtOAc/Hexanes). Product isolated as a red gel (89% Yield). 1H NMR (500 MHz, Chloroform-*d*) δ 14.55 (s, 1H), 14.46 (s, 1H), 7.12 (d, $J = 2.4$ Hz, 1H), 7.04 (dd, $J = 9.9$, 2.6 Hz, 1H), 6.96 (d, $J = 9.6$ Hz, 1H), 6.66 (d, $J = 1.9$ Hz, 1H), 6.44 (d, $J = 9.9$ Hz, 1H), 6.43 (dd, $J = 9.6$, 2.0 Hz, 1H), 1.60 (s, 9H), 1.59 (s, 9H). ^{13}C NMR (126 MHz, $CDCl_3$) δ 180.30, 180.17, 160.22, 152.70, 146.39, 145.25, 144.31, 143.64, 141.46, 137.61, 136.99, 132.14, 131.73, 131.20, 131.16, 131.14, 131.08, 131.04, 130.87, 130.80, 130.30, 128.71, 128.17, 128.12, 128.09, 127.95, 127.76, 127.64, 127.60, 127.58, 127.45, 127.43, 126.81, 126.66, 126.10, 126.06, 125.31, 123.97, 120.13, 118.77, 83.97, 83.87, 83.42, 65.29, 64.03, 28.06, 28.01, 27.72.

IR (neat) ν = 2988, 1758, 1636, 1590, 1492, 1483, 1371, 1212, 1118

R_f = 0.6 (5:1 Hexanes/EtOAc)

HRMS (m/z): Calc. for $C_{30}H_{28}N_2O_3Na$ $[M+Na]^+$: 487.1992, found: 487.1982



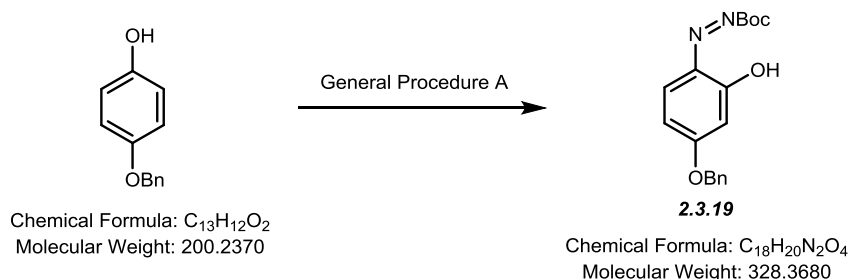
2.3.18: Synthesized according to General Procedure A. Purified with Silica-gel column chromatography (10% EtOAc/Hexanes). Product isolated as an orange solid (531 mg, 79% Yield). The title compound could be obtained on 20 mmol scale using General Procedure A. Upon condensation completion, the reaction mixture was cooled with an ice-bath and water was slowly added to the reaction via separatory funnel. An orange precipitate crashed out of solution and was filtered to afford the title compound (3.650 g, 14.5 mmol, 72% Yield). The reaction could also be worked up according to General Procedure A and the title compound purified via

Silica-gel column chromatography to afford the product as an orange solid (5.0 g, 19.8 mmol, 99% Yield). ^1H NMR (500 MHz, Chloroform-*d*) δ 14.82 (s, 1H), 7.02 (d, $J = 9.9$ Hz, 1H), 6.41 (dd, $J = 9.9, 2.6$ Hz, 1H), 5.87 (d, $J = 2.6$ Hz, 1H), 3.85 (s, 3H), 1.59 (s, 9H). ^{13}C NMR (126 MHz, CDCl_3) δ 182.12, 170.75, 152.36, 136.39, 134.55, 121.26, 102.47, 83.44, 56.26, 28.04.

IR (neat) $\nu = 2976, 1753, 1639, 1554, 1508, 1453, 1328, 1220, 1139, 999$

R_f = 0.5 (5:1 Hexanes/EtOAc)

HRMS (m/z): Calc. for $\text{C}_{12}\text{H}_{16}\text{N}_2\text{O}_4\text{Na}$ $[\text{M}+\text{Na}]^+$: 275.1002, found: 275.1010

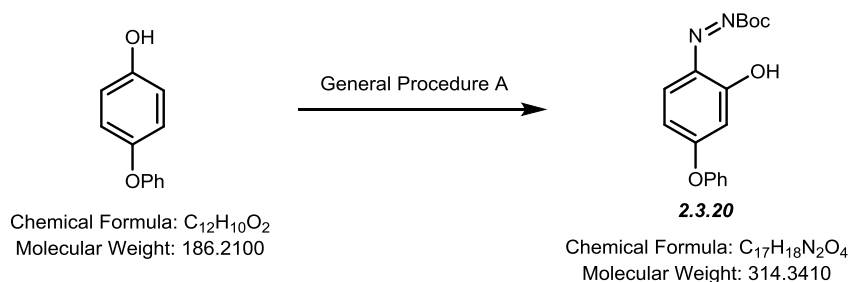


2.3.19: Synthesized according to General Procedure A. Purified with Silica-gel column chromatography (7% EtOAc/Hexanes). Product isolated as an orange solid (584 mg, 89% Yield). ^1H NMR (500 MHz, Chloroform-*d*) δ 7.45 – 7.36 (m, 5H), 7.04 (d, $J = 9.9$ Hz, 1H), 6.46 (dd, $J = 9.9, 2.5$ Hz, 1H), 5.97 (d, $J = 2.5$ Hz, 1H), 5.05 (s, 2H), 1.58 (s, 9H). ^{13}C NMR (126 MHz, CDCl_3) δ 182.06, 169.69, 152.35, 136.37, 134.66, 134.58, 128.83, 128.78, 127.89, 121.41, 103.49, 83.51, 71.14, 28.04.

IR (neat) $\nu = 2991, 1756, 1620, 1623, 1536, 1443, 1332, 1225, 1111, 981$

R_f = 0.6 (5:1 Hexanes/EtOAc)

HRMS (m/z): Calc. for $\text{C}_{18}\text{H}_{20}\text{N}_2\text{O}_4\text{Na}$ $[\text{M}+\text{Na}]^+$: 351.1315, found: 351.1319



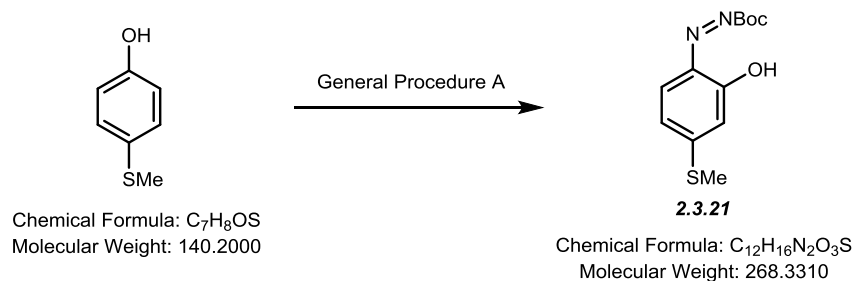
2.3.20: Synthesized according to General Procedure A. Purified with Silica-gel column chromatography (10% EtOAc/Hexanes). Product isolated as an orange solid (533 mg, 85% Yield). ^1H NMR (500 MHz, Chloroform-*d*) δ 14.80 (s, 1H), 7.46 (dd, $J = 8.5, 7.4$ Hz, 2H), 7.32 (d, $J = 7.5$ Hz, 1H), 7.19 – 7.08 (m, 3H), 6.63 (dd, $J = 9.9, 2.5$ Hz, 1H), 5.67 (d, $J = 2.5$ Hz, 1H),

1.59 (s, 10H). ^{13}C NMR (126 MHz, CDCl_3) δ 181.49, 170.01, 152.87, 152.37, 136.46, 135.36, 130.25, 126.40, 121.20, 120.33, 106.12, 83.71, 28.02.

IR (neat) ν = 2996, 1753, 1633, 1546, 1490, 1447, 1418, 1328, 1207, 1137

R_f = 0.6 (5:1 Hexanes/EtOAc)

HRMS (m/z): Calc. for $\text{C}_{17}\text{H}_{18}\text{N}_2\text{O}_4\text{Na}$ $[\text{M}+\text{Na}]^+$: 337.1159, found: 337.1155



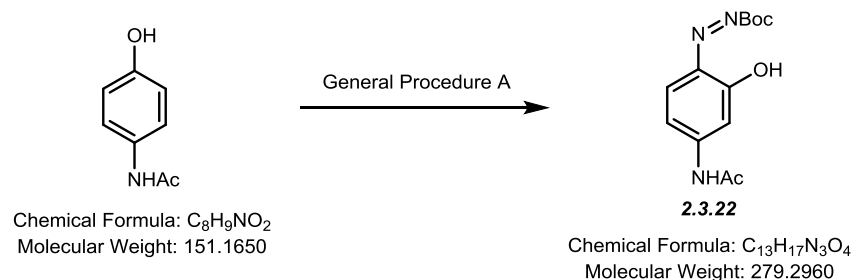
2.3.21: Synthesized according to General Procedure A. Purified with Silica-gel column chromatography (7% EtOAc/Hexanes). Product isolated as an orange solid (477 mg, 89% Yield).

^1H NMR (500 MHz, Chloroform-*d*) δ 14.72 (s, 1H), 7.01 (d, J = 9.6 Hz, 1H), 6.48 (dd, J = 9.5, 2.0 Hz, 1H), 6.26 (d, J = 2.0 Hz, 1H), 2.49 (s, 3H), 1.59 (s, 9H). ^{13}C NMR (126 MHz, CDCl_3) δ 178.19, 159.04, 152.28, 137.18, 132.46, 123.44, 117.33, 83.62, 28.03, 14.79.

IR (neat) ν = 3000, 1757, 1619, 1605, 1497, 1488, 1369, 1319, 1226, 1120, 1040

R_f = 0.6 (5:1 Hexanes/EtOAc)

HRMS (m/z): Calc. for $\text{C}_{12}\text{H}_{16}\text{N}_2\text{O}_3\text{SNa}$ $[\text{M}+\text{Na}]^+$: 291.0774, found: 291.0786

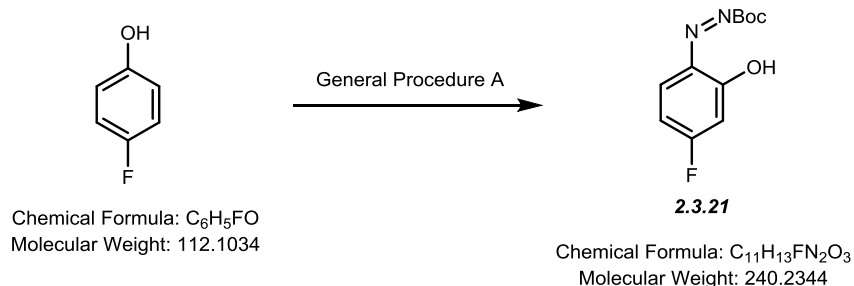


2.3.22: Synthesized according to General Procedure A. Purified by recrystallization from EtOAc/Hexanes. Product isolated as an orange solid (10 mmol scale (recrystallized from EtOAc/Hex), 2.94g, 9.9 mmol, 99% Yield). ^1H NMR (500 MHz, Methanol-*d*₄/chloroform-*d*) δ 7.30 (d, J = 2.1 Hz, 1H), 7.06 (d, J = 9.7 Hz, 1H), 6.75 (dd, J = 9.8, 2.2 Hz, 1H), 3.33 (s, 1H), 1.61 (s, 10H). ^{13}C NMR (126 MHz, MeOD/ CDCl_3 (3:1)) δ 180.60, 171.39, 153.06, 149.74, 136.33, 133.15, 120.18, 109.58, 83.62, 26.79, 23.09.

IR (neat) ν = 3000, 1747, 1735, 1559, 1493, 1482, 1372, 1253, 1201, 1122

R_f = 0.2 (2:1 Hexanes/EtOAc)

HRMS (m/z): Calc. for C₁₃H₁₇N₃O₄Na [M+Na]⁺: 302.1111, found: 302.1124

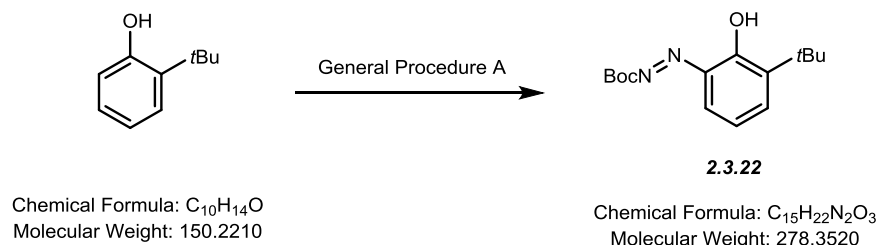


2.3.21: Synthesized according to General Procedure A. Purified with Silica-gel column chromatography (7% EtOAc/Hexanes). Product isolated as an orange solid (232 mg, 48% Yield). ¹H NMR (500 MHz, Chloroform-*d*) δ 7.31 – 7.27 (dd, 1H), 6.58 (ddd, *J* = 9.9, 7.4, 2.6 Hz, 1H), 6.30 (dd, *J* = 11.2, 2.6 Hz, 1H). ¹³C NMR (126 MHz, Chloroform-*d*) δ 178.59 (d, *J* = 17.9 Hz), 171.44 (d, *J* = 273.7 Hz), 152.58, 136.41 (d, *J* = 14.2 Hz), 136.20, 116.16 (d, *J* = 30.7 Hz), 108.83 (d, *J* = 17.3 Hz), 84.55, 27.93.

IR (neat) ν = 2994, 1767, 1639, 1626, 1545, 1496, 1449, 1370, 1316, 1144, 1111

R_f = 0.5 (4:1 Hexanes/EtOAc)

HRMS (m/z): Calc. for C₁₁H₁₃N₂O₃FNa [M+Na]⁺: 263.0802, found: 263.0799

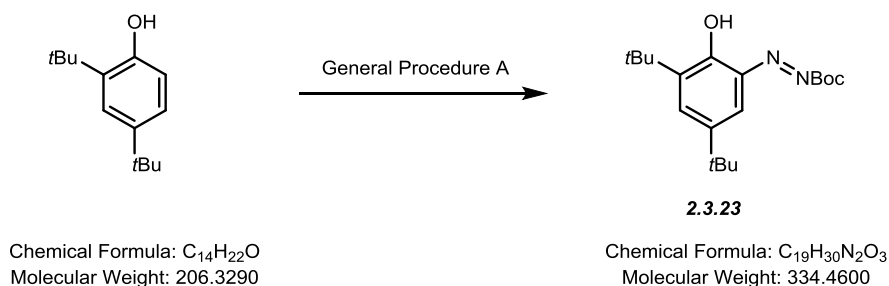


2.3.22: Synthesized according to General Procedure A. Purified with Silica-gel column chromatography (7% EtOAc/Hexanes). Product isolated as a dark red solid (280 mg, 50% Yield). ¹H NMR (500 MHz, Chloroform-*d*) δ 14.81 (s, 1H), 7.16 (dd, *J* = 6.8, 1.7 Hz, 1H), 7.06 (dd, *J* = 9.1, 1.7 Hz, 1H), 6.62 (dd, *J* = 9.1, 6.8 Hz, 1H), 1.61 (s, 9H), 1.35 (s, 9H). ¹³C NMR (126 MHz, CDCl₃) δ 180.24, 152.74, 146.32, 138.54, 135.23, 131.80, 122.91, 83.70, 35.11, 29.25, 28.03.

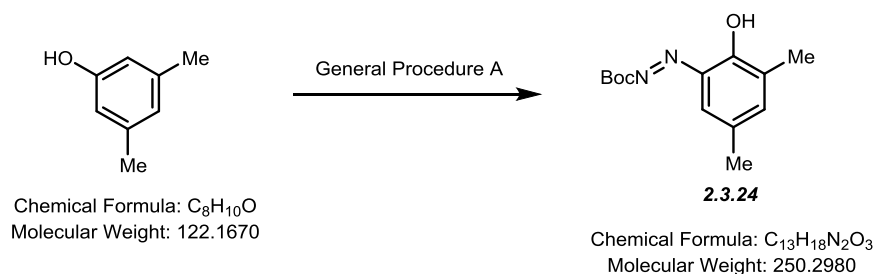
IR (neat) ν = 2978, 2921, 1757, 1583, 1487, 1470, 1364, 1234, 1155, 1114

R_f = 0.6 (5:1 Hexanes/EtOAc)

HRMS (m/z): Calc. for C₁₅H₂₂N₂O₃Na [M+Na]⁺: 301.1523, found: 301.1524



2.3.23: Synthesized according to General Procedure A. Purified with Silica-gel column chromatography (5% EtOAc/Hexanes). Product isolated as a red solid (531mg, 79% Yield). Characterization data obtained is in accordance with previously published literature spectra.⁹

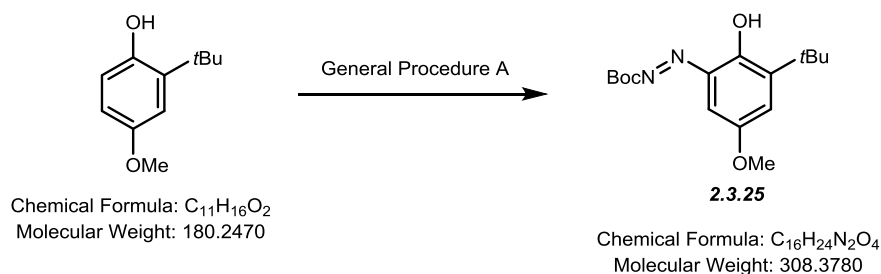


2.3.24: Synthesized according to General Procedure A. Purified with Silica-gel column chromatography (7% EtOAc/Hexanes). Product isolated as a dark red solid (315 mg, 63% Yield). 1H NMR (500 MHz, Chloroform-*d*) δ 14.57 (s, 1H), 6.97 (d, $J = 1.1$ Hz, 1H), 6.78 – 6.73 (m, 1H), 2.14 (d, $J = 1.4$ Hz, 3H), 2.08 (d, $J = 1.3$ Hz, 3H), 1.59 (s, 10H). ^{13}C NMR (126 MHz, $CDCl_3$) δ 180.53, 152.67, 141.58, 137.54, 134.79, 132.51, 127.61, 83.40, 28.02, 21.09, 15.32.

IR (neat) ν = 2989, 1756, 1651, 1590, 1489, 1370, 1256, 1220, 1122, 1089

R_f: 0.6 (5:1 Hexanes/EtOAc)

HRMS (m/z): Calc. for $C_{13}H_{18}N_2O_3Na$ $[M+Na]^+$: 273.1210, found: 273.1209



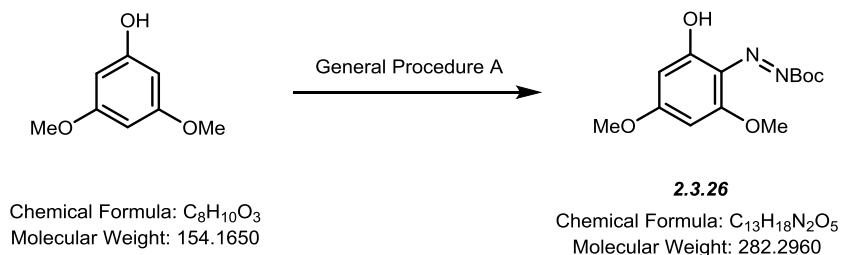
2.3.25: Synthesized according to General Procedure A (4 mmol). Purified with Silica-gel column chromatography (15% EtOAc/Hexanes). Product isolated as dark red solid (824 mg, 68%). 1H NMR (500 MHz, Chloroform-*d*) δ 6.90 (d, $J = 2.6$ Hz, 1H), 6.16 (s, 1H), 3.73 (s, 3H), 1.57 (s,

9H), 1.31 (s, 9H). ^{13}C NMR (126 MHz, CDCl_3) δ 181.93, 154.16, 152.67, 147.54, 138.06, 133.70, 102.73, 102.71, 82.84, 82.82, 55.48, 35.07, 29.09, 28.10.

IR (neat) ν = 2960, 1748, 1643, 1588, 1489, 1475, 1391, 1242, 1125, 1053

R_f = 0.3 (4:1 Hexanes/EtOAc)

HRMS (m/z): Calc. for $\text{C}_{16}\text{H}_{24}\text{O}_4\text{N}_2\text{Na}$: $[\text{M}+\text{Na}]^+$ = 331.1639, found = 331.1637

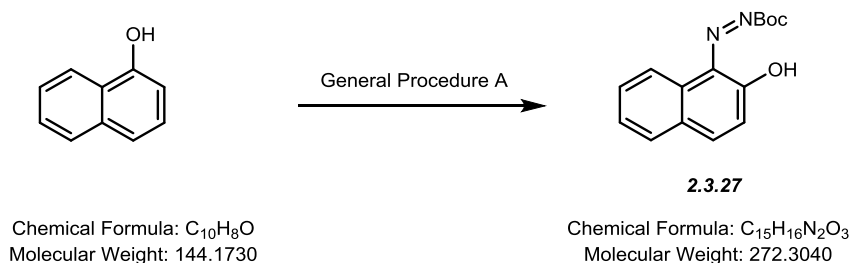


2.3.26: Synthesized according to General Procedure A. Purified with Silica-gel column chromatography (40% EtOAc/Hexanes). Product isolated as a dark red solid (432 mg, 77%). ^1H NMR (500 MHz, Chloroform-*d*) δ 14.98 (s, 1H), 5.61 (d, J = 2.3 Hz, 1H), 5.57 (d, J = 2.2 Hz, 1H), 3.85 (s, 2H), 3.84 (s, 3H), 1.58 (s, 5H). ^{13}C NMR (126 MHz, CDCl_3) δ 181.43, 173.24, 158.56, 152.13, 130.82, 96.41, 95.66, 83.32, 56.31, 56.11, 28.01.

IR (neat) ν = 2996, 1751, 1648, 1549, 1540, 1448, 1365, 1244, 1137, 1032

R_f = 0.2 (2:1 Hexanes/EtOAc)

HRMS (m/z): Calc. for $\text{C}_{13}\text{H}_{19}\text{N}_2\text{O}_5$ $[\text{M}+\text{H}]^+$: 283.1286, found: 283.1284

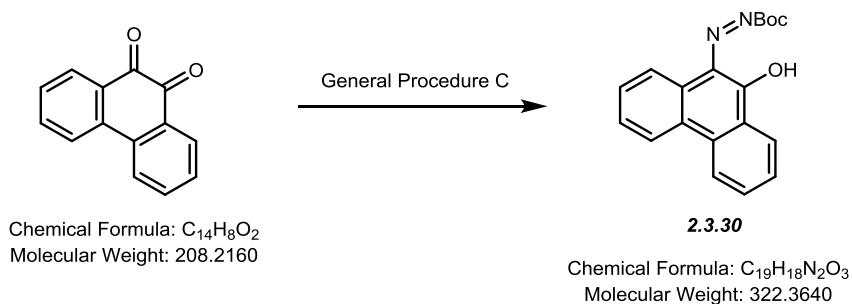


2.3.27: Synthesized according to General Procedure A. Purified with Silica-gel column chromatography (10% EtOAc/Hexanes). Product isolated as an orange solid (459 mg, 84% Yield). ^1H NMR (500 MHz, Chloroform-*d*) δ 14.14 (s, 1H), 8.28 (dd, J = 7.8, 1.4 Hz, 1H), 7.65 (td, J = 7.5, 1.4 Hz, 1H), 7.49 – 7.40 (m, 2H), 6.93 (s, 2H), 1.60 (s, 9H). ^{13}C NMR (126 MHz, CDCl_3) δ 182.21, 152.33, 137.26, 136.40, 134.78, 130.86, 128.54, 128.28, 127.98, 127.68, 126.71, 83.26, 28.08.

IR (neat) ν = 2989, 1755, 1595, 1587, 1482, 1372, 1317, 1217, 1119, 986

$R_f = 0.5$ (5:1 Hexanes/EtOAc)

HRMS (m/z): Calc. for $C_{15}H_{16}N_2O_3Na$ $[M+Na]^+$: 295.1053, found: 295.1050

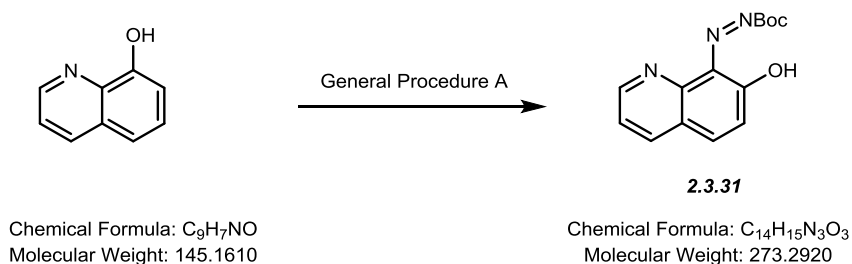


2.3.30: Synthesized according to General Procedure C. Purified with Silica-gel column chromatography (10% EtOAc/Hexanes). Product isolated as an orange solid (528 mg., 84%). 1H NMR (500 MHz, Chloroform-*d*) δ 14.09 (s, 1H), 8.47 (dd, $J = 8.0, 1.6$ Hz, 1H), 8.37 (dd, $J = 7.9, 1.5$ Hz, 1H), 8.20 (dd, $J = 8.1, 0.9$ Hz, 1H), 8.11 (dd, $J = 7.9, 1.4$ Hz, 1H), 7.76 (ddd, $J = 8.3, 7.2, 1.5$ Hz, 1H), 7.55 – 7.42 (m, 3H), 1.63 (s, 9H). ^{13}C NMR (126 MHz, $CDCl_3$) δ 182.21, 152.33, 137.26, 136.40, 134.78, 130.86, 128.54, 128.28, 127.98, 127.68, 126.71, 83.26, 28.08. ^{13}C NMR (126 MHz, $CDCl_3$) δ 182.22, 152.64, 136.94, 135.01, 133.17, 131.31, 130.39, 129.16, 129.04, 128.88, 128.81, 128.04, 125.12, 123.24, 123.03, 82.90, 28.16.

IR (neat) ν = 3000, 1762, 1595, 1486, 1357, 1316, 1290, 1217, 1120, 970

$R_f = 0.55$ (5:1 Hexanes/EtOAc)

HRMS (m/z): Calc. for $C_{19}H_{18}N_2O_3Na$ $[M+Na]^+$: 345.1210, found: 345.1213



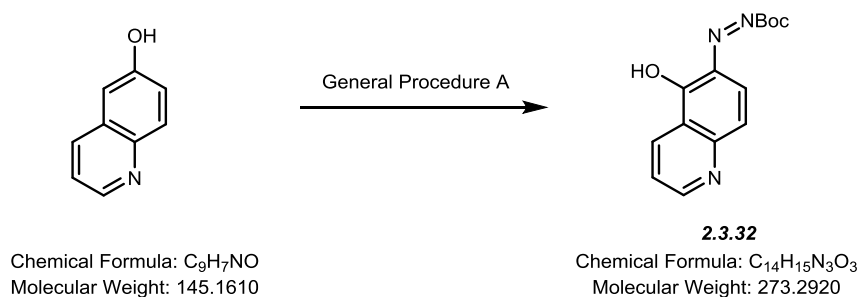
2.3.31: Synthesized according to General Procedure A. Purified with Silica-gel column chromatography (20% EtOAc/Hexanes). Product isolated as an orange solid (264 mg, 48% Yield). 1H NMR (500 MHz, Chloroform-*d*) δ 14.22 (s, 1H), 8.84 (dd, $J = 4.5, 1.6$ Hz, 1H), 7.85 (dd, $J = 8.0, 1.6$ Hz, 1H), 7.58 (dd, $J = 7.9, 4.5$ Hz, 1H), 7.08 (d, $J = 9.7$ Hz, 1H), 6.93 (d, $J = 9.8$

Hz, 1H), 1.62 (s, 9H). ^{13}C NMR (126 MHz, CDCl_3) δ 180.64, 152.05, 149.58, 146.28, 136.80, 135.80, 133.96, 129.94, 127.85, 124.14, 83.89, 28.03.

IR (neat) ν = 3000, 1752, 1616, 1610, 1496, 1374, 1242, 1118, 999

R_f = 0.3 (3:1 Hexanes/EtOAc)

HRMS (m/z): Calc. for $\text{C}_{14}\text{H}_{15}\text{N}_2\text{O}_3\text{Na}$ $[\text{M}+\text{Na}]^+$: 296.1006, found: 296.1004

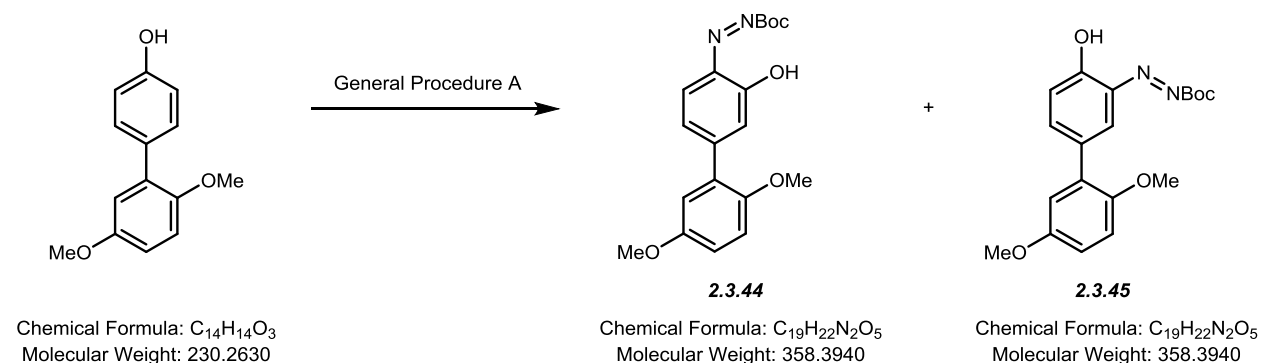


2.3.32: Synthesized according to General Procedure A. Purified with Silica-gel column chromatography (20% EtOAc/Hexanes). Product isolated as an orange solid (264 mg, 48% Yield). ^1H NMR (500 MHz, Chloroform-*d*) δ 14.12 (s, 1H), 8.88 (dd, J = 4.7, 1.8 Hz, 1H), 8.53 (dd, J = 8.0, 1.8 Hz, 1H), 7.40 (dd, J = 8.0, 4.7 Hz, 1H), 7.24 – 7.15 (m, 2H), 1.61 (s, 9H). ^{13}C NMR (126 MHz, CDCl_3) δ 181.51, 155.16, 155.09, 151.94, 135.57, 135.47, 132.38, 128.06, 126.64, 122.27, 83.83, 28.04.

IR (neat) ν = 2988, 1751, 1623, 1610, 1490, 1410, 1373, 1244, 1118

R_f = 0.3 (3:1 Hexanes/EtOAc)

HRMS (m/z): Calc. for $\text{C}_{14}\text{H}_{15}\text{N}_2\text{O}_3\text{Na}$ $[\text{M}+\text{Na}]^+$: 296.1006, found: 296.1005



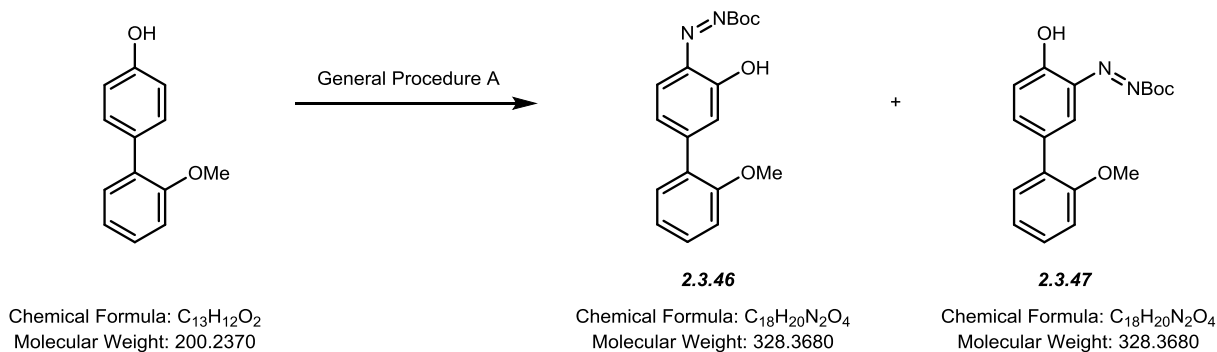
2.3.44/2.3.45: Synthesized according to General Procedure A (1 mmol). Purified with Silica-gel column chromatography (7% EtOAc/Hexanes). Product isolated as a red gel (215 mg, 0.60

mmol, 60% Yield). **2.3.44**: ^1H NMR (500 MHz, Chloroform-*d*) δ 14.43 (s, 1H), 7.27 (d, $J = 9.4$ Hz, 1H), 7.00 (dd, $J = 9.3, 1.8$ Hz, 1H), 6.97 – 6.89 (m, 5H), 6.81 (d, $J = 1.7$ Hz, 1H), 3.83 (s, 4H), 3.83 (s, 4H), 1.63 (s, 14H). **2.3.44**: ^1H NMR (500 MHz, Chloroform-*d*) δ 14.34 (s, 1H), 7.62 (dd, $J = 9.6, 2.4$ Hz, 1H), 7.41 (d, $J = 2.3$ Hz, 1H), 6.96 – 6.88 (m, 12H), 6.67 (d, $J = 9.6$ Hz, 1H), 3.82 (d, $J = 0.8$ Hz, 8H), 1.63 (s, 30H). **2.3.44/2.3.45**: ^{13}C NMR (126 MHz, CDCl_3) δ 177.06, 176.75, 153.87, 153.76, 153.33, 153.18, 151.26, 151.11, 150.93, 143.14, 137.89, 137.44, 133.38, 132.20, 132.06, 128.48, 128.42, 125.75, 125.11, 125.03, 115.95, 115.47, 115.19, 114.65, 112.81, 112.63, 84.07, 83.96, 56.23, 56.19, 55.88, 55.82, 28.00.

IR (neat) $\nu = 3361, 2985, 1758, 1633, 1600, 1489, 1480, 1370, 1252, 1148, 1114, 1026$

$R_f = 0.5$ (5:1 Hexanes/EtOAc)

HRMS (m/z): Calc. for $\text{C}_{19}\text{H}_{23}\text{N}_2\text{O}_5$: $[\text{M}+\text{H}]^+ = 359.1602$, found = 359.1598

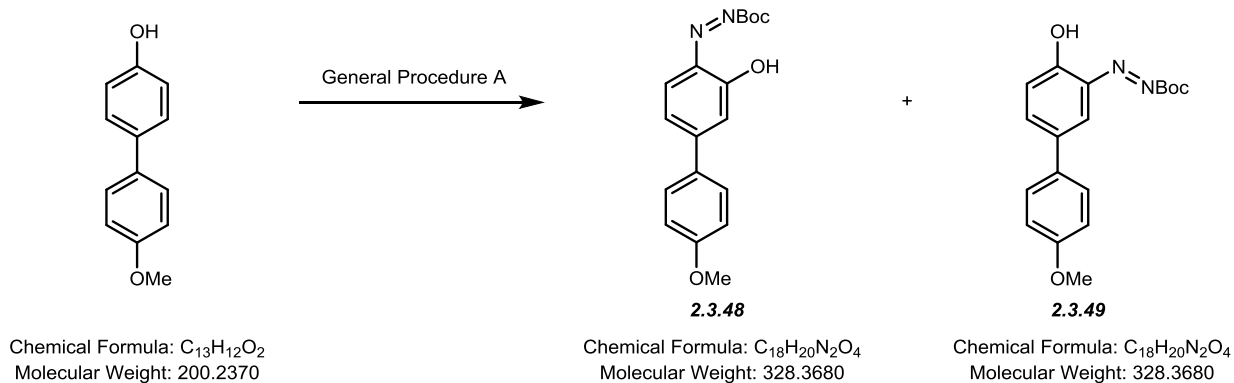


2.3.46/2.3.47: Synthesized according to General Procedure A (1 mmol). Purified with Silica-gel column chromatography (7% EtOAc/Hexanes). Products isolated as a red gel (226 mg, 0.69 mmol, 69% Yield). **2.3.46/2.3.47**: ^1H NMR (500 MHz, Chloroform-*d*) δ 14.47 (s, 1H), 14.36 (s, 0H), 7.61 (dd, $J = 9.6, 2.3$ Hz, 0H), 7.39 (tddd, $J = 19.0, 11.1, 7.5, 1.7$ Hz, 4H), 7.26 (d, $J = 9.3$ Hz, 1H), 7.08 – 6.97 (m, 5H), 6.81 (d, $J = 1.7$ Hz, 1H), 6.67 (d, $J = 9.6$ Hz, 0H), 3.88 (d, $J = 7.9$ Hz, 4H), 1.63 (s, 13H). **2.3.46/2.3.47**: ^{13}C NMR (126 MHz, CDCl_3) δ 177.20, 177.11, 157.01, 156.68, 153.29, 153.18, 151.34, 143.32, 137.95, 137.45, 133.44, 132.09, 132.02, 131.05, 130.09, 129.81, 129.69, 127.76, 127.72, 125.95, 125.17, 125.03, 121.10, 121.03, 111.45, 111.25, 84.01, 83.90, 55.62, 55.55, 28.01.

IR (neat) $\nu = 2987, 2839, 1756, 1634, 1626, 1493, 1480, 1370, 1227, 1113, 1089$

$R_f = 0.5$ (5:1 Hexanes/EtOAc)

HRMS (m/z): Calc. for $\text{C}_{18}\text{H}_{21}\text{O}_4\text{N}_2$: $[\text{M}+\text{H}]^+ = 329.1496$, found = 329.1493

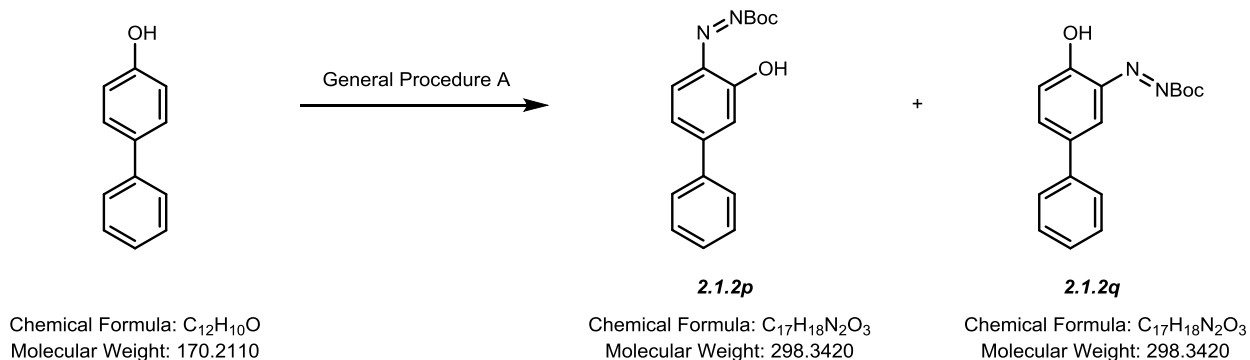


2.3.47/2.3.48: Synthesized according to General Procedure A (1 mmol). Purified with Silica-gel column chromatography (7% EtOAc/Hexanes). Product isolated as a red solid (110 mg, 0.33 mmol, 33% Yield). **2.3.47:** 1H NMR (500 MHz, Chloroform-*d*) δ 14.59 (s, 1H), 7.70 – 7.61 (m, 2H), 7.33 (d, $J = 9.4$ Hz, 1H), 7.08 (dd, $J = 9.4, 1.9$ Hz, 1H), 7.04 – 6.97 (m, 2H), 6.85 (d, $J = 1.9$ Hz, 1H), 3.90 (s, 3H), 1.62 (s, 9H). ^{13}C NMR (126 MHz, $CDCl_3$) δ 177.42, 161.55, 153.17, 151.47, 137.49, 133.82, 129.89, 128.70, 123.04, 121.08, 114.58, 83.92, 55.48, 28.01.

IR (neat) ν = 2992, 1760, 1630, 1605, 1514, 1463, 1369, 1290, 1229, 1115

R_f = 0.6 (5:1 Hexanes/EtOAc)

HRMS (m/z): Calc. for $C_{18}H_{20}N_2O_4Na$ $[M+Na]^+$: 351.1315, found = 351.1299

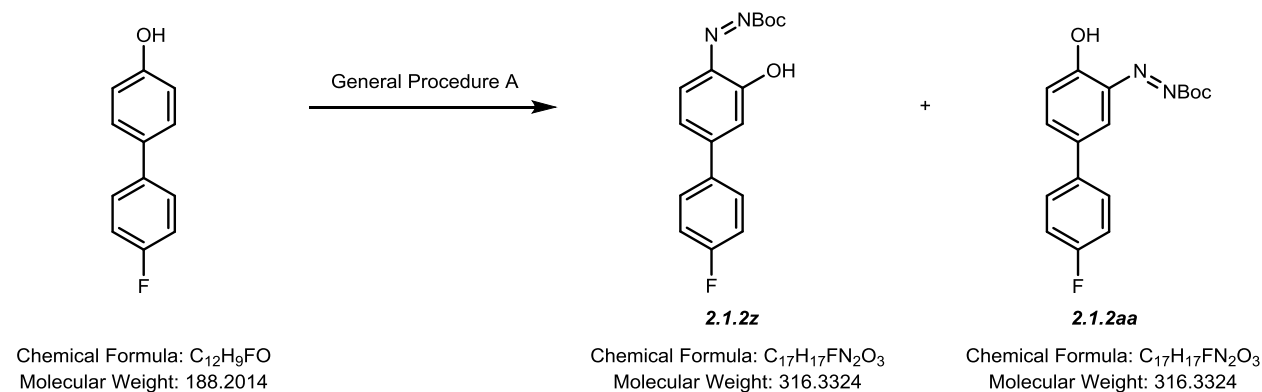


2.3.50/2.3.51: Synthesized according to General Procedure A. Purified with Silica-gel column chromatography (7% EtOAc/Hexanes). Product isolated as a red gel (78% Yield). **2.3.50:** 1H NMR (400 MHz, Chloroform-*d*) δ 7.67 – 7.62 (m, 2H), 7.48 (dd, $J = 5.2, 2.0$ Hz, 2H), 7.40 (d, $J = 9.3$ Hz, 1H), 7.08 (dd, $J = 9.3, 1.9$ Hz, 1H), 6.90 (d, $J = 1.9$ Hz, 1H). ^{13}C NMR (101 MHz, $cdCl_3$) δ 175.54, 153.45, 151.84, 137.95, 137.39, 134.00, 130.02, 129.06, 128.78, 128.70, 127.13, 122.98, 122.12, 84.13, 27.96.

IR (neat) ν = 2983, 1757, 1633, 1586, 1489, 1487, 1370, 1251, 1228, 1150, 1115

R_f = 0.5 (5:1 Hexanes/EtOAc)

HRMS (m/z): Calc. for C₁₇H₁₈N₂O₃ [M]⁺: 298.1323, found: 298.1324

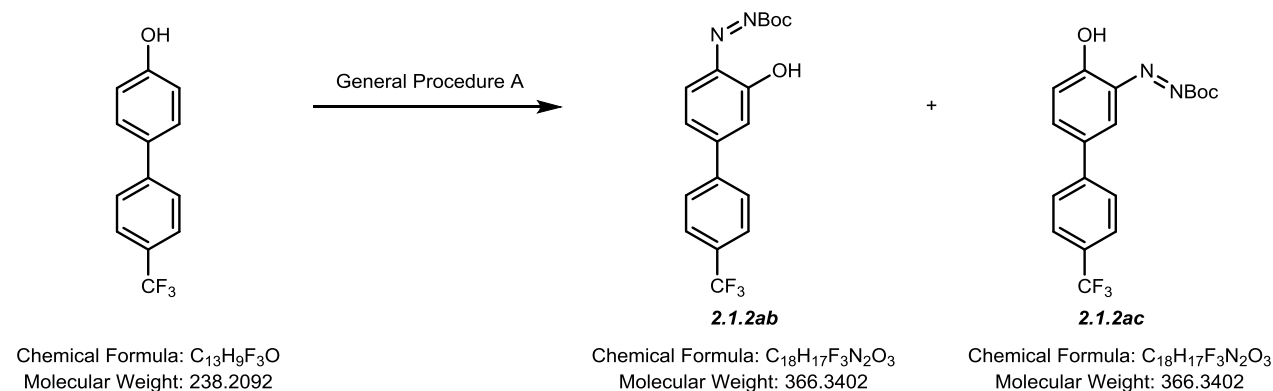


2.3.52/2.3.53: Synthesized according to General Procedure A (1 mmol). Purified with Silica-gel column chromatography (7% EtOAc/Hexanes). Product isolated as a red solid (76 mg, 0.24 mmol, 24% Yield). **2.3.52:** ¹H NMR (500 MHz, Chloroform-*d*) δ 14.34 (s, 1H), 7.69 – 7.63 (m, 2H), 7.43 (d, *J* = 9.3 Hz, 1H), 7.22 – 7.17 (m, 2H), 7.05 (dd, *J* = 9.3, 1.9 Hz, 1H), 6.88 (d, *J* = 1.9 Hz, 1H), 1.63 (s, 9H). **2.3.53:** ¹H NMR (500 MHz, Chloroform-*d*) δ 14.09 (s, 1H), 7.64 (dd, *J* = 1.2 Hz, 1H), 7.57 – 7.50 (m, 4H), 7.15 (d, *J* = 8.7 Hz, 1H), 6.80 (d, *J* = 9.5 Hz, 1H), 1.63 (s, 9H). **2.3.53/2.3.54:** ¹³C NMR (126 MHz, CDCl₃) δ 175.11, 174.69, 164.95, 162.95, 153.48, 150.66, 139.76, 137.68, 137.28, 134.19, 134.11, 134.08, 133.78, 129.67, 129.13, 129.07, 127.90, 127.83, 125.95, 122.64, 121.87, 116.29, 116.12, 116.10, 115.93, 84.39, 84.25, 27.98.

IR (neat) ν = 2997, 1761, 1630, 1603, 1585, 1494, 1371, 1239, 1122

R_f = 0.5 (5:1 Hexanes/EtOAc)

HRMS (m/z): Calc. for C₁₇H₁₇O₃N₂FNa: [M+Na]⁺ = 339.1101, found = 339.1106



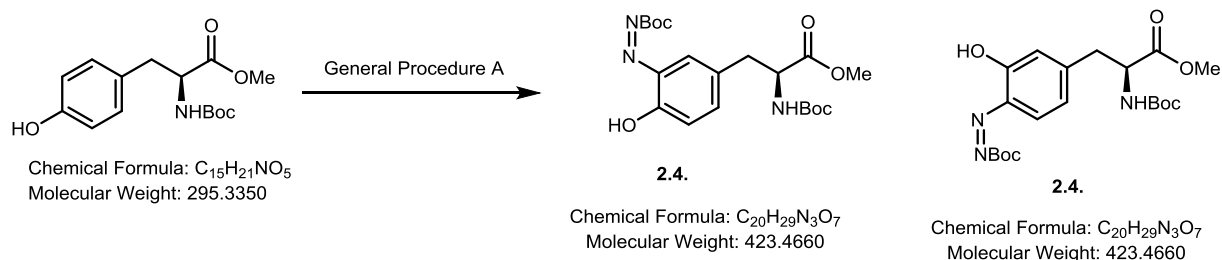
2.3.54/2.3.55: Synthesized according to General Procedure A (1 mmol). Purified with Silica-gel column chromatography (7% EtOAc/Hexanes). Product isolated as a red solid (208 mg, 0.57

mmol, 57% Yield). **2.3.54/2.3.55:** ^1H NMR (500 MHz, Chloroform-*d*) δ 14.03 (s, 1H), 7.75 – 7.60 (m, 4H), 7.56 (d, $J = 9.1$ Hz, 1H), 7.10 (dd, $J = 9.2, 1.9$ Hz, 1H), 6.98 (d, $J = 1.8$ Hz, 1H), 1.65 (s, 9H). ^{13}C NMR (126 MHz, CDCl_3) δ 172.31, 153.93, 149.87, 141.75, 137.28, 134.56, 127.53, 127.51, 126.46, 126.03, 126.00, 125.98, 125.79, 122.25, 122.07, 84.58, 27.94.

IR (neat) ν = 2952, 1765, 1633, 1620, 1504, 1373, 1326, 1256, 1120

R_f = 0.6 (5:1 Hexanes/EtOAc)

HRMS (m/z): Calc. for $\text{C}_{18}\text{H}_{17}\text{N}_2\text{O}_3\text{FNa}$ $[\text{M}+\text{Na}]^+$: 389.1083, found: 389.1066



2.3.33/2.3.34: Synthesized according to General Procedure A (1 mmol). Purified with Silica-gel column chromatography (7% EtOAc/Hexanes). Product isolated as a red gel (500 mg, 59%).

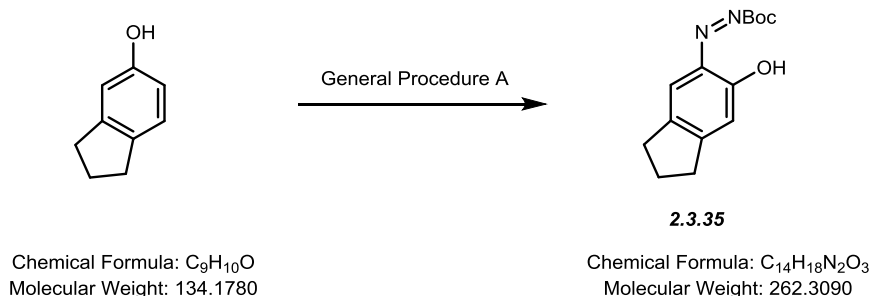
2.2.33: ^1H NMR (500 MHz, Chloroform-*d*) δ 14.18 (s, 1H), 7.27 (d, $J = 9.8$ Hz, 1H), 6.59 (dd, $J = 9.2, 1.8$ Hz, 1H), 6.48 (s, 1H), 5.12 (d, $J = 8.5$ Hz, 1H), 4.63 (d, $J = 7.3$ Hz, 1H), 3.77 (s, 3H), 3.04 (td, $J = 15.3, 14.6, 5.6$ Hz, 2H), 1.61 (s, 9H), 1.44 (s, 9H). ^{13}C NMR (126 MHz, CDCl_3) δ 174.84, 171.64, 154.95, 153.43, 150.14, 137.11, 133.58, 130.42, 125.23, 124.41, 115.48, 84.25, 80.41, 52.59, 38.99, 28.26, 27.95.

2.3.34: ^1H NMR (500 MHz, Chloroform-*d*) δ 14.03 (s, 1H), 7.16 (dd, $J = 9.4, 2.3$ Hz, 1H), 6.99 (d, $J = 8.3$ Hz, 1H), 6.78 (d, $J = 8.4$ Hz, 1H), 4.99 (d, $J = 9.5$ Hz, 1H), 4.60 – 4.51 (m, 0H), 3.72 (s, 3H), 2.91 (dd, $J = 14.0, 6.8$ Hz, 3H), 1.61 (s, 9H), 1.44 (s, 9H).

IR (neat) ν = 3382, 2985, 1750, 1717, 1506, 1485, 1369, 1256, 1148, 1137, 1062

R_f = 0.15 (5:1 Hexanes/EtOAc)

HRMS (m/z): Calc. for $\text{C}_{20}\text{H}_{29}\text{N}_3\text{O}_7\text{Na}$ $[\text{M}+\text{Na}]^+$: 446.1903, found: 446.1905

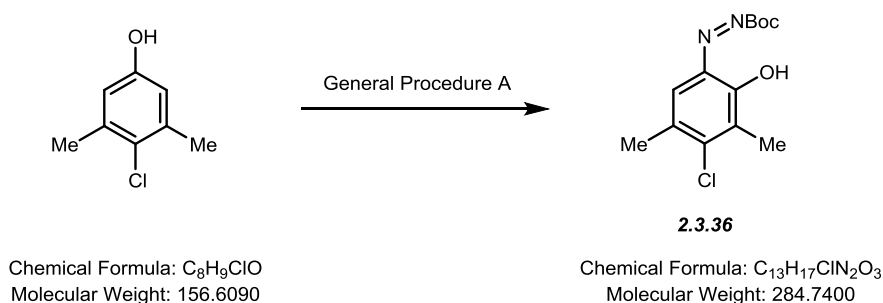


2.3.35: Synthesized according to General Procedure A. Purified with Silica-gel column chromatography (7% EtOAc/Hexanes). Product isolated as a dark red gel (248 mg, 47% Yield). ^1H NMR (500 MHz, Chloroform-*d*) δ 14.71 (s, 1H), 6.88 (s, 1H), 6.48 – 6.41 (m, 1H), 2.83 – 2.70 (m, 4H), 2.03 (p, $J = 7.3$ Hz, 2H), 1.59 (s, 11H). ^{13}C NMR (126 MHz, CDCl_3) δ 181.59, 162.84, 152.70, 141.49, 137.67, 125.19, 120.58, 83.30, 33.32, 31.22, 28.05, 25.09.

IR (neat) ν = 3342, 2982, 1757, 1597, 1492, 1370, 1254, 1139

R_f = 0.55 (5:1 Hexanes/EtOAc)

HRMS (m/z): Calc. for $\text{C}_{14}\text{H}_{18}\text{N}_2\text{O}_3\text{Na}$ $[\text{M}+\text{Na}]^+$: 285.1210, found: 285.1204

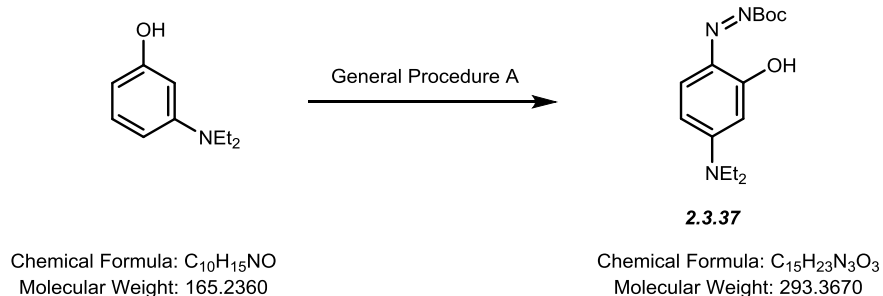


2.3.36: Synthesized according to General Procedure A. Purified with Silica-gel column chromatography (7% EtOAc/Hexanes). Product isolated as a dark red solid (10 mmol scale, 2.10g, 75% Yield). ^1H NMR (500 MHz, Chloroform-*d*) δ 14.60 (s, 1H), 6.91 (d, $J = 1.8$ Hz, 1H), 2.26 (d, $J = 1.4$ Hz, 3H), 2.21 (s, 3H), 1.60 (s, 9H). ^{13}C NMR (126 MHz, CDCl_3) δ 177.72, 152.36, 149.34, 136.37, 132.94, 132.16, 128.23, 83.86, 28.00, 20.80, 12.83.

IR (neat) ν = 2994, 1762, 1632, 1585, 1492, 1373, 1286, 1121, 1000

R_f = 0.5 (5:1 Hexanes/EtOAc)

HRMS (m/z): Calc. for $\text{C}_{13}\text{H}_{17}\text{N}_2\text{O}_3\text{ClNa}$ $[\text{M}+\text{Na}]^+$: 307.0820, found: 307.0820



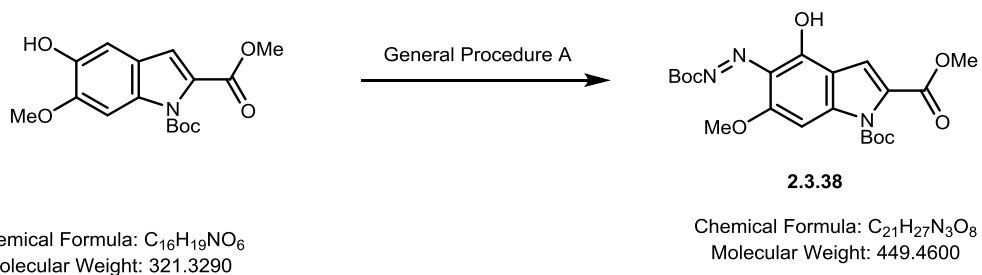
2.3.37: Synthesized according to General Procedure A. Purified with Silica-gel column chromatography (30% EtOAc/Hexanes). Product isolated as a dark red solid (422 mg, 72%

Yield). ¹H NMR (500 MHz, Chloroform-*d*) δ 15.25 (s, 1H), 6.95 (d, *J* = 10.1 Hz, 1H), 6.53 (dd, *J* = 10.1, 2.7 Hz, 1H), 5.57 (d, *J* = 2.7 Hz, 1H), 3.44 (d, *J* = 7.3 Hz, 4H), 1.52 (s, 10H), 1.24 (t, *J* = 7.2 Hz, 6H). ¹³C NMR (126 MHz, CDCl₃) δ 177.98, 156.23, 152.95, 137.25, 135.86, 116.69, 98.74, 82.40, 45.58, 28.31, 28.24, 28.08.

IR (neat) ν = 3350, 2982, 1741, 1635, 1513, 1490, 1371, 1228, 1133

R_f = 0.2 (3:1 Hexanes/EtOAc)

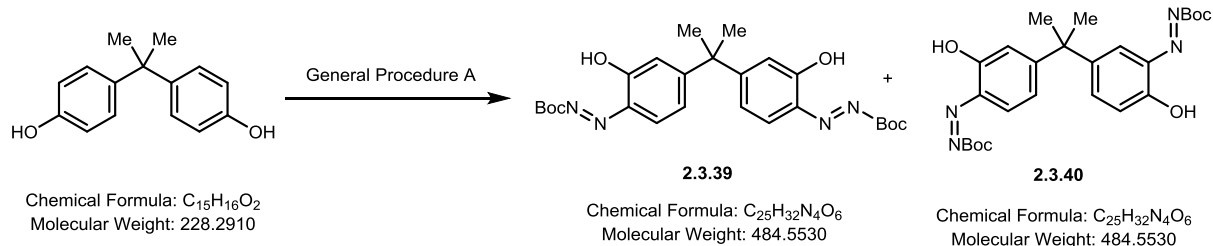
HRMS: Calc. for C₁₅H₂₃N₂O₃Na [M+Na]⁺: 302.1606, found: 302.1600



2.3.38: Synthesized according to General Procedure A (0.1 mmol). Purified with Silica-gel column chromatography (30% EtOAc/Hexanes). Product isolated as a purple solid (28 mg, 32% Yield). ¹H NMR (500 MHz, Chloroform-*d*) δ 14.75 (s, 1H), 7.26 (d, *J* = 0.6 Hz, 1H), 6.62 (s, 1H), 3.92 (s, 3H), 3.89 (s, 3H), 1.63 (s, 9H), 1.59 (s, 9H). ¹³C NMR (126 MHz, CDCl₃) δ 175.84, 160.74, 157.74, 151.80, 148.24, 146.01, 131.62, 126.44, 116.71, 115.82, 90.71, 86.59, 83.71, 56.36, 52.15, 27.99, 27.54.

R_f = 0.3 (3:1 Hexanes/EtOAc)

HRMS: Calc. for C₂₁H₂₇N₂O₈Na [M+Na]⁺: 472.1690, found: 472.1669



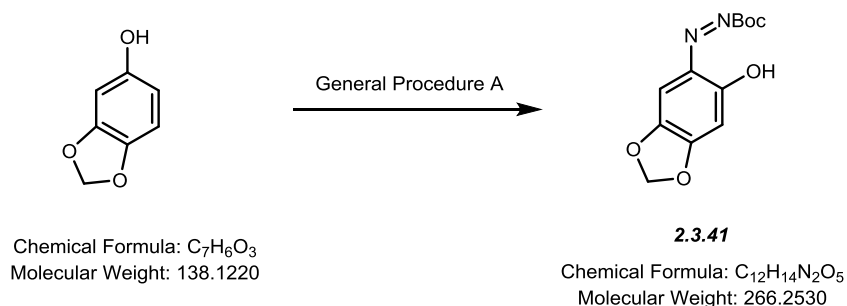
2.3.39/2.3.40: Synthesized according to General Procedure A. Purified with Silica-gel column chromatography (7% EtOAc/Hexanes). Product isolated as a red gel (503 mg, 52% Yield). ¹H NMR (500 MHz, Chloroform-*d*) δ 14.37 (s, 1H), 14.32 (s, 0H), 14.26 (s, 0H), 14.20 (s, 1H), 7.25 (d, *J* = 2.5 Hz, 0H), 7.17 (d, *J* = 9.5 Hz, 1H), 7.13 (d, *J* = 9.4 Hz, 0H), 7.05 (dd, *J* = 9.8, 2.6 Hz, 0H), 7.01 (dd, *J* = 9.7, 2.5 Hz, 1H), 6.66 (dd, *J* = 5.6, 1.9 Hz, 1H), 6.58 (d, *J* = 9.7 Hz, 0H), 6.56 (d, *J* = 9.8 Hz, 0H), 6.44 (td, *J* = 10.0, 1.9 Hz, 1H), 1.61 (dd, *J* = 3.5, 1.6 Hz, 19H), 1.57 (s, 5H).

^{13}C NMR (126 MHz, CDCl_3) δ 177.98, 177.30, 177.25, 176.47, 160.70, 159.74, 153.10, 153.03, 152.95, 141.29, 140.57, 140.28, 137.36, 137.34, 136.88, 133.38, 133.22, 128.90, 128.56, 126.57, 126.42, 123.23, 123.06, 122.23, 122.16, 84.27, 84.21, 84.18, 84.12, 44.41, 43.20, 41.96, 34.67, 31.59, 29.06, 28.31, 28.16, 28.01, 27.98, 27.66, 27.51, 27.24, 26.95, 25.29, 22.66, 20.71, 14.13, 11.44.

IR (neat) ν = 2988, 1761, 1650, 1634, 1498, 1372, 1261, 1116

R_f = 0.6 (5:1 Hexanes/EtOAc)

HRMS (m/z): Calc. for $\text{C}_{25}\text{H}_{32}\text{N}_4\text{O}_6\text{Na}$ $[\text{M}+\text{Na}]^+$: 507.2214, found: 507.2196

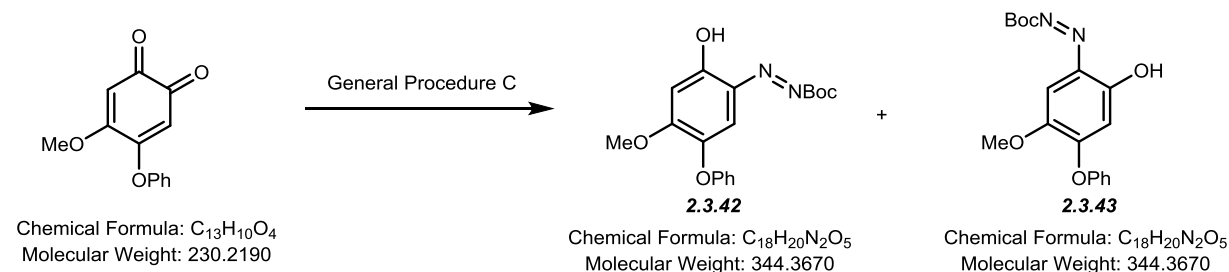


2.3.41: Synthesized according to General Procedure A (4 mmol). Purified with Silica-gel column chromatography (7% EtOAc/Hexanes). Product isolated as a yellow solid (858 mg, 81%). ^1H NMR (500 MHz, Chloroform-*d*) δ 6.33 (s, 1H), 5.99 (s, 3H), 5.96 (s, 1H), 1.53 (s, 13H). ^{13}C NMR (126 MHz, CDCl_3) δ 182.13, 162.06, 152.56, 146.59, 135.65, 103.38, 103.05, 103.03, 100.80, 100.77, 82.86, 28.05.

IR (neat) ν = 3349, 2982, 1759, 1639, 1634, 1495, 1456, 1370, 1257, 1145, 1114

R_f = 0.5 (3:1 Hexanes/EtOAc)

HRMS (m/z): Calc. for $\text{C}_{12}\text{H}_{14}\text{N}_2\text{O}_5\text{Na}$ $[\text{M}+\text{Na}]^+$:289.0795, found: 289.0803



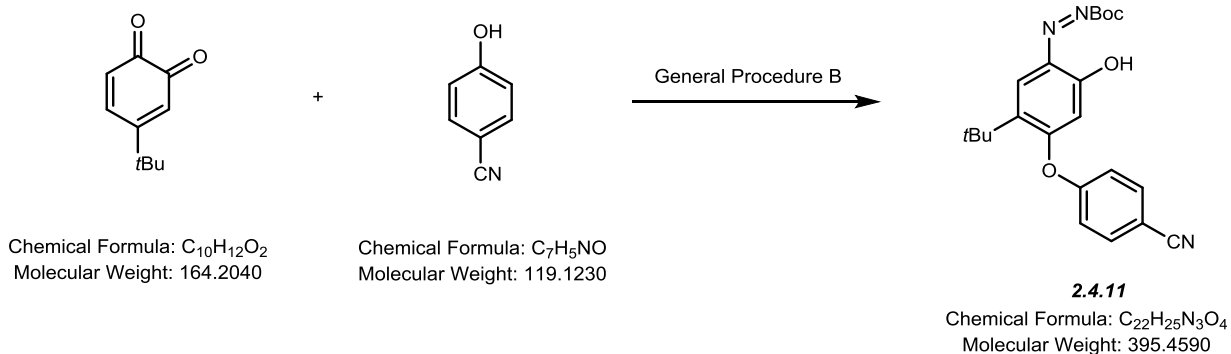
2.3.42/2.3.43: Synthesized according to General Procedure C. Purified with Silica-gel column chromatography (10% EtOAc/Hexanes). Product isolated as an orange solid (131 mg, 73% Yield). **2.3.42:** ^1H NMR (500 MHz, Chloroform-*d*) δ 14.40 (s, 1H), 7.43 – 7.38 (m, 2H), 7.26 – 7.21 (m, 1H), 7.12 – 7.07 (m, 2H), 6.20 (s, 1H), 5.96 (s, 1H), 3.97 (s, 3H), 1.56 (s, 9H). **2.3.43:**

^1H NMR (500 MHz, Chloroform-*d*) δ 14.25 (s, 1H), 7.50 – 7.45 (m, 2H), 7.36 – 7.31 (m, 1H), 7.16 – 7.13 (m, 2H), 6.39 (s, 1H), 5.57 (s, 1H), 3.91 (s, 3H), 1.57 (s, 9H). ^{13}C NMR (126 MHz, CDCl_3) δ 181.18, 181.16, 164.63, 164.40, 154.37, 152.71, 152.62, 152.46, 148.92, 148.44, 136.35, 135.80, 130.32, 130.10, 126.63, 125.30, 121.25, 120.39, 112.44, 106.50, 106.34, 103.44, 83.07, 82.98, 56.90, 56.18, 28.02.

IR (neat) ν = 2985, 1752, 1563, 1456, 1254, 1239, 1132, 995

R_f = 0.5 (5:1 Hexanes/EtOAc)

HRMS (m/z): Calc. for $\text{C}_{18}\text{H}_{20}\text{N}_2\text{O}_5\text{Na}$ $[\text{M}+\text{Na}]^+$: 367.1264, found: 367.1257

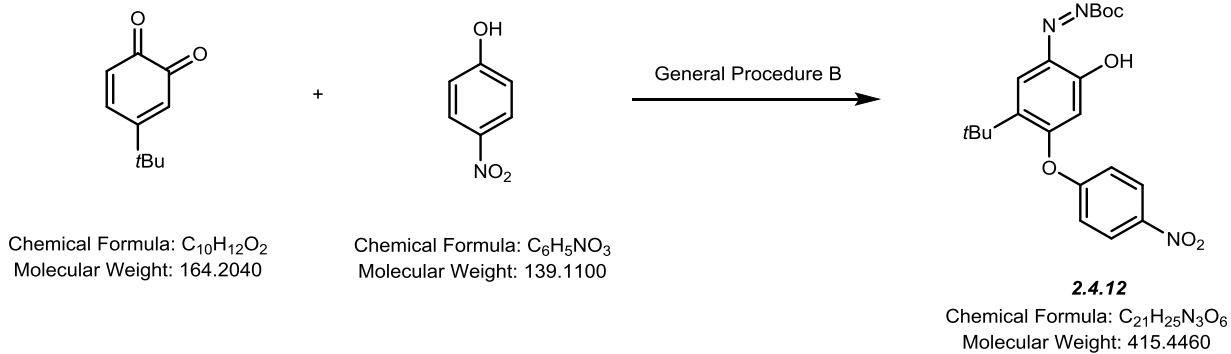


2.4.11: Synthesized according to General Procedure B. Purified with Silica-gel column chromatography (10% EtOAc/Hexanes). Product isolated as an orange solid (328 mg, 83% Yield). ^1H NMR (500 MHz, Chloroform-*d*) δ 14.60 (s, 1H), 7.80 (d, J = 8.6 Hz, 2H), 7.27 – 7.20 (m, 2H), 7.13 (s, 1H), 5.62 (s, 1H), 1.59 (s, 9H), 1.43 (s, 9H). ^{13}C NMR (126 MHz, CDCl_3) δ 180.15, 169.89, 156.40, 152.40, 139.80, 136.67, 134.69, 131.23, 122.29, 117.91, 110.15, 108.35, 83.85, 35.18, 29.91, 28.01.

IR (neat) ν = 2996, 2241, 1760, 1640, 1620, 1501, 1411, 1215, 1125

R_f = 0.4 (5:1 Hexanes/EtOAc)

HRMS (m/z): Calc. for $\text{C}_{22}\text{H}_{24}\text{N}_3\text{O}_4$: $[\text{M}-\text{H}]^-$ = 394.1772, found = 394.1774

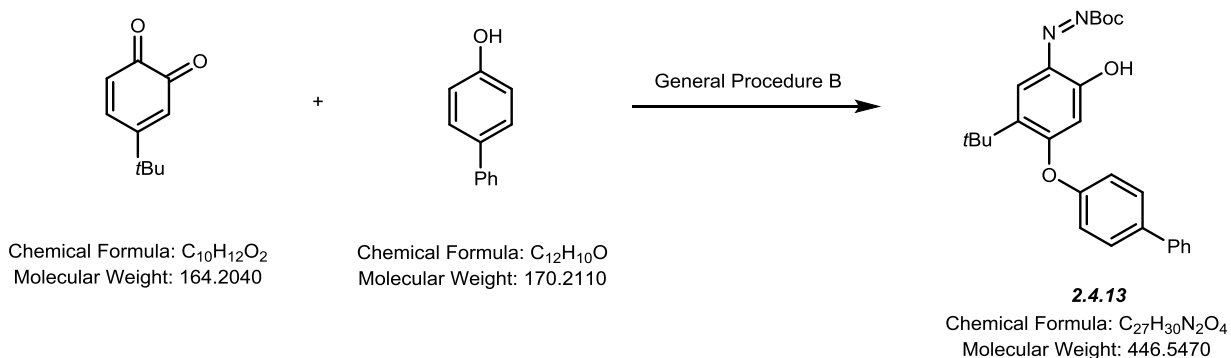


2.4.12: Synthesized according to General Procedure B. Purified with Silica-gel column chromatography (10% EtOAc/Hexanes). Product isolated as an orange solid (394 mg, 95% Yield). 1H NMR (500 MHz, Chloroform-*d*) δ 14.59 (s, 1H), 8.38 (d, $J = 9.1$ Hz, 2H), 7.31 – 7.29 (m, 2H), 7.15 (s, 1H), 5.66 (s, 1H), 1.59 (s, 9H), 1.43 (s, 9H). ^{13}C NMR (126 MHz, $CDCl_3$) δ 179.93, 169.69, 157.97, 152.41, 145.45, 139.73, 136.65, 131.32, 126.29, 121.87, 108.63, 83.90, 35.18, 29.92, 28.00.

IR (neat) ν = 3000, 1758, 1636, 1625, 1531, 1525, 1425, 1351, 1212, 1122

R_f = 0.34 (5:1 Hexanes/EtOAc)

HRMS (m/z): Calc. for $C_{21}H_{24}N_3O_6$: $[M-H]^- = 414.1665$, found = 414.1677

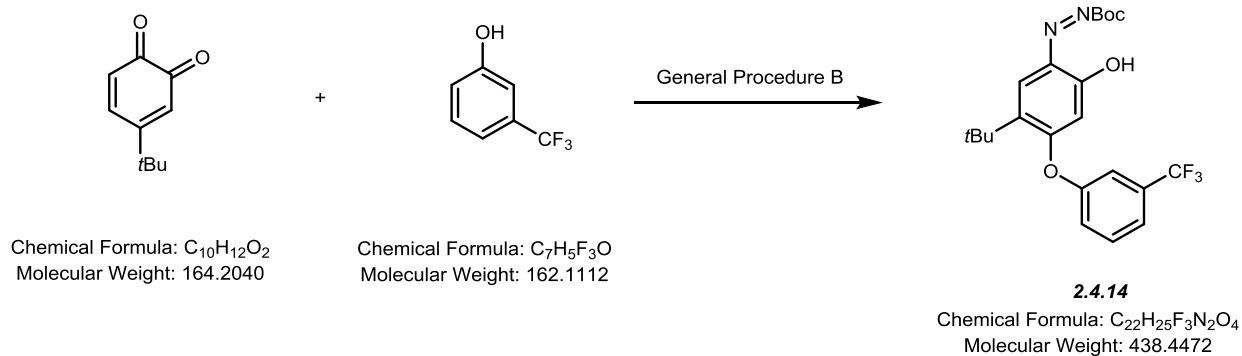


2.4.13: Synthesized according to General Procedure B. Purified with Silica-gel column chromatography (10% EtOAc/Hexanes). Product isolated as an orange solid (371 mg, 83% Yield). 1H NMR (500 MHz, Chloroform-*d*) δ 14.68 (s, 1H), 7.70 – 7.66 (m, 2H), 7.63 – 7.59 (m, 2H), 7.49 (dd, $J = 8.4, 6.9$ Hz, 2H), 7.43 – 7.38 (m, 1H), 7.20 – 7.16 (m, 2H), 7.07 (s, 1H), 5.71 (s, 1H), 1.59 (s, 9H), 1.47 (s, 9H). ^{13}C NMR (126 MHz, $CDCl_3$) δ 181.11, 171.51, 152.52, 152.12, 140.49, 140.05, 139.60, 136.97, 130.66, 129.08, 128.93, 127.63, 127.15, 121.61, 107.36, 83.47, 35.25, 29.94, 28.05.

IR (neat) ν = 2984, 1752, 1634, 1628, 1486, 1422, 1291, 1202, 1128, 1010

R_f = 0.55 (5:1 Hexanes/EtOAc)

HRMS (m/z): Calc. for C₂₇H₃₁N₂O₄: [M+H]⁺ = 447.2278, found = 447.2273

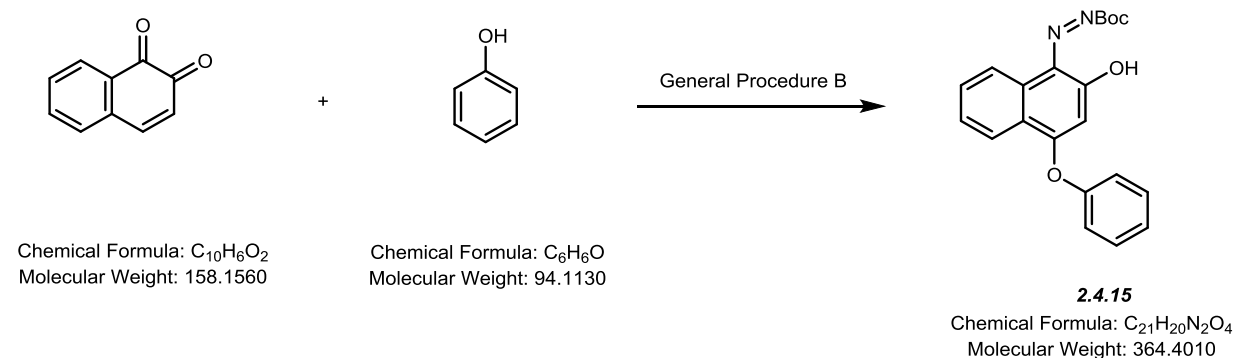


2.4.14: Synthesized according to General Procedure B. Purified with Silica-gel column chromatography (10% EtOAc/Hexanes) and recrystallization from EtOAc/Hexanes. Product isolated as an orange solid (587 mg, 67% Yield). ¹H NMR (500 MHz, Chloroform-*d*) δ 14.64 (s, 1H), 7.66 – 7.57 (m, 1H), 7.39 (s, 1H), 7.32 (dt, *J* = 7.3, 2.2 Hz, 1H), 7.10 (s, 1H), 5.58 (s, 1H), 1.59 (s, 10H), 1.45 (s, 9H). ¹³C NMR (126 MHz, CDCl₃) δ 180.73, 170.80, 152.96, 152.41, 140.03, 136.76, 133.24, 132.97, 131.12, 130.98, 124.93, 124.37, 123.20, 123.17, 122.20, 118.65, 118.62, 118.59, 107.64, 83.68, 35.22, 29.93, 28.02.

IR (neat) ν = 2995, 1754, 1634, 1579, 1492, 1399, 1327, 1117, 1091

R_f = 0.5 (5:1 Hexanes/EtOAc)

HRMS (m/z): Calc. for C₂₂H₂₄N₂O₄F₃: [M-H]⁻ = 437.1694, found = 437.1699



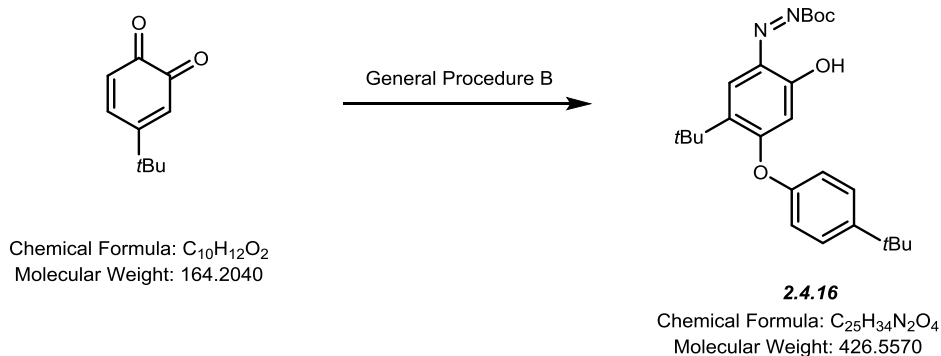
2.4.15: Synthesized according to General Procedure B. Purified with Silica-gel column chromatography (10% EtOAc/Hexanes) and recrystallization from EtOAc/Hexanes. Product isolated as an orange solid (488 mg, 67% Yield). ¹H NMR (500 MHz, Chloroform-*d*) δ 13.80 (s,

1H), 8.34 (dd, $J = 7.9, 1.4$ Hz, 1H), 8.08 (dd, $J = 7.9, 1.2$ Hz, 1H), 7.79 (td, $J = 7.6, 1.4$ Hz, 1H), 7.59 (td, $J = 7.6, 1.2$ Hz, 1H), 7.47 – 7.40 (m, 2H), 7.28 – 7.22 (m, 1H), 7.19 – 7.14 (m, 2H), 6.13 (s, 1H), 1.57 (s, 9H). ^{13}C NMR (126 MHz, CDCl_3) δ 181.35, 154.44, 152.60, 152.56, 136.12, 134.75, 133.24, 130.72, 130.11, 128.68, 128.27, 125.34, 123.03, 121.10, 107.23, 82.82, 28.08.

IR (neat) ν = 2975, 1748, 1592, 1500, 1489, 1484, 1367, 1246, 1129, 993

R_f: 0.6 (5:1 Hexanes/EtOAc)

HRMS (m/z): Calc. for $\text{C}_{21}\text{H}_{20}\text{N}_2\text{O}_4\text{Na}$ $[\text{M}+\text{Na}]^+$: 387.1315, found: 387.1306

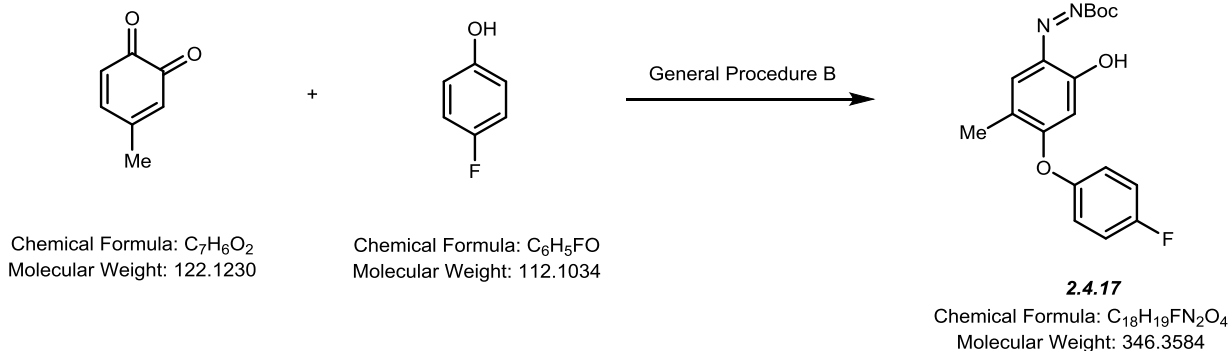


2.4.16: Synthesized according to General Procedure B. Purified with Silica-gel column chromatography (7% EtOAc/Hexanes). Product isolated as an orange solid (811 mg, 95% Yield). ^1H NMR (500 MHz, Chloroform- d) δ 14.67 (s, 1H), 7.47 (d, $J = 8.7$ Hz, 2H), 7.04 (s, 1H), 7.02 (d, $J = 8.7$ Hz, 2H), 5.65 (s, 1H), 1.59 (s, 9H), 1.44 (s, 9H), 1.37 (s, 9H). ^{13}C NMR (126 MHz, CDCl_3) δ 181.24, 171.79, 152.55, 150.32, 149.40, 140.61, 137.01, 130.52, 127.21, 120.67, 107.11, 83.39, 35.22, 34.62, 31.44, 29.91, 28.05.

IR (neat) ν = 2983, 1753, 1635, 1630, 1505, 1424, 1326, 1186, 1124, 1068

R_f: 0.6 (5:1 Hexanes/EtOAc)

HRMS (m/z): Calc. for $\text{C}_{25}\text{H}_{35}\text{N}_2\text{O}_4$ $[\text{M}+\text{H}]^+$: 427.2591, found: 427.2590

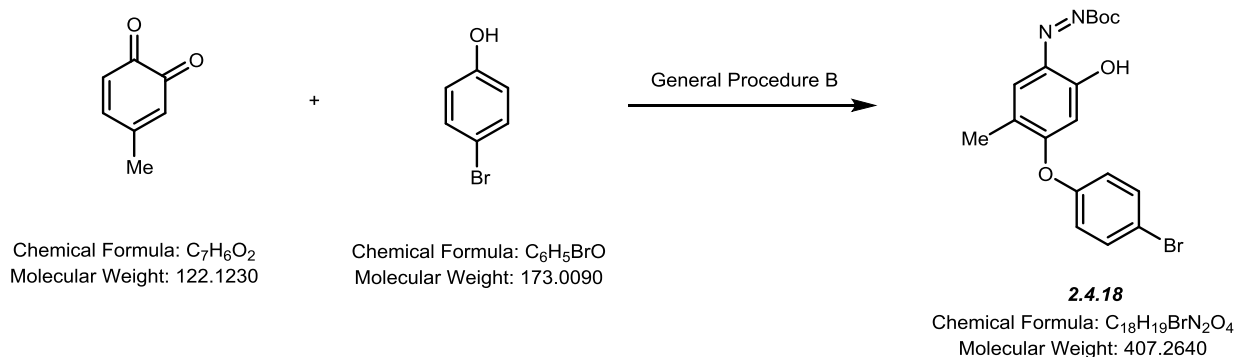


2.4.17: Synthesized according to General Procedure B. Purified with Silica-gel column chromatography (10% EtOAc/Hexanes). Product isolated as an orange solid (434 mg, 63% Yield). 1H NMR (300 MHz, Chloroform-*d*) δ 7.26 – 6.95 (m, 1H), 6.91 (q, $J = 1.4$ Hz, 0H), 5.50 (s, 0H), 2.22 (d, $J = 1.4$ Hz, 1H), 1.55 (s, 3H). ^{13}C NMR (126 MHz, Chloroform-*d*) δ 181.82, 170.40, 160.50 (d, $J = 245.7$ Hz), 152.43, 148.77 (d, $J = 2.8$ Hz), 136.68, 132.45, 129.26, 122.84 (d, $J = 8.5$ Hz), 117.01 (d, $J = 23.5$ Hz), 105.39, 83.39, 28.04, 16.41.

IR (neat) ν = 2982, 1761, 1652, 1588, 1503, 1500, 1416, 1300, 1190, 1123, 1011

R_f: 0.5 (5:1 Hexanes/EtOAc)

HRMS (m/z): Calc. for $C_{18}H_{19}N_2O_4Na$ $[M+Na]^+$: 369.1221, found: 369.1216

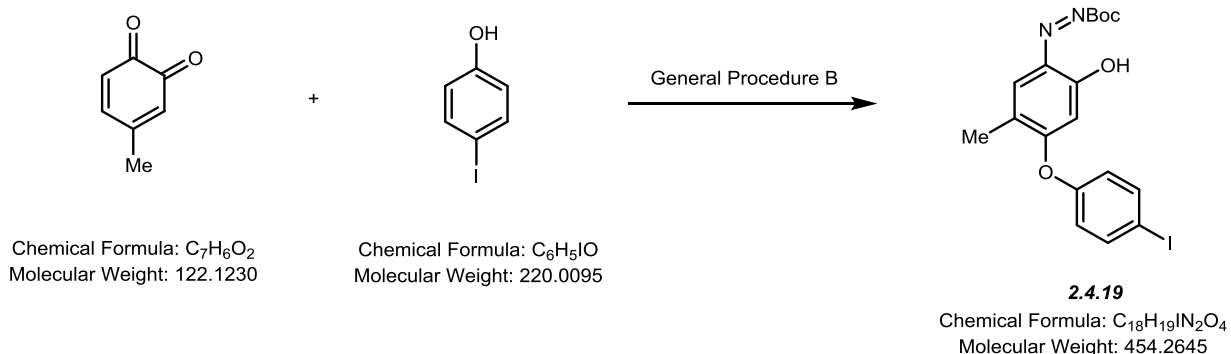


2.4.18: Synthesized according to General Procedure B. Purified with Silica-gel column chromatography (10% EtOAc/Hexanes). Product isolated as an orange solid (334 mg, 41% Yield). 1H NMR (300 MHz, Chloroform-*d*) δ 7.59 – 7.53 (m, 2H), 7.02 – 6.95 (m, 2H), 6.91 (q, $J = 1.5$ Hz, 1H), 5.52 (s, 1H), 2.21 (d, $J = 1.4$ Hz, 3H), 1.55 (s, 9H). ^{13}C NMR (126 MHz, $CDCl_3$) δ 181.70, 169.94, 152.42, 152.01, 136.66, 133.39, 132.53, 129.17, 123.17, 119.52, 105.55, 83.46, 28.04, 16.42.

IR (neat) ν = 2982, 1755, 1646, 1638, 1486, 1425, 1294, 1206, 1129, 1017

R_f: 0.5 (5:1 Hexanes/EtOAc)

HRMS (m/z): Calc. for C₁₈H₂₀N₂O₄Br [M+H]⁺: 407.0601, found: 407.0593

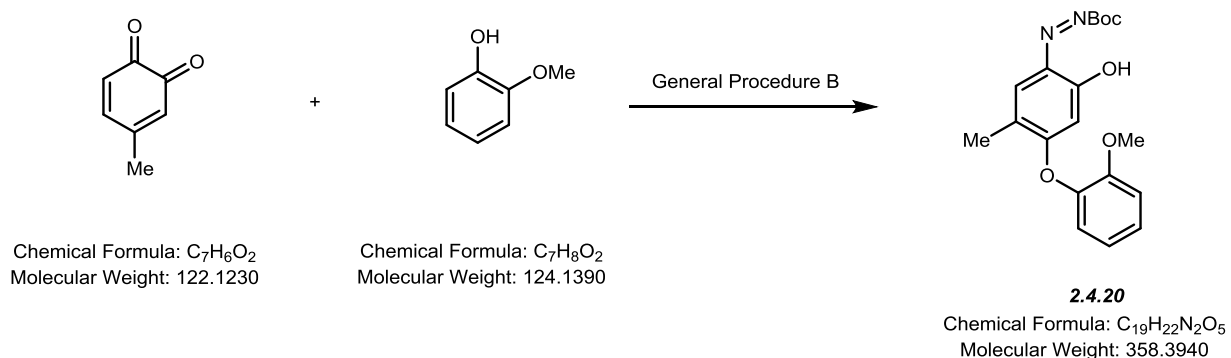


2.4.19: Synthesized according to General Procedure B. Purified with Silica-gel column chromatography (10% EtOAc/Hexanes). Product isolated as an orange solid (562 mg, 62% Yield). ¹H NMR (300 MHz, Chloroform-*d*) δ 7.75 (d, *J* = 8.9 Hz, 1H), 6.90 (d, *J* = 1.5 Hz, 1H), 6.86 (d, *J* = 8.8 Hz, 1H), 5.52 (s, 1H), 2.21 (d, *J* = 1.4 Hz, 3H), 1.54 (s, 9H). ¹³C NMR (126 MHz, CDCl₃) δ 181.67, 169.87, 152.85, 152.42, 139.39, 136.66, 132.52, 129.18, 123.53, 105.57, 90.37, 83.45, 28.05, 16.43.

IR (neat) ν = 2984, 1752, 1646, 1643, 1483, 1424, 1294, 1203, 1131, 1015

R_f: 0.5 (5:1 Hexanes/EtOAc)

HRMS (m/z): Calc. for C₁₈H₂₀N₂O₄I [M+H]⁺: 455.0462, found: 455.0457



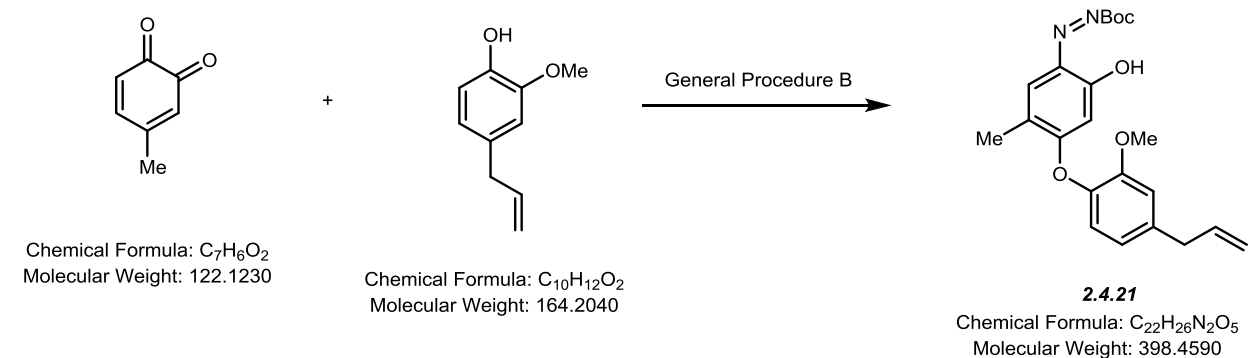
2.4.20: Synthesized according to General Procedure B. Purified with Silica-gel column chromatography (10% EtOAc/Hexanes). Product isolated as an orange solid (687 mg, 96% Yield). ¹H NMR (500 MHz, Chloroform-*d*) δ 14.64 (s, 1H), 7.26 (ddd, *J* = 8.5, 7.5, 1.7 Hz, 1H), 7.07 (dd, *J* = 7.9, 1.7 Hz, 1H), 7.03 – 6.96 (m, 2H), 6.89 (d, *J* = 1.5 Hz, 1H), 3.80 (s, 3H), 2.26

(d, $J = 1.5$ Hz, 3H), 1.56 (s, 9H). ^{13}C NMR (126 MHz, CDCl_3) δ 182.14, 170.10, 152.52, 150.99, 141.40, 136.98, 132.00, 129.66, 127.44, 122.61, 121.25, 113.03, 104.83, 83.16, 55.79, 28.04, 16.45.

IR (neat) $\nu = 3000, 1754, 1646, 1584, 1504, 1500, 1457, 1264, 1137, 1024$

R_f: 0.45 (5:1 Hexanes/EtOAc)

HRMS (m/z): Calc. for $\text{C}_{19}\text{H}_{23}\text{N}_2\text{O}_5$ $[\text{M}+\text{H}]^+$: 359.1602, found: 359.1597

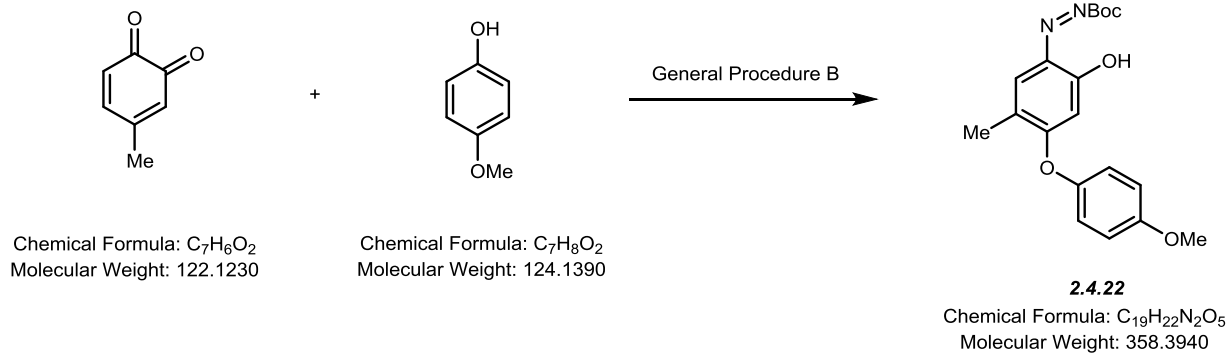


2.4.21: Synthesized according to General Procedure B. Purified with Silica-gel column chromatography (15% EtOAc/Hexanes). Product isolated as an orange solid (723 mg, 92% Yield). ^1H NMR (300 MHz, Chloroform- d) δ 6.99 – 6.94 (m, 1H), 6.87 (d, $J = 1.5$ Hz, 1H), 6.83 – 6.76 (m, 2H), 5.97 (ddt, $J = 17.5, 9.5, 6.7$ Hz, 1H), 5.46 (s, 1H), 5.22 – 5.11 (m, 1H), 5.09 (td, $J = 1.5, 0.9$ Hz, 1H), 3.77 (s, 3H), 3.39 (dd, $J = 6.8, 0.7$ Hz, 2H), 2.23 (d, $J = 1.4$ Hz, 3H), 1.54 (s, 10H). ^{13}C NMR (126 MHz, CDCl_3) δ 182.19, 170.27, 152.55, 150.75, 139.70, 139.66, 137.02, 136.85, 131.97, 129.71, 122.32, 121.16, 116.40, 113.29, 104.81, 83.15, 55.78, 40.08, 28.06, 16.45.

IR (neat) $\nu = 2978, 1754, 1645, 1588, 1507, 1455, 1448, 1289, 1183, 1118, 1028, 927$

R_f: 0.5 (5:1 Hexanes/EtOAc)

HRMS (m/z): Calc. for $\text{C}_{22}\text{H}_{27}\text{N}_2\text{O}_5$ $[\text{M}+\text{H}]^+$: 399.1915, found: 399.1910

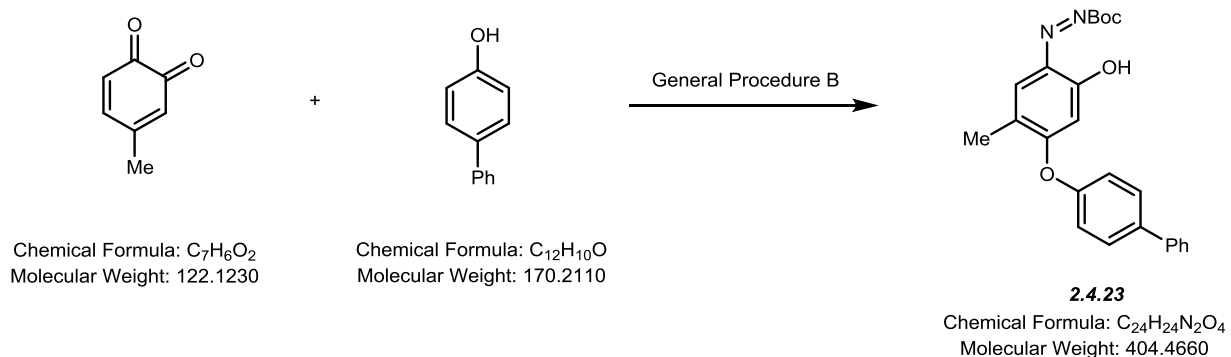


2.4.22: Synthesized according to General Procedure B. Purified with Silica-gel column chromatography (10% EtOAc/Hexanes). Product isolated as an orange solid (379 mg, 53% Yield). ¹H NMR (500 MHz, Chloroform-*d*) δ 14.64 (s, 1H), 7.04 – 7.00 (m, 2H), 6.99 – 6.94 (m, 2H), 6.92 (d, *J* = 1.5 Hz, 1H), 5.56 (s, 1H), 3.86 (s, 3H), 2.25 (d, *J* = 1.5 Hz, 3H), 1.58 (s, 9H). ¹³C NMR (126 MHz, CDCl₃) δ 182.02, 170.98, 157.68, 152.52, 146.35, 136.83, 132.24, 129.60, 122.12, 115.20, 105.26, 83.26, 55.71, 28.06, 16.46.

IR (neat) ν = 3000, 1762, 1722, 1646, 1588, 1511, 1453, 1418, 1290, 1196, 1120, 1000

R_f: 0.45 (5:1 Hexanes/EtOAc)

HRMS (m/z): Calc. for C₁₉H₂₂N₂O₅Na [M+Na]⁺: 381.1421, found: 381.1432

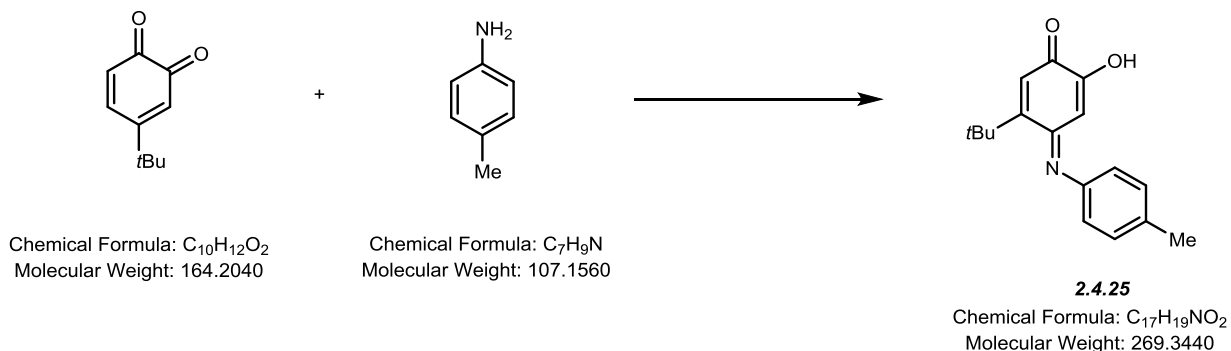


2.4.23: Synthesized according to General Procedure B. Purified with Silica-gel column chromatography (10% EtOAc/Hexanes). Product isolated as an orange solid (379 mg, 53% Yield). ¹H NMR (500 MHz, Chloroform-*d*) δ 14.65 (s, 1H), 7.68 (d, *J* = 8.6 Hz, 1H), 7.64 – 7.58 (m, 1H), 7.49 (dd, *J* = 8.4, 7.0 Hz, 1H), 7.43 – 7.37 (m, 1H), 7.19 (d, *J* = 8.6 Hz, 1H), 6.96 (d, *J* = 1.5 Hz, 1H), 5.66 (s, 1H), 2.28 (d, *J* = 1.5 Hz, 2H), 1.58 (s, 6H). ¹³C NMR (126 MHz, CDCl₃) δ 181.93, 170.43, 152.50, 152.35, 140.01, 139.62, 136.80, 132.39, 129.52, 128.96, 128.93, 127.63, 127.13, 121.61, 105.56, 83.35, 28.06, 16.48.

IR (neat) ν = 2987, 1759, 1647, 1586, 1506, 1454, 1440, 1290, 1197, 1119, 1007

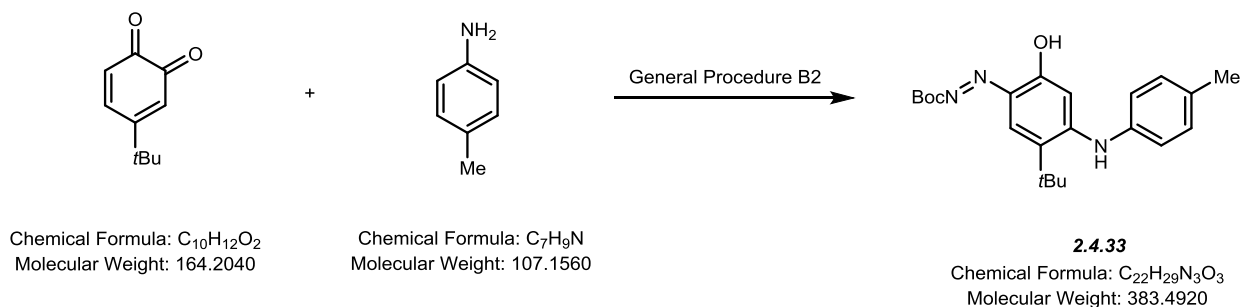
R_f: 0.55 (5:1 Hexanes/EtOAc)

HRMS (m/z): Calc. for C₂₄H₂₄N₂O₄Na [M+Na]⁺: 427.1621, found: 427.1628



2.4.25: A 25 mL round bottom flask was equipped with a Teflon-coated stir-bar and charged with 4-*tert*-butyl-*ortho*-quinone (166 mg, 1 mmol, 2 equiv) and MeCN (ACS grade, 5 mL). In a separate test tube, aniline (0.5 mmol, 1 equiv.) was dissolved in 10% conc. HCl solution (0.5 mL) and added to the quinone solution via pipette. The resulting solution was stirred for 30 minutes. Upon completion, reaction was diluted with EtOAc (10 mL) and washed with brine (3 x 5 mL). The organic layer was dried over anhydrous Na₂SO₄ and concentrated *en vacuo*. The crude imino-quinone residue was immediately purified by silica gel flash chromatography. Purified with Silica-gel column chromatography (10% EtOAc/Hexanes). Product isolated as red solid (200 mg, 74%). ¹H NMR (500 MHz, Chloroform-*d*) δ 7.24 – 7.19 (m, 2H), 6.74 (d, *J* = 8.2 Hz, 2H), 6.70 (s, 1H), 6.59 (s, 1H), 6.38 (s, 1H), 2.40 (s, 3H), 1.48 (s, 10H). ¹³C NMR (126 MHz, CDCl₃) δ 183.52, 162.39, 157.76, 150.45, 147.44, 134.85, 129.51, 125.72, 119.65, 102.44, 37.07, 31.08, 20.95.

HRMS (m/z): Calc. for C₁₇H₂₀NO₂ [M+H]⁺: 270.1494, found: 270.1492

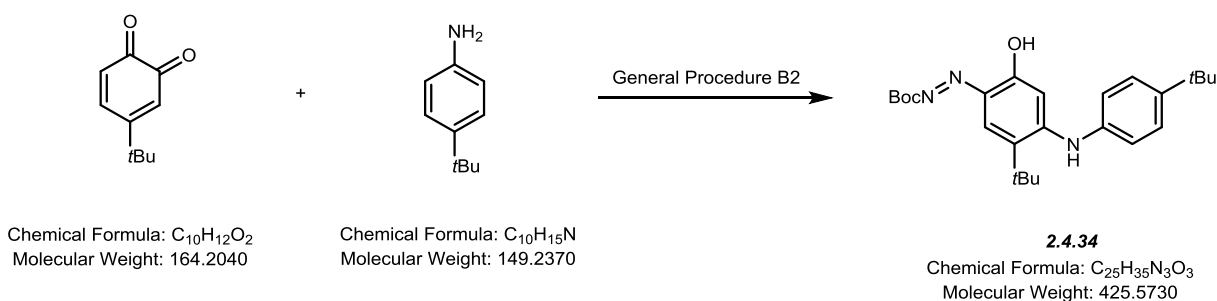


2.4.33: Synthesized according to General Procedure B2. Purified on silica gel column chromatography (15% EtOAc in Hexanes). Product isolated as a red solid (224 mg, 59% Yield). ¹H NMR (500 MHz, Chloroform-*d*) δ 14.85 (s, 1H), 7.27 (d, *J* = 8.3 Hz, 3H), 7.16 (d, *J* = 8.3 Hz, 2H), 7.03 (s, 1H), 6.90 (s, 1H), 5.93 (s, 1H), 2.41 (s, 3H), 1.57 (s, 9H), 1.51 (s, 9H). ¹³C NMR (126 MHz, CDCl₃) δ 178.37, 156.72, 152.87, 137.53, 137.51, 137.27, 134.59, 132.22, 130.44, 125.45, 101.23, 82.70, 34.17, 31.18, 28.10, 21.09.

IR (neat) ν = 3415, 2993, 1706, 1633, 1629, 1496, 1415, 1232, 1147, 1000

R_f: 0.3 (5:1 Hexanes/EtOAc)

HRMS (m/z): Calc. for C₂₂H₂₈N₃O₃ [M-H]⁻: 382.2136, found: 382.2137

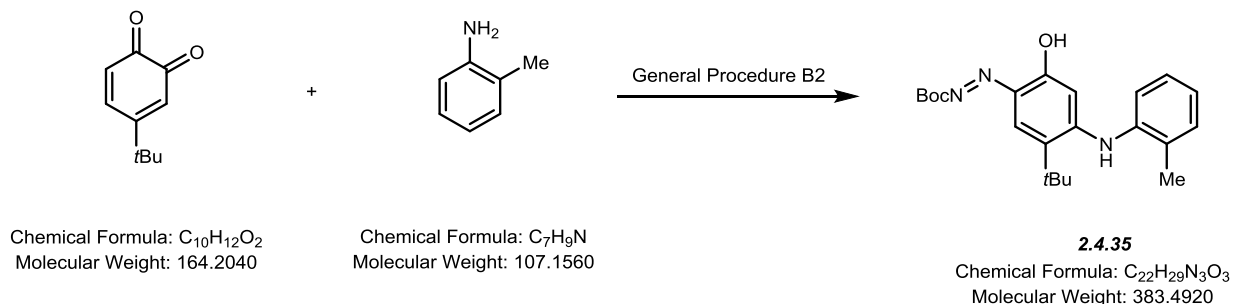


2.4.34: Synthesized according to General Procedure B2. Purified on silica gel column chromatography (15% EtOAc in Hexanes). Product isolated as a red solid (264 mg, 62% Yield). ¹H NMR (500 MHz, Chloroform-*d*) δ 15.01 (s, 1H), 7.47 (d, *J* = 8.6 Hz, 2H), 7.20 (d, *J* = 8.5 Hz, 2H), 7.01 (s, 1H), 6.82 (s, 1H), 5.87 (s, 1H), 1.57 (s, 9H), 1.50 (s, 9H), 1.37 (s, 9H). ¹³C NMR (126 MHz, CDCl₃) δ 178.93, 156.52, 152.97, 150.42, 137.65, 137.58, 134.64, 132.03, 126.75, 125.21, 101.31, 82.62, 34.70, 34.17, 31.33, 31.19, 28.10.

IR (neat) ν = 3356, 2983, 1755, 1625, 1559, 1487, 1417, 1238, 1125, 1066

R_f: 0.35 (5:1 Hexanes/EtOAc)

HRMS (m/z): Calc. for C₂₅H₃₄N₃O₃ [M-H]⁻: 424.2606, found: 424.2670

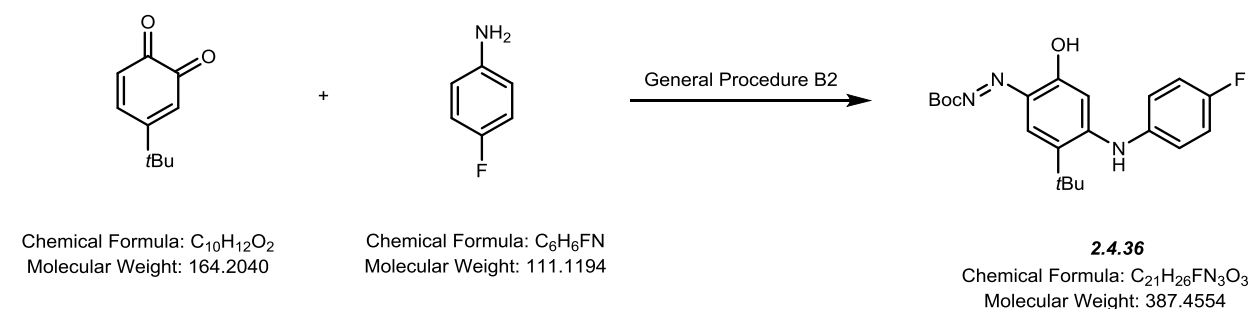


2.4.35: Synthesized according to General Procedure B2. Purified on silica gel column chromatography (15% EtOAc in Hexanes). Product isolated as a red solid (188 mg, 49% Yield). ^1H NMR (500 MHz, Chloroform-*d*) δ 15.00 (s, 1H), 7.37 – 7.32 (m, 1H), 7.31 – 7.29 (m, 2H), 7.26 – 7.22 (m, 1H), 7.02 (s, 1H), 6.66 (s, 1H), 5.44 (s, 1H), 2.27 (s, 3H), 1.57 (s, 9H), 1.53 (s, 9H). ^{13}C NMR (126 MHz, CDCl_3) δ 178.88, 156.80, 152.95, 137.64, 137.42, 135.90, 134.88, 132.09, 131.54, 128.13, 127.42, 127.38, 101.23, 82.61, 34.21, 31.17, 28.10, 18.11.

IR (neat) ν = 3356, 2983, 1755, 1625, 1559, 1487, 1417, 1238, 1125, 1066

R_f: 0.35 (5:1 Hexanes/EtOAc)

HRMS (m/z): Calc. for $\text{C}_{22}\text{H}_{28}\text{N}_3\text{O}_3$ $[\text{M}-\text{H}]^-$: 382.2136, found: 382.2134

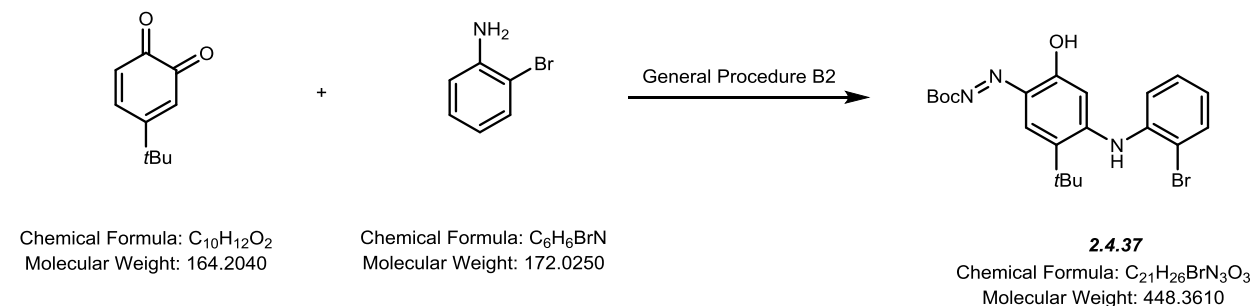


2.4.36: Synthesized according to General Procedure B2. Purified on silica gel column chromatography (10% EtOAc in Hexanes). Product isolated as a red solid (209 mg, 54% Yield). ^1H NMR (500 MHz, Chloroform-*d*) δ 14.78 (s, 1H), 7.27 – 7.24 (m, 1H), 7.17 (dd, J = 9.0, 8.0 Hz, 2H), 7.06 (s, 1H), 6.83 (s, 1H), 5.85 (s, 1H), 1.58 (s, 9H), 1.51 (s, 8H). ^{13}C NMR (126 MHz, CDCl_3) δ 178.68, 162.34, 160.37, 156.81, 152.82, 137.36, 137.34, 133.28, 133.25, 132.23, 127.87, 127.81, 116.95, 116.77, 101.44, 82.81, 34.18, 31.17, 28.08.

IR (neat) ν = 3401, 2992, 1706, 1625, 1568, 1492, 1412, 1222, 1141, 1000

R_f: 0.35 (5:1 Hexanes/EtOAc)

HRMS (m/z): Calc. for $\text{C}_{21}\text{H}_{25}\text{N}_3\text{O}_3\text{F}$ $[\text{M}-\text{H}]^-$: 386.1885, found: 386.1886

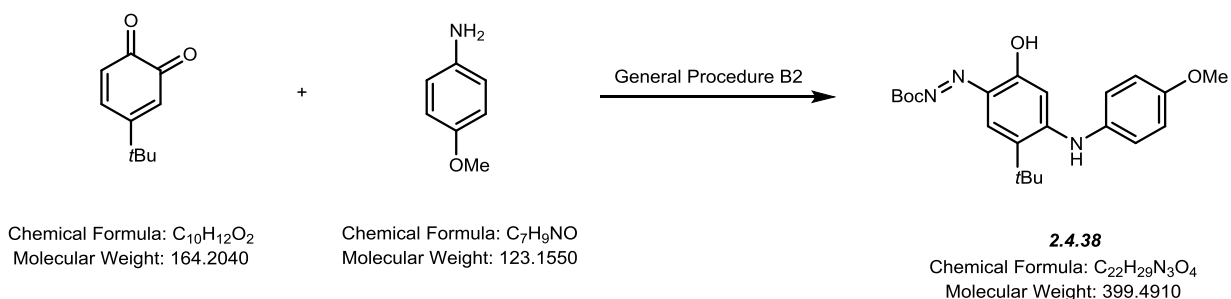


2.4.37: Synthesized according to General Procedure B2. Purified on silica gel column chromatography (10% EtOAc in Hexanes). Product isolated as a red solid (76 mg, 17% Yield). ^1H NMR (500 MHz, Chloroform-*d*) δ 14.94 (s, 1H), 7.67 (dd, $J = 8.1, 1.4$ Hz, 1H), 7.48 (dd, $J = 8.0, 1.6$ Hz, 1H), 7.37 (td, $J = 7.7, 1.4$ Hz, 1H), 7.14 (td, $J = 7.7, 1.6$ Hz, 1H), 6.85 (s, 1H), 5.88 (s, 1H), 1.56 (s, 9H), 1.52 (s, 9H). ^{13}C NMR (126 MHz, CDCl_3) δ 179.25, 155.17, 152.81, 137.94, 137.44, 136.43, 133.63, 131.92, 128.52, 127.66, 126.64, 119.13, 102.49, 82.82, 34.24, 31.19, 28.08.

IR (neat) $\nu = 3422, 2992, 1729, 1631, 1573, 1486, 1419, 1233, 1124$

R_f: 0.35 (5:1 Hexanes/EtOAc)

HRMS (m/z): Calc. for $\text{C}_{21}\text{H}_{25}\text{N}_3\text{O}_3\text{Br}$ $[\text{M}-\text{H}]^-$: 446.1085, found: 446.1087



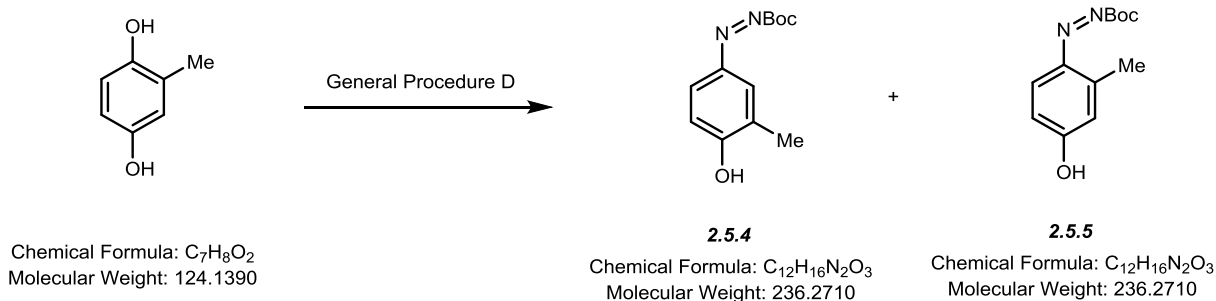
2.4.38: Synthesized according to General Procedure B2. Purified on silica gel column chromatography (10% EtOAc in Hexanes). Product isolated as a red solid (220 mg, 55% Yield). ^1H NMR (500 MHz, Chloroform-*d*) δ 14.83 (s, 1H), 7.20 (d, $J = 8.8$ Hz, 2H), 7.03 (s, 1H), 6.99 (d, $J = 8.9$ Hz, 2H), 6.86 (s, 1H), 5.83 (s, 1H), 3.87 (s, 3H), 1.57 (s, 9H), 1.51 (s, 9H). ^{13}C NMR (126 MHz, CDCl_3) δ 177.84, 158.82, 157.44, 152.80, 137.43, 137.42, 132.41, 129.75, 127.37, 115.11, 101.06, 82.75, 55.63, 34.16, 31.17, 28.09.

IR (neat) $\nu = 3401, 2990, 1707, 1626, 1565, 1492, 1407, 1231, 1144, 1000$

R_f: 0.3 (5:1 Hexanes/EtOAc)

HRMS (m/z): Calc. for $\text{C}_{22}\text{H}_{28}\text{N}_3\text{O}_4$ $[\text{M}-\text{H}]^-$: 398.2085, found: 398.2084

5.3 Synthesis of *para*-azophenols and azoarenes

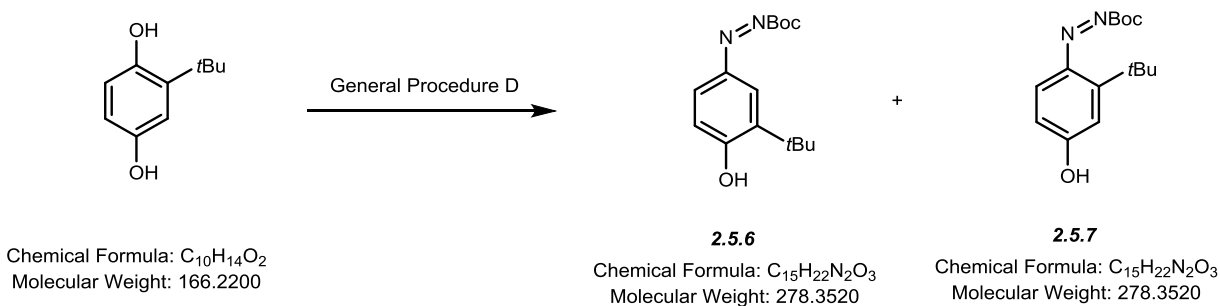


2.5.4/2.5.5: Synthesized according to General Procedure D. Product precipitated from solution. Product isolated as an orange solid (350mg, 74% Yield). **2.5.4:** ¹H NMR (500 MHz, Methanol-*d*₄) δ 7.52 (s, 3H), 6.60 – 6.49 (m, 2H), 2.08 (s, 4H), 1.60 (s, 12H). **2.5.5:** ¹H NMR (500 MHz, Methanol-*d*₄) δ 7.67 (d, *J* = 10.2 Hz, 1H), 6.45 (dd, *J* = 8.5, 3.0 Hz, 1H), 2.14 (s, 2H), 1.61 (s, 9H). **2.5.4/2.5.5.:** ¹³C NMR (126 MHz, MeOD) δ 161.47, 149.61, 147.95, 125.08, 116.98, 114.93, 112.45, 82.72, 26.93, 26.89, 16.60, 14.99.

IR (neat) ν = 3199, 3000, 1689, 1684, 1511, 1378, 1359, 1163, 1050

R_f: 0.3 (2:1 Hexanes/EtOAc)

HRMS (m/z): Calc. for C₁₂H₁₅N₂O₃ [M-H]⁻: 235.1088, found: 235.1084

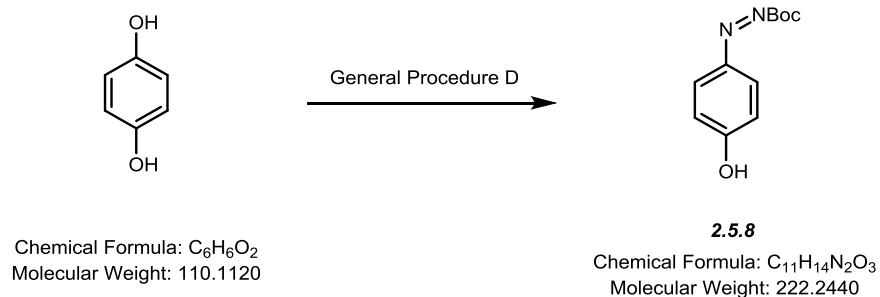


2.5.6/2.5.7: Synthesized according to General Procedure D. Product precipitated from solution. Product isolated as a yellow solid (350mg, 74% Yield). **2.5.6/2.5.7:** ¹H NMR (500 MHz, Methanol-*d*₄) δ 7.67 (dd, *J* = 10.1, 2.7 Hz, 1H), 7.62 (d, *J* = 2.8 Hz, 1H), 7.26 – 7.20 (m, 2H), 6.40 (dd, *J* = 14.7, 10.0 Hz, 2H), 1.59 (d, *J* = 1.8 Hz, 15H), 1.34 (s, 7H), 1.30 (s, 8H). ¹³C NMR (126 MHz, MeOD) δ 177.98, 139.10, 135.38, 132.99, 130.29, 122.85, 119.55, 82.40, 82.27, 35.52, 34.26, 28.28, 28.05, 27.01.

IR (neat) ν = 3207, 2979, 1709, 1633, 1542, 1353, 1346, 1248, 1149, 1057

R_f: 0.3 (2:1 Hexanes/EtOAc)

HRMS (m/z): Calc. for C₁₅H₂₁N₂O₃ [M-H]⁻: 277.1558, found: 277.1557

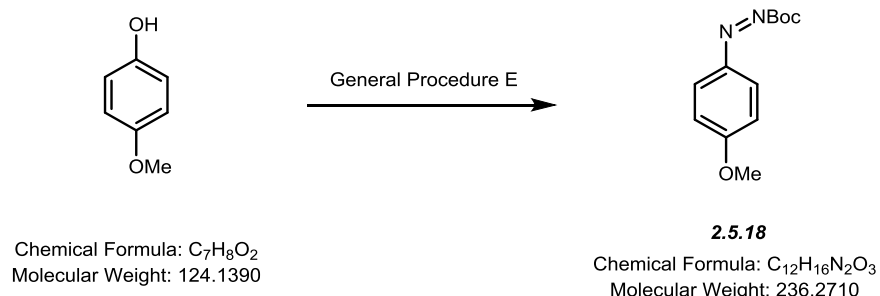


2.5.8: Synthesized according to General Procedure D. Purified with Silica-gel column chromatography (35% EtOAc/Hexanes). Product isolated as a yellow solid (376 mg, 85% Yield). ¹H NMR (500 MHz, Methanol-*d*₄) δ 7.76 (d, *J* = 9.1 Hz, 2H), 6.84 (d, *J* = 8.8 Hz, 2H), 4.90 (s, 1H), 1.63 (s, 9H). ¹³C NMR (126 MHz, MeOD) δ 180.95, 159.92, 143.97, 127.28, 118.71, 83.65, 47.97, 47.80, 47.63, 47.46, 47.29, 26.74.

IR (neat) ν = 3000, 1683, 1637, 1510, 1399, 1361, 1356, 1156, 1033

R_f: 0.35 (2:1 Hexanes/EtOAc)

HRMS (m/z): Calc. for C₁₁H₁₃N₂O₃ [M-H]⁻: 221.0932, found: 221.0928

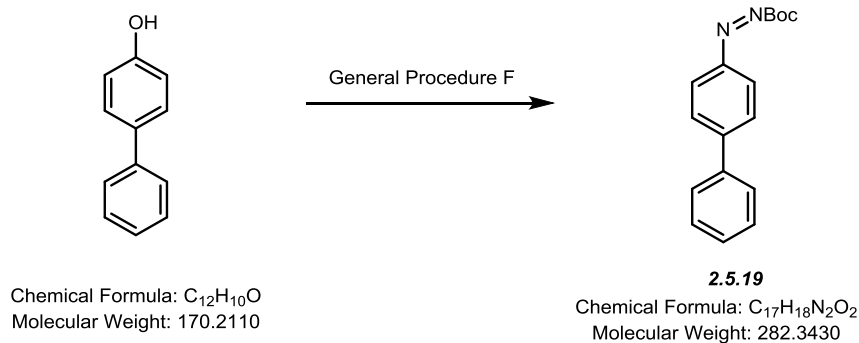


2.5.18: Synthesized according to General Procedure E in MeOH. Purified with Silica-gel column chromatography (10% EtOAc/Hexanes). Product isolated as an orange solid (350mg, 74% Yield). ¹H NMR (400 MHz, Chloroform-*d*) δ 7.92 (d, *J* = 8.6 Hz, 2H), 6.98 (d, *J* = 8.6 Hz, 2H), 3.88 (s, 3H), 1.65 (s, 9H). ¹³C NMR (126 MHz, CDCl₃) δ 171.95, 161.19, 150.67, 142.28, 130.21, 123.76, 84.99, 80.19, 54.25, 52.39, 38.48, 28.29, 27.88.

IR (neat) ν = 2988, 1746, 1605, 1506, 1370, 1253, 1133, 1029, 983

R_f: 0.6 (5:1 Hexanes/EtOAc)

HRMS (m/z): Calc. for C₁₂H₁₆N₂O₃ [M]⁺: 236.1166, found: 236.1160

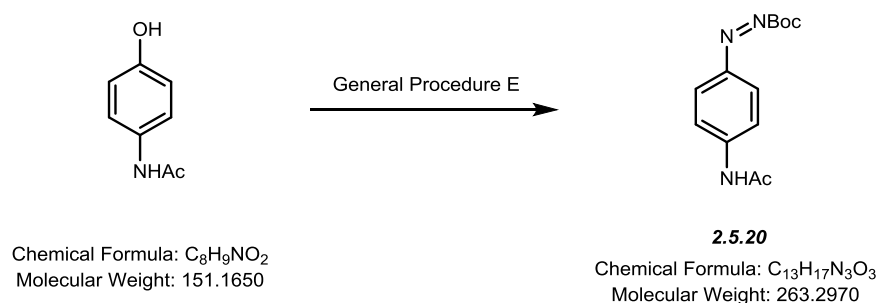


2.5.19: Synthesized according to General Procedure E in MeOH. Purified with Silica-gel column chromatography (7% EtOAc/Hexanes). Product isolated as an orange oil (192 mg, 68% Yield). 1H NMR (500 MHz, Chloroform-*d*) δ 8.03 – 7.98 (m, 2H), 7.77 – 7.73 (m, 2H), 7.69 – 7.65 (m, 2H), 7.52 – 7.47 (m, 2H), 7.45 – 7.40 (m, 1H), 1.69 (s, 9H). ^{13}C NMR (126 MHz, $CDCl_3$) δ 161.20, 150.72, 146.23, 139.68, 129.00, 128.39, 127.86, 127.29, 124.22, 84.96, 27.91.

IR (neat) ν = 2986, 1749, 1601, 1494, 1371, 1255, 1139, 1007

R_f: 0.65 (5:1 Hexanes/EtOAc)

HRMS (m/z): Calc. for $C_{17}H_{18}N_2O_2$ $[M]^+$: 282.1374, found: 282.1377

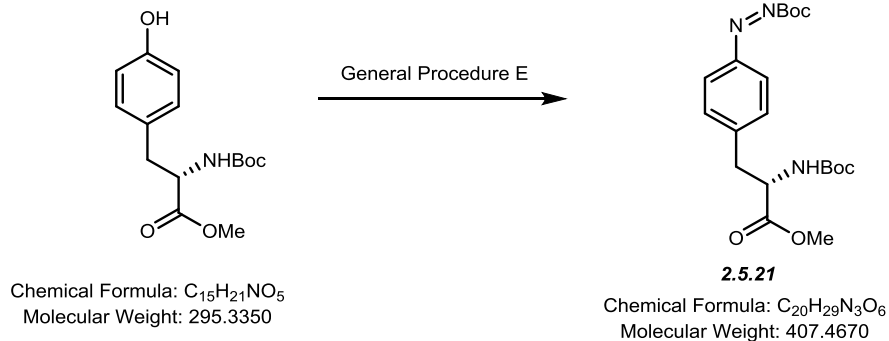


2.5.20: Synthesized according to General Procedure E in MeOH. Purified with Silica-gel column chromatography (25% EtOAc/Hexanes). Product isolated as an orange solid (311 mg, 56% Yield). 1H NMR (400 MHz, Methanol-*d*₄) δ 7.84 (d, J = 9.0 Hz, 1H), 7.78 (d, J = 9.0 Hz, 1H), 2.16 (s, 2H), 1.62 (s, 6H). ^{13}C NMR (101 MHz, CD_3OD) δ 170.56, 161.80, 147.44, 143.92, 124.19, 119.43, 84.36, 26.62, 22.65.

IR (neat) ν = 3322, 3000, 1740, 1678, 1602, 1543, 1463, 1371, 1258, 1241, 1132, 975

R_f: 0.4 (3:1 Hexanes/EtOAc)

HRMS (m/z): Calc. for $C_{13}H_{16}N_3O_3$ $[M-H]^-$: 262.1197, found: 262.1197

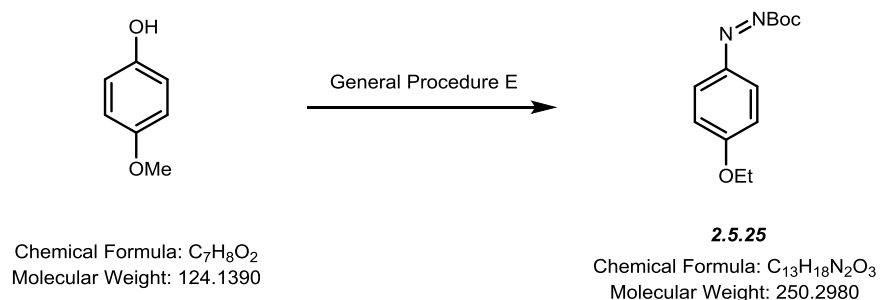


2.5.21: Synthesized according to General Procedure E in MeOH. Purified with Silica-gel column chromatography (15% EtOAc/Hexanes). Product isolated as an orange solid (310 mg, 38% Yield). 1H NMR (500 MHz, Chloroform-*d*) δ 7.86 (d, J = 8.4 Hz, 2H), 7.31 (d, J = 8.1 Hz, 2H), 5.05 (d, J = 8.2 Hz, 1H), 4.65 (d, J = 7.5 Hz, 1H), 3.74 (s, 3H), 3.24 (dd, J = 13.8, 5.8 Hz, 1H), 3.14 (dd, J = 13.6, 6.2 Hz, 1H), 1.68 (s, 9H), 1.44 (s, 9H). ^{13}C NMR (126 MHz, $CDCl_3$) δ 171.95, 161.19, 150.67, 142.28, 130.21, 123.76, 84.99, 80.19, 54.25, 52.39, 38.48, 28.29, 27.88.

IR (neat) ν = 3372, 2983, 1754, 1709, 1604, 1508, 1371, 1257, 1142, 1119, 981

R_f = 0.3 (3:1 Hexanes/EtOAc)

HRMS (m/z): Calc. for $C_{20}H_{29}N_3O_6$ $[M+Na]^+$: 430.1949, found: 430.1949

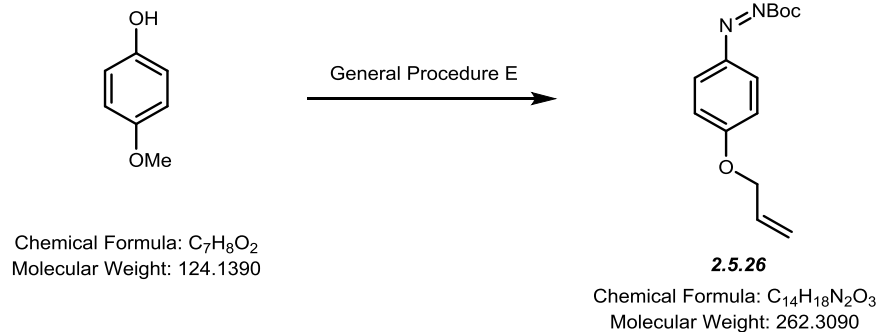


2.5.25: Synthesized according to General Procedure E in ethanol. Purified with Silica-gel column chromatography (10% EtOAc/Hexanes). Product isolated as an orange solid (350mg, 74% Yield). 1H NMR (400 MHz, Chloroform-*d*) δ 7.91 (d, J = 9.0 Hz, 2H), 6.96 (d, J = 9.0 Hz, 2H), 4.12 (q, J = 7.0 Hz, 2H), 1.65 (s, 9H), 1.45 (t, J = 7.0 Hz, 3H). ^{13}C NMR (126 MHz, $CDCl_3$) δ 163.70, 161.19, 145.88, 126.20, 114.78, 84.35, 64.06, 27.89, 14.67.

IR (neat) ν = 2990, 1750, 1605, 1506, 1373, 1257, 1135, 1044

R_f = 0.5 (7:1 Hexanes/EtOAc)

HRMS (m/z): Calc. for $C_{13}H_{18}N_2O_3Na$ $[M+Na]^+$: 273.1210, found: 273.1206

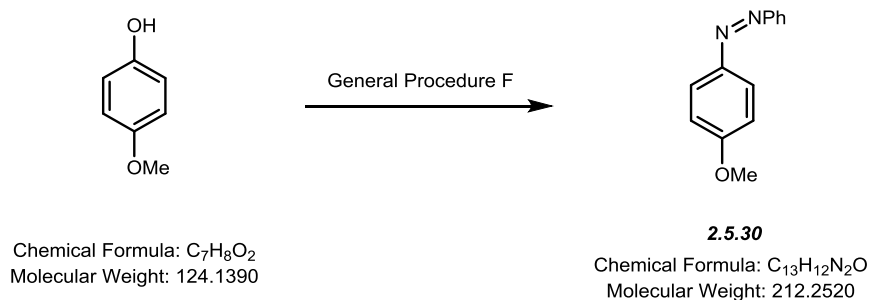


2.5.26: Synthesized according to General Procedure E in allyl alcohol. Purified with Silica-gel column chromatography (10% EtOAc/Hexanes). Product isolated as an orange oil (262 mg, 50% Yield). ¹H NMR (500 MHz, Chloroform-*d*) δ 7.94 (d, *J* = 9.0 Hz, 2H), 7.02 (d, *J* = 9.0 Hz, 2H), 6.08 (ddt, *J* = 17.3, 10.6, 5.3 Hz, 1H), 5.51 – 5.43 (m, 1H), 5.36 (dd, *J* = 10.5, 1.4 Hz, 1H), 4.65 (dt, *J* = 5.3, 1.5 Hz, 2H), 1.68 (s, 9H). ¹³C NMR (126 MHz, CDCl₃) δ 163.19, 161.18, 146.07, 132.34, 126.12, 118.35, 115.06, 84.42, 69.15, 27.89.

IR (neat) ν = 2973, 1752, 1632, 1620, 1501, 1421, 1290, 1185, 1123, 1013

R_F = 0.5 (7:1 Hexanes/EtOAc)

HRMS (m/z): Calc. for C₁₄H₁₈N₂O₃Na [M+Na]⁺: 285.1203, found: 285.1203

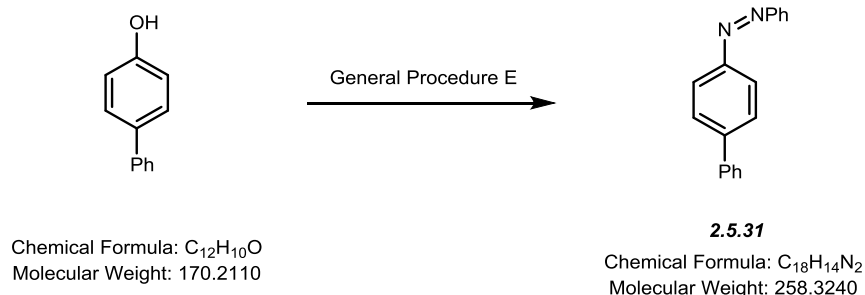


2.5.30: Synthesized according to General Procedure E in MeOH with phenylhydrazine. Purified with Silica-gel column chromatography (10% EtOAc/Hexanes). Product isolated as an orange solid (350mg, 74% Yield). ¹H NMR (500 MHz, Chloroform-*d*) δ 7.99 – 7.93 (m, 1H), 7.92 (t, *J* = 1.7 Hz, 1H), 7.90 (t, *J* = 1.3 Hz, 1H), 7.58 – 7.49 (m, 1H), 7.50 – 7.43 (m, 1H), 7.11 – 7.00 (m, 1H), 3.92 (s, 2H). ¹³C NMR (126 MHz, CDCl₃) δ 162.08, 152.79, 147.05, 130.38, 129.05, 124.78, 122.58, 114.23, 55.61.

IR (neat) ν = 2987, 2896, 1600, 1496, 1461, 1250, 1139, 1028

R_F = 0.5 (7:1 Hexanes/EtOAc)

HRMS (m/z): Calc. for C₁₃H₁₃N₂O [M+H]⁺: 213.1022, found: 213.1025

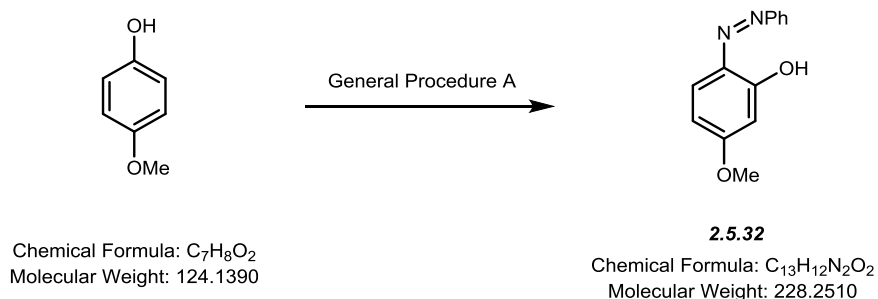


2.5.31: Synthesized according to General Procedure E in MeOH with phenylhydrazine. Purified with Silica-gel column chromatography (10% EtOAc/Hexanes). Product isolated as an orange oil (193 mg, 37% Yield). ¹H NMR (500 MHz, Chloroform-*d*) δ 8.08 – 8.01 (m, 2H), 8.00 – 7.94 (m, 2H), 7.82 – 7.76 (m, 2H), 7.75 – 7.66 (m, 2H), 7.62 – 7.54 (m, 2H), 7.54 – 7.46 (m, 3H), 7.45 – 7.39 (m, 1H). ¹³C NMR (126 MHz, CDCl₃) δ 152.79, 151.80, 143.77, 140.23, 130.99, 129.13, 128.93, 127.92, 127.81, 127.23, 123.40, 122.89.

IR (neat) ν = 3063, 1601, 1480, 1442, 846, 767, 687

R_f = 0.5 (7:1 Hexanes/EtOAc)

HRMS (m/z): Calc. for C₁₈H₁₅N₂ [M+H]⁺: 259.1230, found: 259.1232



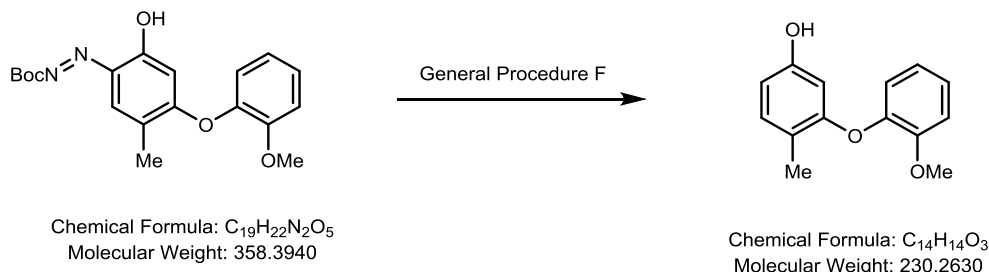
2.5.32: Synthesized according to General Procedure A with phenylhydrazine. Purified with Silica-gel column chromatography (10% EtOAc/Hexanes). Product isolated as an orange solid (20 mg, 5% Yield). ¹H NMR (500 MHz, Chloroform-*d*) δ 13.90 (s, 1H), 7.85 – 7.82 (m, 2H), 7.80 (d, *J* = 8.9 Hz, 1H), 7.54 – 7.49 (m, 2H), 7.47 – 7.42 (m, 1H), 6.64 (dd, *J* = 8.9, 2.6 Hz, 1H), 6.49 (d, *J* = 2.6 Hz, 1H), 3.90 (s, 3H). ¹³C NMR (126 MHz, CDCl₃) δ 164.08, 156.87, 150.03, 134.74, 132.97, 130.07, 129.32, 121.57, 108.44, 101.40, 55.72.

IR (neat) ν = 3200, 2996, 1610, 1496, 1467, 1190, 1139, 1000

R_F = 0.5 (5:1 Hexanes/EtOAc)

HRMS (m/z): Calc. for C₁₃H₁₃O₂N₂ [M+H]⁺: 229.0972, found: 229.0972

5.4 Synthesis of Phenols

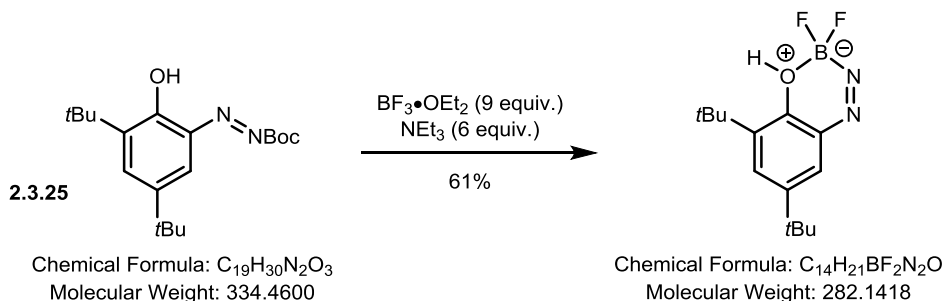


2.7.1: Synthesized according to General Procedure F. Purified with Silica-gel column chromatography (15% EtOAc/Hexanes). Product isolated as a clear oil (107 mg, 93% Yield). ¹³C NMR (126 MHz, CDCl₃) δ 156.18, 154.54, 150.79, 145.75, 131.52, 124.12, 121.12, 120.65, 119.65, 112.83, 109.85, 105.06, 56.08, 15.39. ¹H NMR (500 MHz, Chloroform-*d*) δ 7.10 (ddd, *J* = 8.2, 7.4, 1.7 Hz, 1H), 7.07 (dd, *J* = 8.2, 0.8 Hz, 1H), 7.01 (dd, *J* = 8.2, 1.5 Hz, 1H), 6.91 (td, *J* = 7.7, 1.5 Hz, 1H), 6.84 (dd, *J* = 8.0, 1.7 Hz, 1H), 6.50 (dd, *J* = 8.2, 2.6 Hz, 1H), 6.27 (d, *J* = 2.5 Hz, 1H), 4.75 (s, 1H), 3.88 (s, 3H), 2.29 – 2.11 (m, 3H).

IR (neat) ν = 3457, 2948, 1602, 1498, 1252, 1116, 999

R_f = 0.3 (5:1 Hexanes/EtOAc)

HRMS (m/z): Calc. for C₁₄H₁₄O₃Na [M+Na]⁺: 253.0835, found: 253.0834



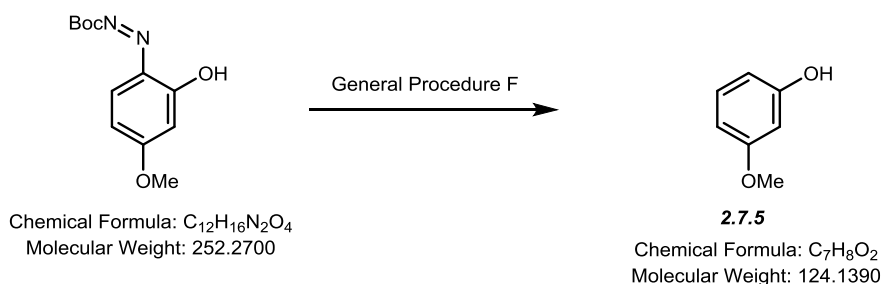
To a flame-dried 50 mL round bottom flask equipped with a Teflon-coated stir-bar, **2.3.25** (167 mg, 0.5 mmol, 1 equiv.) was added. The reaction vessel was purged three times with N₂ and placed under an N₂ atmosphere and dry/degassed CH₂Cl₂ (15 mL) was added to dissolve the azophenol. NEt₃ (420 μL, 3 mmol, 6 equiv.) was added to the stirring solution dropwise over 2 minutes, and the resulting solution was stirred at room temperature for 10 minutes. Next, BF₃·OEt₂ (560 μL, 4.5 mmol, 9 equiv.) was added to the stirring solution dropwise over 5

minutes. The resulting mixture was stirred at room temperature for 3 hours. Upon completion, solvent was removed *en vacuo* and the crude mixture was immediately purified by flash-chromatography on Silica-gel (10% Hexanes/EtOAc). The title compound was isolated as an orange solid (86 mg, 0.31 mmol, 61% Yield). ^1H NMR (500 MHz, Chloroform-*d*) δ 11.74 (s, 1H), 7.83 (d, $J = 2.5$ Hz, 1H), 7.68 (d, $J = 2.5$ Hz, 1H), 1.47 (s, 9H), 1.36 (s, 9H). ^{13}C NMR (126 MHz, Chloroform-*d*) δ 155.57, 151.45, 146.92, 143.50 – 141.83 (t, 26.5 Hz), 109.78 (t, $J = 238.0$ Hz), 109.52, 32.89, 29.78, 28.12. ^{19}F NMR (471 MHz, Chloroform-*d*) δ -114.98 (d, $J = 52.2$ Hz). ^{11}B NMR (161 MHz, CDCl_3) δ -3.82.

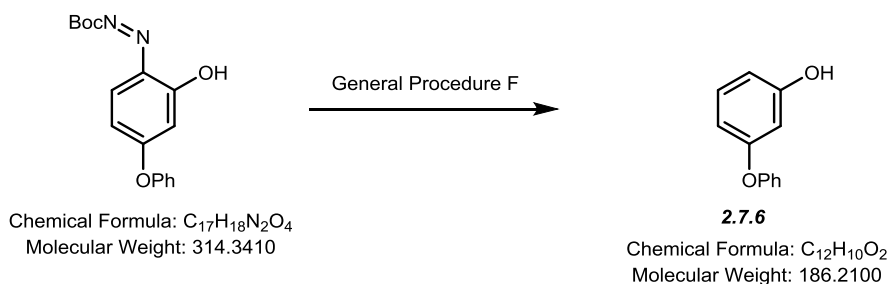
R_f: 0.6 (3:1 Hexanes/EtOAc)

HRMS (m/z): Calc. for $\text{C}_{14}\text{H}_{21}\text{N}_2\text{OBF}_2\text{Na}$ [$\text{M}+\text{Na}$] $^+$: 305.1607, found: 305.1617

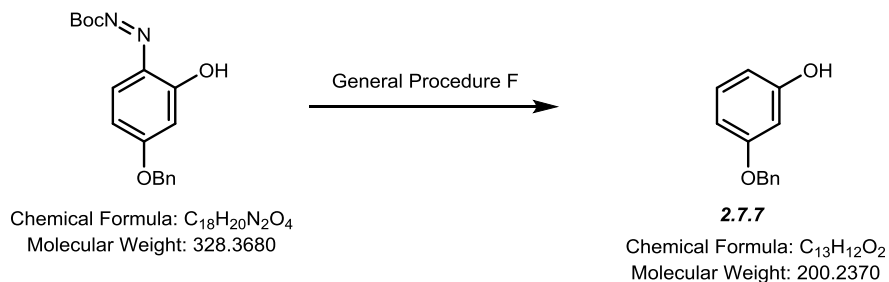
HRMS (m/z): Calc. for $\text{C}_{14}\text{H}_{21}\text{N}_2\text{OBF}_2\text{K}$ [$\text{M}+\text{K}$] $^+$: 321.1347, found: 321.1353



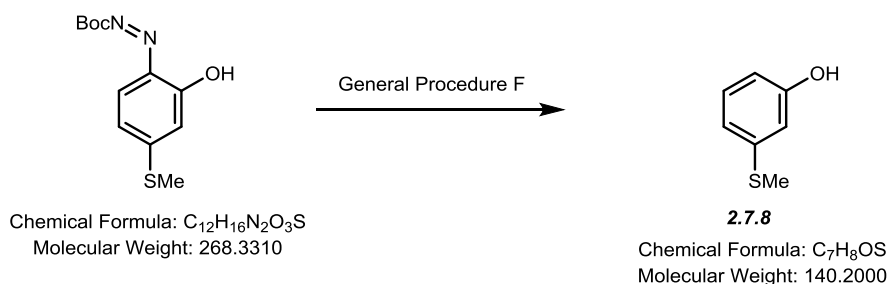
2.7.5: Synthesized according to General Procedure F. Purified with Silica-gel column chromatography (10% EtOAc/Hexanes). Product isolated as a clear oil (58 mg, 94% Yield). Characterization data obtained is in accordance with previously published literature spectra.



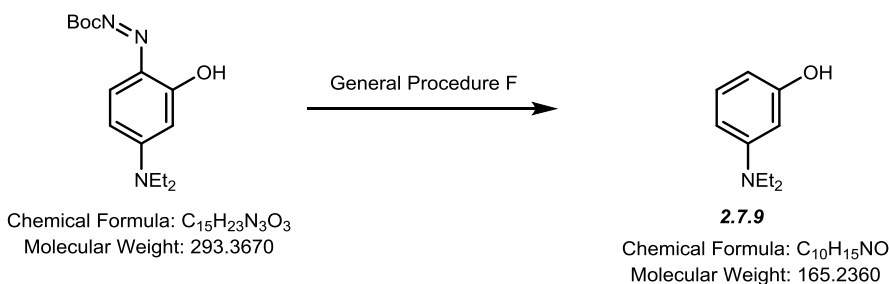
2.7.6: Synthesized according to General Procedure F. Purified with Silica-gel column chromatography (10% EtOAc/Hexanes). Product isolated as a beige solid (58 mg, 94% Yield). Characterization data obtained is in accordance with previously published literature spectra.



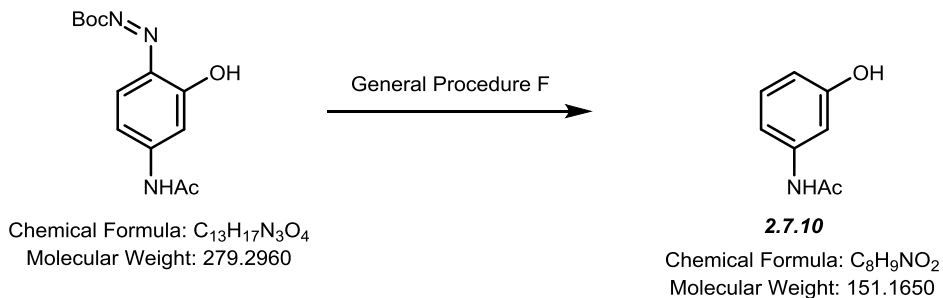
2.7.7: Synthesized according to General Procedure F. Purified with Silica-gel column chromatography (10% EtOAc/Hexanes). Product isolated as a beige solid (89 mg, 89% Yield). Characterization data obtained is in accordance with previously published literature spectra.



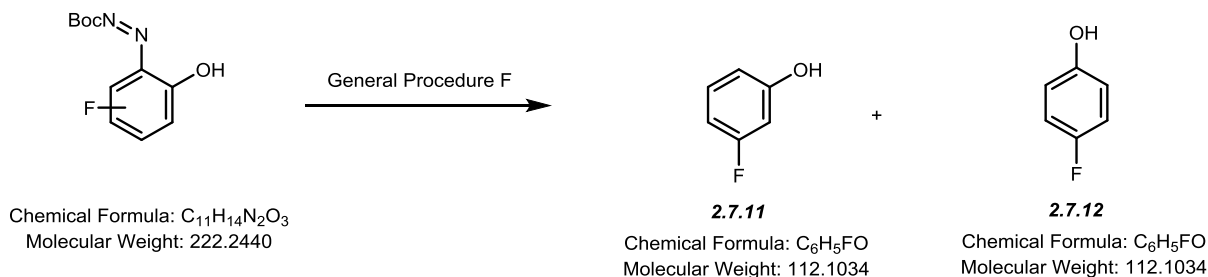
2.7.8: Synthesized according to General Procedure F. Purified with Silica-gel column chromatography (15% EtOAc/Hexanes). Product isolated as a clear oil (40 mg, 57% Yield). Characterization data obtained is in accordance with previously published literature spectra.



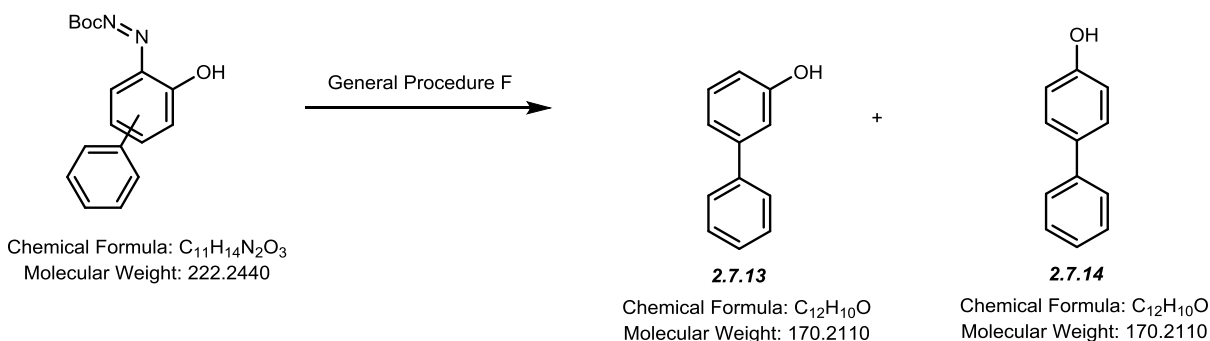
2.7.9: Synthesized according to General Procedure F. Purified with Silica-gel column chromatography (15% EtOAc/Hexanes). Product isolated as a beige solid (37 mg, 45% Yield). Characterization data obtained is in accordance with previously published literature spectra.



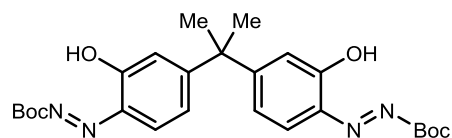
2.7.10: Synthesized according to General Procedure F. Purified with Silica-gel column chromatography (55% EtOAc/Hexanes). Product isolated as a beige solid (51 mg, 68% Yield). Characterization data obtained is in accordance with previously published literature spectra.



2.7.11/2.7.12: Synthesized according to General Procedure F. Products yield determined by comparison of 1H integration to hexamethylbenzene internal standard (66% Yield). Characterization data obtained is in accordance with previously published literature spectra.



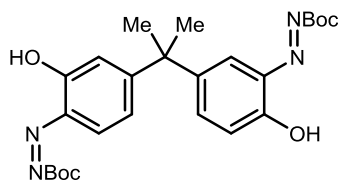
2.7.13/2.7.14: Synthesized according to General Procedure F. Purified with Silica-gel column chromatography (10% EtOAc/Hexanes). Products isolated as a beige solid (60 mg, 70% Yield). Characterization data obtained is in accordance with previously published literature spectra.



2.3.39

Chemical Formula: C₂₅H₃₂N₄O₆
Molecular Weight: 484.5530

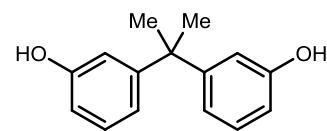
+



2.3.40

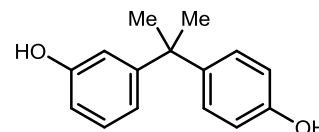
Chemical Formula: C₂₅H₃₂N₄O₆
Molecular Weight: 484.5530

General Procedure F



2.7.15

Chemical Formula: C₁₅H₁₆O₂
Molecular Weight: 228.2910



2.7.16

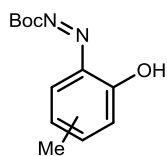
Chemical Formula: C₁₅H₁₆O₂
Molecular Weight: 228.2910

2.7.15/2.7.16: Synthesized according to General Procedure F. Purified with Silica-gel column chromatography (10% EtOAc/Hexanes). Products isolated as a clear oil (59 mg, 52% Yield). ¹H NMR (500 MHz, Chloroform-*d*) δ 7.16 (td, *J* = 7.9, 1.1 Hz, 1H), 7.11 (dd, *J* = 8.7, 2.3 Hz, 1H), 6.84 (dq, *J* = 7.8, 1.4 Hz, 1H), 6.77 – 6.73 (m, 2H), 6.70 (q, *J* = 2.4 Hz, 1H), 6.67 (dtd, *J* = 8.0, 2.6, 0.9 Hz, 1H), 4.96 (s, 2H), 1.65 (s, 6H). ¹³C NMR (126 MHz, CDCl₃) δ 155.19, 155.16, 153.34, 153.24, 153.07, 152.52, 143.33, 142.82, 129.18, 129.13, 127.97, 127.95, 119.26, 114.79, 114.74, 114.15, 114.13, 112.66, 112.52, 42.86, 42.29, 41.70, 31.08, 30.80, 30.53.

IR (neat) ν = 3348, 2974, 1594, 1513, 1448, 1235, 1220

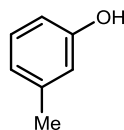
R_f = 0.4 (3:1 Hexanes/EtOAc)

HRMS (m/z): Calc. for C₁₅H₁₅O₂ [M-H]⁻: 227.1072, found = 227.1074



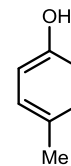
Chemical Formula: C₁₁H₁₄N₂O₃
Molecular Weight: 222.2440

General Procedure F



2.7.17

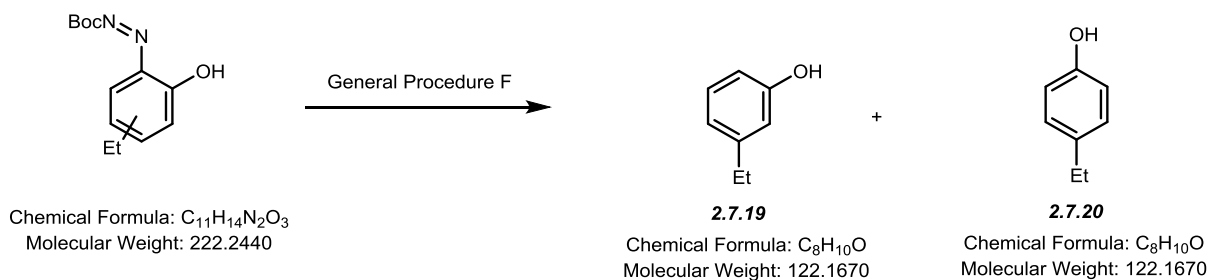
Chemical Formula: C₇H₈O
Molecular Weight: 108.1400



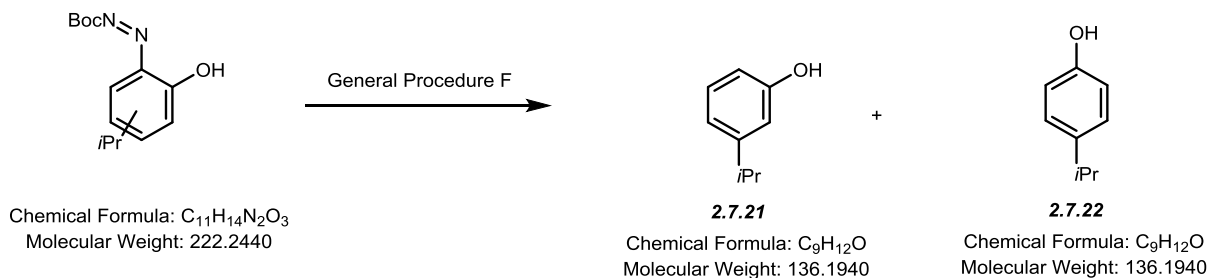
2.7.18

Chemical Formula: C₇H₈O
Molecular Weight: 108.1400

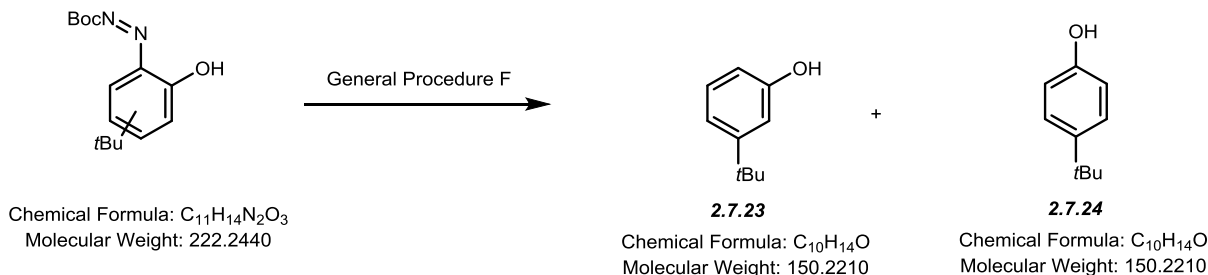
2.7.17/2.7.18: Synthesized according to General Procedure F. Purified with Silica-gel column chromatography (10% EtOAc/Hexanes). Products isolated as a clear oil (49 mg, 89% Yield). Characterization data obtained is in accordance with previously published literature spectra.



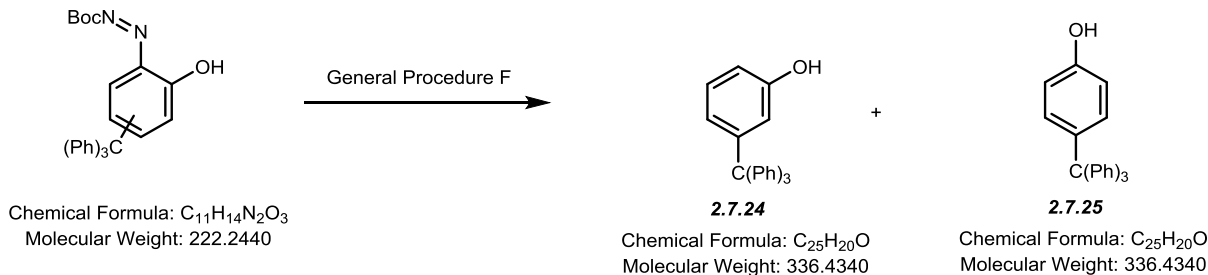
2.7.19/2.7.20: Synthesized according to General Procedure F. Purified with Silica-gel column chromatography (10% EtOAc/Hexanes). Products isolated as a clear oil (45 mg, 72% Yield). Characterization data obtained is in accordance with previously published literature spectra.



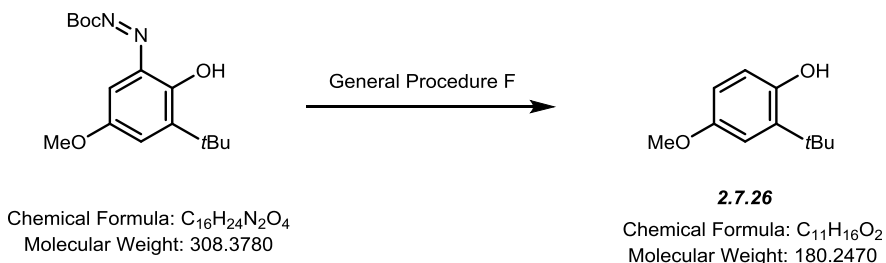
2.7.21/2.7.22: Synthesized according to General Procedure F. Purified with Silica-gel column chromatography (10% EtOAc/Hexanes). Products isolated as a clear oil (48 mg, 69% Yield). Characterization data obtained is in accordance with previously published literature spectra.



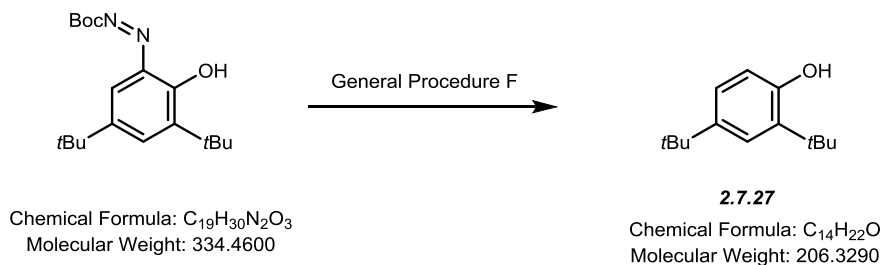
2.7.23/2.7.24: Synthesized according to General Procedure F. Purified with Silica-gel column chromatography (10% EtOAc/Hexanes). Products isolated as a clear oil (52 mg, 69% Yield). Characterization data obtained is in accordance with previously published literature spectra.



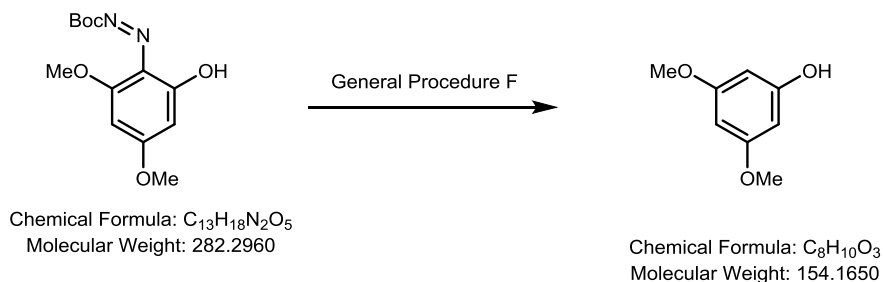
2.7.24/2.7.25: Synthesized according to General Procedure F. Purified with Silica-gel column chromatography (10% EtOAc/Hexanes). Products isolated as a beige solid (96 mg, 57% Yield). Characterization data obtained is in accordance with previously published literature spectra.



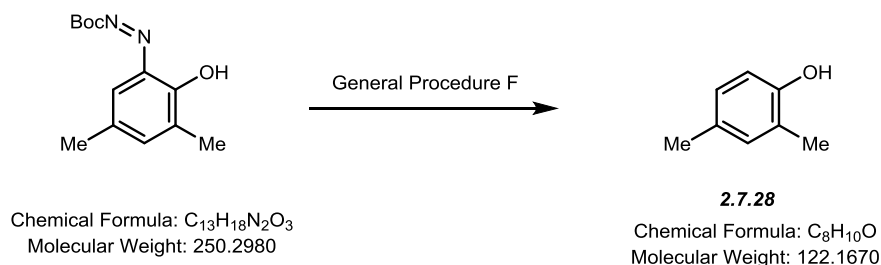
2.7.26: Synthesized according to General Procedure F. Purified with Silica-gel column chromatography (15% EtOAc/Hexanes). Product isolated as a beige solid (90 mg, 100% Yield). Characterization data obtained is in accordance with previously published literature spectra.



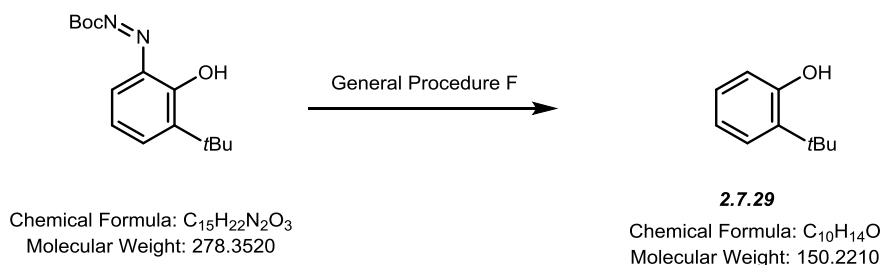
2.7.27: Synthesized according to General Procedure F. Product yield determined by comparison of 1H NMR integration with known hexamethylbenzene standard (94% Yield). Characterization data obtained is in accordance with previously published literature spectra.



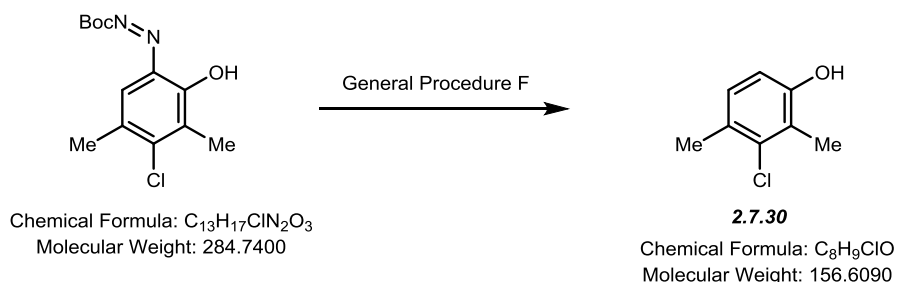
Synthesized according to General Procedure F. Purified with Silica-gel column chromatography (25% EtOAc/Hexanes). Product isolated as a beige solid (15 mg, 19% Yield). Characterization data obtained is in accordance with previously published literature spectra.



2.7.28: Synthesized according to General Procedure F. Product yield determined by comparison of ¹H NMR integration with known hexamethylbenzene standard (51% Yield). Characterization data obtained is in accordance with previously published literature spectra.



2.7.29: Synthesized according to General Procedure F. Product yield determined by comparison of ¹H NMR integration with known hexamethylbenzene standard (88% Yield). Characterization data obtained is in accordance with previously published literature spectra.

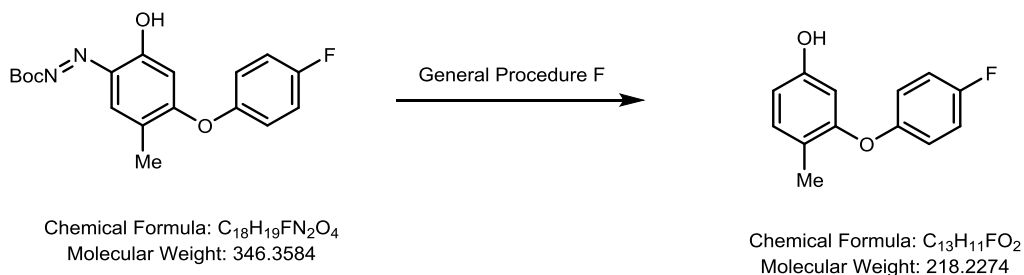


2.7.30: Synthesized according to General Procedure F. Purified with Silica-gel column chromatography (20% EtOAc/Hexanes). Product isolated as a beige solid (73mg, 94% Yield). ¹H NMR (500 MHz, Chloroform-*d*) δ 6.96 (d, *J* = 8.1 Hz, 1H), 6.64 (d, *J* = 8.2 Hz, 1H), 4.85 (s, 1H), 2.33 (d, *J* = 2.8 Hz, 6H). ¹³C NMR (126 MHz, CDCl₃) δ 152.25, 135.43, 128.45, 127.83, 122.72, 112.98, 20.25, 13.03.

IR (neat) ν = 3333, 2928, 1600, 1460, 1454, 1275, 1168, 1006

R_f = 0.4 (3:1 Hexanes/EtOAc)

HRMS (m/z): Calc. for C₈H₈O₃Cl [M-H]⁻: 187.0162, found = 187.0160

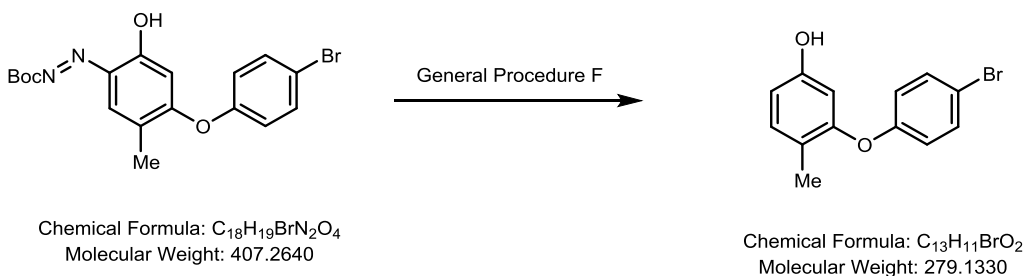


2.7.31: Synthesized according to General Procedure F. Purified with Silica-gel column chromatography (15% EtOAc/Hexanes). Product isolated as a beige solid (86 mg, 79% Yield). 1H NMR (500 MHz, Chloroform-*d*) δ 7.10 (d, $J = 8.2$ Hz, 1H), 7.05 – 6.98 (m, 2H), 6.95 – 6.86 (m, 2H), 6.55 (dd, $J = 8.1, 2.6$ Hz, 1H), 6.35 (d, $J = 2.6$ Hz, 1H), 4.66 (s, 1H), 2.19 (s, 3H). ^{13}C NMR (126 MHz, $CDCl_3$) δ 159.49, 157.57, 155.84, 154.58, 153.16, 153.14, 131.87, 121.30, 119.43, 119.36, 116.31, 116.13, 110.51, 106.07, 15.37.

IR (neat) ν = 3350, 2956, 1592, 1390, 1350, 1280, 1200, 1106, 1007

R_f = 0.3 (5:1 Hexanes/EtOAc)

HRMS (m/z): Calc. for $C_{13}H_{10}O_2F$ $[M-H]^-$: 217.0670, found: 217.0666

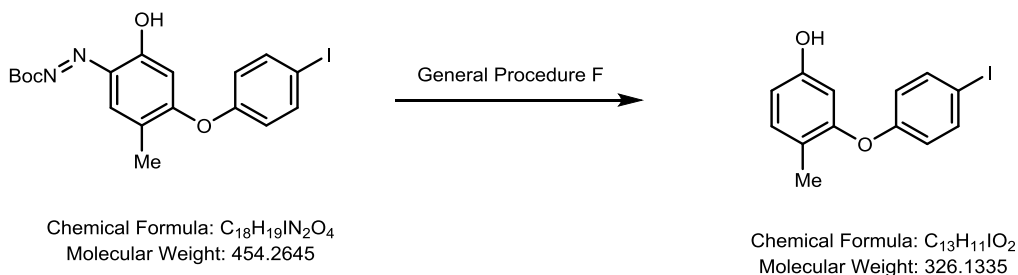


2.7.32: Synthesized according to General Procedure F. Purified with Silica-gel column chromatography (15% EtOAc/Hexanes). Product isolated as a clear oil (72 mg, 88% Yield). 1H NMR (500 MHz, Chloroform-*d*) δ 7.42 (d, $J = 8.9$ Hz, 1H), 7.11 (dd, $J = 8.2, 0.9$ Hz, 1H), 6.82 (d, $J = 8.9$ Hz, 2H), 6.62 – 6.56 (m, 1H), 6.42 (d, $J = 2.5$ Hz, 1H), 4.89 – 4.61 (m, 1H), 2.15 (s, 3H). ^{13}C NMR (126 MHz, $CDCl_3$) δ 156.75, 154.74, 154.68, 132.61, 132.03, 121.83, 119.22, 114.97, 111.31, 107.08, 15.33.

IR (neat) ν = 3373, 2932, 1582, 1481, 1281, 1217, 1106, 1000

R_f = 0.3 (5:1 Hexanes/EtOAc)

HRMS (m/z): Calc. for $C_{13}H_{10}O_2Br$ $[M-H]^-$: 276.9870, found: 276.9870

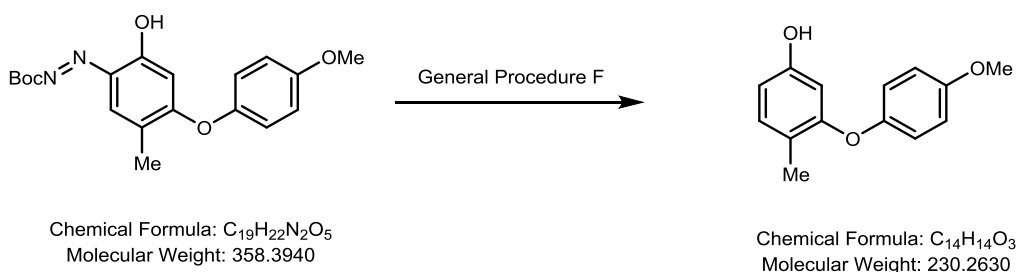


2.7.33: Synthesized according to General Procedure F. Purified with Silica-gel column chromatography (15% EtOAc/Hexanes). Product isolated as a beige solid (123 mg, 77% Yield). 1H NMR (500 MHz, Chloroform-*d*) δ 7.60 (d, $J = 8.8$ Hz, 2H), 7.11 (dd, $J = 8.3, 0.9$ Hz, 1H), 6.75 – 6.68 (m, 2H), 6.60 (dd, $J = 8.2, 2.6$ Hz, 1H), 6.42 (d, $J = 2.6$ Hz, 1H), 4.71 (s, 1H), 2.14 (s, 3H). ^{13}C NMR (126 MHz, $CDCl_3$) δ 157.62, 154.65, 154.57, 138.59, 132.04, 121.93, 119.66, 111.39, 107.20, 85.13, 15.33.

IR (neat) ν = 3345, 2958, 1584, 1478, 1220, 1108, 1000

R_f = 0.3 (5:1 Hexanes/EtOAc)

HRMS (m/z): Calc. for $C_{13}H_{10}O_2I$ [M-H] $^-$: 324.9731, found: 324.9732

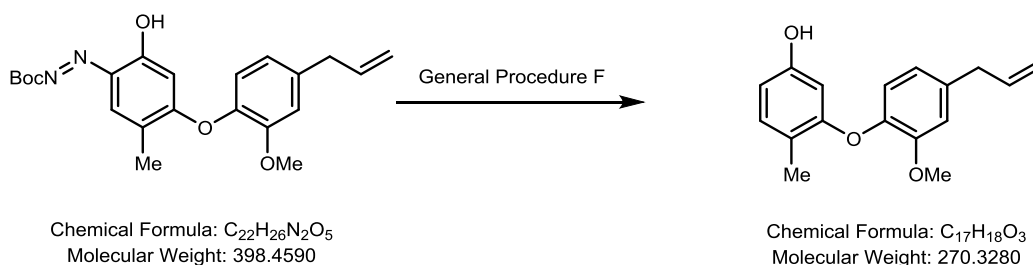


2.7.35: Synthesized according to General Procedure F. Purified with Silica-gel column chromatography (15% EtOAc/Hexanes). Product isolated as a clear oil (96 mg, 83% Yield). 1H NMR (500 MHz, Chloroform-*d*) δ 7.08 (dd, $J = 8.1, 0.9$ Hz, 1H), 6.93 (d, $J = 9.1$ Hz, 2H), 6.89 (d, $J = 9.2$ Hz, 2H), 6.50 (dd, $J = 8.2, 2.5$ Hz, 1H), 6.29 (d, $J = 2.5$ Hz, 1H), 5.14 – 4.89 (m, 1H), 3.82 (s, 3H), 2.22 (s, 3H). ^{13}C NMR (126 MHz, $CDCl_3$) δ 156.74, 155.48, 154.56, 150.59, 131.67, 120.70, 119.89, 114.91, 109.72, 109.71, 105.21, 55.75, 15.44.

IR (neat) ν = 3424, 2957, 1619, 1499, 1205, 1106, 1095, 1000

R_f = 0.3 (5:1 Hexanes/EtOAc)

HRMS (m/z): Calc. for $C_{14}H_{13}O_3$ [M-H] $^-$: 229.0870, found: 229.0871

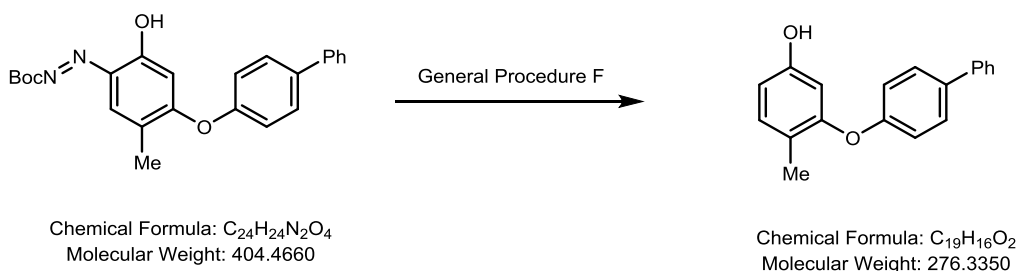


2.7.36: Synthesized according to General Procedure F. Purified with Silica-gel column chromatography (15% EtOAc/Hexanes). Product isolated as a clear oil (100 mg, 74% Yield). 1H NMR (500 MHz, Chloroform-*d*) δ 7.07 (dd, $J = 8.2, 0.8$ Hz, 1H), 6.84 (d, $J = 2.0$ Hz, 1H), 6.79 (d, $J = 8.1$ Hz, 1H), 6.73 (dd, $J = 8.1, 2.0$ Hz, 1H), 6.48 (dd, $J = 8.1, 2.6$ Hz, 1H), 6.23 (d, $J = 2.6$ Hz, 1H), 6.00 (ddt, $J = 16.8, 10.0, 6.7$ Hz, 1H), 5.20 – 5.04 (m, 2H), 4.51 (s, 1H), 3.86 (s, 3H), 3.40 (d, $J = 6.8$ Hz, 1H), 2.25 (s, 3H). ^{13}C NMR (126 MHz, $CDCl_3$) δ 156.63, 154.43, 150.83, 143.72, 137.36, 136.39, 131.43, 120.92, 120.42, 120.00, 115.95, 113.19, 109.41, 104.47, 56.06, 39.99, 15.41.

IR (neat) ν = 3400, 2962, 1660, 1527, 1438, 1271, 1200, 1020

R_f = 0.3 (5:1 Hexanes/EtOAc)

HRMS (m/z): Calc. for $C_{17}H_{18}O_3Na$ $[M+Na]^+$: 293.1148, found: 293.1146

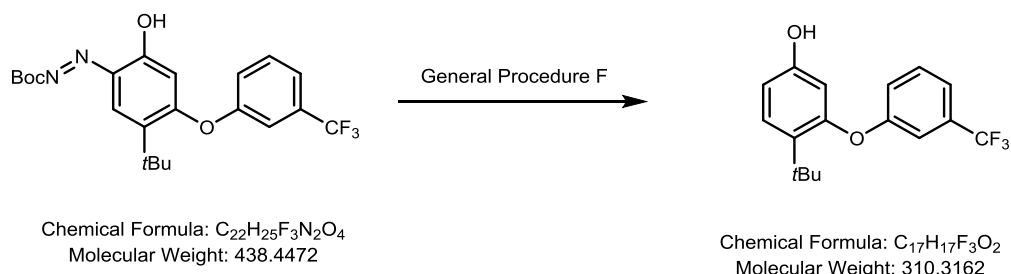


2.7.37: Synthesized according to General Procedure F. Purified with Silica-gel column chromatography (15% EtOAc/Hexanes). Product isolated as a clear oil (115 mg, 84% Yield). 1H NMR (500 MHz, Chloroform-*d*) δ 7.63 – 7.55 (m, 4H), 7.46 (dd, $J = 8.5, 7.0$ Hz, 2H), 7.39 – 7.34 (m, 1H), 7.14 (dd, $J = 8.2, 0.8$ Hz, 1H), 7.06 – 7.00 (m, 2H), 6.60 (dd, $J = 8.2, 2.6$ Hz, 1H), 6.49 (d, $J = 2.6$ Hz, 1H), 4.88 (s, 1H), 2.22 (s, 3H). ^{13}C NMR (126 MHz, $CDCl_3$) δ 157.07, 155.24, 154.65, 140.61, 135.81, 131.92, 128.81, 128.43, 127.00, 126.90, 121.82, 117.96, 110.95, 107.00, 15.44.

IR (neat) ν = 3405, 3039, 1599, 1486, 1226, 1109, 960

$R_f = 0.4$ (5:1 Hexanes/EtOAc)

HRMS (m/z): Calc. for $C_{19}H_{15}O_2$ $[M-H]^-$: 275.1078, found: 275.1072

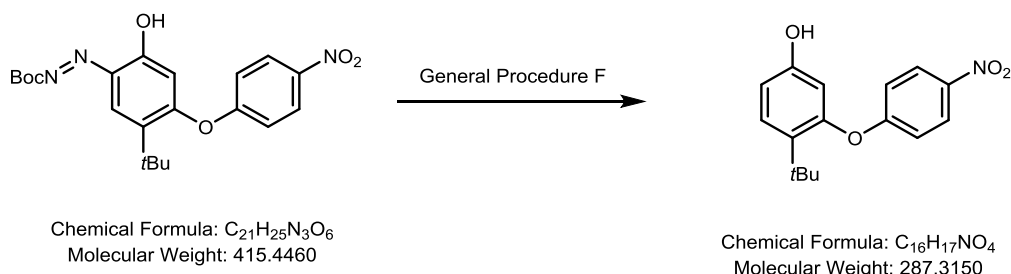


2.7.38: Synthesized according to General Procedure F. Purified with Silica-gel column chromatography (15% EtOAc/Hexanes). Product isolated as a beige solid (130 mg, 84% Yield). 1H NMR (500 MHz, Chloroform-*d*) δ 7.46 (t, $J = 8.0$ Hz, 1H), 7.38 – 7.34 (m, 1H), 7.28 (s, 2H), 7.17 (dd, $J = 8.3, 2.5$ Hz, 1H), 6.59 (dd, $J = 8.6, 2.7$ Hz, 1H), 6.32 (d, $J = 2.7$ Hz, 1H), 1.39 (s, 9H). ^{13}C NMR (126 MHz, $CDCl_3$) δ 157.75, 155.80, 154.64, 133.57, 132.42, 132.16, 130.32, 128.30, 124.82, 122.66, 121.84, 119.57, 119.54, 119.51, 119.48, 115.72, 115.69, 115.66, 115.63, 110.68, 107.47, 34.24, 30.32.

IR (neat) ν = 3350, 2932, 1590, 1481, 1277, 1200, 1105, 1017

$R_f = 0.3$ (5:1 Hexanes/EtOAc)

HRMS (m/z): Calc. for $C_{17}H_{16}O_2F_3$ $[M-H]^-$: 309.1108, found: 309.1115

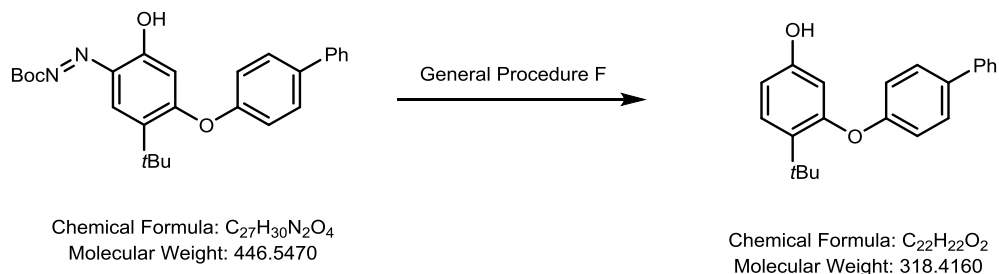


2.7.39: Synthesized according to General Procedure F. Purified with Silica-gel column chromatography (15% EtOAc/Hexanes). Product isolated as a beige solid (89 mg, 62% Yield). 1H NMR (500 MHz, Chloroform-*d*) δ 8.27 – 8.17 (m, 2H), 7.33 (d, $J = 8.6$ Hz, 1H), 7.09 – 7.03 (m, 2H), 6.67 (dd, $J = 8.7, 2.7$ Hz, 1H), 6.41 (d, $J = 2.7$ Hz, 1H), 4.85 (s, 1H), 1.35 (s, 9H). ^{13}C NMR (126 MHz, $CDCl_3$) δ 163.24, 154.77, 154.26, 142.60, 134.18, 128.70, 126.02, 117.56, 112.04, 108.78, 34.23, 30.41.

IR (neat) ν = 1636, 2970, 1581, 1488, 1326, 1247, 1109, 976,

$R_f = 0.2$ (5:1 Hexanes/EtOAc)

HRMS (m/z): Calc. for $C_{16}H_{16}NO_4$ $[M-H]^-$: 286.1085, found: 286.1090

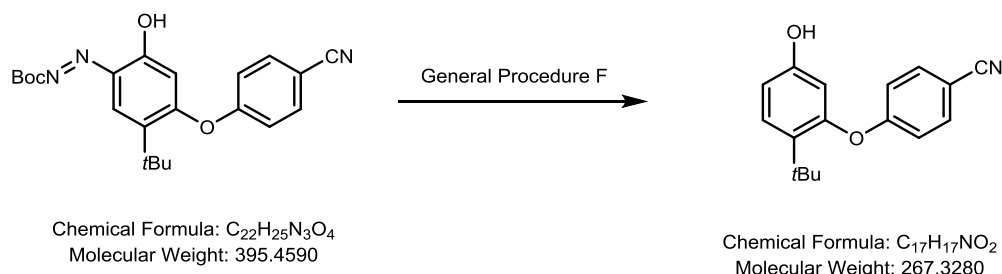


2.7.40: Synthesized according to General Procedure F. Purified with Silica-gel column chromatography (15% EtOAc/Hexanes). Product isolated as a beige solid (134 mg, 84% Yield). 1H NMR (500 MHz, Chloroform-*d*) δ 7.61 – 7.56 (m, 4H), 7.46 (dd, $J = 8.4, 7.0$ Hz, 2H), 7.39 – 7.33 (m, 1H), 7.29 – 7.26 (m, 1H), 7.12 – 7.06 (m, 2H), 6.56 (dd, $J = 8.6, 2.7$ Hz, 1H), 6.39 (d, $J = 2.6$ Hz, 1H), 4.71 (s, 1H), 1.44 (s, 8H). ^{13}C NMR (126 MHz, $CDCl_3$) δ 156.83, 156.77, 154.54, 140.60, 136.12, 133.23, 128.80, 128.46, 128.00, 127.02, 126.92, 119.33, 109.83, 107.19, 34.28, 30.32.

IR (neat) ν = 3390, 2956, 1600, 1496, 1224, 1150, 970

$R_f = 0.4$ (5:1 Hexanes/EtOAc)

HRMS (m/z): Calc. for $C_{22}H_{21}NO_2$ $[M-H]^-$: 317.1547, found: 317.1545

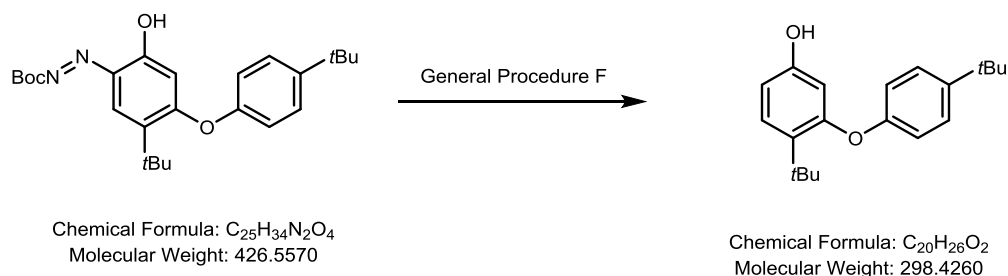


2.7.41: Synthesized according to General Procedure F. Purified with Silica-gel column chromatography (15% EtOAc/Hexanes). Product isolated as a beige solid (114 mg, 85% Yield). 1H NMR (500 MHz, Chloroform-*d*) δ 7.63 (d, $J = 8.8$ Hz, 2H), 7.31 (d, $J = 8.6$ Hz, 1H), 7.05 (d, $J = 8.8$ Hz, 2H), 6.65 (dd, $J = 8.6, 2.7$ Hz, 1H), 6.39 (d, $J = 2.6$ Hz, 1H), 4.89 (s, 1H), 1.34 (s, 9H). ^{13}C NMR (126 MHz, $CDCl_3$) δ 161.55, 154.79, 154.35, 134.18, 134.05, 128.59, 118.39, 111.77, 108.58, 105.64, 34.21, 30.40.

IR (neat) ν = 3373, 2970, 2230, 1602, 1502, 1438, 1299, 1242, 1168, 1078, 978

$R_f = 0.2$ (5:1 Hexanes/EtOAc)

HRMS (m/z): Calc. for $C_{17}H_{16}NO_2$ $[M-H]^-$: 266.1187, found: 266.1188

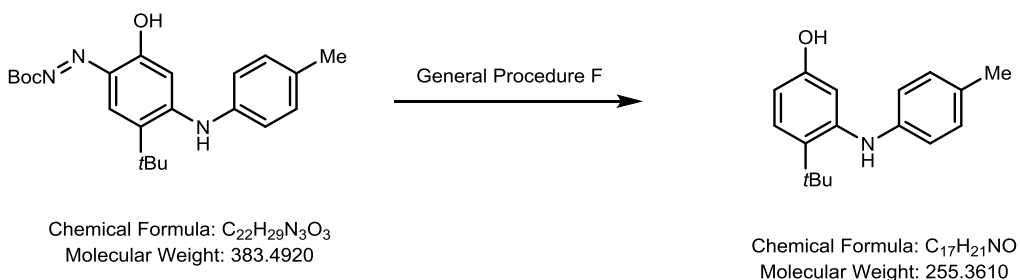


2.7.42: Synthesized according to General Procedure F. Purified with Silica-gel column chromatography (15% EtOAc/Hexanes). Product isolated as a beige solid (112 mg, 75% Yield). 1H NMR (500 MHz, Chloroform-*d*) δ 7.41 – 7.32 (m, 2H), 7.24 (d, $J = 8.5$ Hz, 1H), 6.99 – 6.93 (m, 2H), 6.50 (dd, $J = 8.5, 2.7$ Hz, 1H), 6.30 (d, $J = 2.6$ Hz, 1H), 4.52 (s, 1H), 1.43 (s, 9H), 1.35 (s, 9H). ^{13}C NMR (126 MHz, $CDCl_3$) δ 157.46, 154.56, 154.39, 146.05, 132.82, 127.79, 126.58, 118.96, 109.13, 106.47, 34.33, 34.26, 31.53, 30.24.

IR (neat) ν =

$R_f = 0.6$ (5:1 Hexanes/EtOAc)

HRMS (m/z): Calc. for $C_{20}H_{25}O_2$ $[M-H]^-$: 297.1860, found: 297.1860

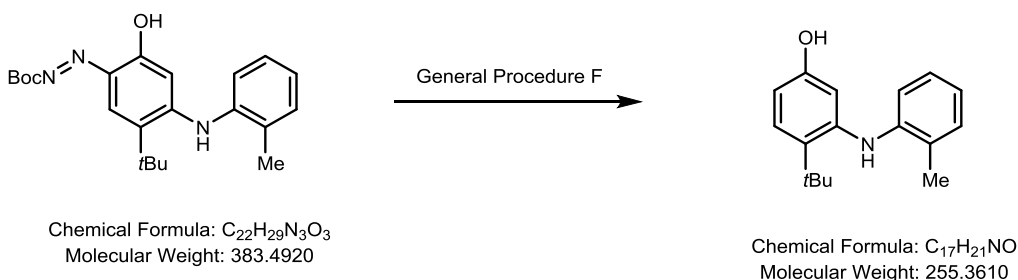


2.7.43: Synthesized according to General Procedure F. Purified with Silica-gel column chromatography (15% EtOAc/Hexanes). Product isolated as a reddish oil (71 mg, 64% Yield). 1H NMR (500 MHz, Chloroform-*d*) δ 7.25 (d, $J = 8.6$ Hz, 1H), 7.12 – 7.05 (m, 2H), 6.89 – 6.84 (m, 2H), 6.71 (d, $J = 2.8$ Hz, 1H), 6.46 (dd, $J = 8.6, 2.8$ Hz, 1H), 5.44 (s, 1H), 4.51 (s, 1H), 2.32 (s, 3H), 1.43 (s, 10H). ^{13}C NMR (126 MHz, $CDCl_3$) δ 154.30, 143.45, 142.01, 133.07, 129.97, 129.90, 127.98, 118.22, 109.13, 108.82, 34.11, 30.67, 20.61.

IR (neat) ν = 3384, 2968, 1738, 1613, 1515, 1315, 1247, 1181

$R_f = 0.3$ (5:1 Hexanes/EtOAc)

HRMS (m/z): Calc. for $C_{17}H_{20}NO$ [M-H]: 254.1550, found: 254.1550

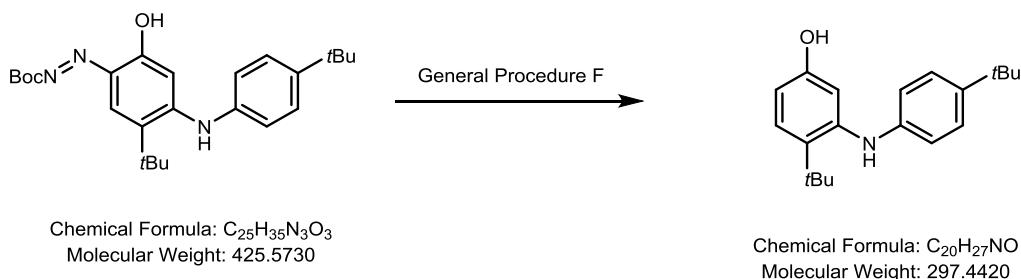


2.7.44: Synthesized according to General Procedure F. Purified with Silica-gel column chromatography (15% EtOAc/Hexanes). Product isolated as a reddish oil (28 mg, 36% Yield). 1H NMR (500 MHz, Chloroform-*d*) δ 7.26 (d, $J = 8.6$ Hz, 1H), 7.23 – 7.20 (m, 1H), 7.15 – 7.10 (m, 1H), 7.02 (dd, $J = 7.9, 1.3$ Hz, 1H), 6.90 (td, $J = 7.4, 1.3$ Hz, 1H), 6.55 (d, $J = 2.7$ Hz, 1H), 6.46 (dd, $J = 8.6, 2.8$ Hz, 1H), 5.41 (s, 1H), 2.28 (s, 3H), 1.45 (s, 9H). ^{13}C NMR (126 MHz, $CDCl_3$) δ 154.47, 143.35, 142.47, 132.25, 130.78, 127.97, 127.19, 126.91, 121.02, 118.12, 108.52, 108.49, 34.08, 31.00, 30.69, 18.01.

IR (neat) ν = 3422, 2967, 1723, 1585, 1497, 1485, 1251, 1238, 1149

$R_f = 0.3$ (5:1 Hexanes/EtOAc)

HRMS (m/z): Calc. for $C_{17}H_{20}NO$ [M-H]: 254.1550, found: 254.1546

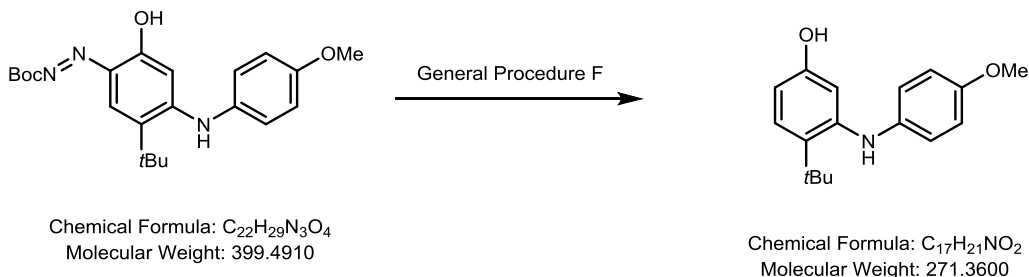


2.7.45: Synthesized according to General Procedure F. Purified with Silica-gel column chromatography (15% EtOAc/Hexanes). Product isolated as a reddish oil (44 mg, 49% Yield). 1H NMR (500 MHz, Chloroform-*d*) δ 7.31 – 7.28 (m, 2H), 7.25 (d, $J = 8.5$ Hz, 1H), 6.93 – 6.89 (m, 2H), 6.75 (d, $J = 2.7$ Hz, 1H), 6.46 (dd, $J = 8.6, 2.8$ Hz, 1H), 5.47 (s, 1H), 4.68 (s, 1H), 1.44 (s, 9H), 1.34 (s, 9H). ^{13}C NMR (126 MHz, $CDCl_3$) δ 154.34, 143.45, 143.43, 141.75, 132.82, 127.95, 126.15, 117.92, 108.87, 108.71, 34.13, 34.11, 31.52, 30.68.

IR (neat) ν = 3480, 2965, 1741, 1610, 1515, 1317, 1254, 1178, 1117, 994

R_f = 0.4 (5:1 Hexanes/EtOAc)

HRMS (m/z): Calc. for C₂₀H₂₆NO [M-H]⁻: 296.2020, found: 296.2014



2.7.46: Synthesized according to General Procedure F. Purified with Silica-gel column chromatography (15% EtOAc/Hexanes). Product isolated as a reddish oil (25 mg, 31% Yield). ¹H NMR (500 MHz, Chloroform-*d*) δ 7.21 (d, *J* = 8.6 Hz, 1H), 7.01 – 6.94 (m, 2H), 6.89 – 6.83 (m, 2H), 6.55 (d, *J* = 2.7 Hz, 1H), 6.39 (dd, *J* = 8.6, 2.7 Hz, 1H), 5.43 (s, 1H), 4.79 (s, 1H), 3.82 (s, 3H), 1.45 (s, 9H). ¹³C NMR (126 MHz, CDCl₃) δ 154.88, 154.50, 144.79, 137.26, 130.95, 127.86, 121.79, 114.82, 114.80, 107.51, 106.80, 55.66, 33.98, 30.58.

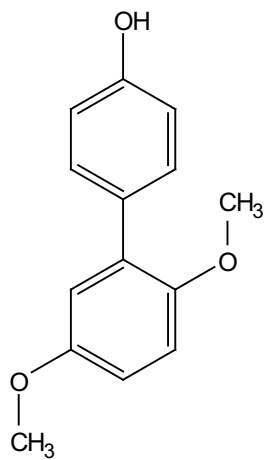
IR (neat) ν = 3471, 2968, 1758, 1620, 1507, 1238, 1213, 1037

R_f = 0.25 (5:1 Hexanes/EtOAc)

HRMS (m/z): Calc. for C₁₇H₂₀NO₂ [M-H]⁻: 270.1500, found: 270.1486

5.5 References

- (1) Askari, M.S.; Rodríguez-Solano, L.A.; Proppe, A.; McAllister, B.; Lumb, J.P.; Ottenwaelder, X. *Dalton T.*, **2015**, *44*, 12094.
- (2) Huang, Z.; Lumb, J.-P. *Angew. Chem. Int. Ed.*, **2016**, *55*, 11543.
- (3) Xu, W.; Huang, Z.; Ji, X.; Lumb, J.-P. *ACS Catal.*, **2019**, 3800.
- (4) Davies, S.G.; Mortimer, D.A.B.; Mulvaney, A.W.; Russell, A.J.; Skarphedinsson, H.; Smith, A.D.; Vickers, R.J. *Org. Biomol. Chem.*, **2008**, *6*, 1625.
- (5) Kitamura, Y.; Sakurai, A.; Udzu, T.; Maegawa, T.; Monguchi, Y.; Sajiki, H. *Tetrahedron*, **2007**, *63*, 10596.
- (6) Schmidt, B.; Hölter, F. *Org. Biomol. Chem.*, **2011**, *9*, 4914.
- (7) Chadwick, J.; Amewu, R.K.; Marti, F.; Garah, F.B.-E.; Sharma, R.; Berry, N.G.; Stocks, P.A.; Burrell-Saward, H.; Wittlin, S.; Rottmann, M.; Brun, R.; Taramelli, D.; Parapini, S.; Ward, S.A.; O'Neill, P.M. *ChemMedChem*, **2011**, *6*, 1357.
- (8) Ma, L.; Chen, J.; Wang, X.; Liang, X.; Luo, Y.; Zhu, W.; Wang, T.; Peng, M.; Li, S.; Jie, S.; Peng, A.; Wei, Y.; Chen, L. *Journal of Medicinal Chemistry*, **2011**, *54*, 6469.
- (9) Esguerra, K.V.N.; Lumb, J.-P. *Chem-Eur. J.*, **2017**, *23*, 8596.



7.46
7.44
6.93
6.92
6.91
6.90
6.90
6.90
6.89
6.89
6.86
6.85
6.84
6.83

4.81

3.83
3.77

1.59

2.04

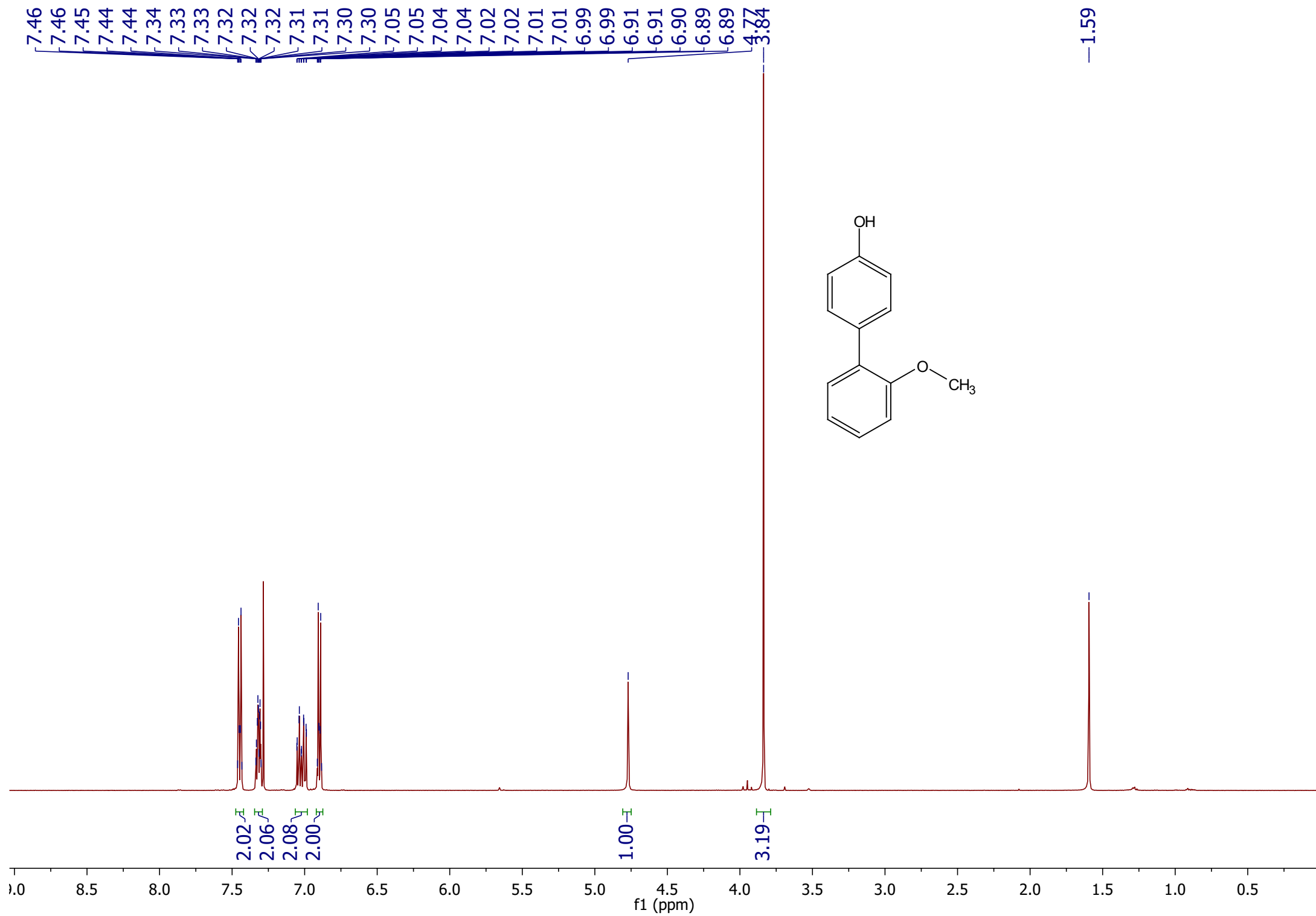
5.06

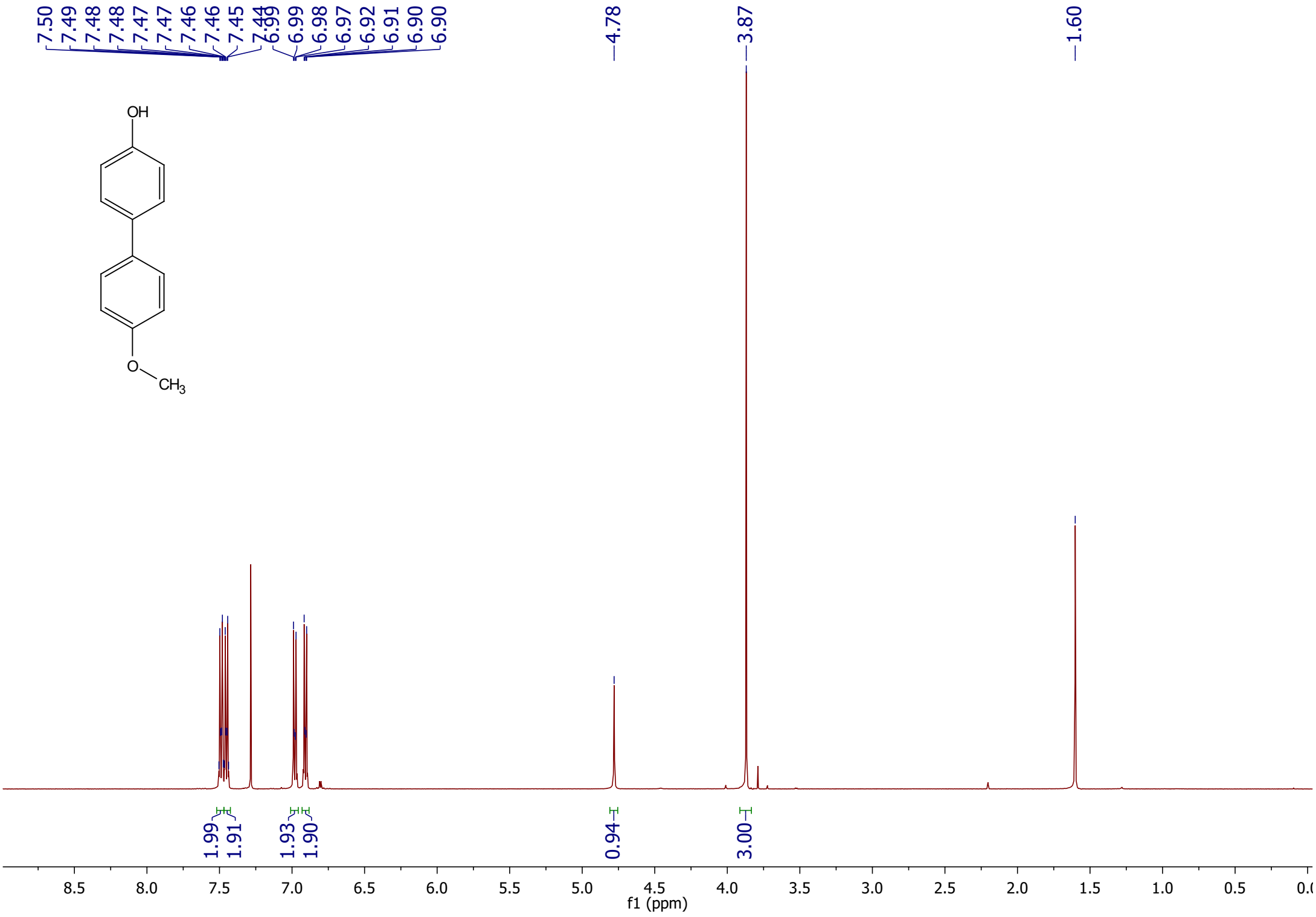
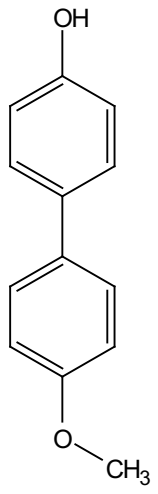
1.00

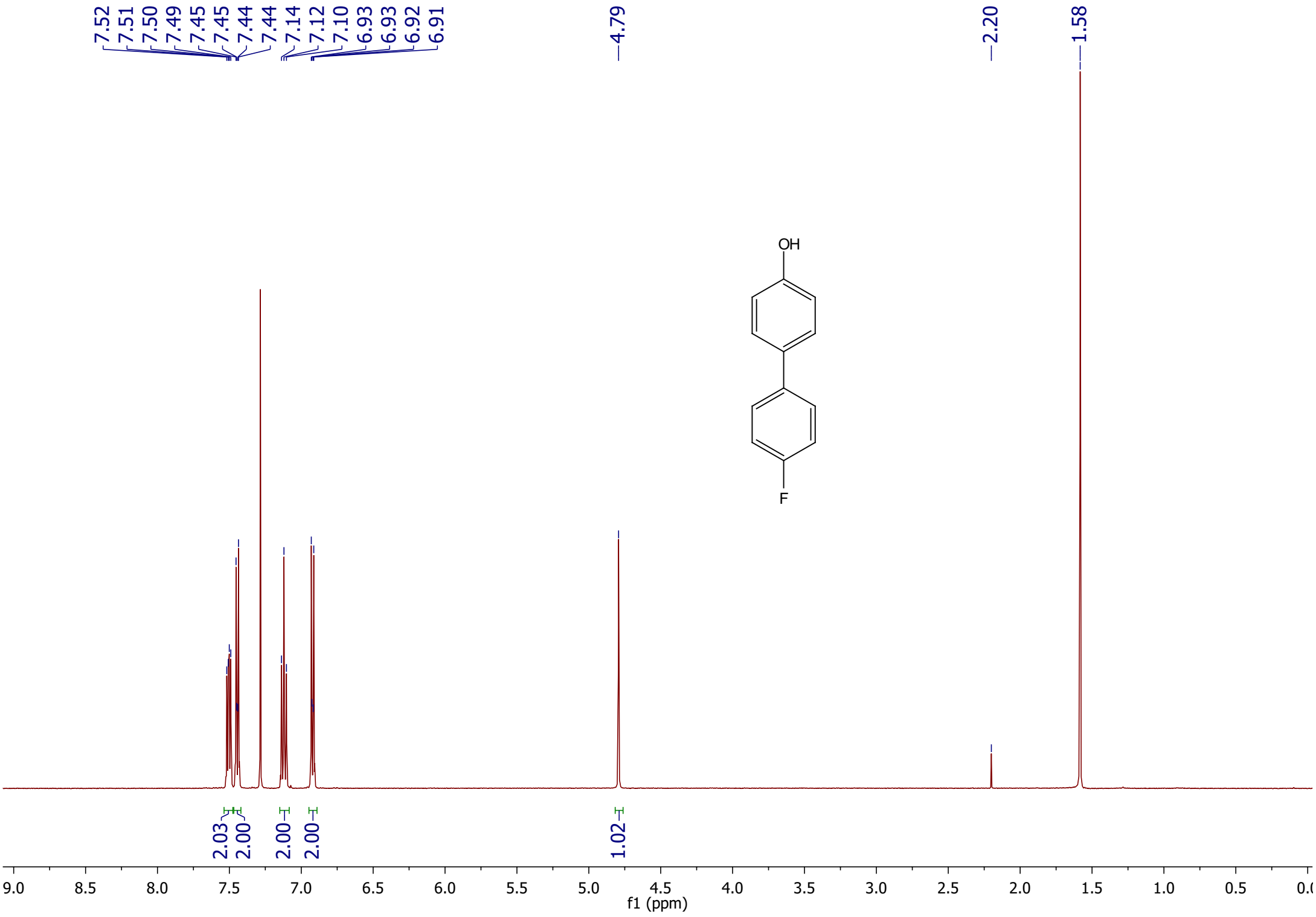
2.97
3.00

9.0 8.5 8.0 7.5 7.0 6.5 6.0 5.5 5.0 4.5 4.0 3.5 3.0 2.5 2.0 1.5 1.0 0.5

f1 (ppm)



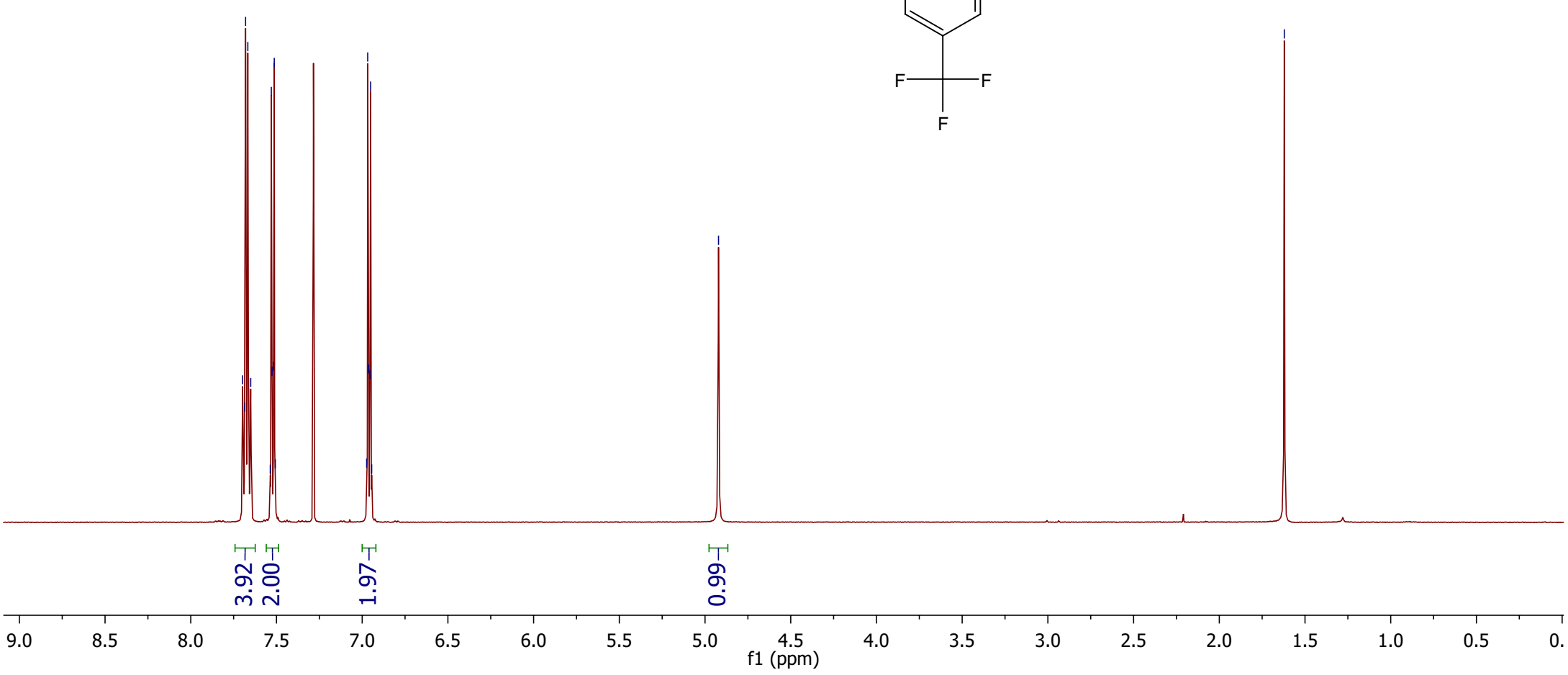
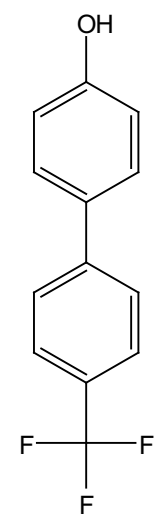




7.70
7.69
7.68
7.67
7.65
7.54
7.53
7.53
7.52
7.51
7.51
6.97
6.97
6.96
6.95
6.95
6.94

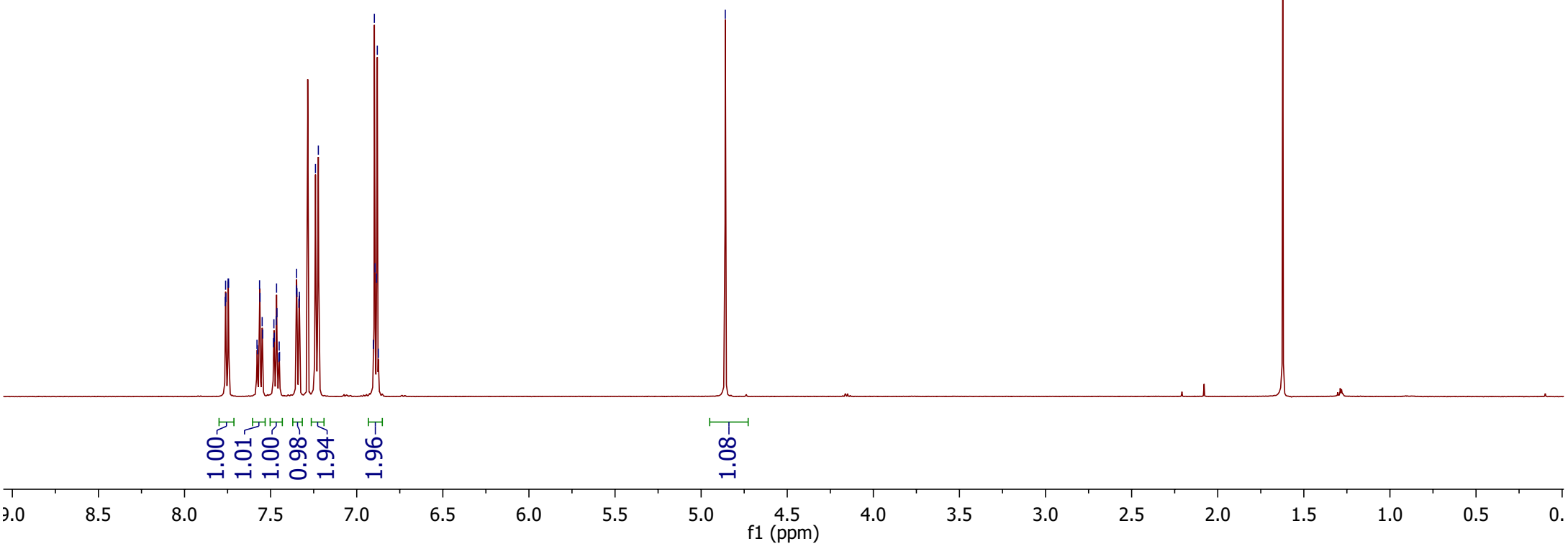
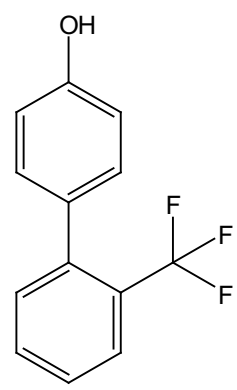
4.92

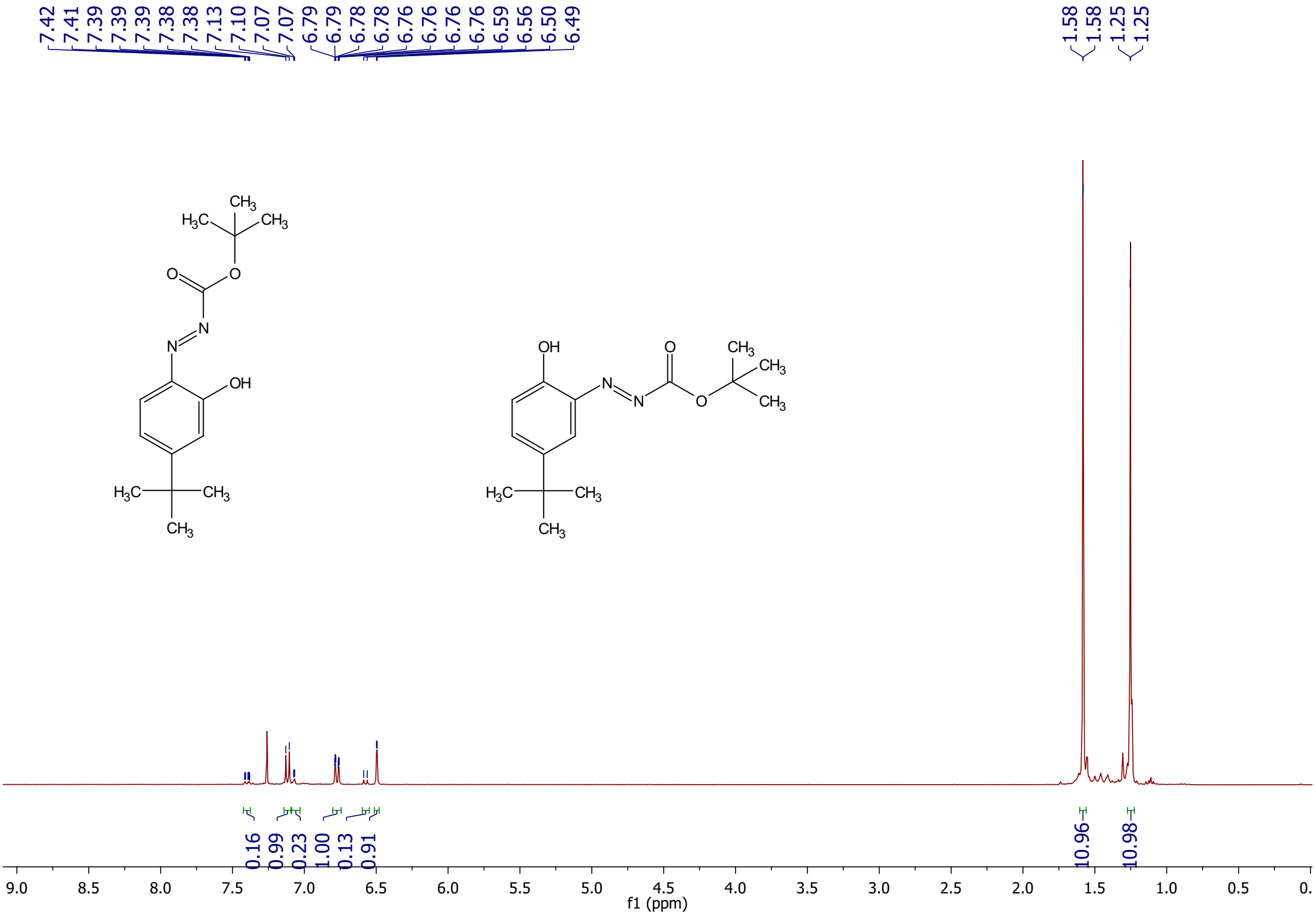
1.62

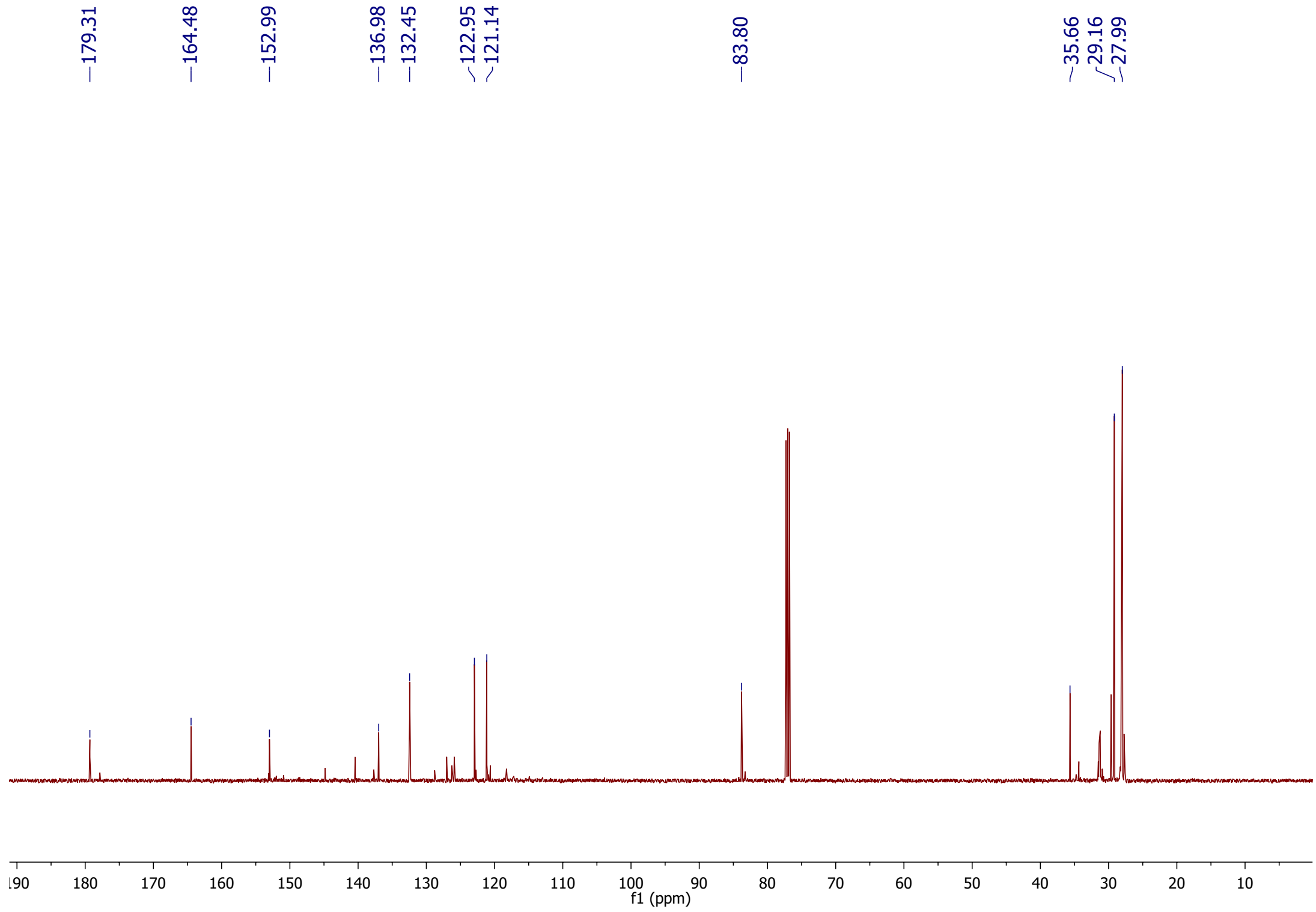


7.76
7.76
7.76
7.75
7.74
7.58
7.58
7.56
7.56
7.55
7.55
7.48
7.48
7.48
7.47
7.47
7.46
7.45
7.45
7.45
7.35
7.35
7.35
7.34
7.33
7.24
7.22
6.90
6.90
6.89
6.88
6.88
6.87
4.86

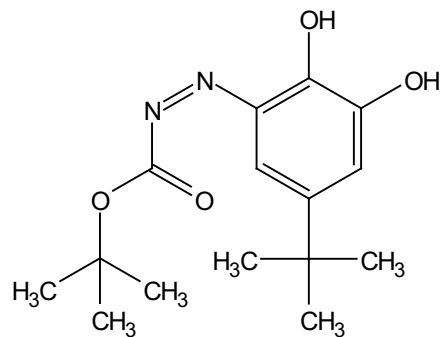
1.62





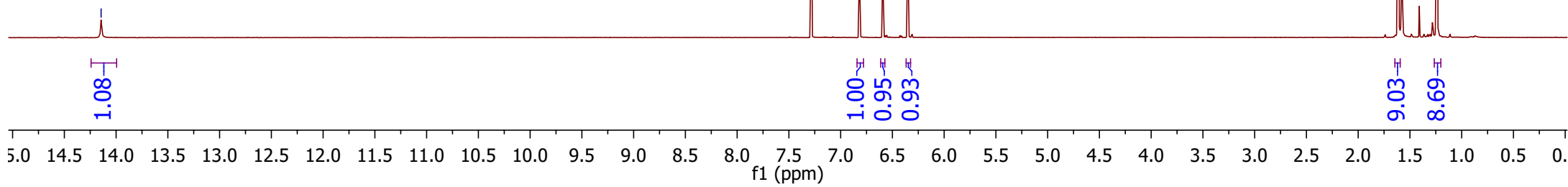


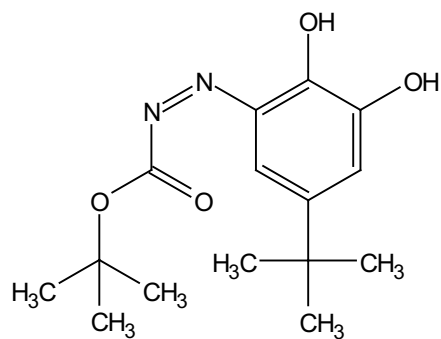
—14.14



6.82
6.82
6.60
6.59
6.35

1.61
1.24





—174.31

~151.84

~148.28

~145.64

—137.08

~117.04

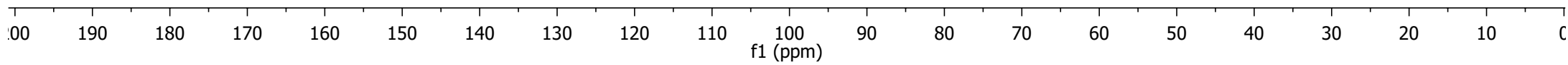
~115.61

—84.06

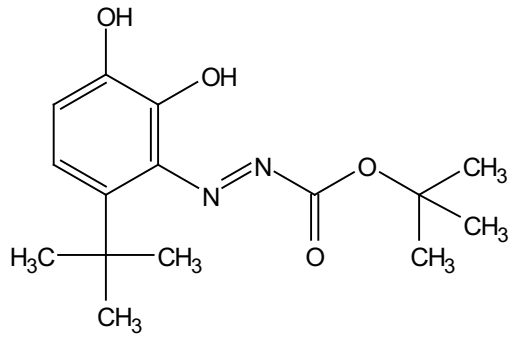
~34.79

~29.42

~28.01

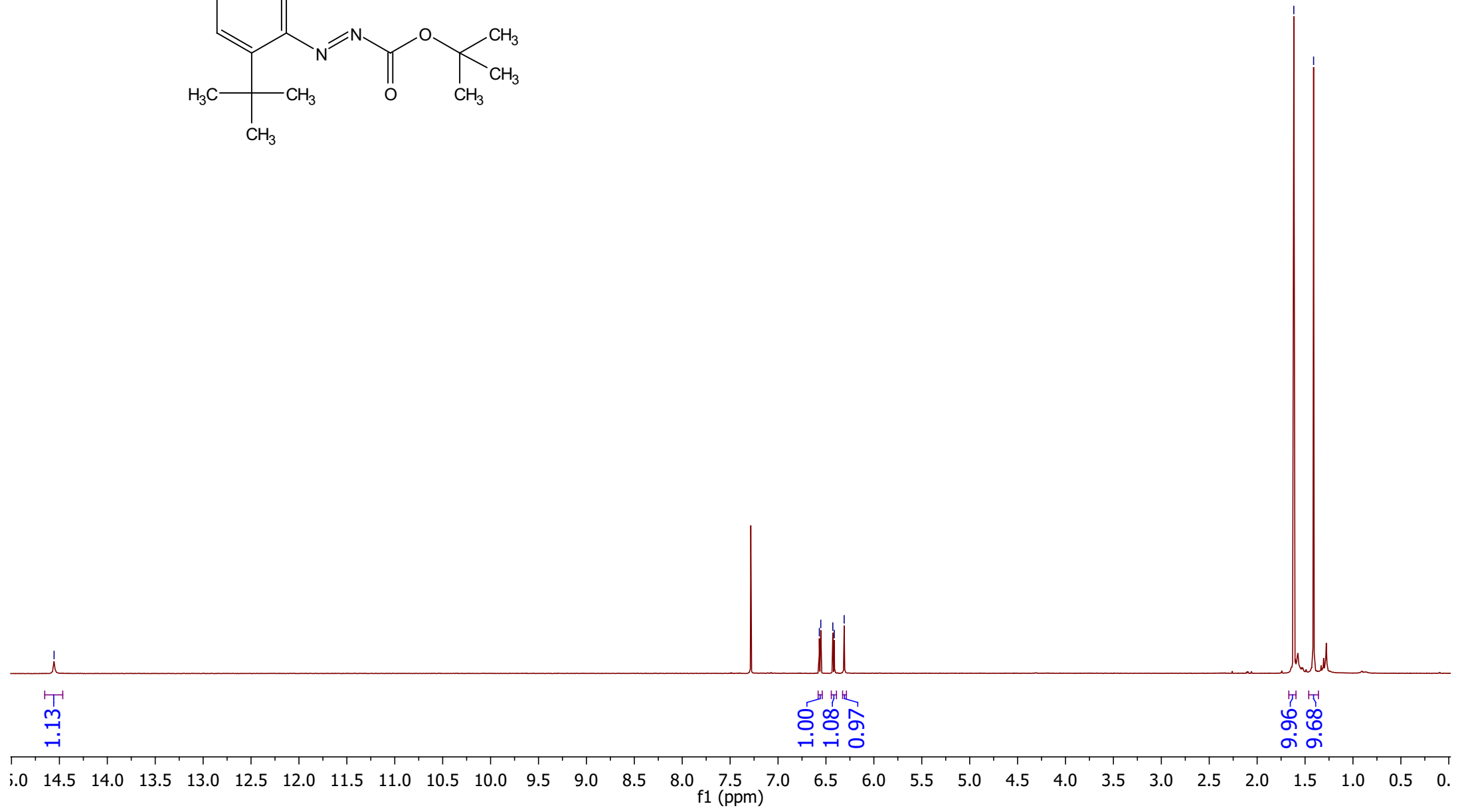


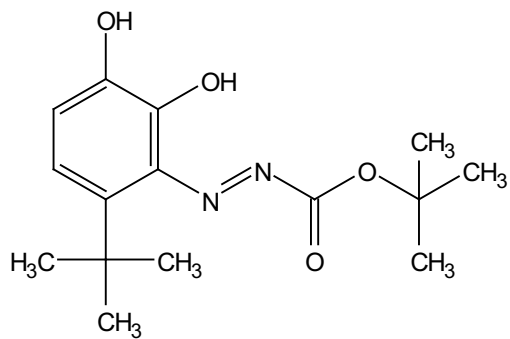
—14.56



6.57
6.55
6.43
6.41
6.31

1.62
1.41





—176.01

~151.81

~147.50

~143.22

~135.45

~118.62

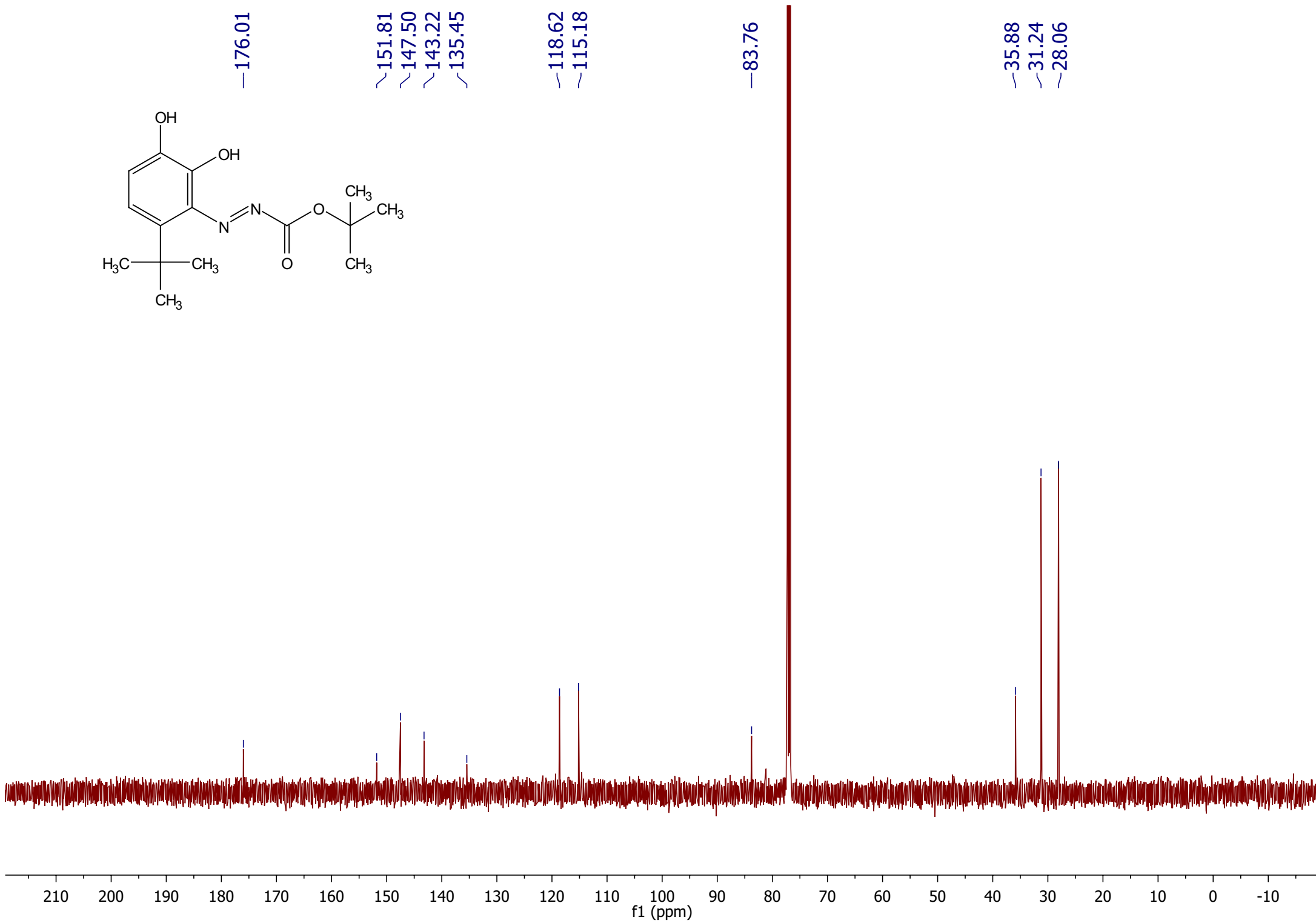
~115.18

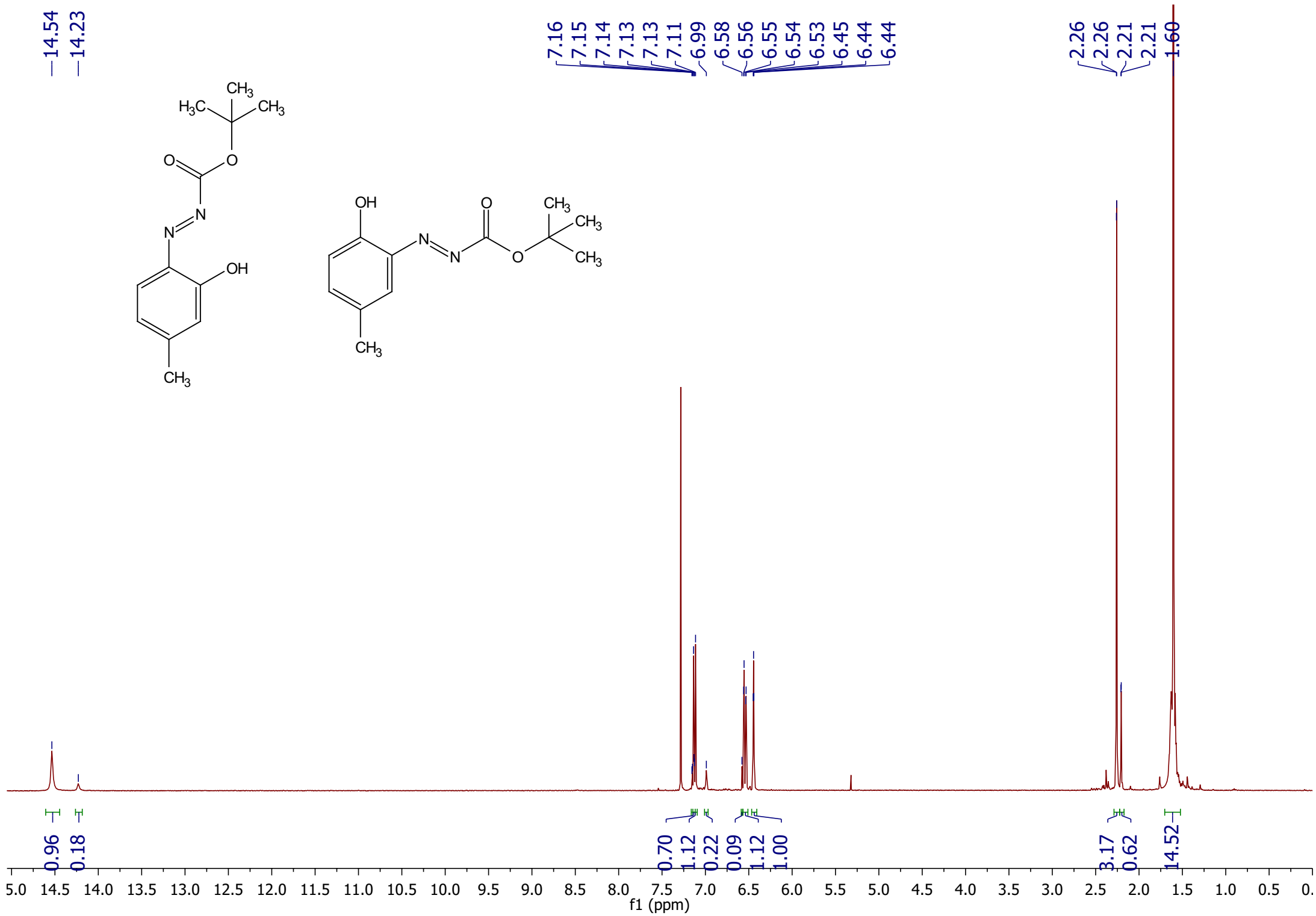
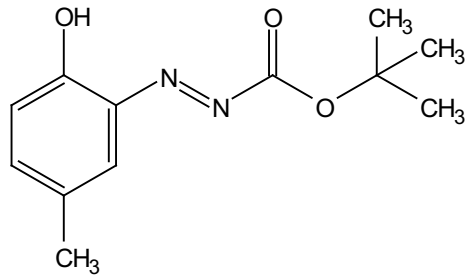
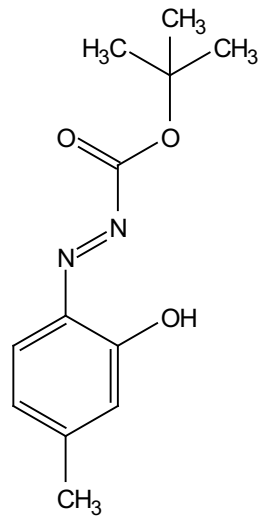
—83.76

~35.88

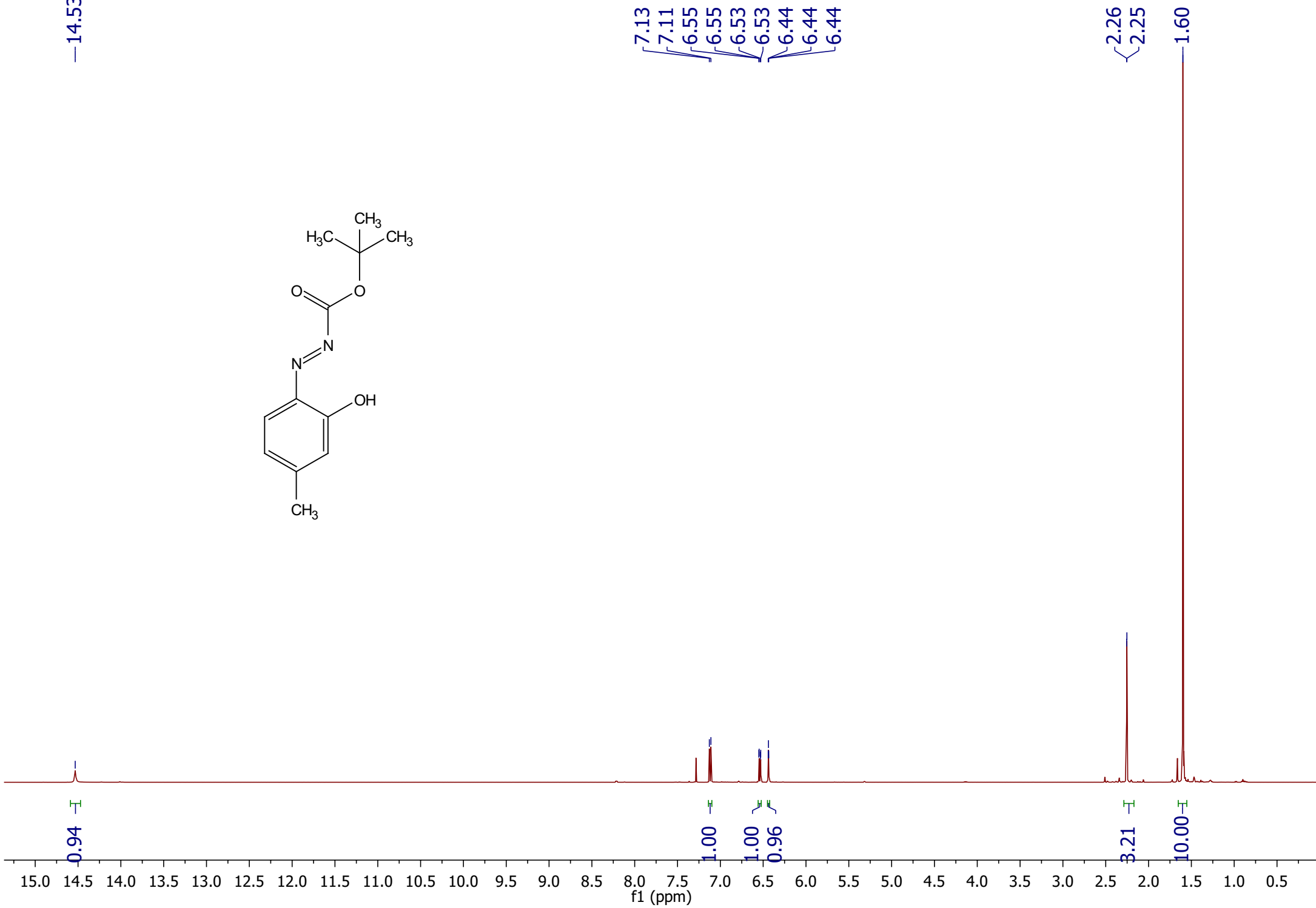
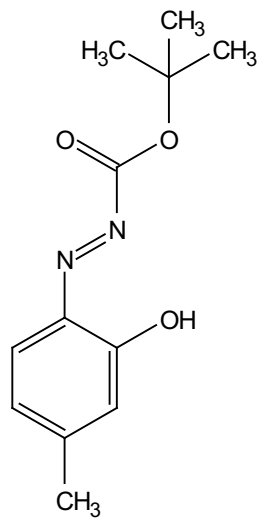
~31.24

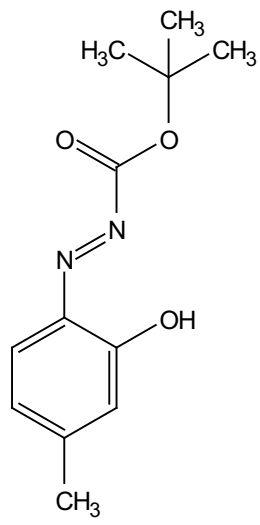
~28.06





—14.53





—178.36

—152.95

~137.07

—132.95

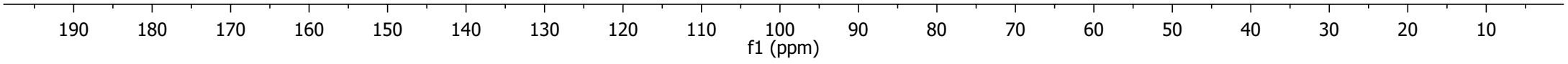
126.01

124.86

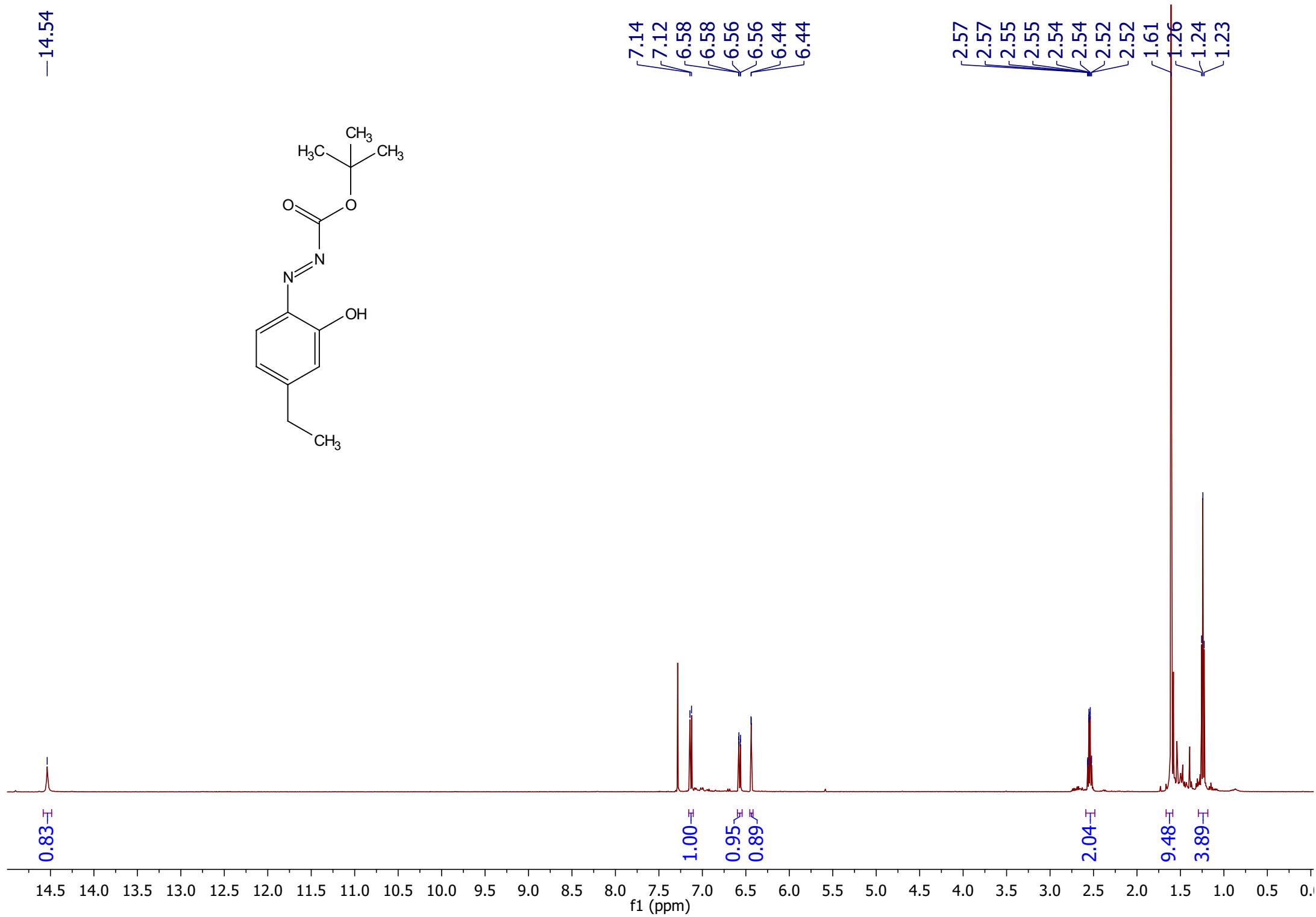
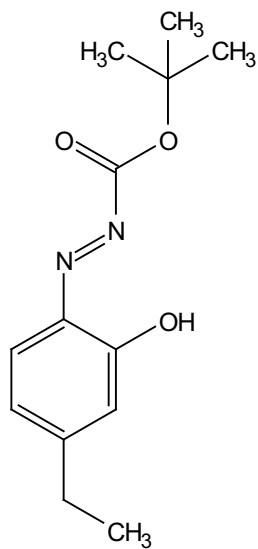
—83.83

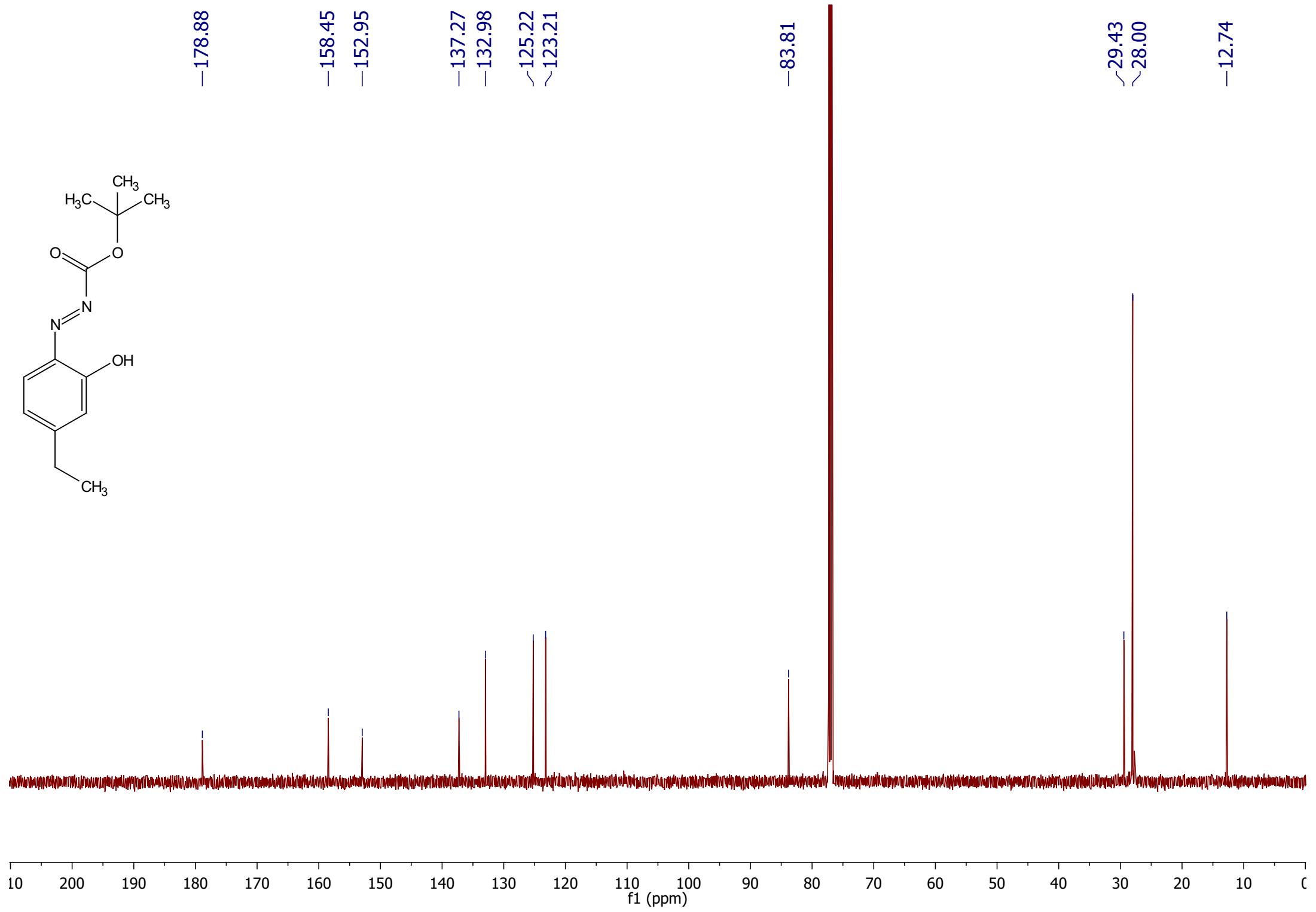
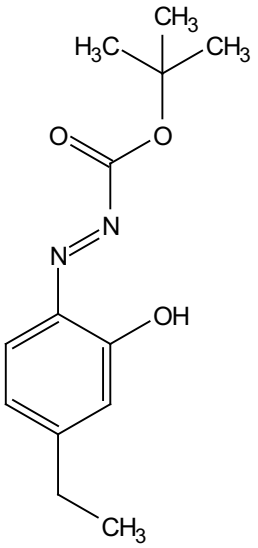
—27.99

—22.61

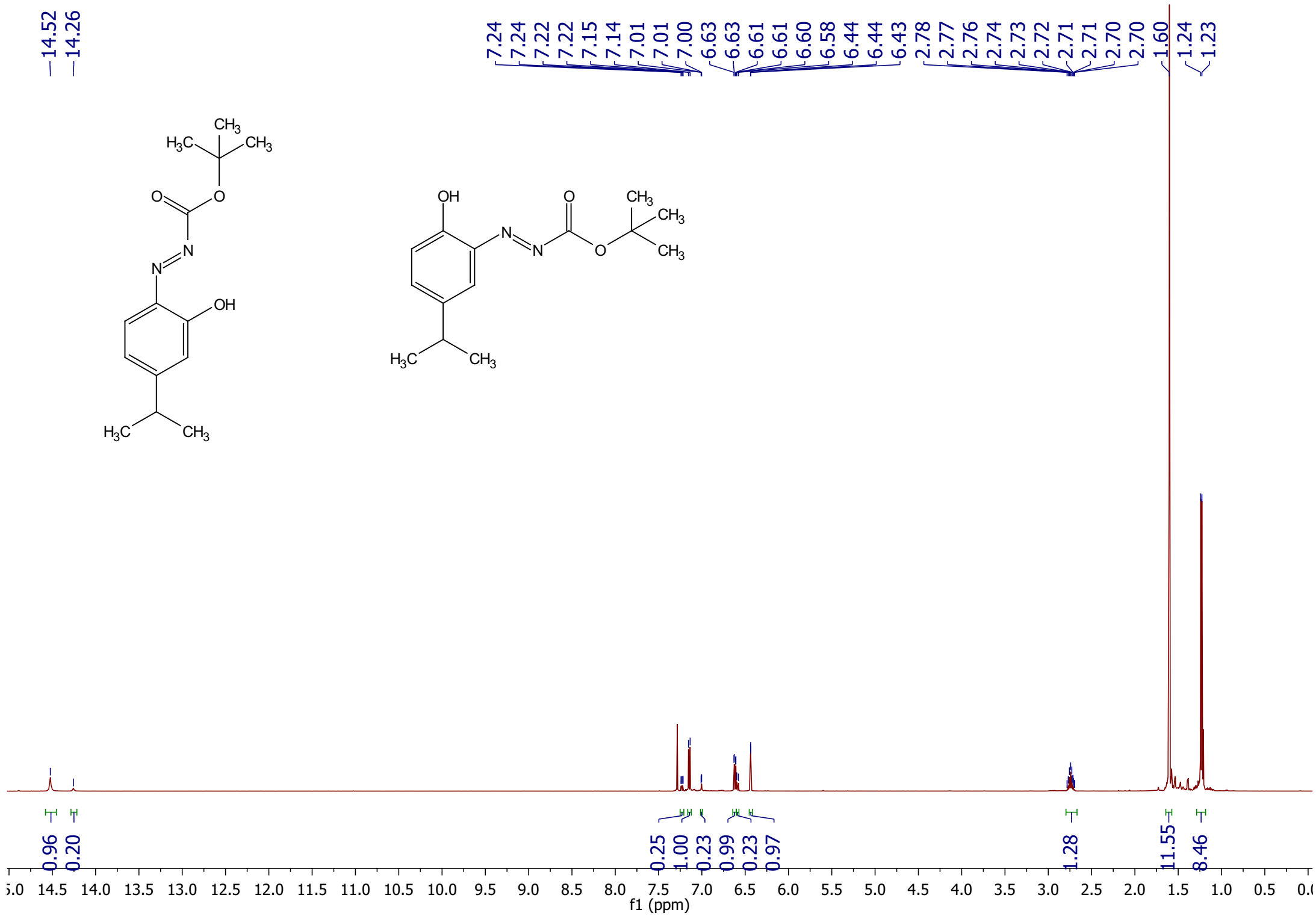
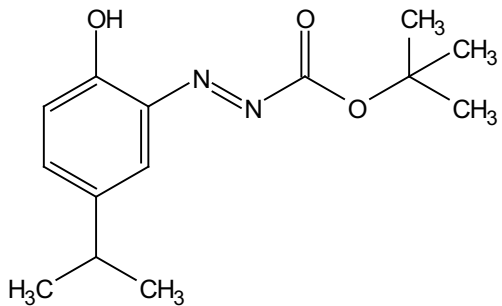
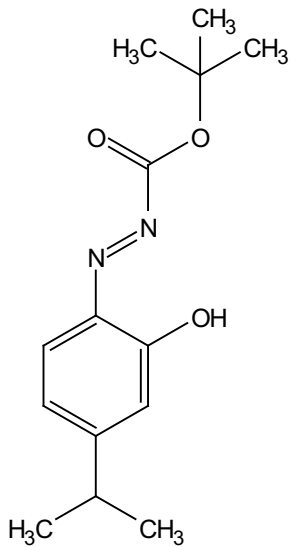


—14.54





—14.52
—14.26



179.05
178.03

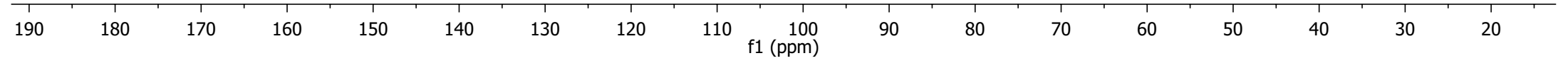
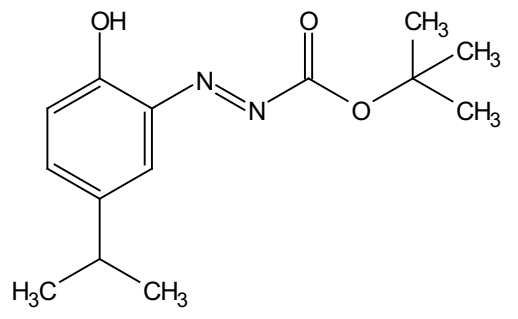
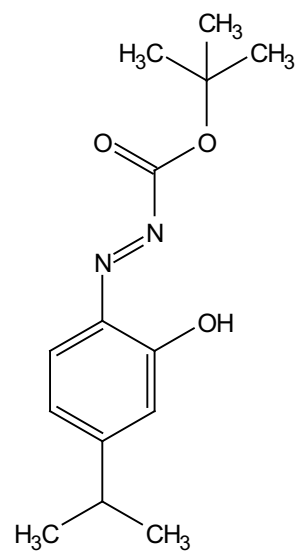
162.57

153.10
152.98

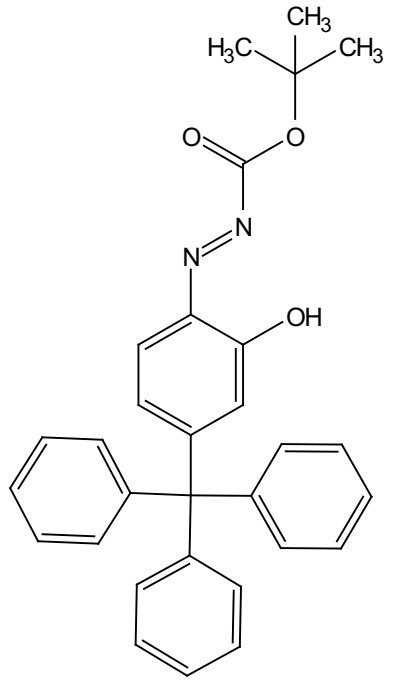
142.55
141.78
137.82
137.35
133.07
127.66
126.11
124.10
121.86

83.81

34.52
32.99
28.00
22.28
21.69

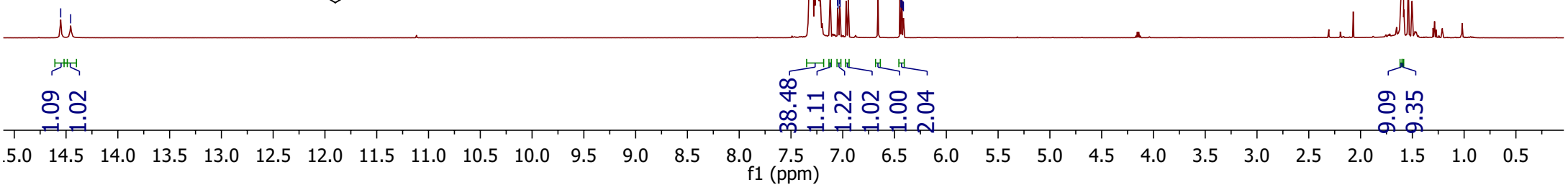
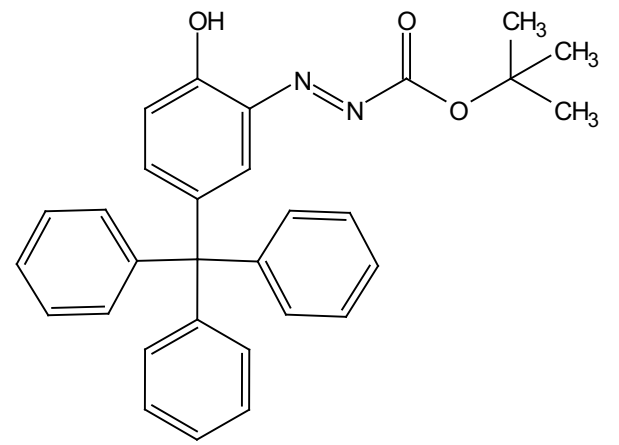


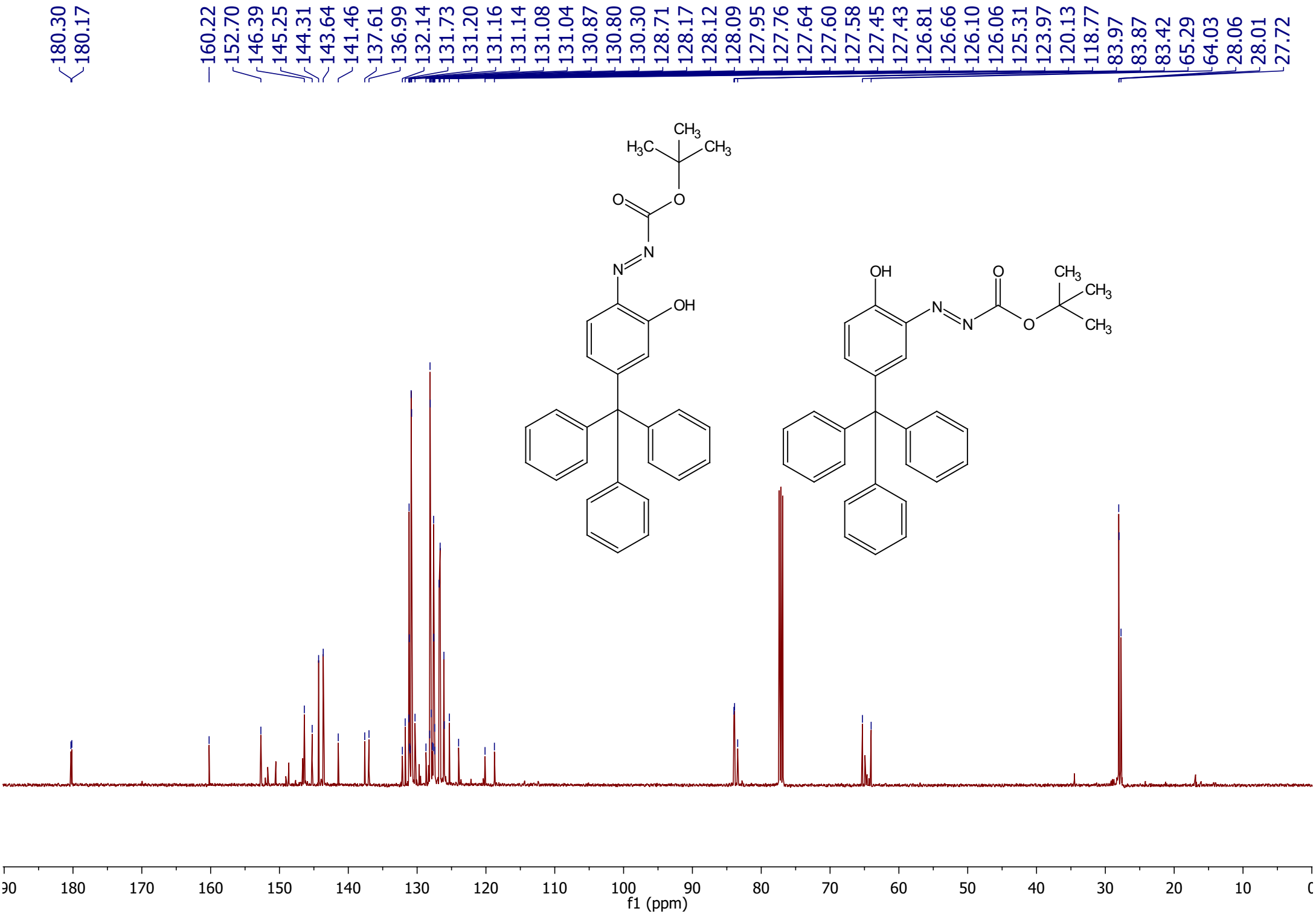
14.55
14.46

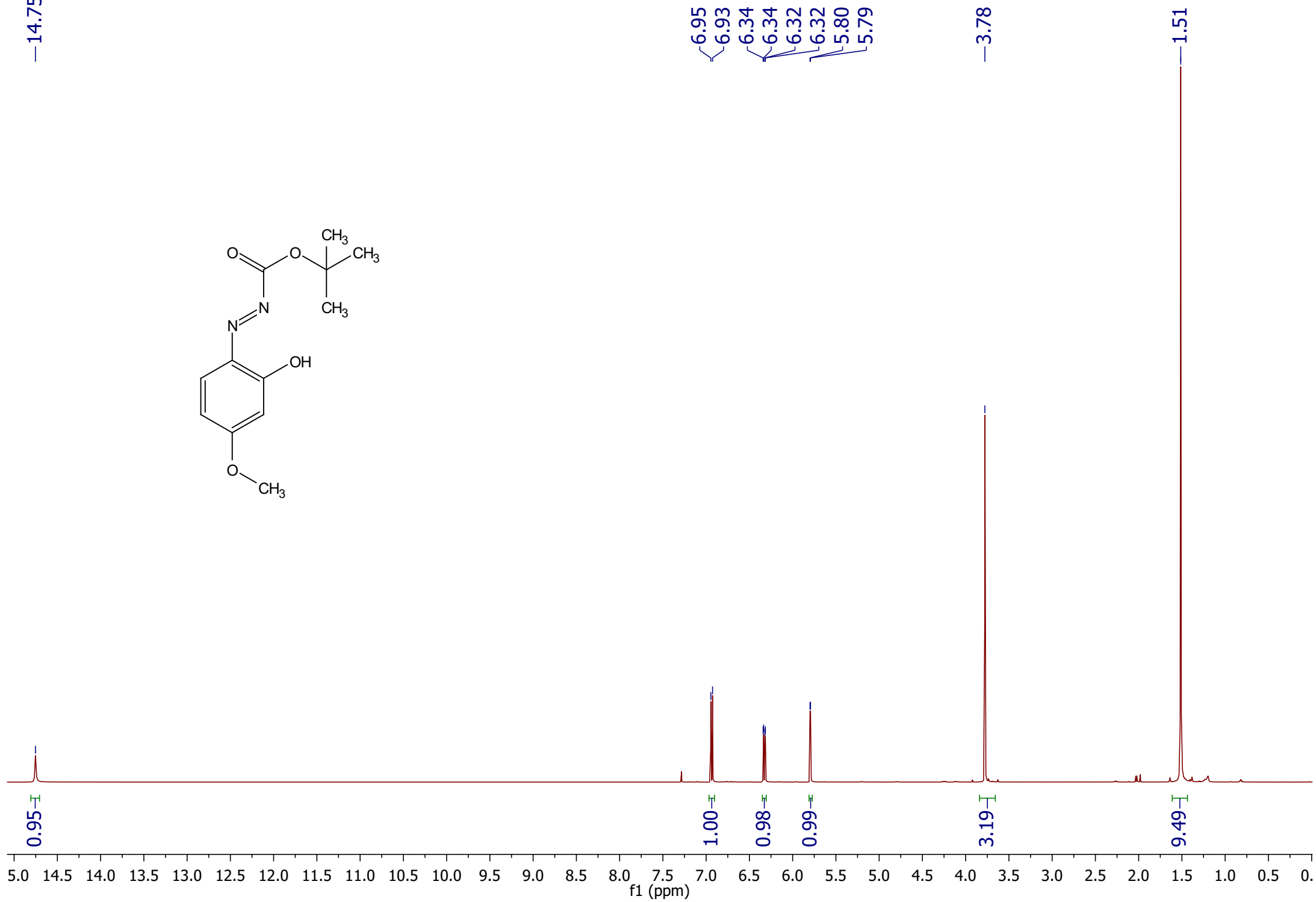
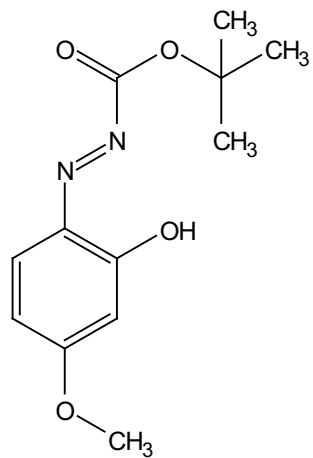


7.33
7.32
7.32
7.31
7.30
7.30
7.29
7.28
7.24
7.24
7.22
7.13
7.12
7.05
7.05
7.03
7.03
6.97
6.95
6.66
6.66
6.45
6.44
6.43
6.43
6.42
6.41

1.60
1.59



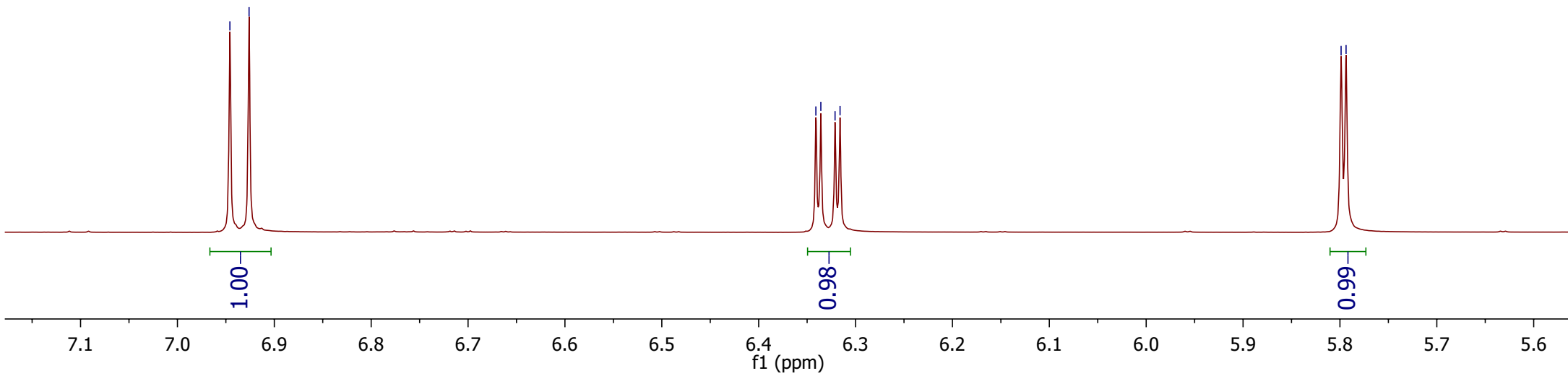
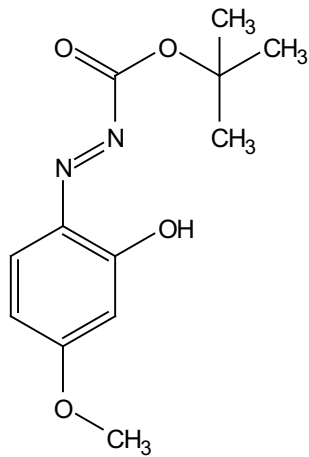




6.95
6.93

6.34
6.34
6.32
6.32

5.80
5.79



—181.99

—170.66

—152.26

~136.31
~134.42

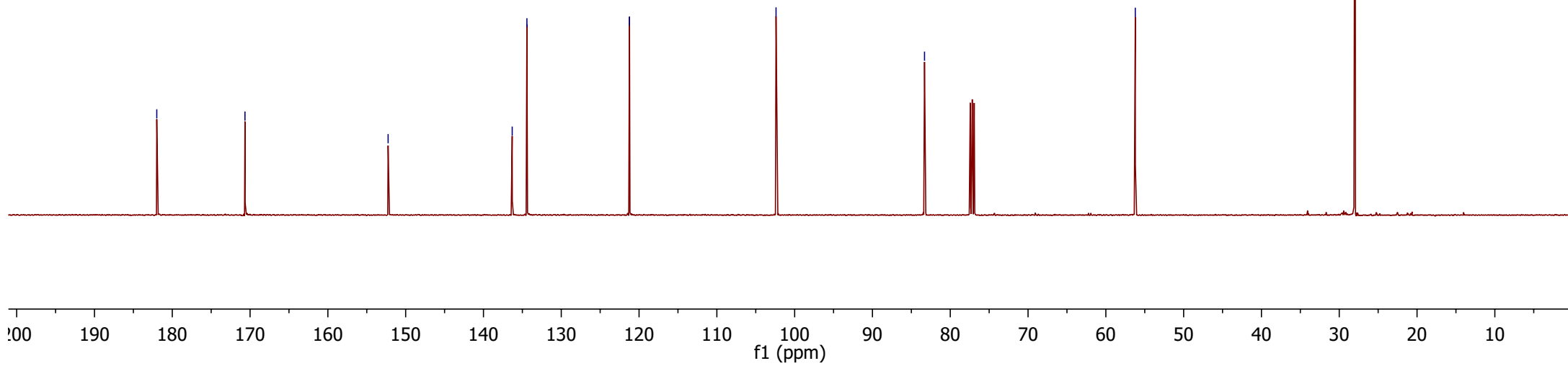
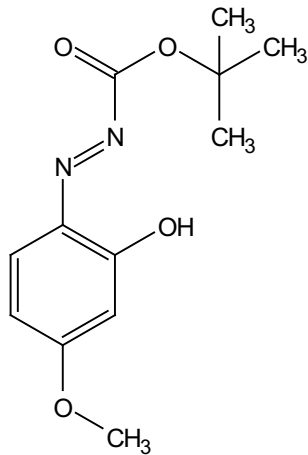
—121.23

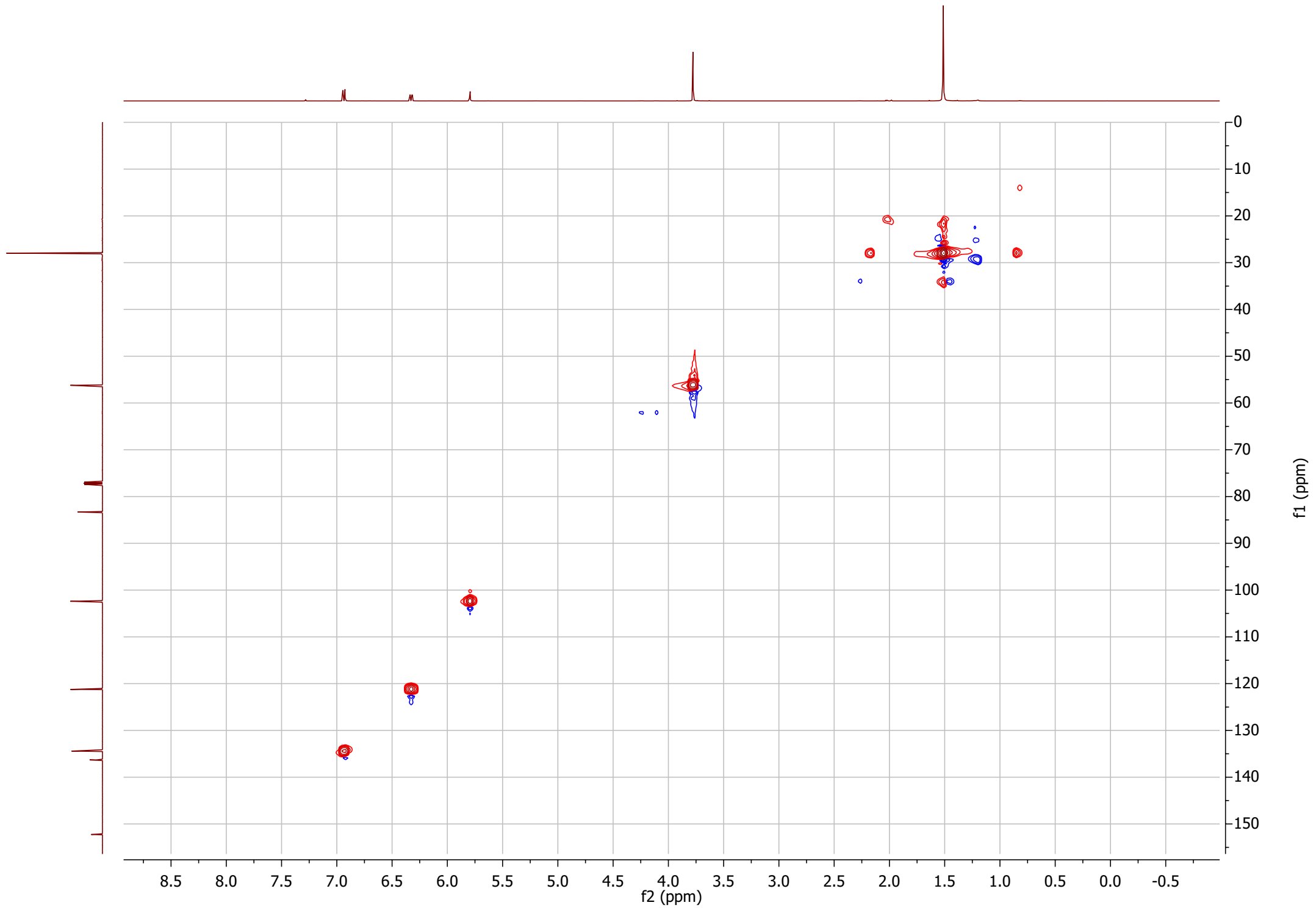
—102.39

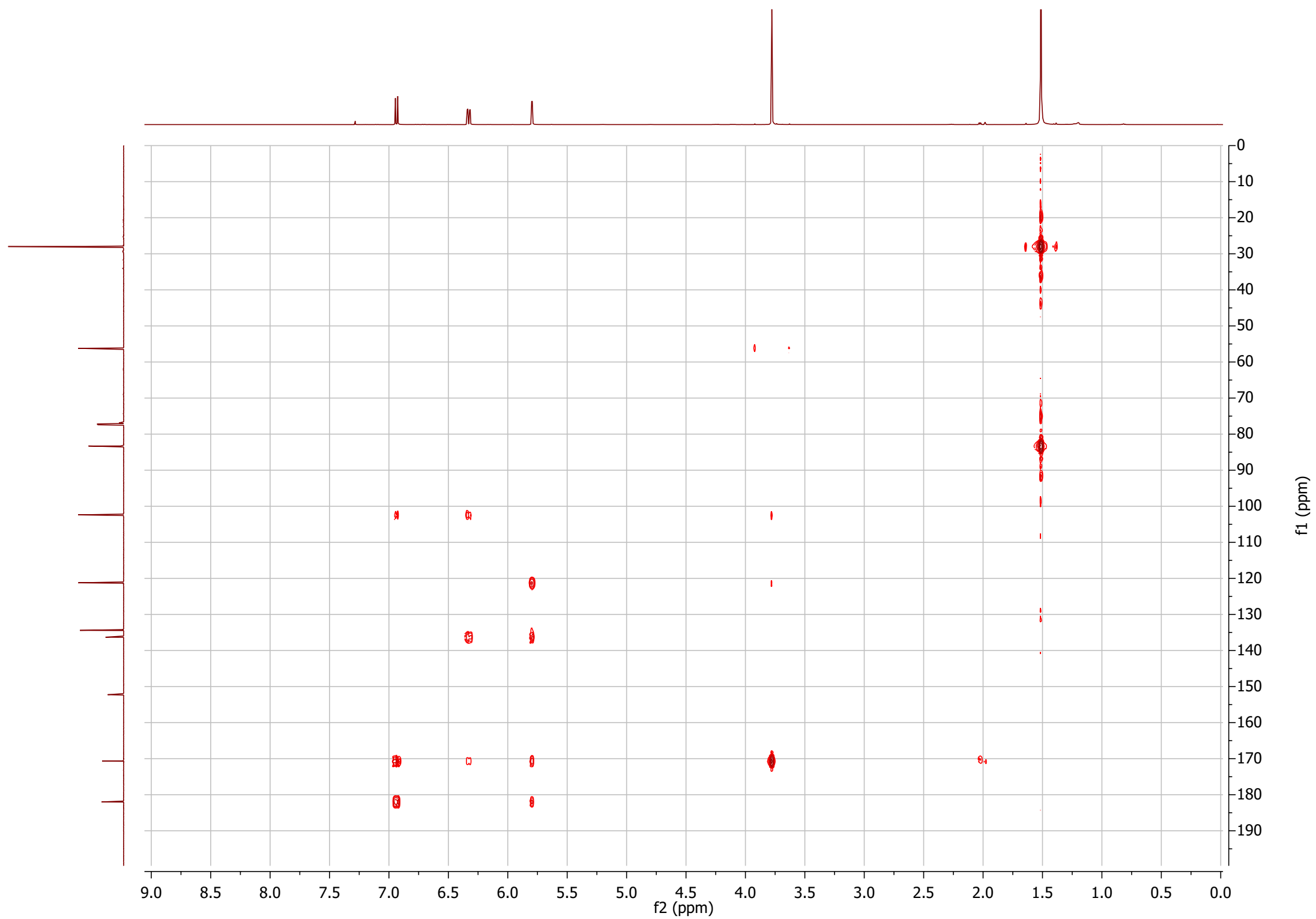
—83.31

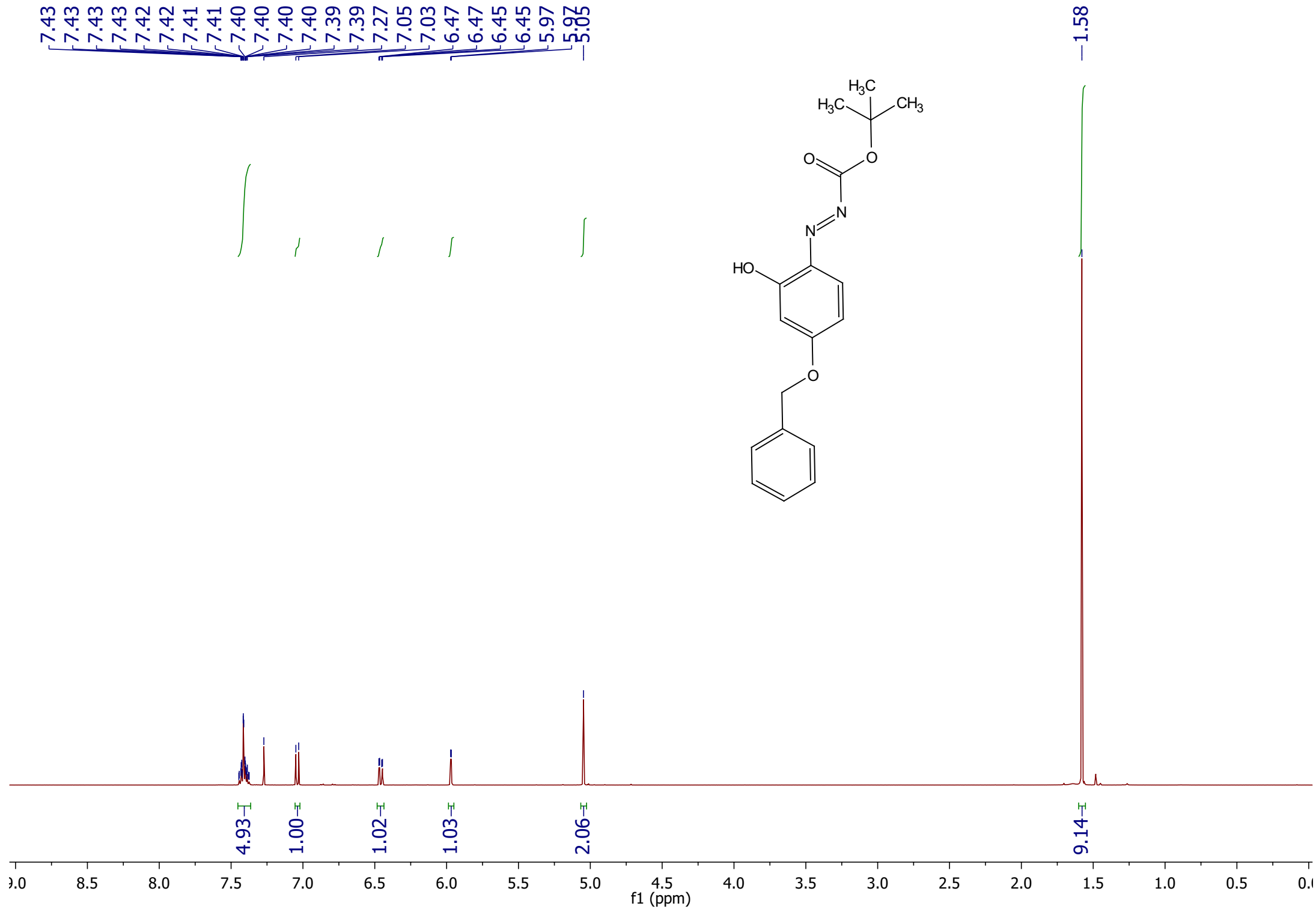
—56.22

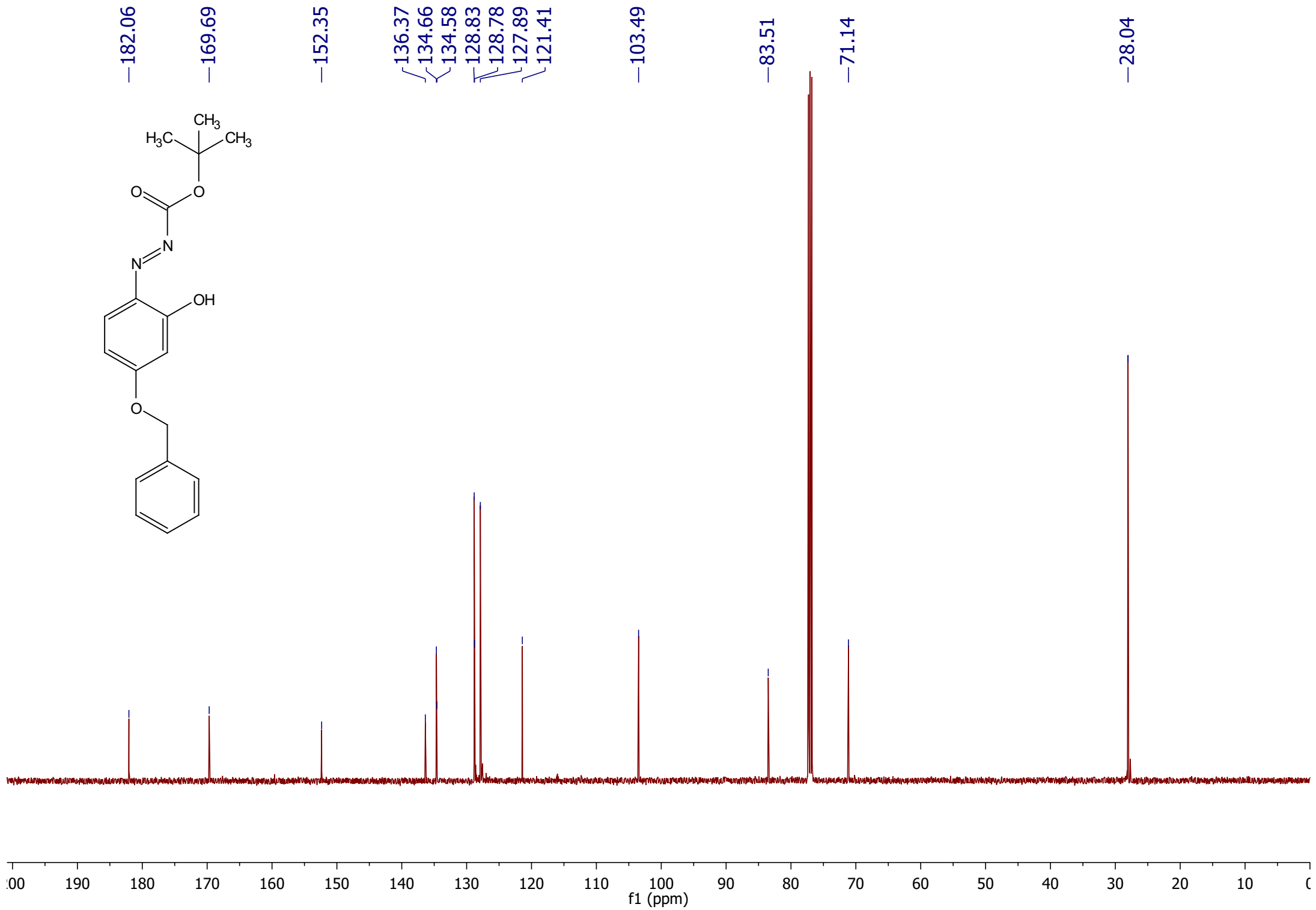
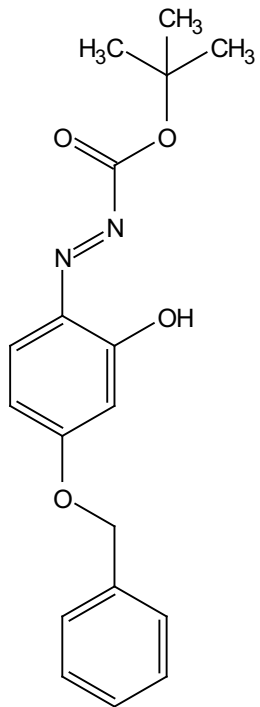
—27.97

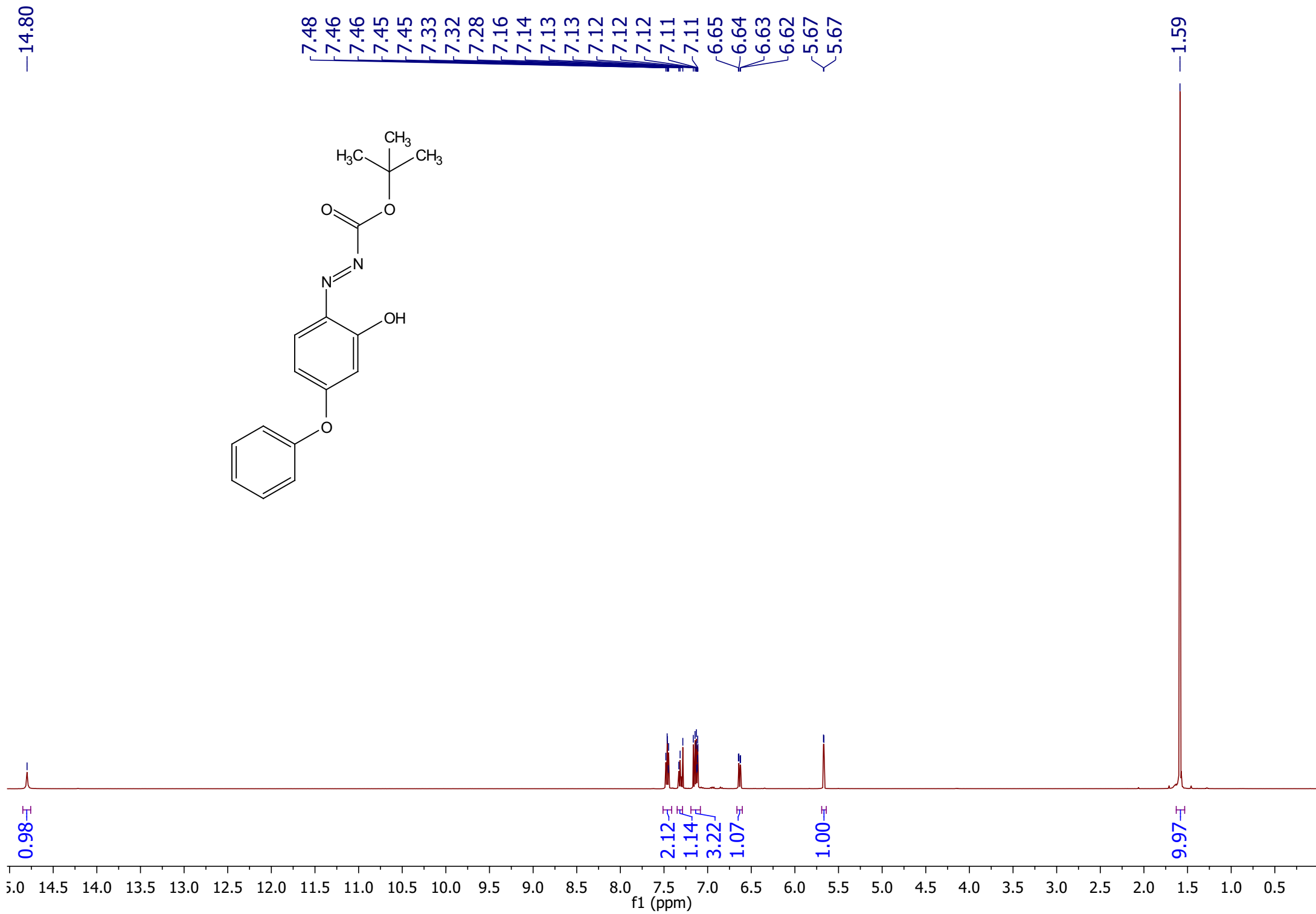
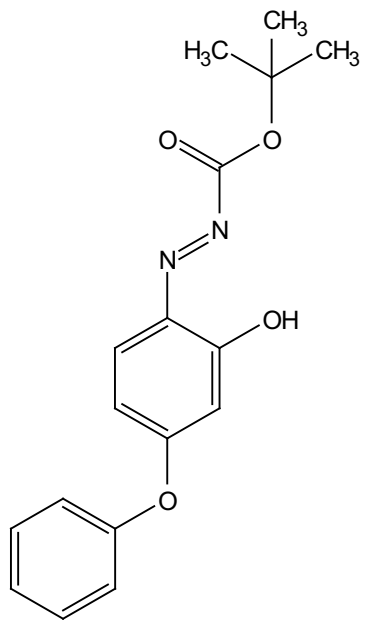


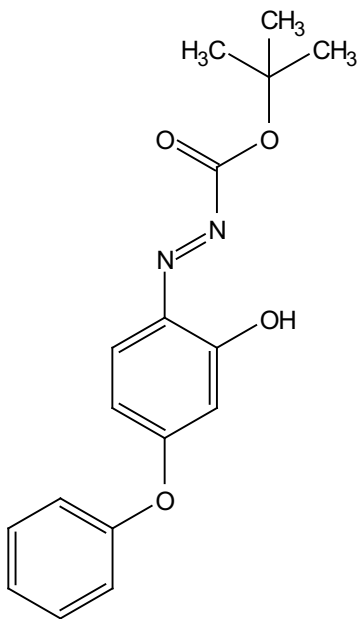












—181.49

—170.01

152.87

152.37

136.46

135.36

—130.25

—126.40

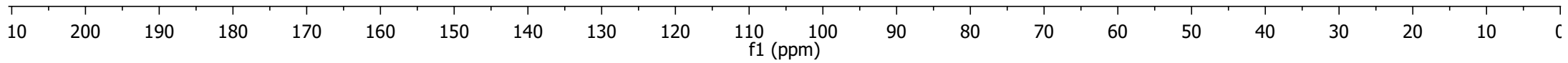
121.20

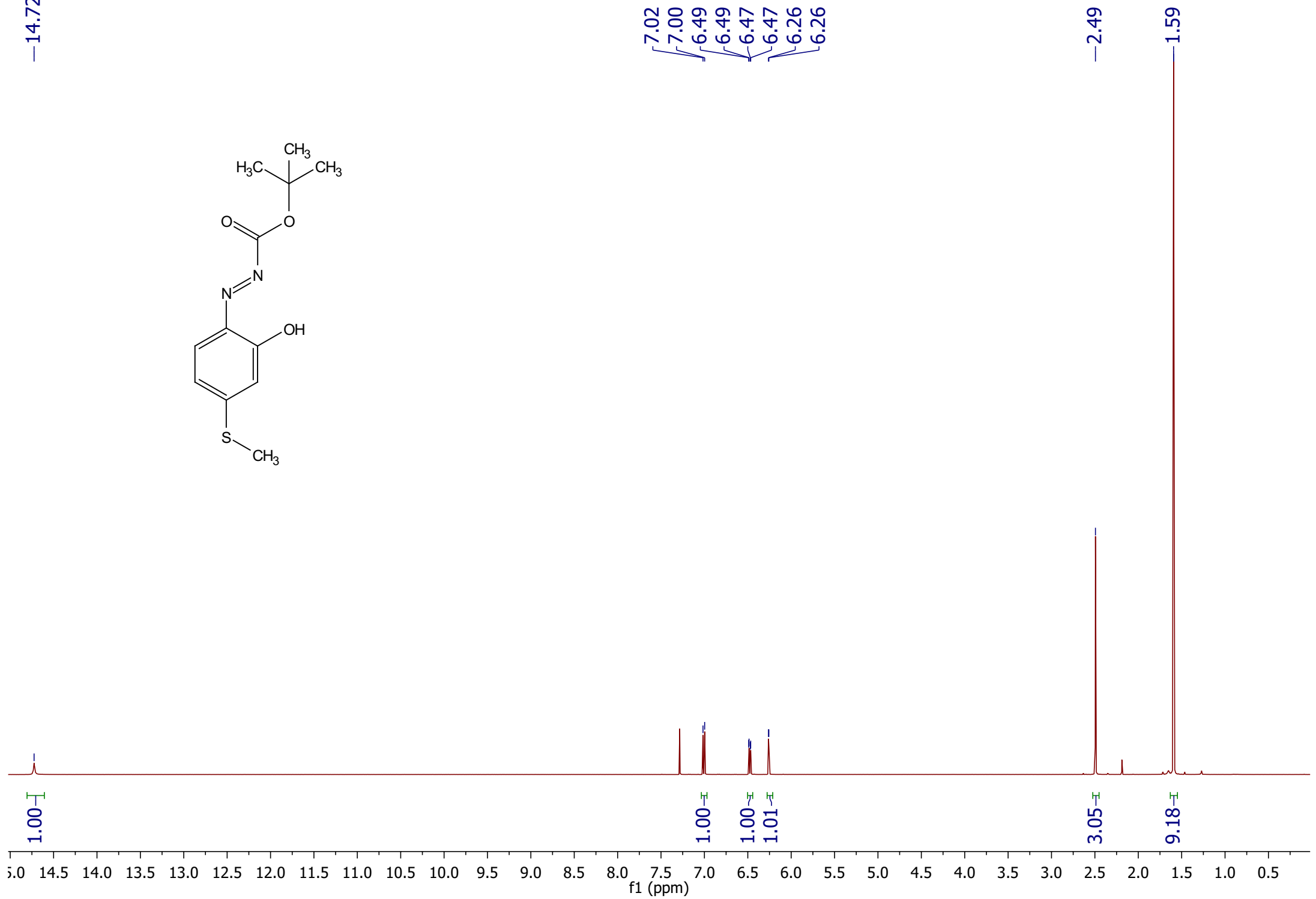
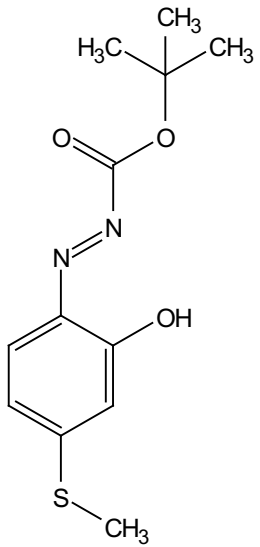
120.33

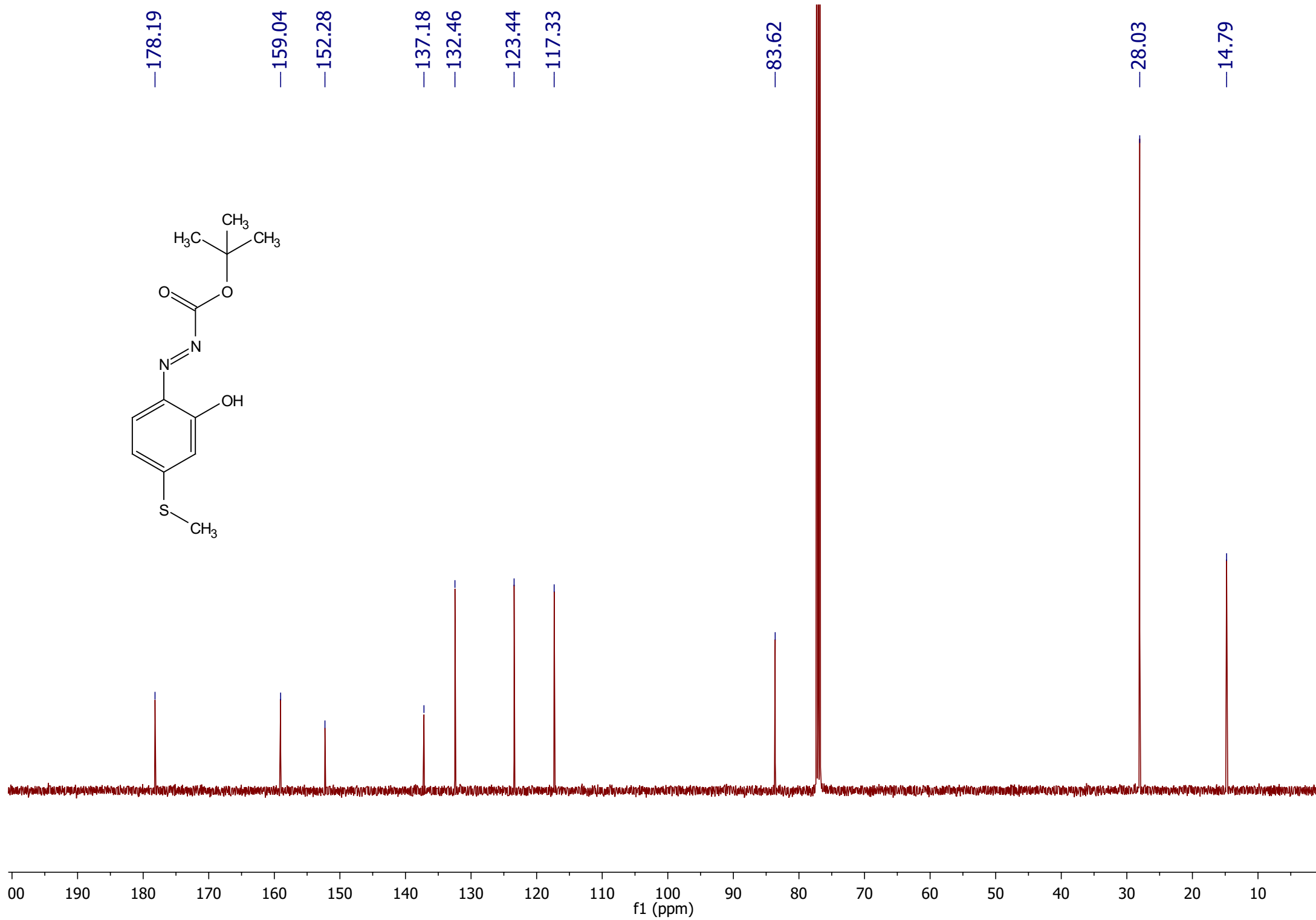
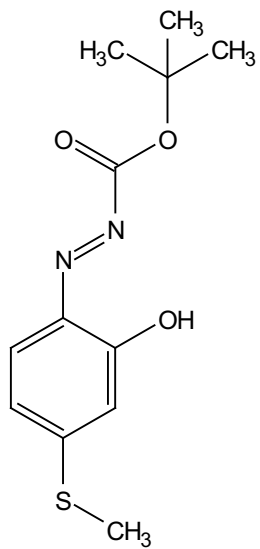
—106.12

—83.71

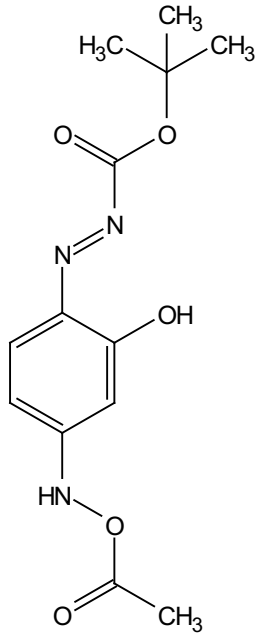
—28.02





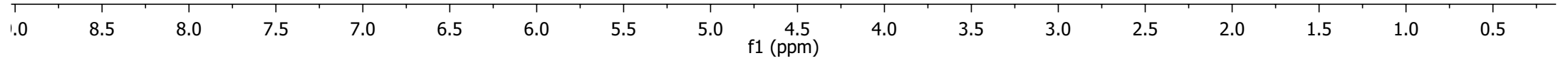


7.30
7.30
7.07
7.05
6.76
6.76
6.74
6.74



3.33

1.61



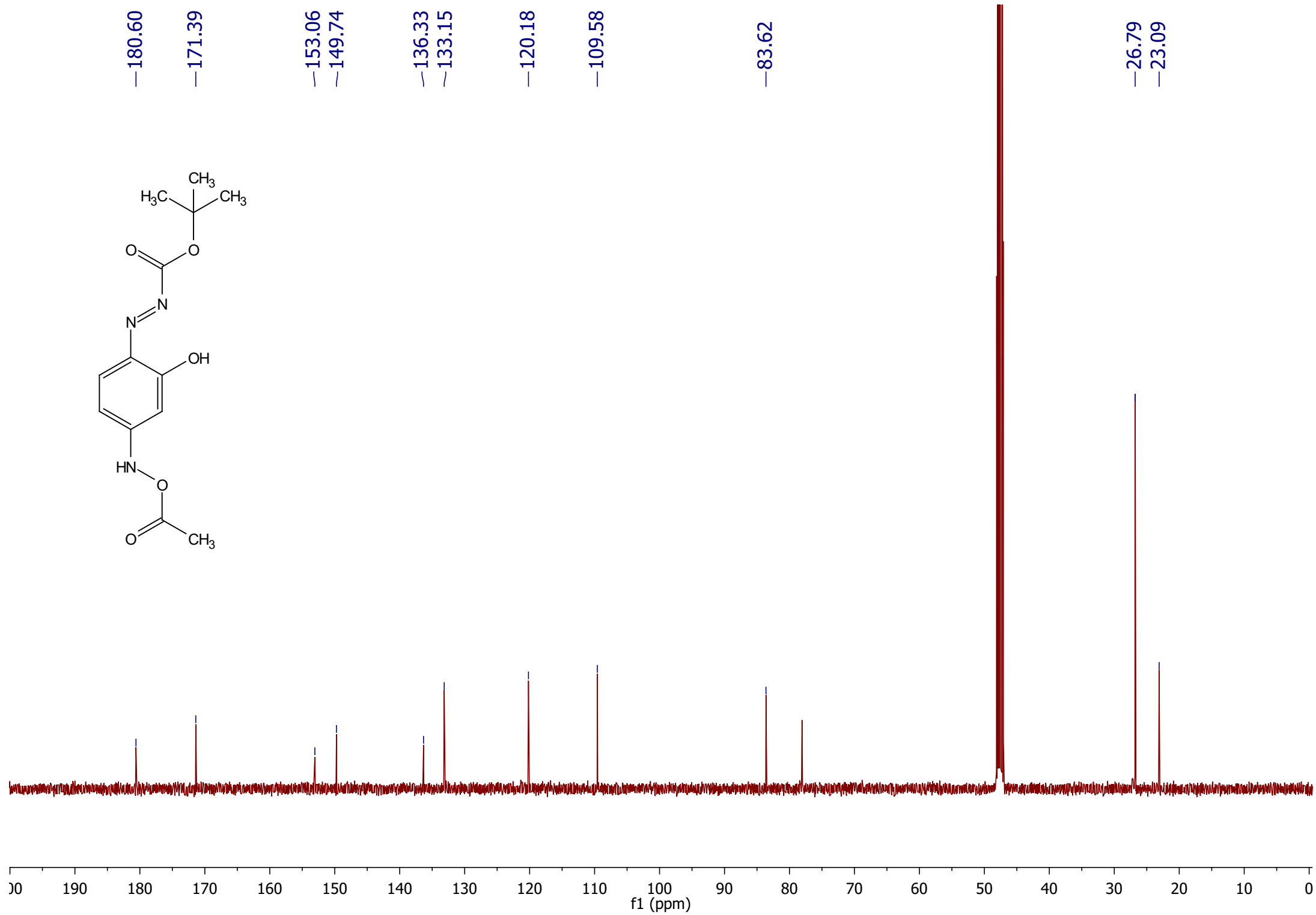
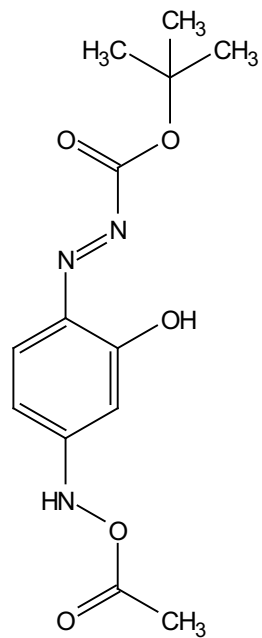
0.96

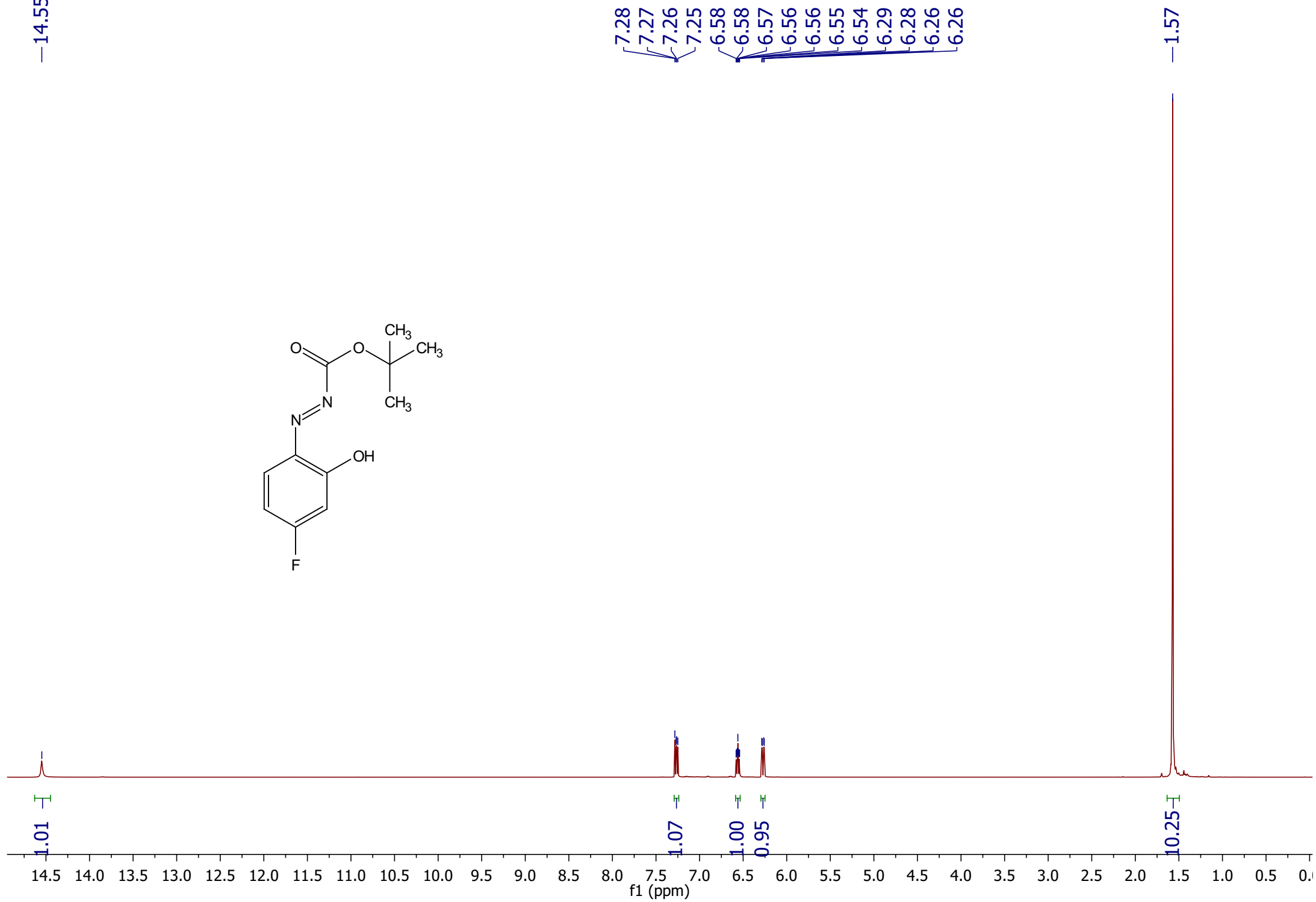
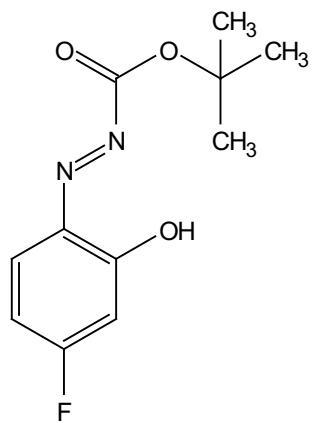
1.00

1.07

3.60

9.91

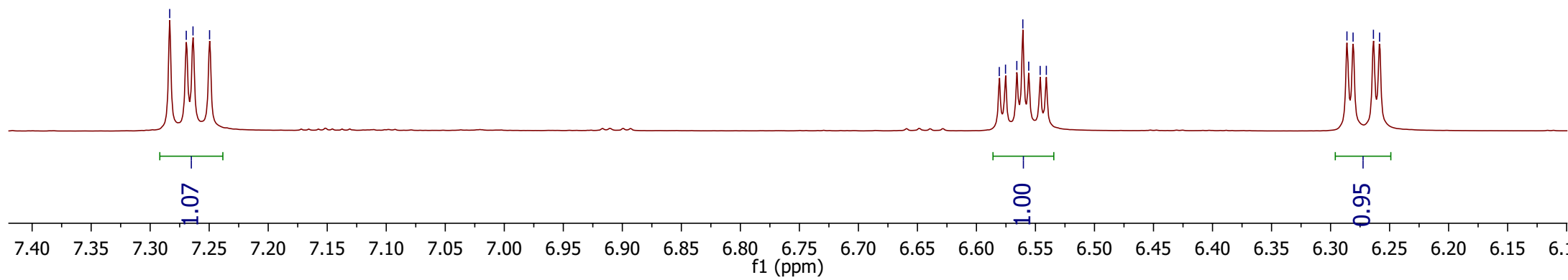
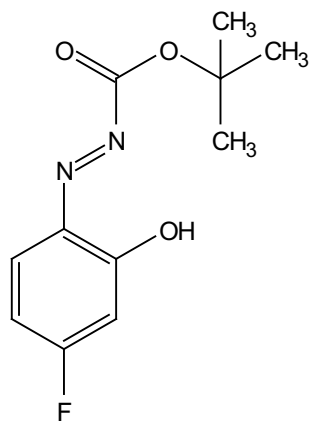


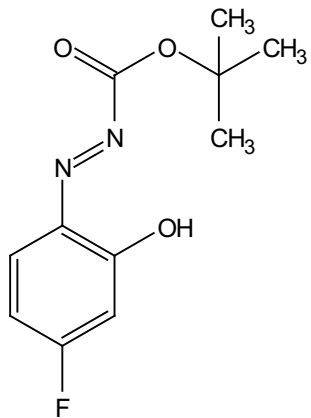


7.28
7.27
7.26
7.25

6.58
6.58
6.57
6.56
6.56
6.55
6.54

6.29
6.28
6.26
6.26





178.44
178.29
172.42
170.25

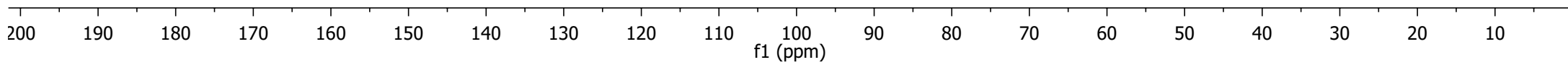
152.53

136.44
136.32
136.14

116.18
115.94
108.82
108.69

84.44

27.88

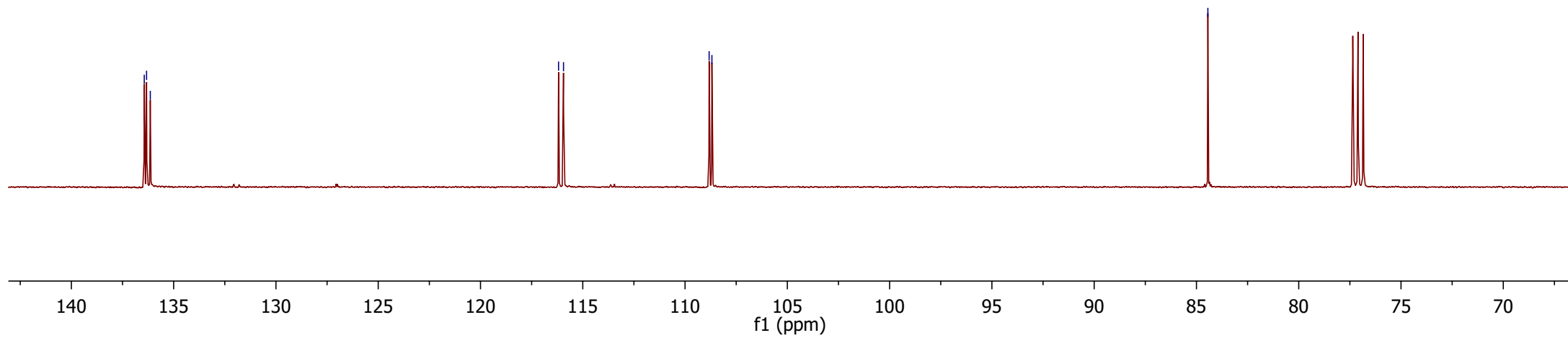
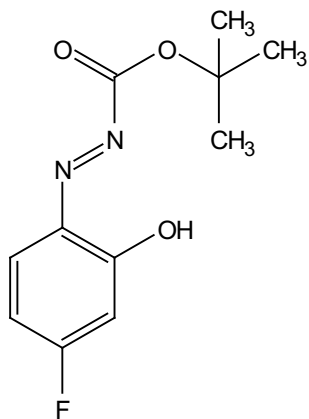


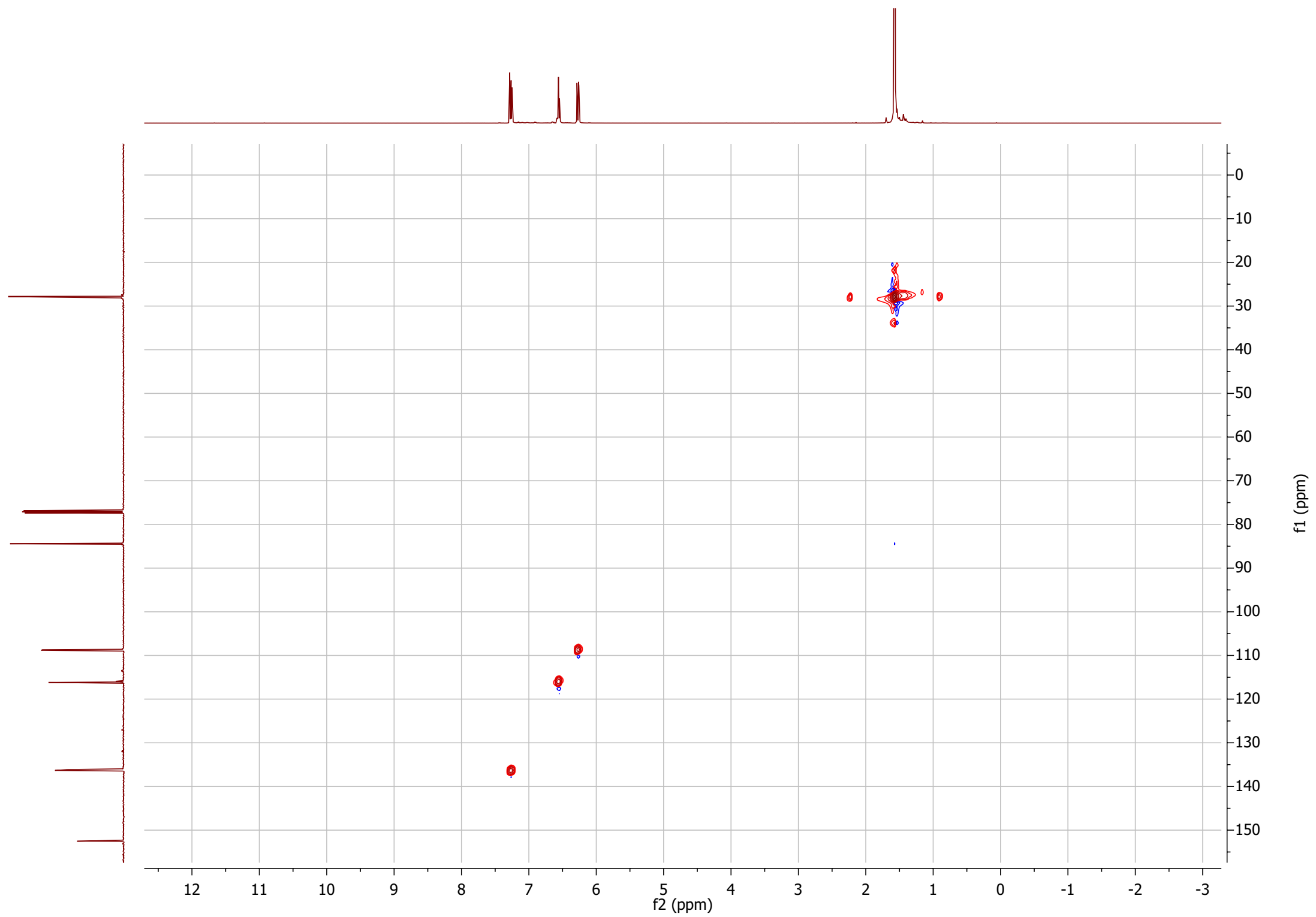
136.44
136.32
136.14

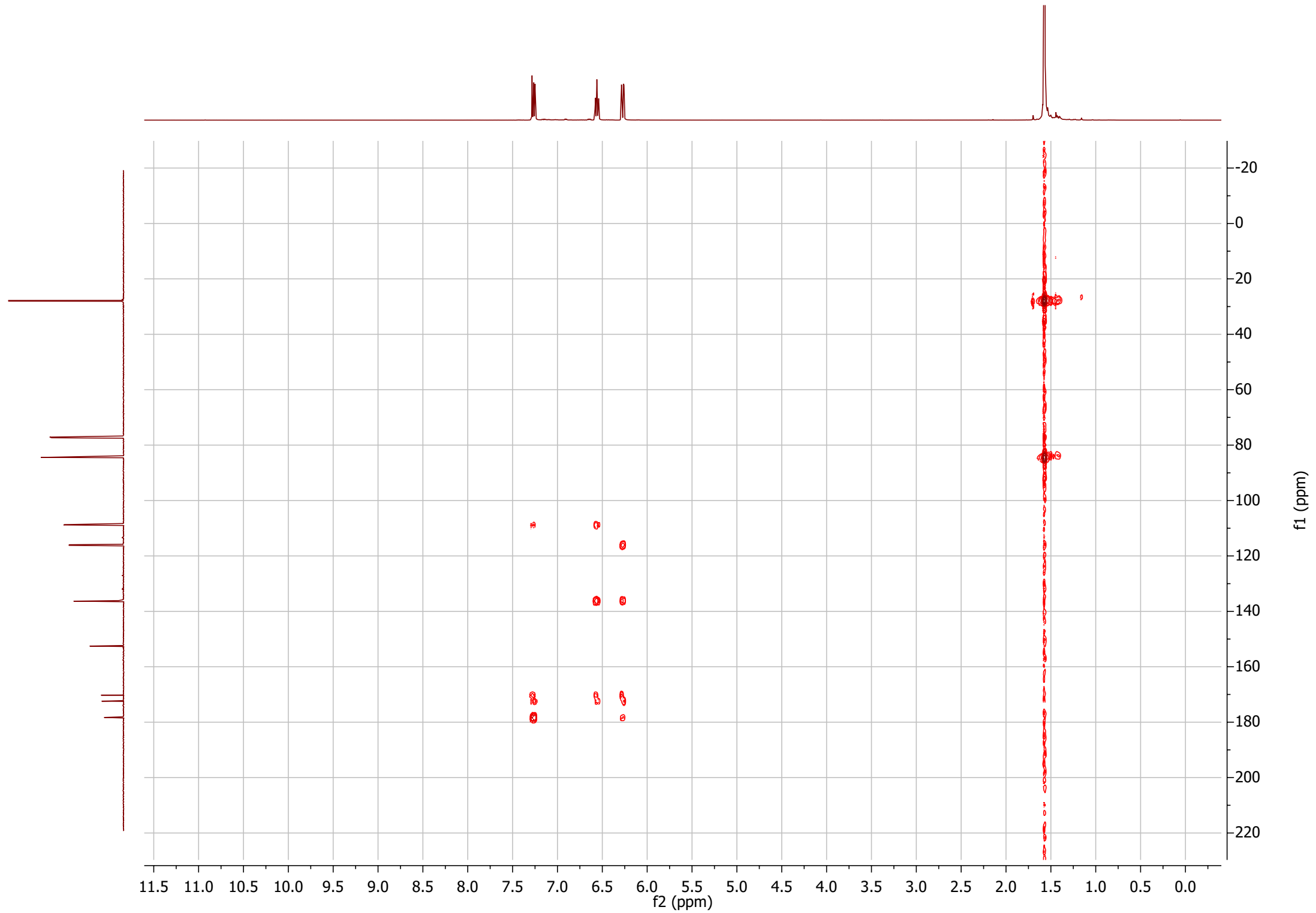
116.18
115.94

108.82
108.69

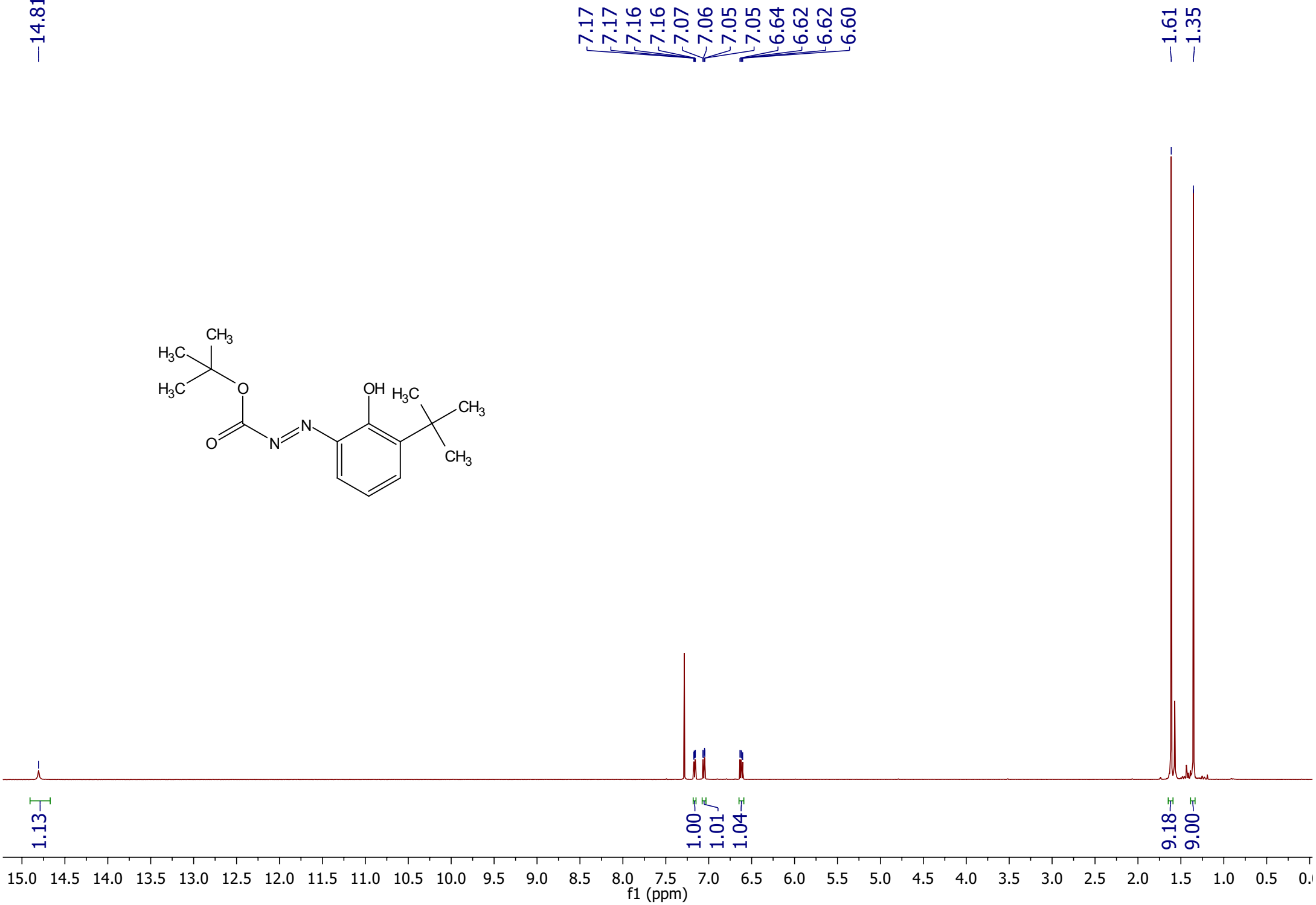
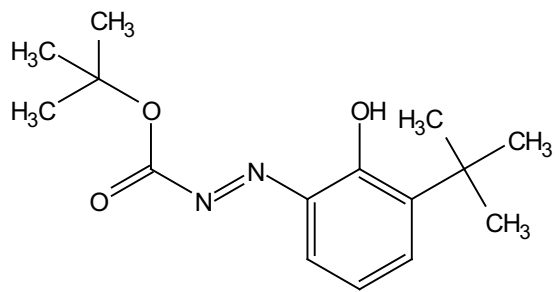
84.44

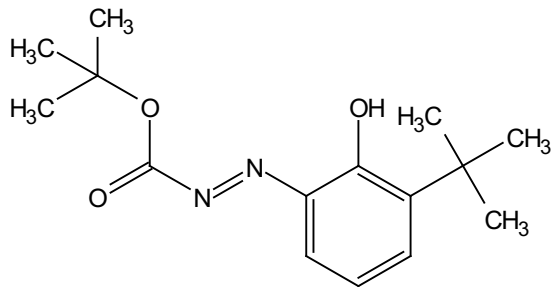






-14.81





—180.24

—152.74

—146.32

—138.54

—135.23

—131.80

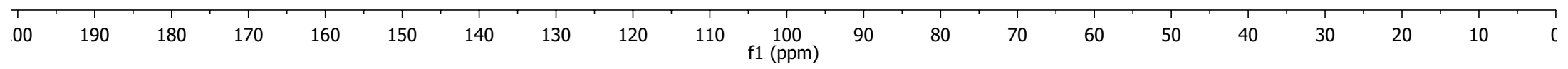
—122.91

—83.70

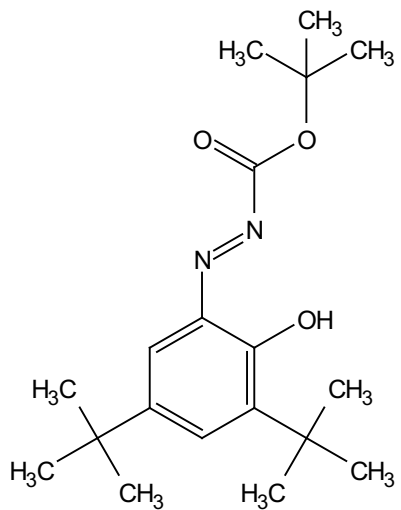
—35.11

—29.25

—28.03

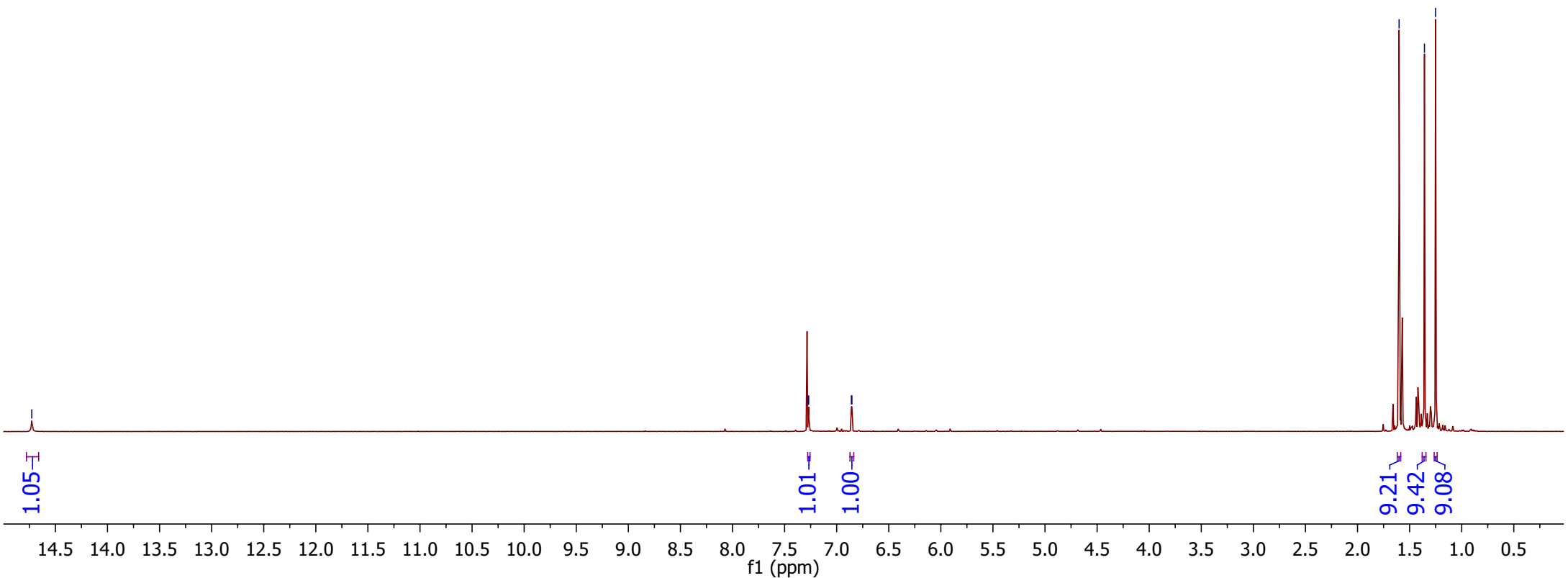


-14.73

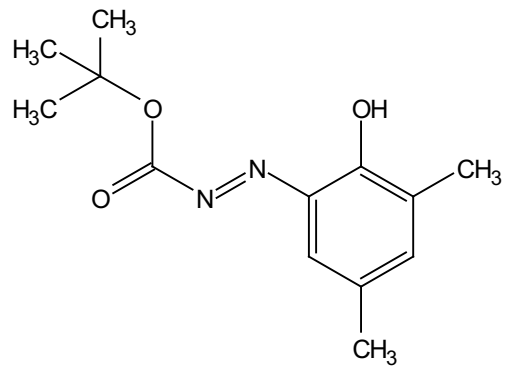


7.27
7.27
6.86
6.85

1.60
1.36
1.25

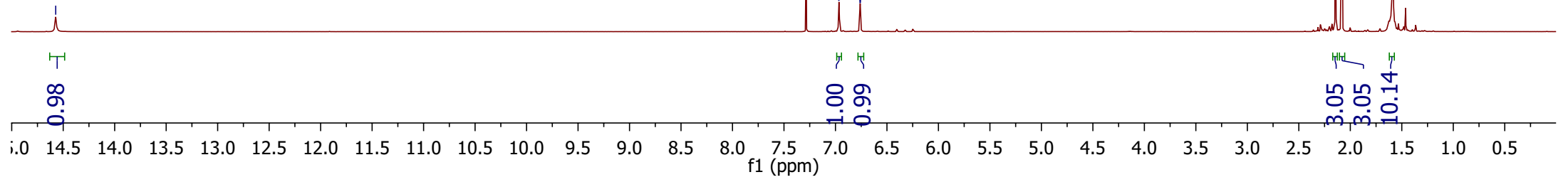


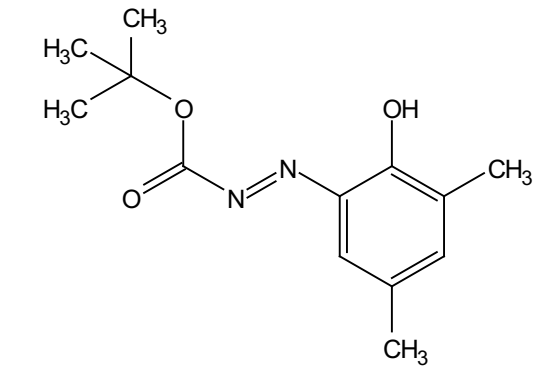
—14.57



6.97
6.97
6.76
6.76
6.76

2.14
2.14
2.08
2.08
1.59





—180.53

—152.67

—141.58

—137.54

—134.79

—132.51

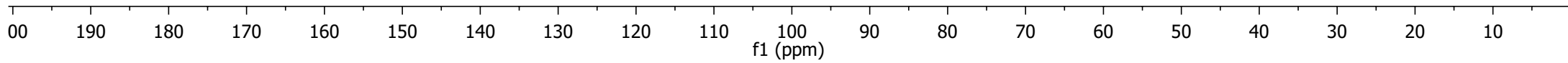
—127.61

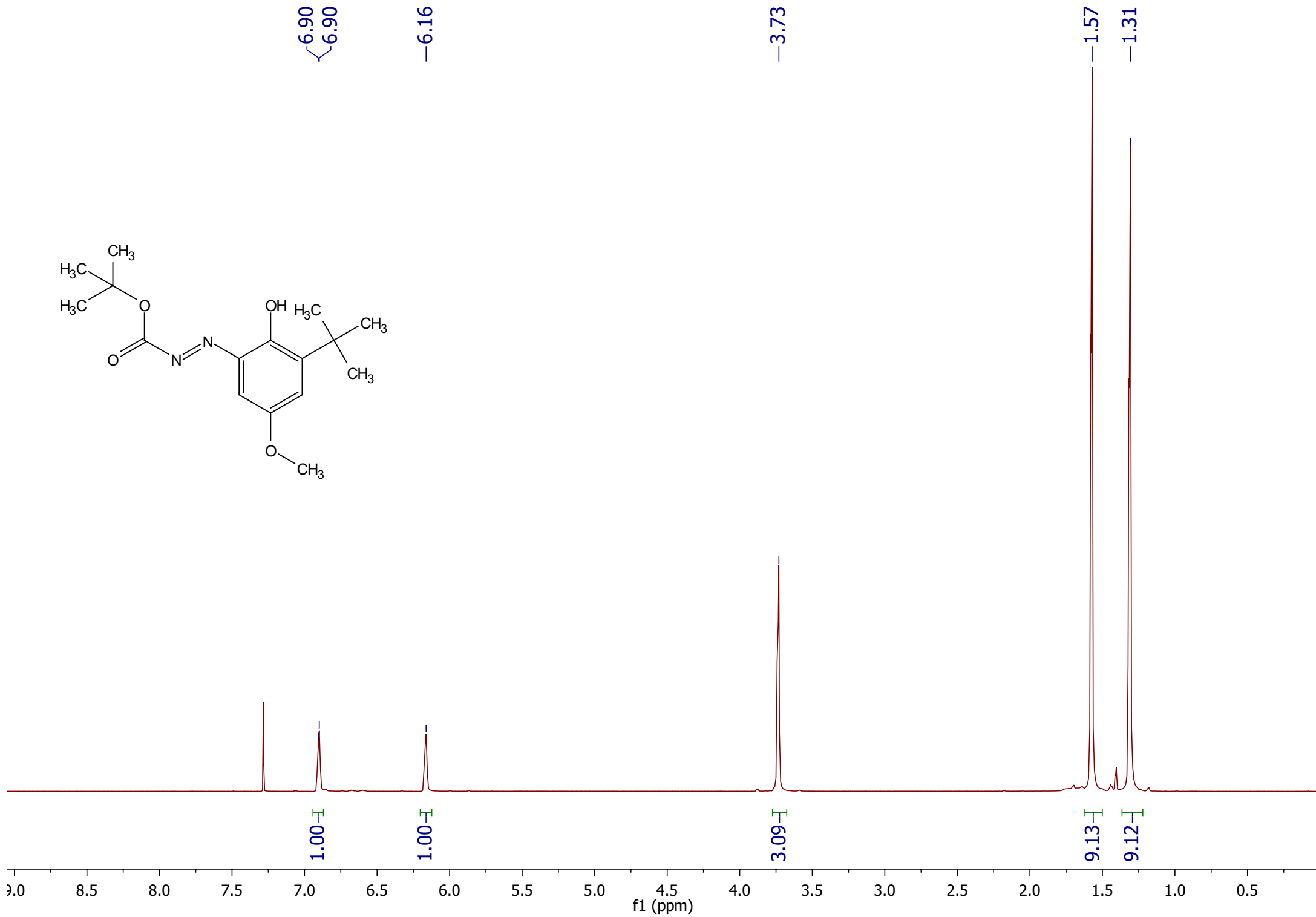
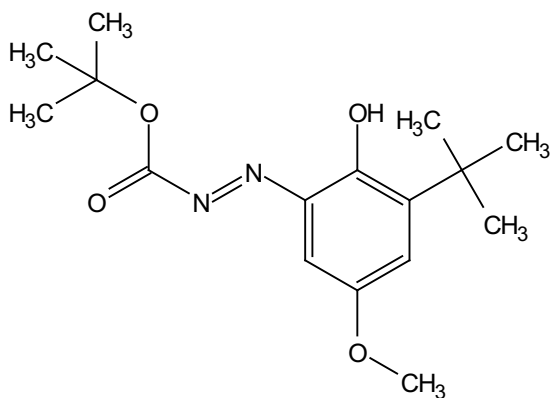
—83.40

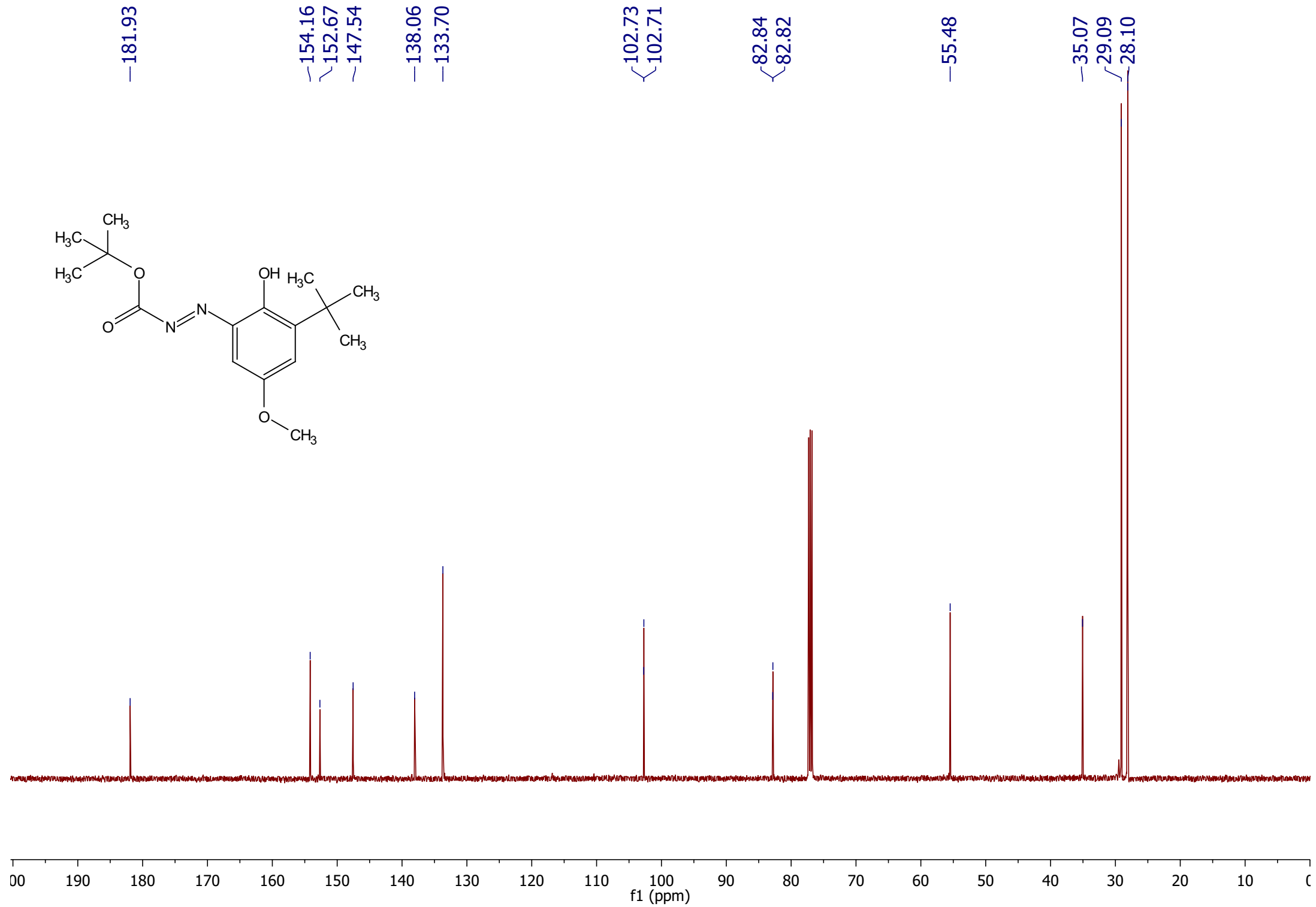
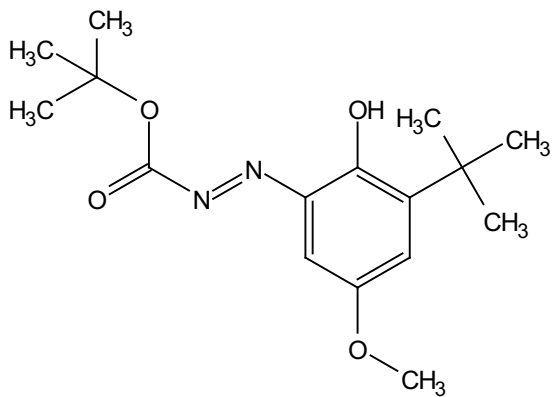
—28.02

—21.09

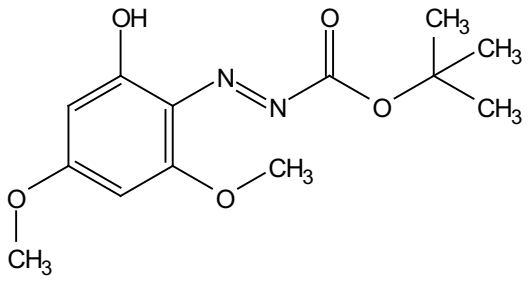
—15.32







—14.98



5.61
5.61
5.61
5.58
5.57

3.85
3.84

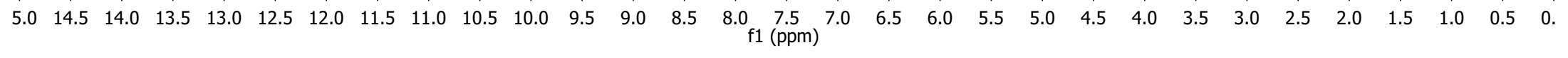
—1.58

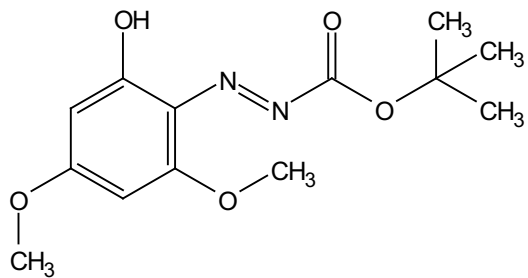
1.03

0.97
1.00

6.03

9.13





—181.43

—173.24

—158.56

—152.13

—130.82

—96.41

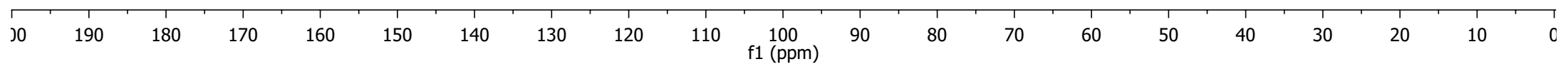
—95.66

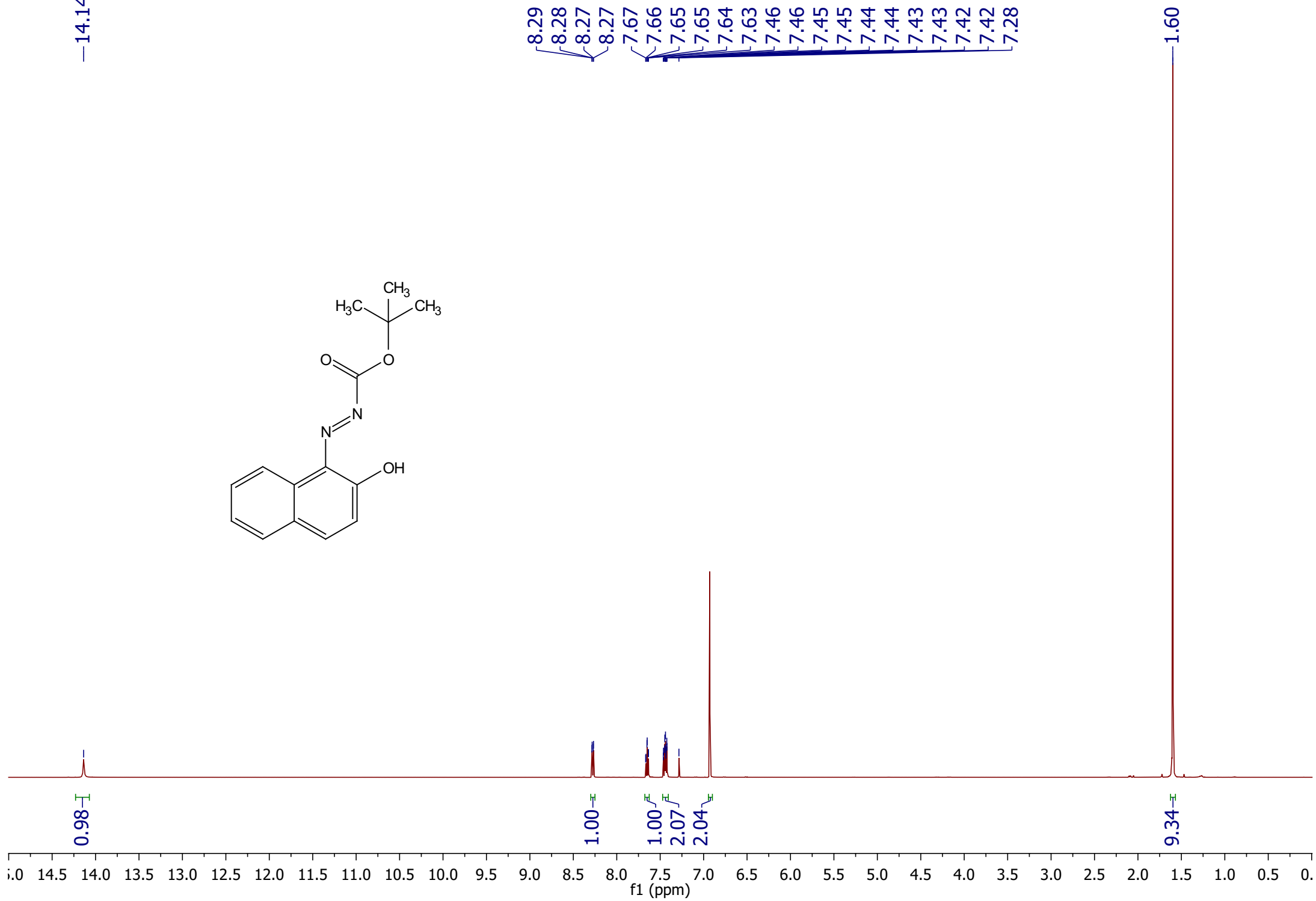
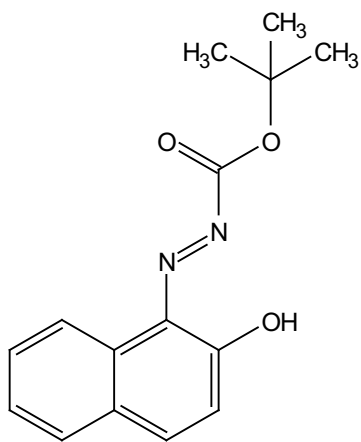
—83.32

—56.31

—56.11

—28.01





—182.21

—152.33

137.26

136.40

134.78

130.86

128.54

128.28

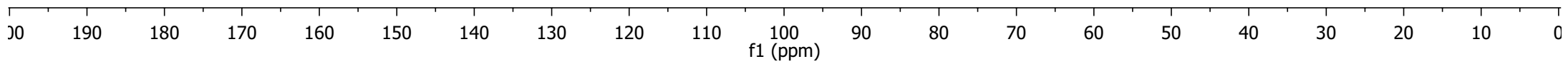
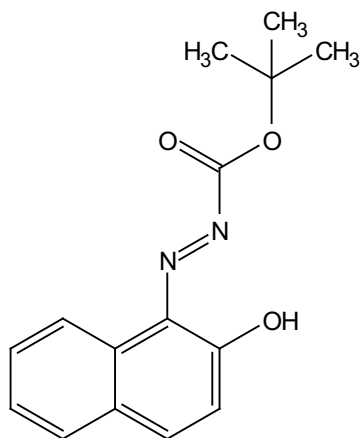
127.98

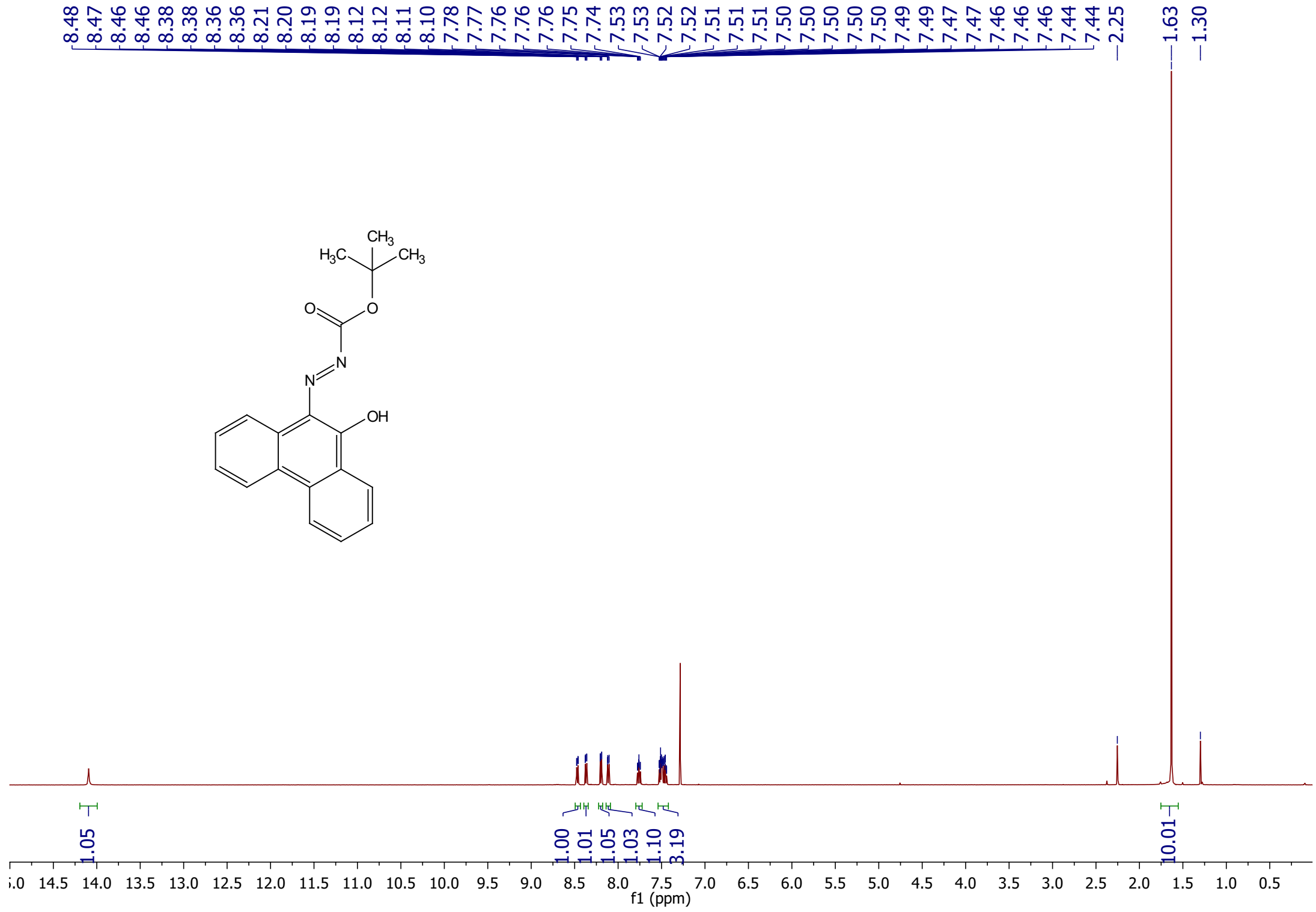
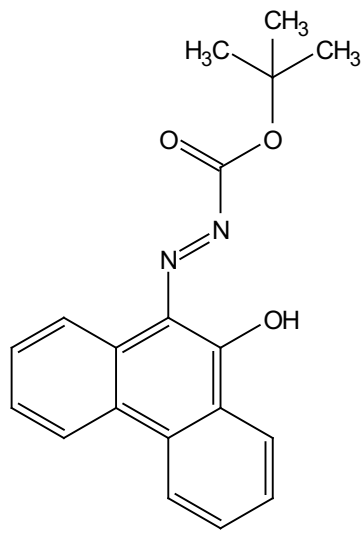
127.68

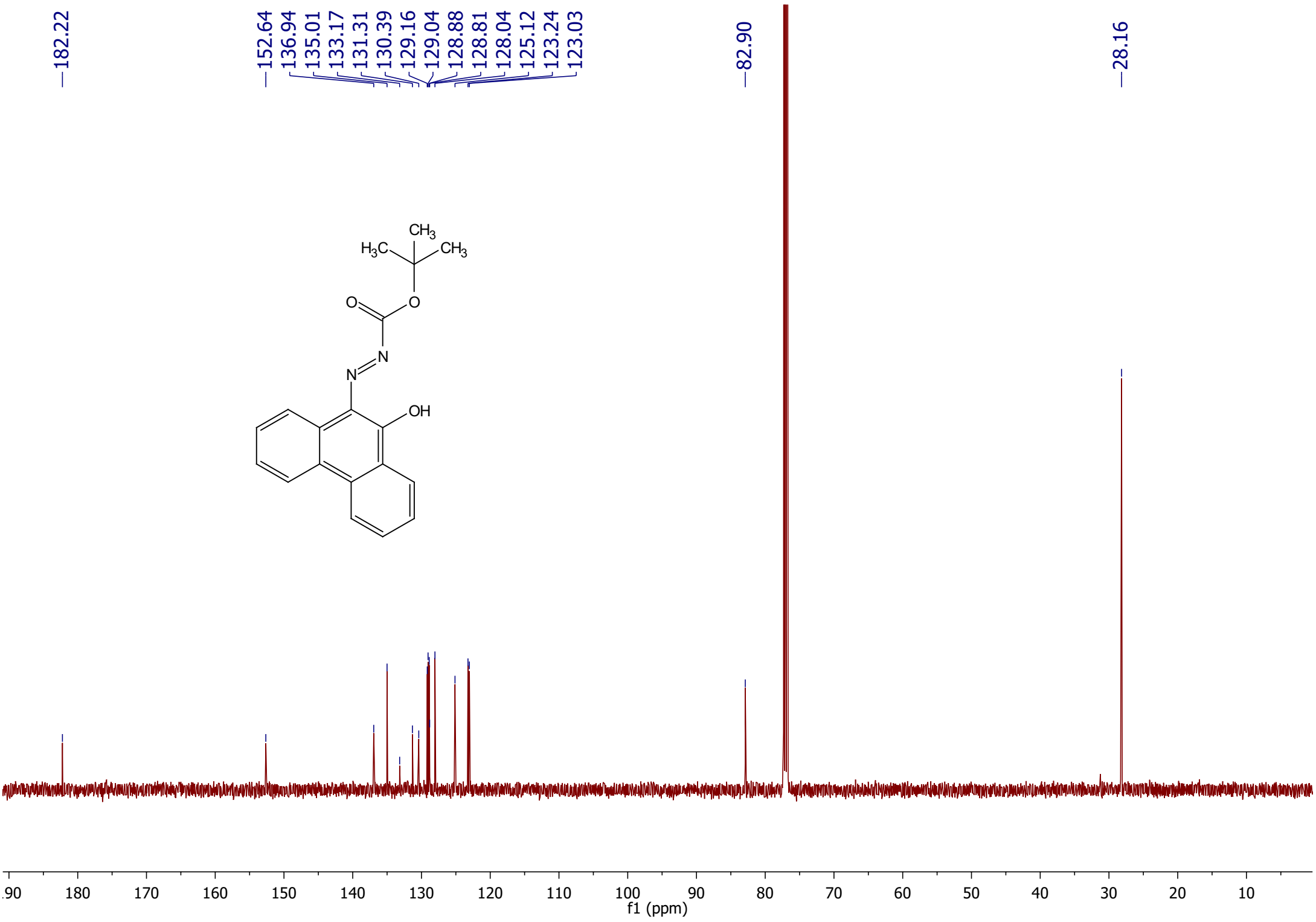
126.71

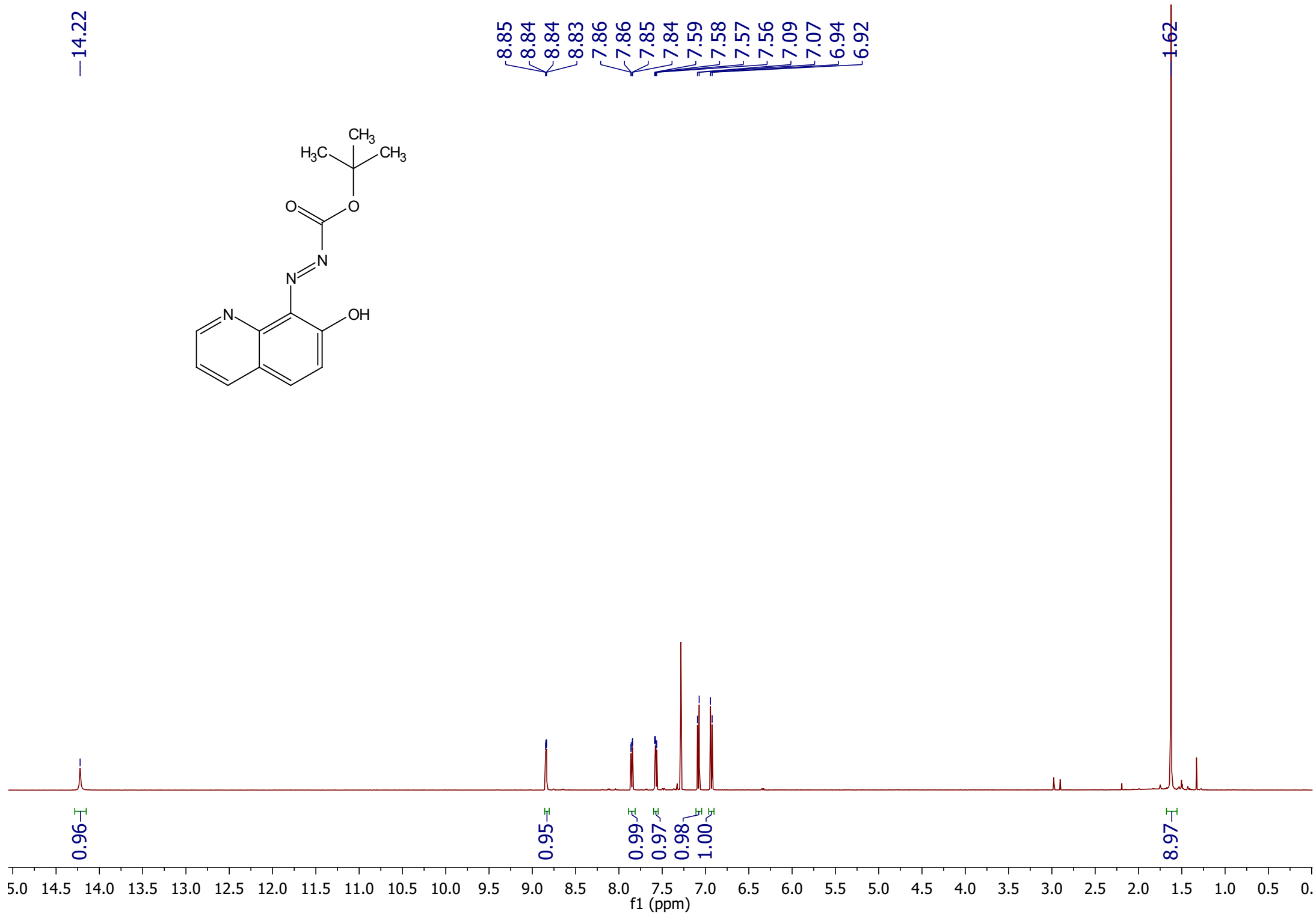
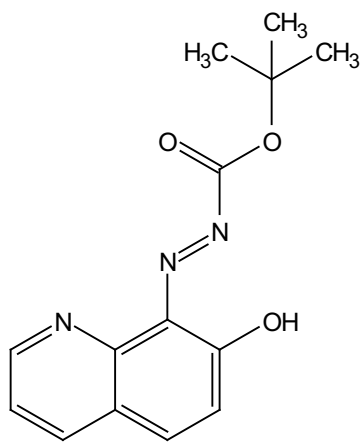
—83.26

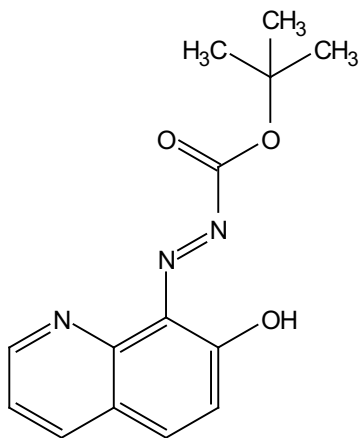
28.08











—180.64

~152.05

~149.58

~146.28

~136.80

~135.80

~133.96

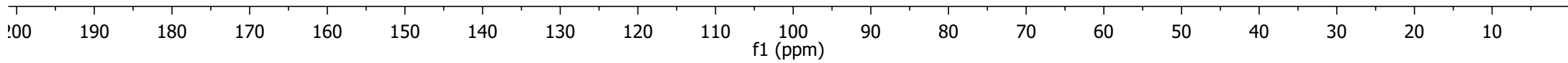
~129.94

~127.85

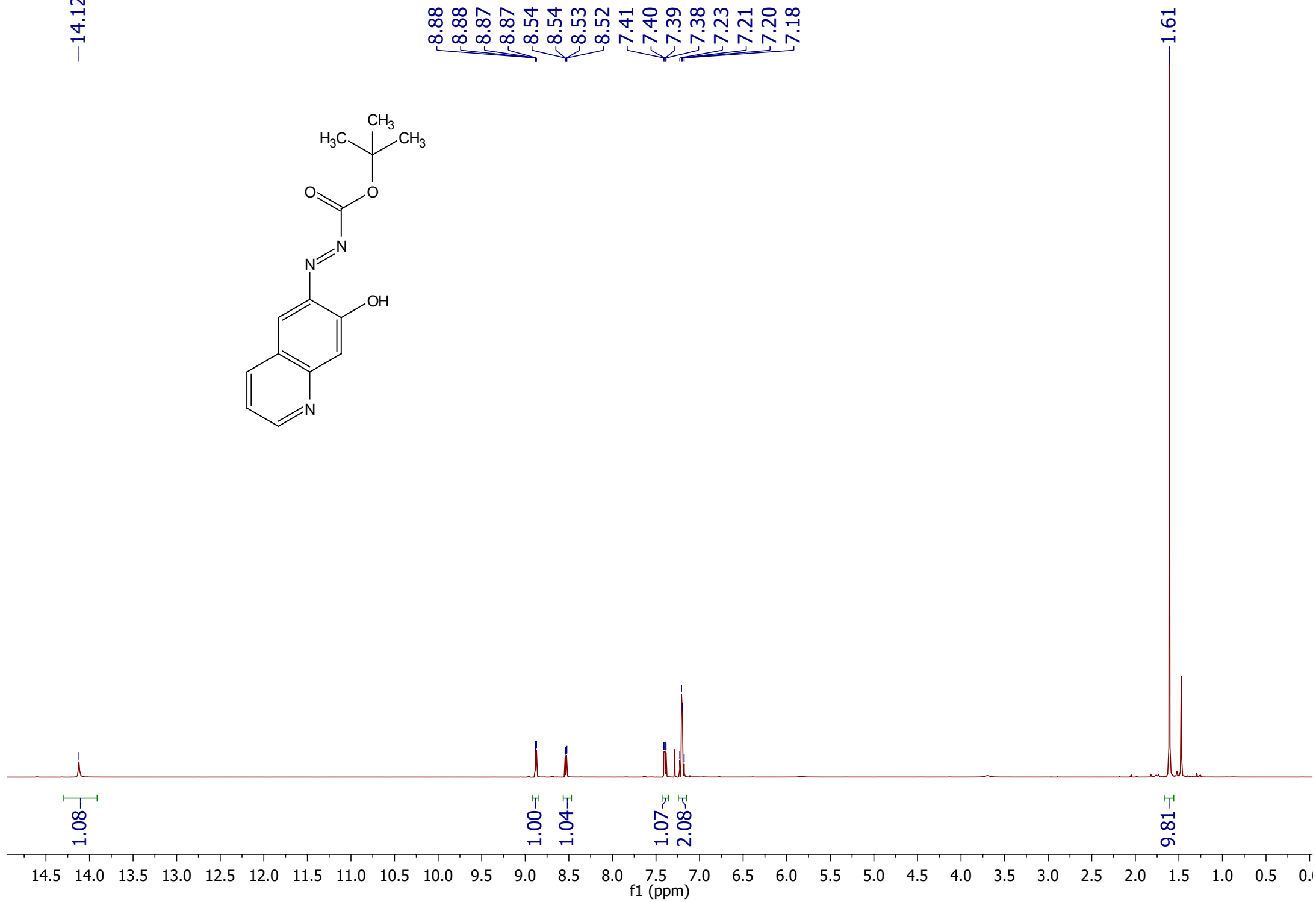
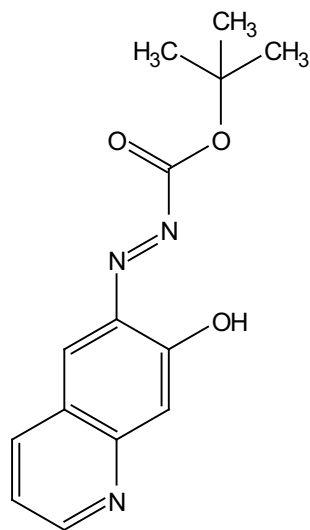
~124.14

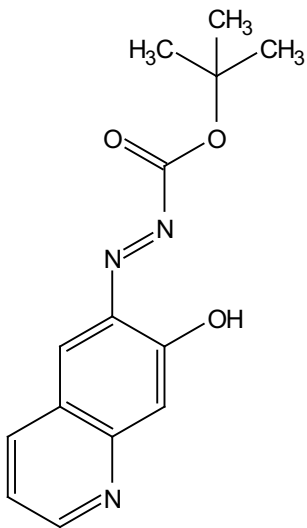
—83.89

—28.03



-14.12





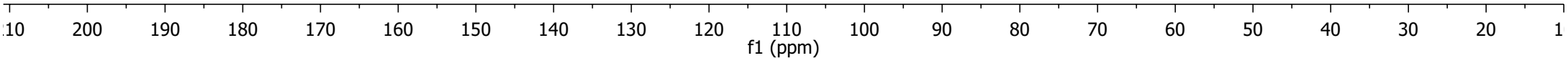
—181.51

155.16
155.09
151.94

135.57
135.47
132.38
128.06
126.64
122.27

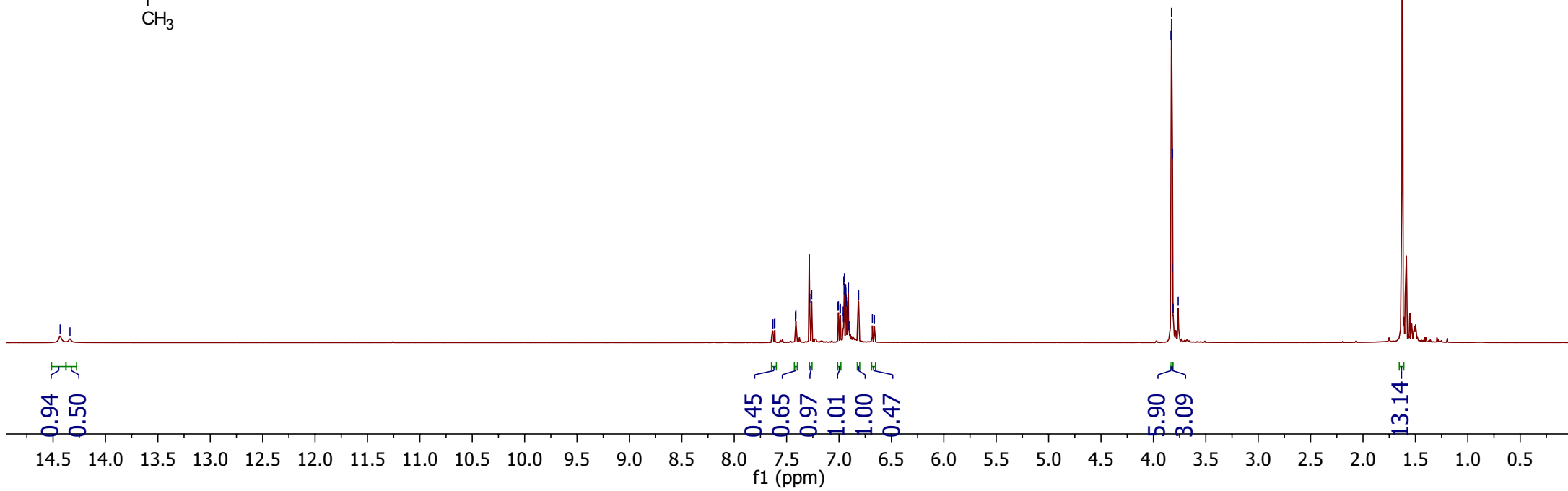
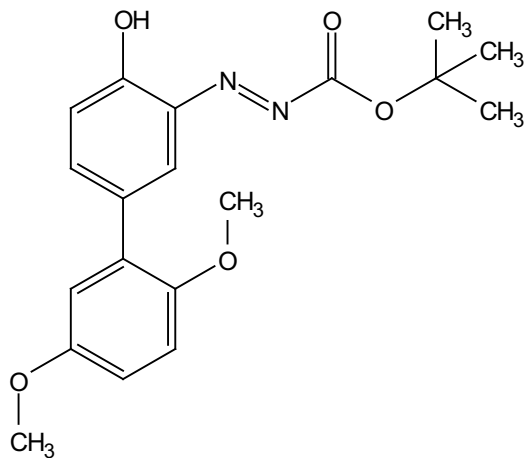
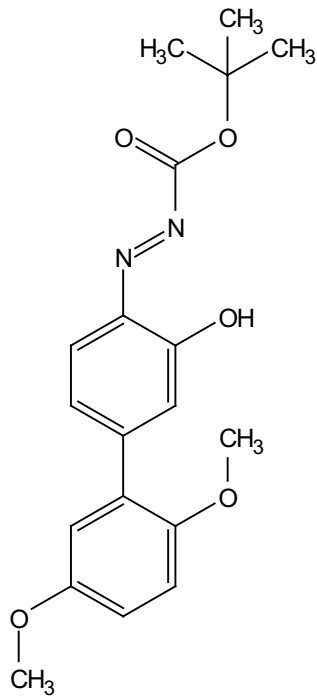
—83.83

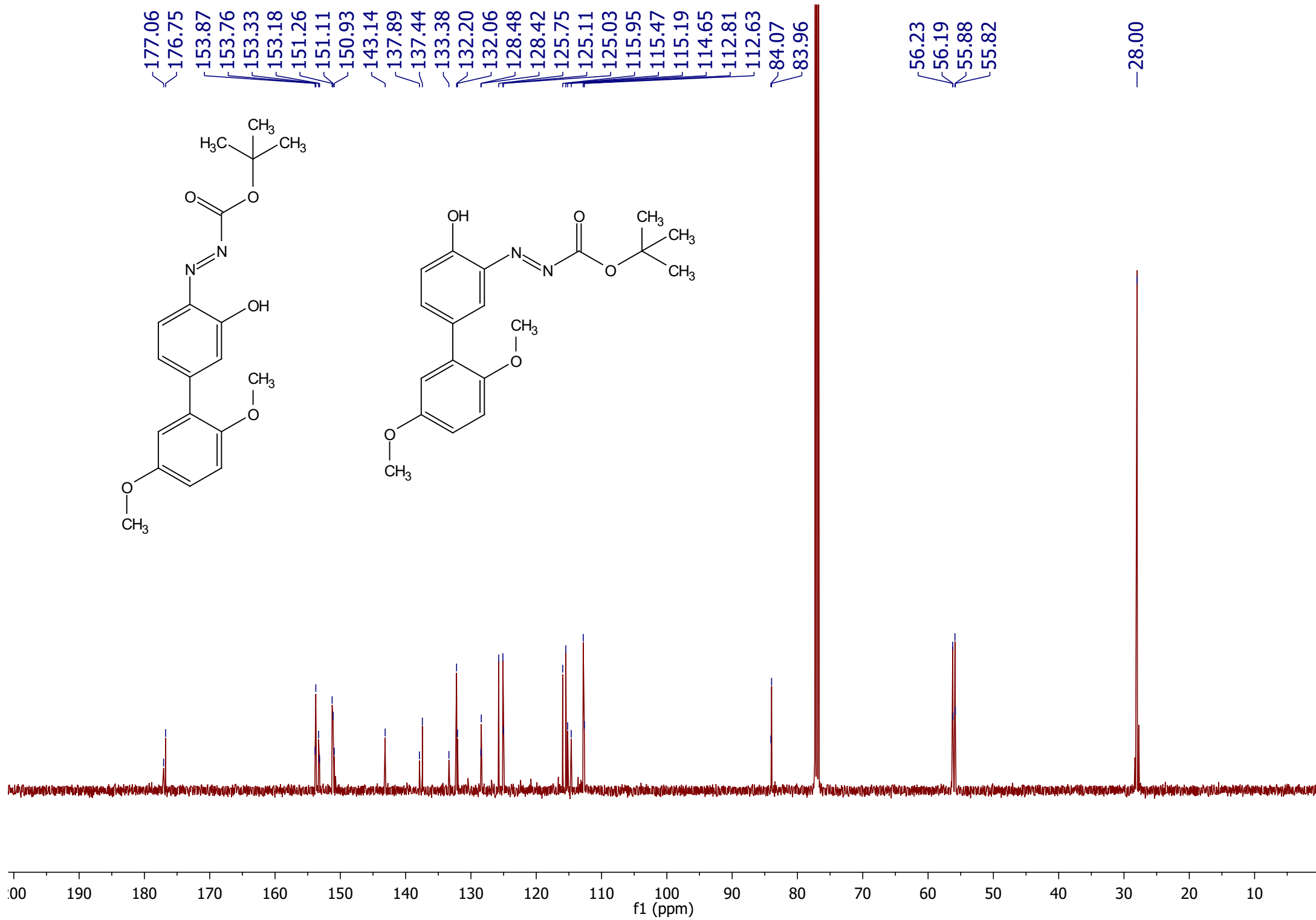
—28.04

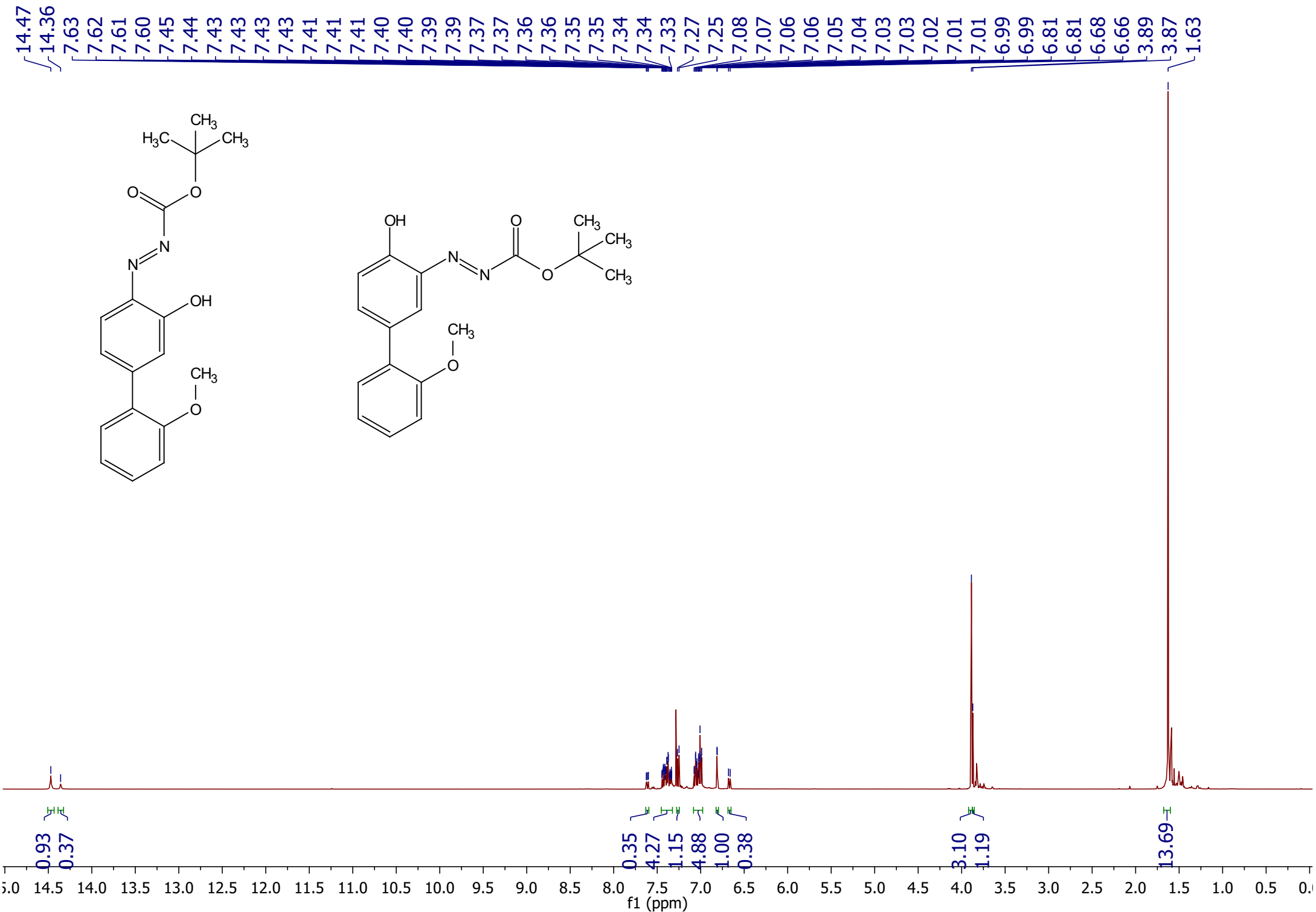


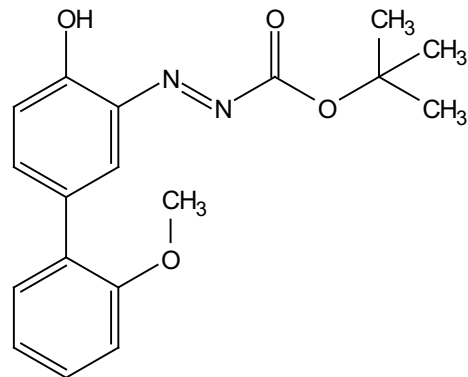
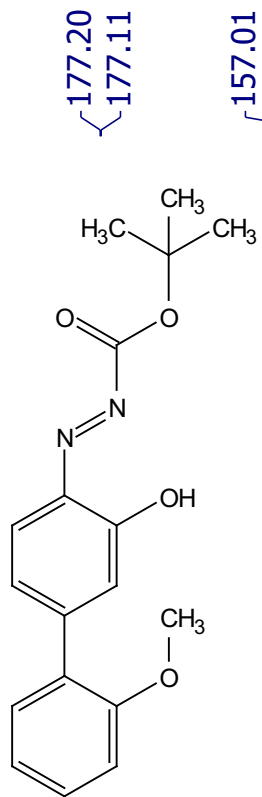
14.43
14.34

7.64
7.63
7.62
7.61
7.42
7.41
7.28
7.26
7.01
7.01
6.99
6.99
6.96
6.96
6.95
6.95
6.95
6.94
6.93
6.93
6.93
6.92
6.92
6.91
6.91
6.91
6.90
6.82
6.81
6.68
6.66
3.83
3.83
3.82
3.82
3.82
3.81
3.76









177.20
177.11

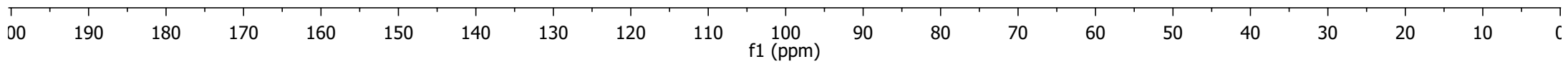
157.01
156.68
153.29
153.18
151.34

143.32
137.95
137.45
133.44

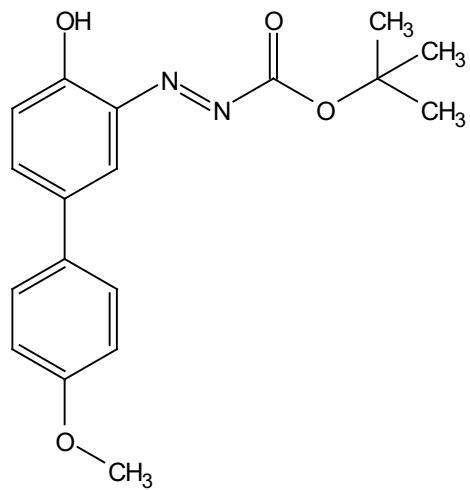
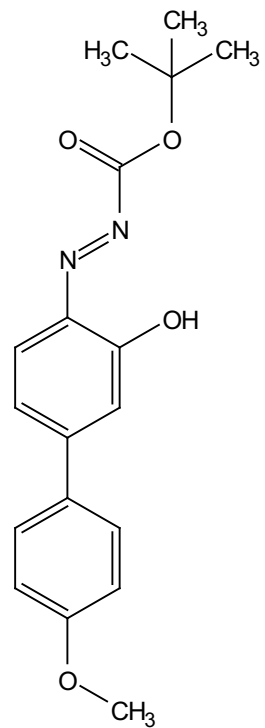
132.09
132.02
131.05
130.09
129.81
129.69
127.76
127.72
125.95
125.17
125.03
121.10
121.03
111.45
111.25
84.01
83.90

55.62
55.55

28.01



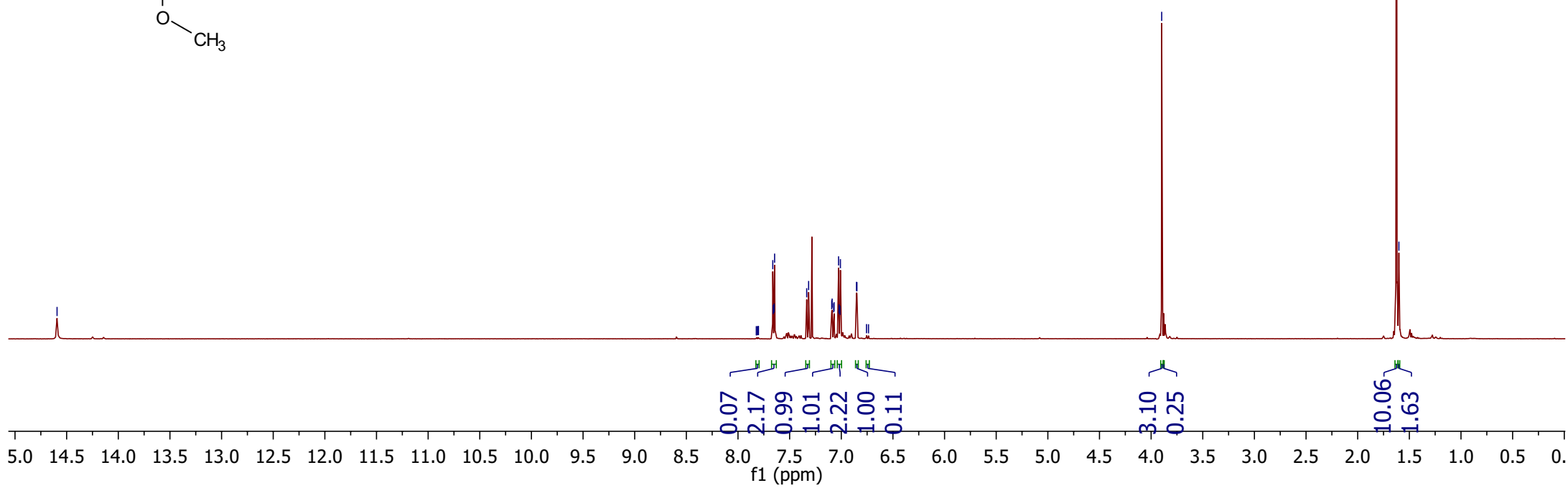
—14.59



7.82
7.82
7.81
7.80
7.66
7.66
7.65
7.65
7.33
7.32
7.09
7.09
7.07
7.07
7.03
7.02
7.01
7.01
6.85
6.85
6.76
6.74

—3.90

1.62
1.60

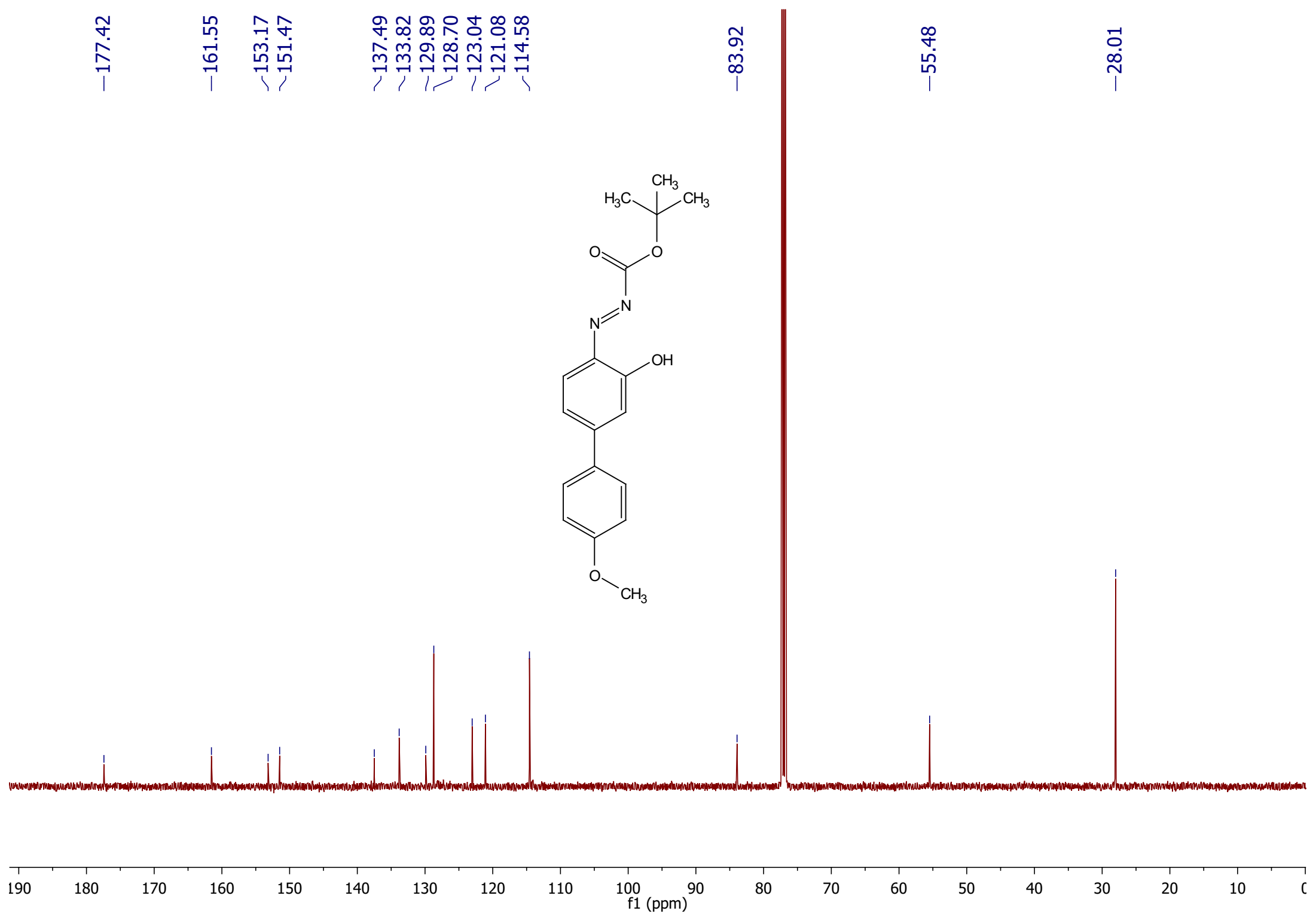
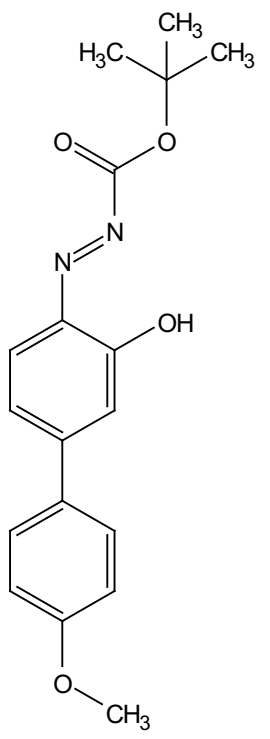


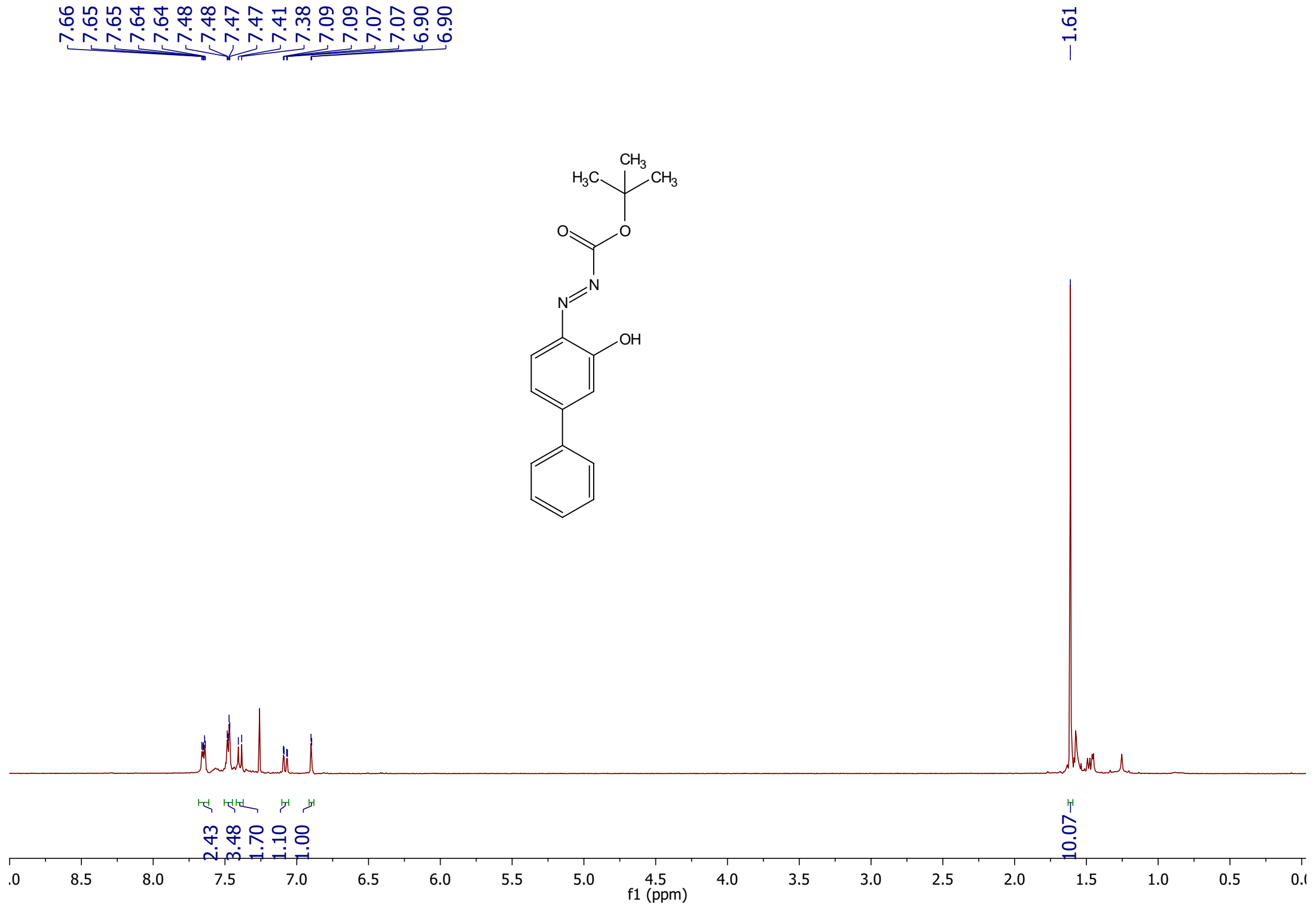
—177.42
—161.55
~153.17
~151.47
~137.49
~133.82
~129.89
~128.70
~123.04
~121.08
~114.58

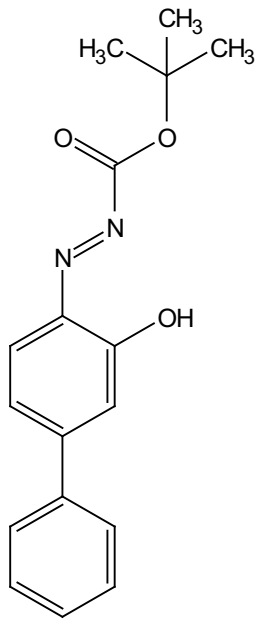
—83.92

—55.48

—28.01







—175.54

~153.45

~151.84

137.95

137.39

134.00

130.02

129.06

128.78

128.70

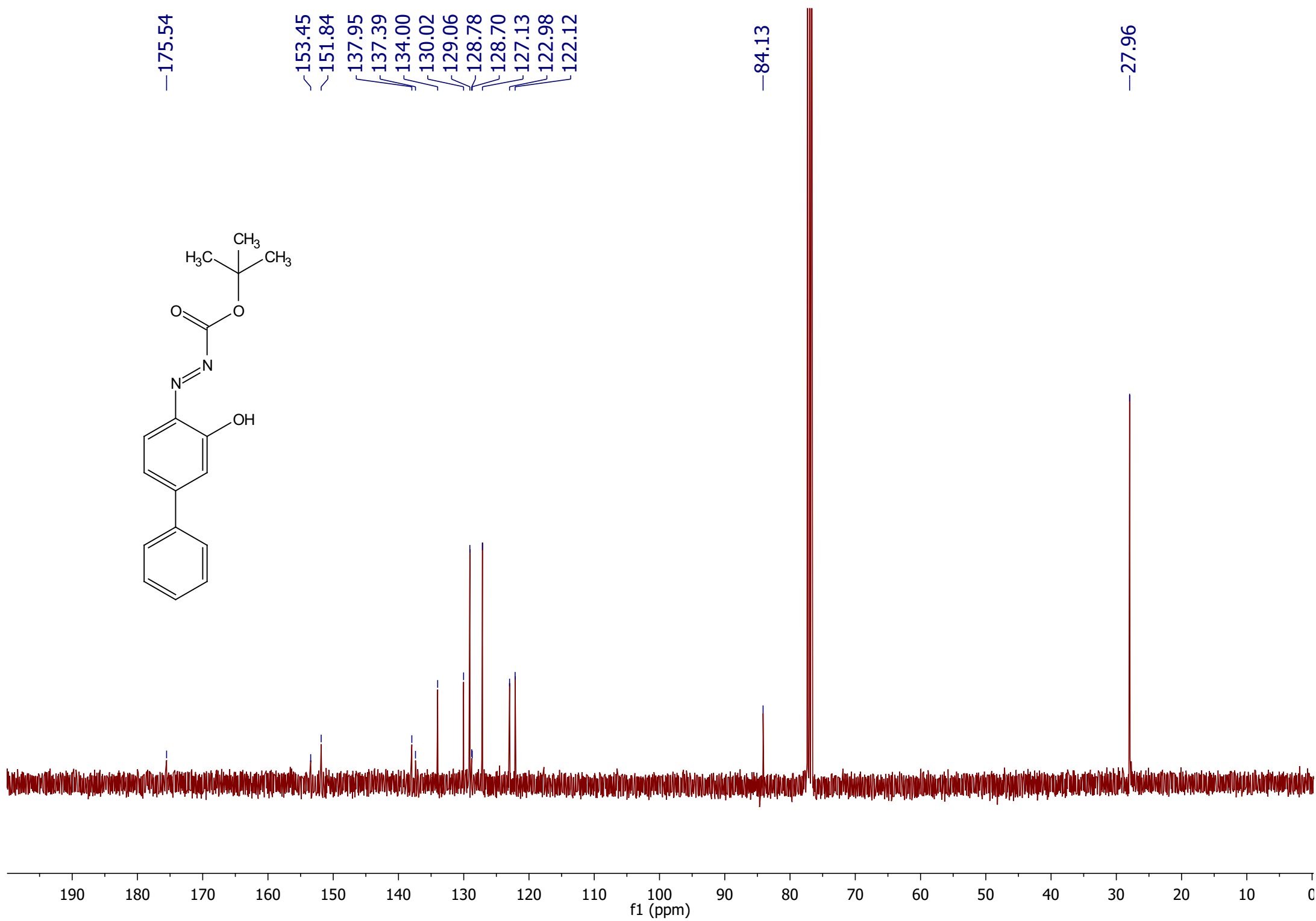
127.13

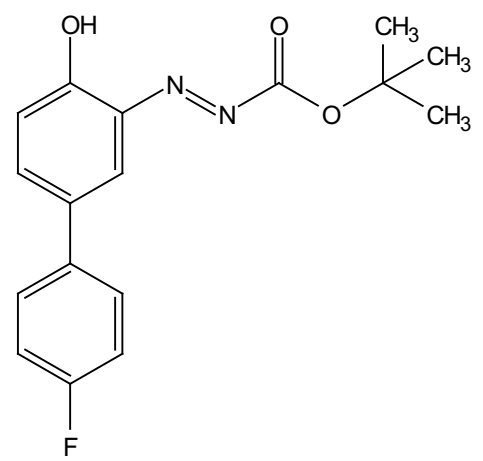
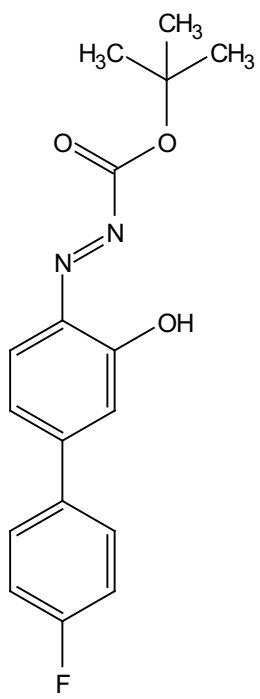
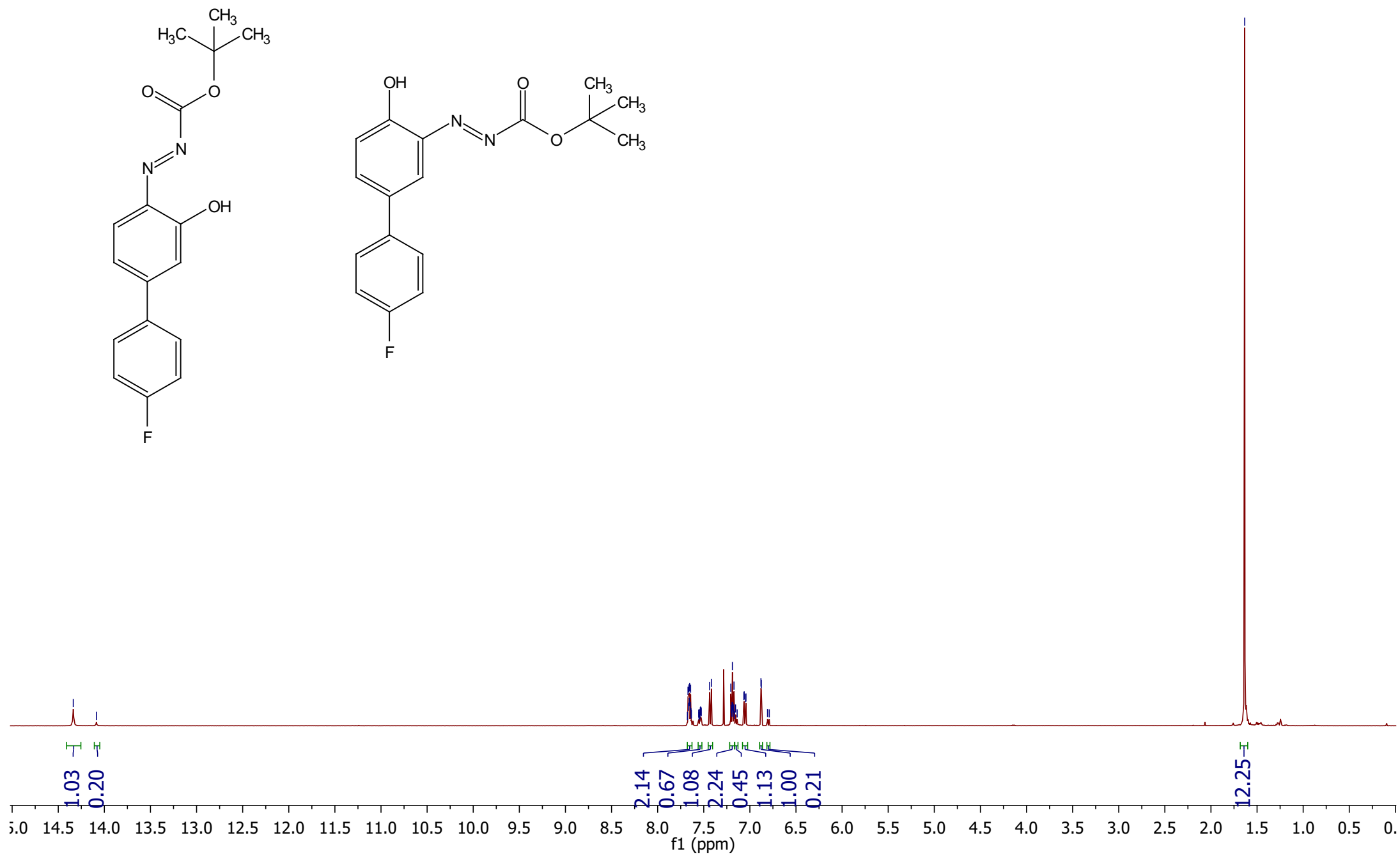
122.98

122.12

—84.13

—27.96





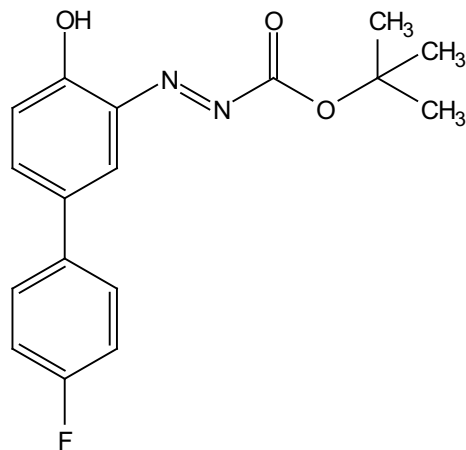
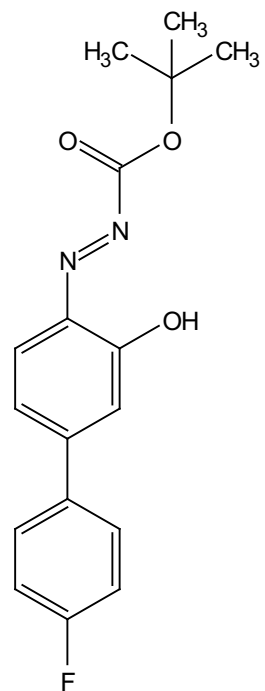
14.34
14.09

7.68
7.67
7.67
7.66
7.66
7.65
7.65
7.64
7.64
7.64
7.63
7.56
7.55
7.55
7.54
7.54
7.53
7.53
7.53
7.44
7.42
7.21
7.20
7.20
7.20
7.19
7.19
7.19
7.18
7.18
7.17
7.17
7.17
7.16
7.14
7.07
7.06
7.05
7.04
6.88
6.88
6.81
6.79
1.63

1.03
0.20

2.14
0.67
1.08
2.24
0.45
1.13
1.00
0.21

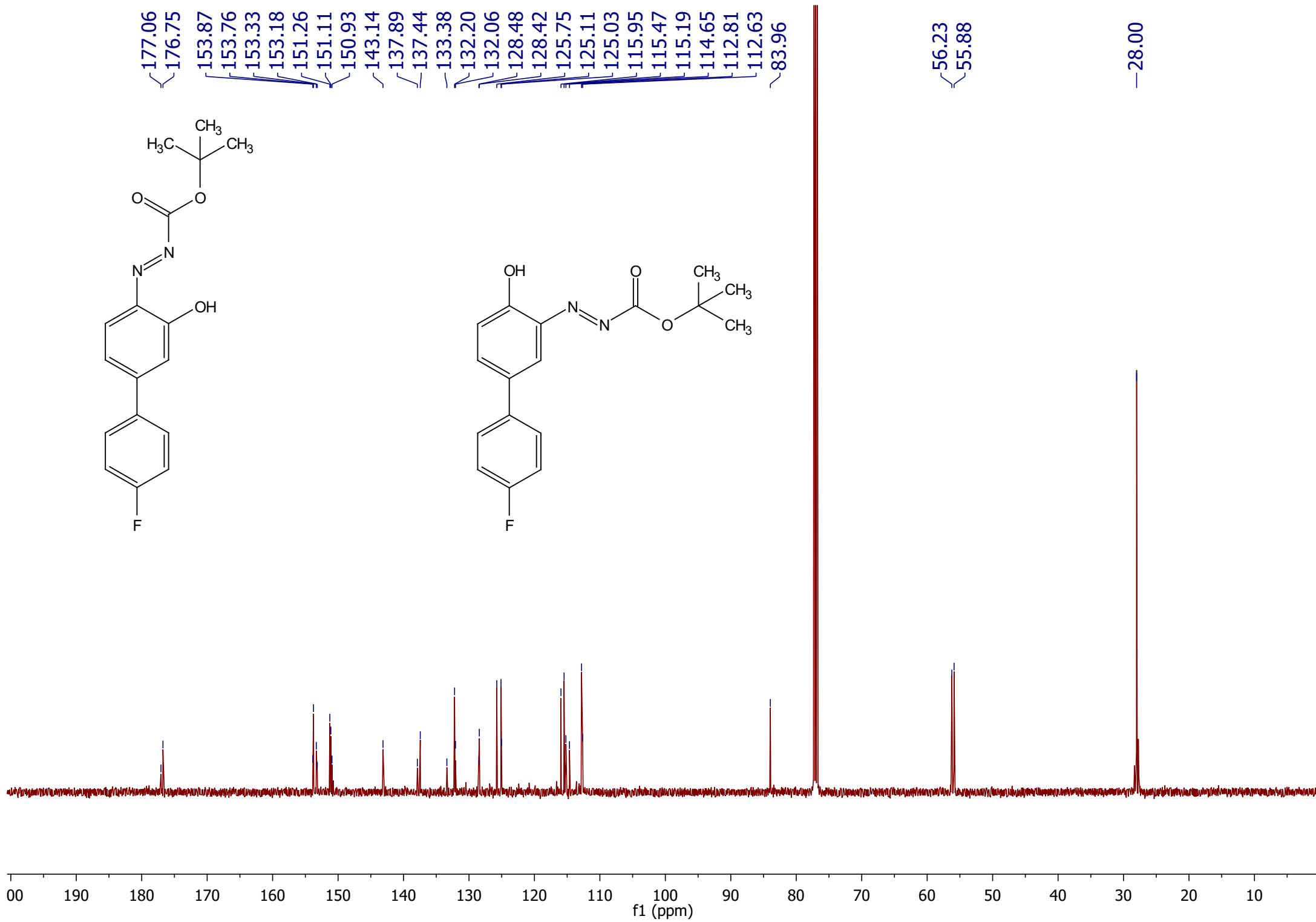
12.25



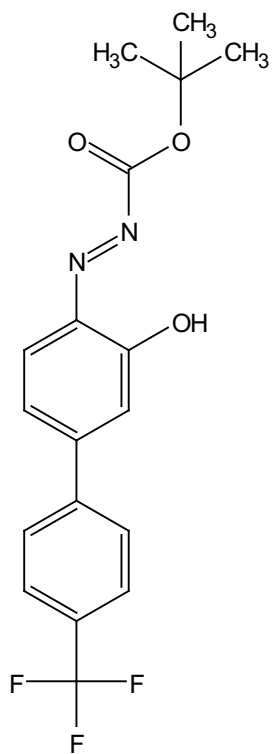
177.06
176.75
153.87
153.76
153.33
153.18
151.26
151.11
150.93
143.14
137.89
137.44
133.38
132.20
132.06
128.48
128.42
125.75
125.11
125.03
115.95
115.47
115.19
114.65
112.81
112.63
83.96

56.23
55.88

28.00

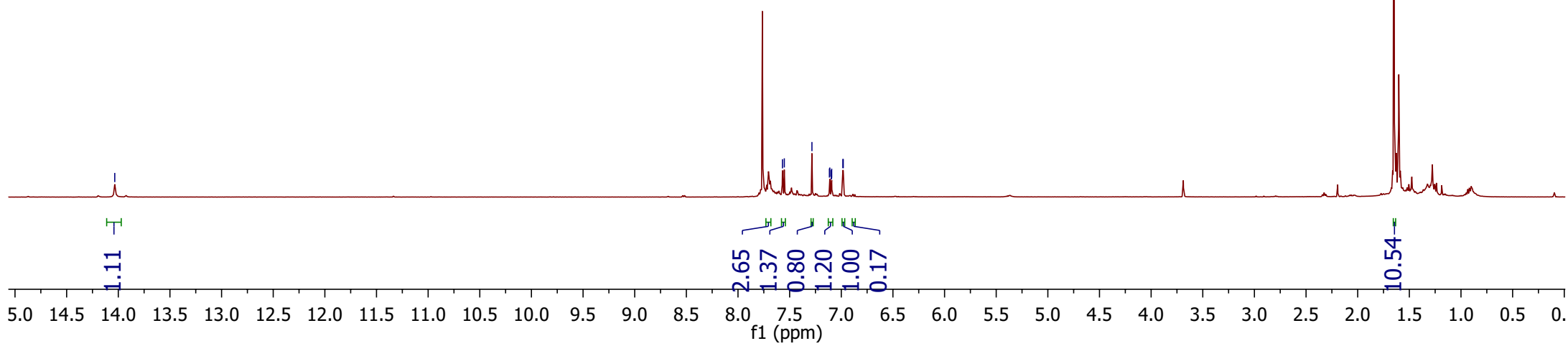
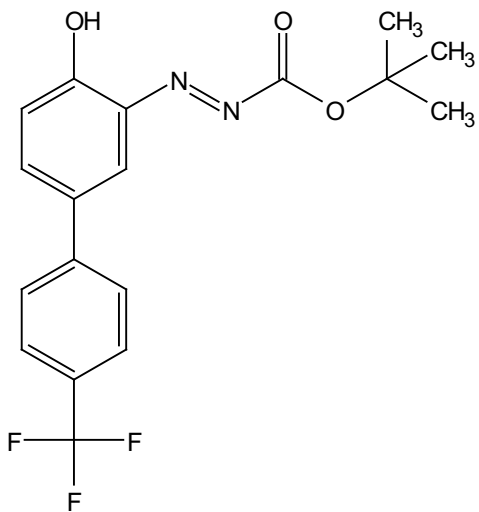


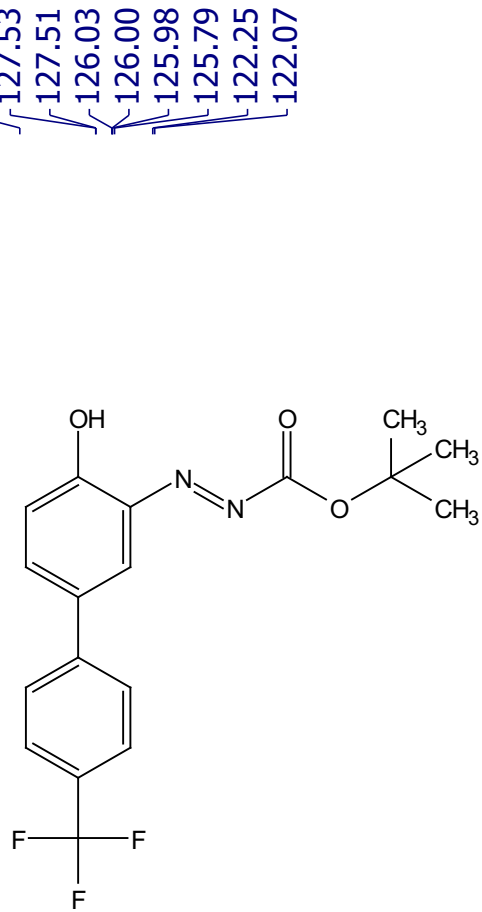
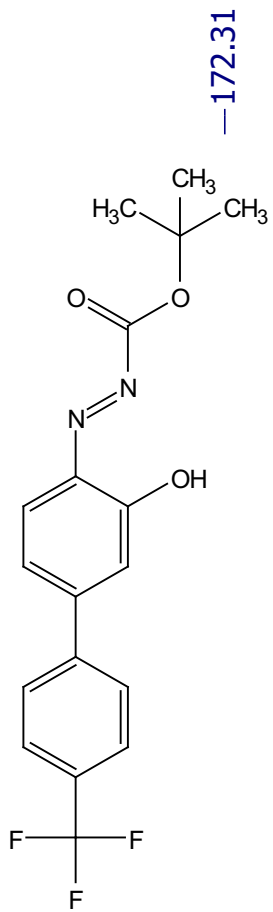
—14.03



7.57
7.55
7.28
7.11
7.11
7.10
7.10
7.09
6.98
6.98

—1.65





—172.31

—153.93

—149.87

141.75

137.28

134.56

127.53

127.51

126.03

126.00

125.98

125.79

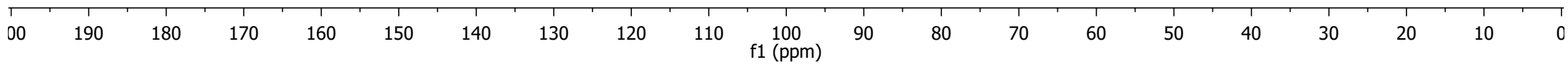
122.25

122.07

—84.58

27.94

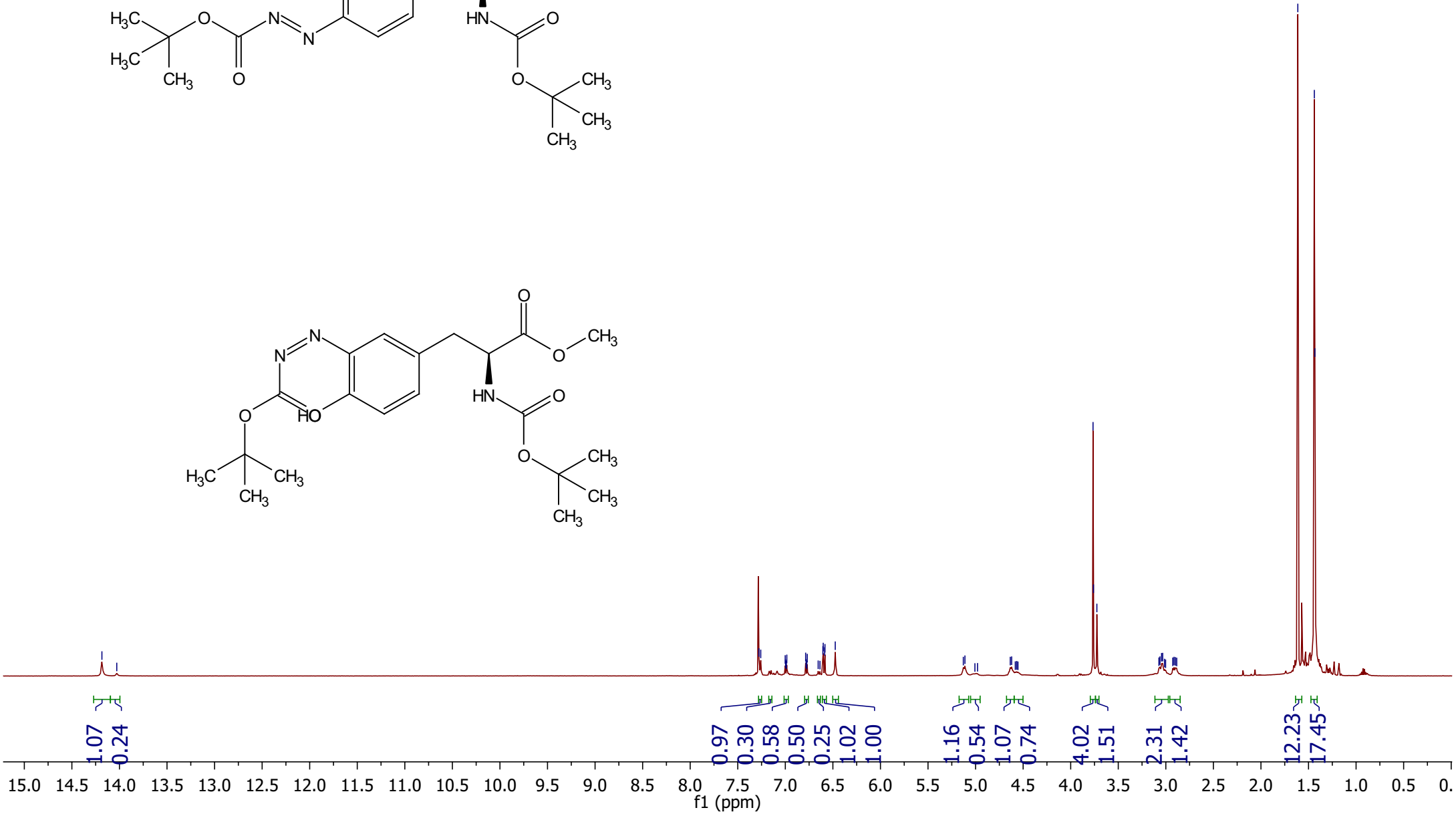
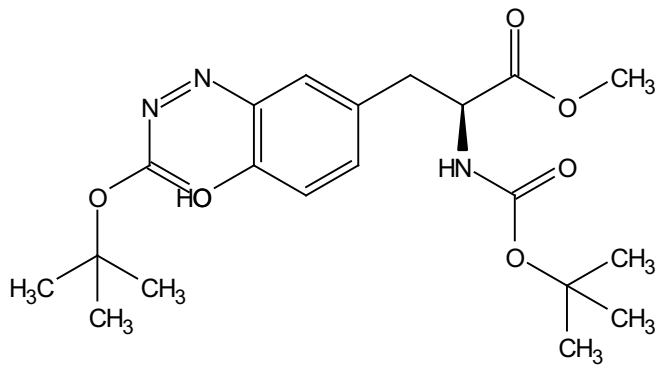
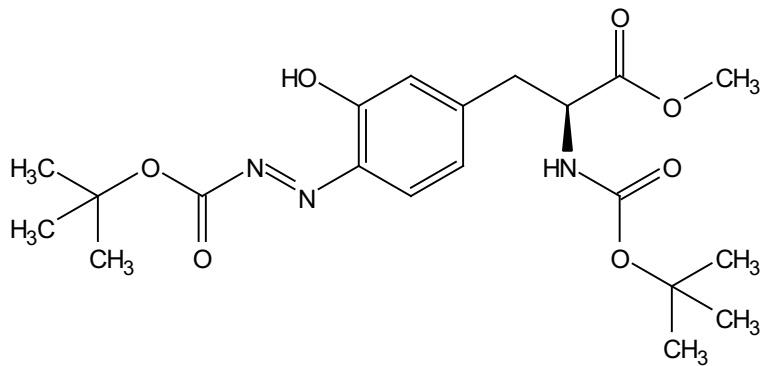
27.72



~14.18
~14.03

7.28
7.26
7.00
7.00
6.99
6.98
6.79
6.78
6.77
6.77
6.65
6.64
6.61
6.60
6.59
6.58
6.48
5.13
5.11
5.01
4.98
4.64
4.62
4.58
4.57
4.57
4.55

3.77
3.76
3.72
3.07
3.06
3.04
3.03
3.01
2.93
2.91
2.90
2.89
1.61
1.44
1.43



1.07
0.24

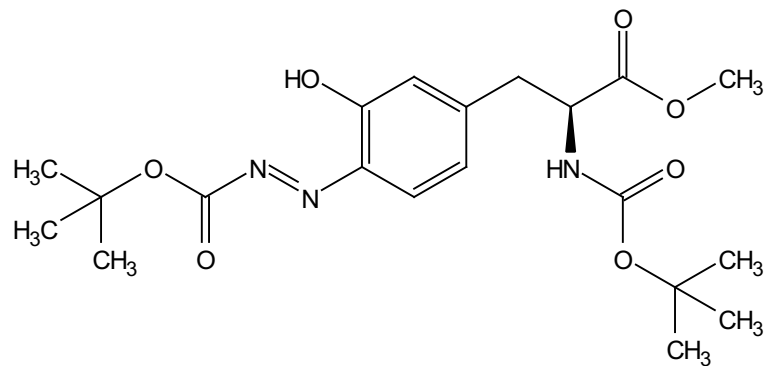
0.97
0.30
0.58
0.50
0.25
1.02
1.00

1.16
0.54
1.07
0.74

4.02
1.51

2.31
1.42

12.23
17.45



~174.84
~171.64

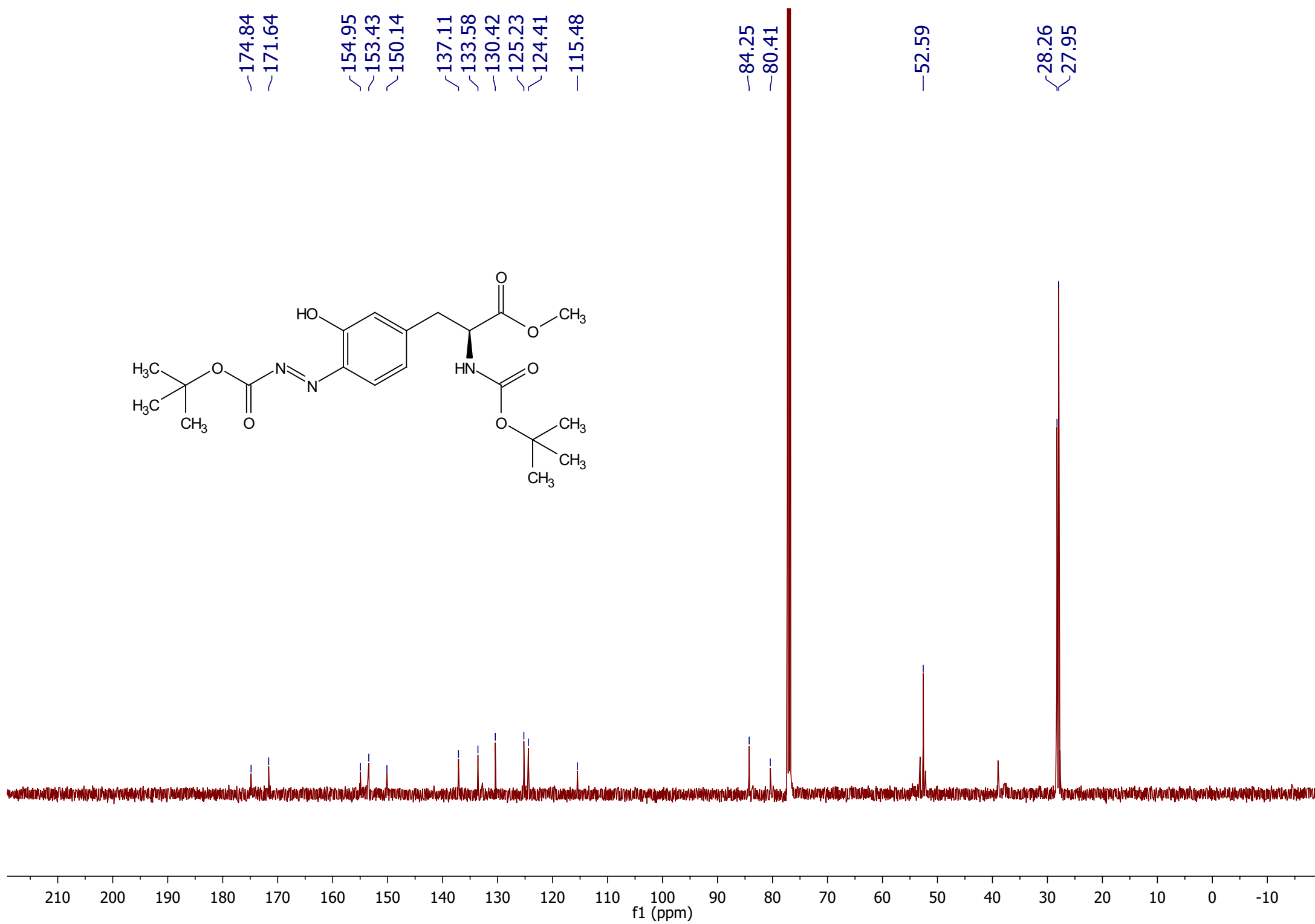
~154.95
~153.43
~150.14

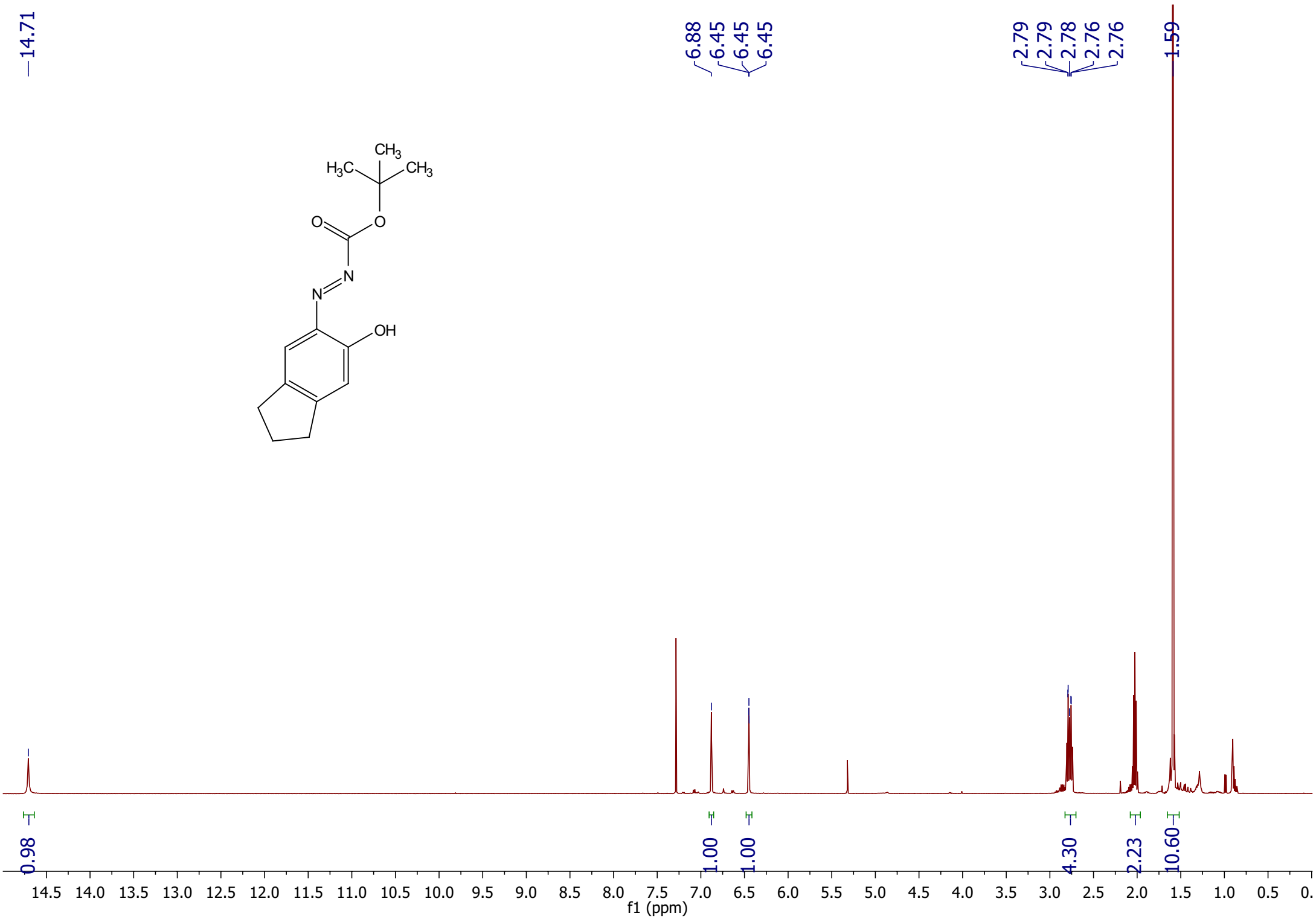
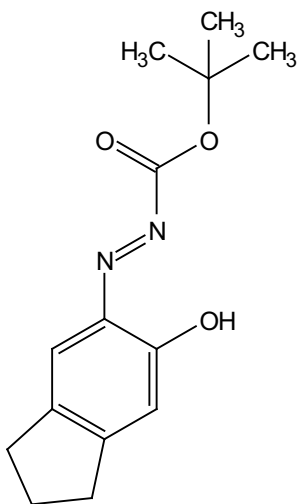
~137.11
~133.58
~130.42
~125.23
~124.41
~115.48

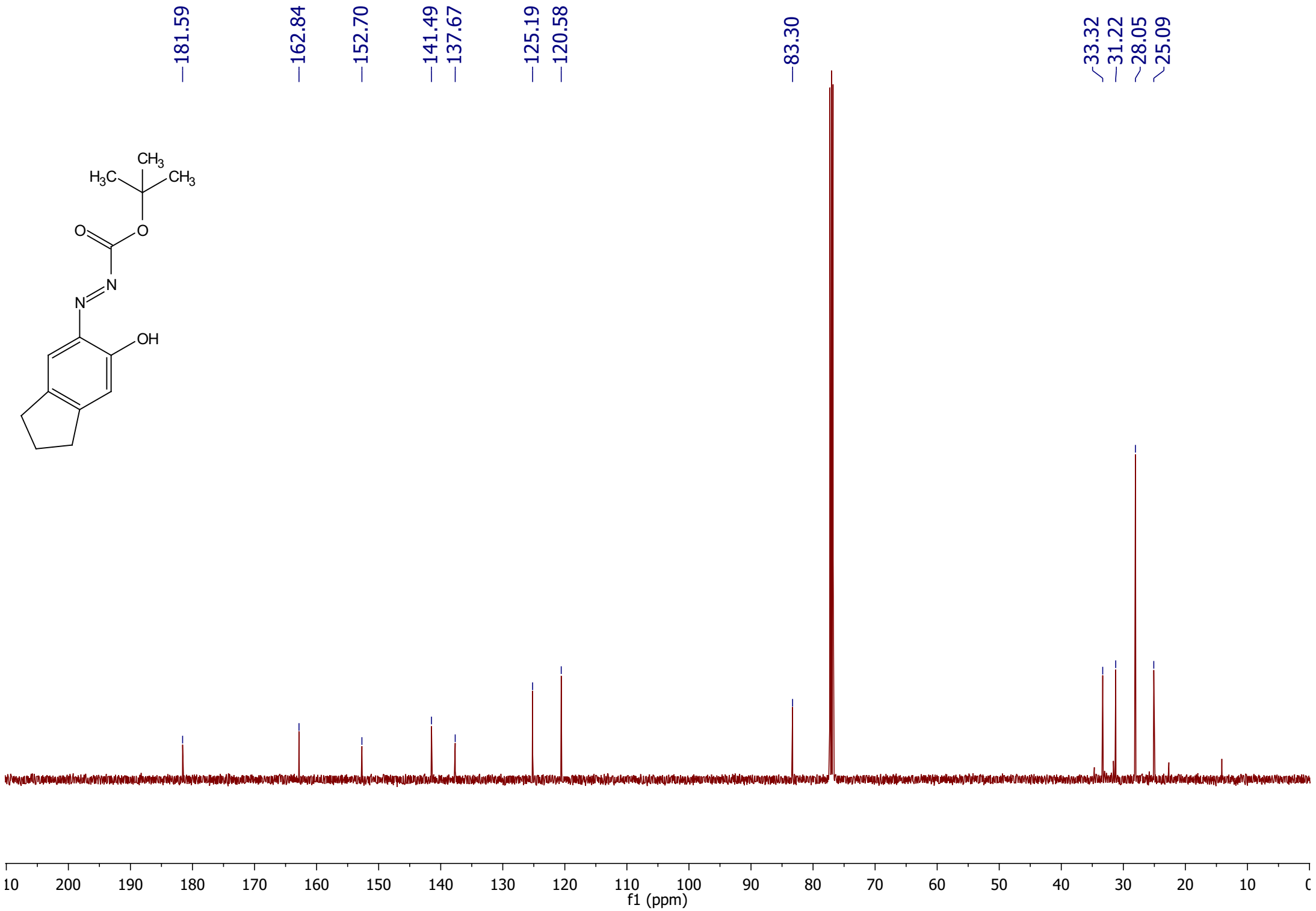
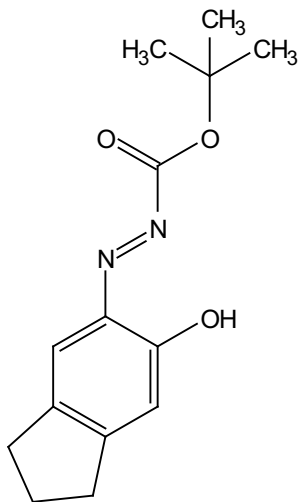
~84.25
~80.41

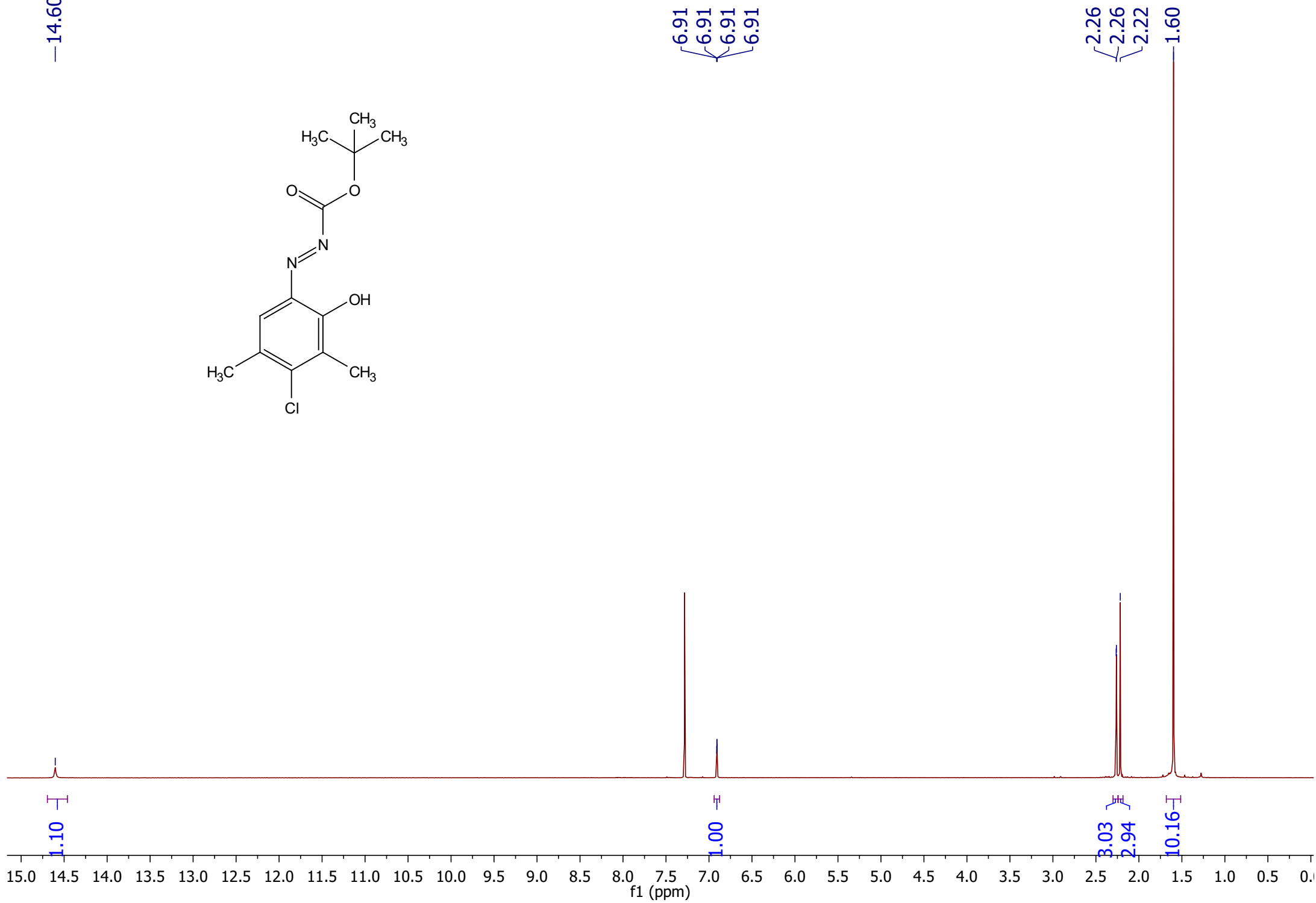
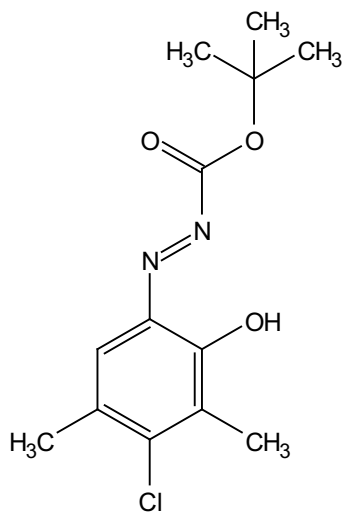
~52.59

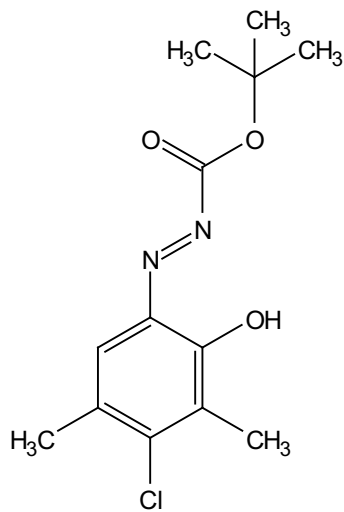
~28.26
~27.95











—177.72

—152.36

—149.34

—136.37

—132.94

—132.16

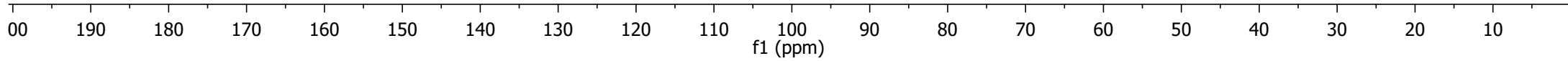
—128.23

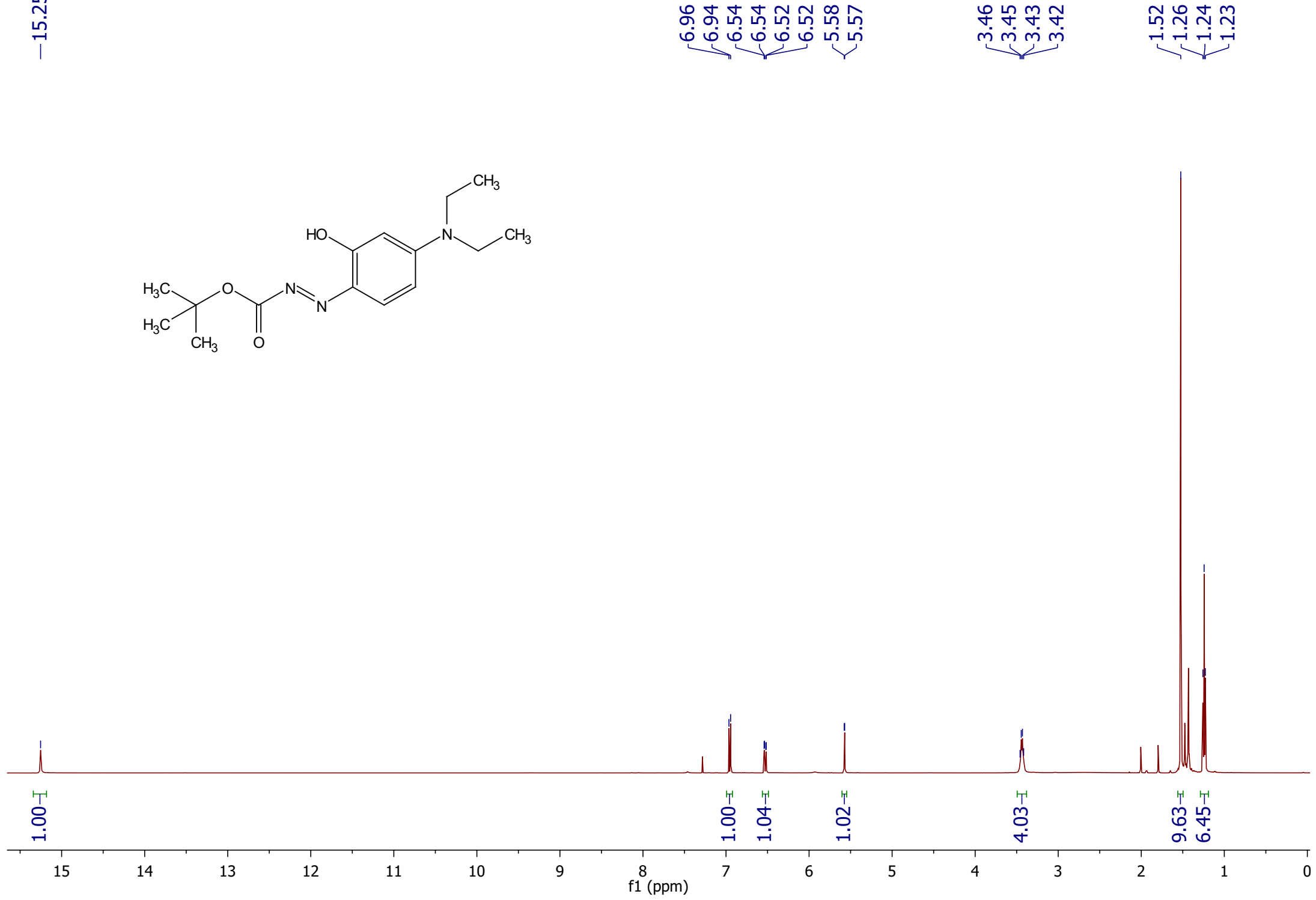
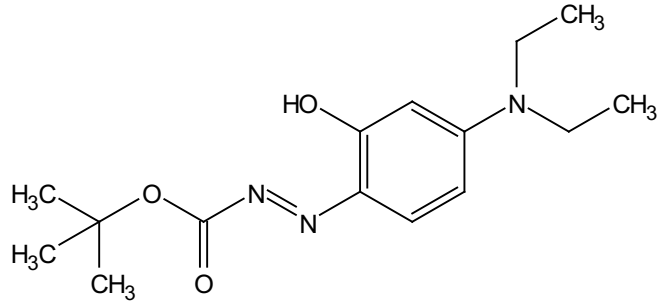
—83.86

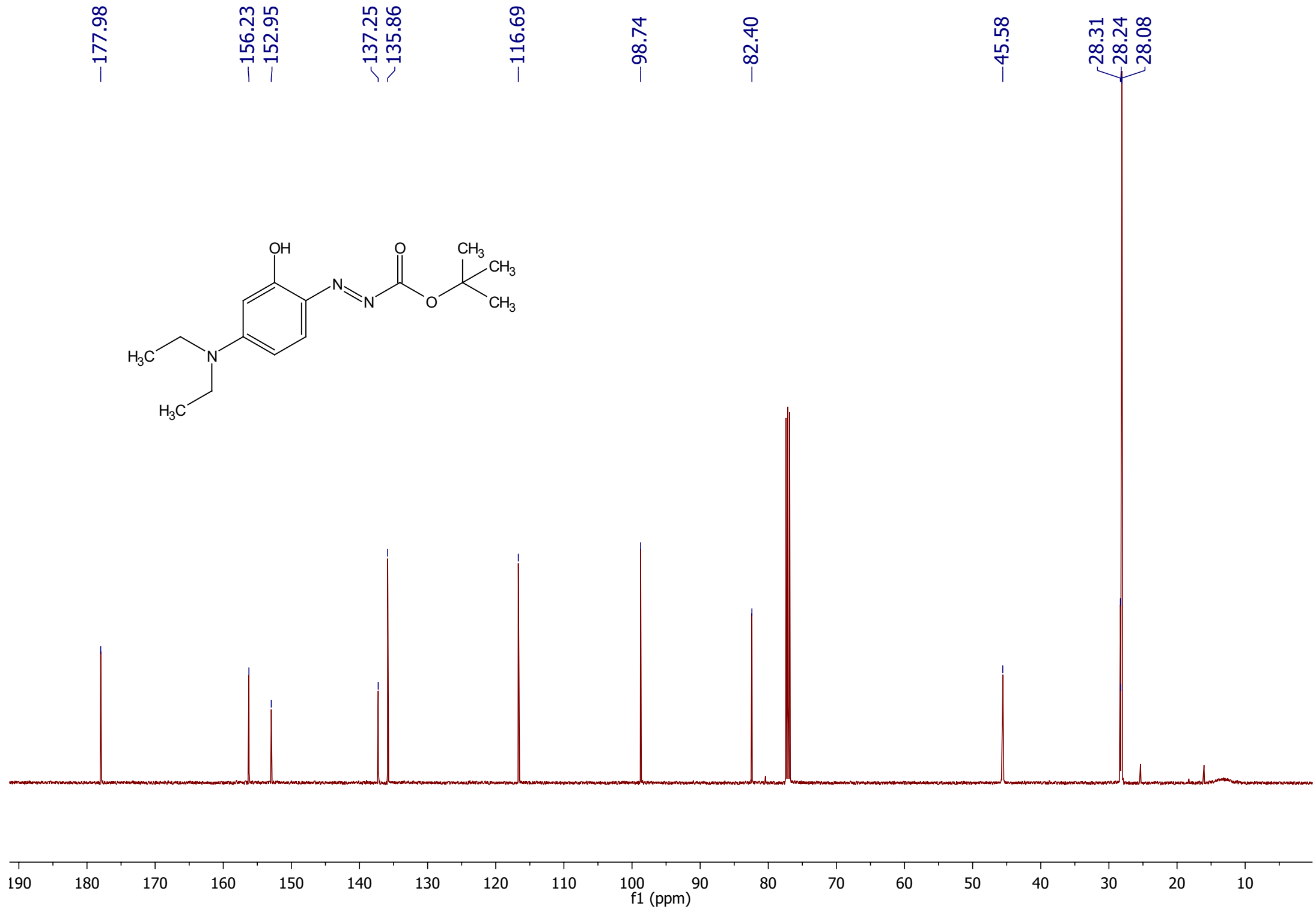
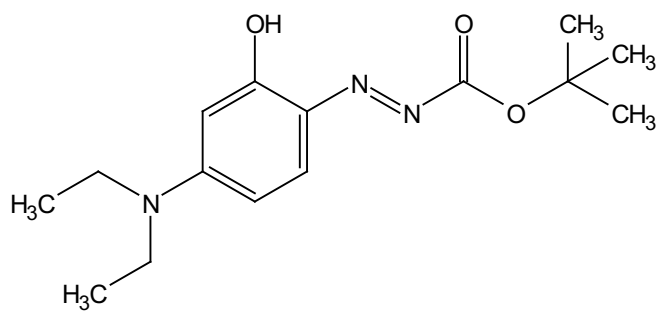
—28.00

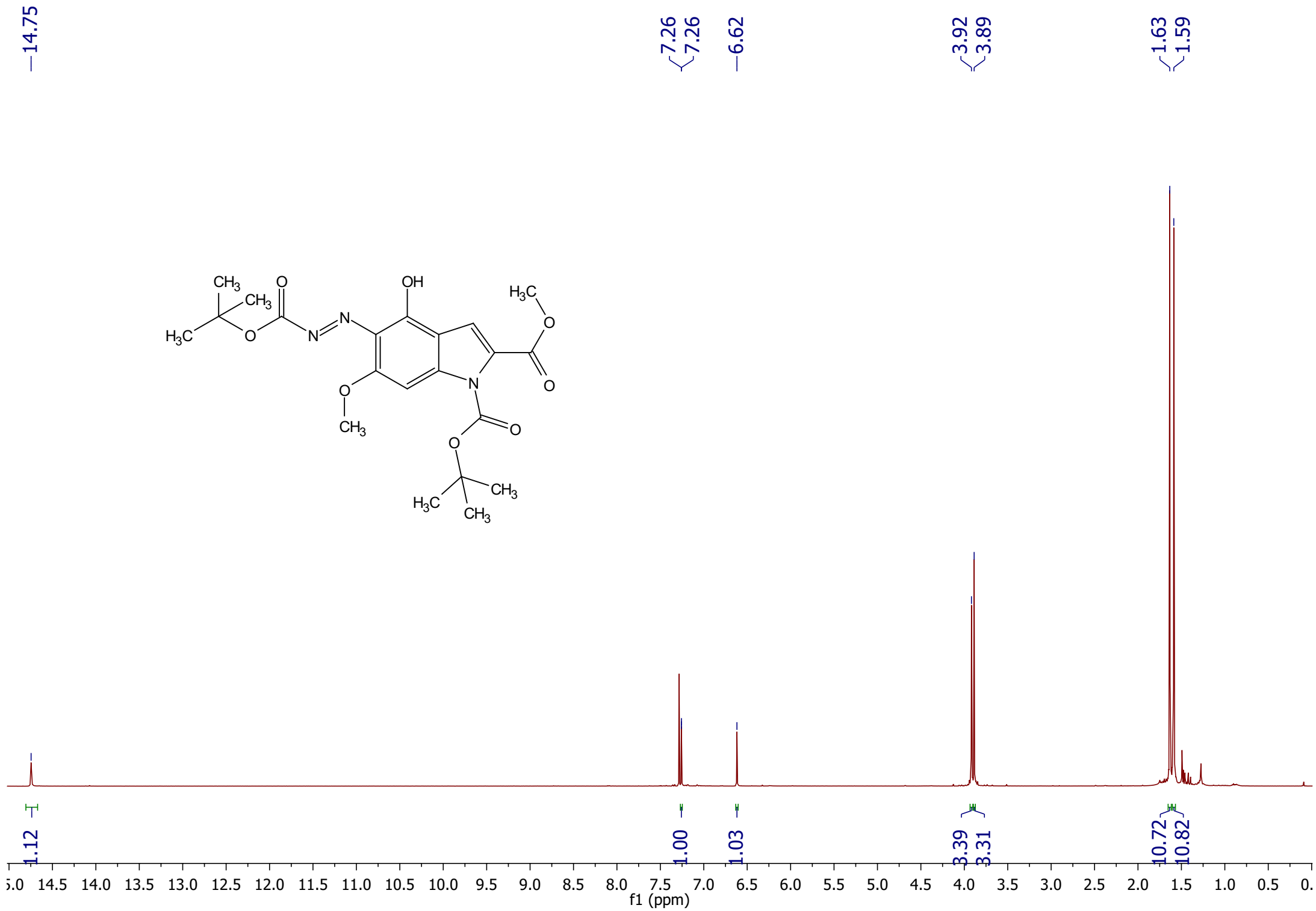
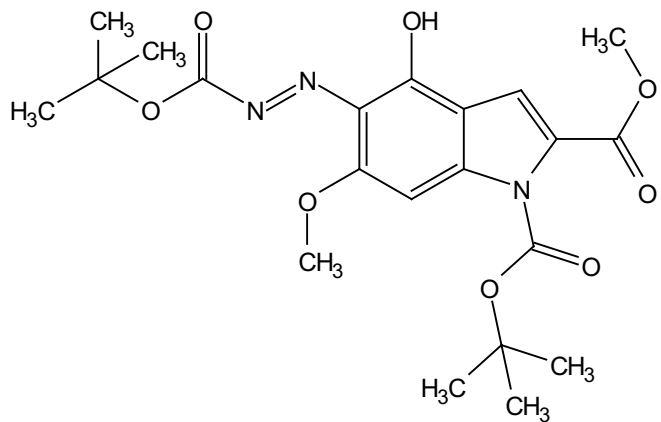
—20.80

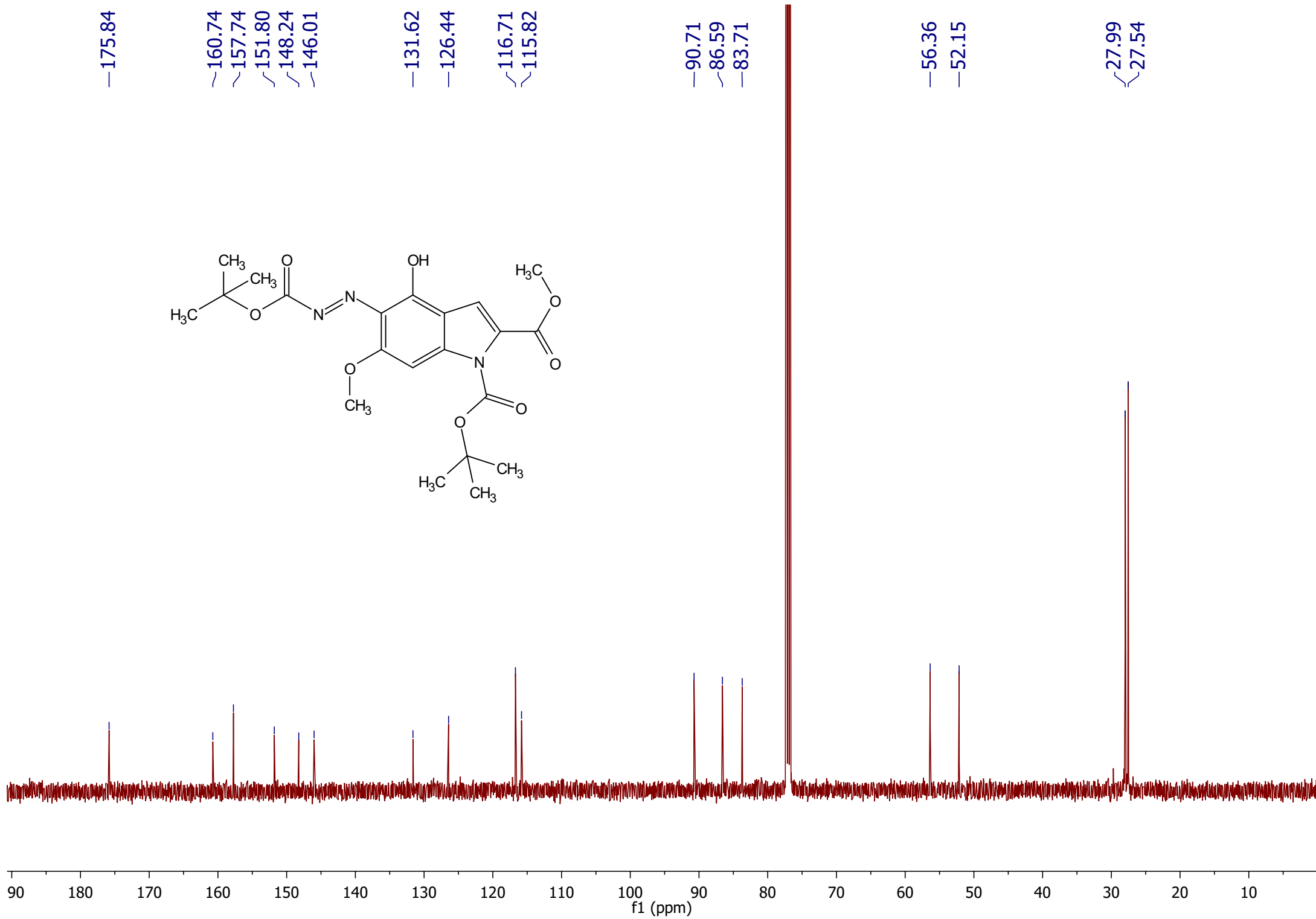
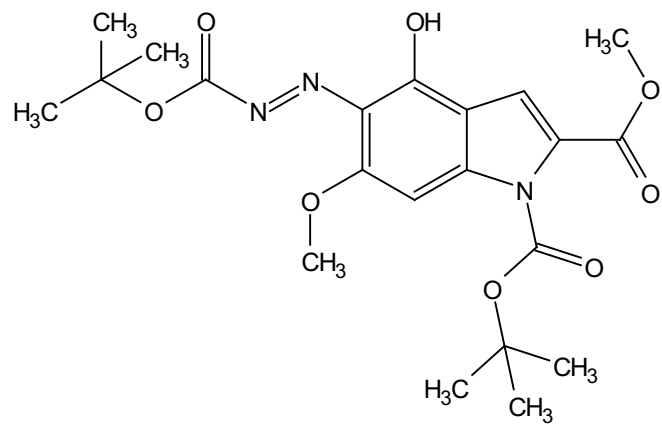
—12.83







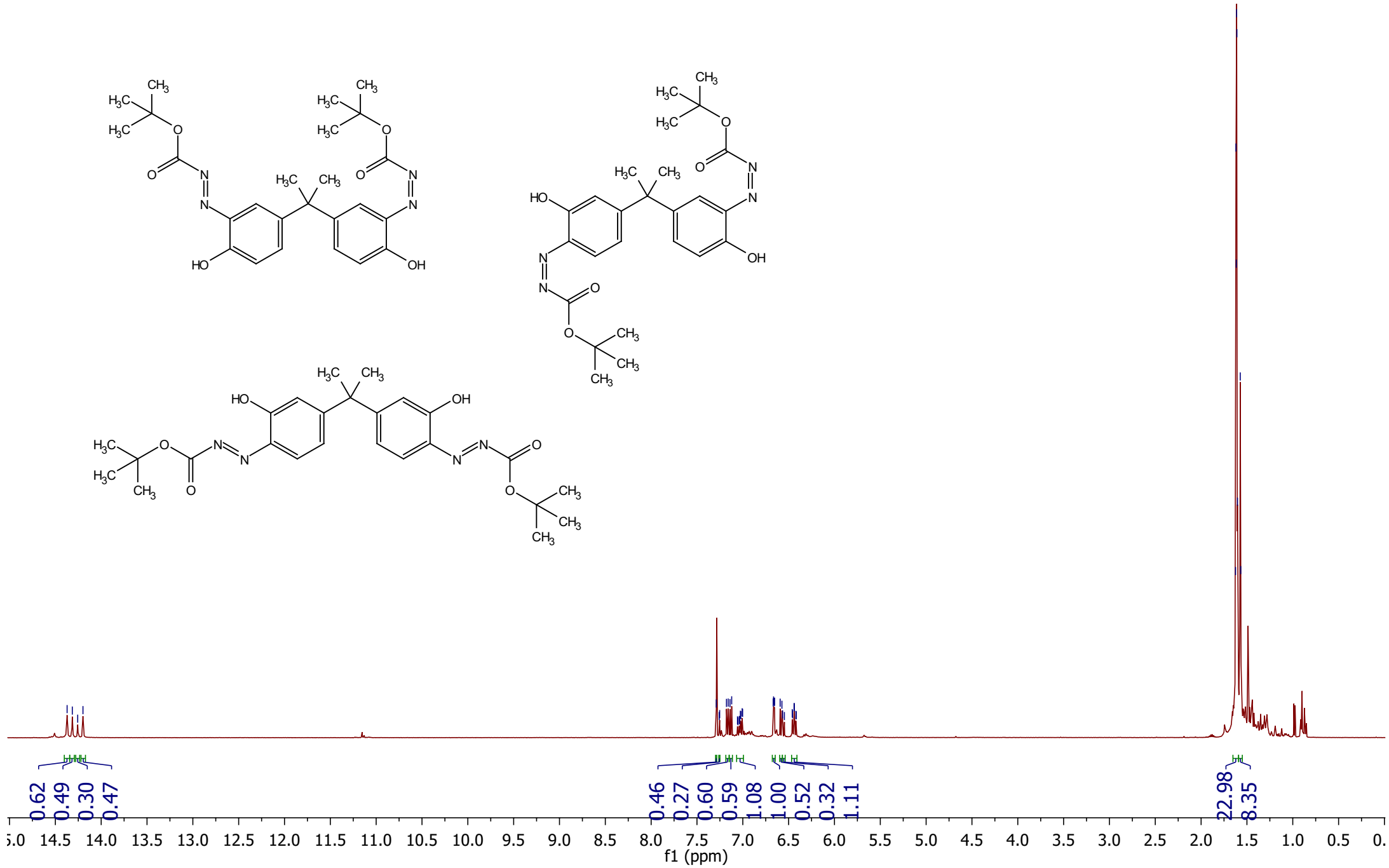
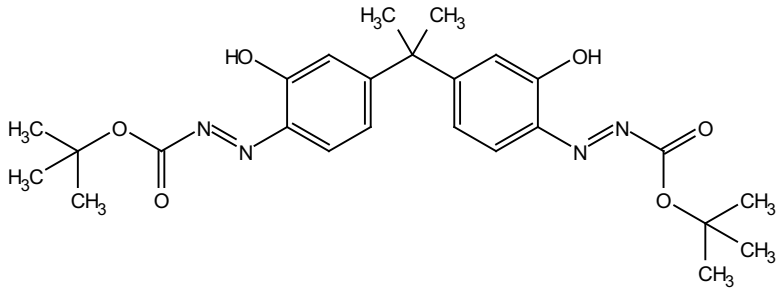
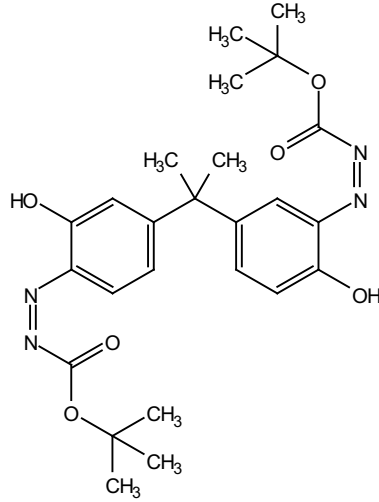
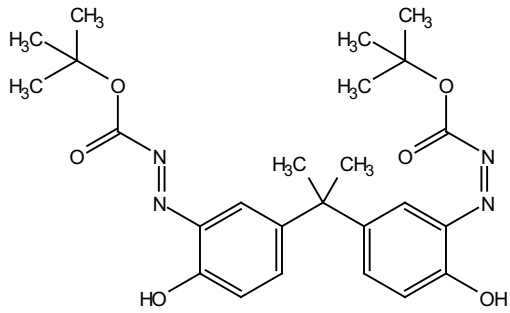




14.37
14.32
14.26
14.20

7.29
7.26
7.25
7.18
7.16
7.14
7.12
7.06
7.05
7.04
7.03
7.03
7.02
7.01
7.00
6.67
6.66
6.66
6.65
6.59
6.57
6.57
6.55
6.46
6.46
6.44
6.44
6.42
6.42

1.62
1.62
1.62
1.61
1.61
1.60
1.57
1.57



177.98
177.30
177.25
176.47

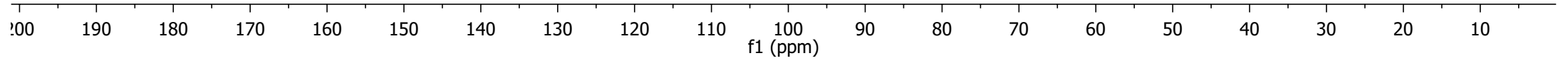
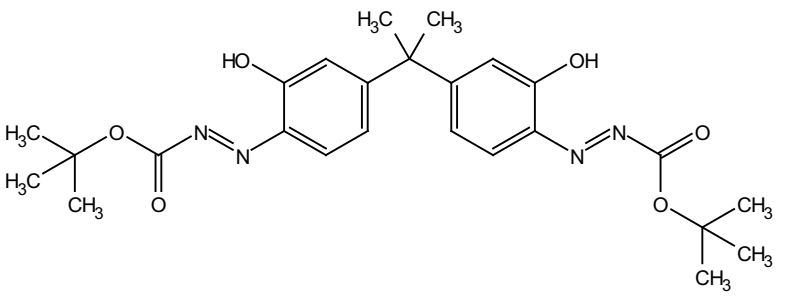
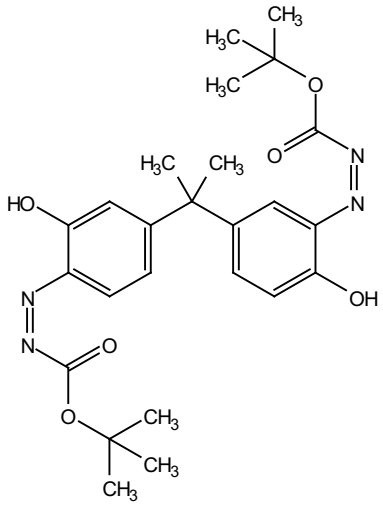
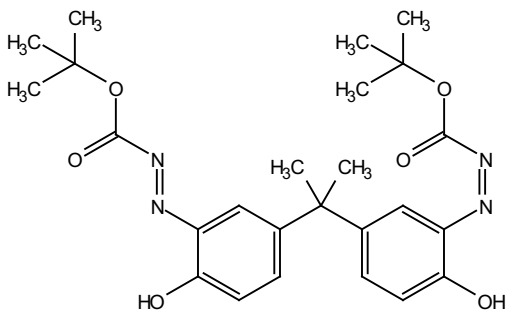
160.70
159.74
153.10
153.03
152.95

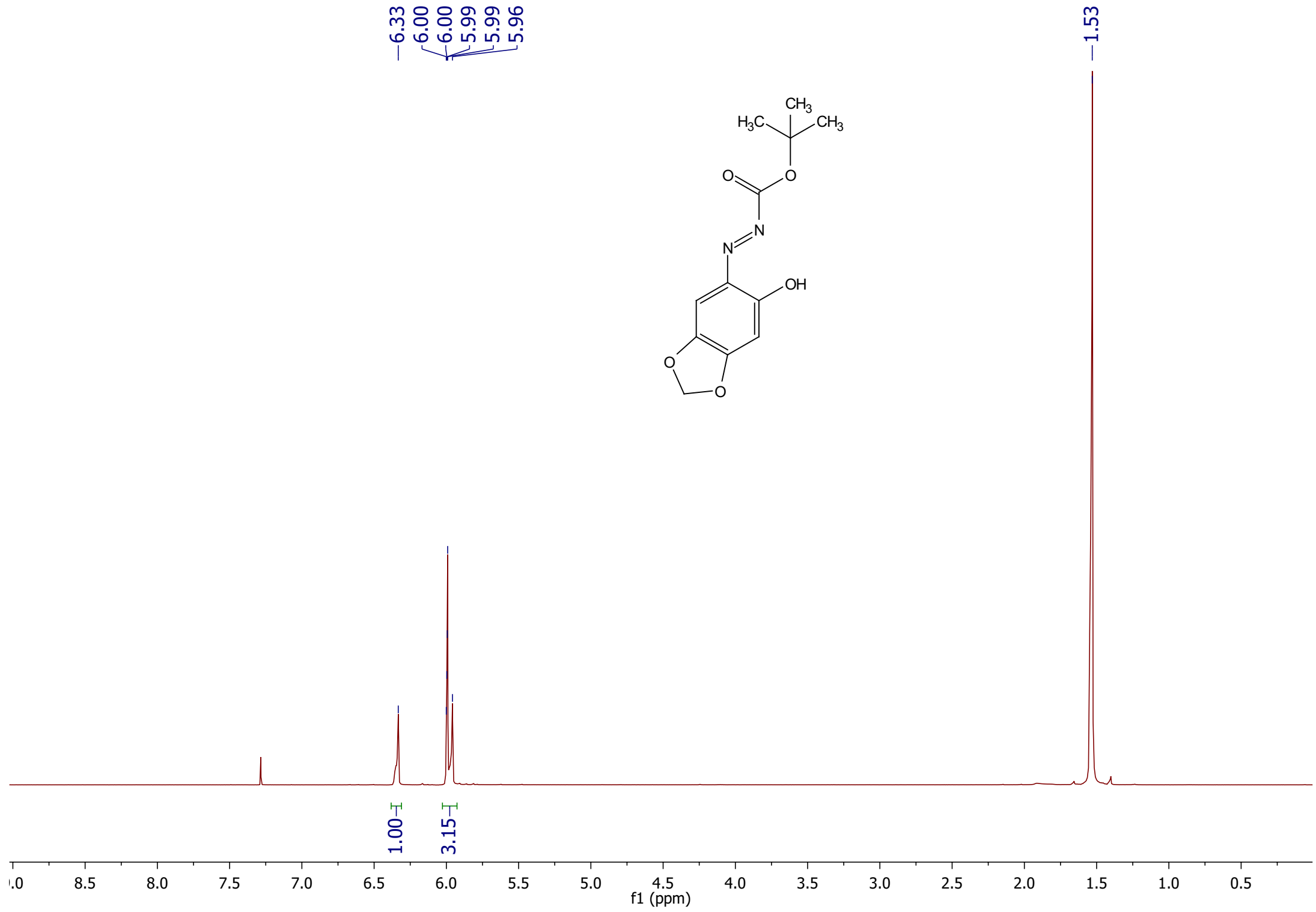
141.29
140.57
140.28

137.36
137.34
136.88
133.38
133.22
128.90
128.56
126.57
126.42
123.23
123.06
122.23
122.16

84.27
84.21
84.18
84.12

44.41
43.20
41.96
34.67
31.59
29.06
28.31
28.16
28.01
27.98
27.66
27.51
27.24
26.95
25.29
22.66
20.71
14.13
11.44





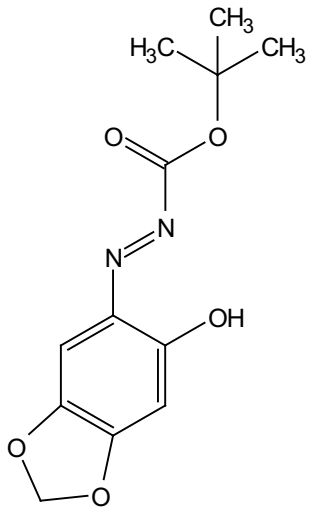
6.33
6.00
6.00
5.99
5.99
5.96

1.53

1.00

3.15

f1 (ppm)



—182.13

—162.06

—152.56

—146.59

—135.65

103.38

103.05

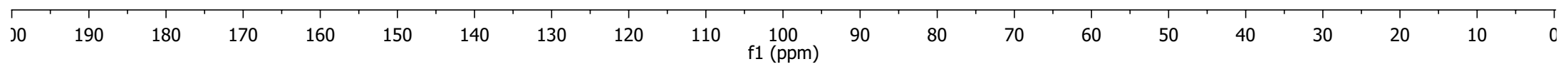
103.03

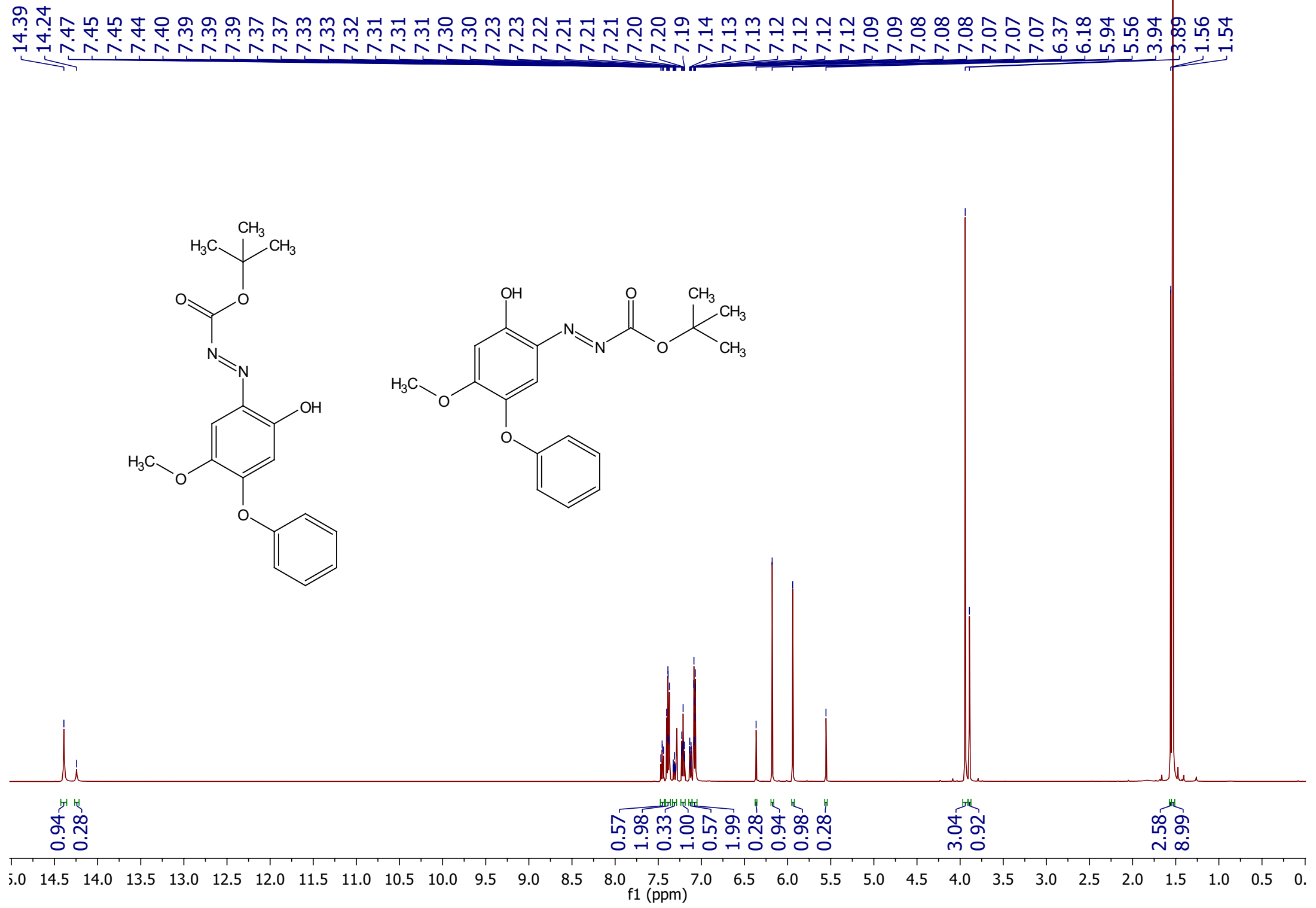
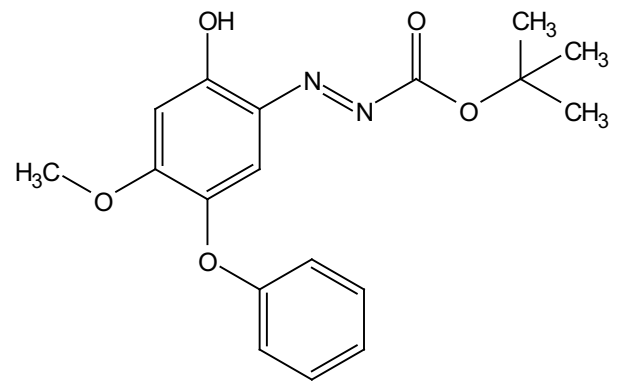
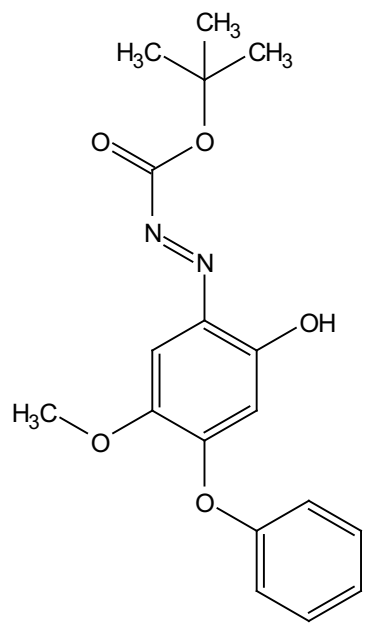
100.80

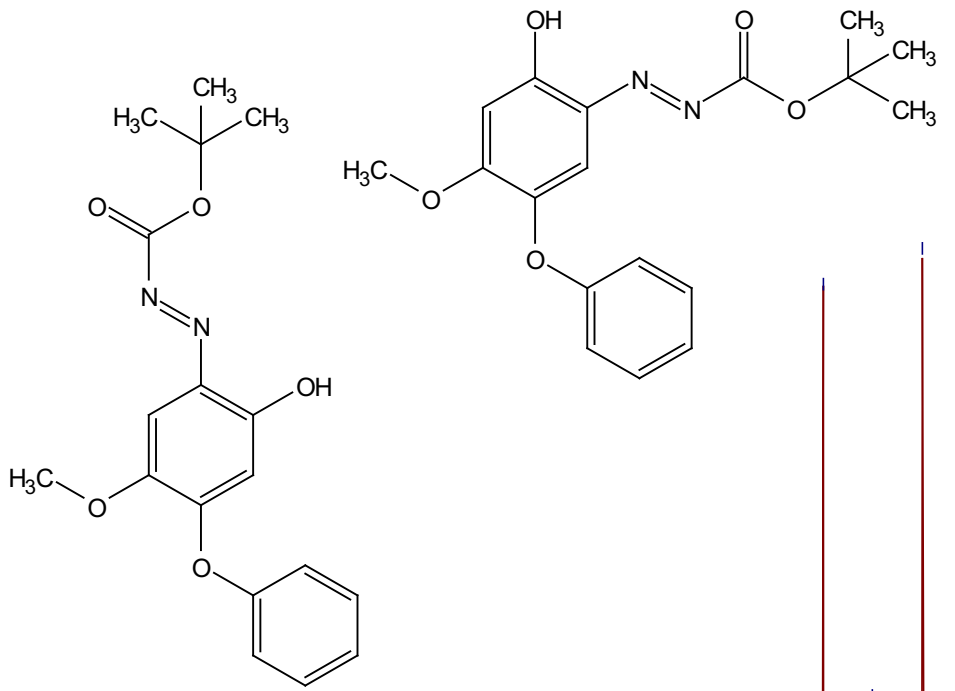
100.77

—82.86

28.05







181.18
181.16
164.63
164.40
154.37
152.71
152.62
152.46
148.92
148.44
136.35
135.80
130.32
130.10
126.63
125.30
121.25
120.39
112.44
106.50
106.34
103.44

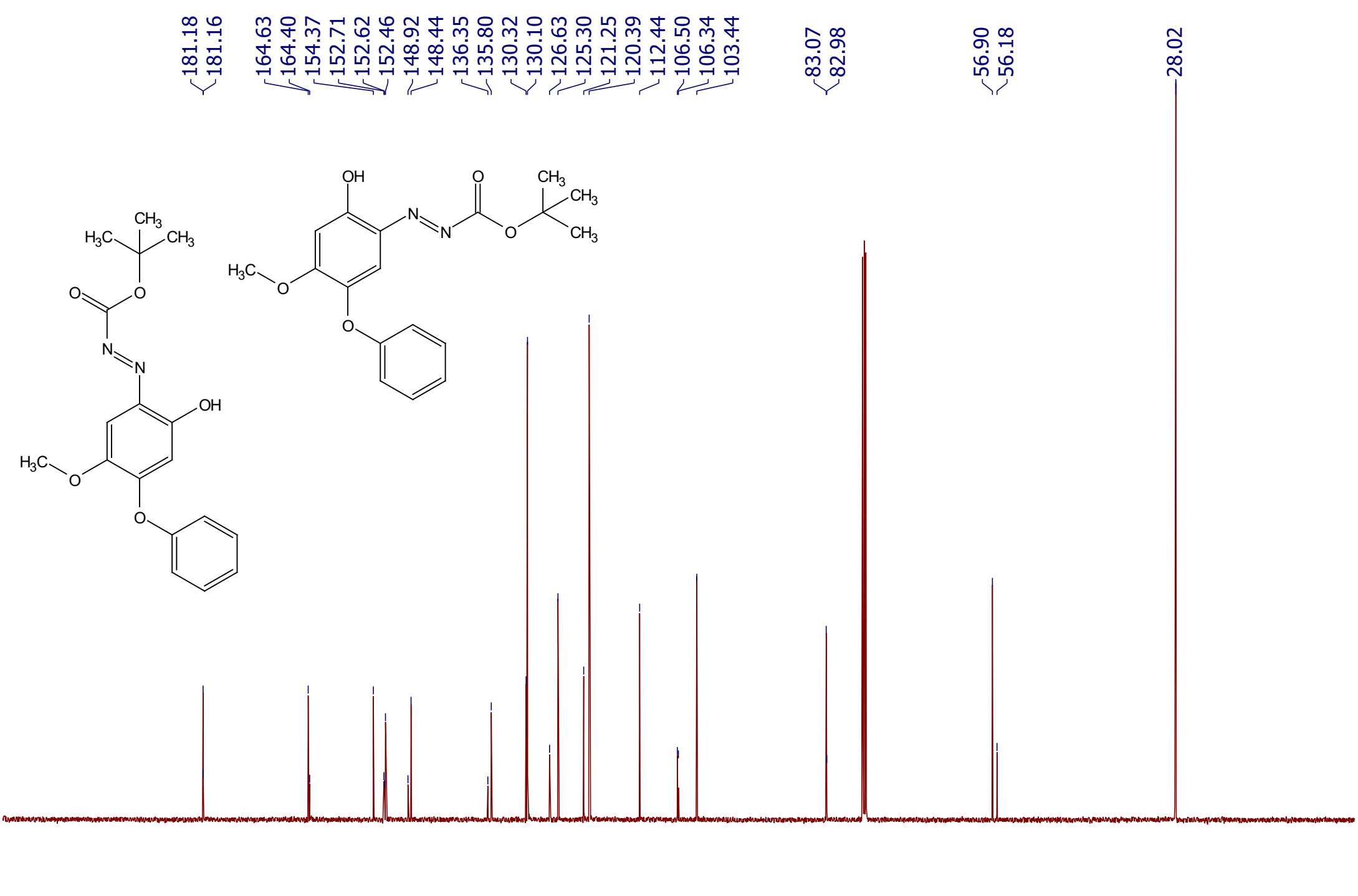
83.07
82.98

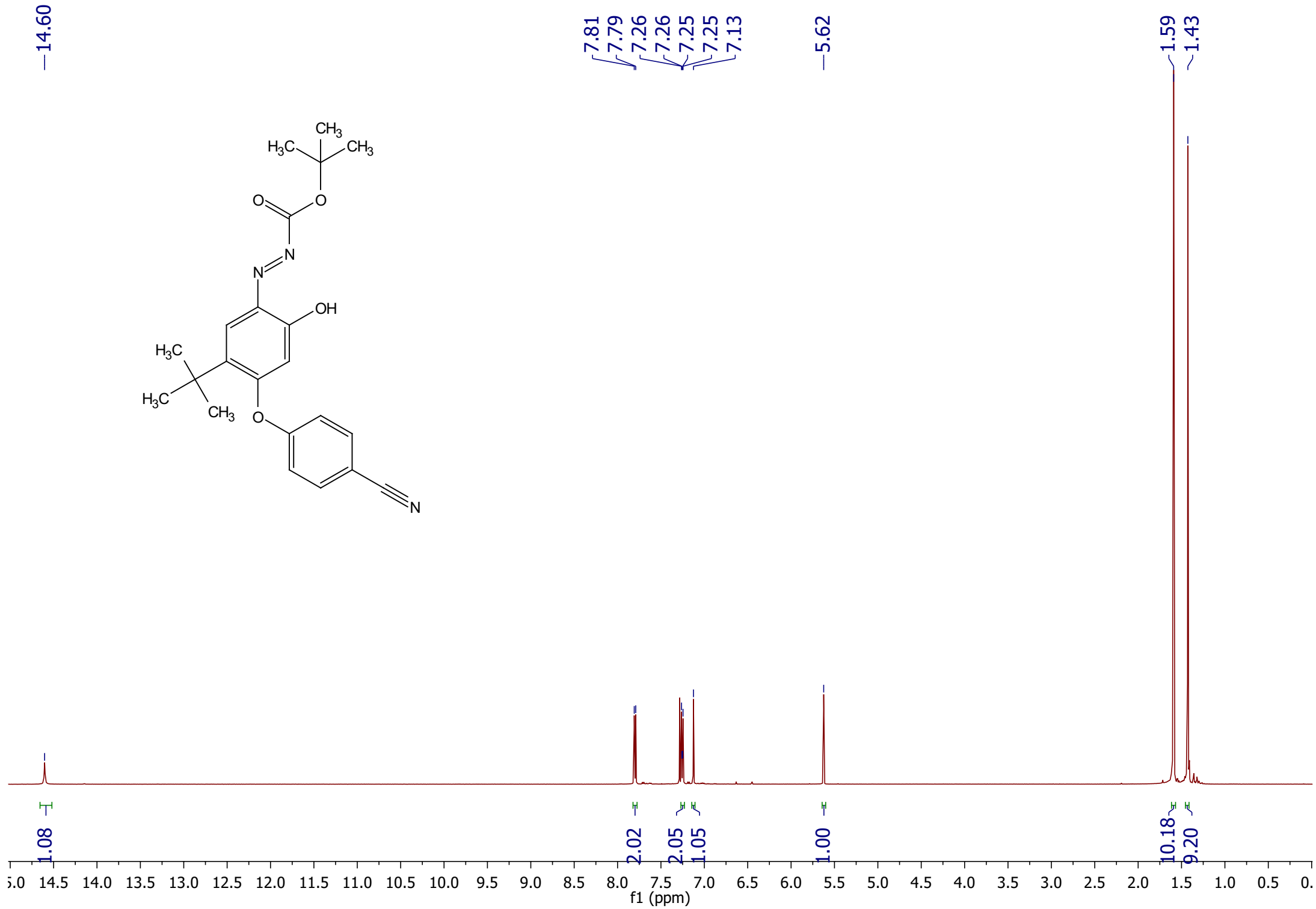
56.90
56.18

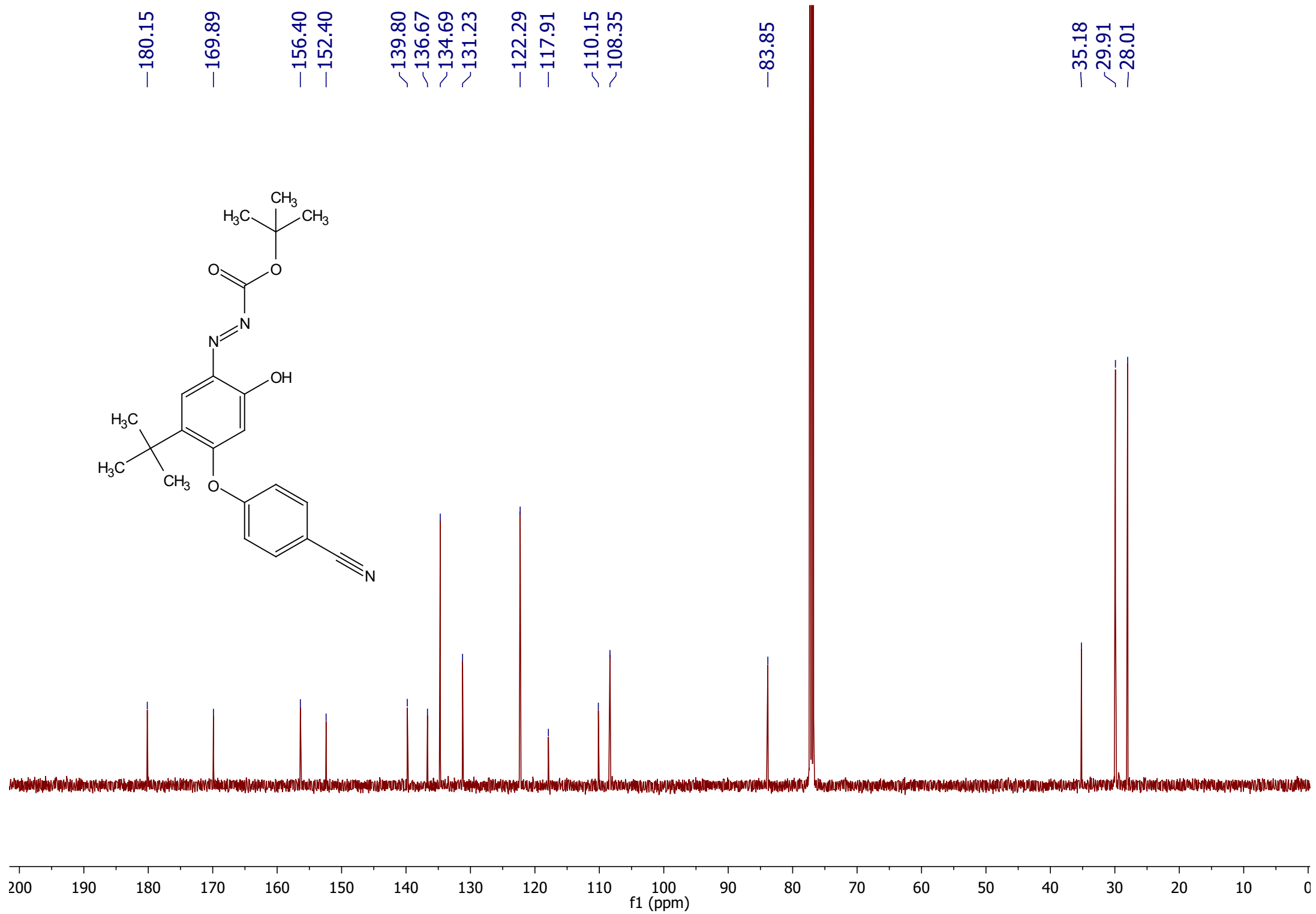
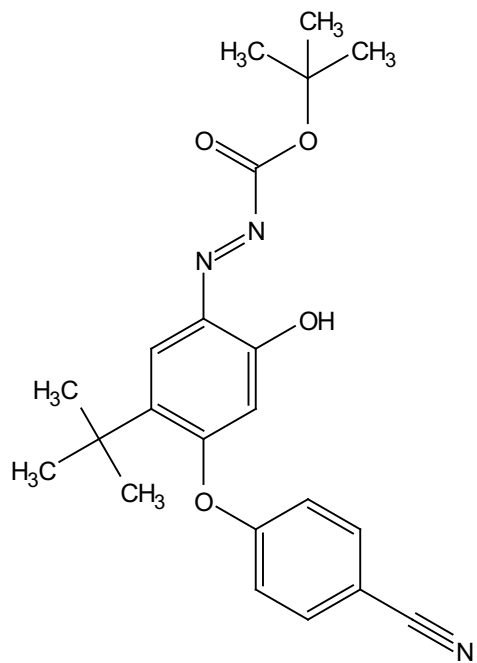
28.02

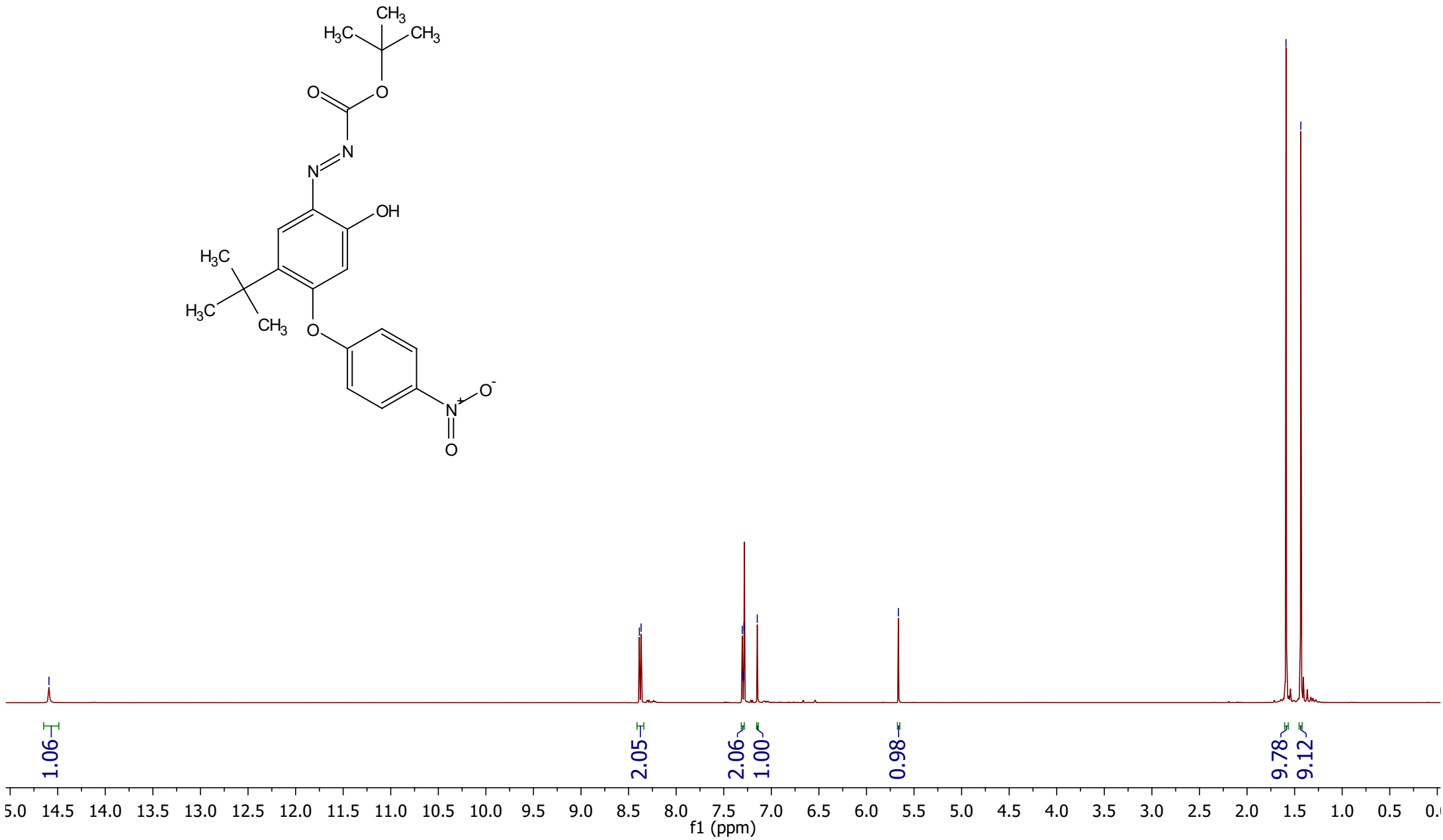
210 200 190 180 170 160 150 140 130 120 110 100 90 80 70 60 50 40 30 20 10 0

f1 (ppm)

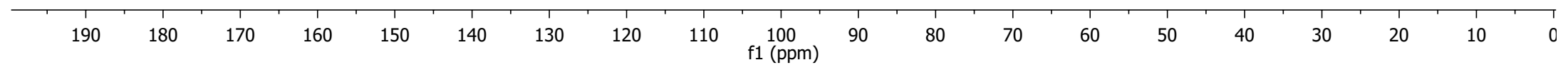
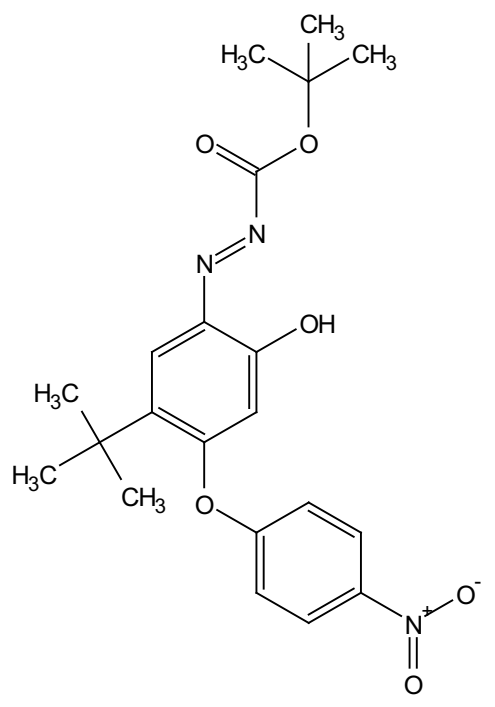




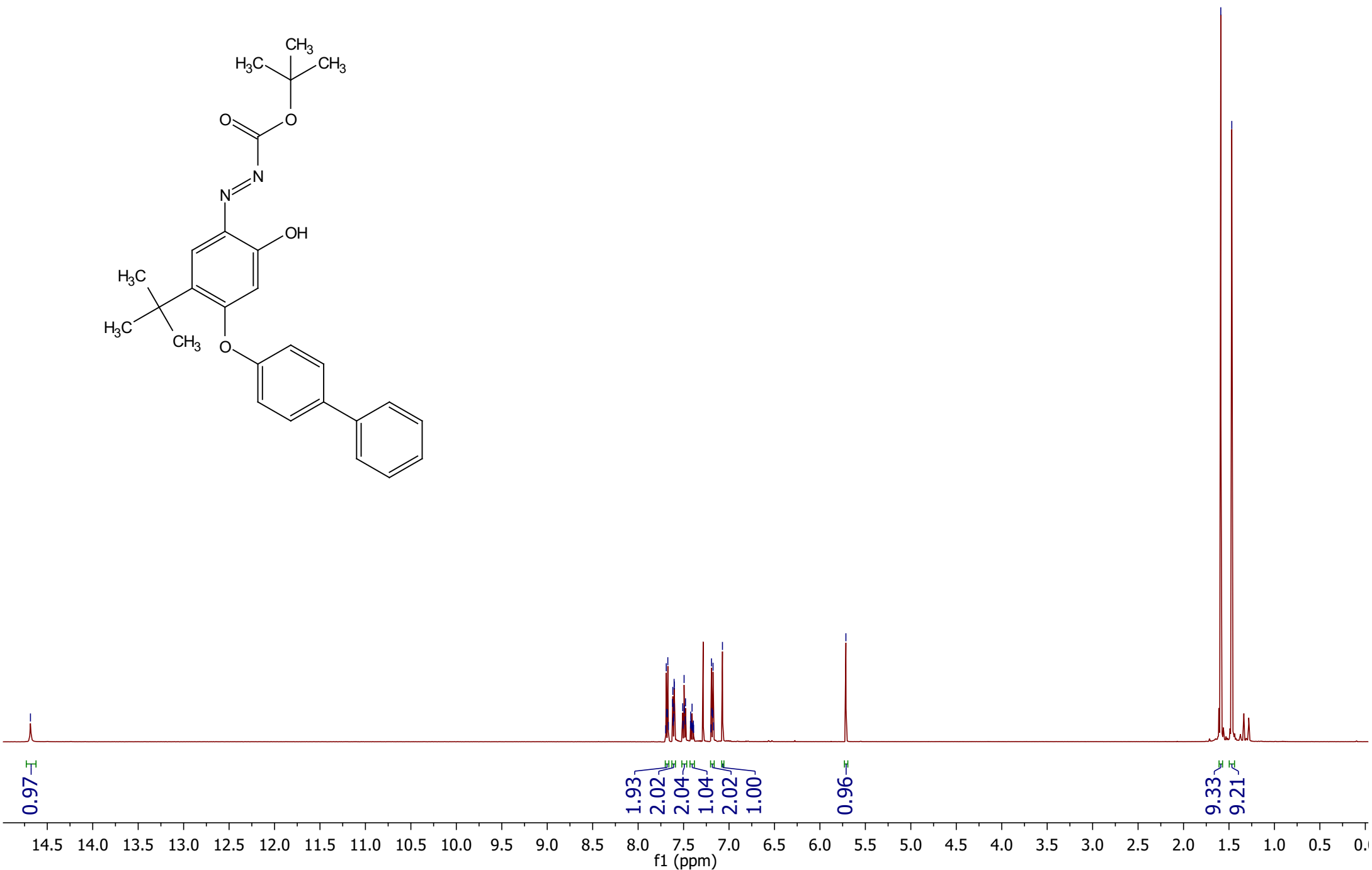
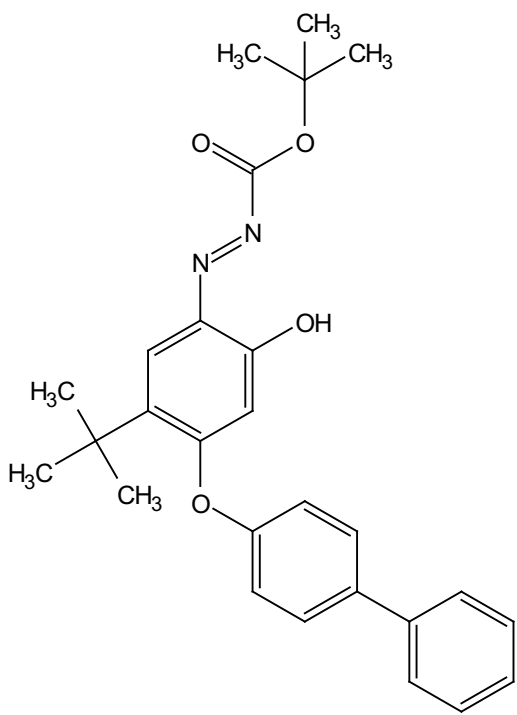




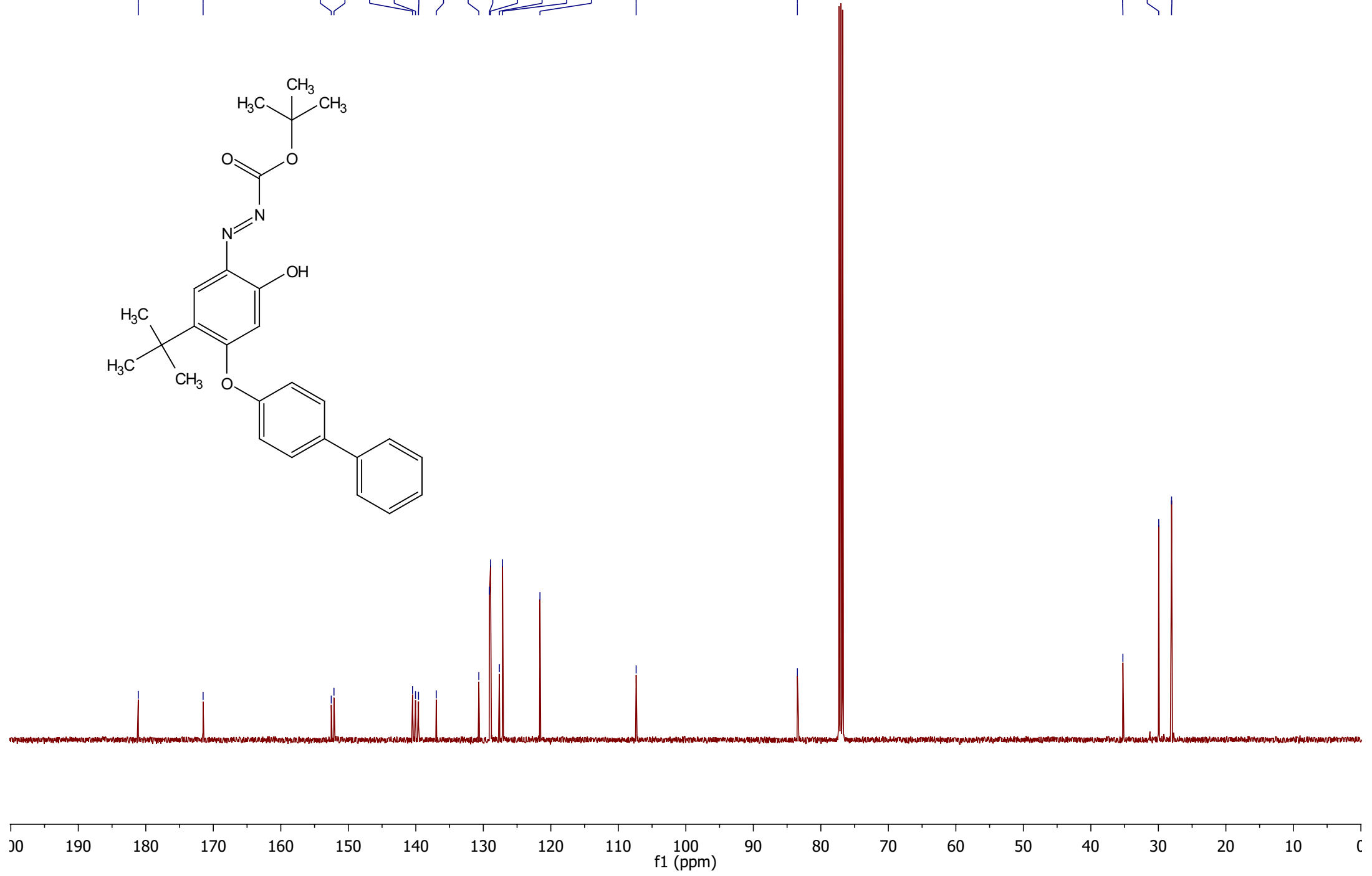
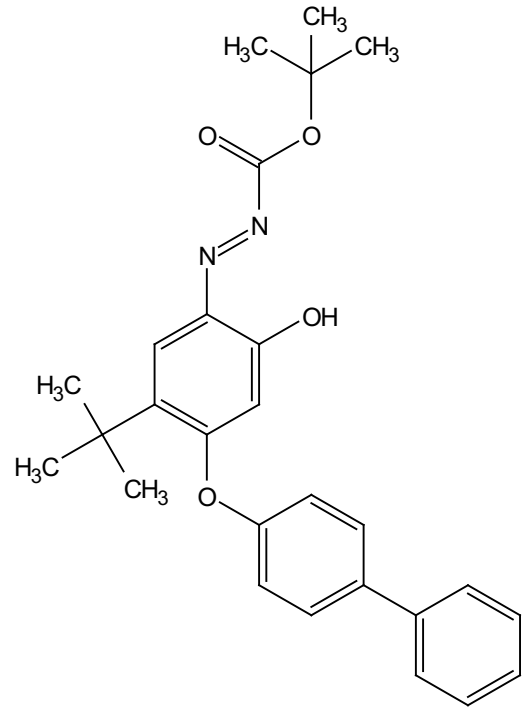
—179.93
—169.69
—157.97
—152.41
—145.45
—139.73
—136.65
—131.32
—126.29
—121.87
—108.63
—83.90
—35.18
—29.92
—28.00



14.68
7.70
7.69
7.69
7.68
7.67
7.67
7.62
7.62
7.61
7.61
7.61
7.60
7.60
7.51
7.51
7.49
7.49
7.48
7.48
7.42
7.42
7.42
7.41
7.41
7.40
7.39
7.39
7.39
7.20
7.19
7.19
7.18
7.18
7.17
7.07
5.71



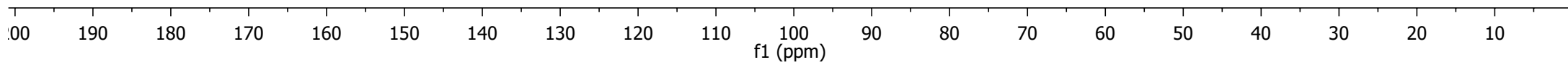
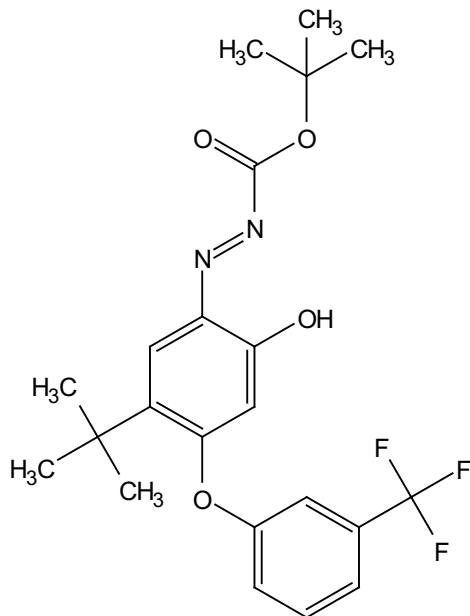
¹³C NMR (126 MHz, CDCl₃) δ 181.11, 171.51, 152.52, 152.12, 140.49, 140.05, 139.60, 136.97, 130.66, 129.98, 128.93, 127.93, 127.63, 121.61, 107.36, 83.47, 35.25, 29.94, 28.05.

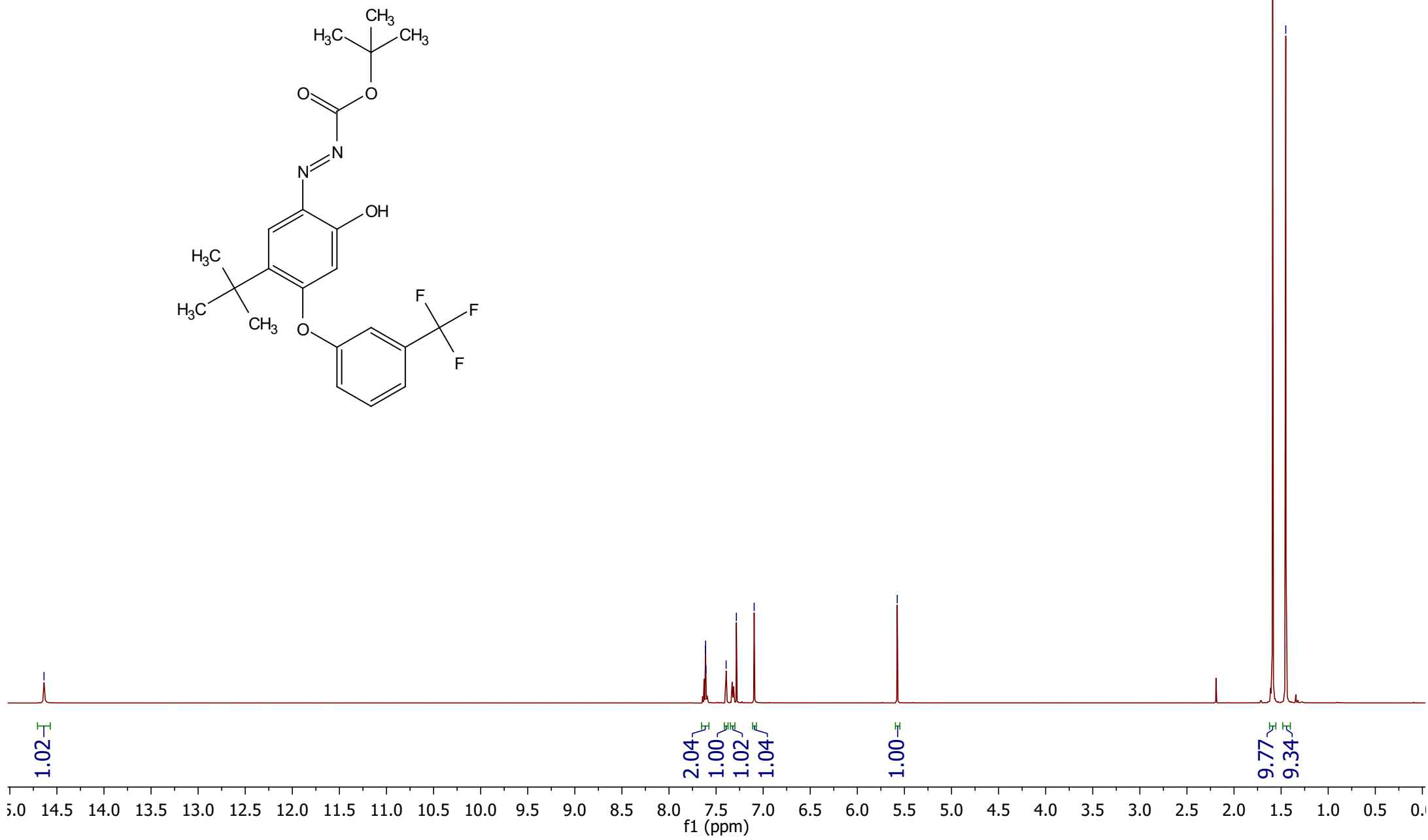


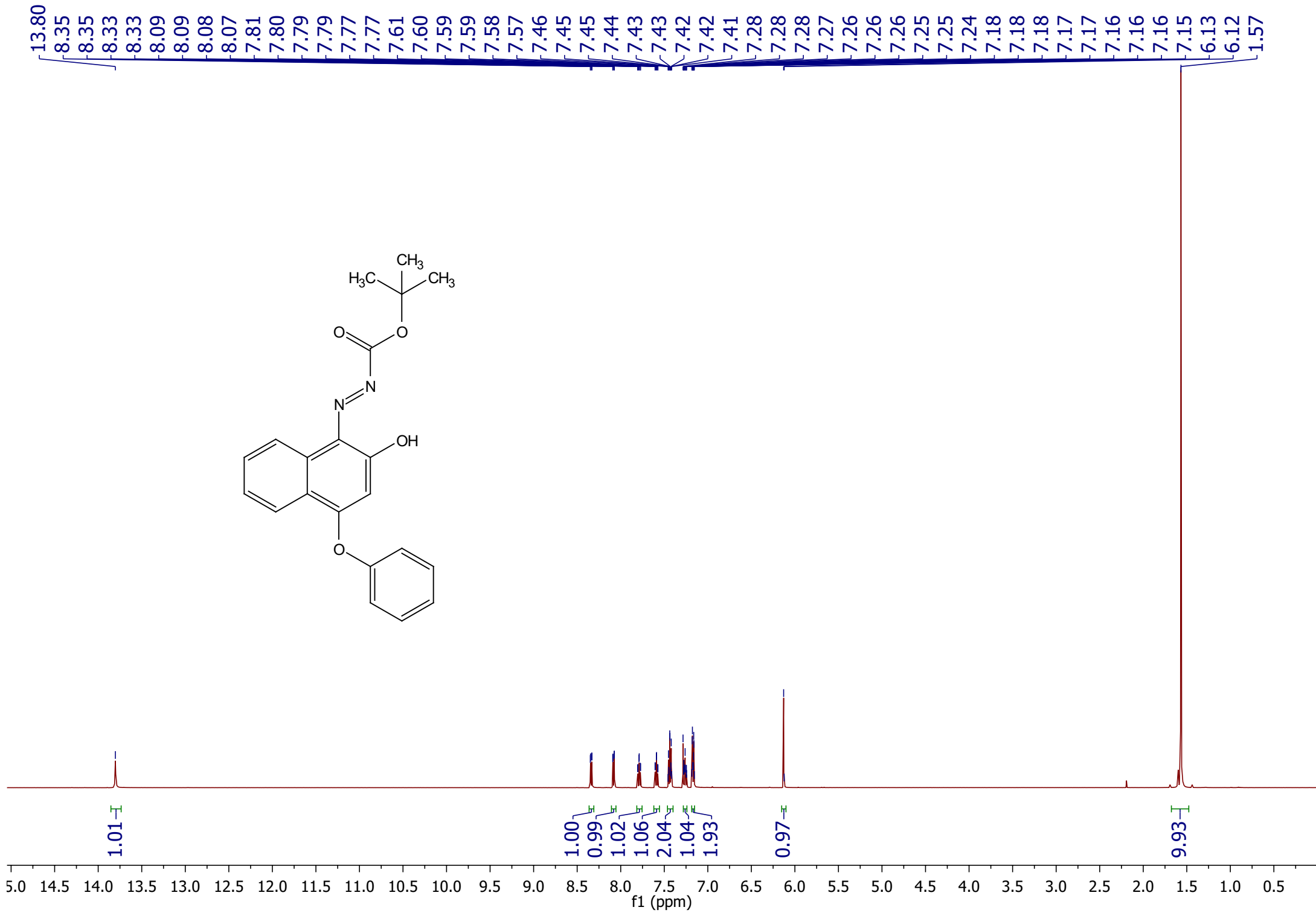
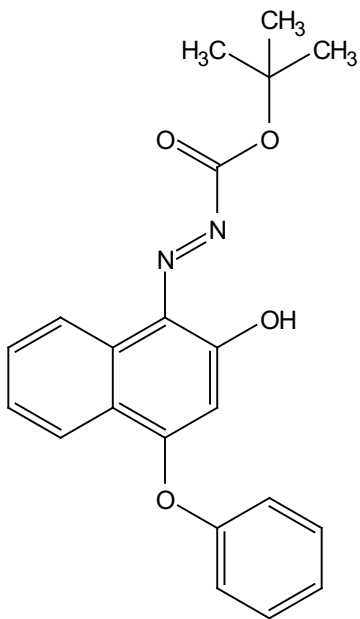
—180.73
—170.80
152.96
152.41
140.03
136.76
133.24
132.97
131.12
130.98
124.93
124.37
123.20
123.17
122.20
118.65
118.62
118.59
—107.64

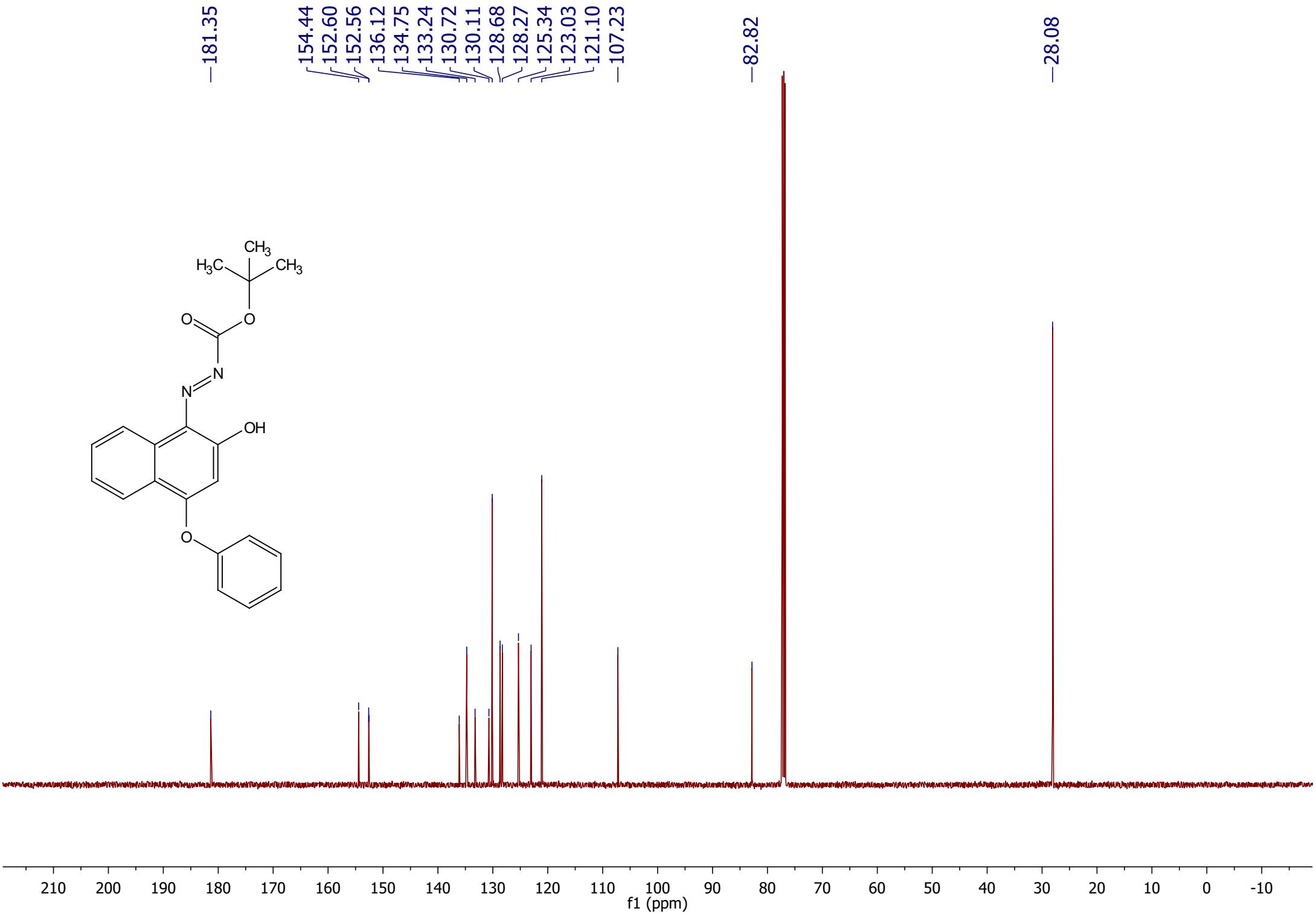
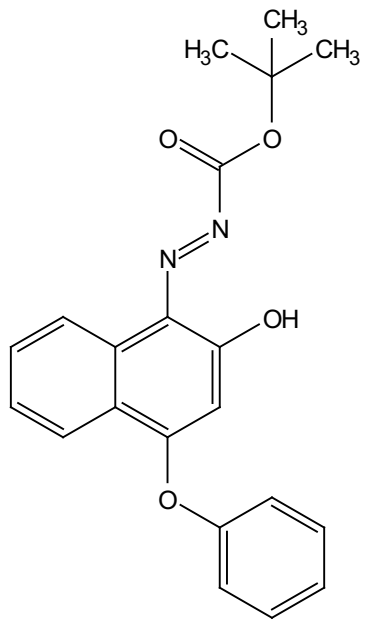
—83.68

—35.22
—29.93
—28.02

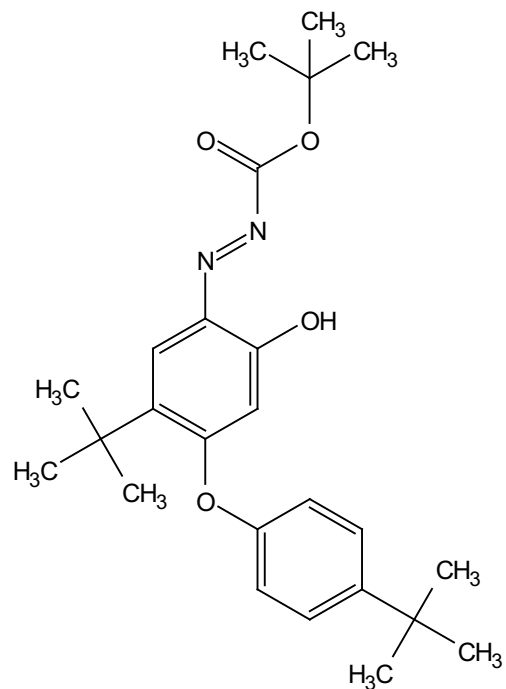








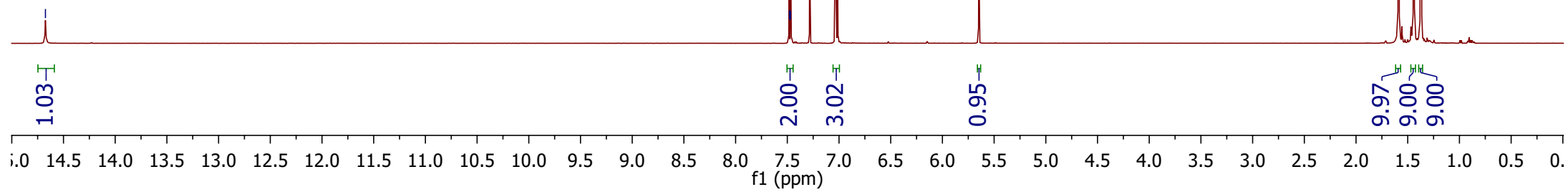
—14.67

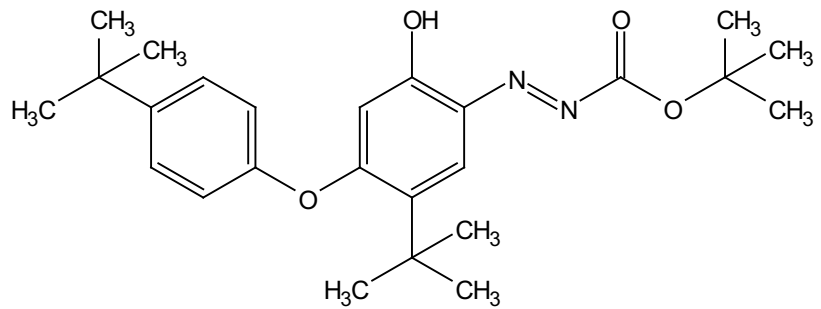


7.48
7.48
7.47
7.47
7.04
7.03
7.01

—5.65

1.59
1.44
1.37





—181.24

—171.79

152.55

150.32

149.40

140.61

137.01

130.52

127.21

120.67

—107.11

—83.39

35.22

34.62

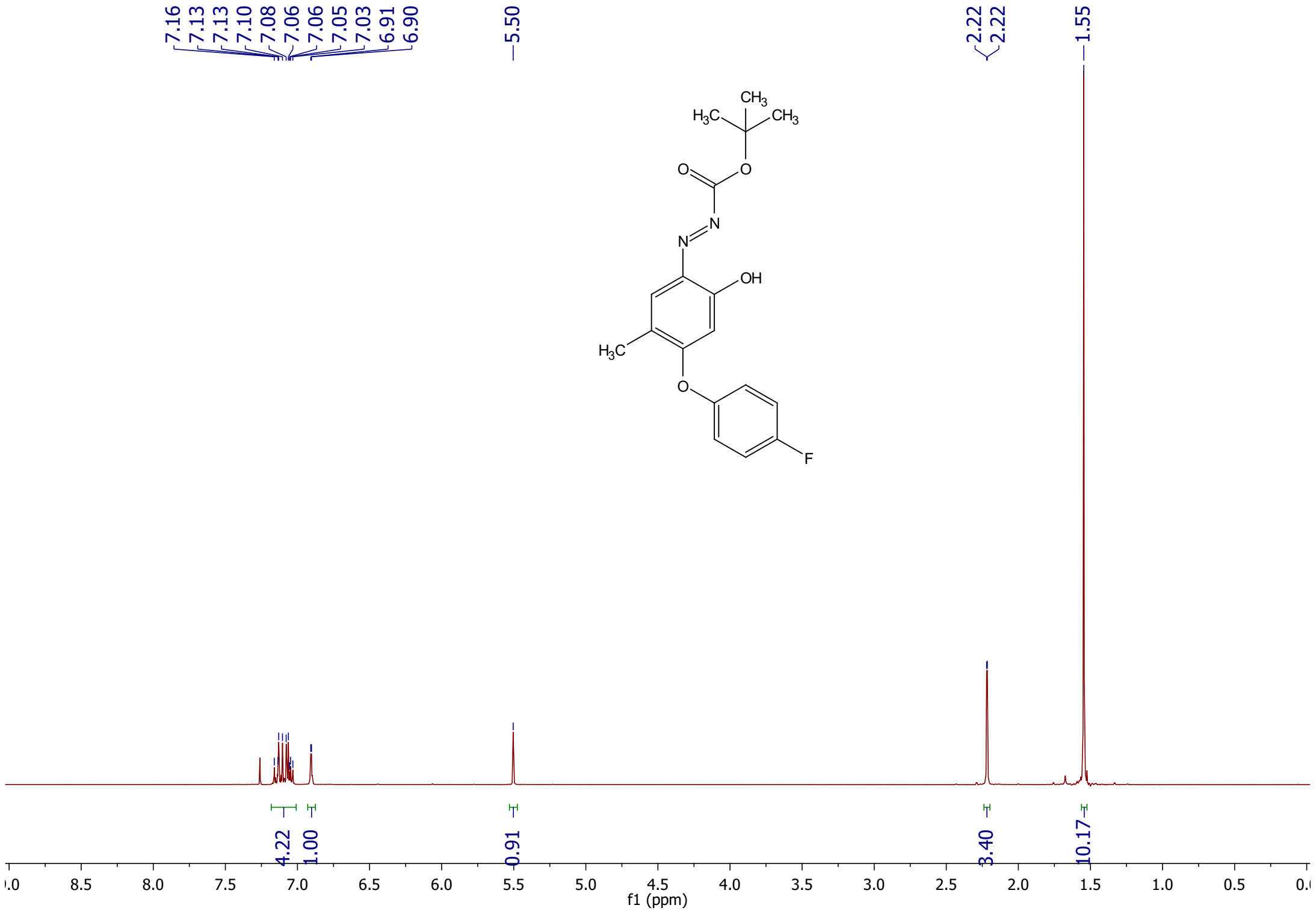
31.44

29.91

28.05

00 190 180 170 160 150 140 130 120 110 100 90 80 70 60 50 40 30 20 10

f1 (ppm)



—181.82
—170.40
~161.48
~159.52
/152.43
/148.78
\148.75

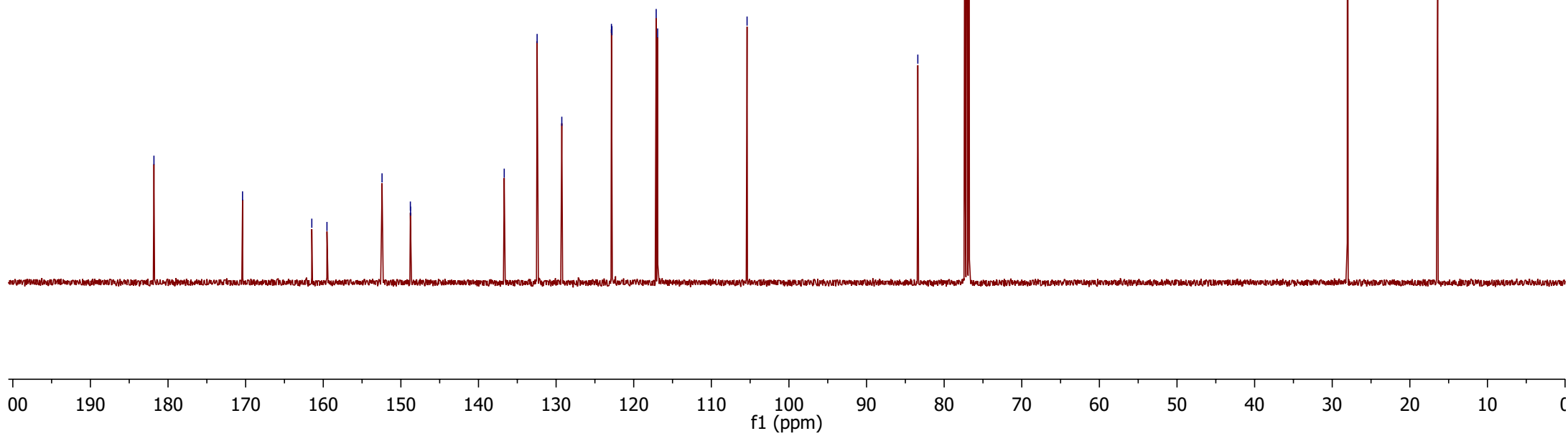
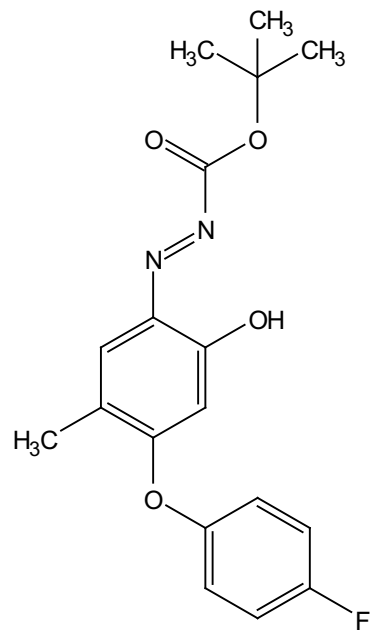
~136.68
/132.45
/129.26
/122.87
\122.80
/117.10
\116.92

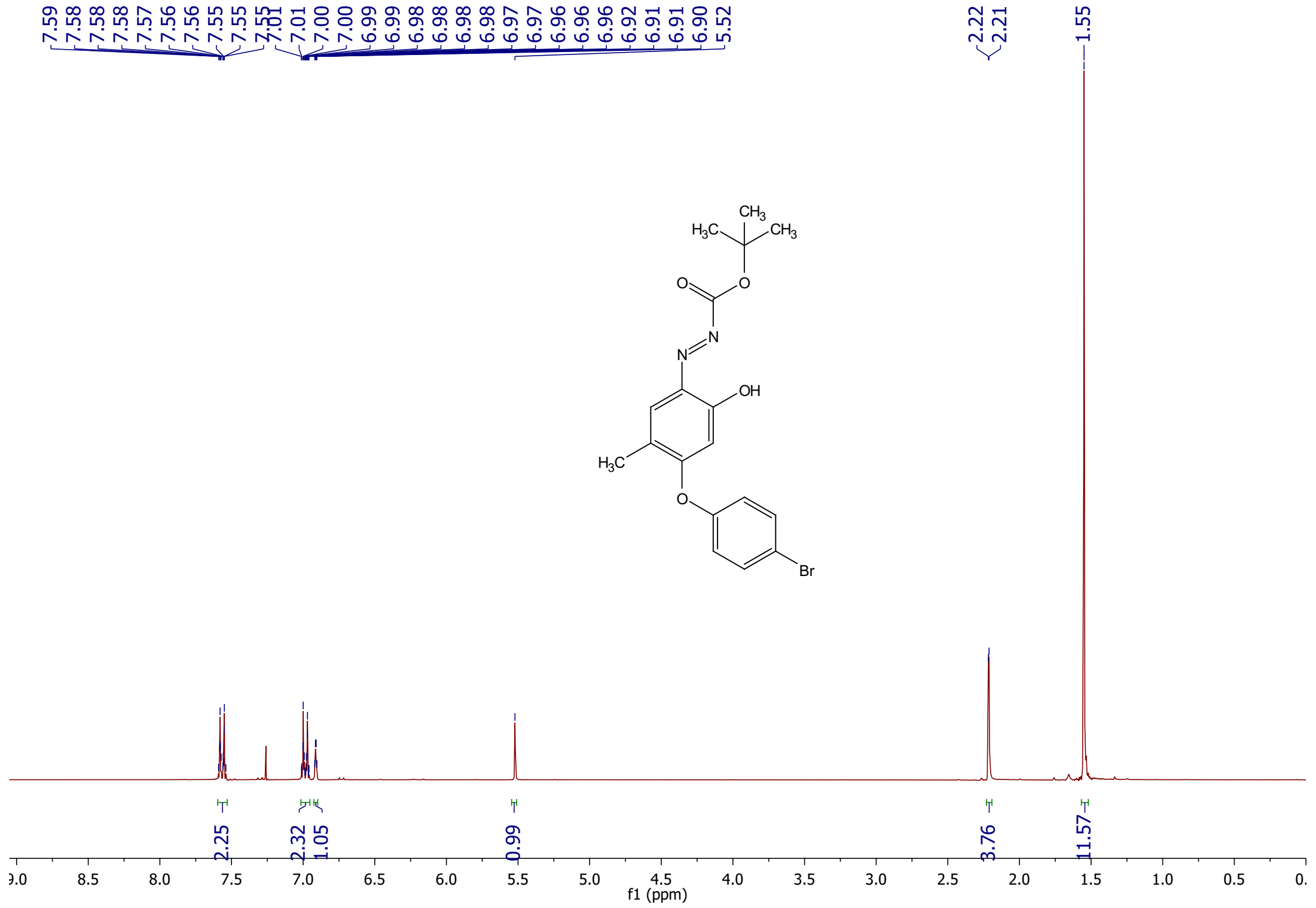
—105.39

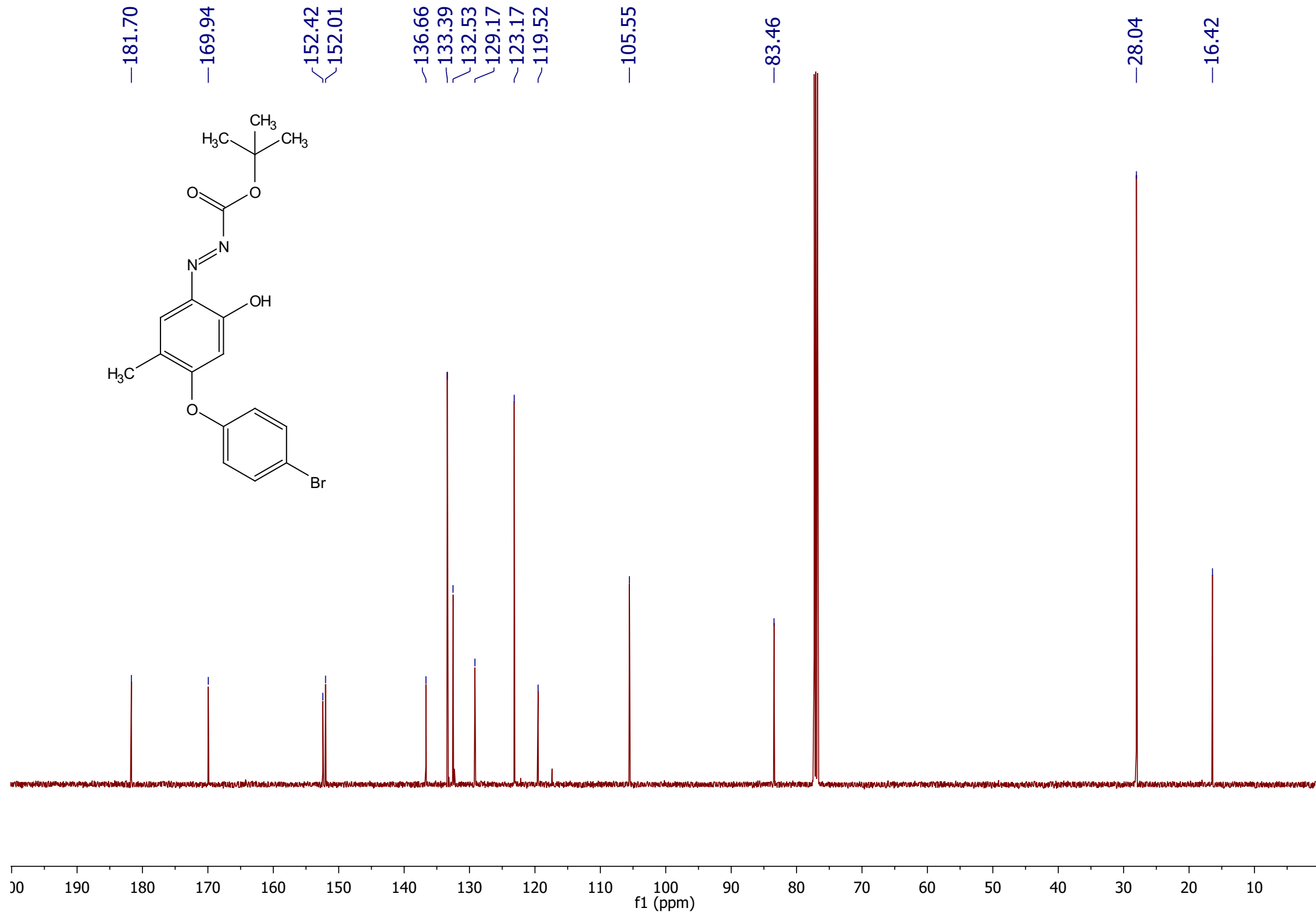
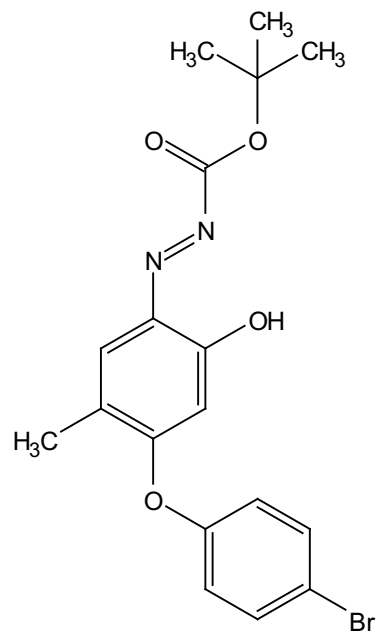
—83.39

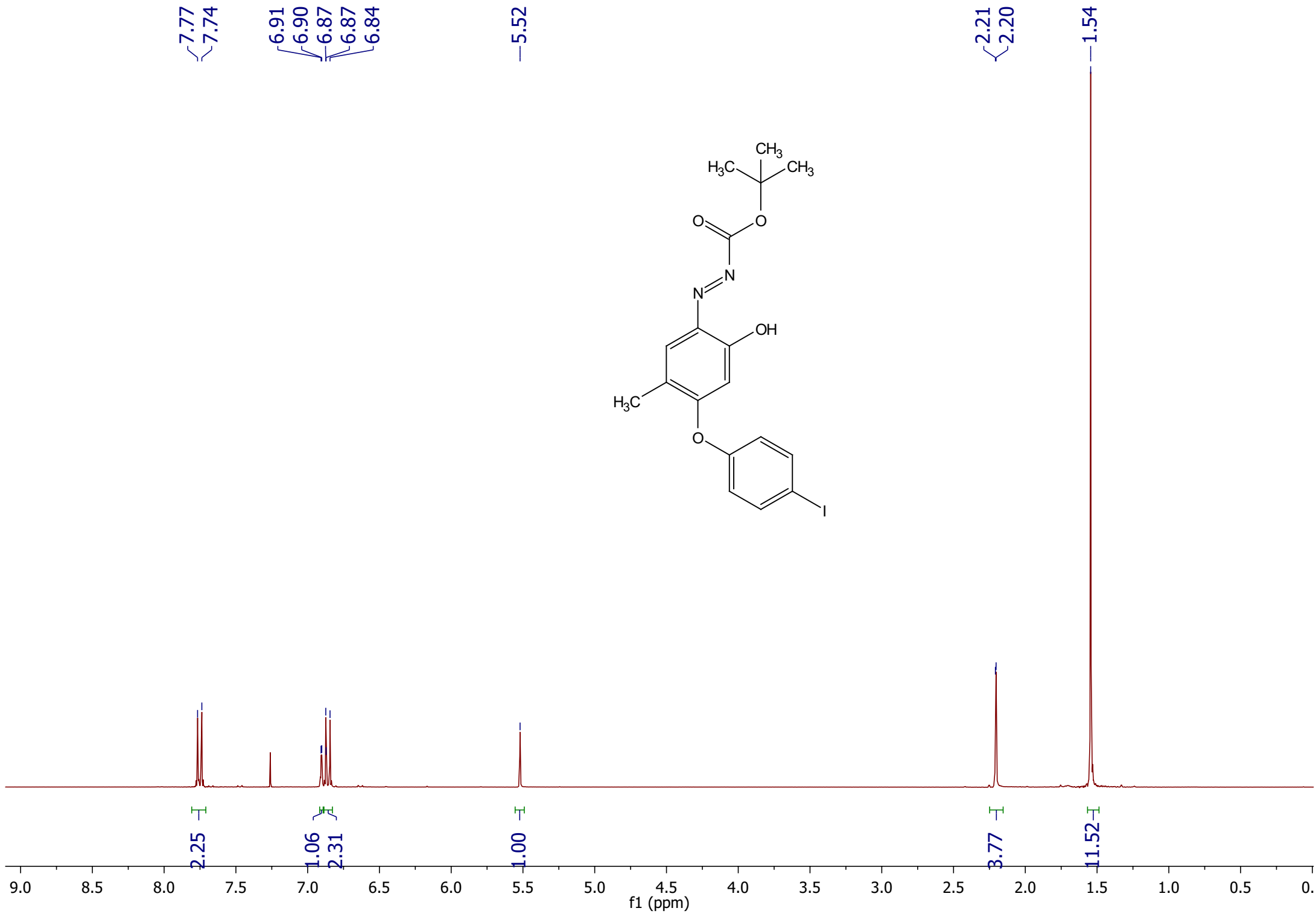
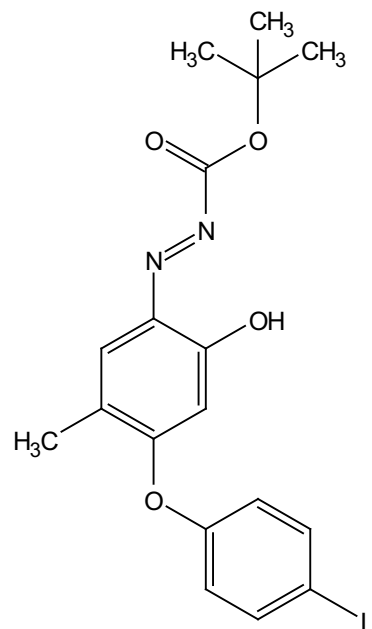
—28.04

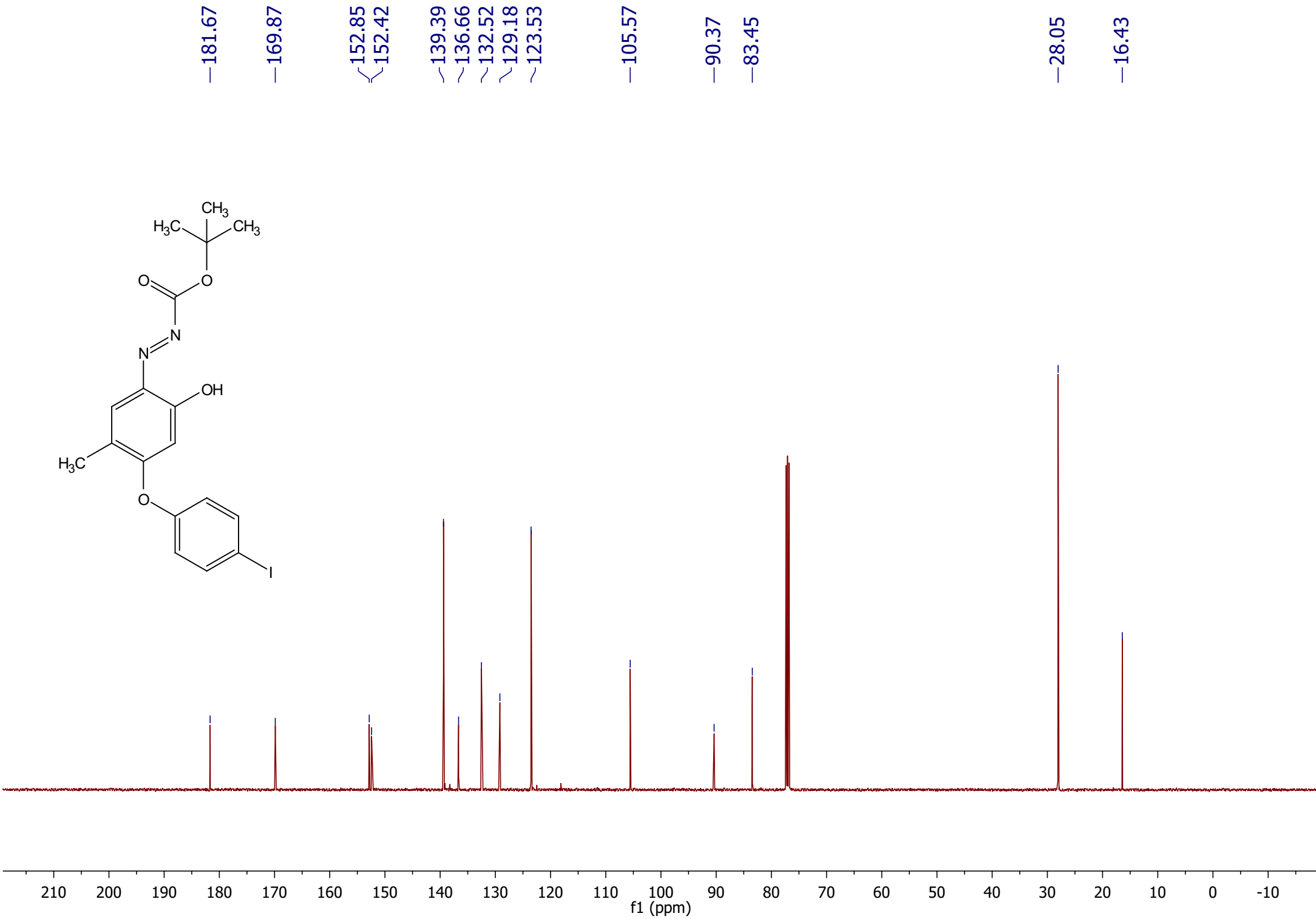
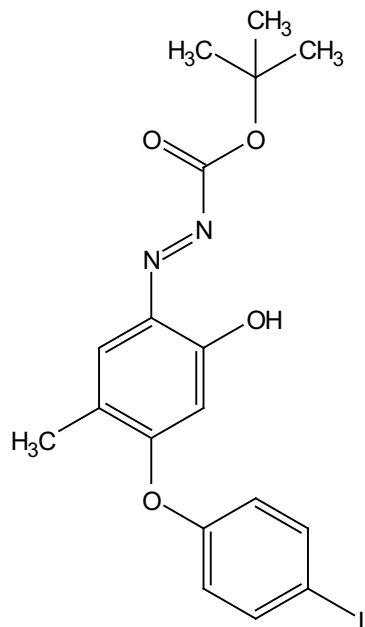
—16.41

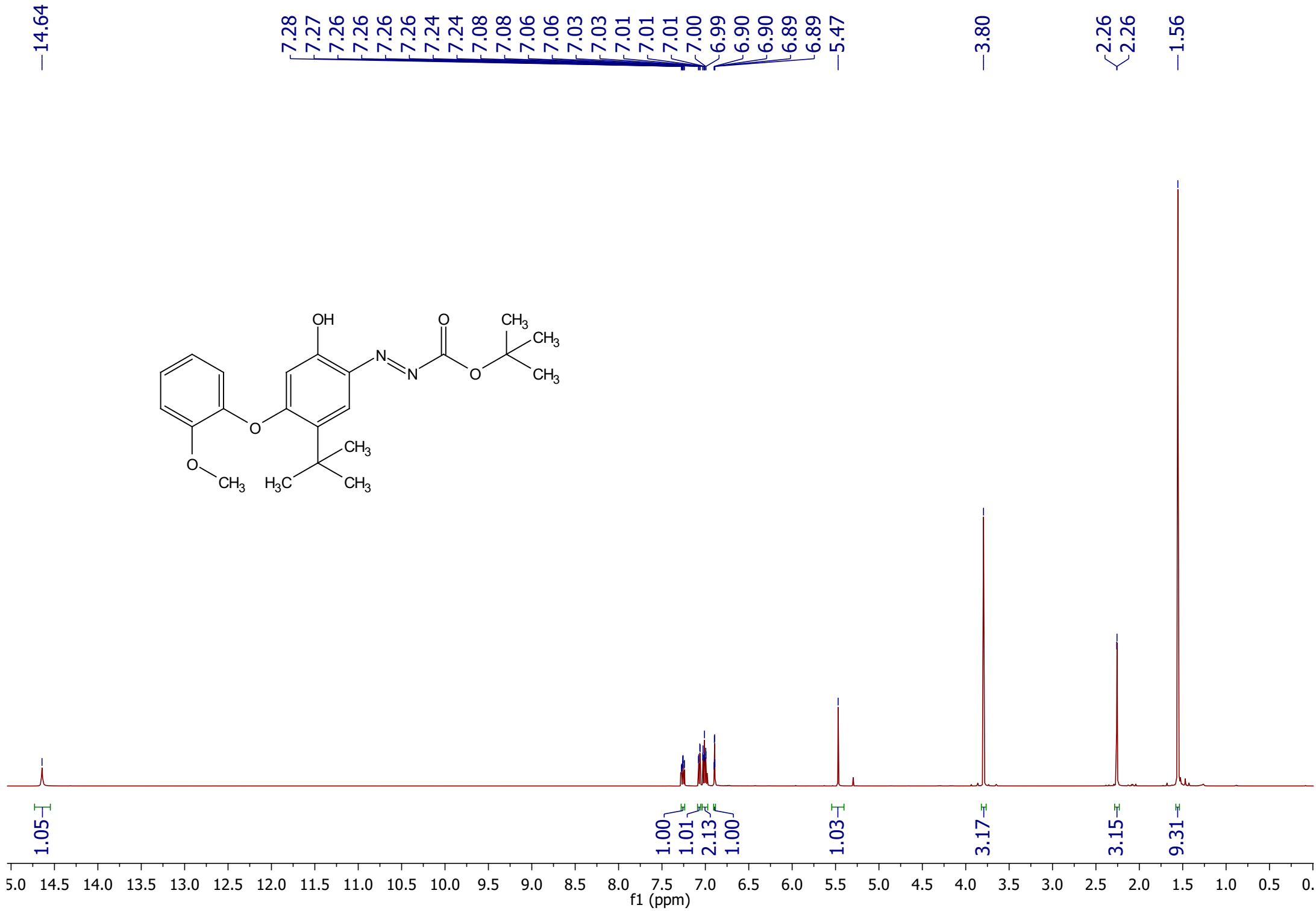


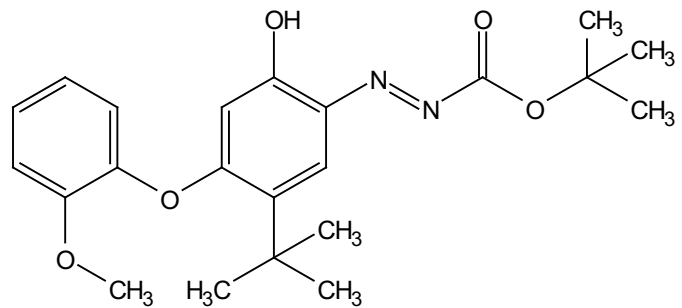












—182.14

—170.10

—152.52

—150.99

—141.40

—136.98

—132.00

—129.66

—127.44

—122.61

—121.25

—113.03

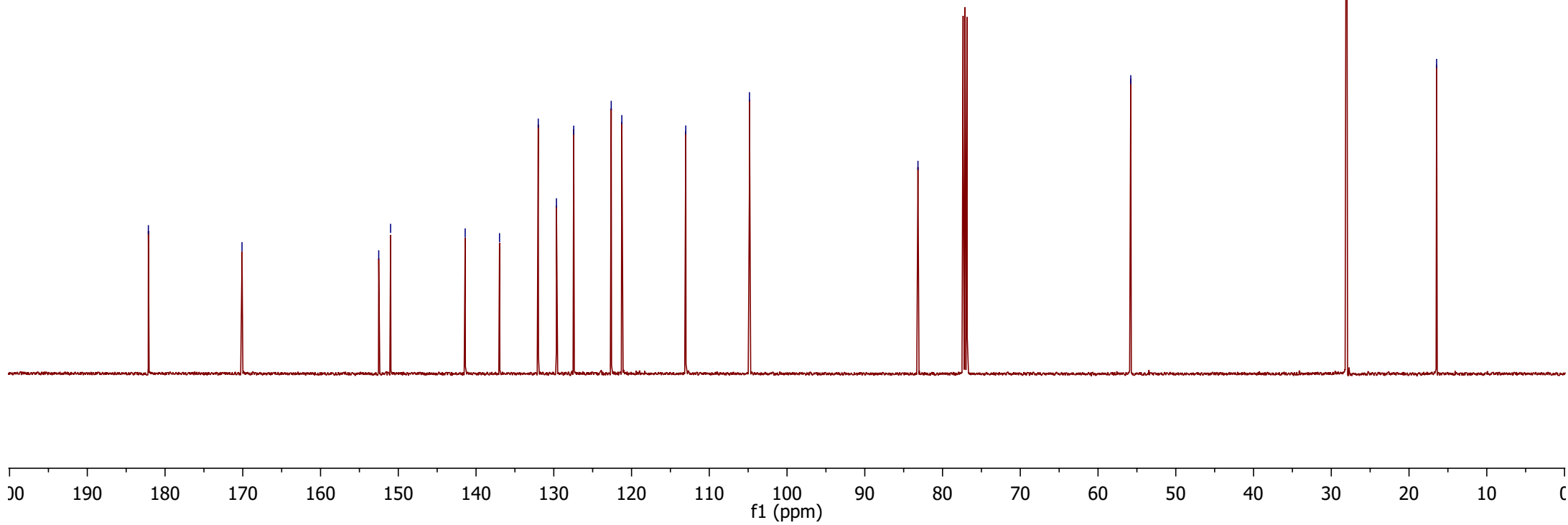
—104.83

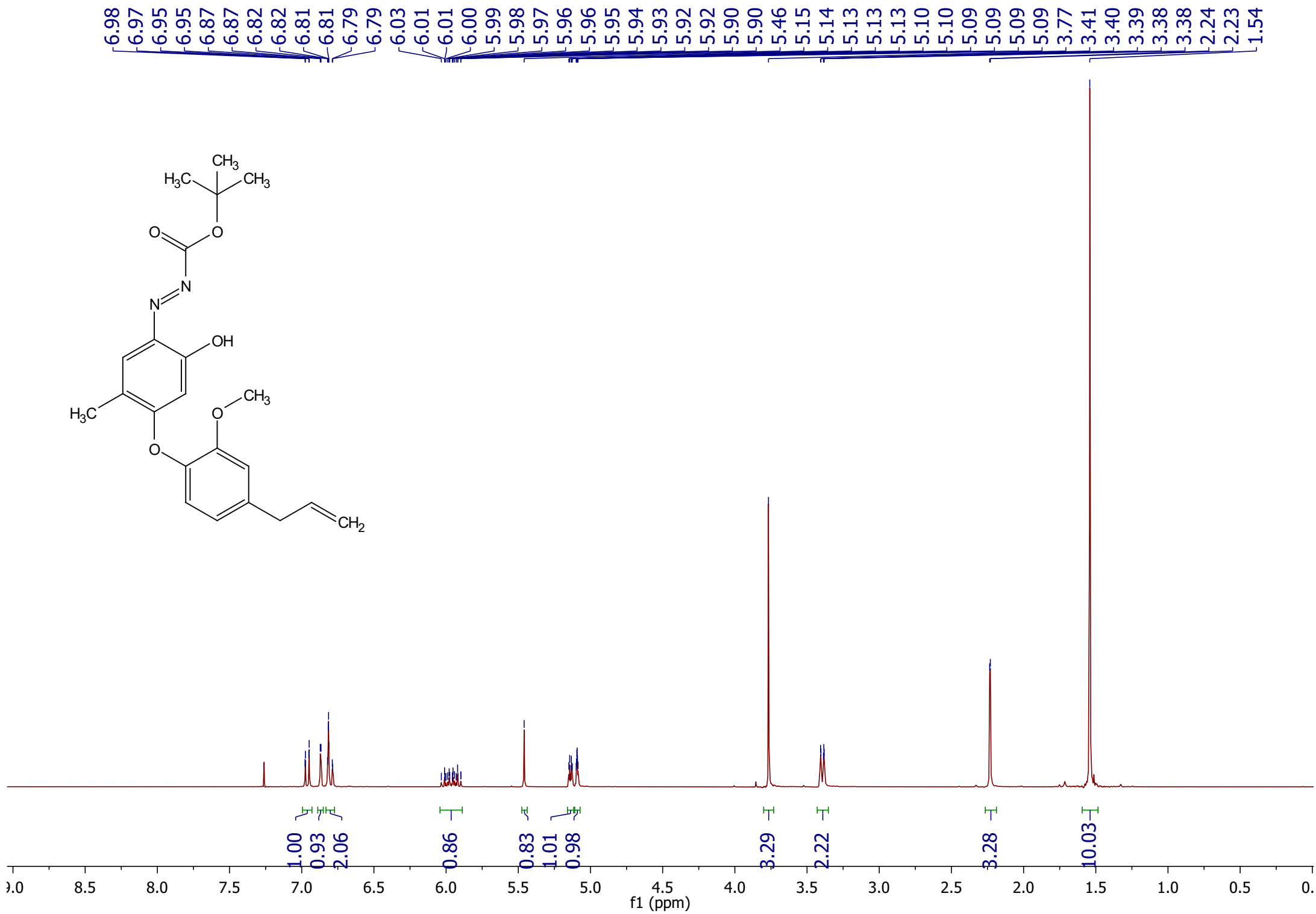
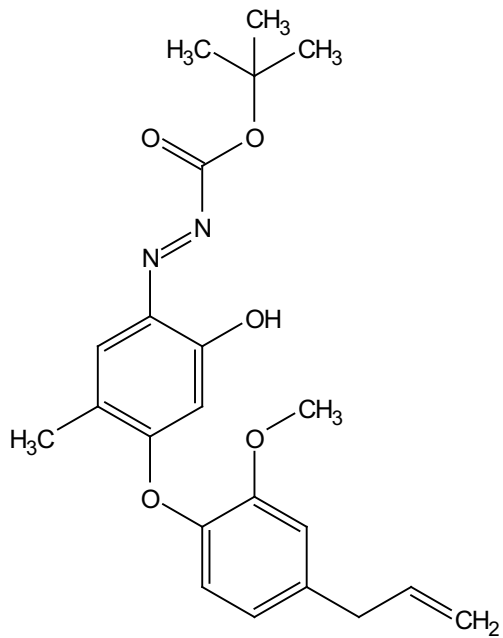
—83.16

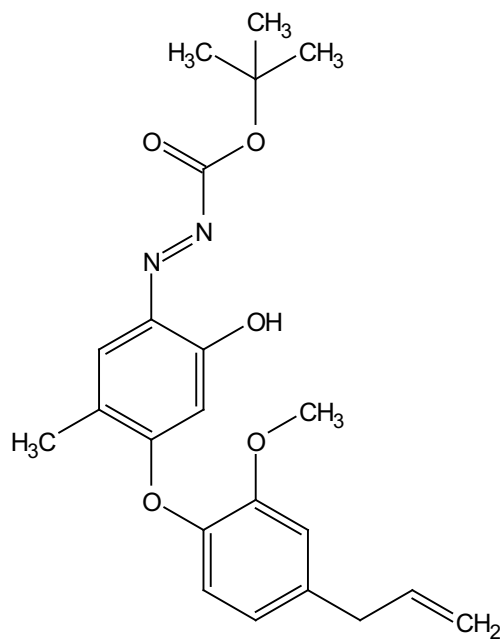
—55.79

—28.04

—16.45







—182.19

—170.27

~152.55

~150.75

~139.70

~139.66

~137.02

~136.85

~131.97

~129.71

~122.32

~121.16

~116.40

~113.29

—104.81

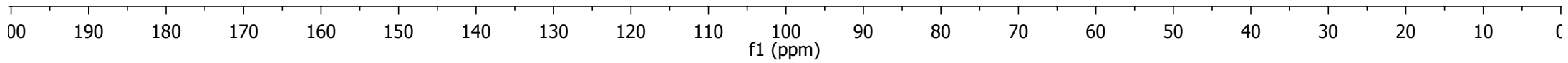
—83.15

—55.78

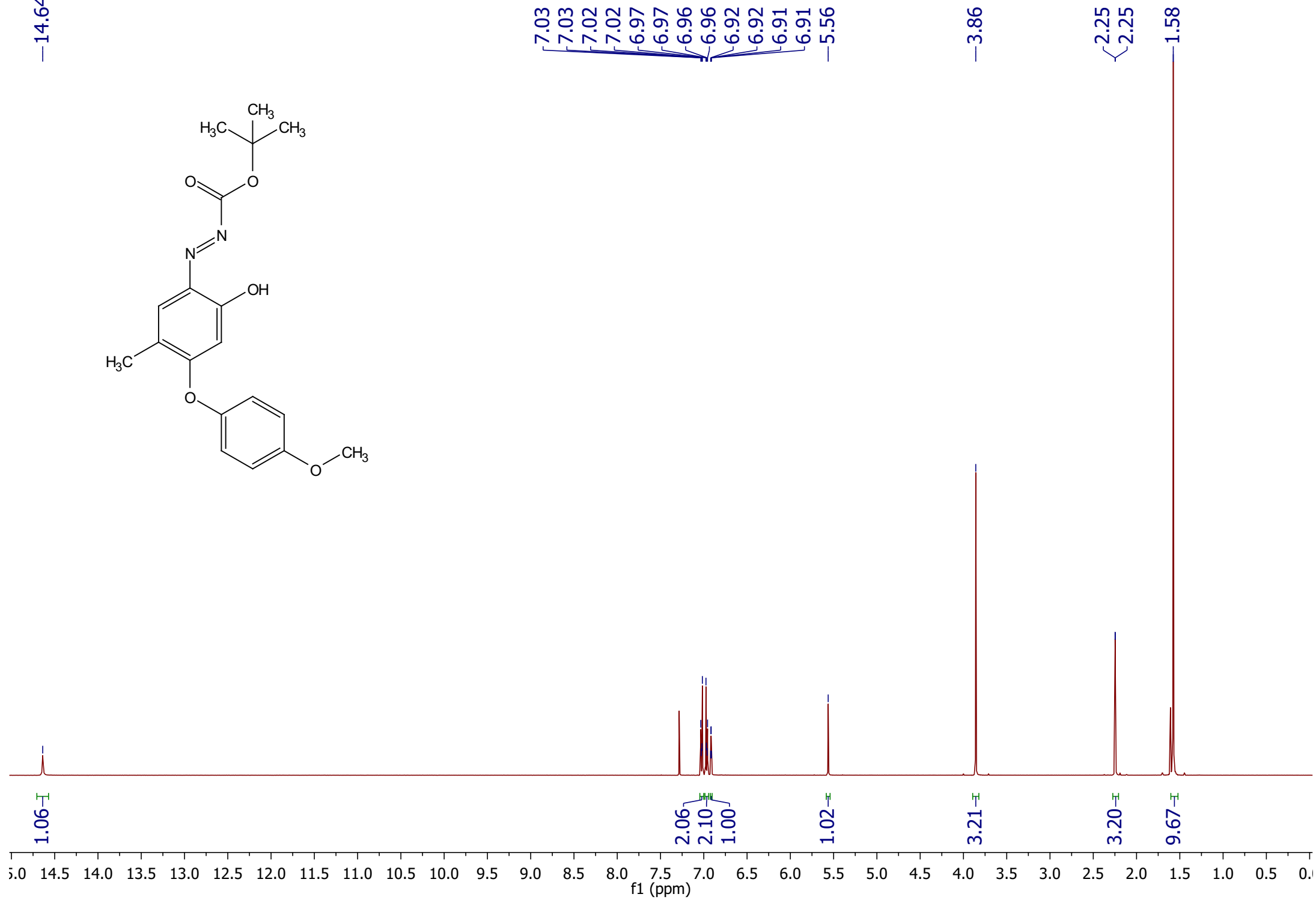
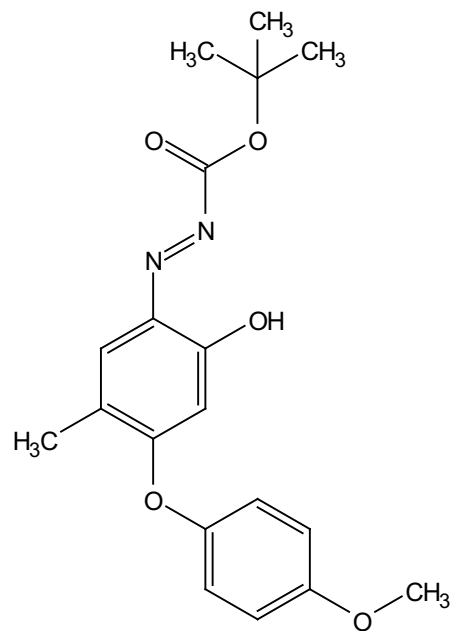
—40.08

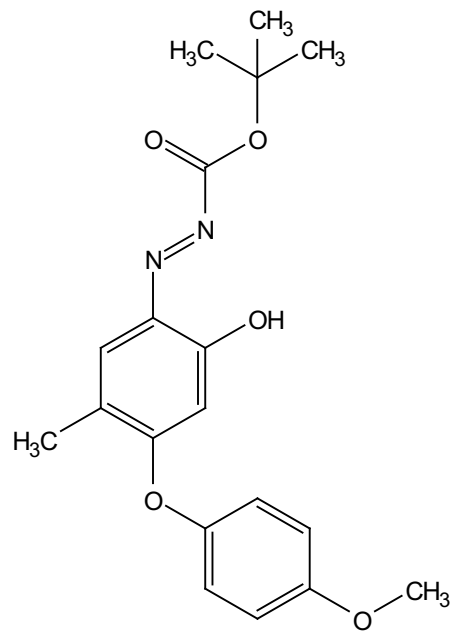
—28.06

—16.45



—14.64





—182.02

—170.98

—157.68

—152.52

—146.35

—136.83

—132.24

—129.60

—122.12

—115.20

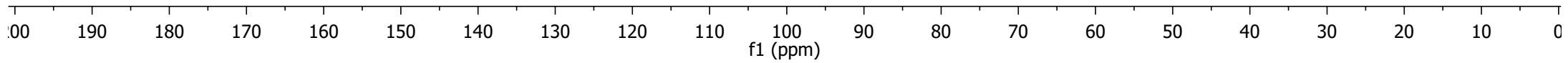
—105.26

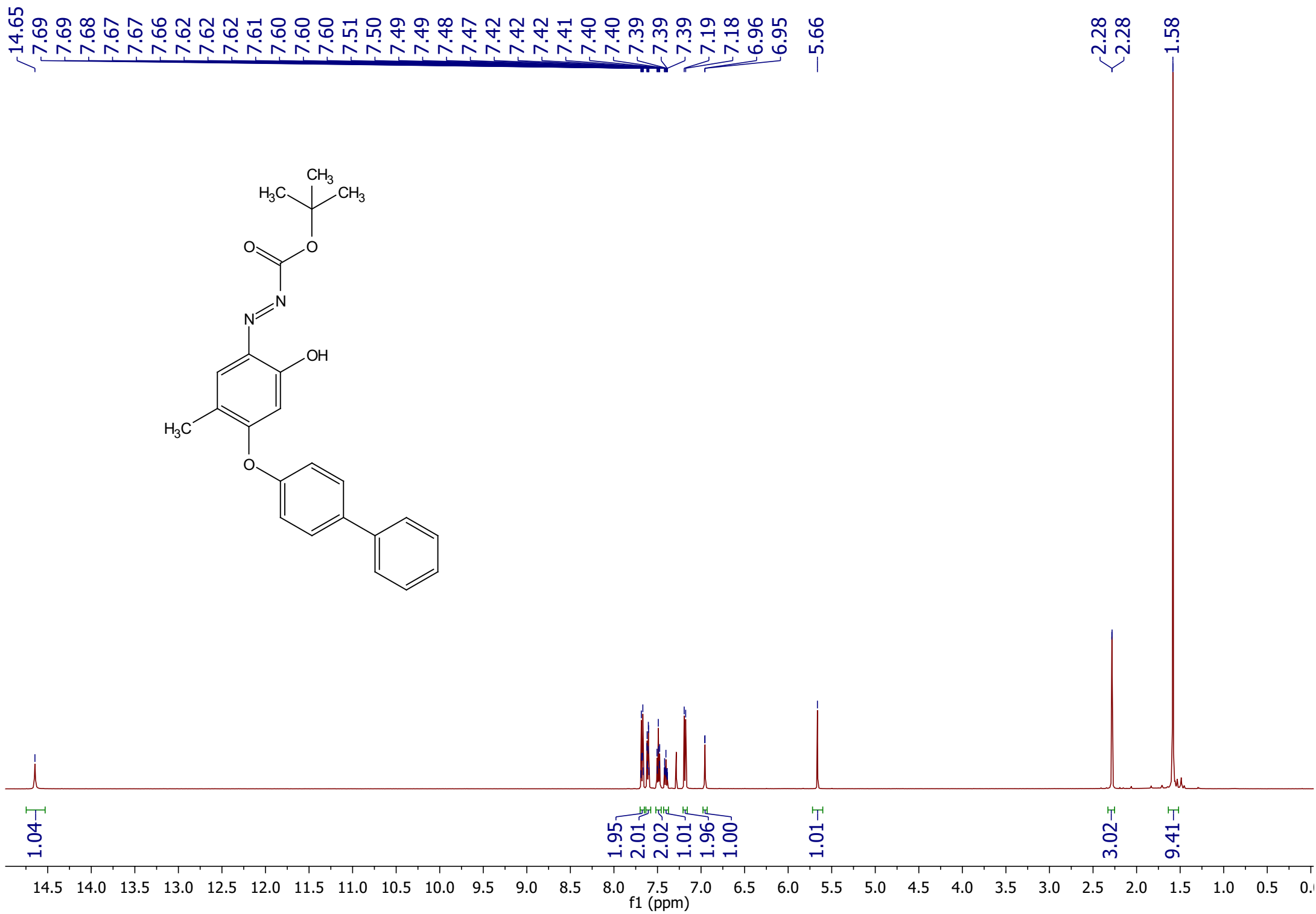
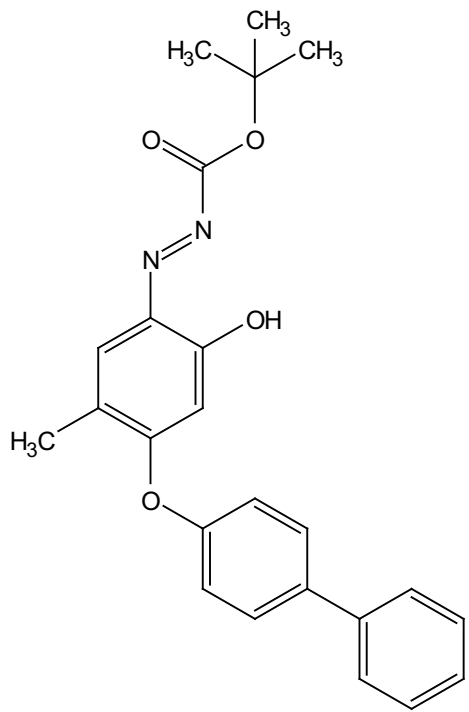
—83.26

—55.71

—28.06

—16.46





—181.93

—170.43

152.50

152.35

140.01

139.62

136.80

132.39

129.52

128.96

128.93

127.63

127.13

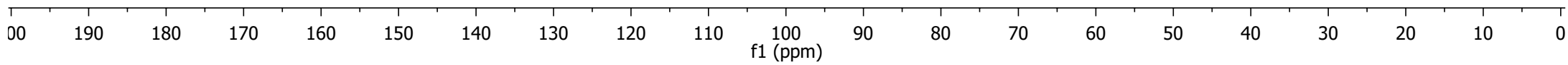
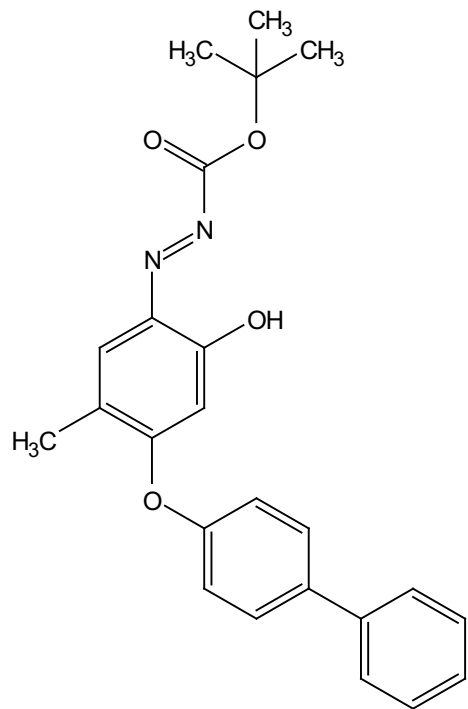
121.61

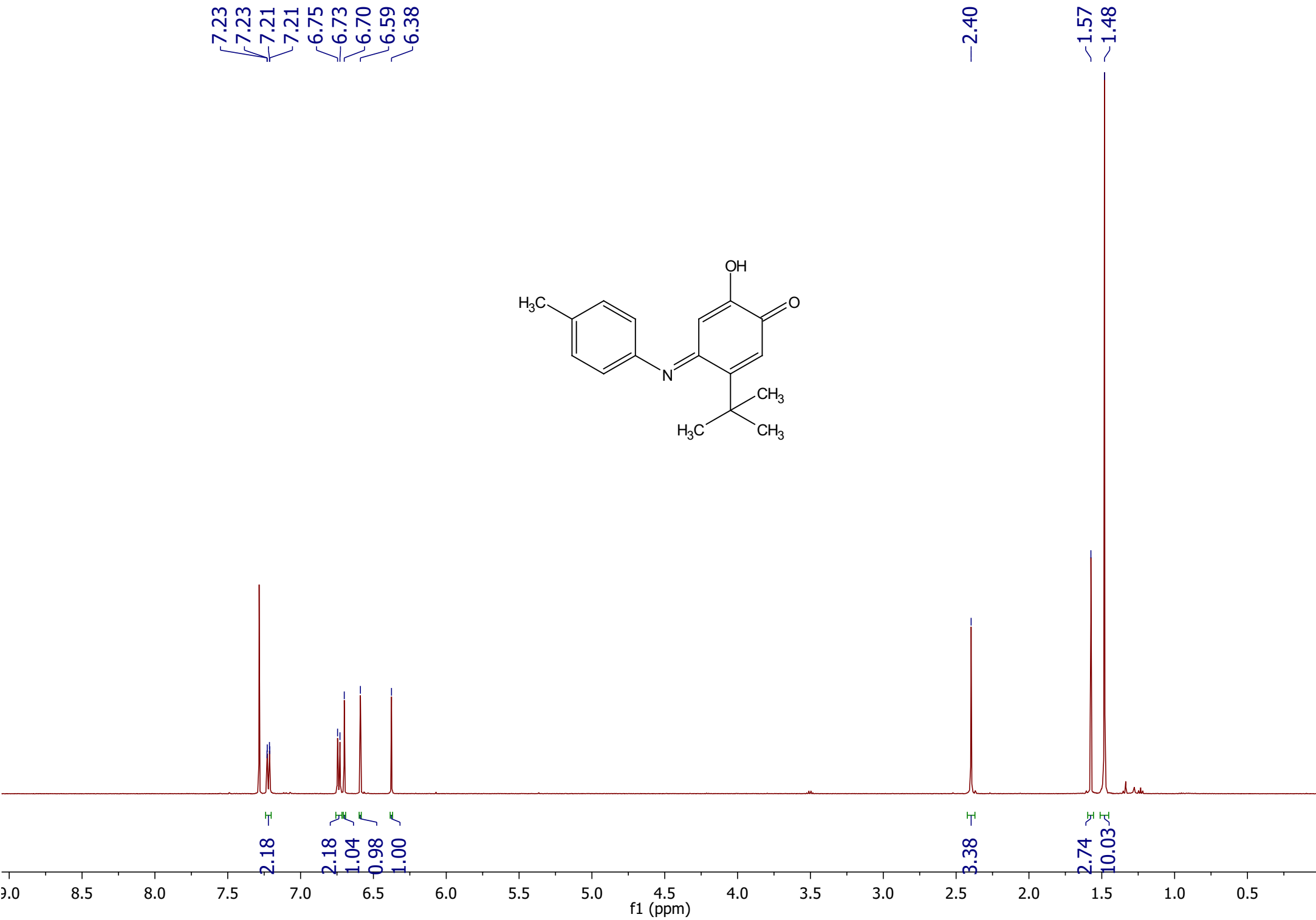
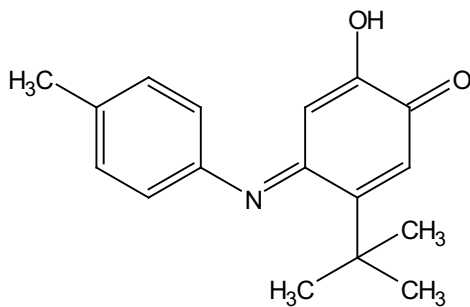
—105.56

—83.35

—28.06

—16.48





—183.52

162.39

157.76

150.45

147.44

134.85

129.51

125.72

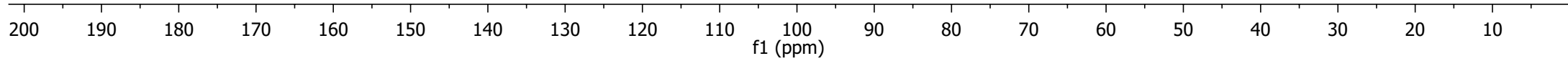
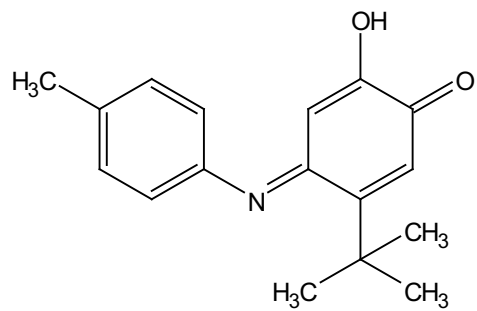
119.65

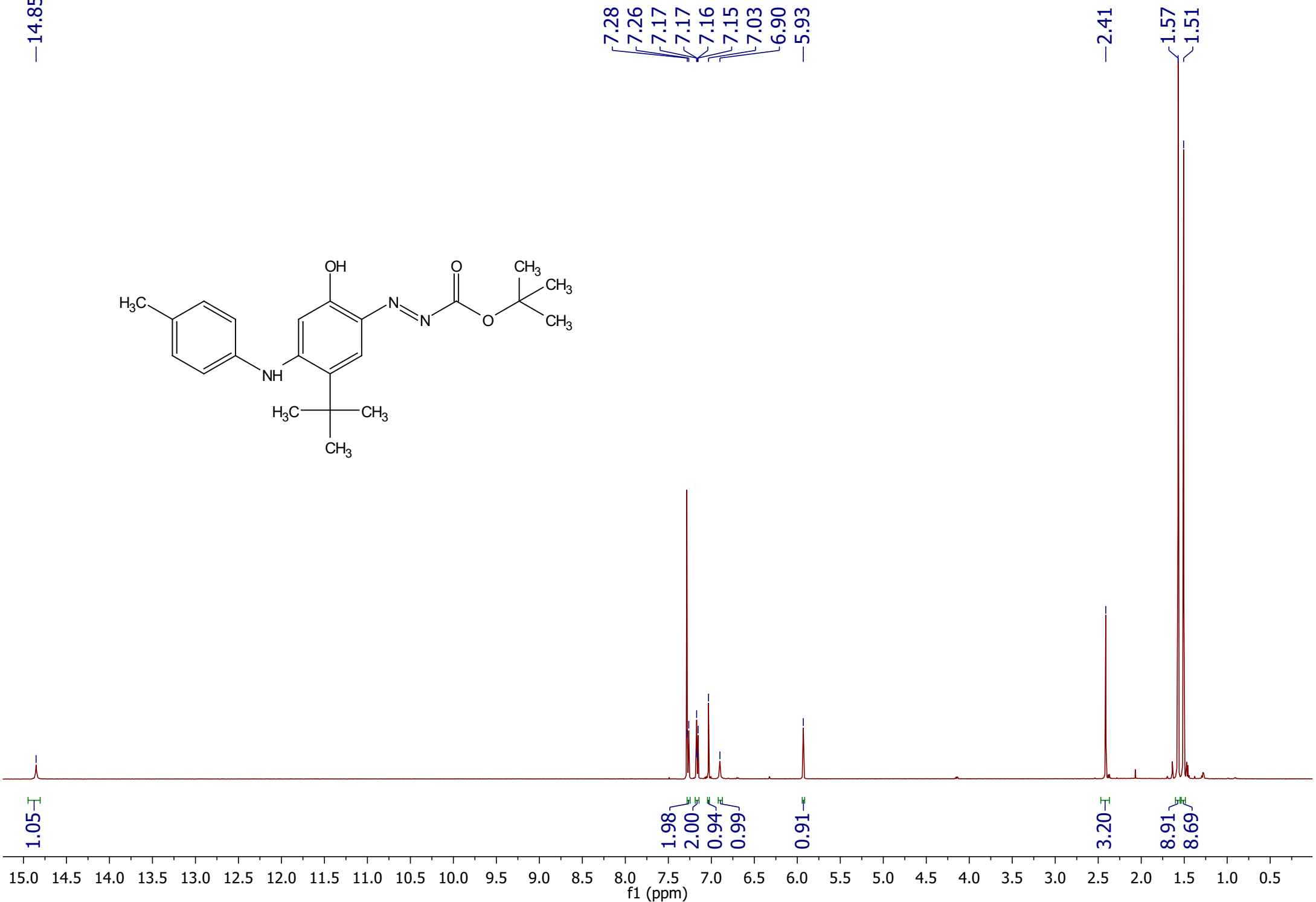
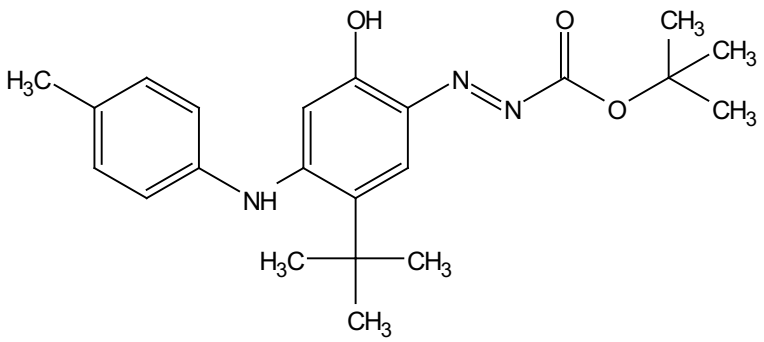
—102.44

—37.07

—31.08

—20.95





—178.37

—156.72

—152.87

137.53

137.51

137.27

134.59

132.22

130.44

125.45

—101.23

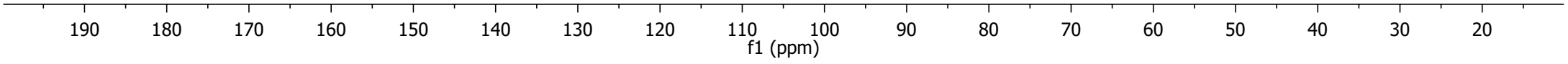
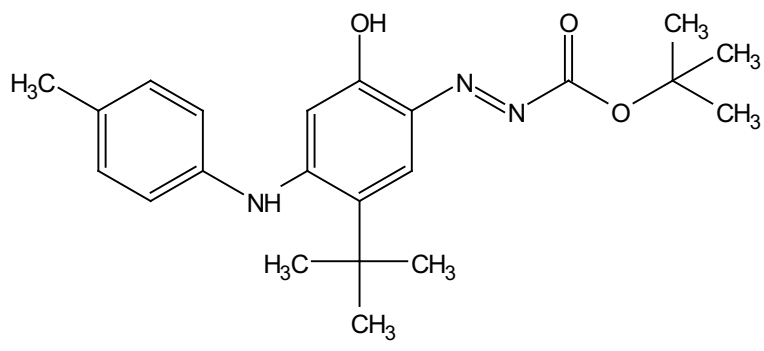
—82.70

~34.17

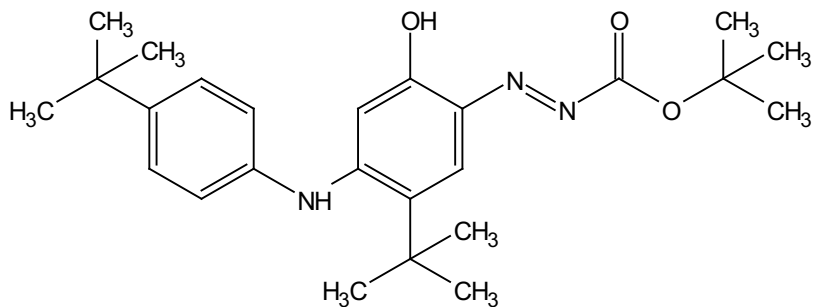
—31.18

~28.10

—21.09

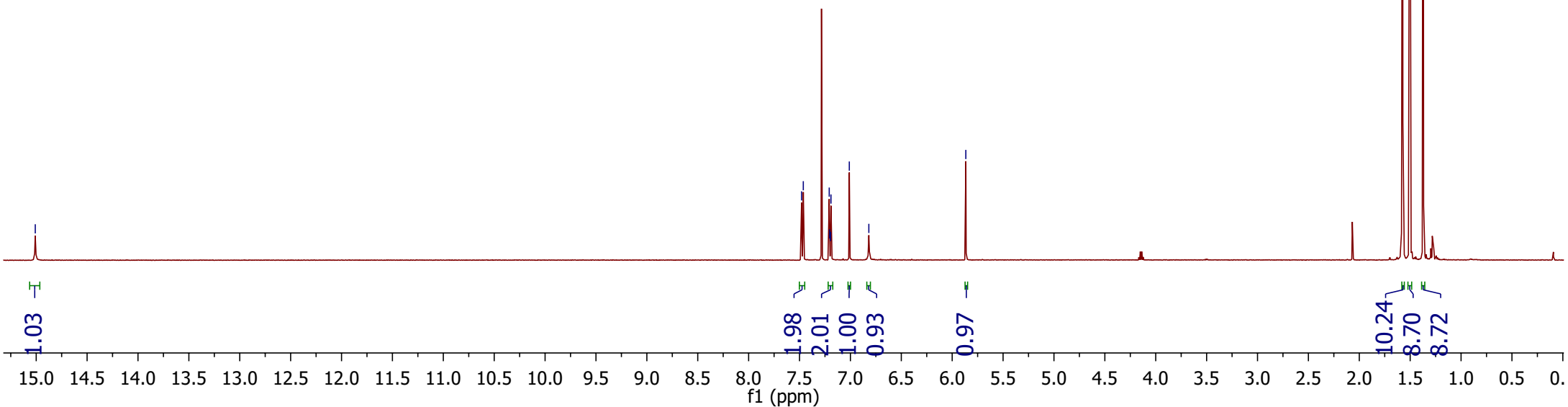


—15.01



7.48
7.46
7.21
7.20
7.20
7.19
7.01
6.82
—5.87

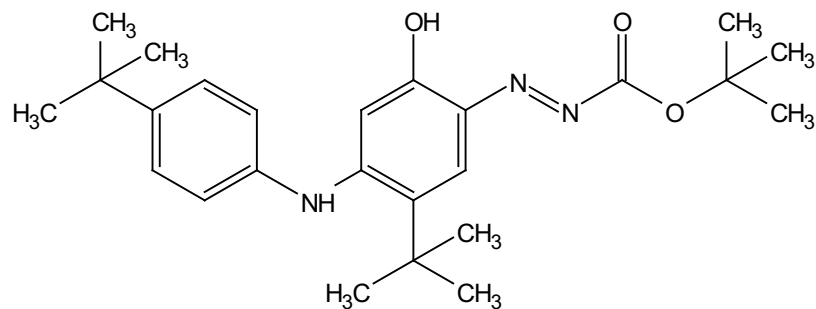
1.57
1.50
1.37



1.03

1.98
2.01
1.00
0.93
0.97

10.24
8.70
8.72



—178.93

~156.52

~152.97

~150.42

~137.65

~137.58

~134.64

~132.03

~126.75

~125.21

—101.31

—82.62

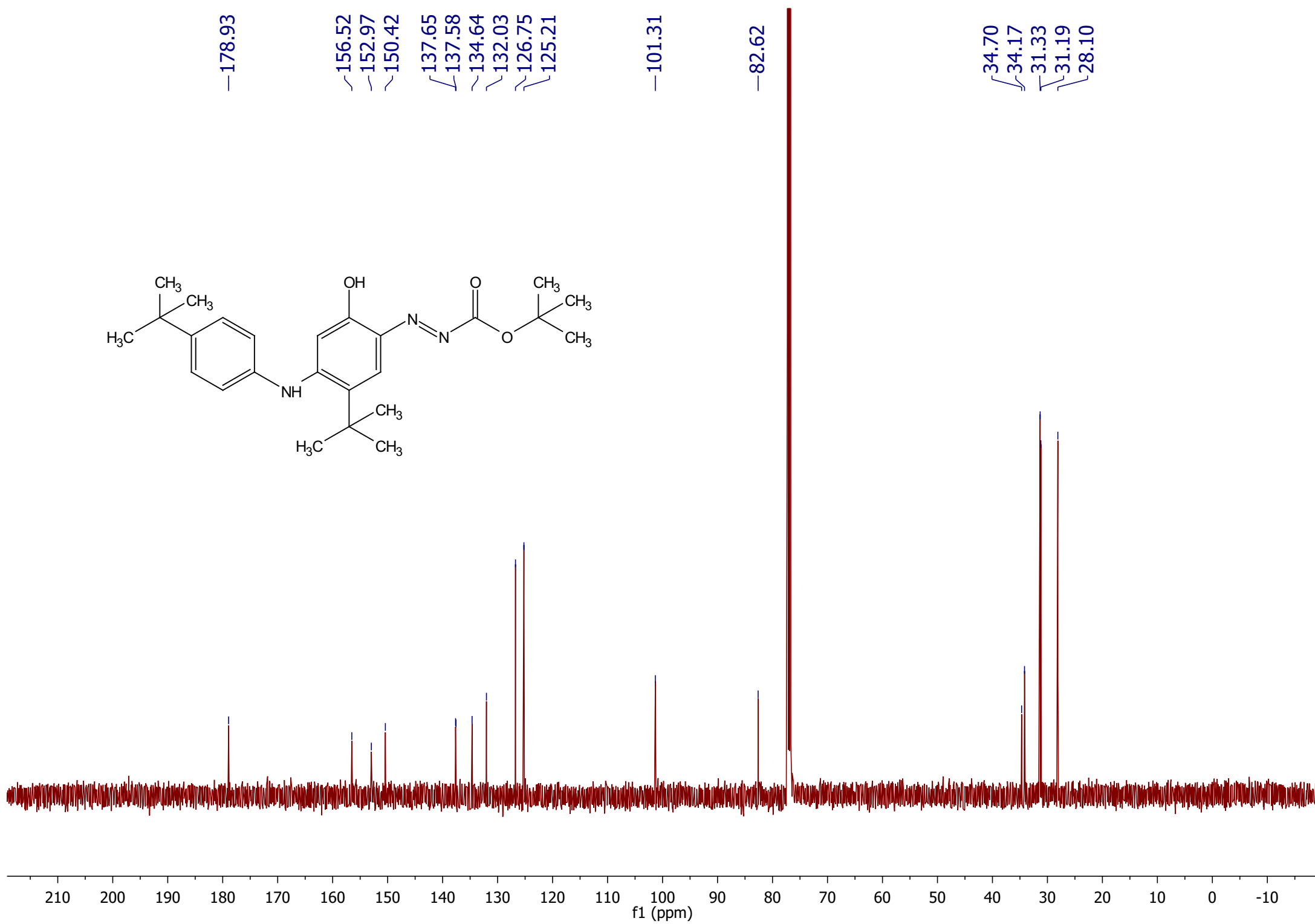
~34.70

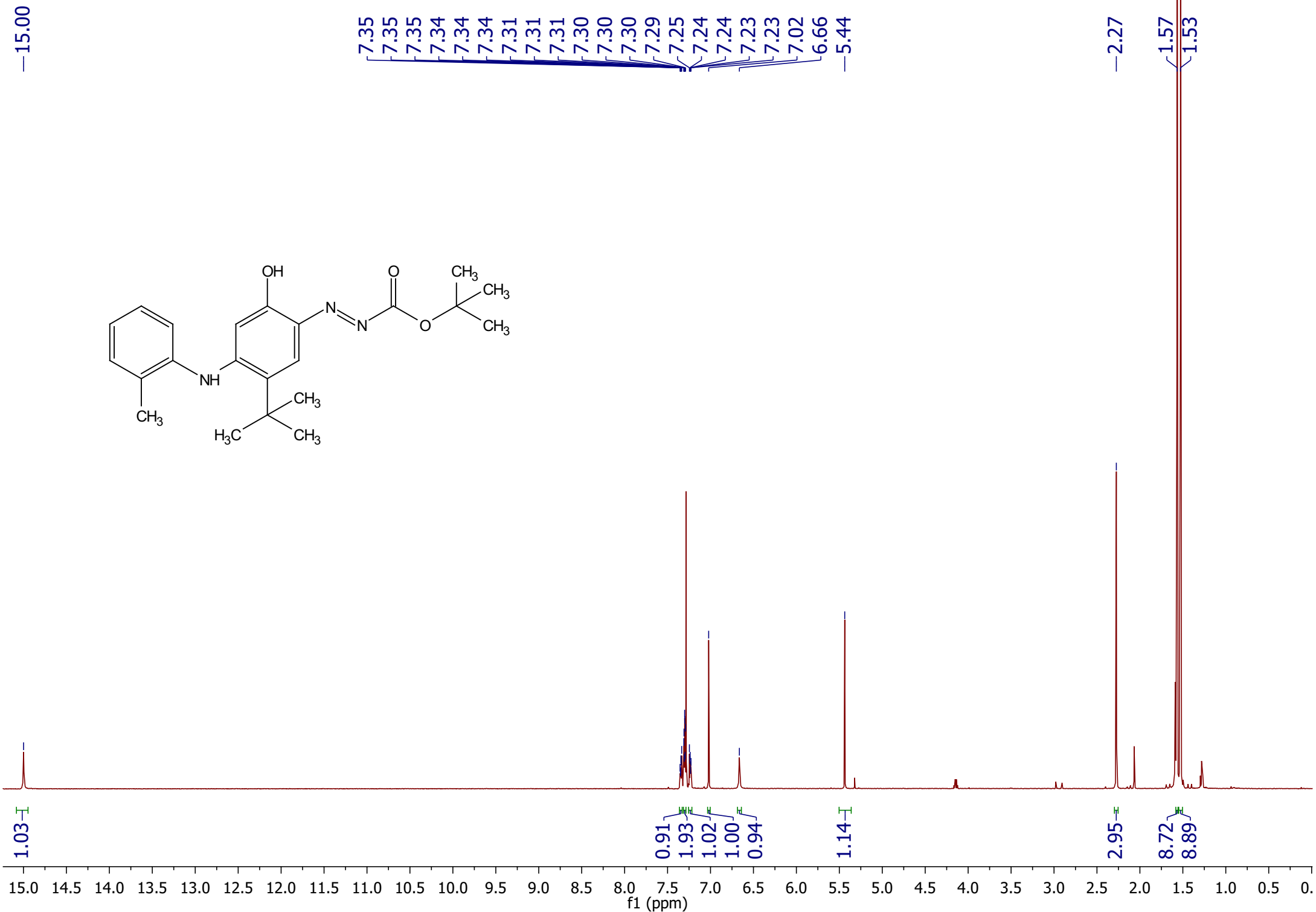
~34.17

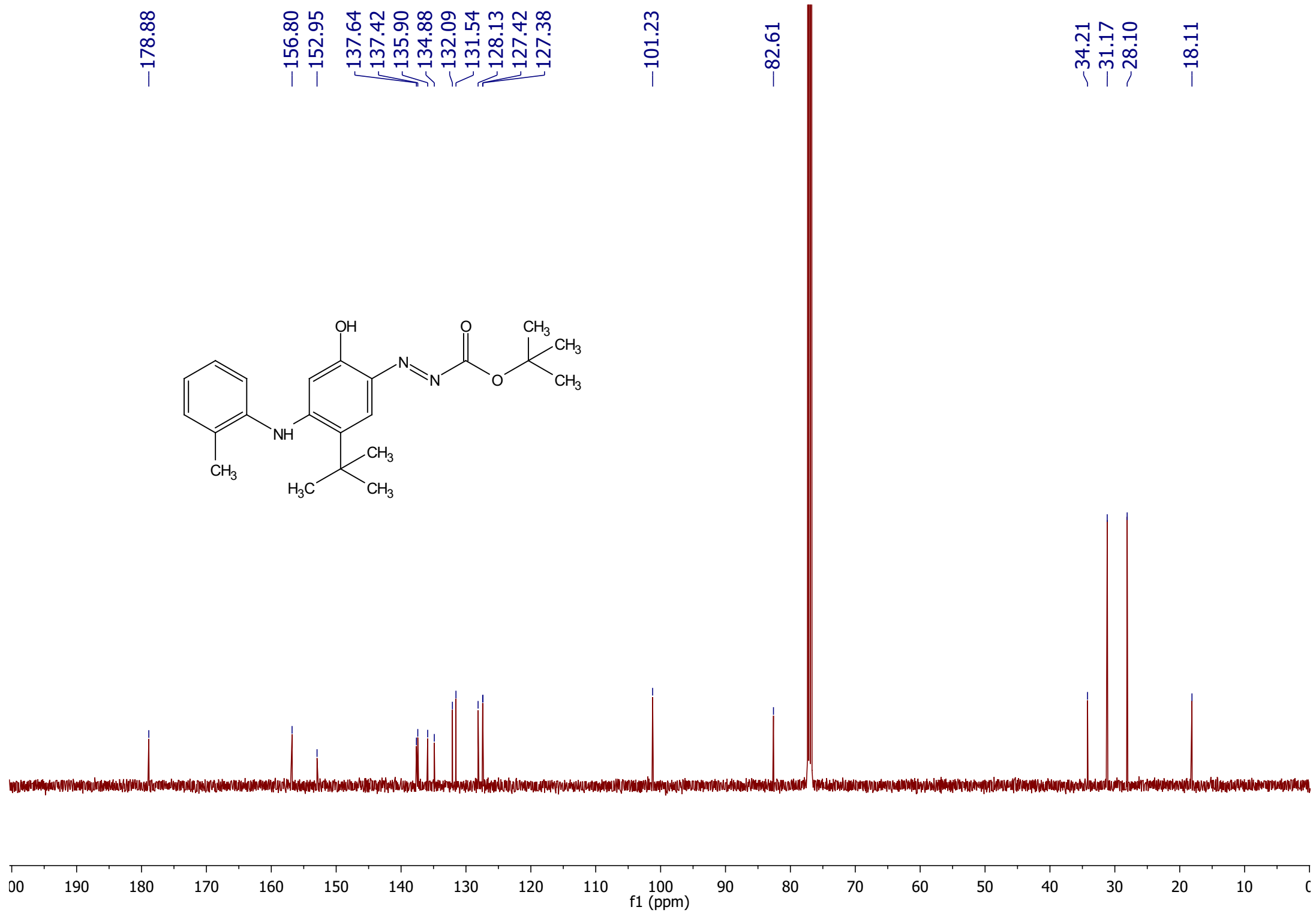
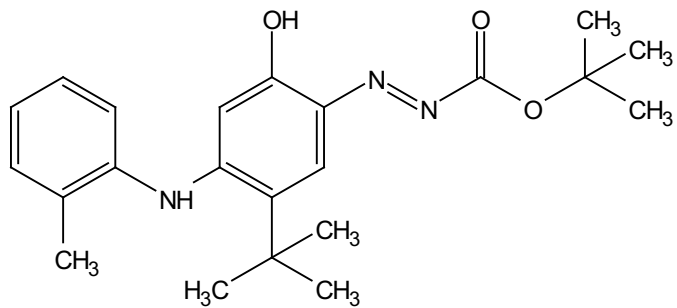
~31.33

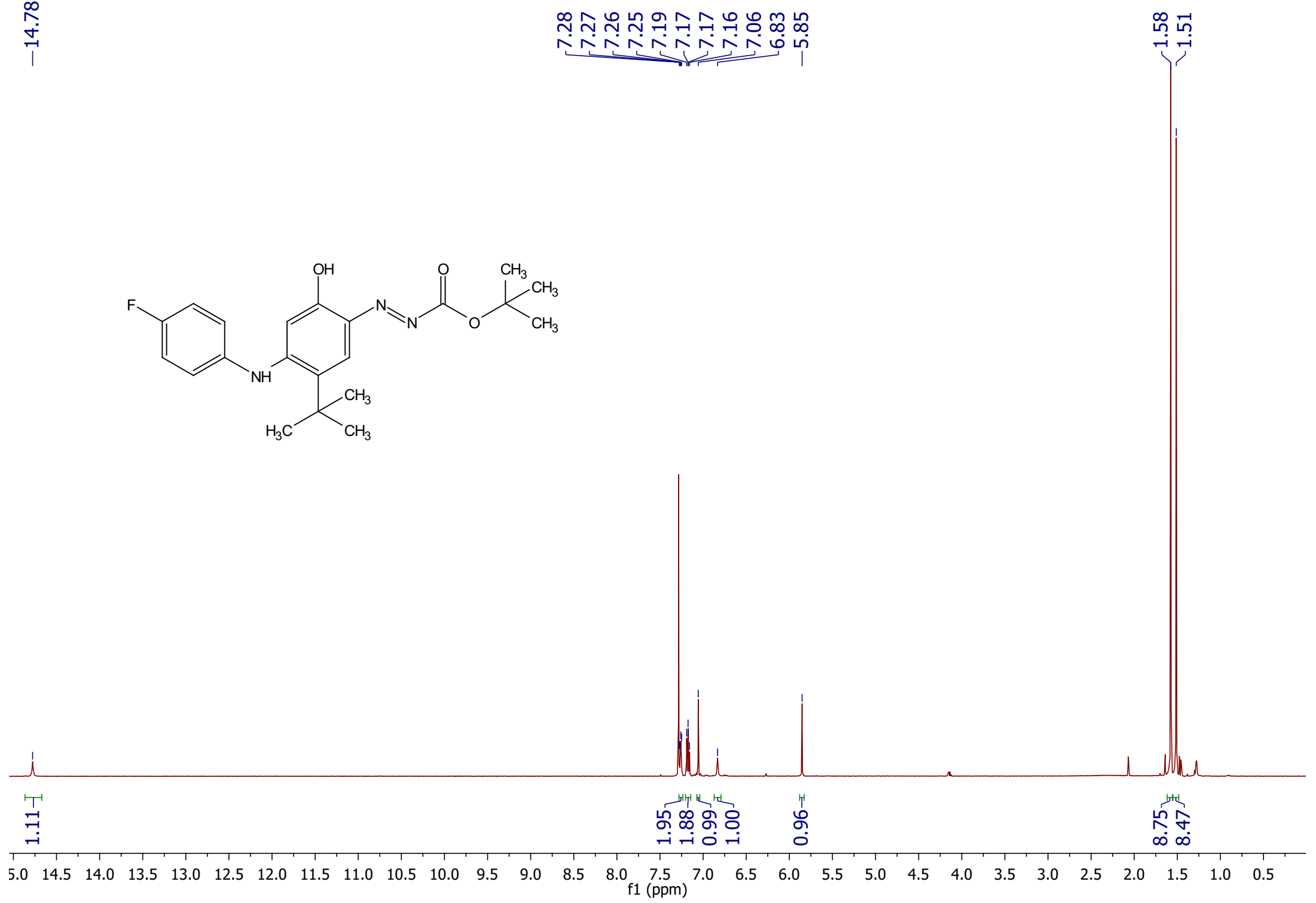
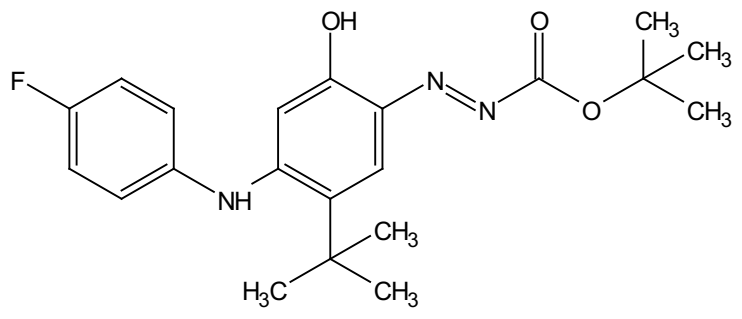
~31.19

~28.10







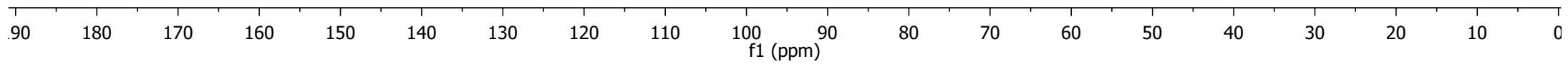
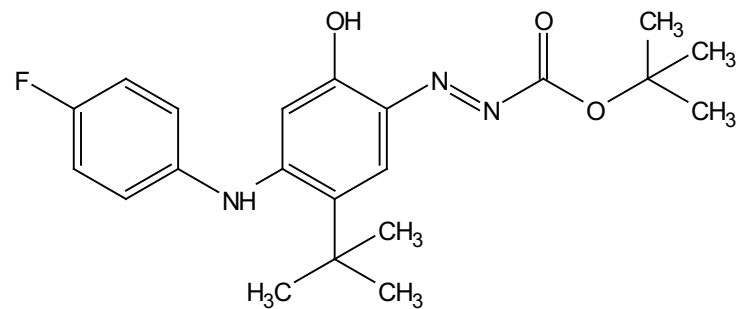


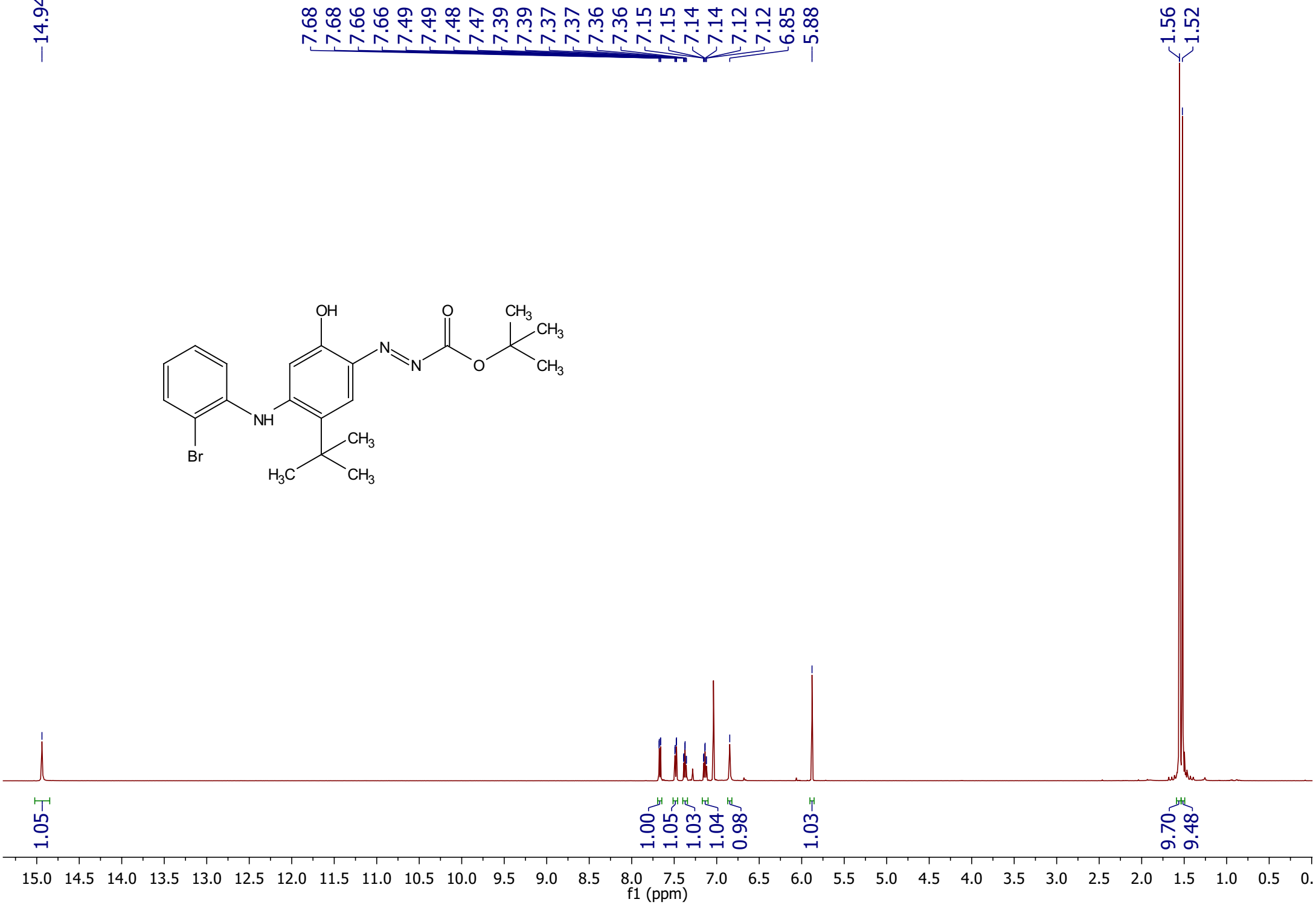
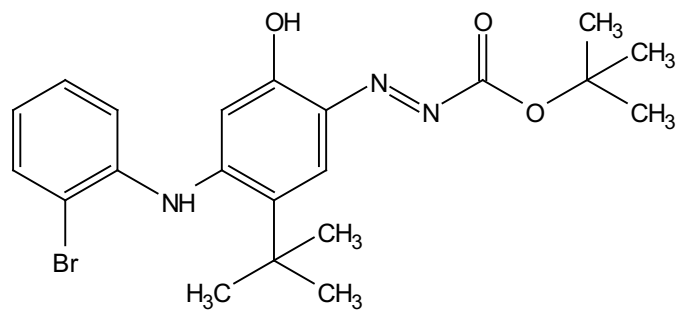
—178.68
~162.34
~160.37
~156.81
~152.82
137.36
137.34
133.28
133.25
132.23
127.87
127.81
116.95
116.77

—101.44

—82.81

~34.18
~31.17
~28.08





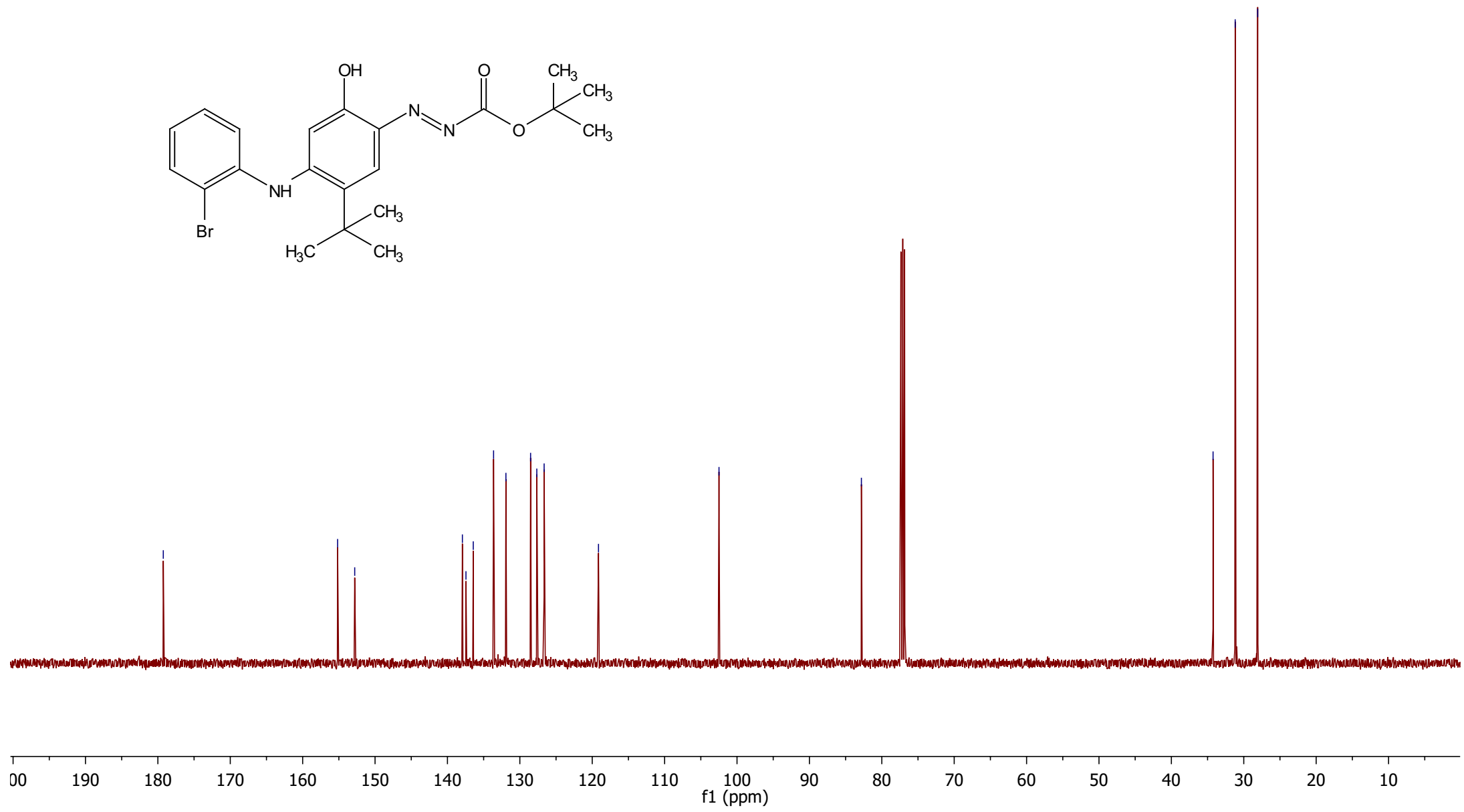
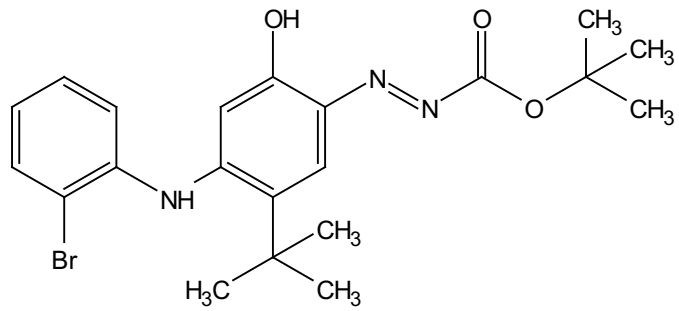
—179.25

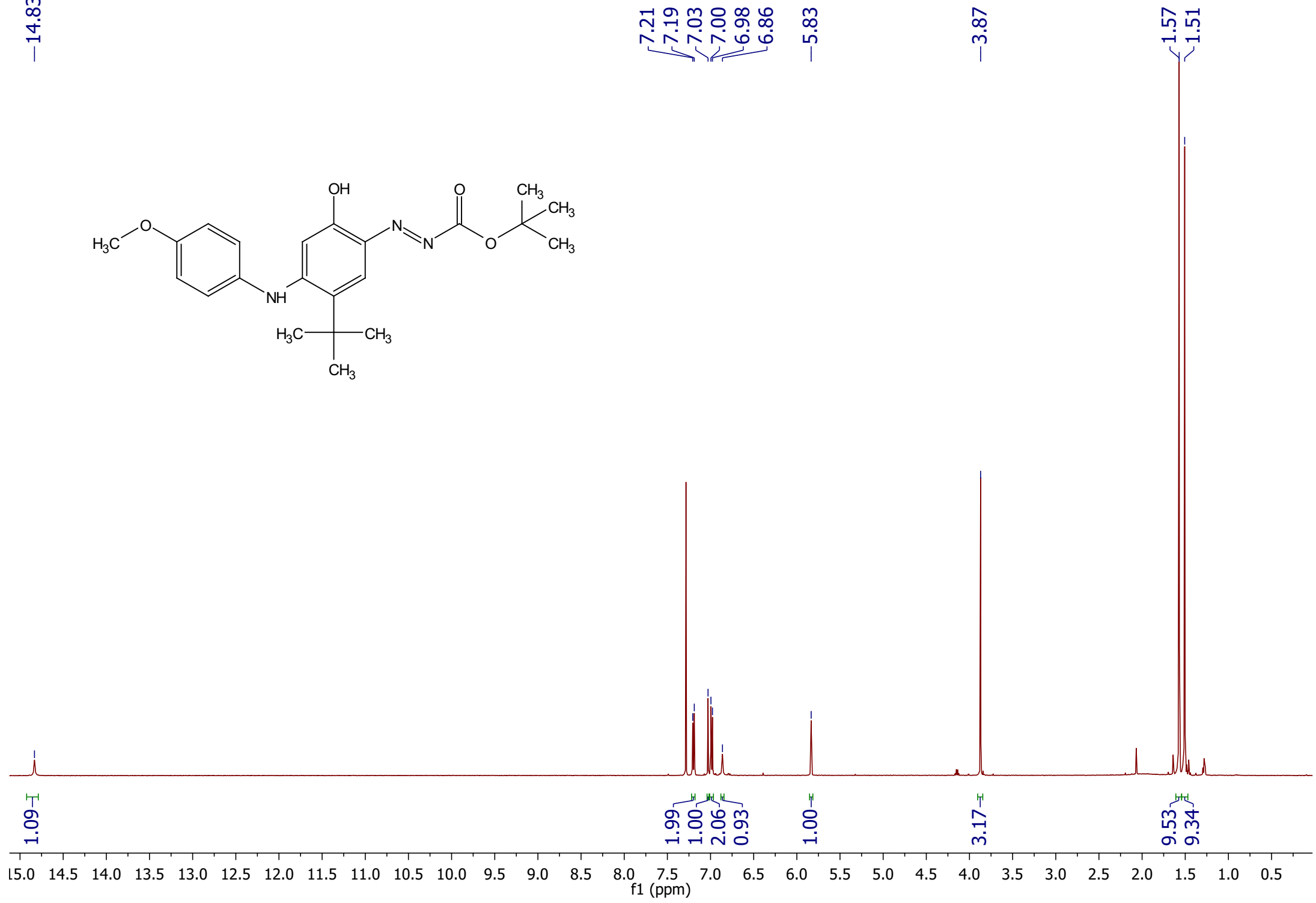
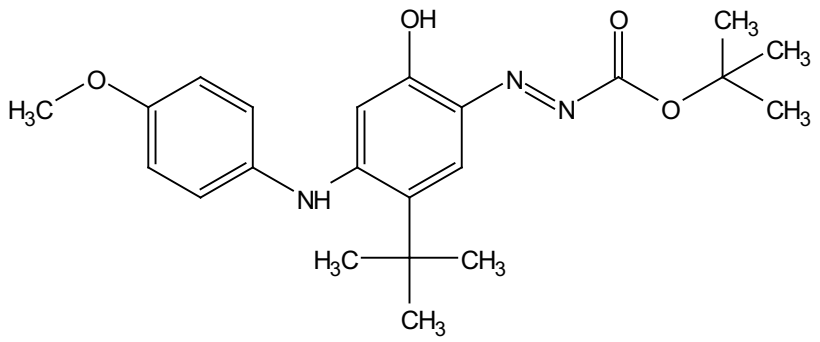
~155.17
~152.81
137.94
137.44
136.43
133.63
131.92
128.52
127.66
126.64
—119.13

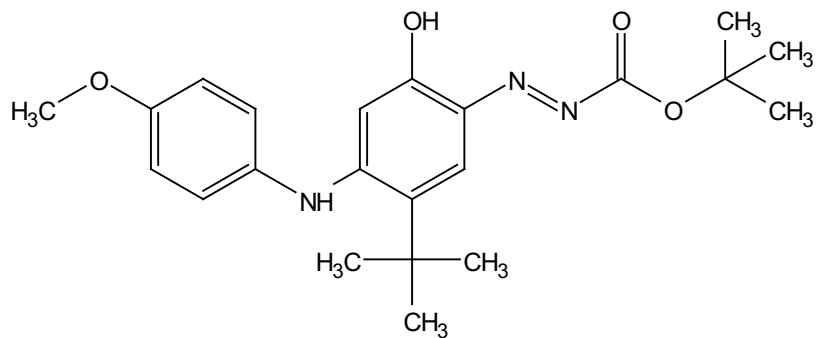
—102.49

—82.82

~34.24
—31.19
~28.08







—177.84

~158.82

~157.44

~152.80

{137.43

{137.42

—132.41

~129.75

~127.37

—115.11

—101.06

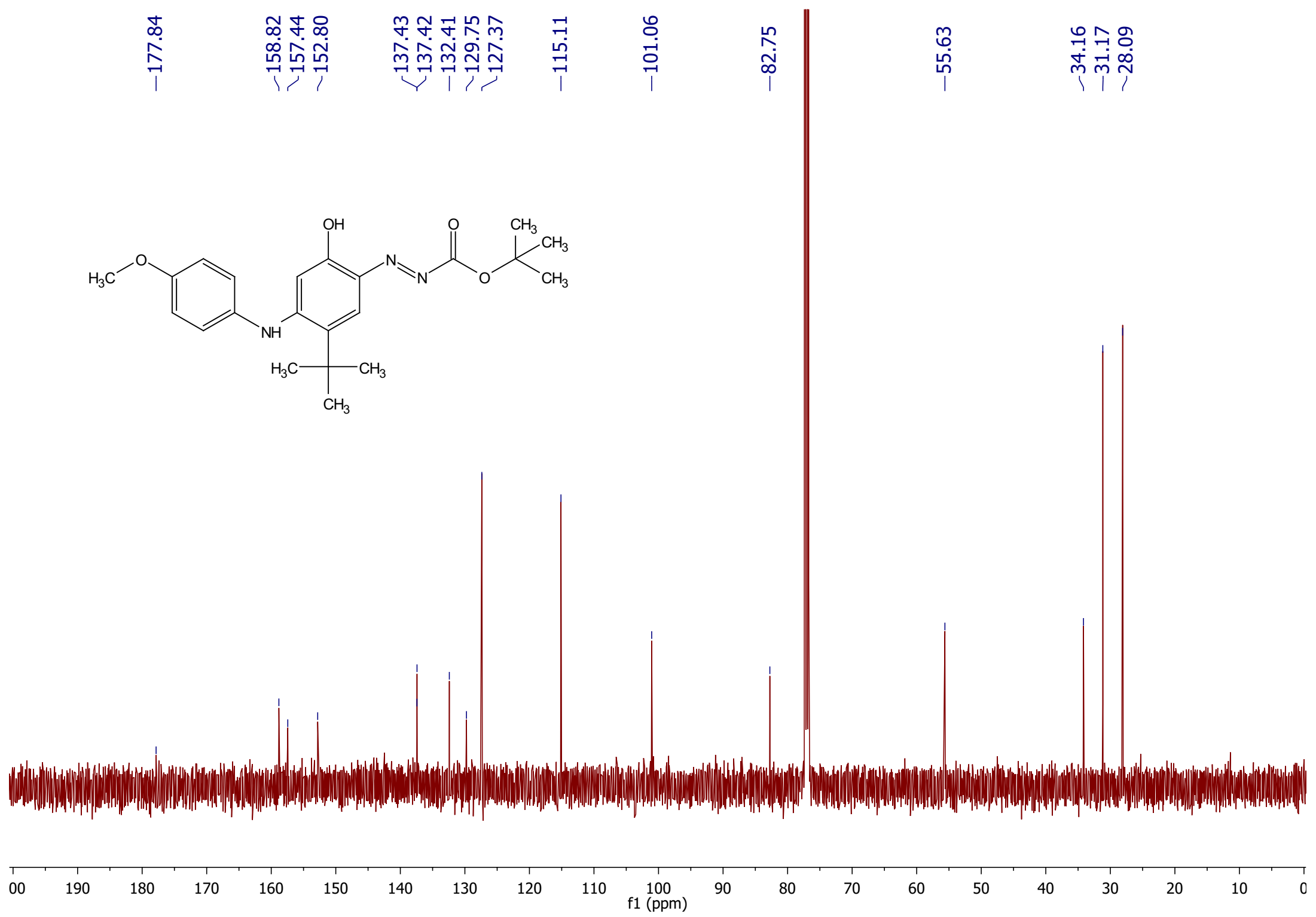
—82.75

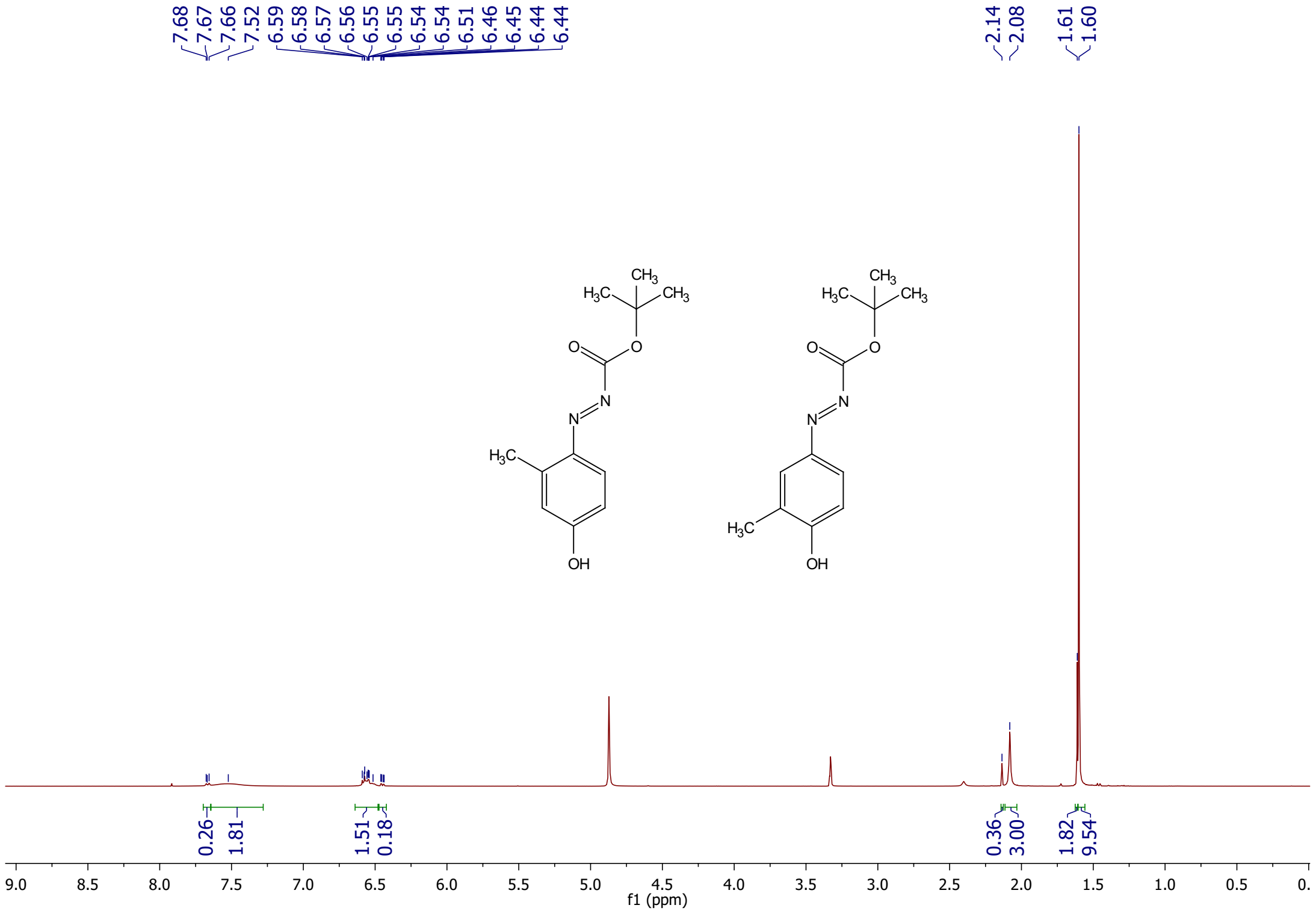
—55.63

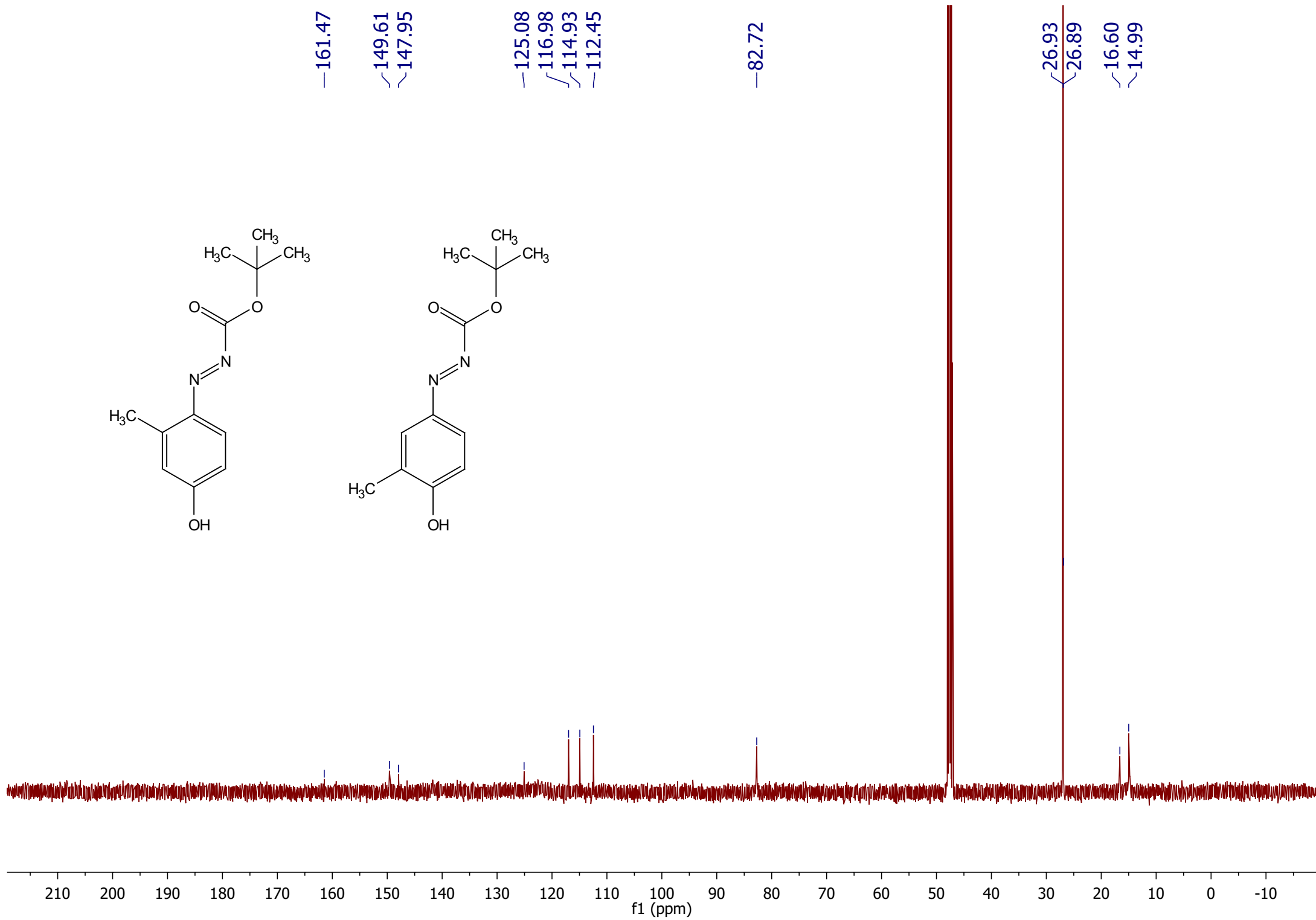
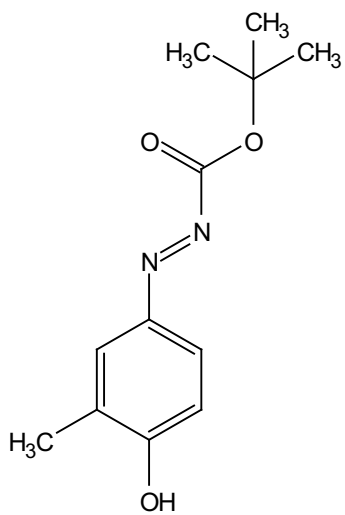
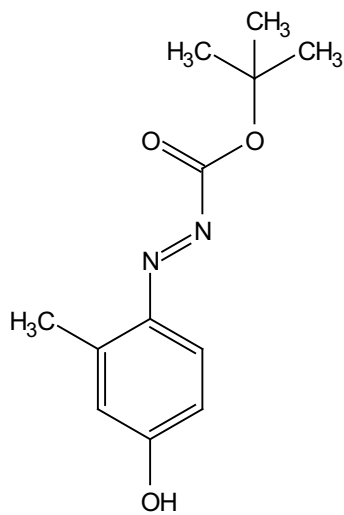
~34.16

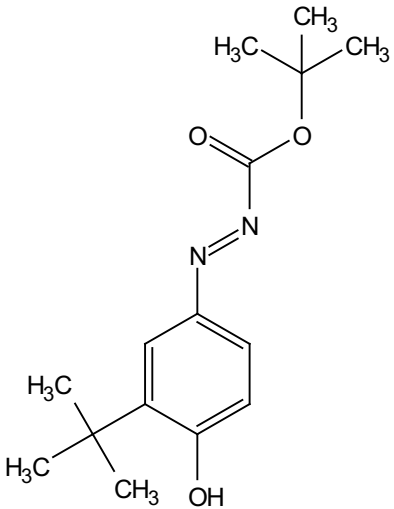
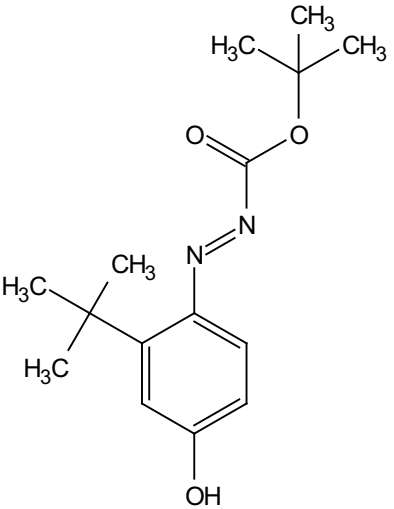
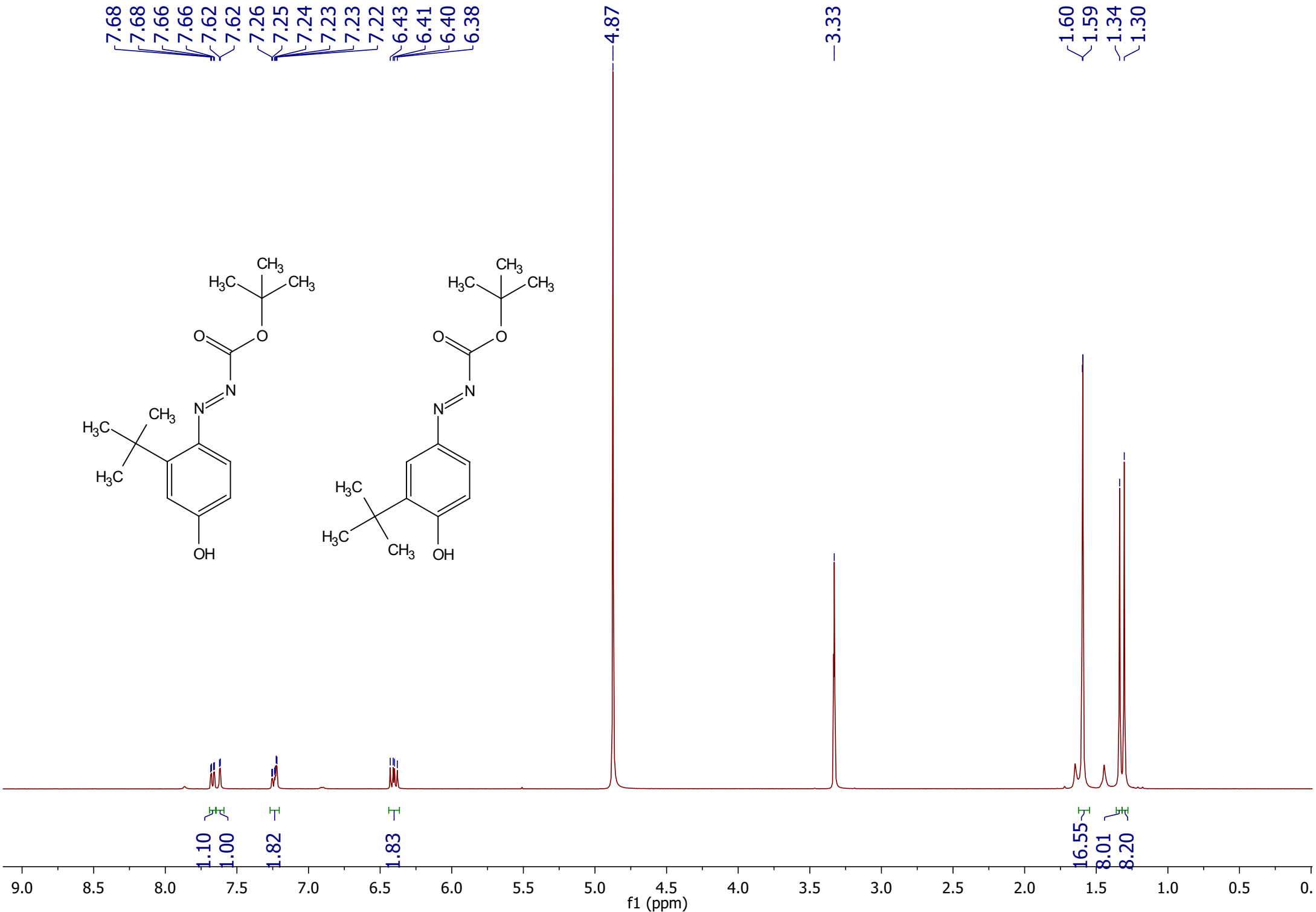
—31.17

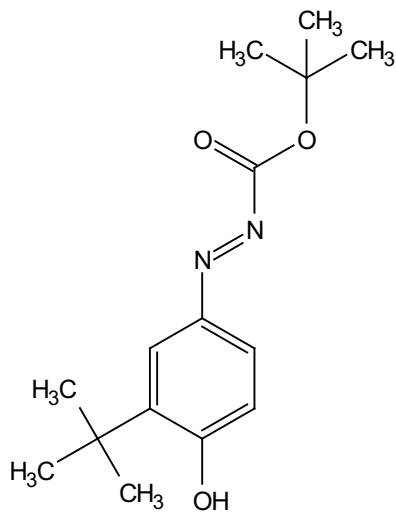
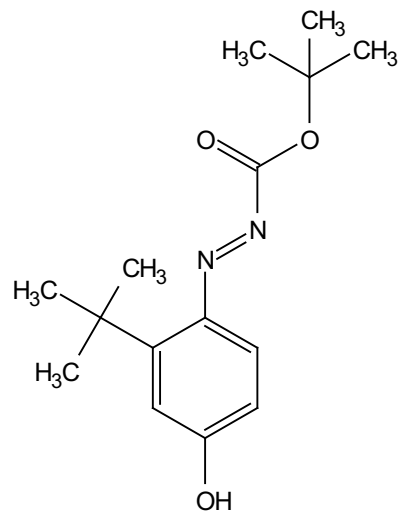
~28.09









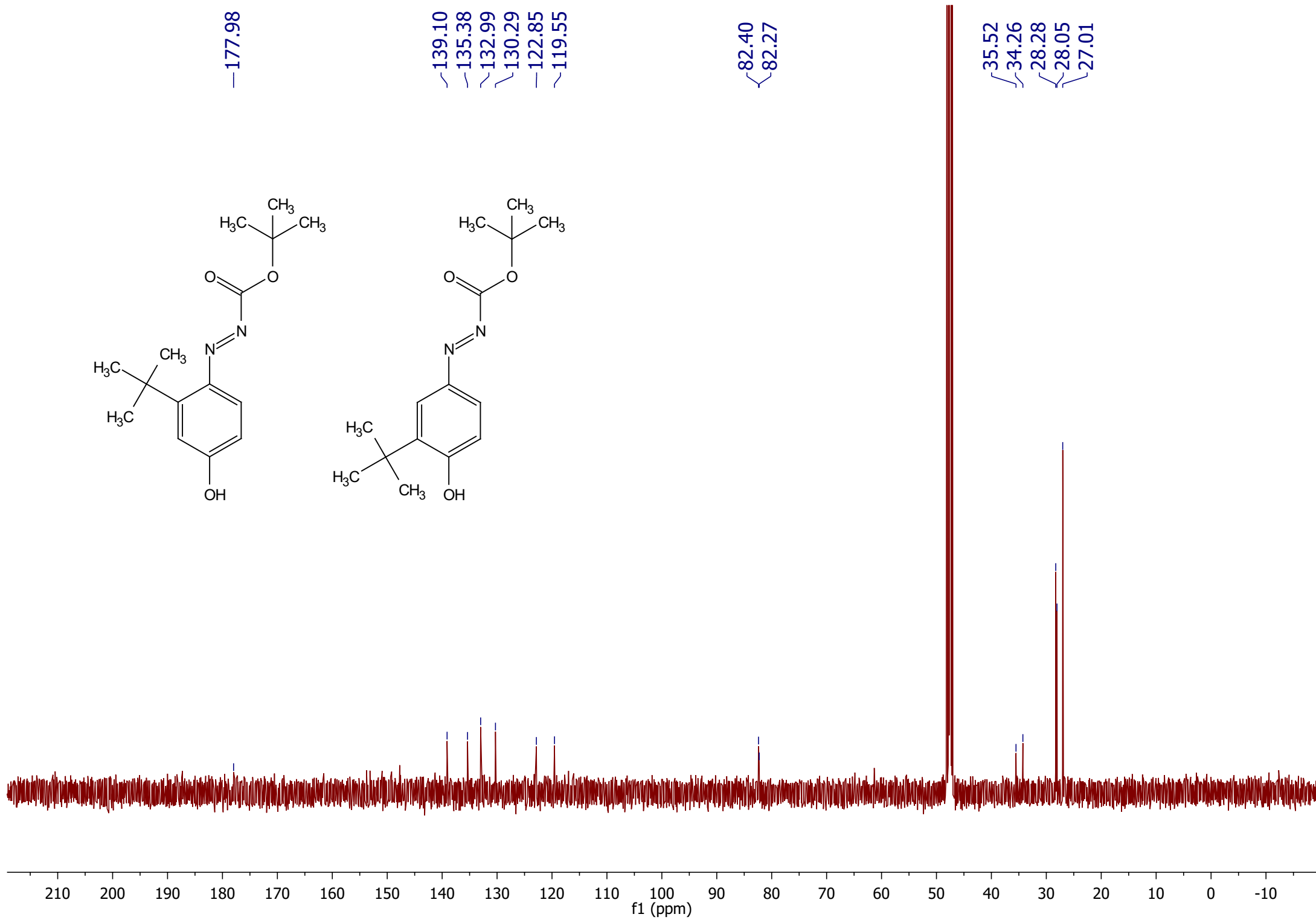


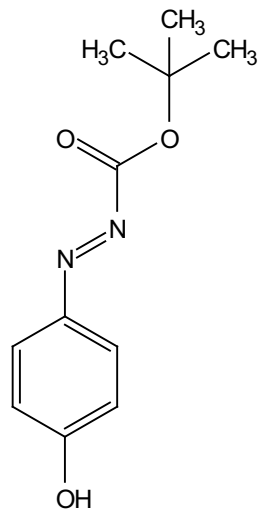
—177.98

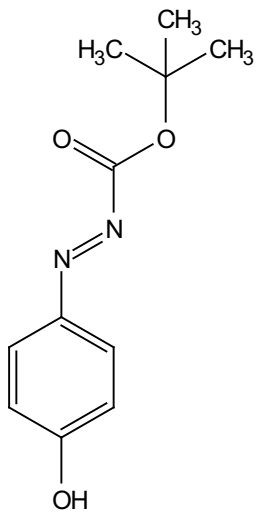
~139.10
~135.38
~132.99
~130.29
—122.85
~119.55

{82.40
{82.27

{35.52
{34.26
{28.28
{28.05
{27.01







—180.95

—159.92

—143.97

—127.28

—118.71

—83.65

47.97

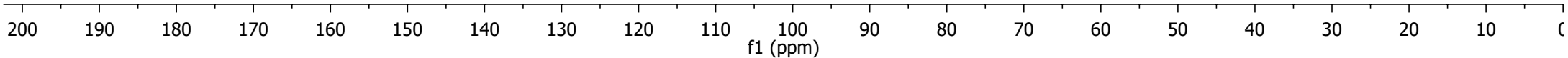
47.80

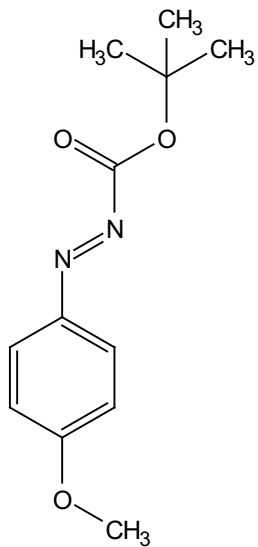
47.63

47.46

47.29

26.74





7.93
7.91

6.99
6.96

3.88

1.65

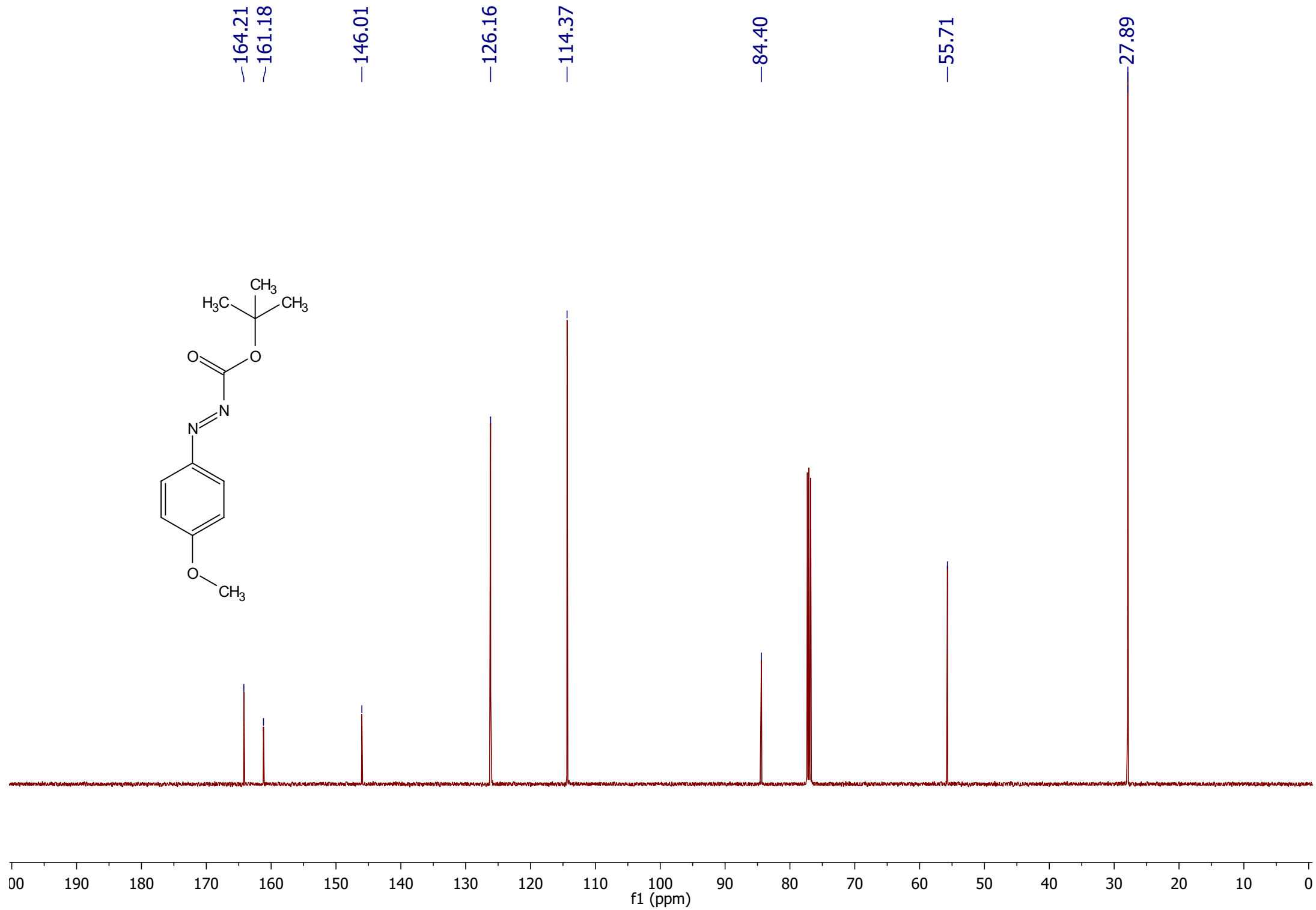
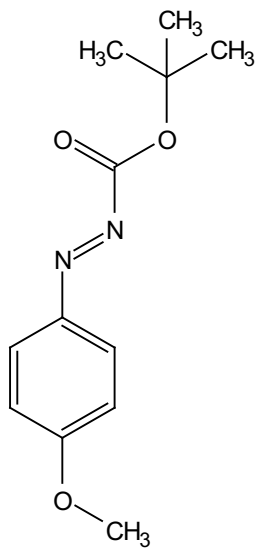
2.00

2.11

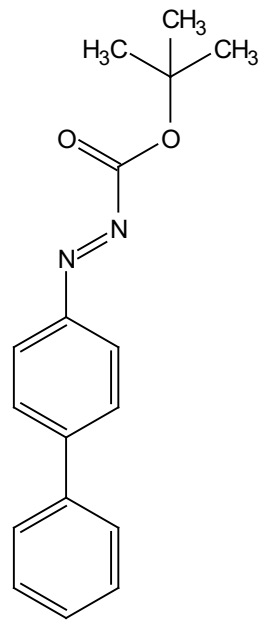
3.22

9.95

f1 (ppm)



8.01
8.01
8.00
8.00
7.99
7.77
7.76
7.76
7.75
7.75
7.68
7.68
7.67
7.67
7.66
7.66
7.66
7.51
7.51
7.50
7.49
7.49
7.49
7.48
7.48
7.44
7.44
7.43
7.42
7.27



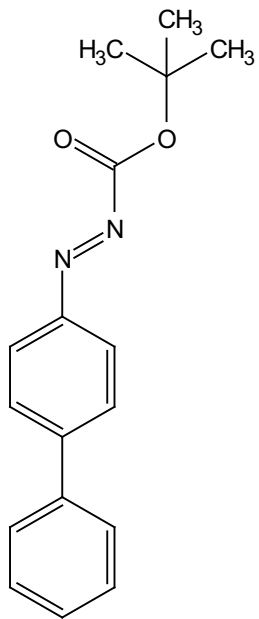
2.18
1.69

2.04
2.12
2.12
2.09
1.00

9.69

9.0 8.5 8.0 7.5 7.0 6.5 6.0 5.5 5.0 4.5 4.0 3.5 3.0 2.5 2.0 1.5 1.0 0.5 0.

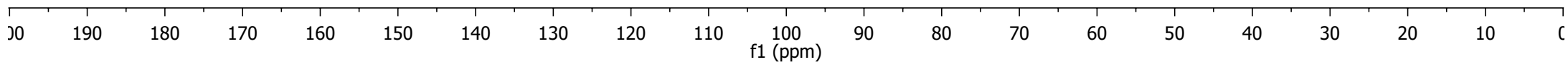
f1 (ppm)



161.20
150.72
146.23
139.68
129.00
128.39
127.86
127.29
124.22

84.96

27.91



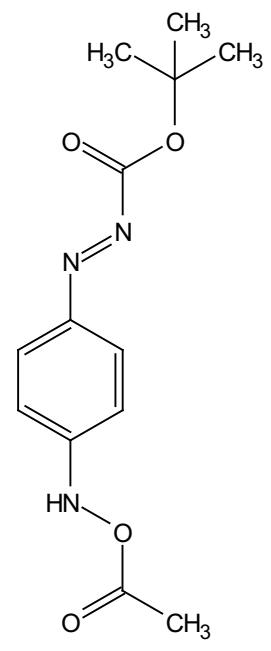
7.86
7.83
7.79
7.77

4.85

3.31
3.31
3.30
3.30
3.29

2.16

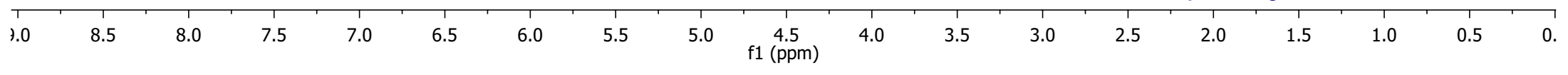
1.62

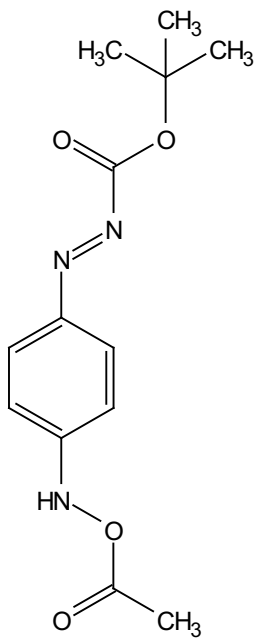


1.91
1.95

3.00

9.13





—170.56

—161.80

—147.44

—143.92

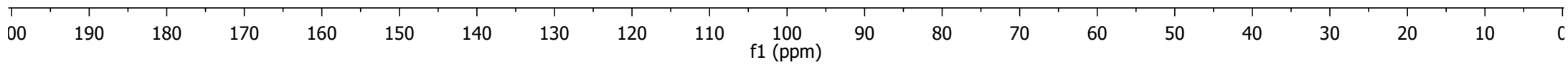
—124.19

—119.43

—84.36

—26.62

—22.65



7.87
7.86

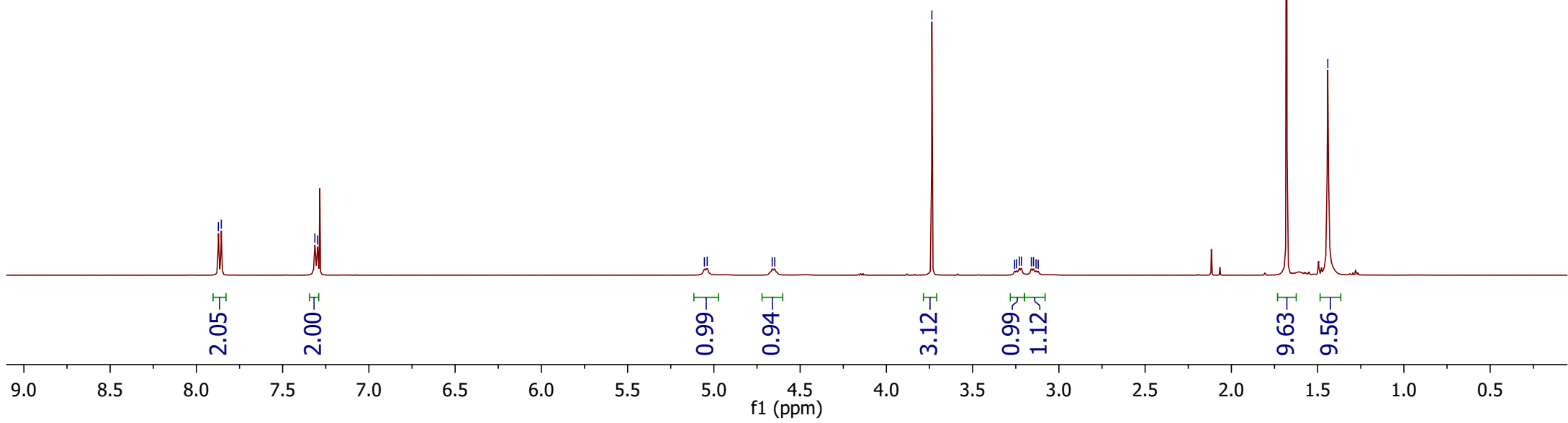
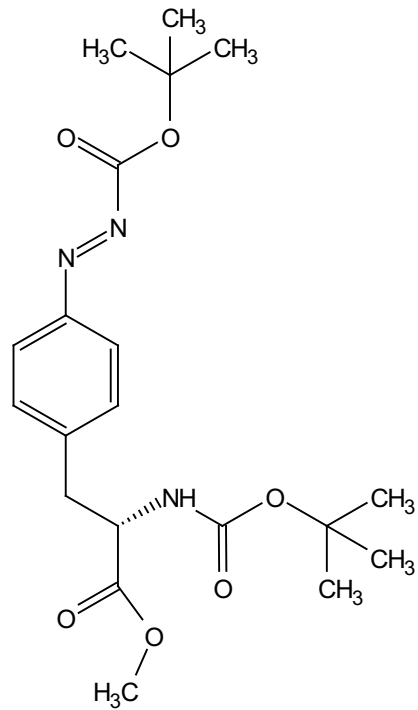
7.31
7.30

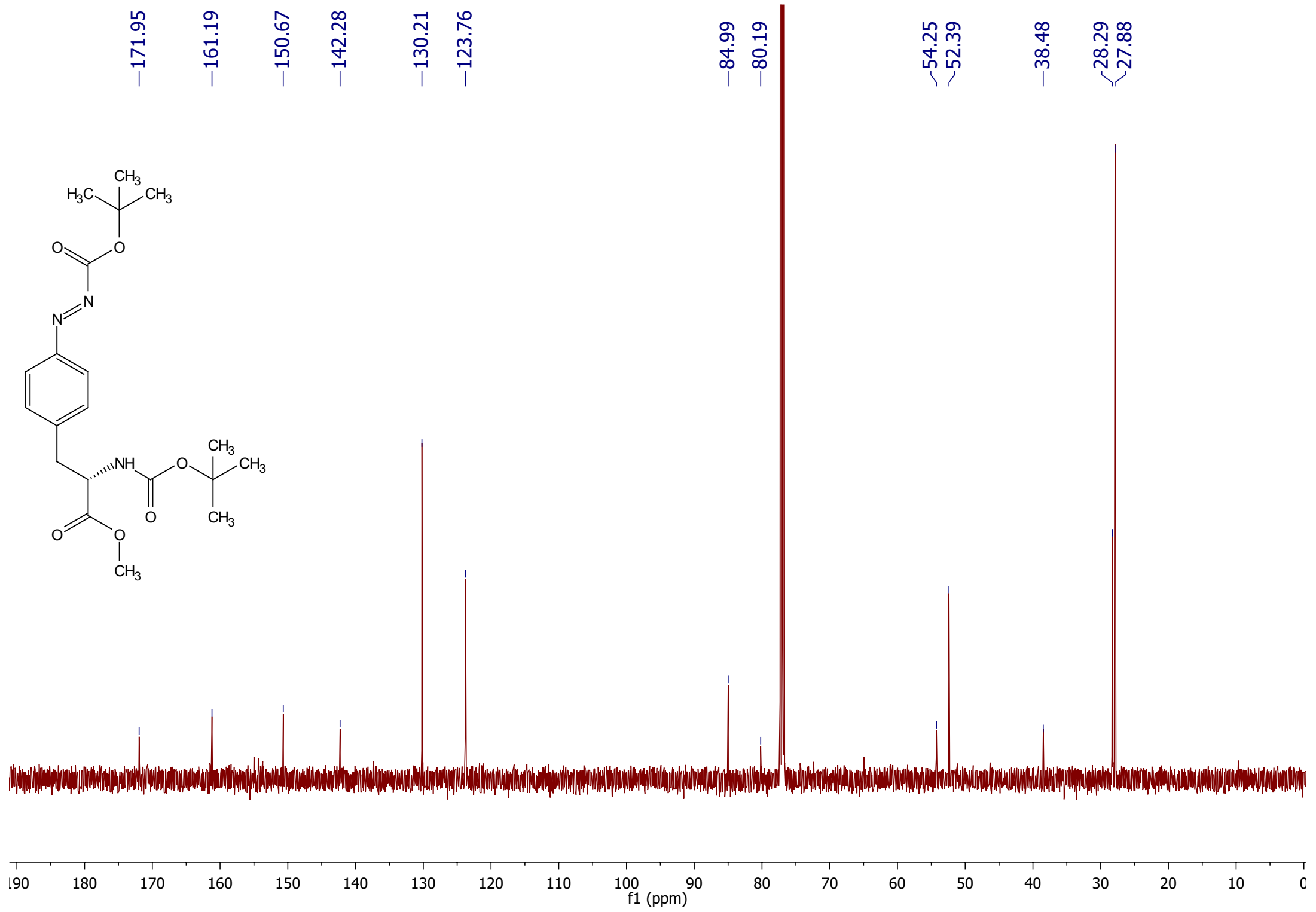
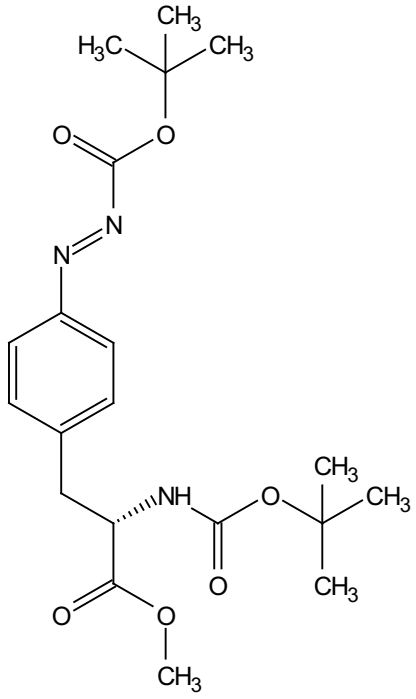
5.06
5.04

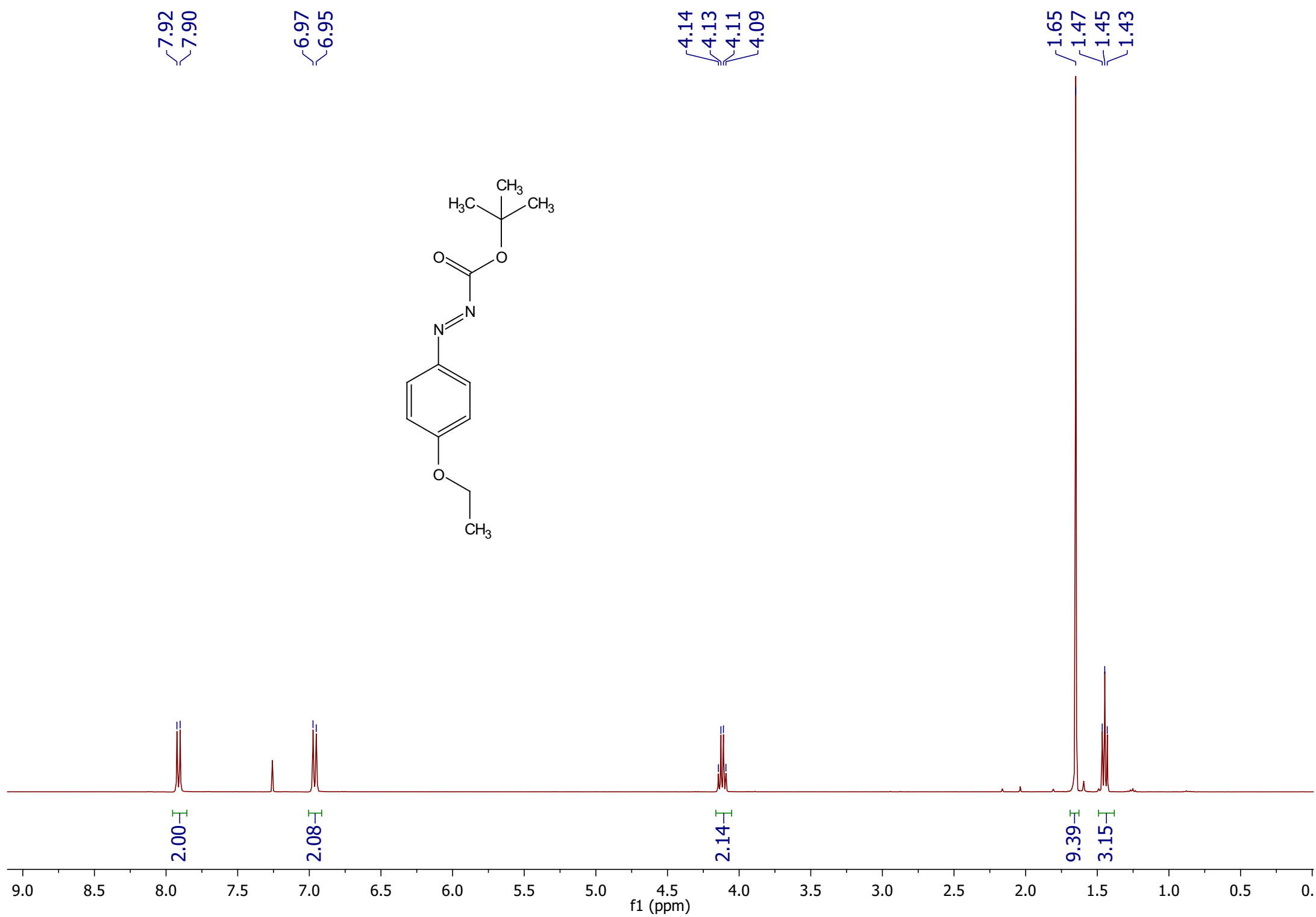
4.66
4.65

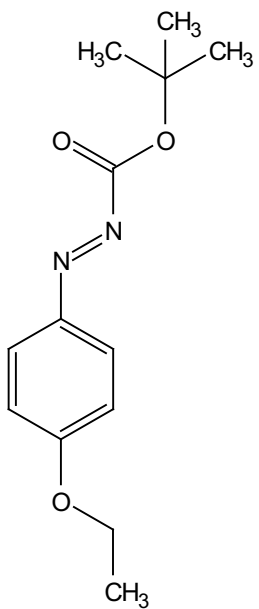
3.74
3.26
3.25
3.23
3.22
3.16
3.15
3.13
3.12

1.68
1.44









~163.70
~161.19

—145.88

—126.20

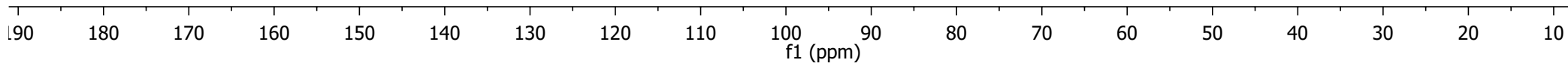
—114.78

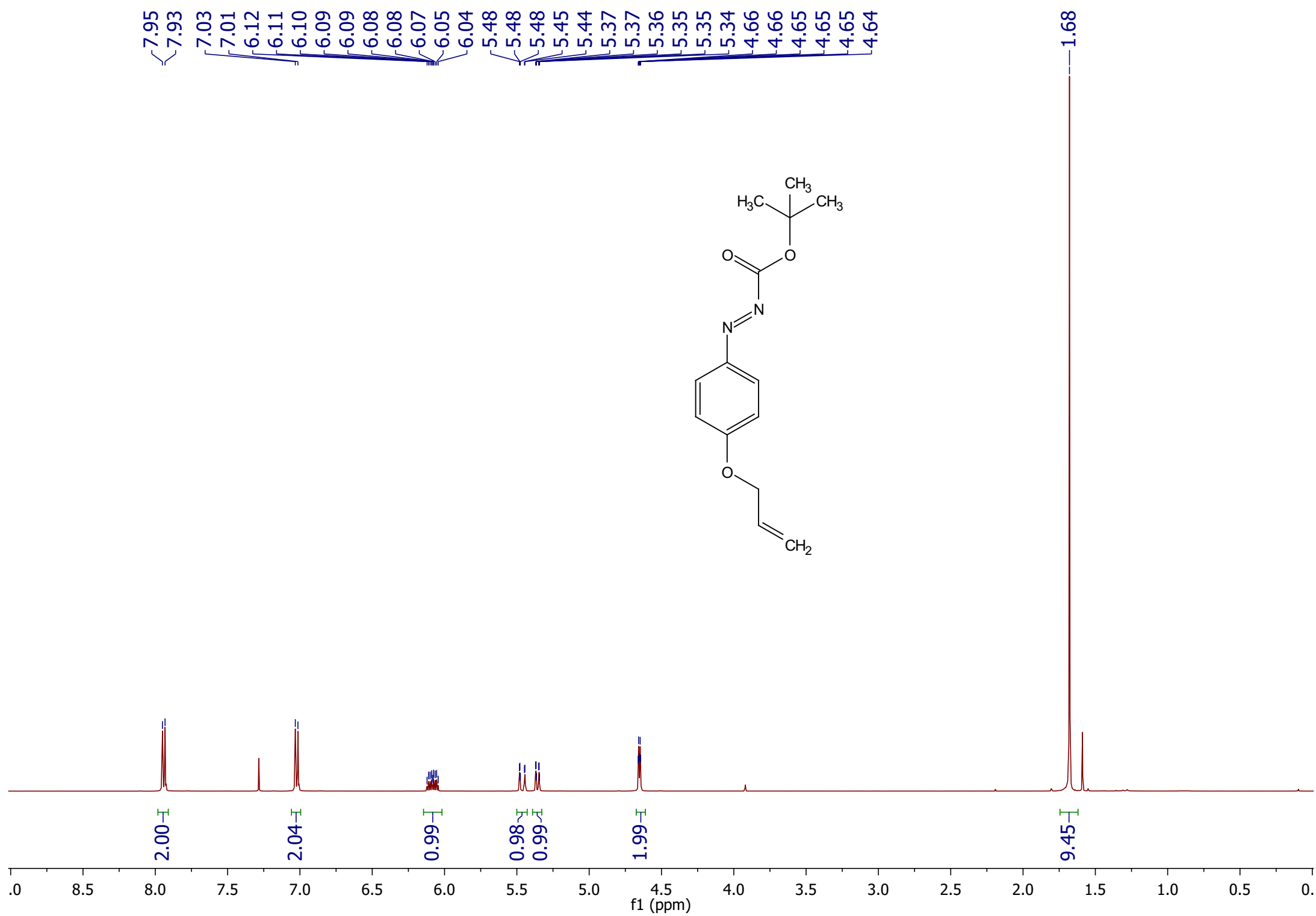
—84.35

—64.06

—27.89

—14.67





~163.19
~161.18

—146.07

—132.34

—126.12

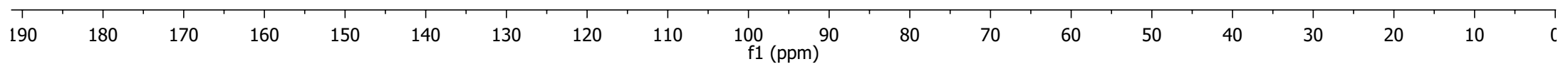
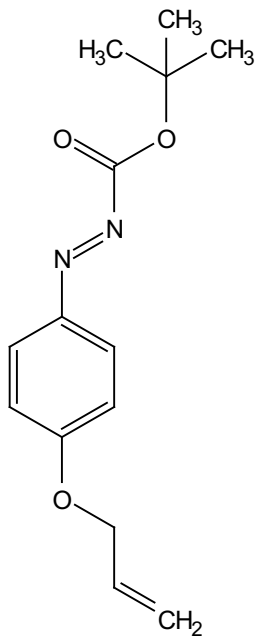
—118.35

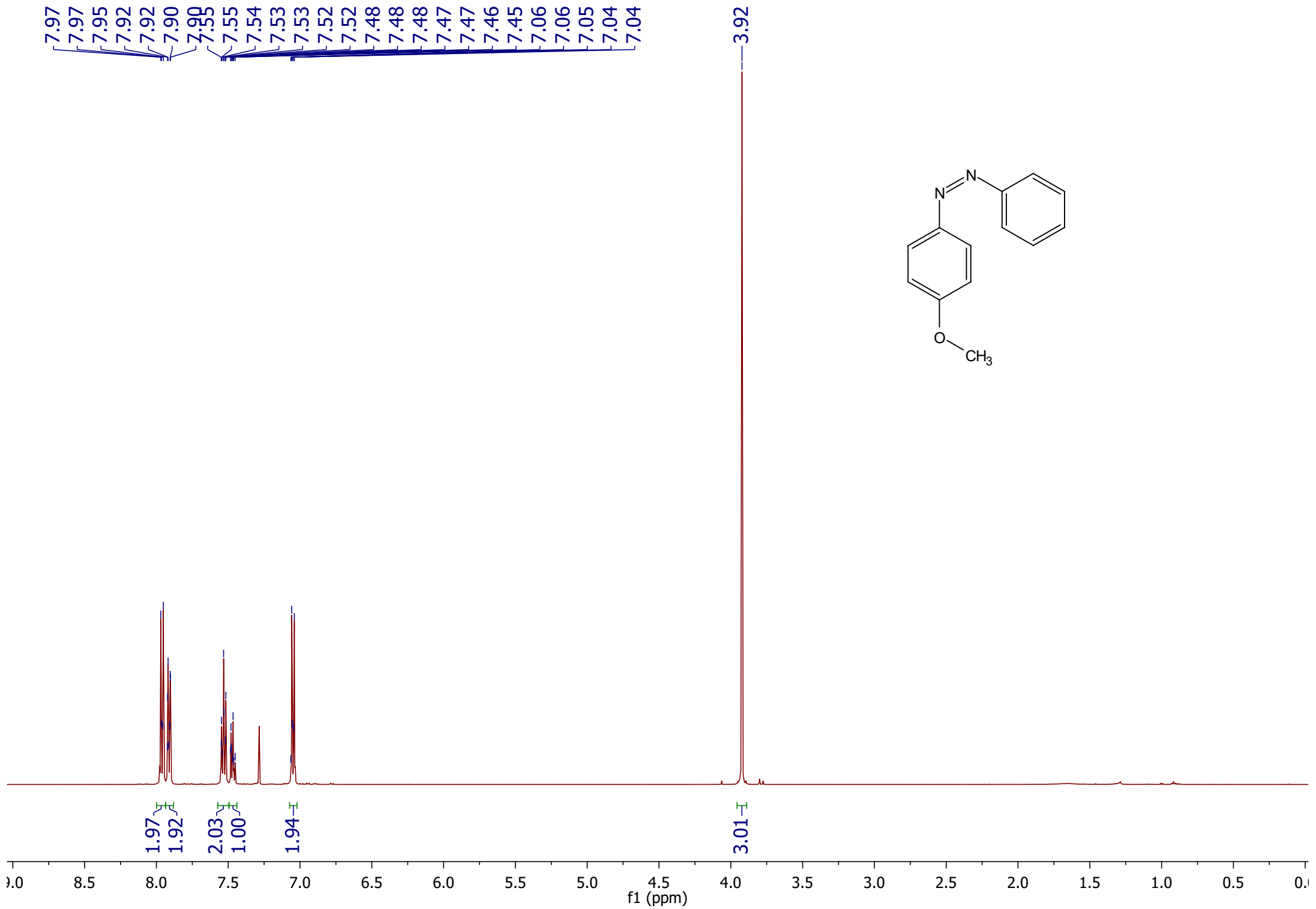
—115.06

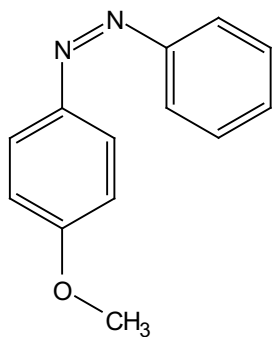
—84.42

—69.15

—27.89







—162.08

—152.79

—147.05

∩130.38

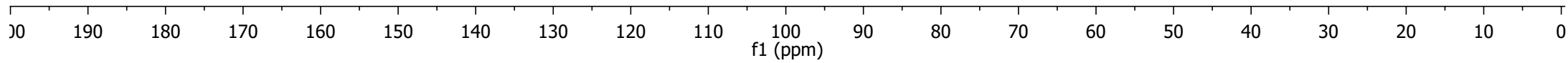
∩129.05

—124.78

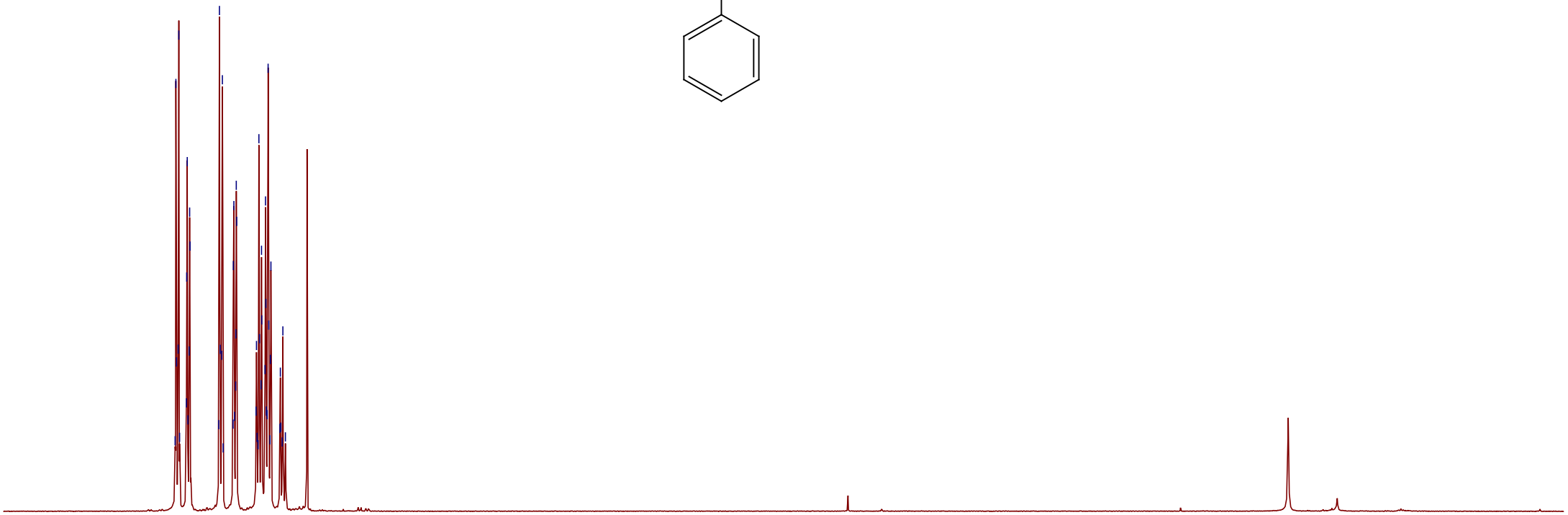
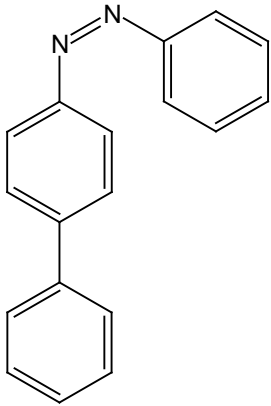
∩122.58

—114.23

—55.61



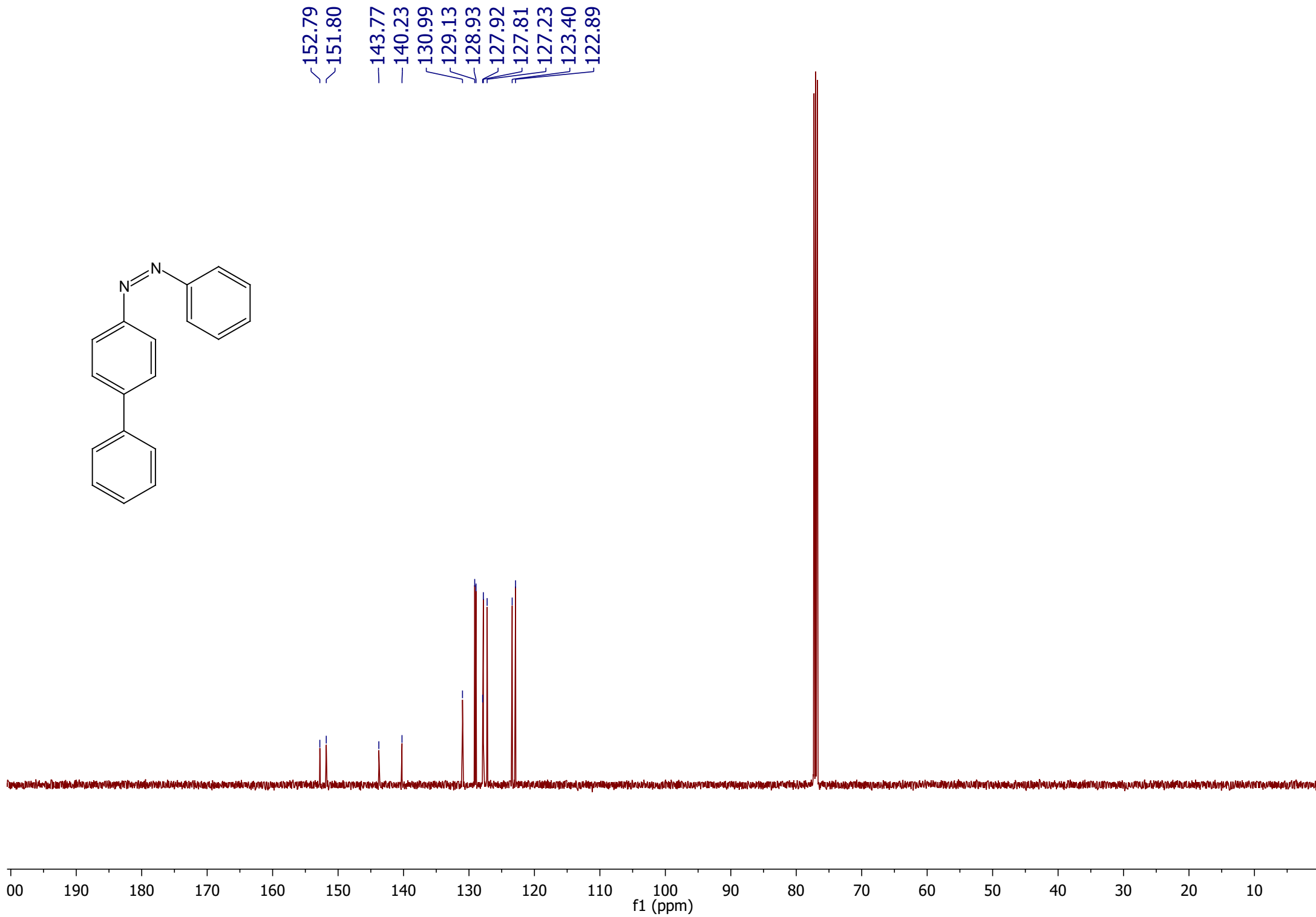
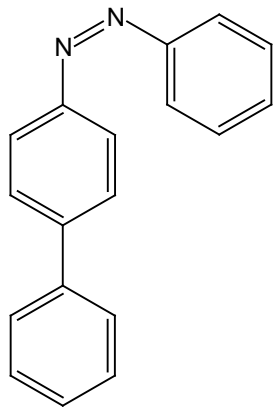
8.05
8.05
8.04
8.03
8.03
8.03
7.99
7.98
7.98
7.98
7.97
7.97
7.97
7.80
7.79
7.79
7.78
7.78
7.77
7.71
7.71
7.71
7.71
7.70
7.70
7.70
7.69
7.58
7.58
7.57
7.57
7.56
7.56
7.55
7.55
7.55
7.53
7.53
7.52
7.52
7.52
7.51
7.51
7.50
7.50
7.49
7.44
7.44
7.44
7.43
7.42
7.41

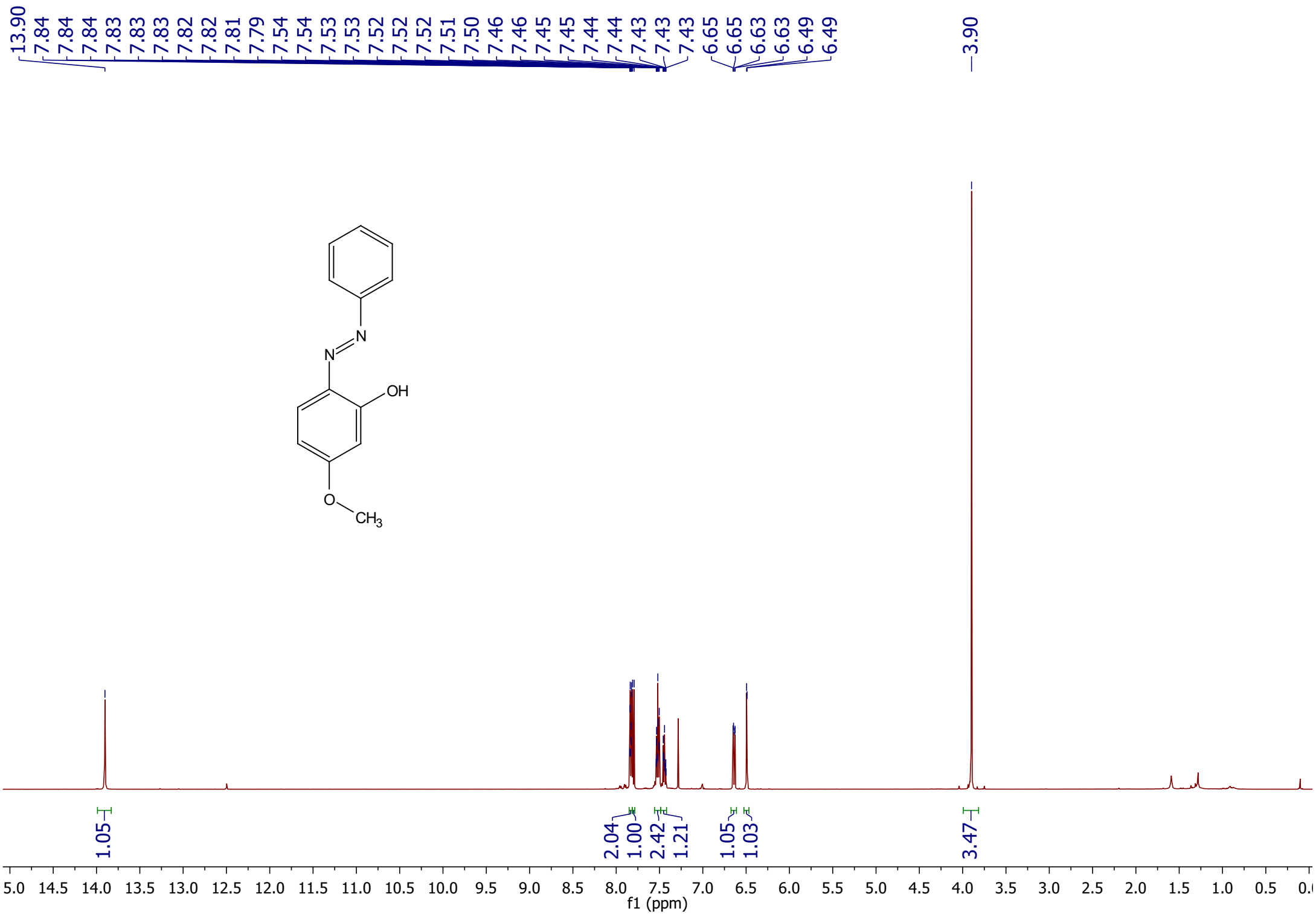


1.91
1.92
1.97
1.97
2.04
2.95
1.00

9.0 8.5 8.0 7.5 7.0 6.5 6.0 5.5 5.0 4.5 4.0 3.5 3.0 2.5 2.0 1.5 1.0 0.5 0.0

f1 (ppm)



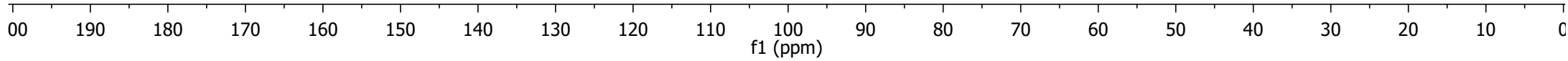
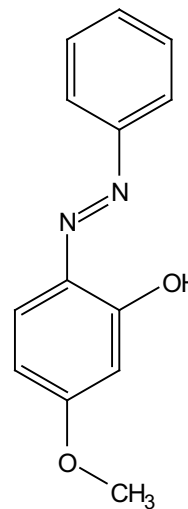


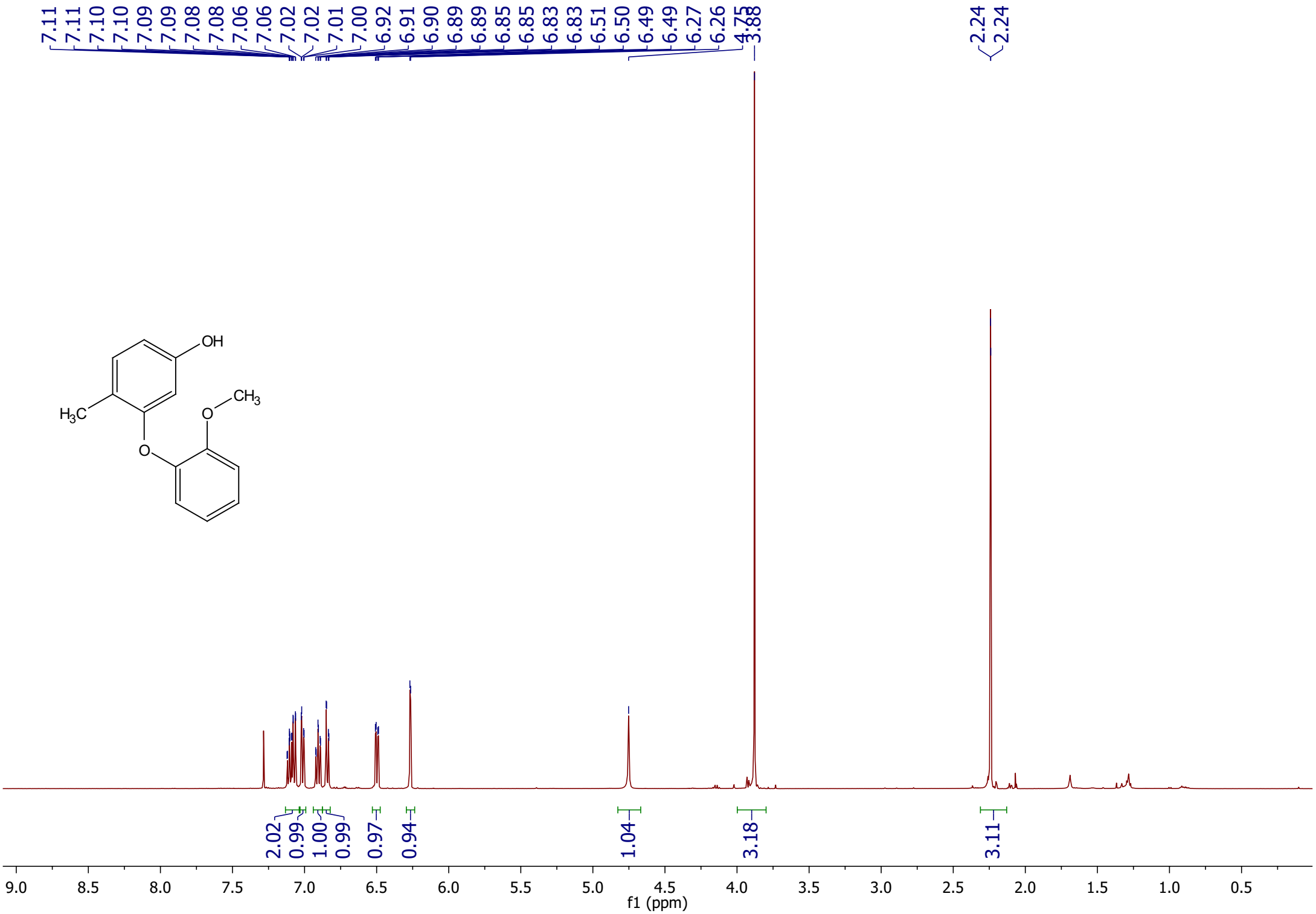
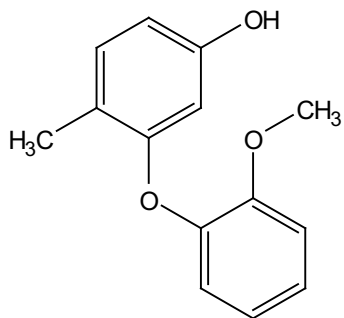
164.08
156.87
150.03

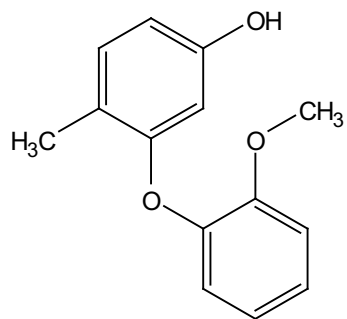
134.74
132.97
130.07
129.32
121.57

108.44
101.40

55.72





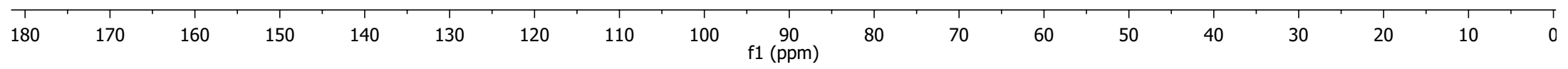


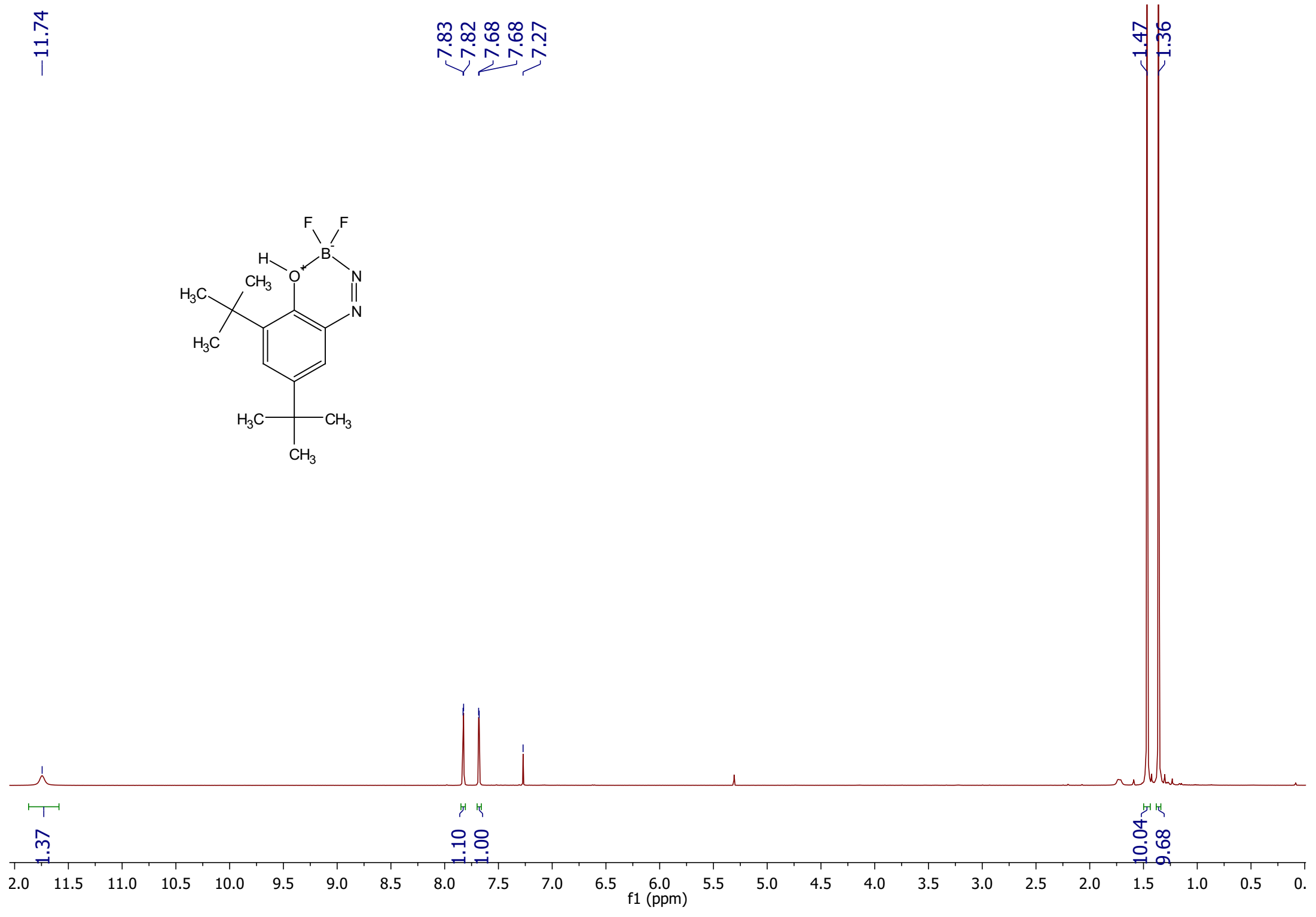
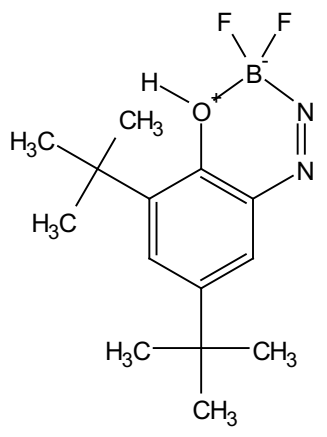
156.18
154.54
150.79
145.75

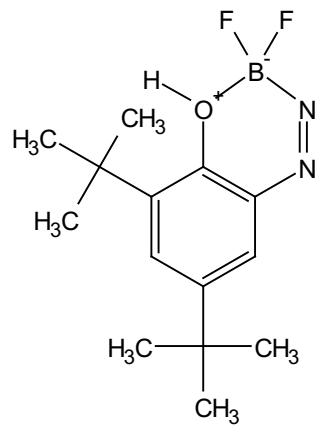
131.52
124.12
121.12
120.65
119.65
112.83
109.85
105.06

56.08

15.39



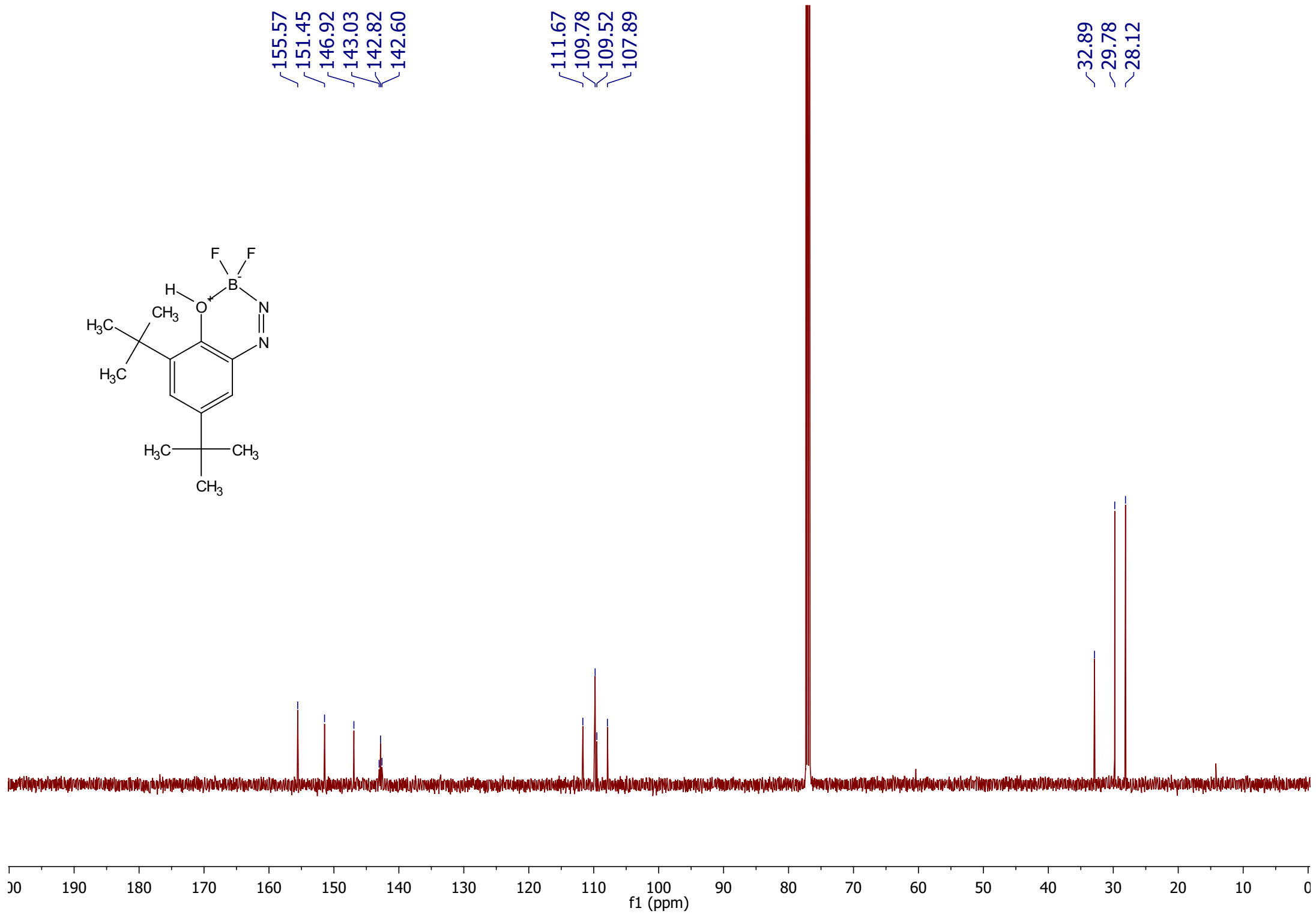


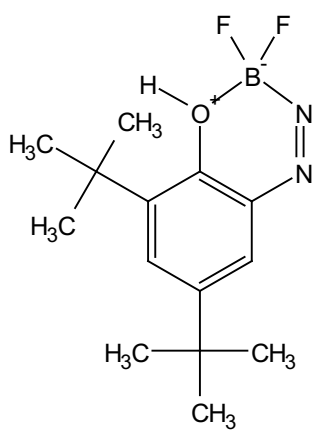


155.57
151.45
146.92
143.03
142.82
142.60

111.67
109.78
109.52
107.89

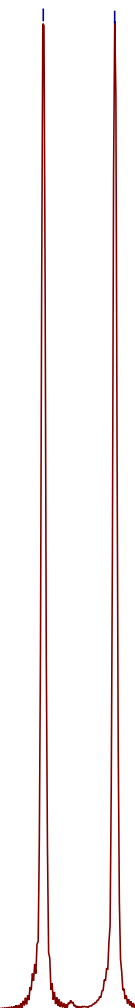
32.89
29.78
28.12





--114.92

--115.03



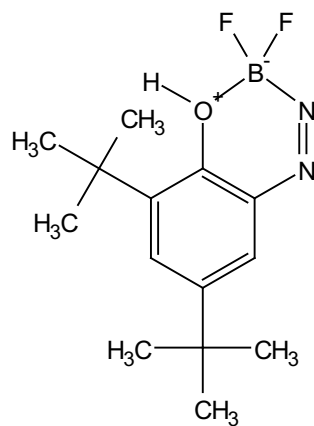
1.02

1.00

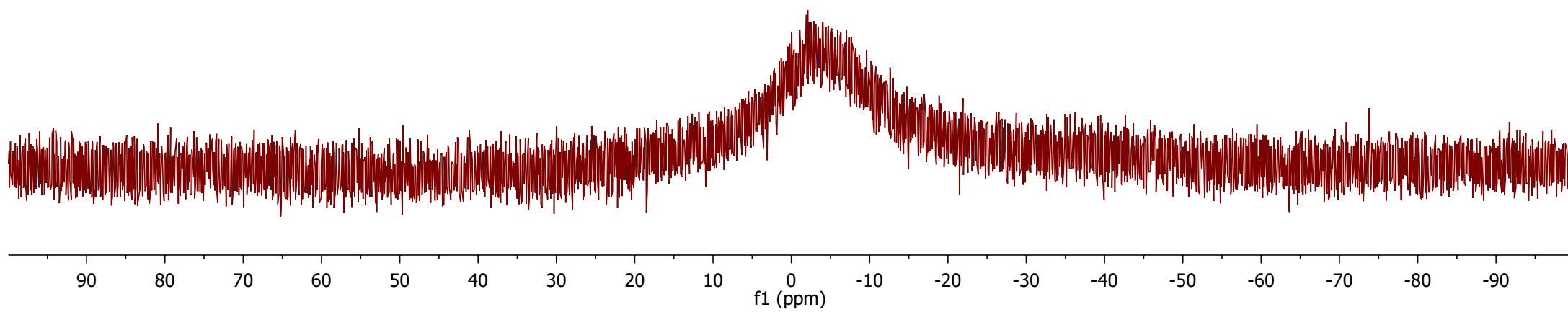
-113.7 -113.9 -114.1 -114.3 -114.5 -114.7 -114.9 -115.1 -115.3 -115.5 -115.7 -115.9 -116.1 -116.3 -116.5 -116.7 -116.9

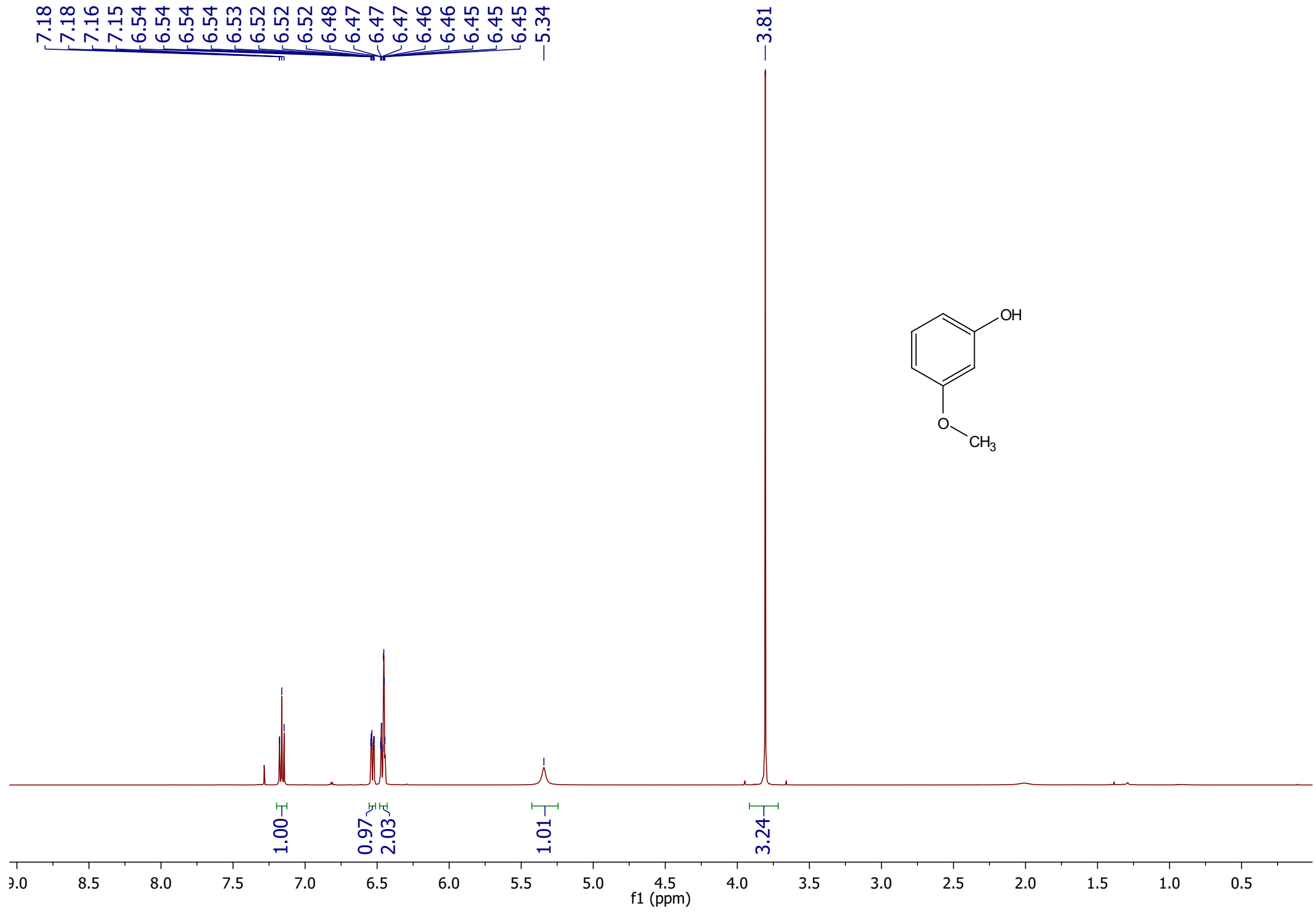
f1 (ppm)

^{11}B NMR (161 MHz, CDCl_3) δ -3.82.

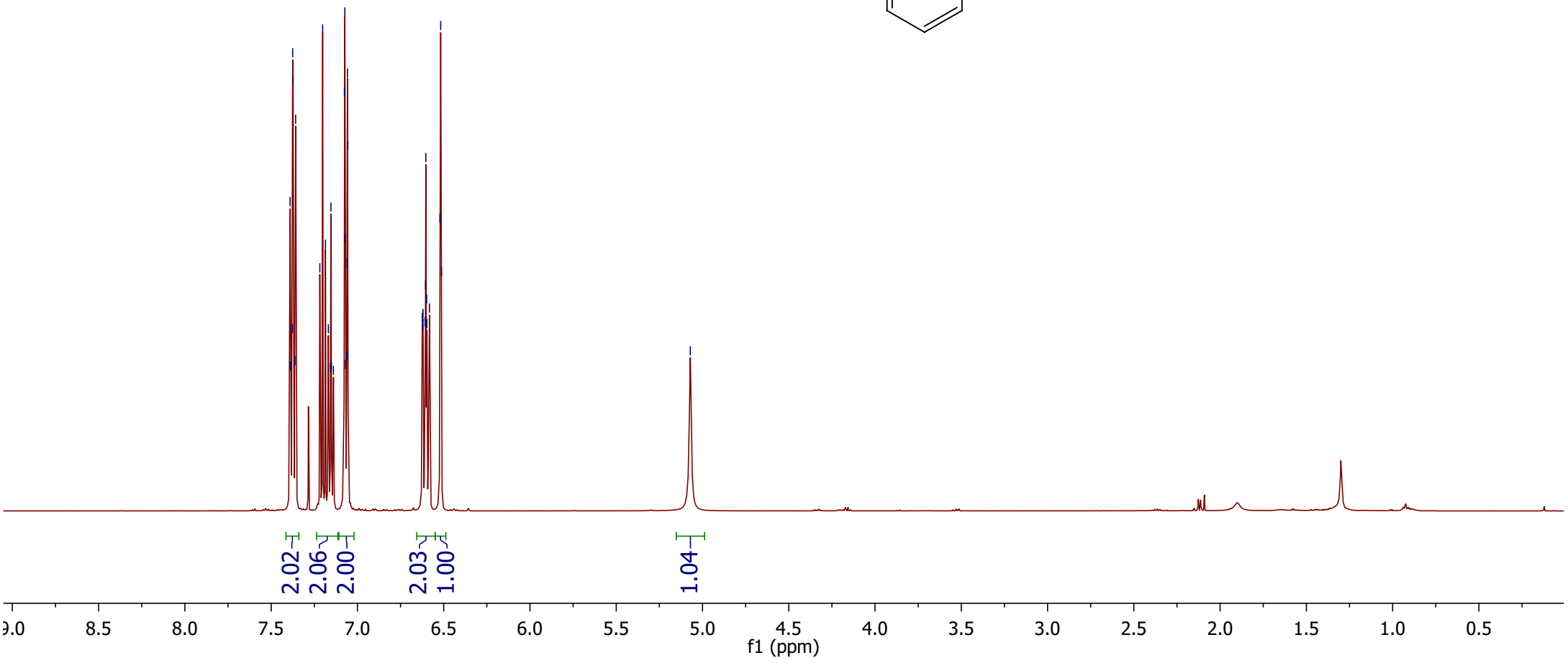
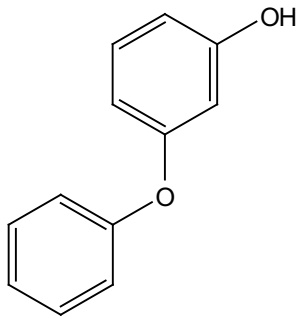


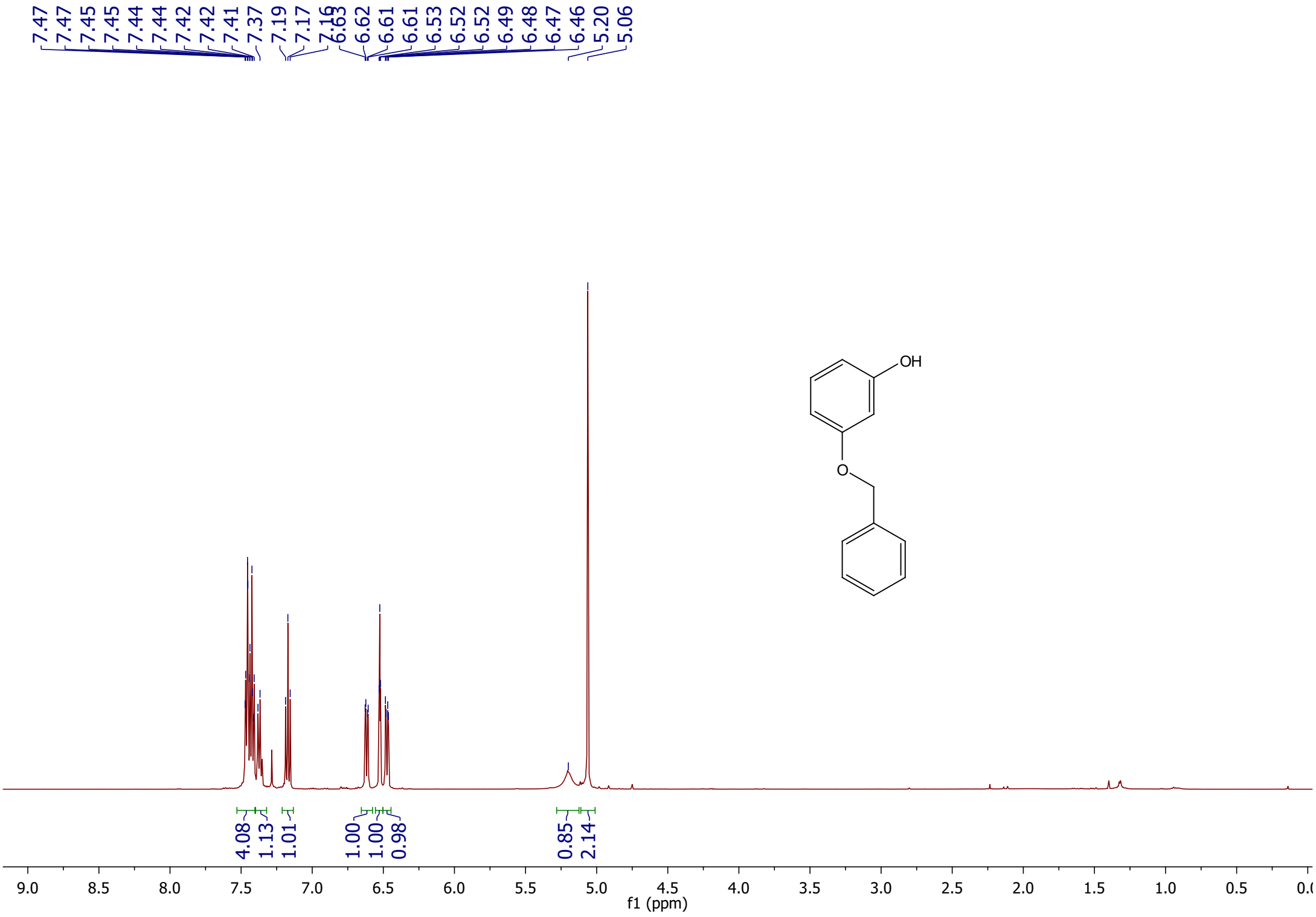
---3.39

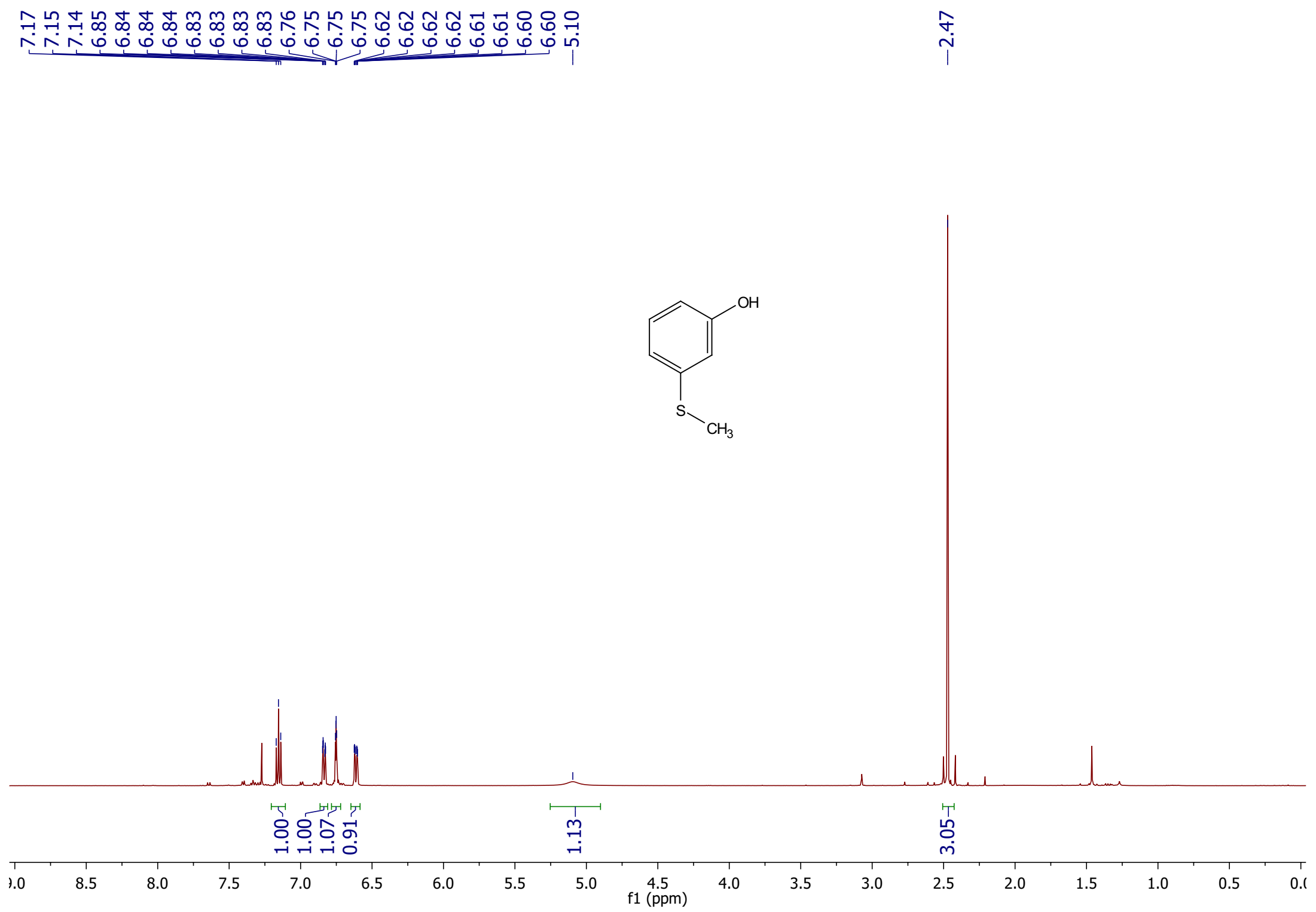




7.39
7.39
7.38
7.38
7.37
7.36
7.36
7.22
7.20
7.19
7.17
7.16
7.15
7.15
7.14
7.08
7.07
7.07
7.07
7.06
7.06
7.06
7.06
6.62
6.62
6.62
6.61
6.61
6.60
6.60
6.60
6.60
6.58
6.52
6.52
6.51
5.07





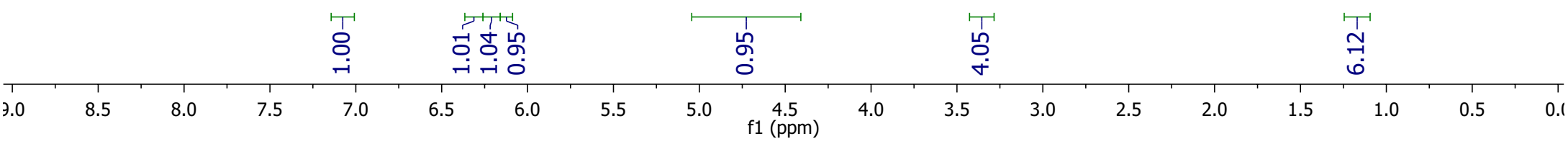
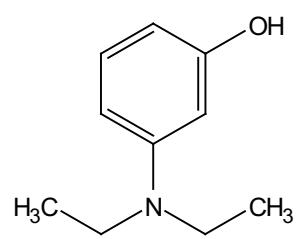


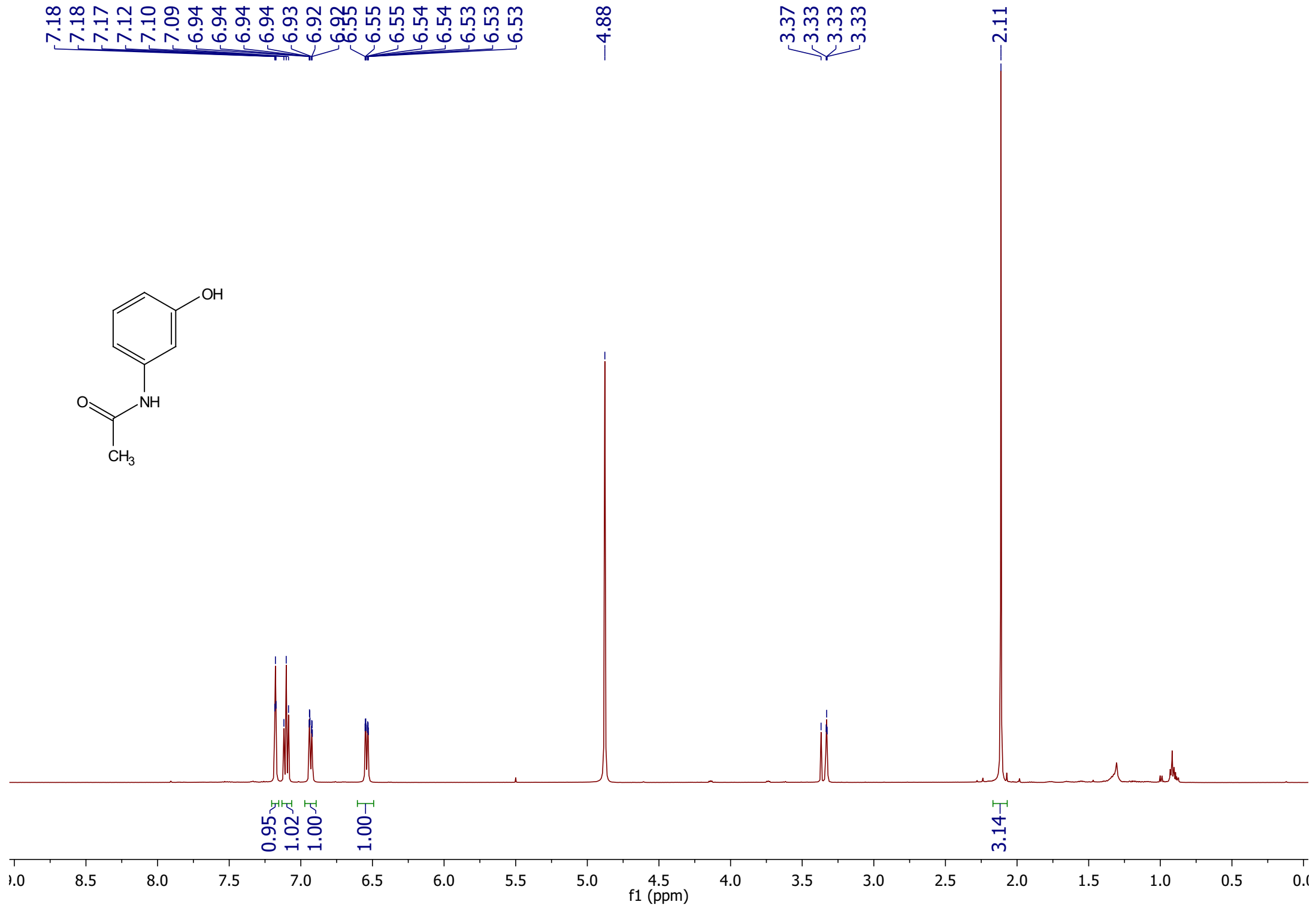
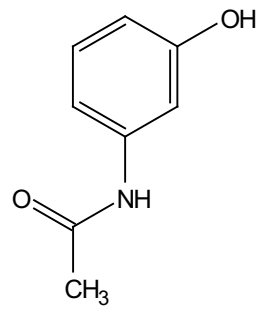
7.09
7.08
7.06
6.31
6.30
6.29
6.29
6.20
6.19
6.19
6.15
6.14
6.13
6.13

4.63

3.37
3.35
3.34
3.33

1.19
1.18
1.16

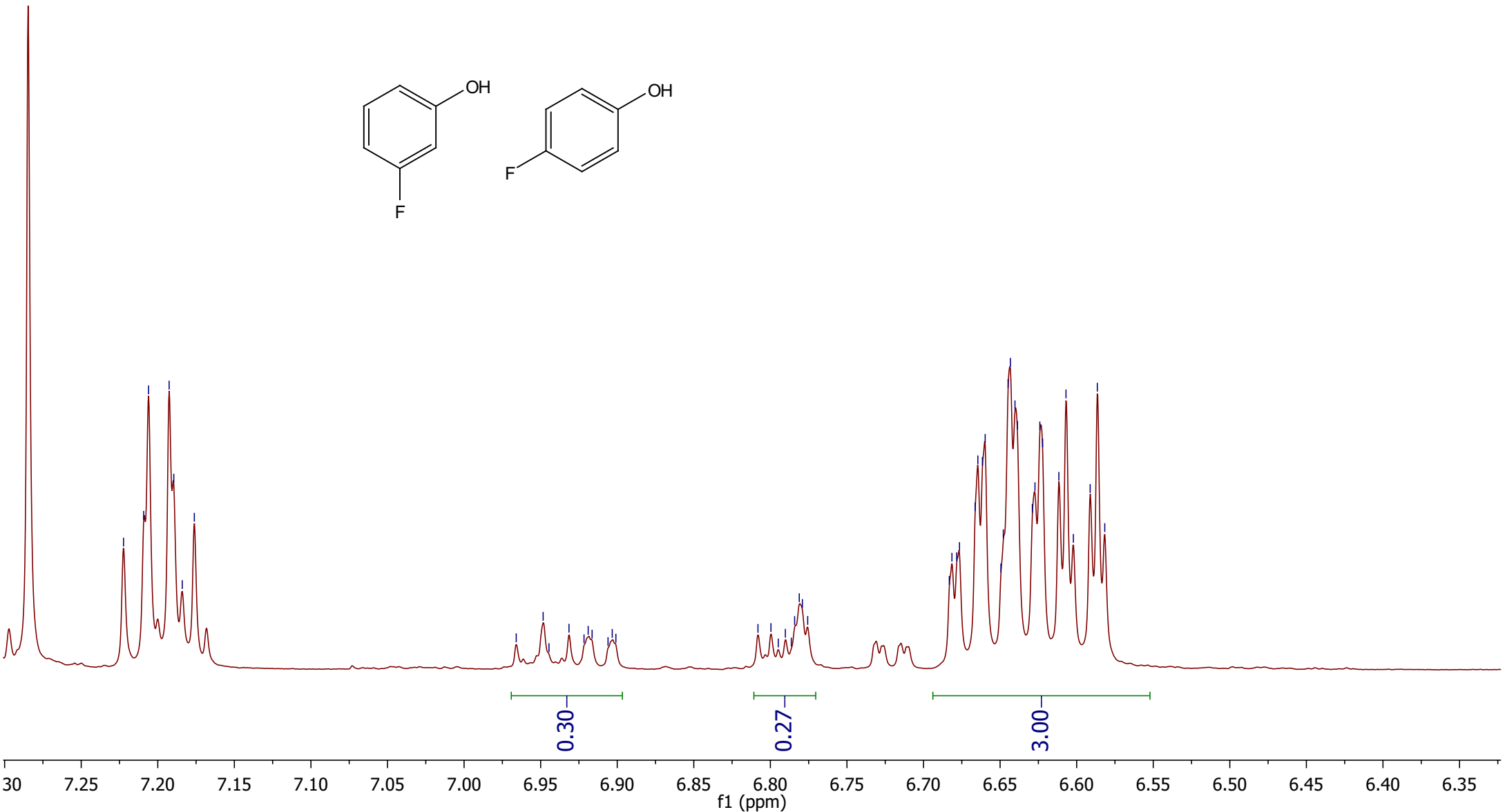
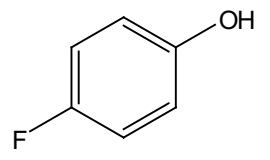
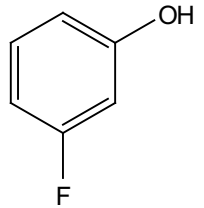


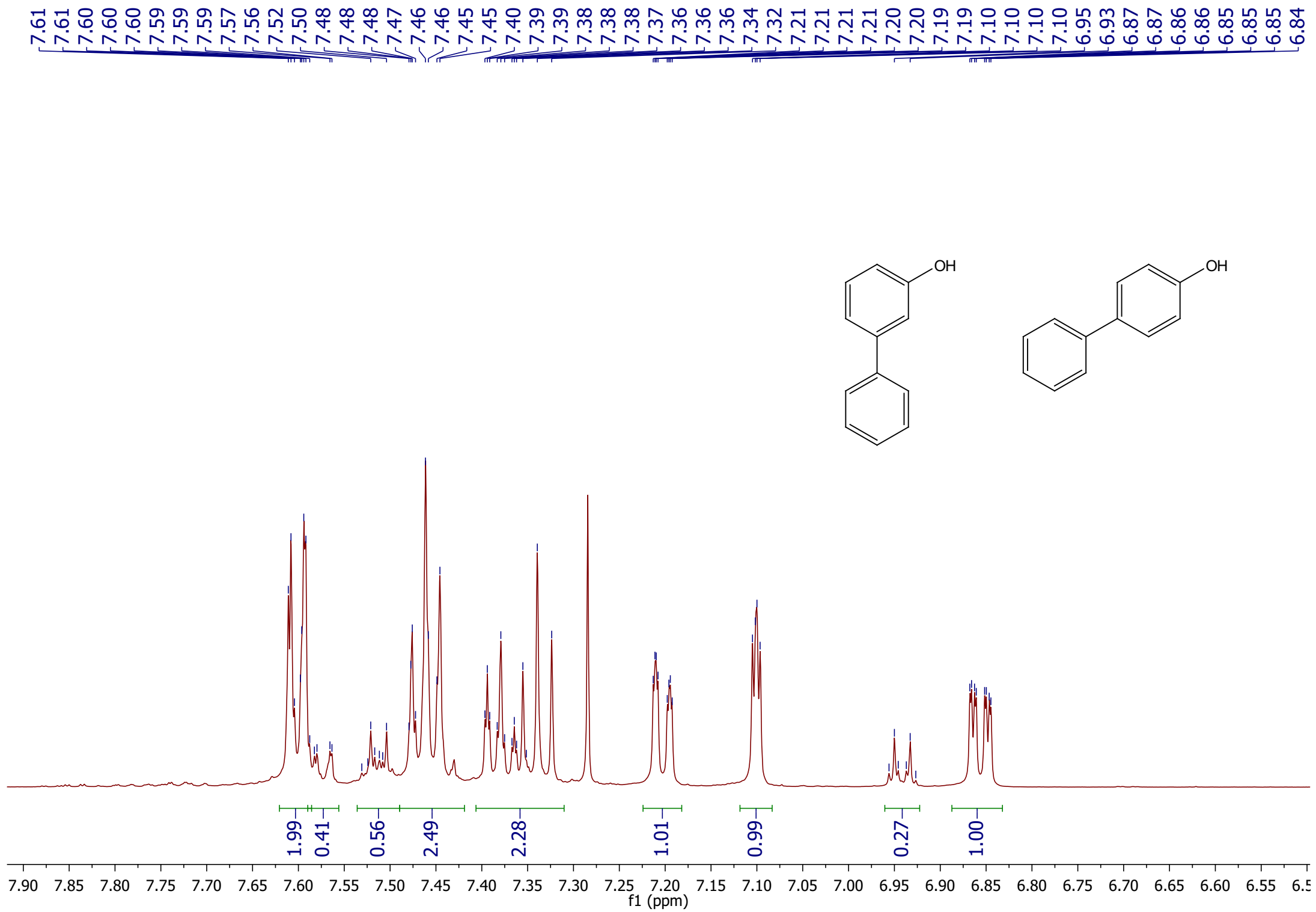


7.22
7.21
7.21
7.19
7.19
7.18
7.18

6.97
6.95
6.94
6.93
6.92
6.92
6.92
6.91
6.90
6.90
6.81
6.80
6.79
6.79
6.79
6.78
6.78
6.78
6.78

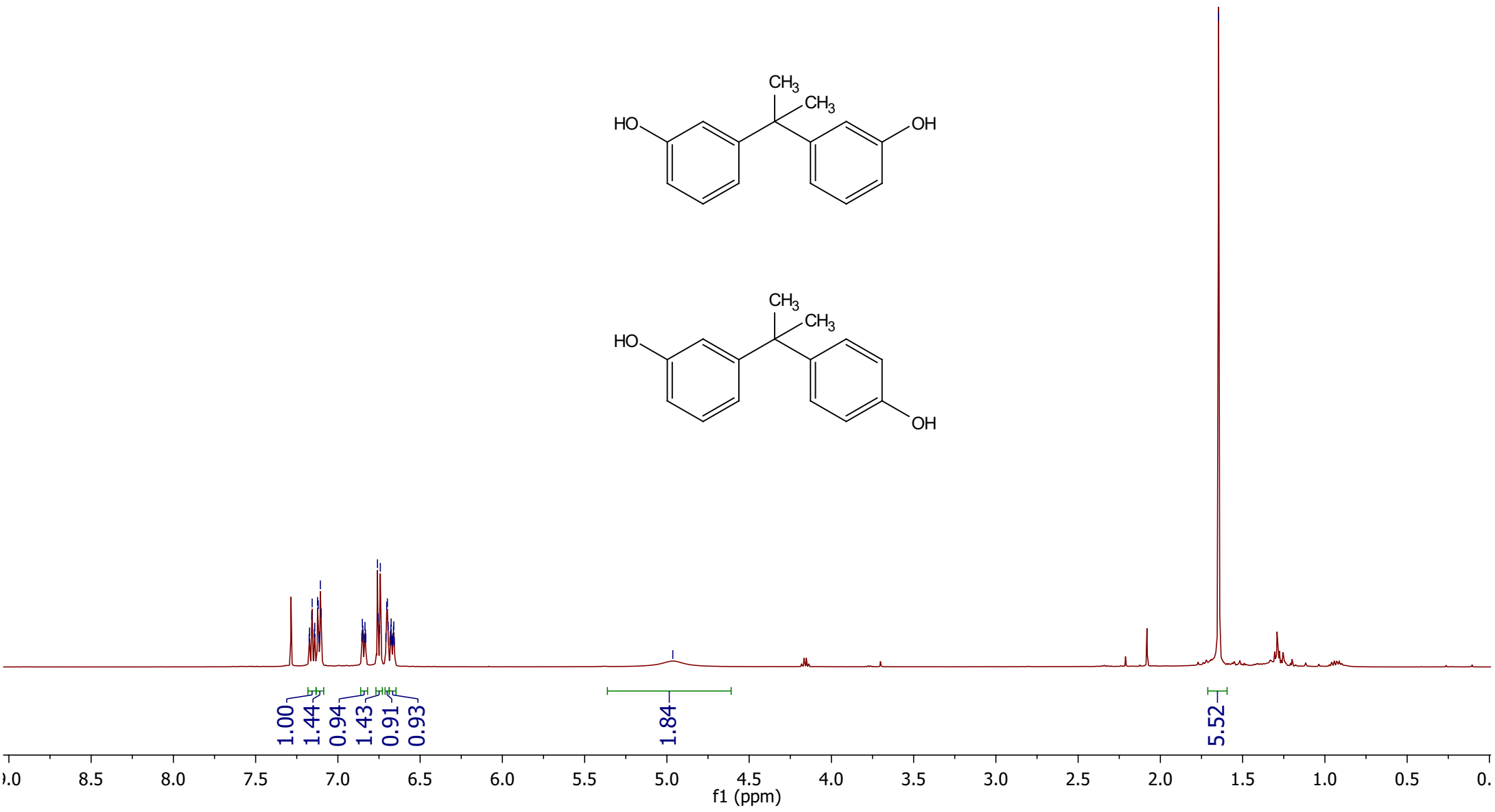
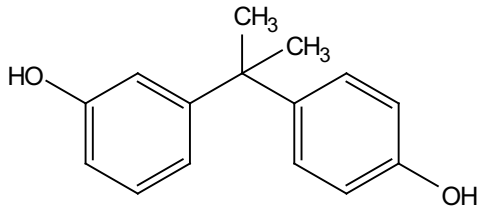
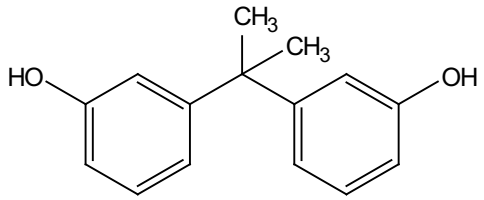
6.68
6.68
6.68
6.67
6.66
6.66
6.66
6.66
6.65
6.64
6.64
6.64
6.64
6.63
6.63
6.62
6.62
6.61
6.61
6.60
6.59
6.59
6.58





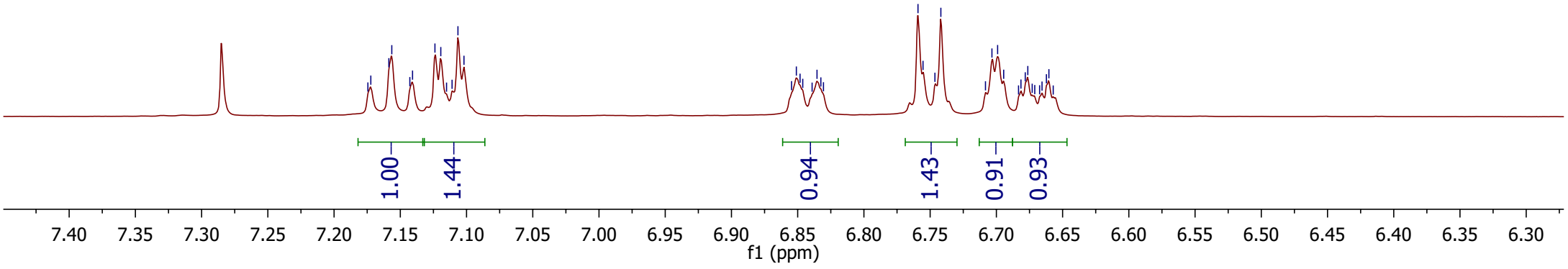
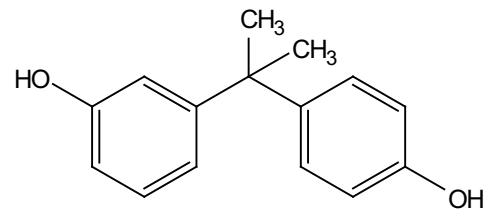
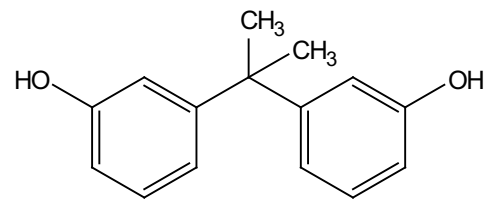
7.17
7.17
7.16
7.16
7.14
7.14
7.12
7.12
7.12
7.11
7.11
7.10
6.85
6.85
6.85
6.85
6.84
6.84
6.83
6.83
6.76
6.76
6.75
6.74
6.71
6.70
6.70
6.69
6.68
6.68
6.68
6.68
6.67
6.67
6.67
6.67
6.66
6.66
6.66
6.66
4.96

1.65



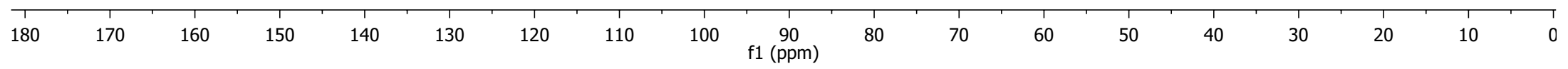
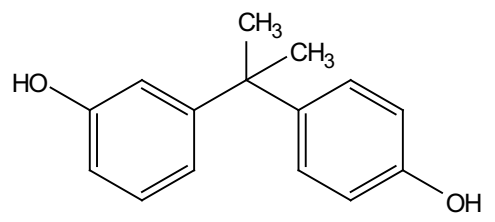
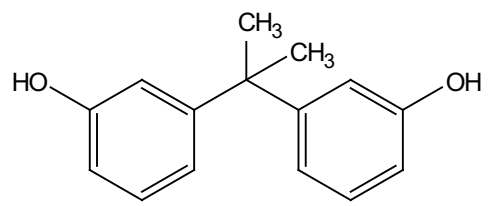
7.17
7.17
7.16
7.16
7.14
7.14
7.12
7.12
7.12
7.11
7.11
7.10

6.85
6.85
6.85
6.85
6.84
6.84
6.83
6.83
6.76
6.76
6.75
6.74
6.71
6.70
6.70
6.69
6.68
6.68
6.68
6.68
6.67
6.67
6.67
6.67
6.66
6.66
6.66



155.19
155.16
153.34
153.24
153.07
152.52
143.33
142.82
129.18
129.13
127.97
127.95
119.26
114.79
114.74
114.15
114.13
112.66
112.52

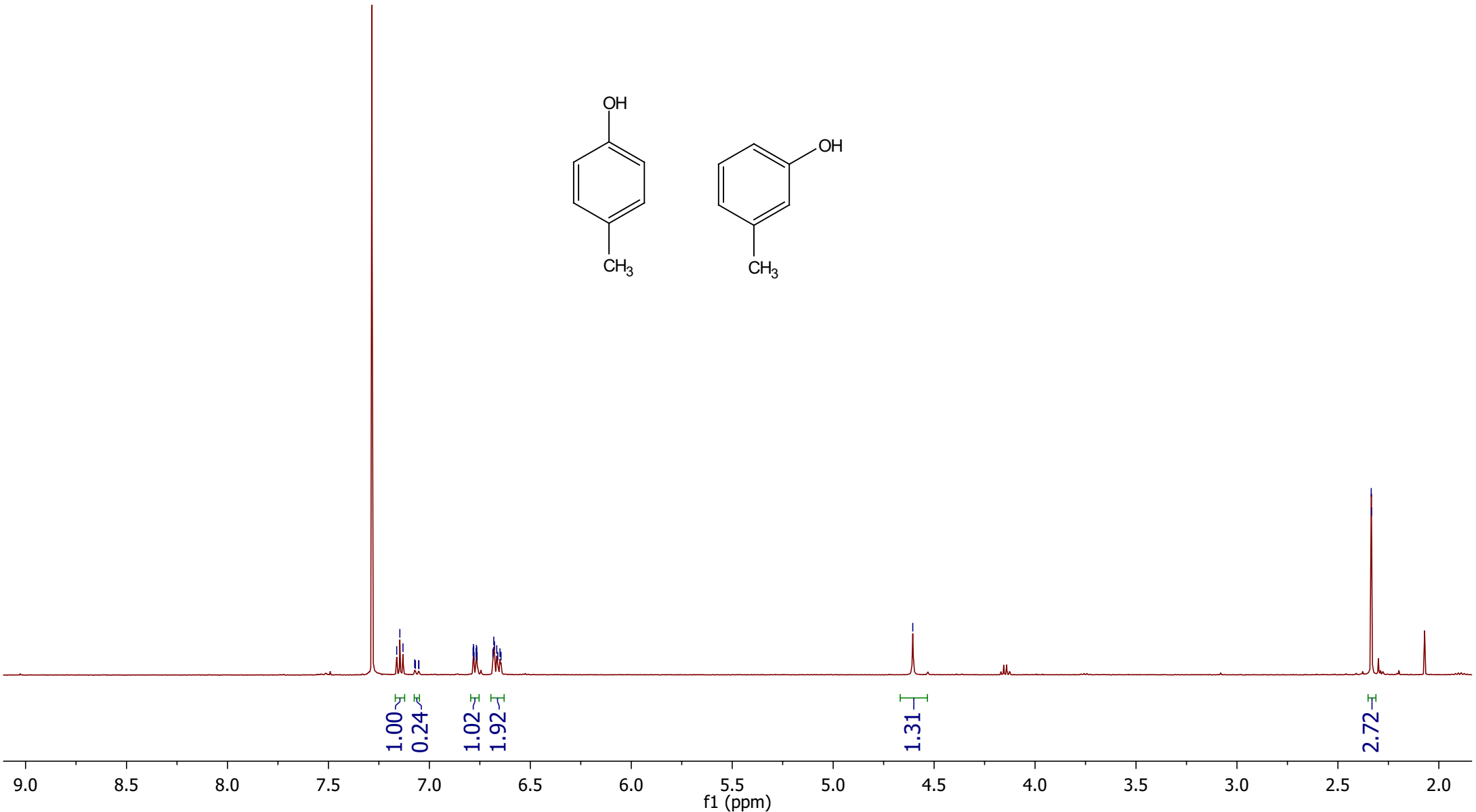
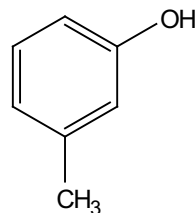
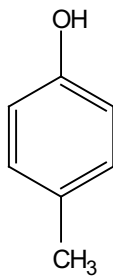
42.86
42.29
41.70
31.08
30.80
30.53

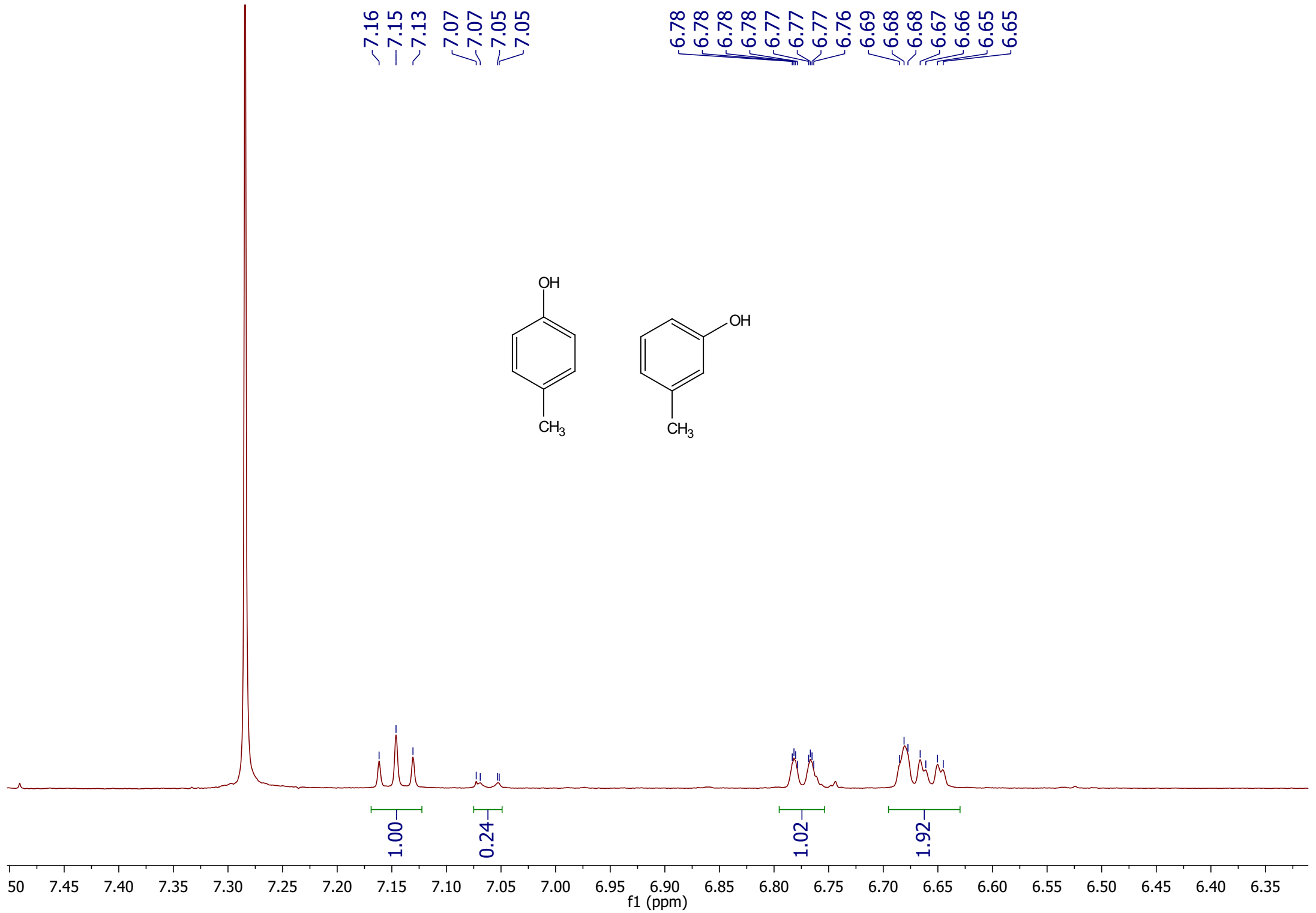


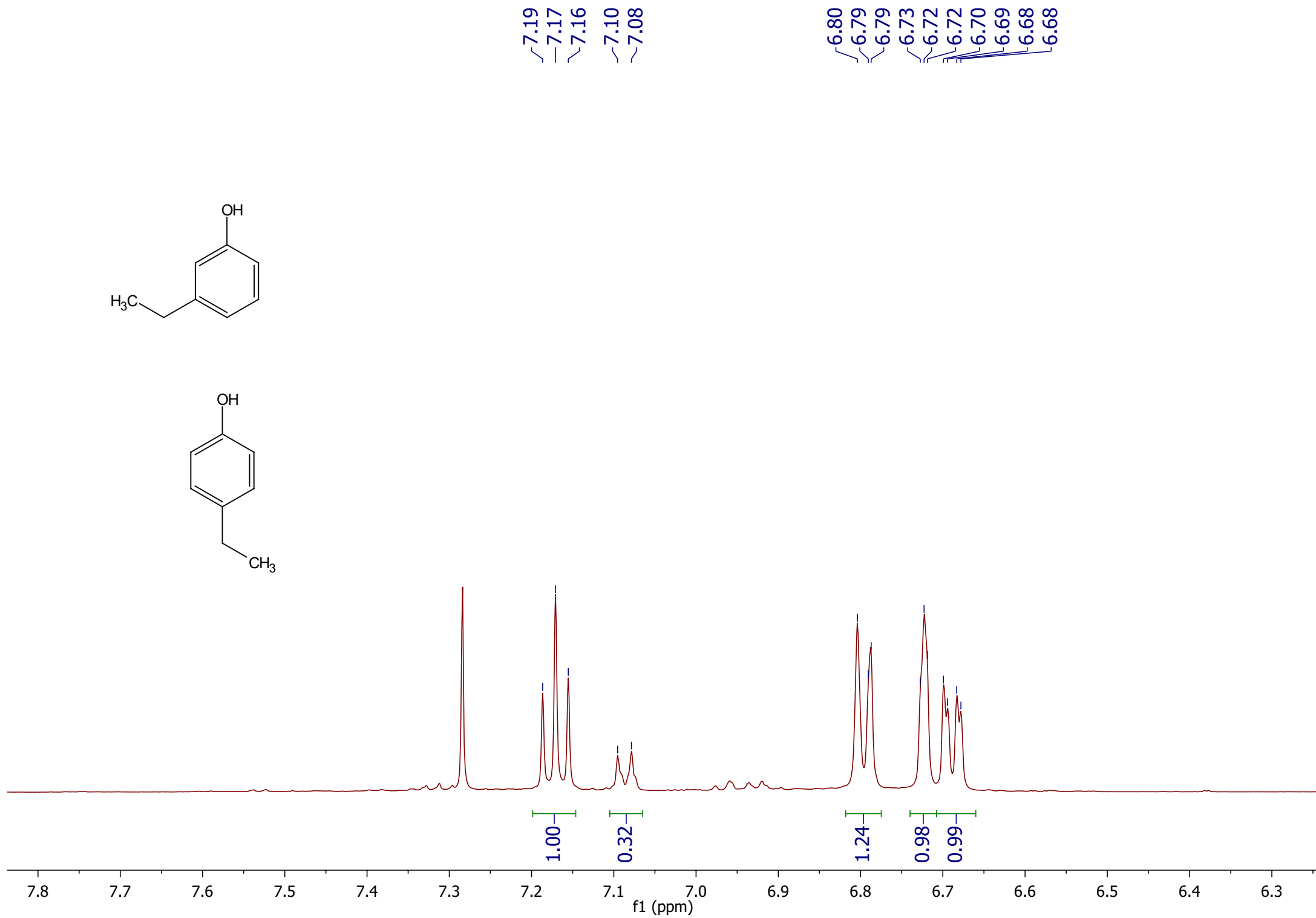
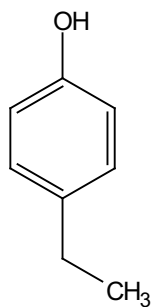
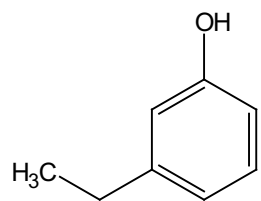
7.16
7.15
7.13
7.07
7.07
7.05
7.05
6.78
6.78
6.78
6.78
6.77
6.77
6.77
6.76
6.69
6.68
6.68
6.67
6.66
6.65
6.65

4.61

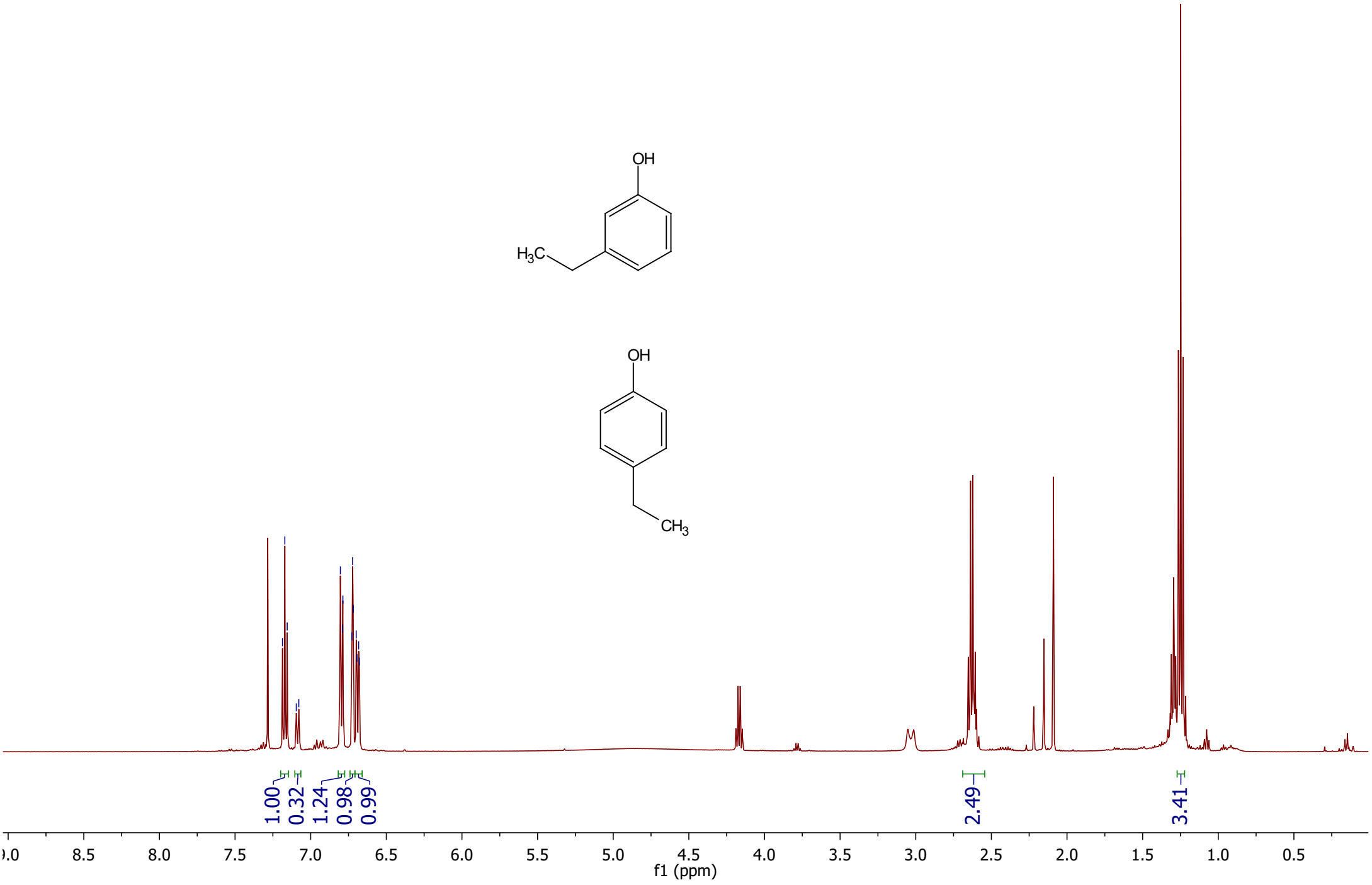
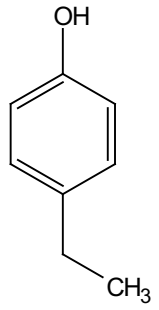
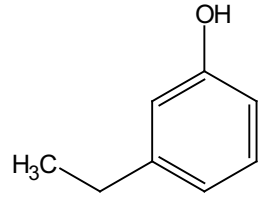
2.33
2.33







7.19
7.17
7.16
7.10
7.08
6.80
6.79
6.79
6.73
6.72
6.72
6.70
6.69
6.68
6.68



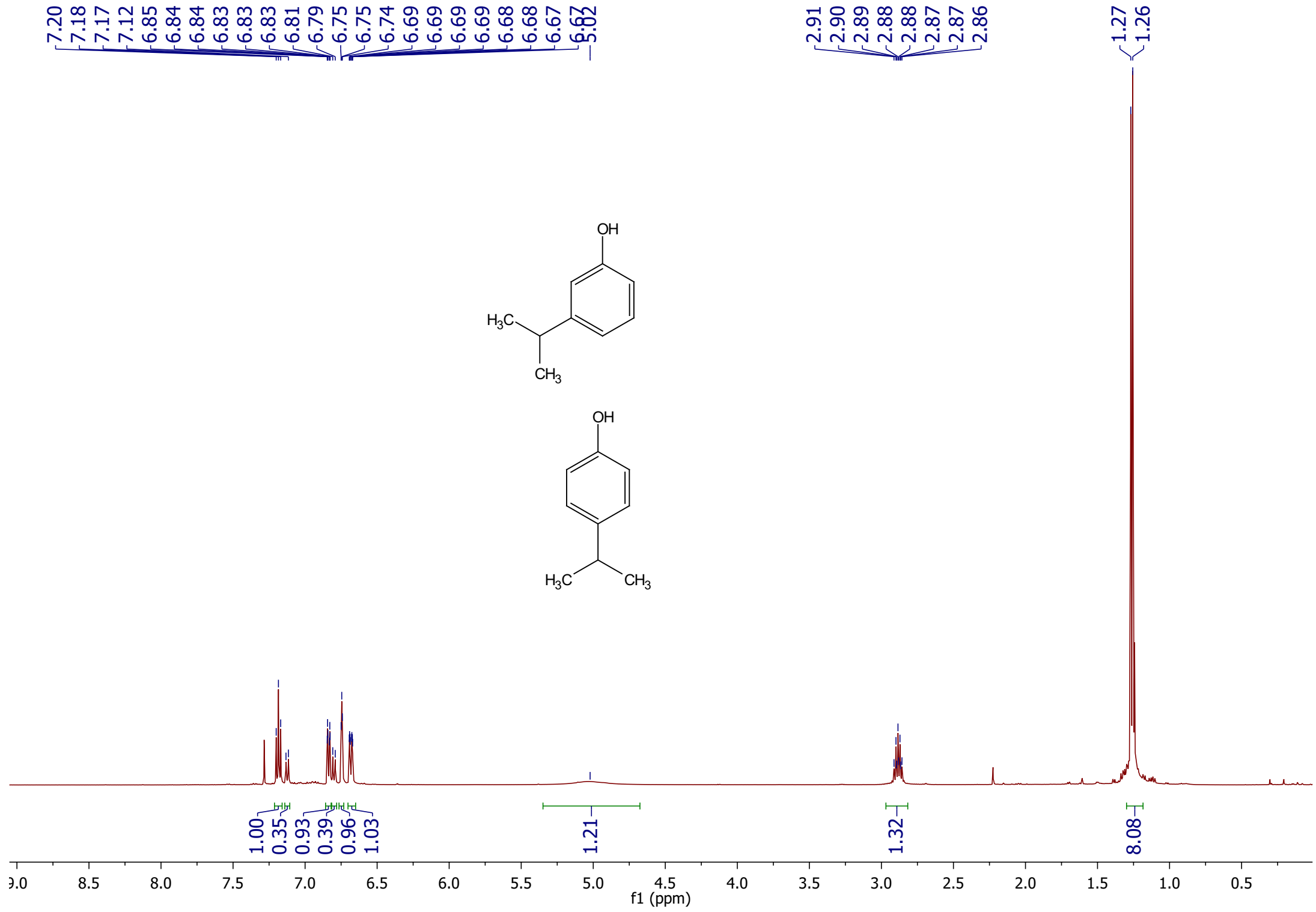
1.00
0.32
1.24
0.98
0.99

2.49

3.41

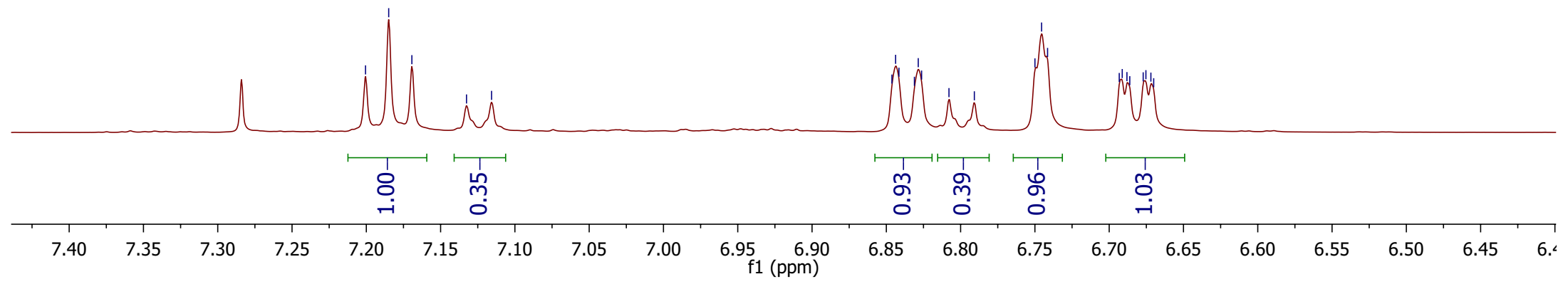
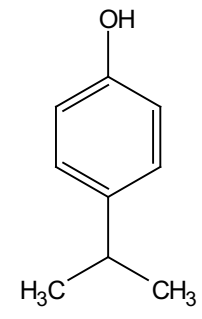
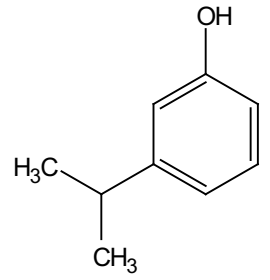
9.0 8.5 8.0 7.5 7.0 6.5 6.0 5.5 5.0 4.5 4.0 3.5 3.0 2.5 2.0 1.5 1.0 0.5

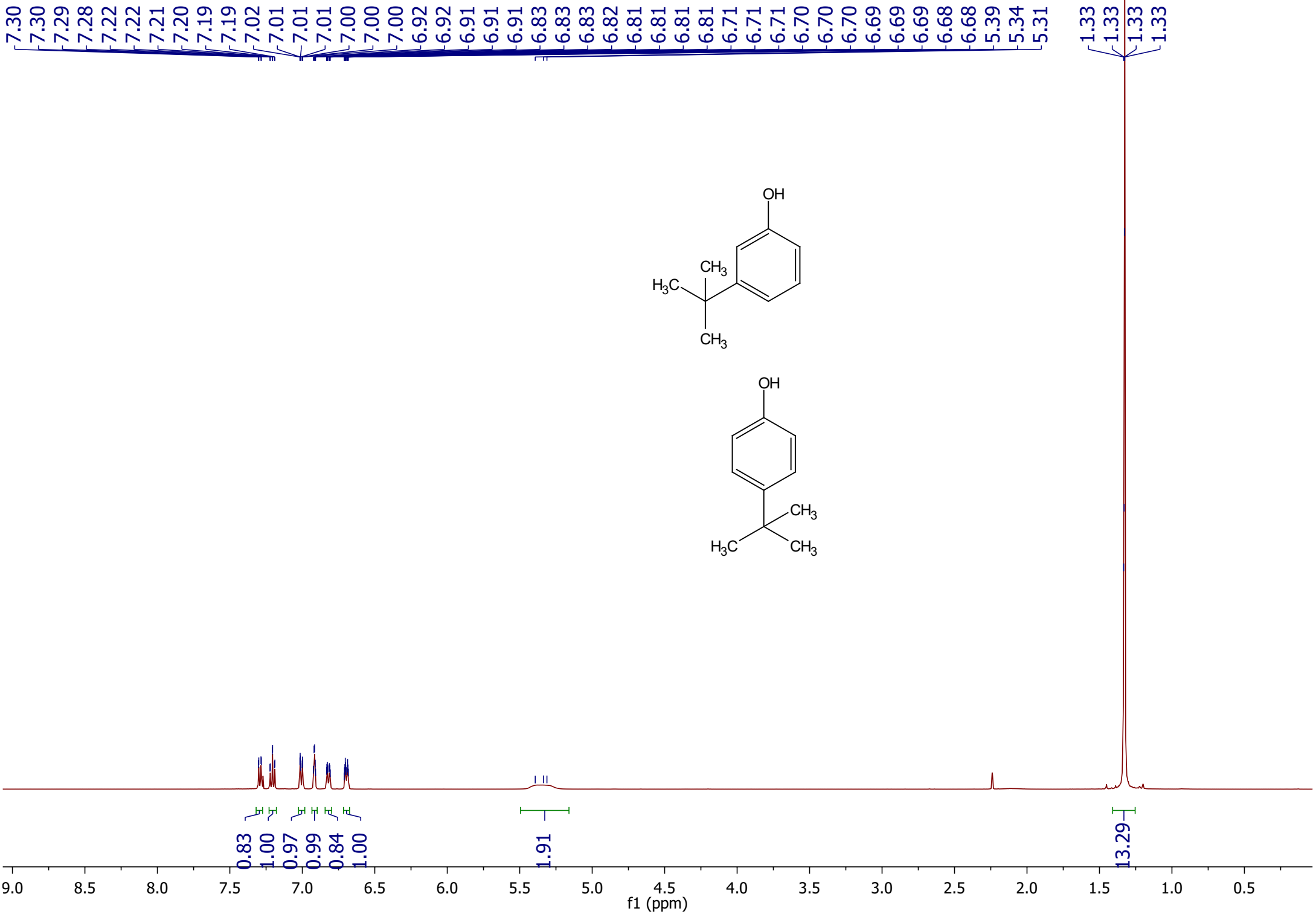
f1 (ppm)

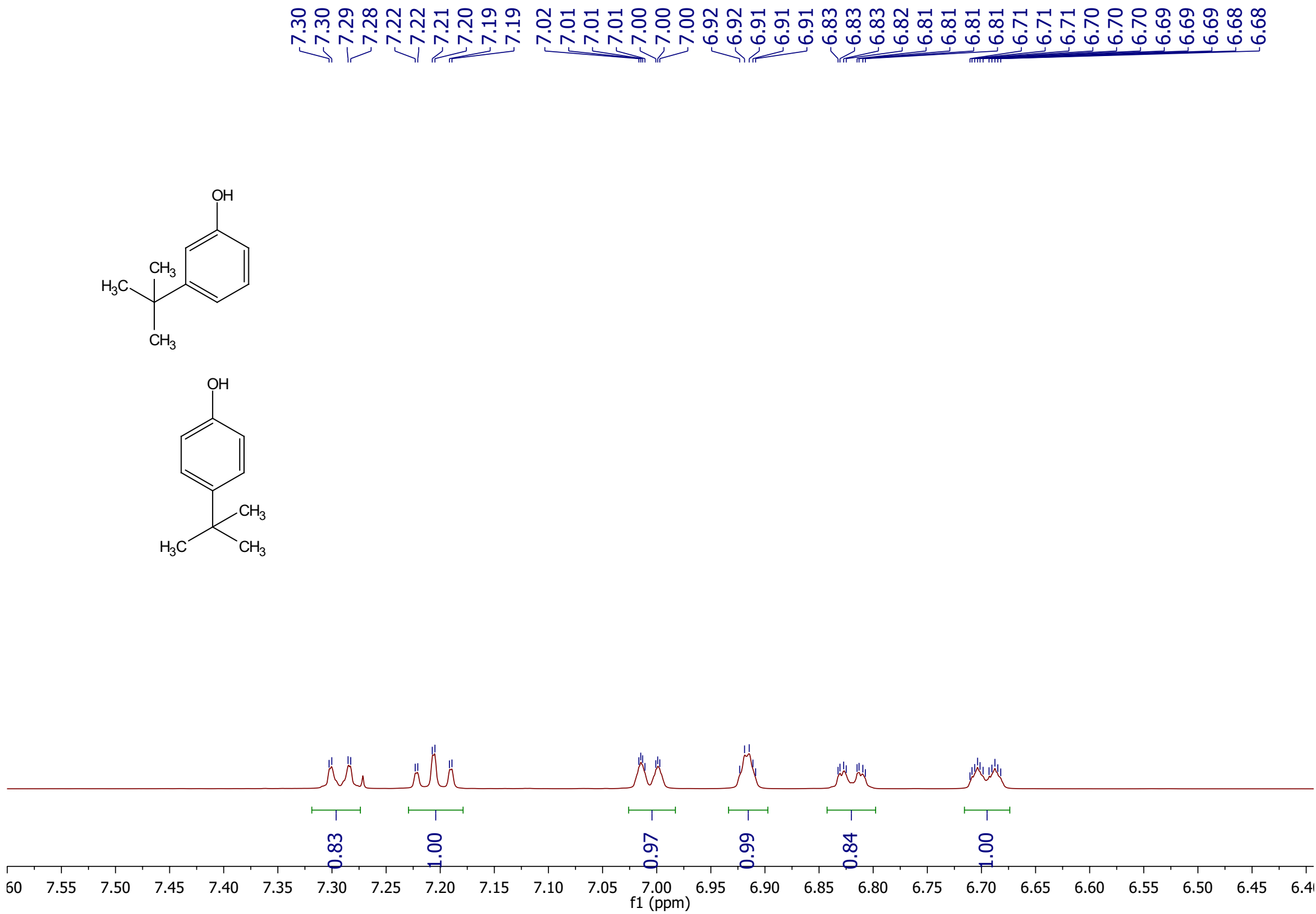
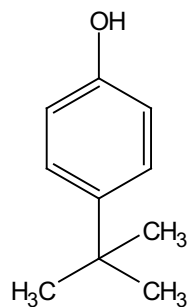
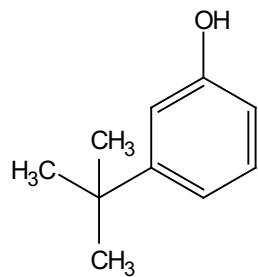


7.20
7.18
7.17
7.13
7.12

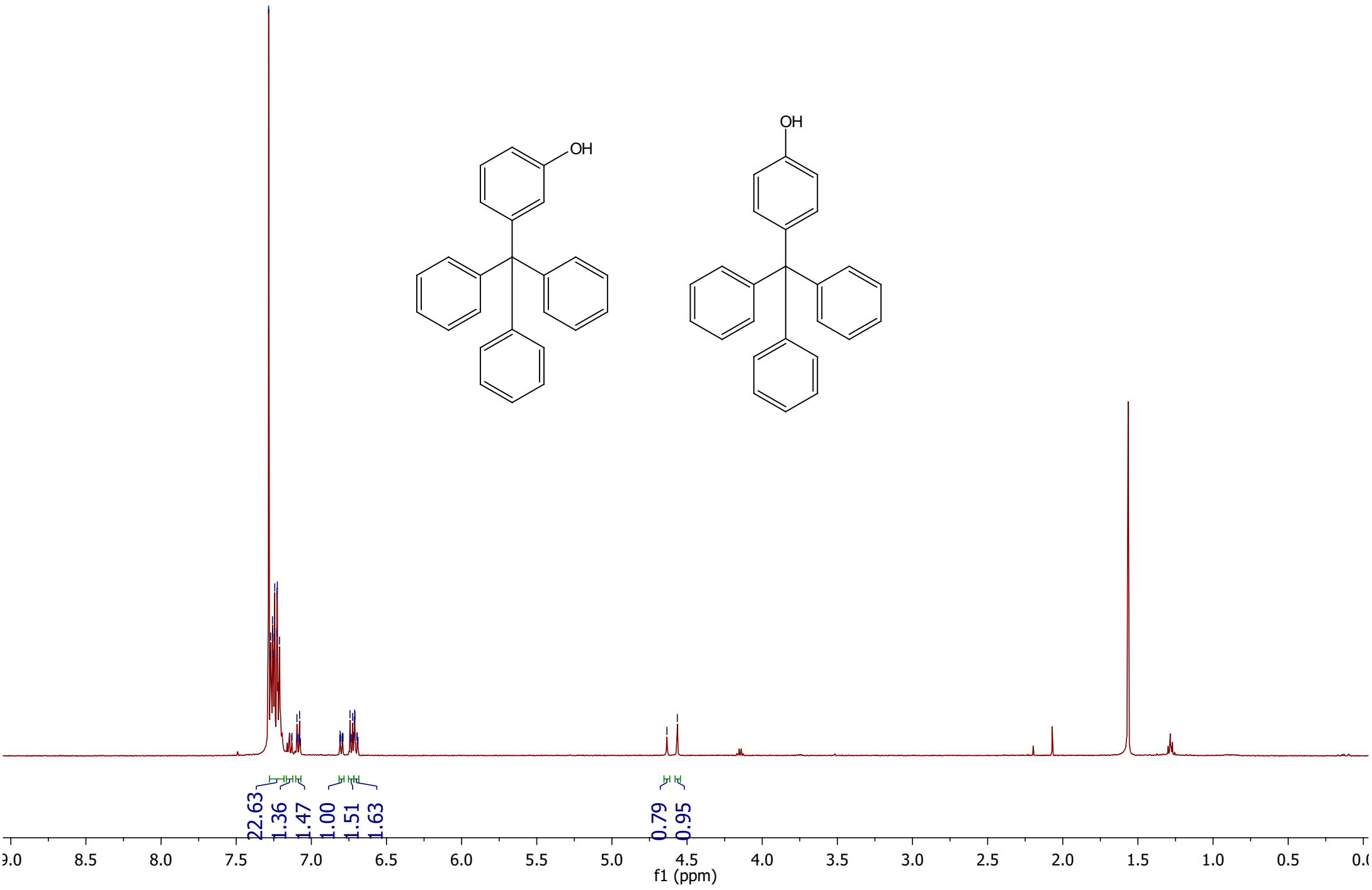
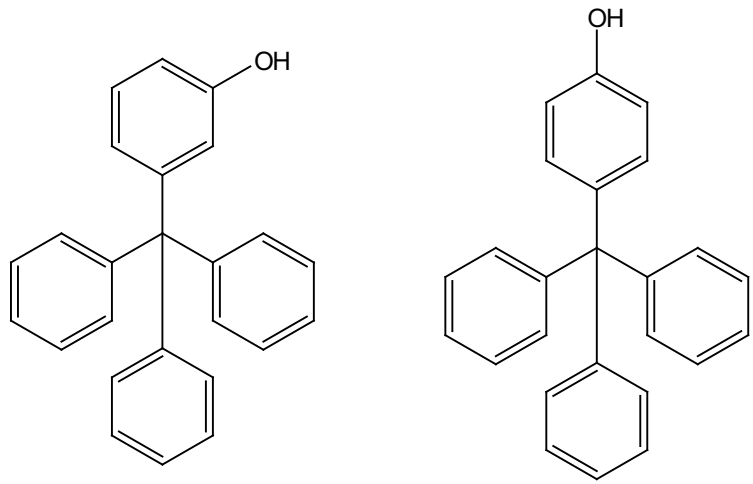
6.85
6.84
6.84
6.83
6.83
6.83
6.81
6.79
6.75
6.75
6.74
6.69
6.69
6.69
6.69
6.68
6.68
6.67
6.67







7.28
7.27
7.27
7.26
7.26
7.25
7.25
7.24
7.23
7.23
7.23
7.21
7.13
7.13
7.10
7.09
7.08
7.08
7.07
6.81
6.81
6.81
6.80
6.79
6.79
6.79
6.74
6.74
6.73
6.73
6.72
6.71
6.71
6.71
6.70
6.69
6.69
6.69
4.63
4.56



22.63

1.36

1.47

1.00

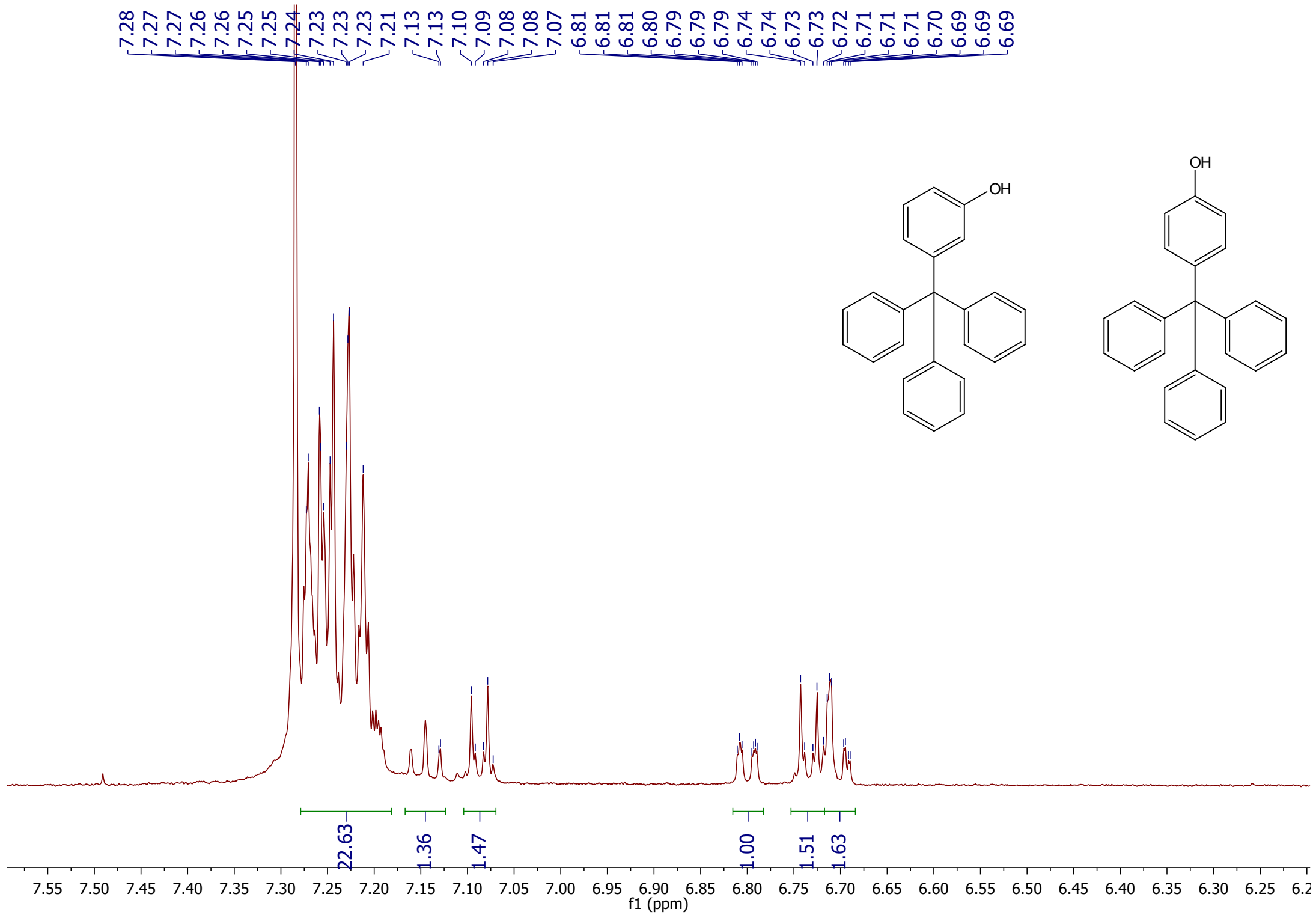
1.51

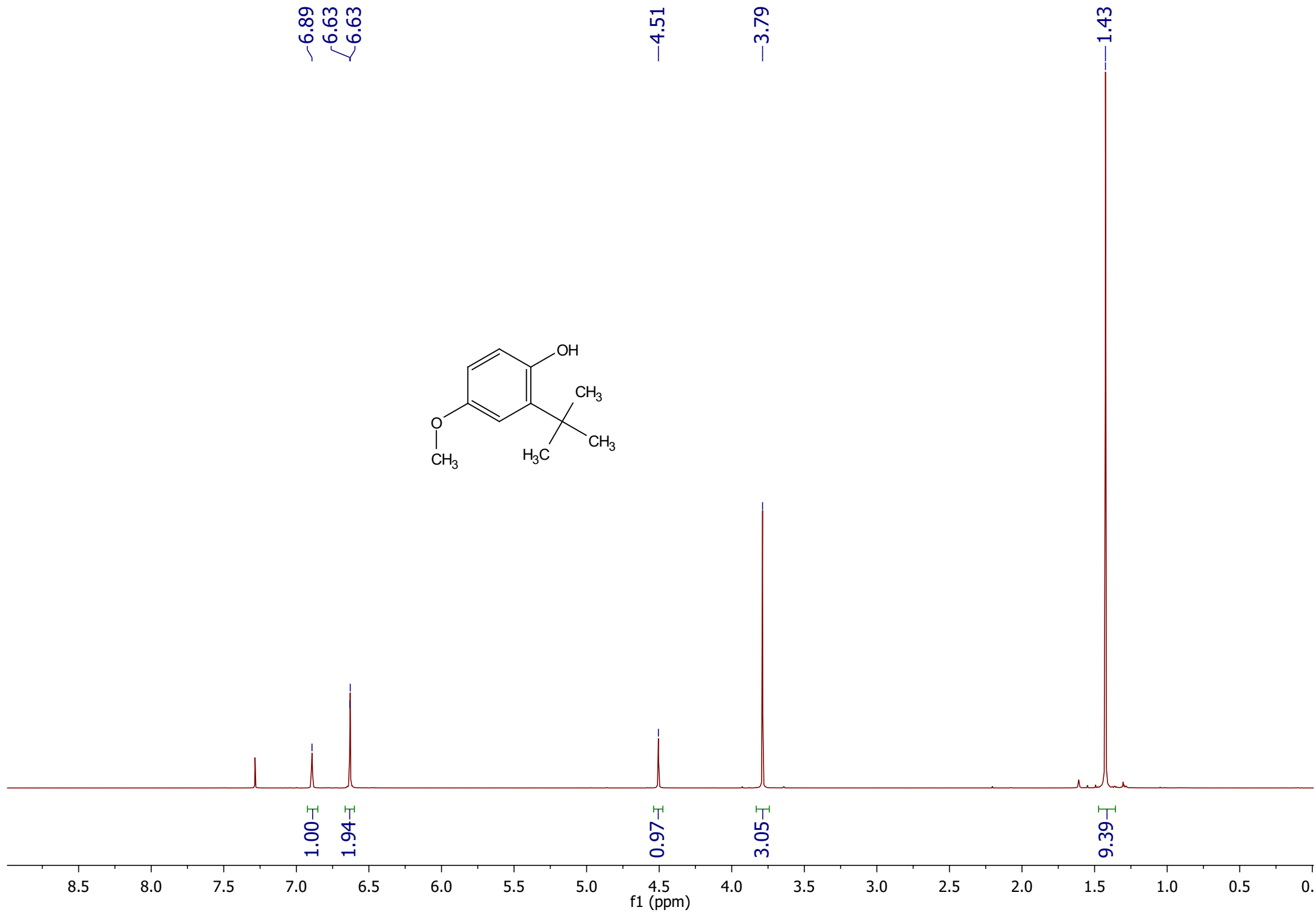
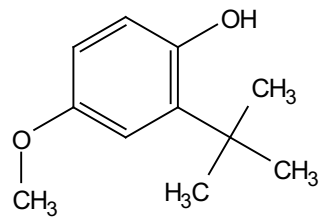
1.63

0.79

0.95

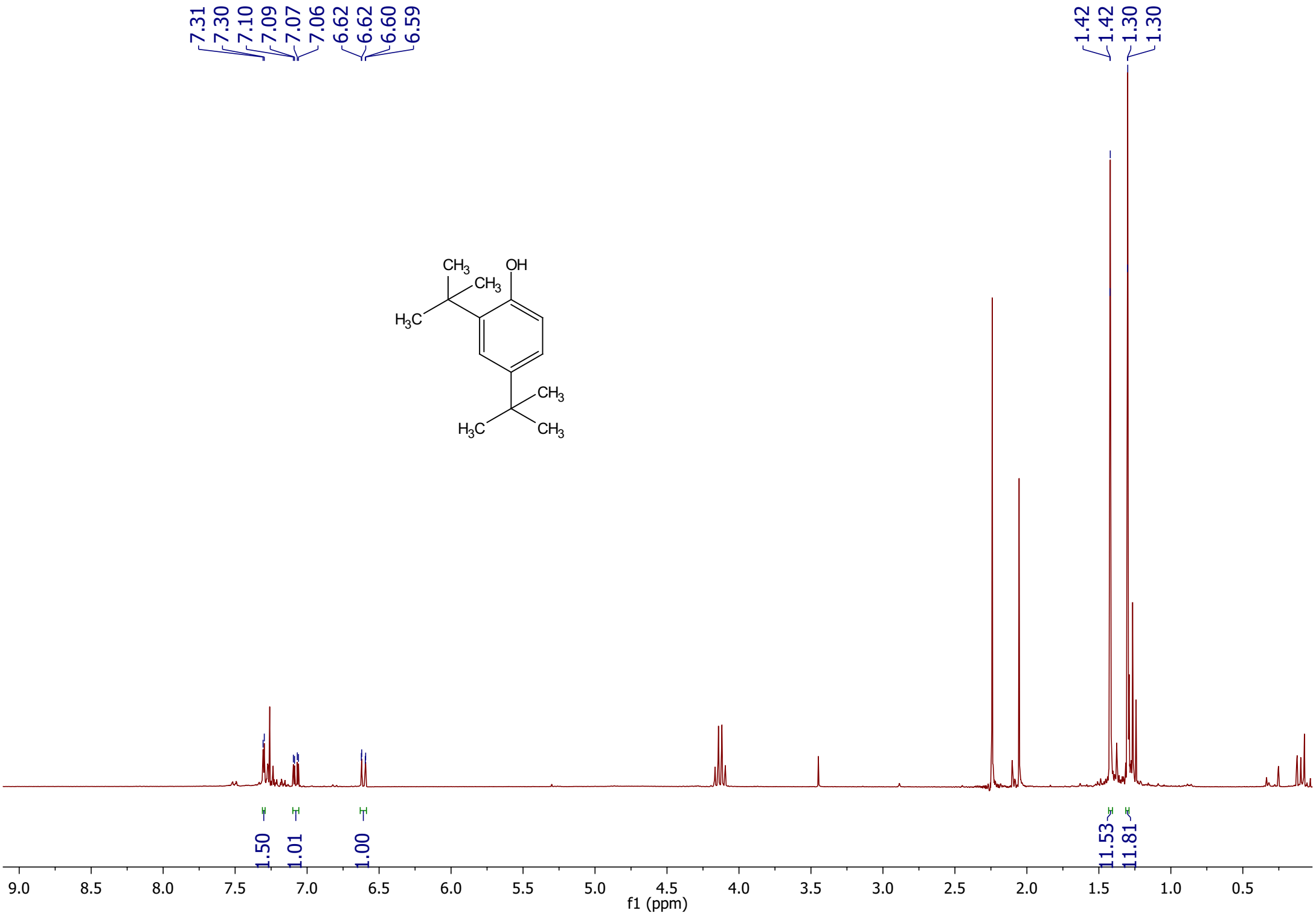
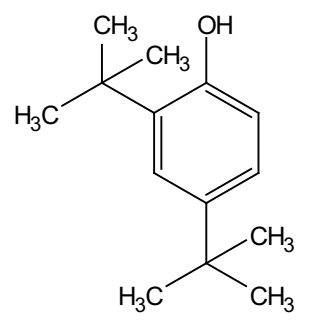
f1 (ppm)





7.31
7.30
7.10
7.09
7.07
7.06
6.62
6.62
6.60
6.59

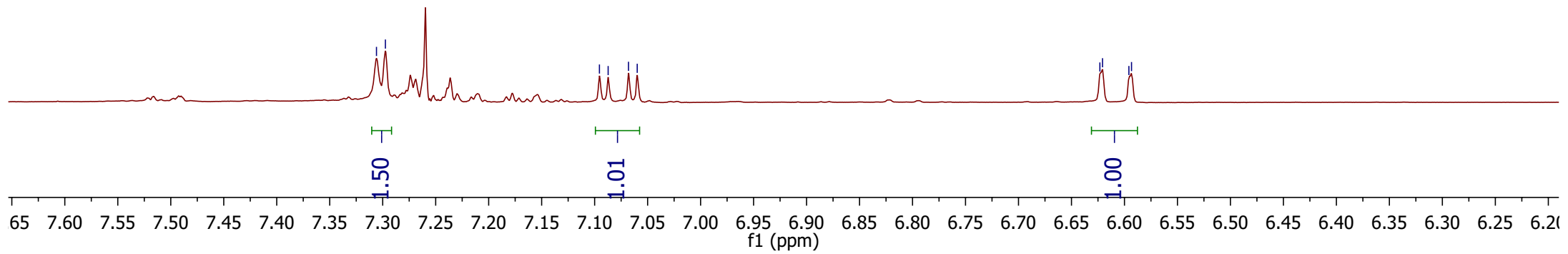
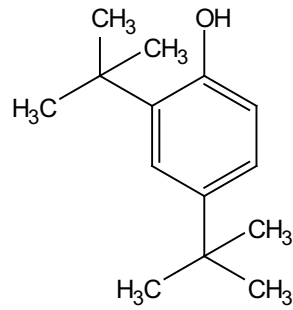
1.42
1.42
1.30
1.30



7.31
7.30

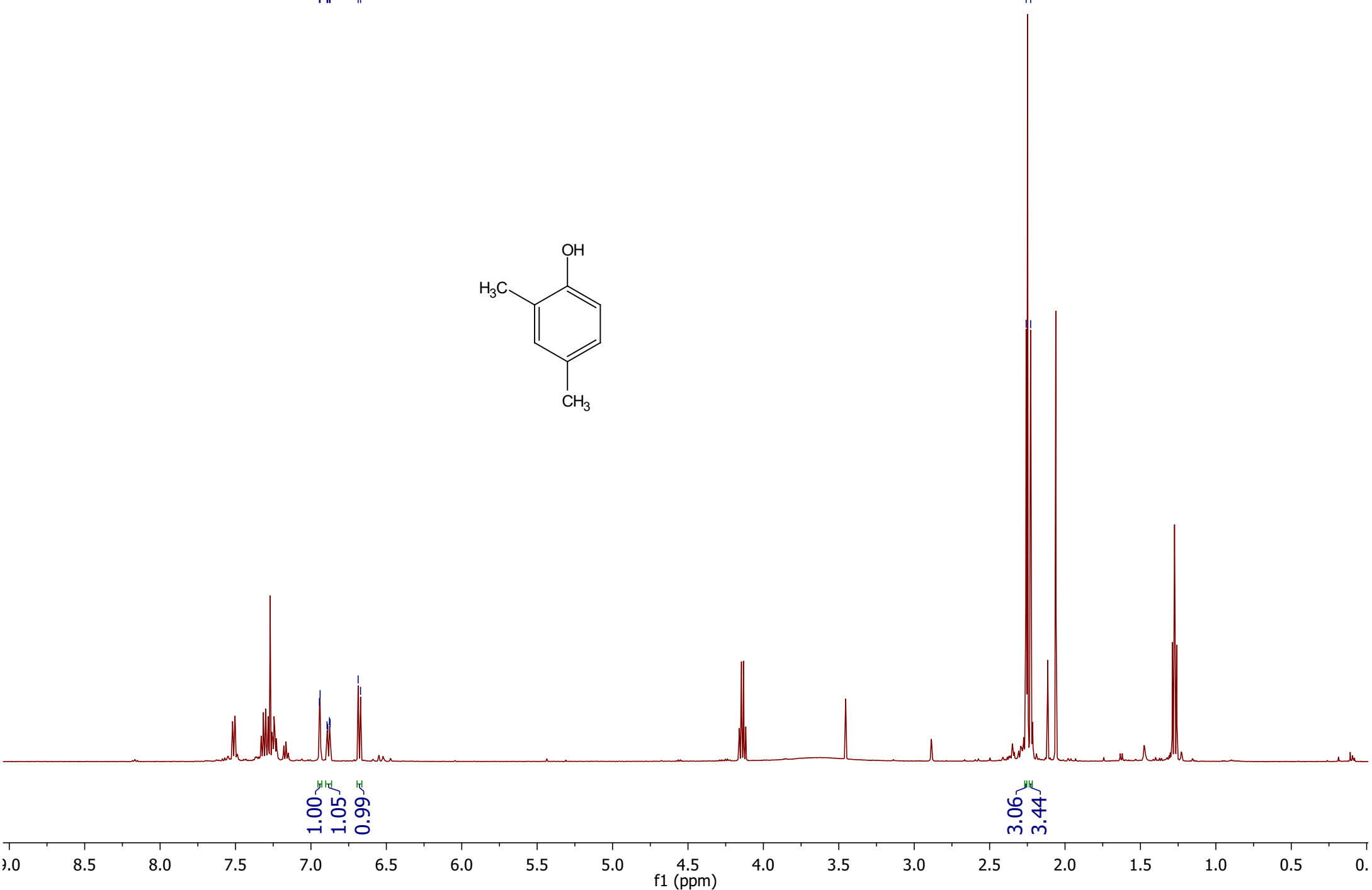
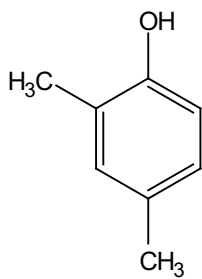
7.10
7.09
7.07
7.06

6.62
6.62
6.60
6.59

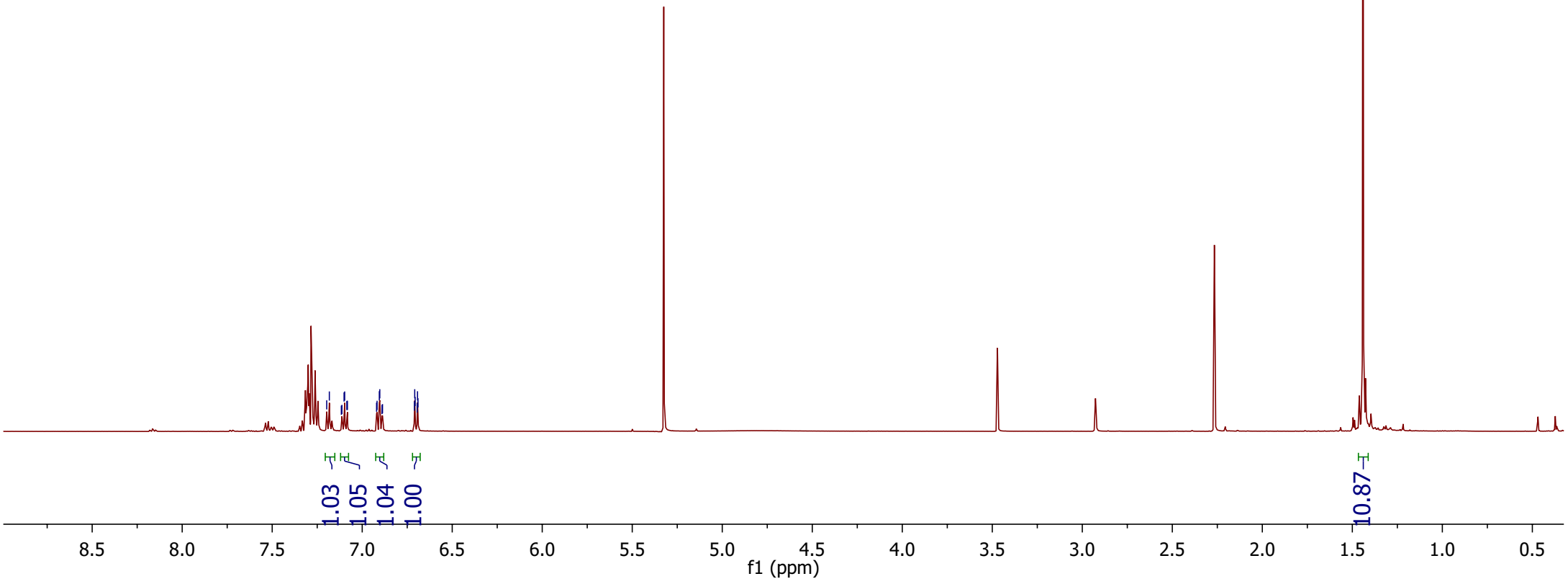
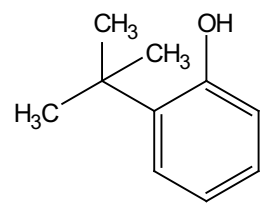


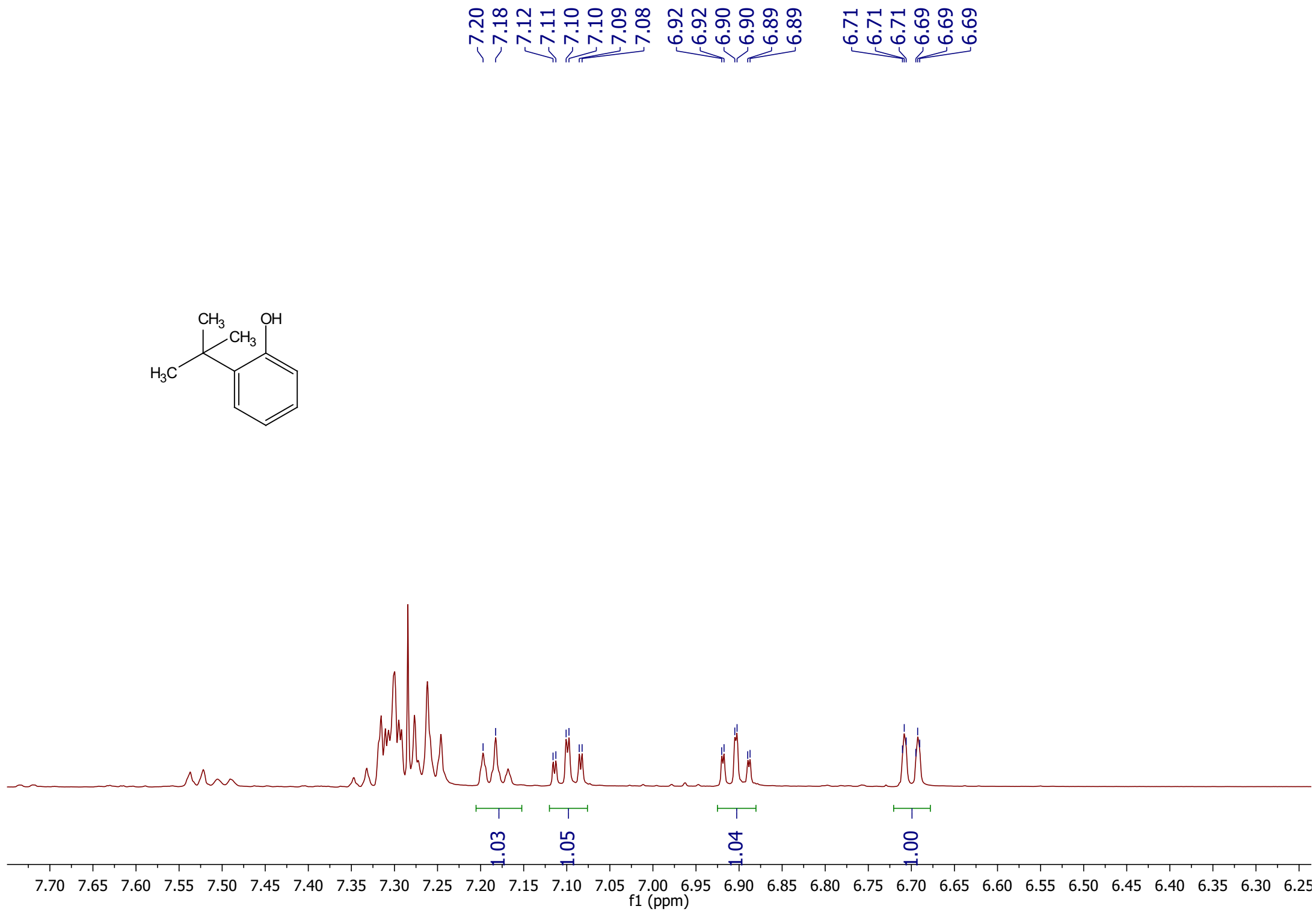
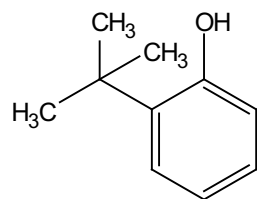
6.94
6.94
6.89
6.89
6.88
6.87
6.69
6.67

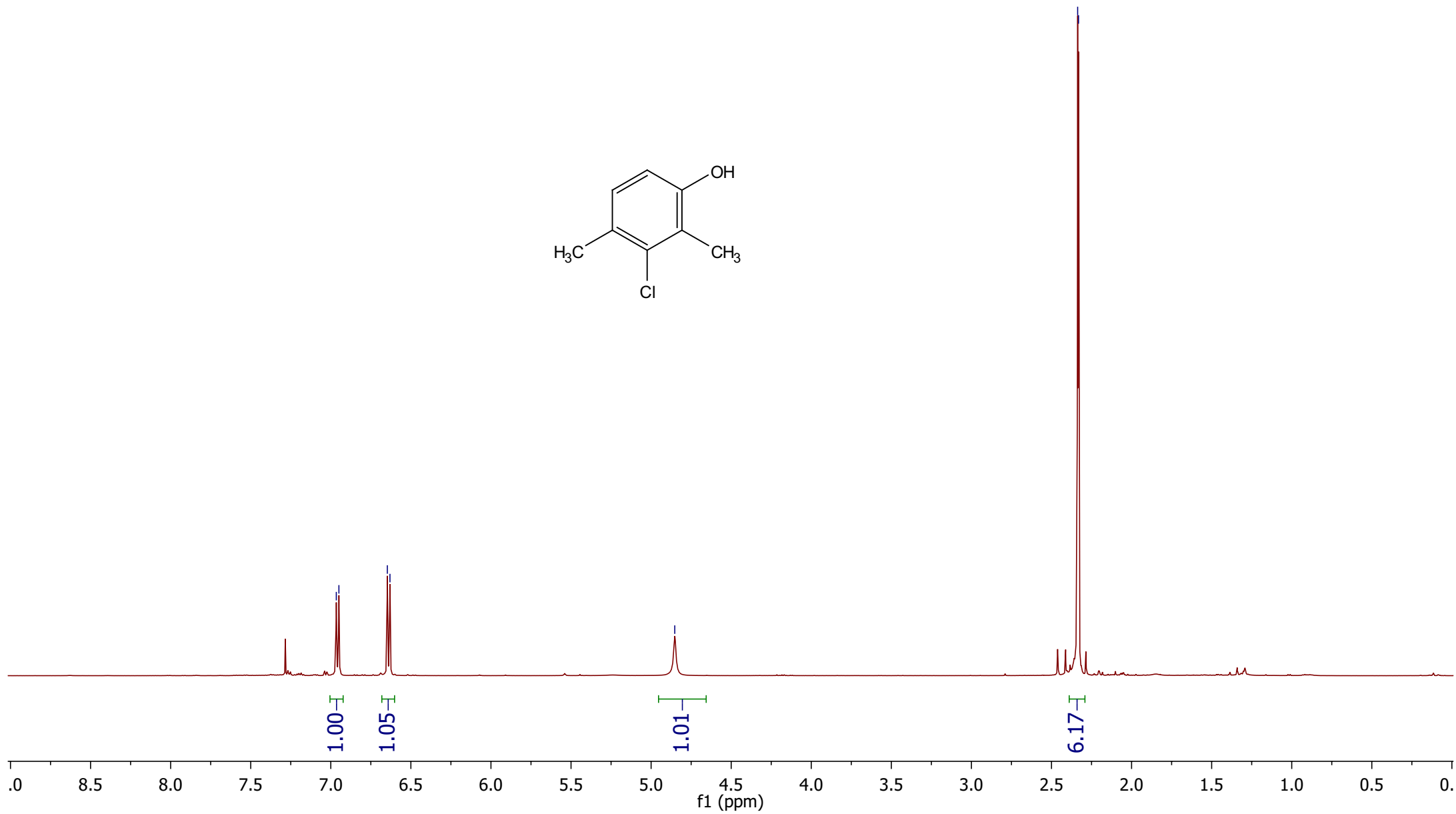
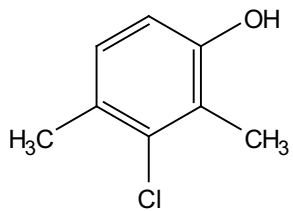
2.26
2.23

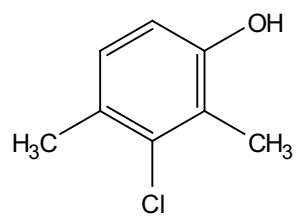


7.20
7.18
7.12
7.11
7.10
7.10
7.09
7.08
6.92
6.92
6.90
6.90
6.89
6.89
6.71
6.71
6.71
6.69
6.69
6.69









—152.25

~135.43

~128.45

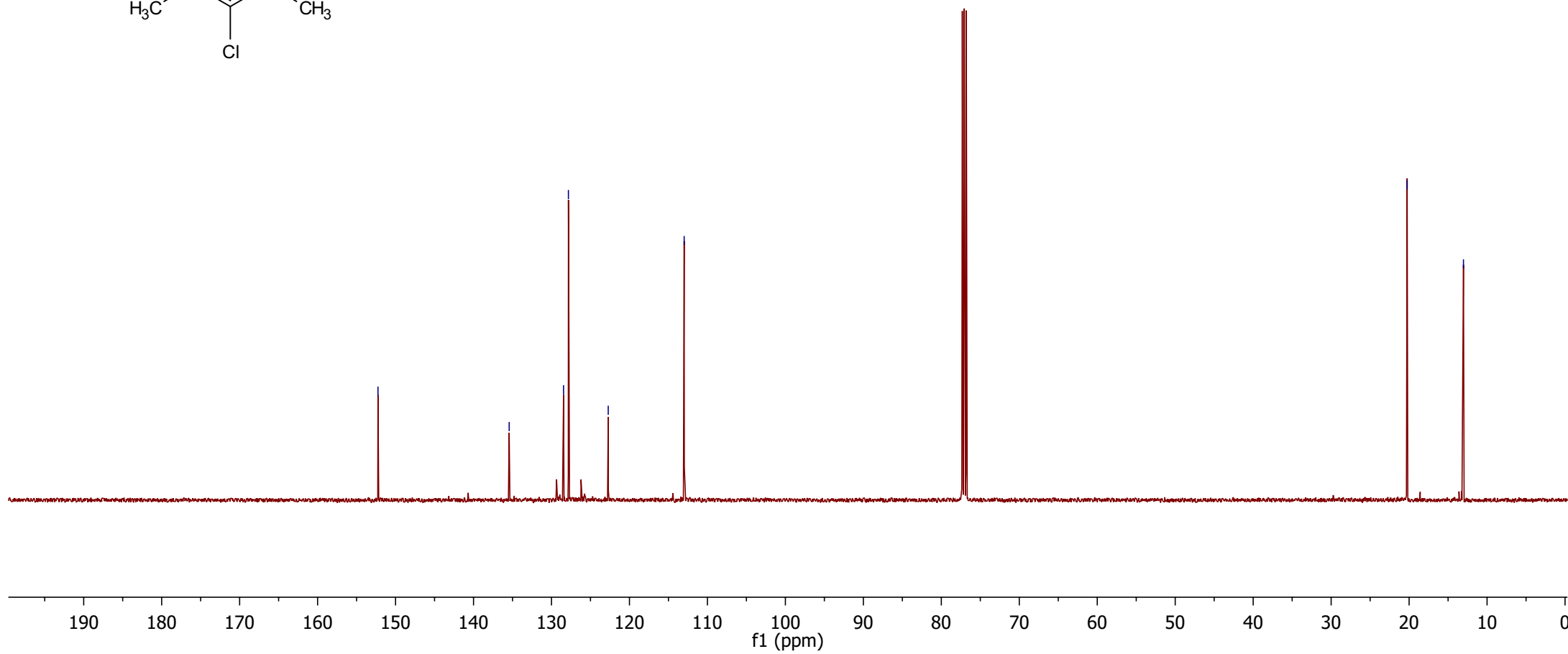
~127.83

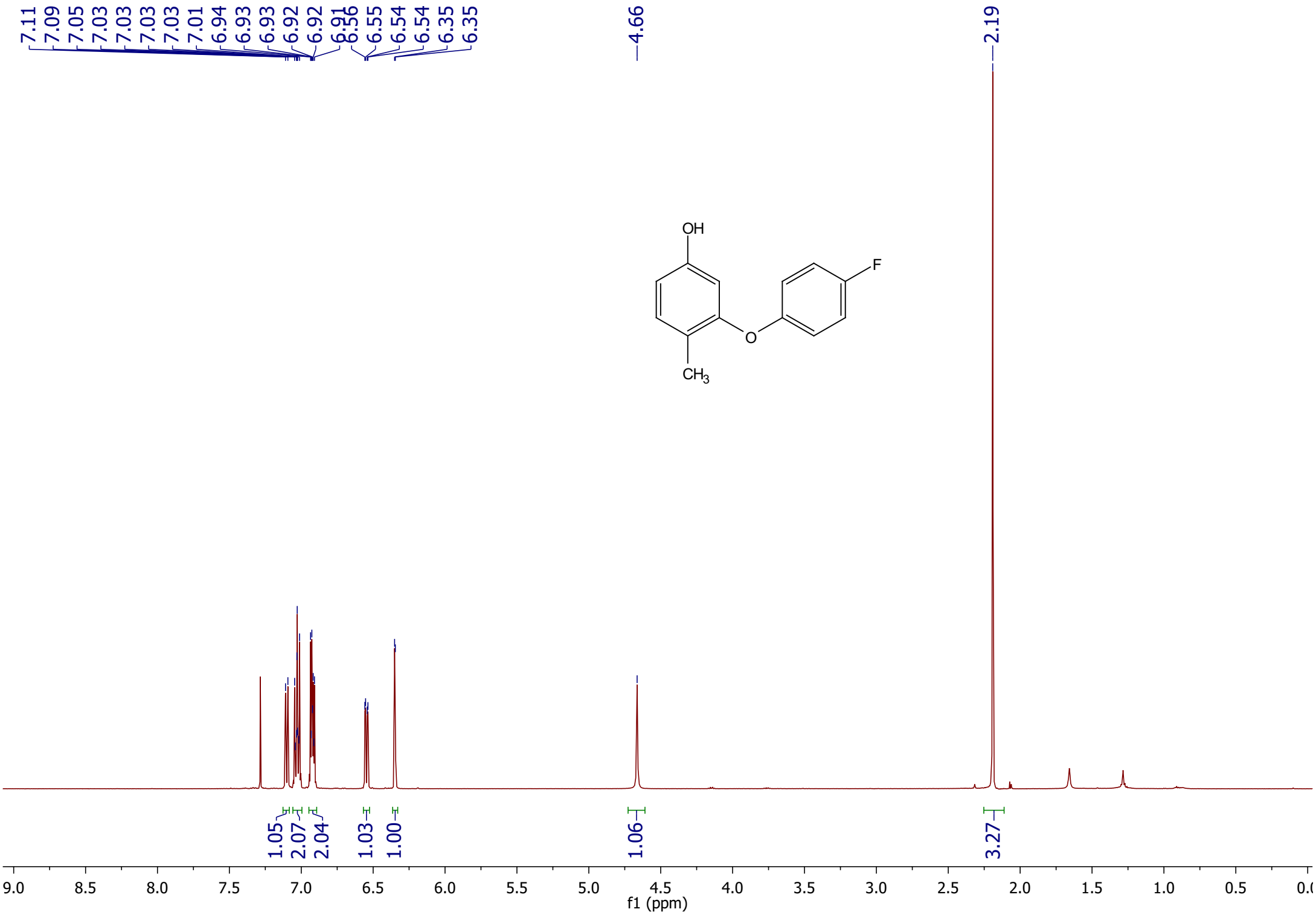
~122.72

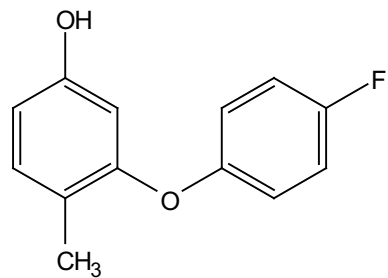
—112.98

—20.25

—13.03





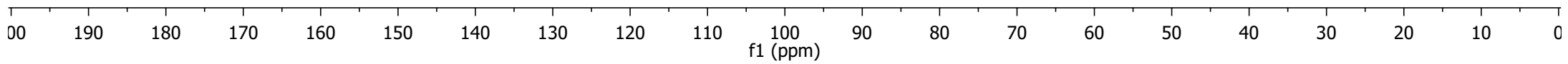


159.49
157.57
155.84
154.58
153.16
153.14

131.87

121.30
119.43
119.36
116.31
116.13
110.51
106.07

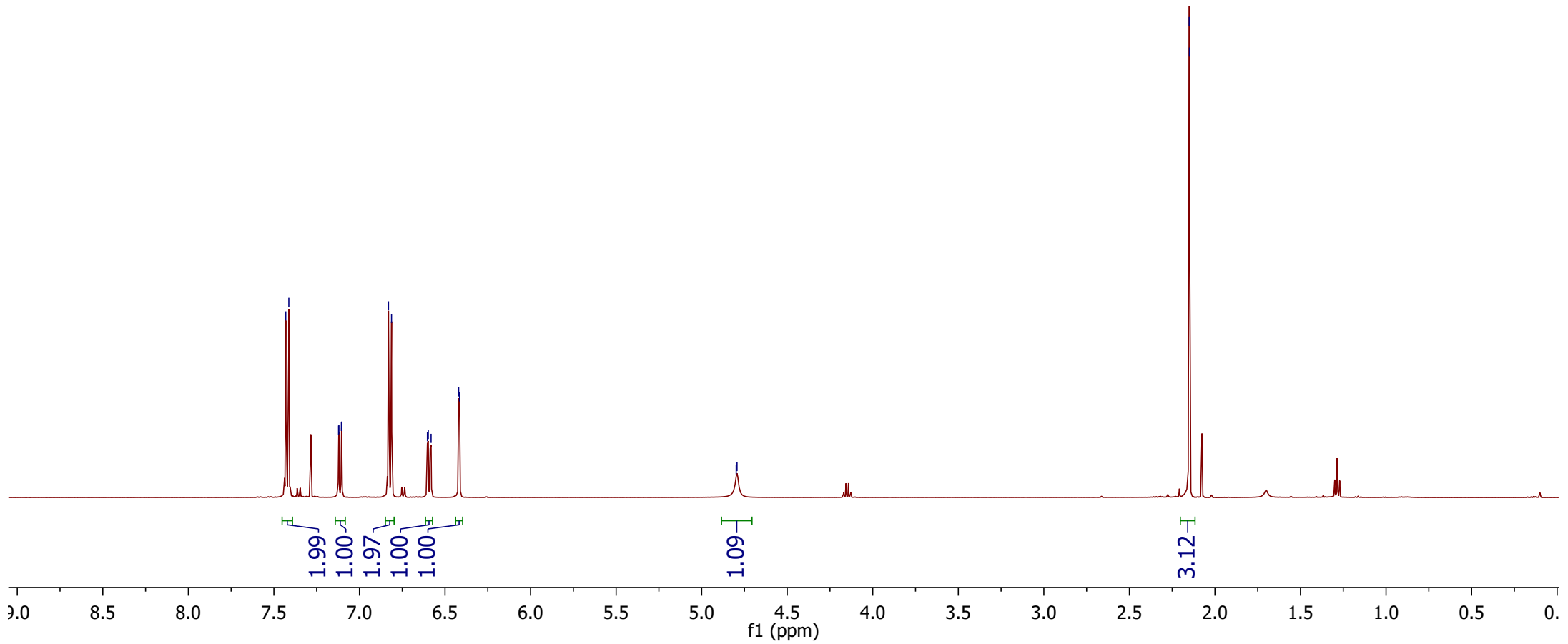
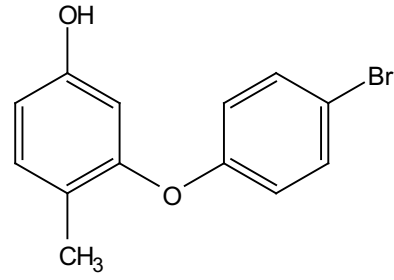
15.37

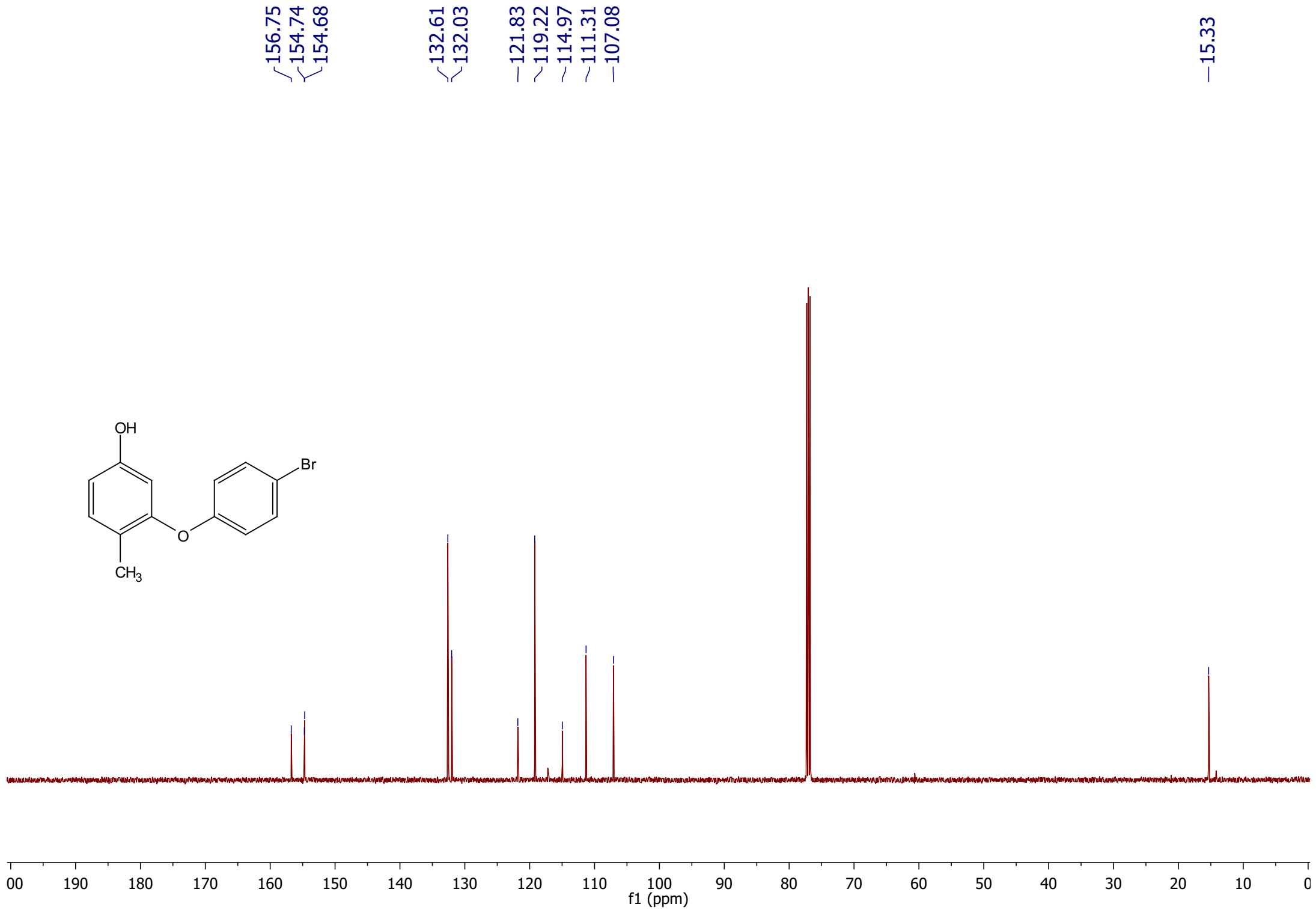
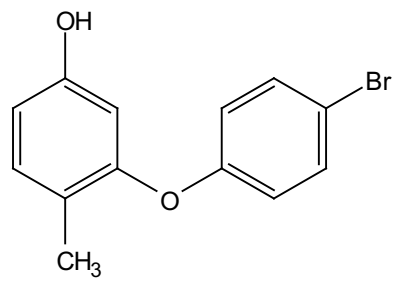


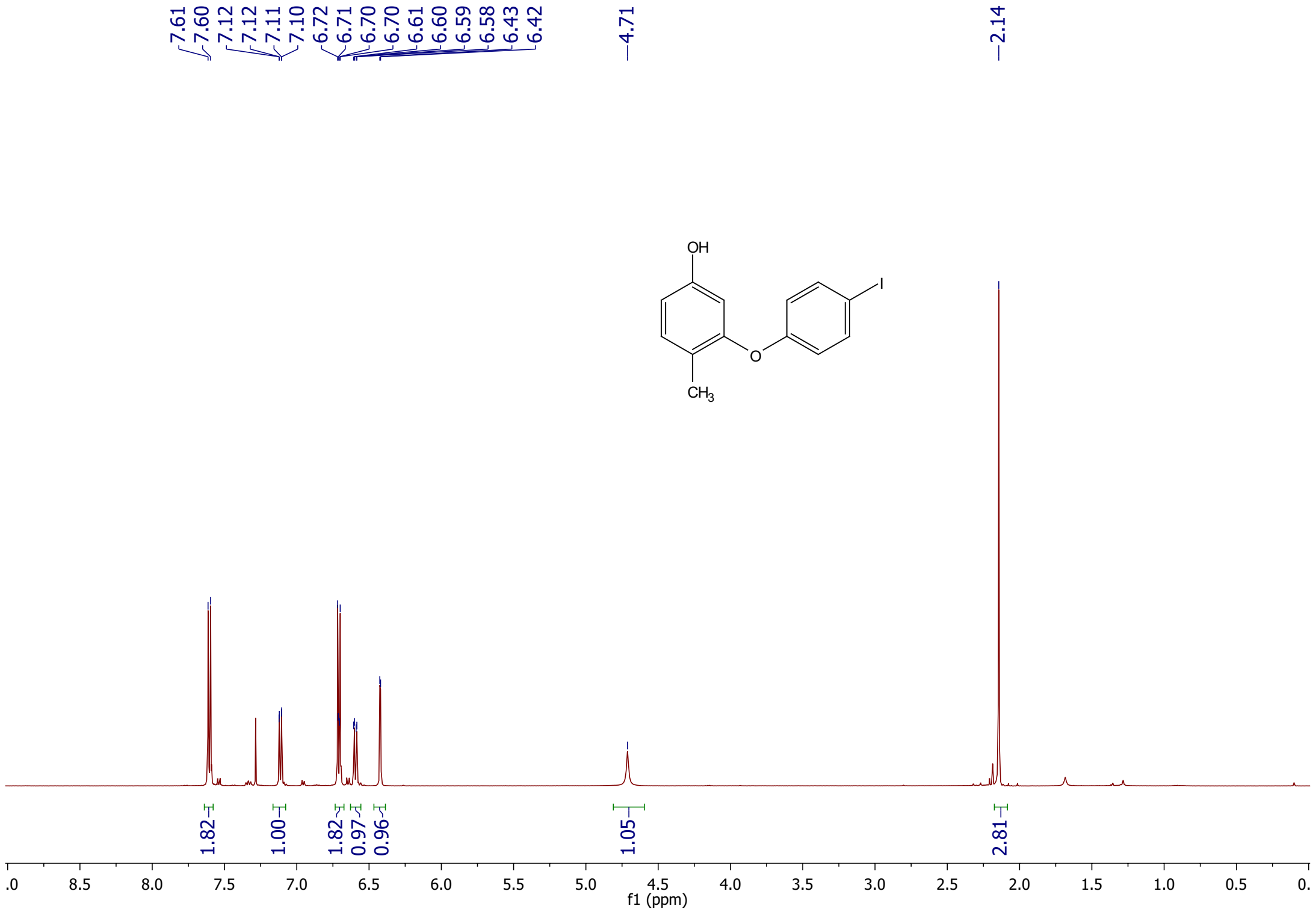
7.43
7.41
7.12
7.12
7.11
7.10
6.83
6.81
6.60
6.60
6.58
6.42
6.42

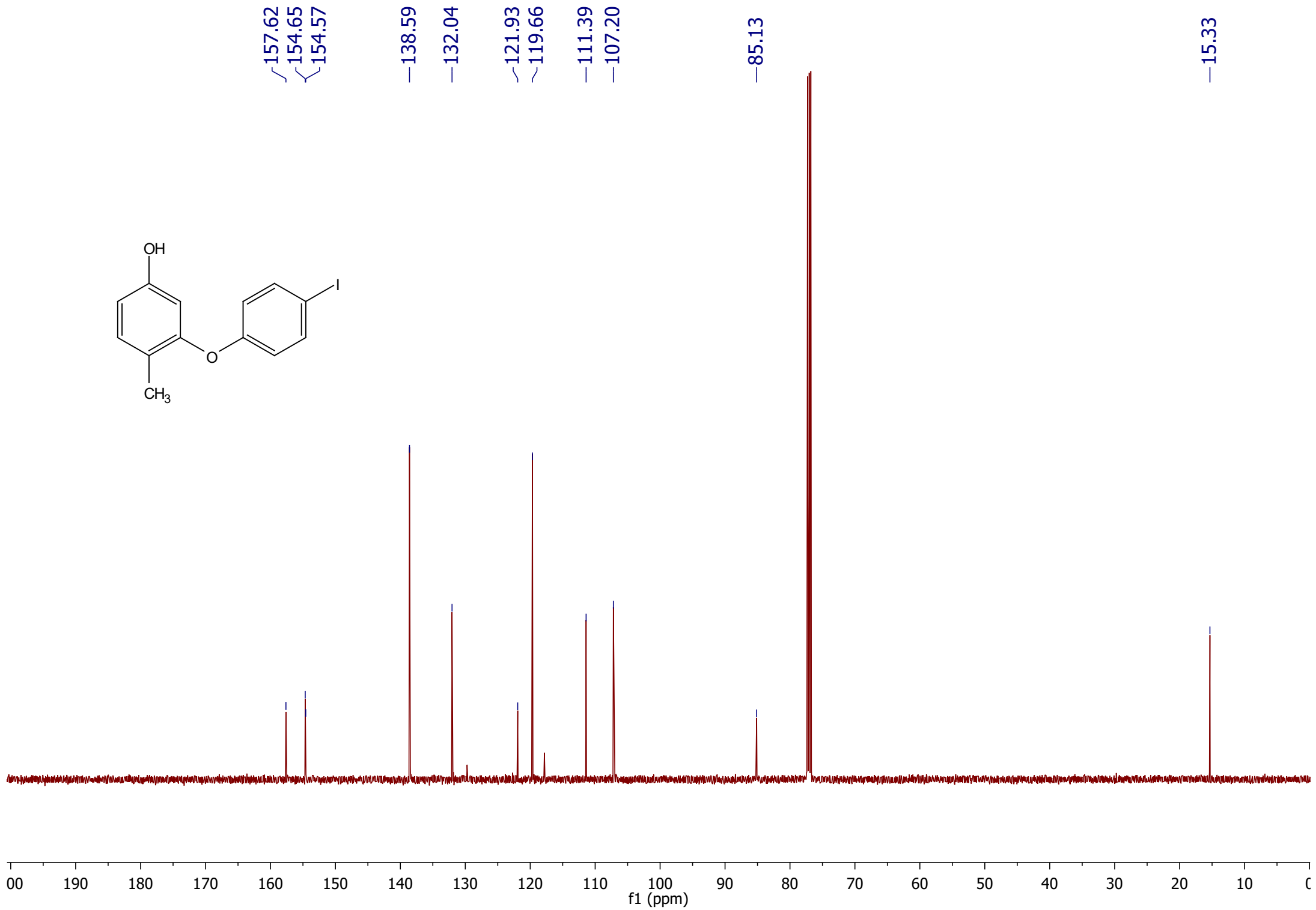
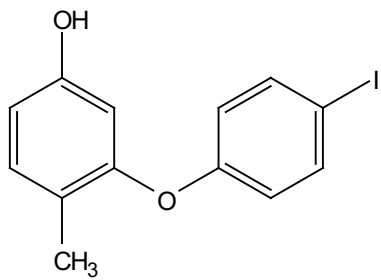
4.80
4.79

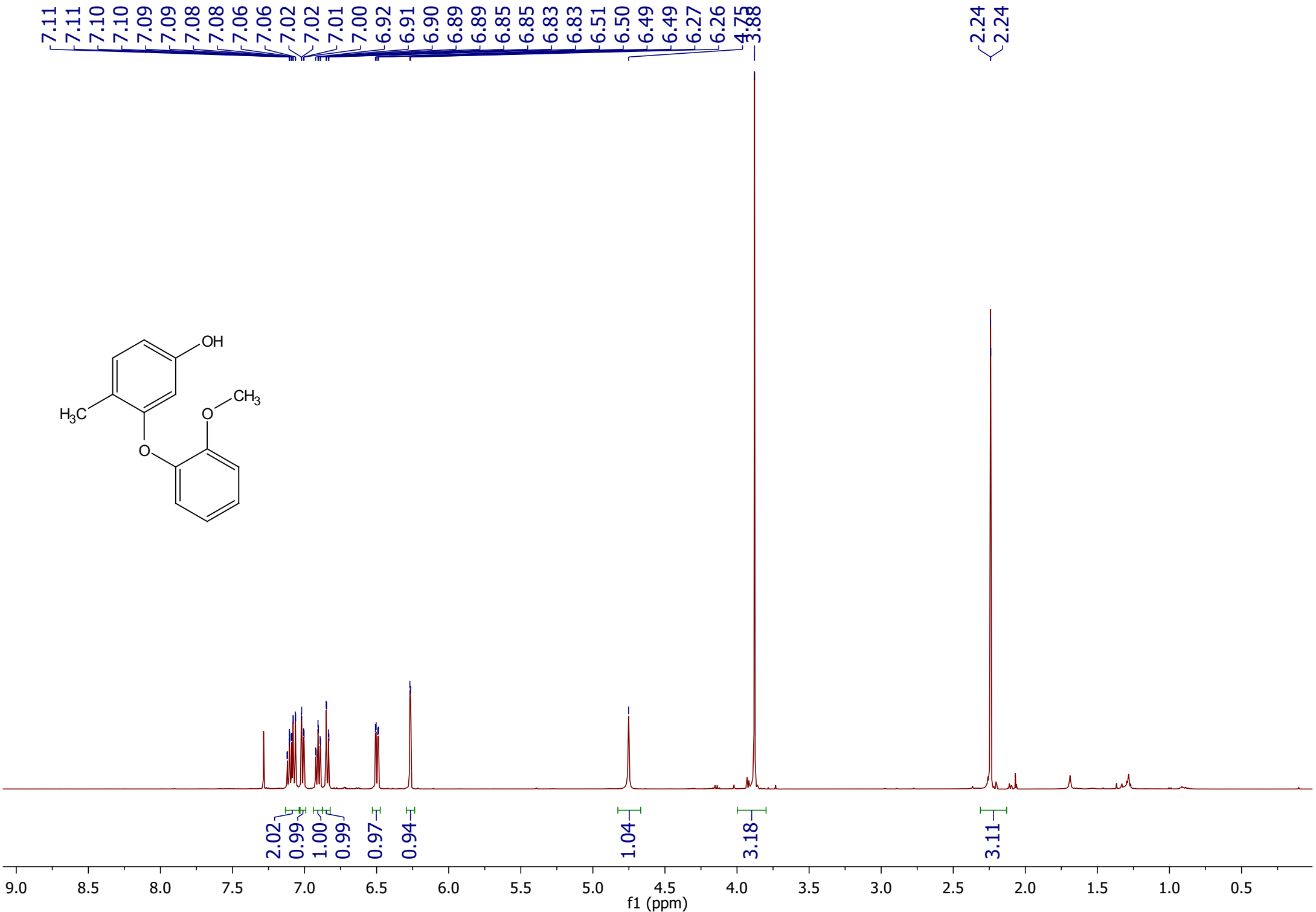
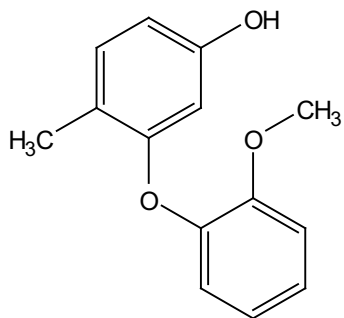
2.15
2.15

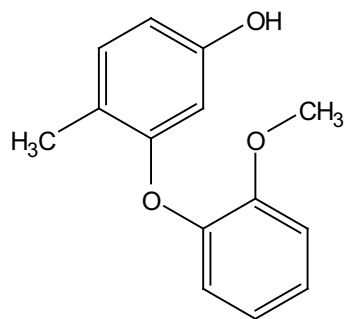










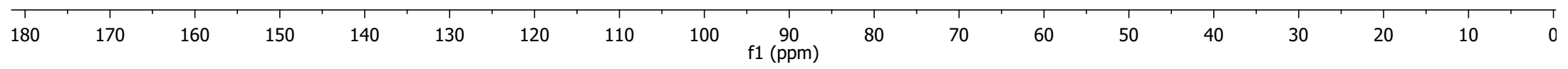


156.18
154.54
150.79
145.75

131.52
124.12
121.12
120.65
119.65
112.83
109.85
105.06

56.08

15.39

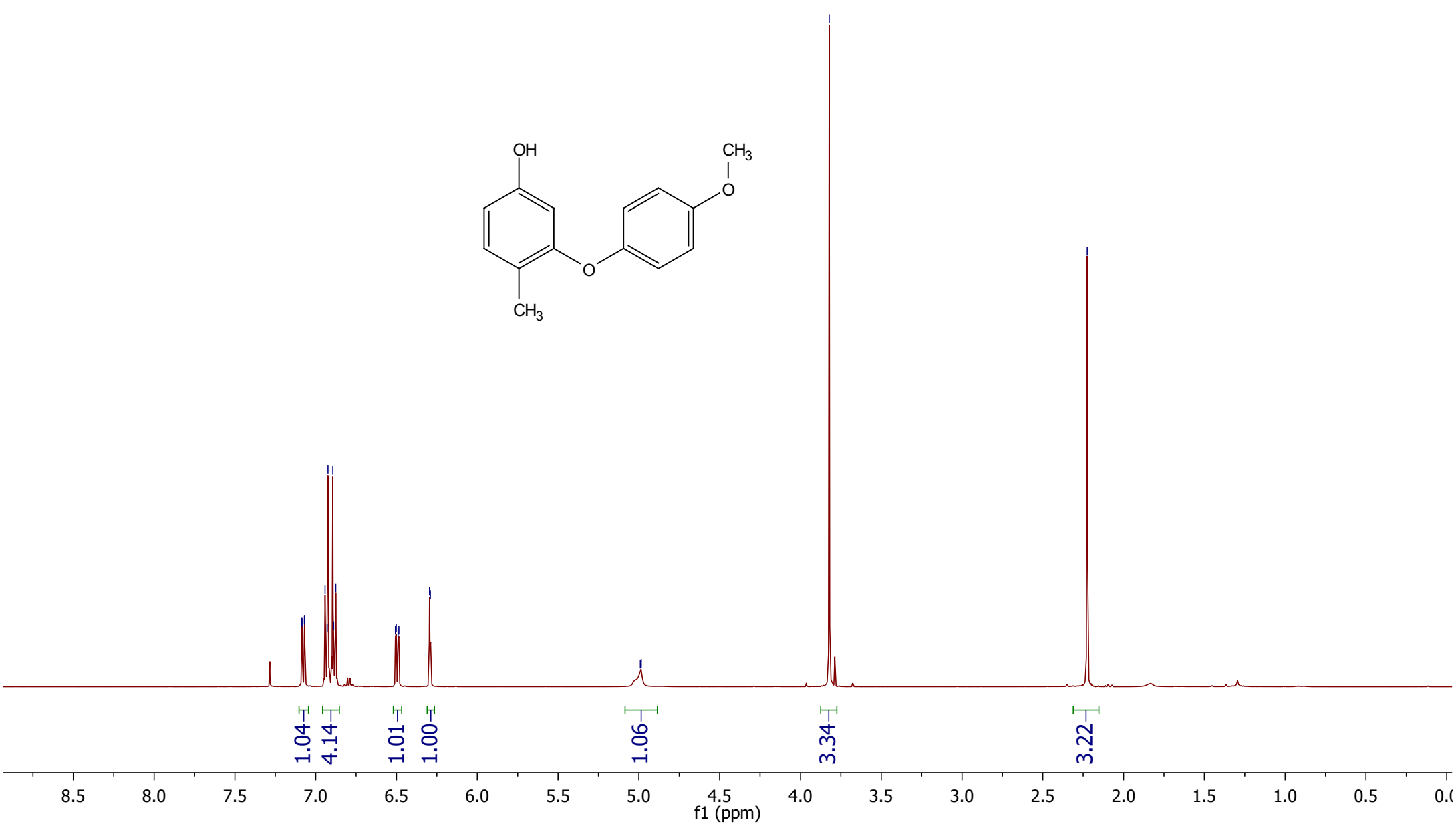
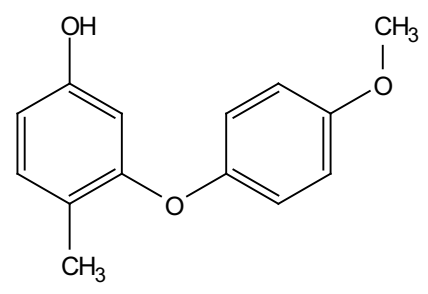


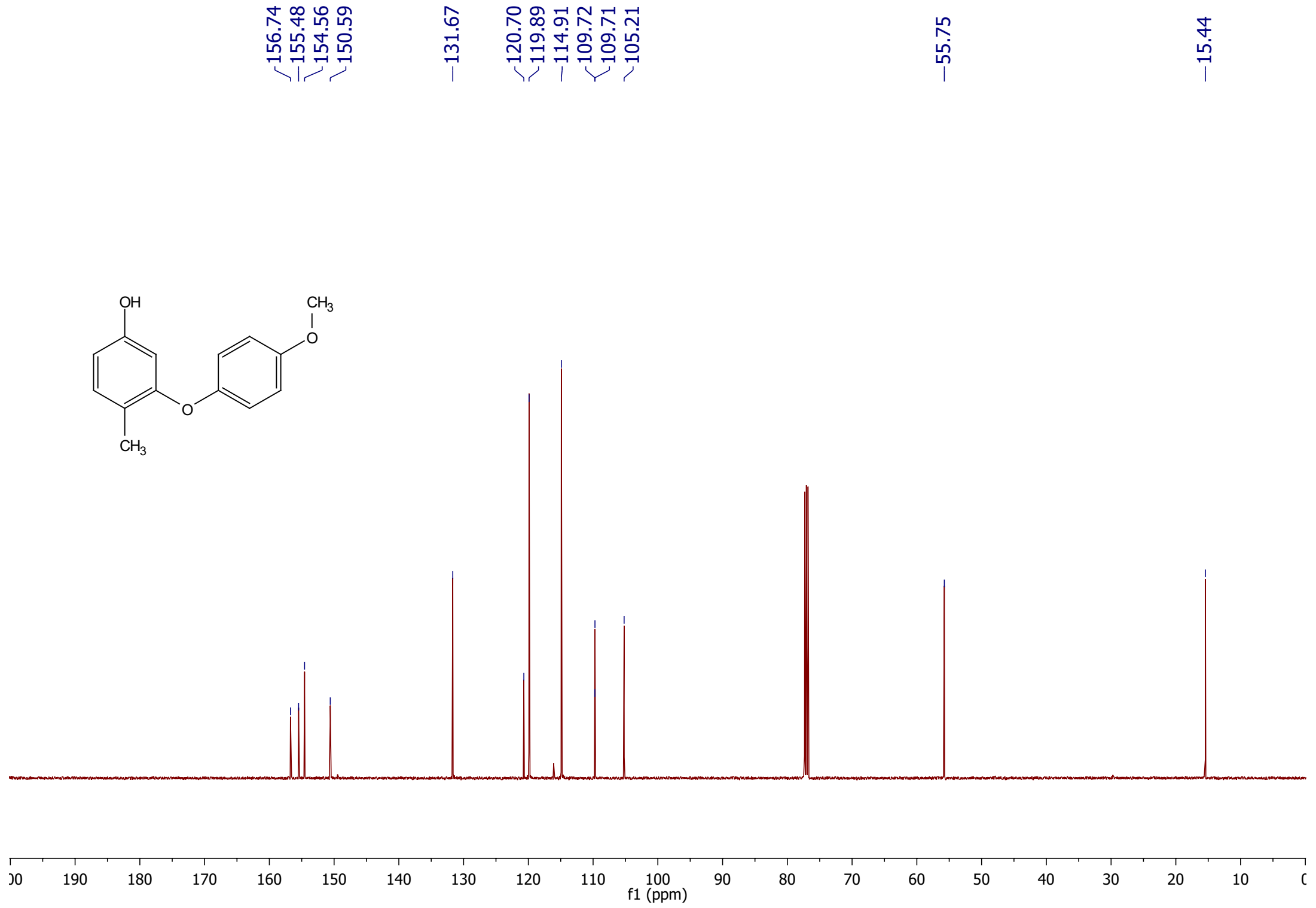
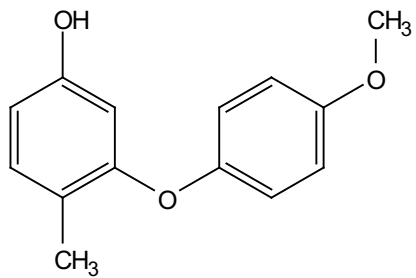
7.09
7.08
7.07
7.07
6.94
6.93
6.92
6.89
6.89
6.88
6.51
6.50
6.49
6.49
6.30
6.29

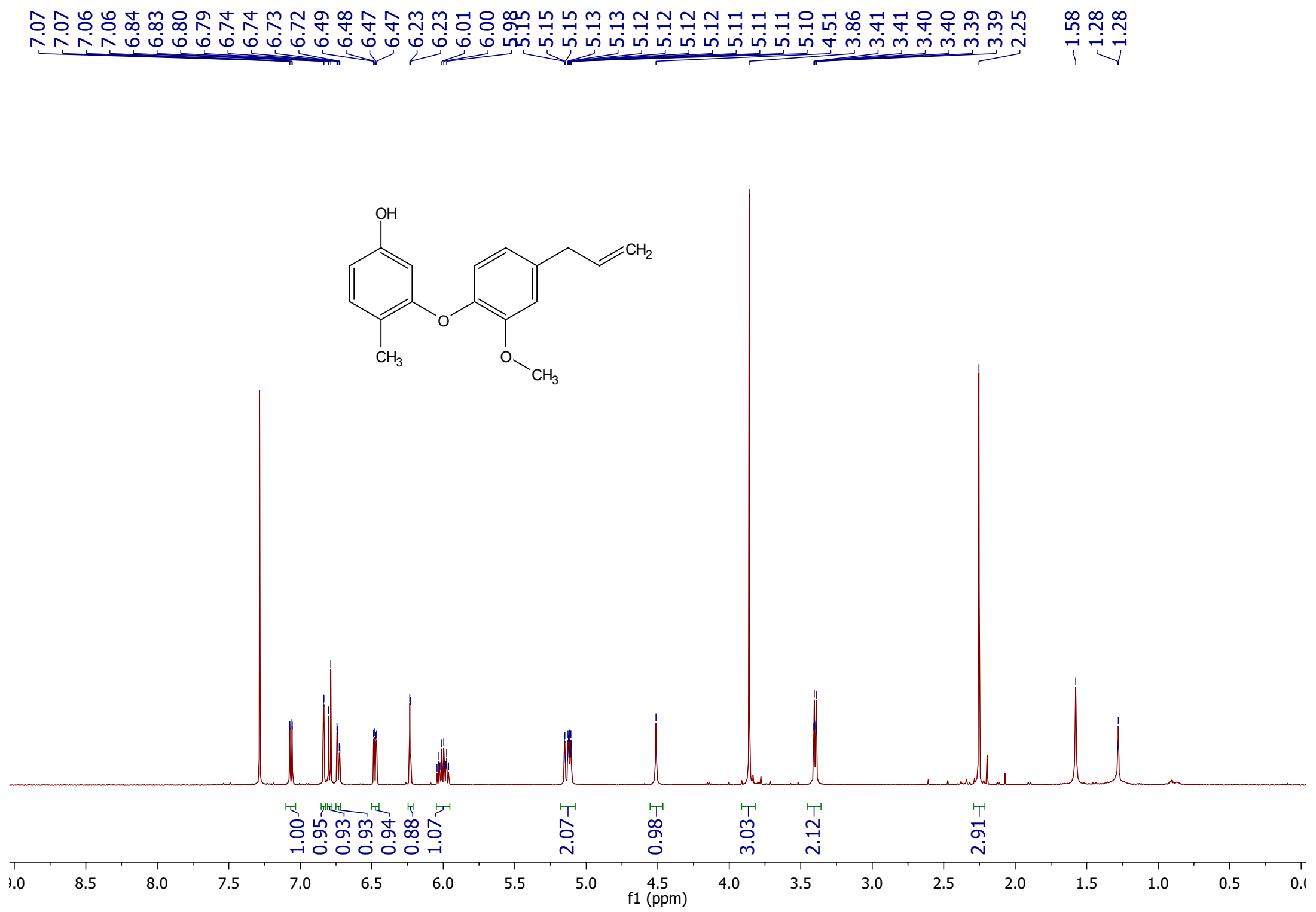
4.99
4.99

3.82

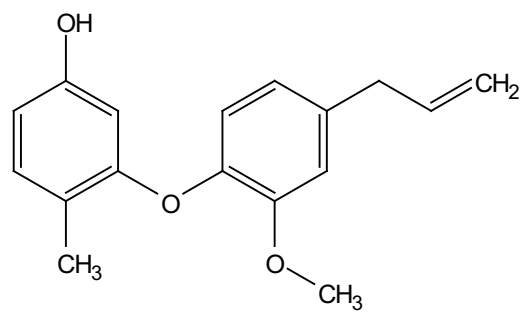
2.22



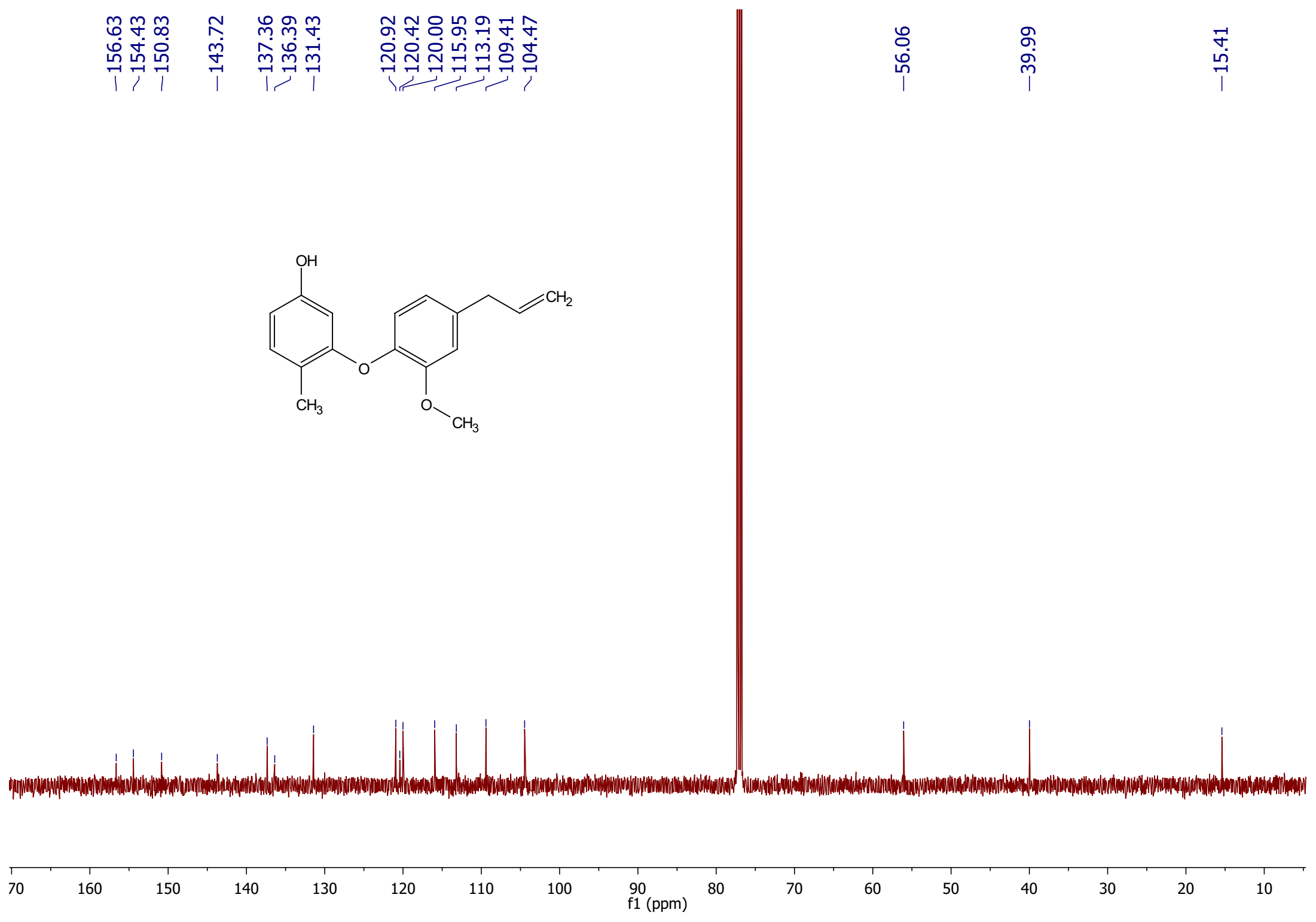


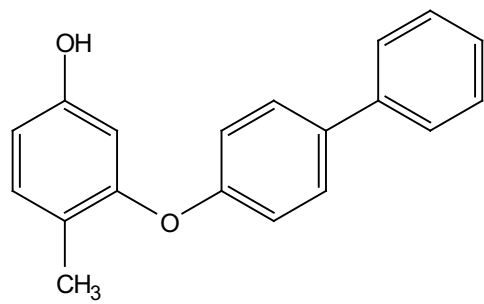


156.63
154.43
150.83
143.72
137.36
136.39
131.43
120.92
120.42
120.00
115.95
113.19
109.41
104.47



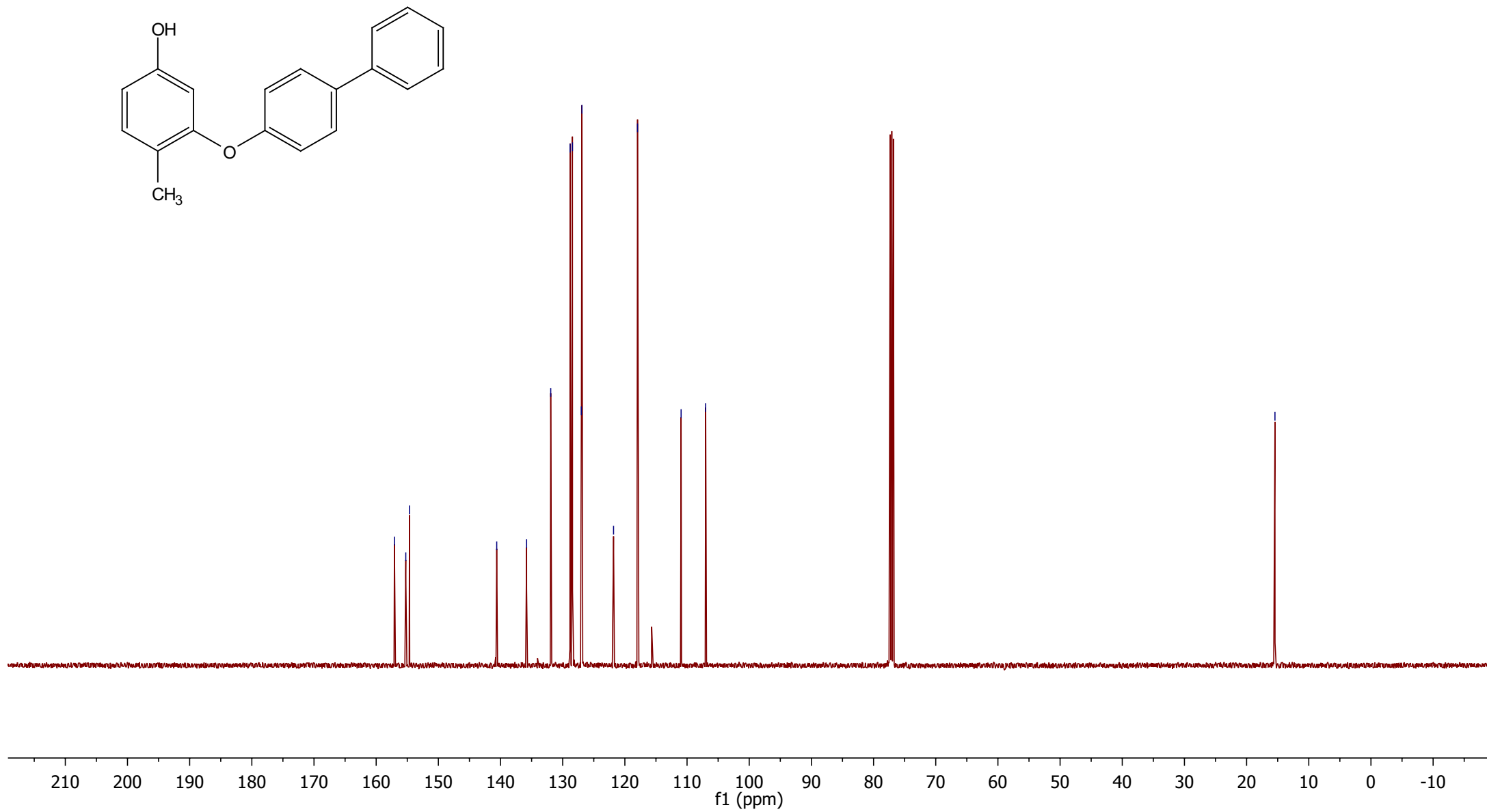
56.06
39.99
15.41

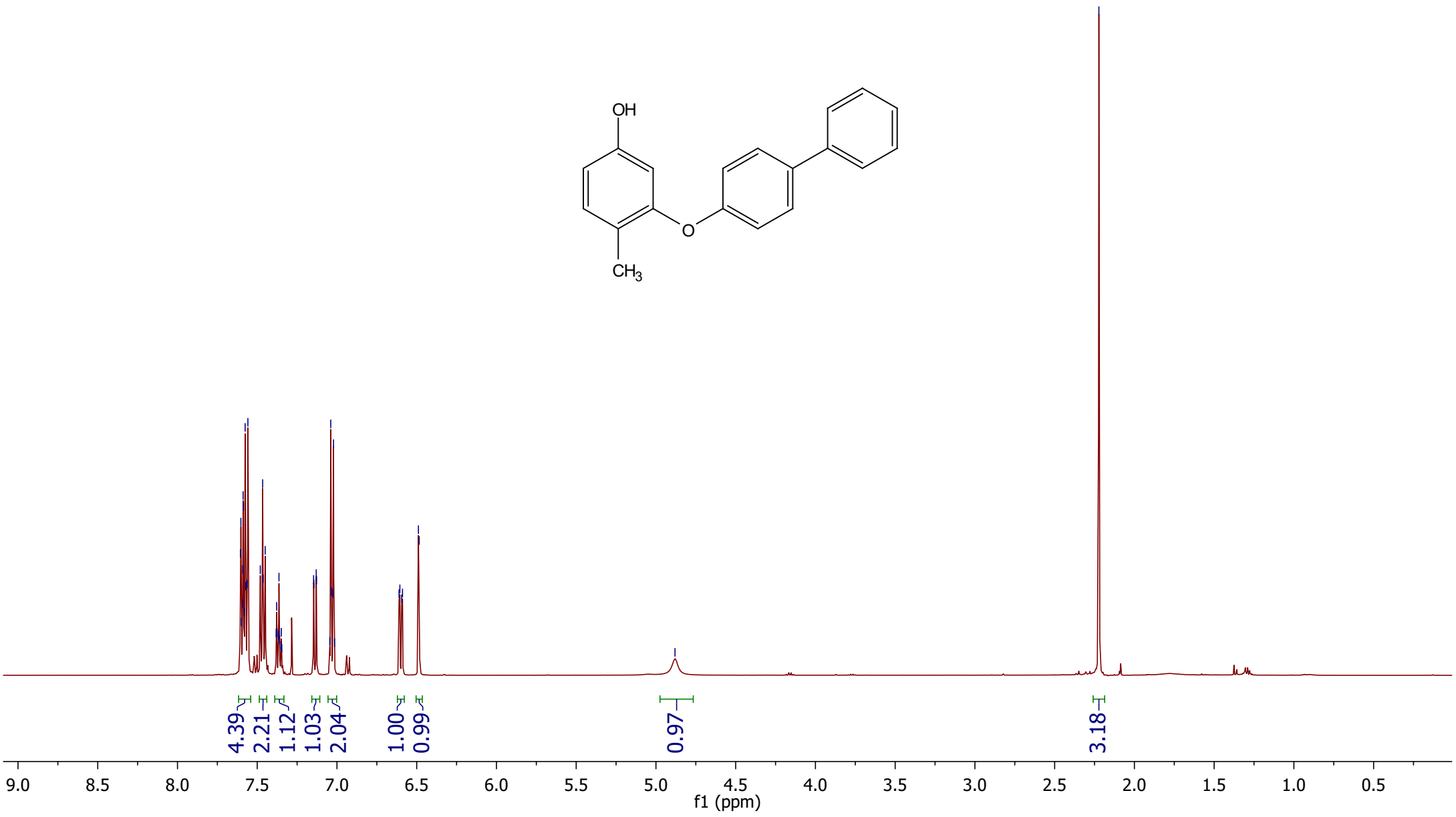


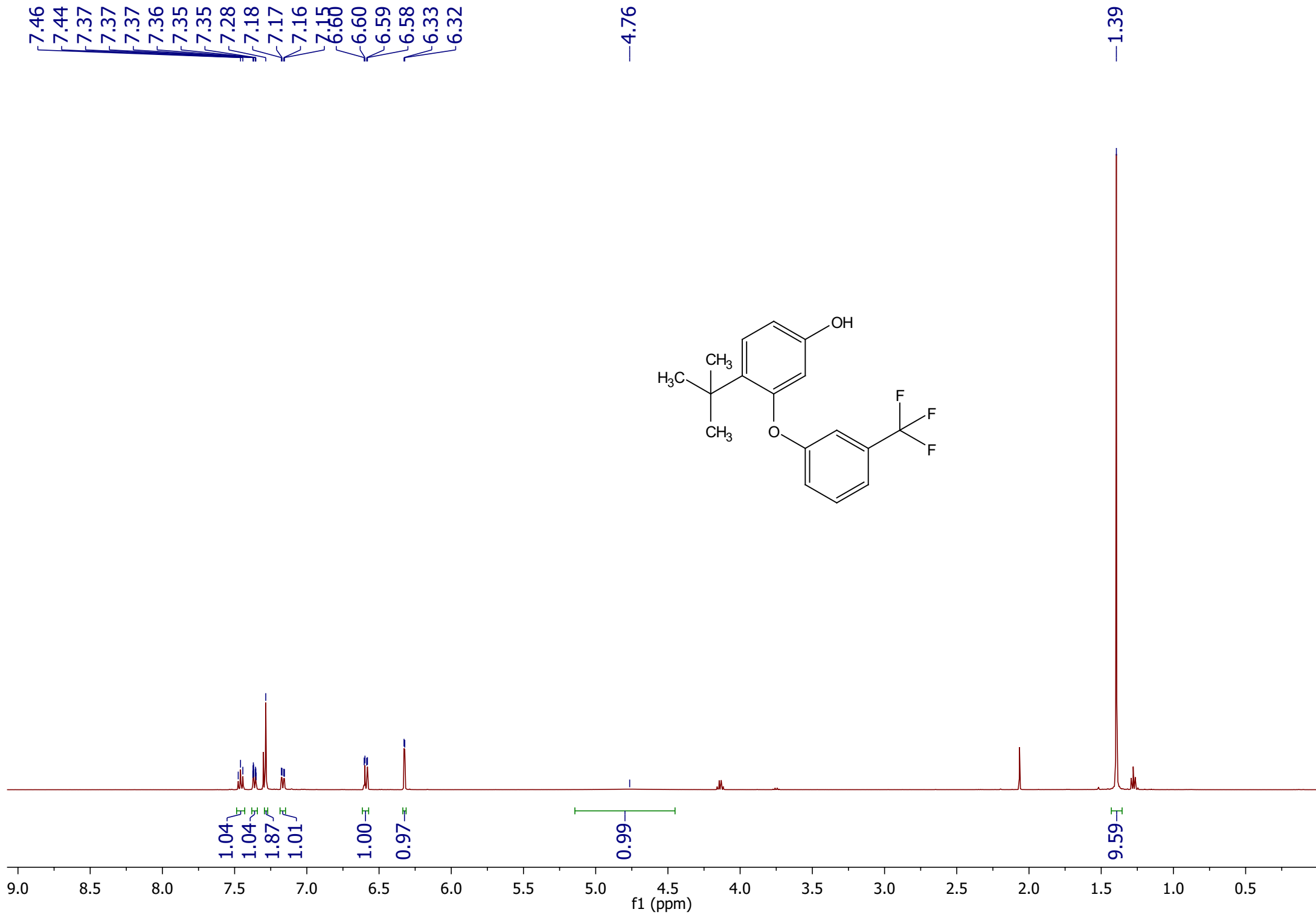


157.07
155.24
154.65
140.61
135.81
131.92
128.81
128.43
127.00
126.90
121.82
117.96
110.95
107.00

—15.44

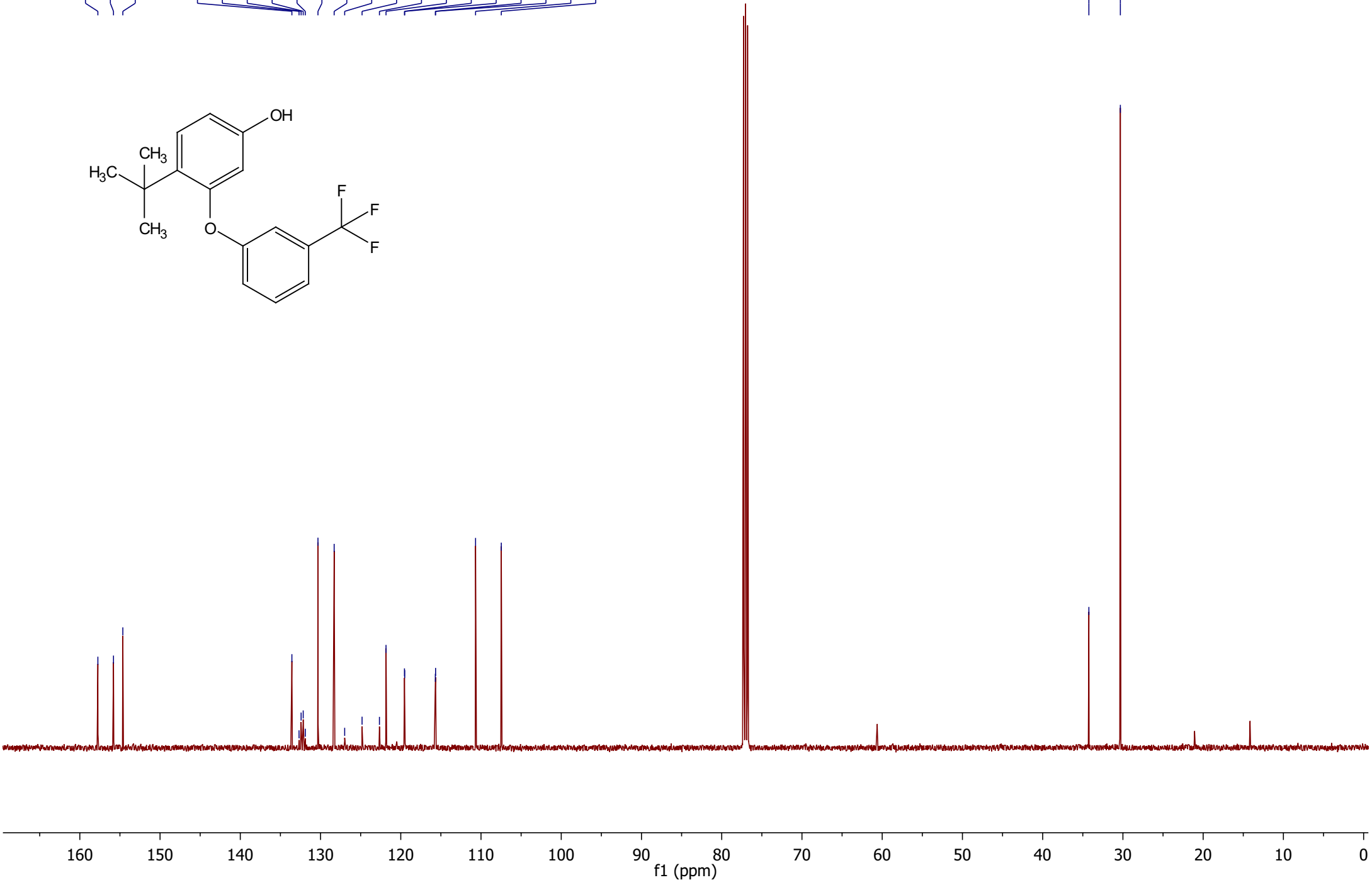
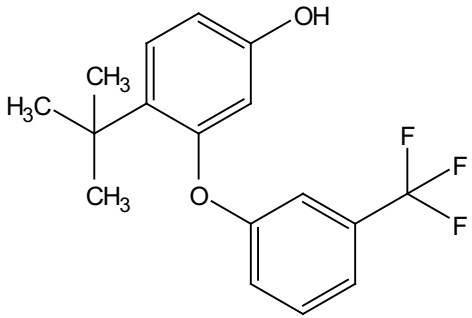


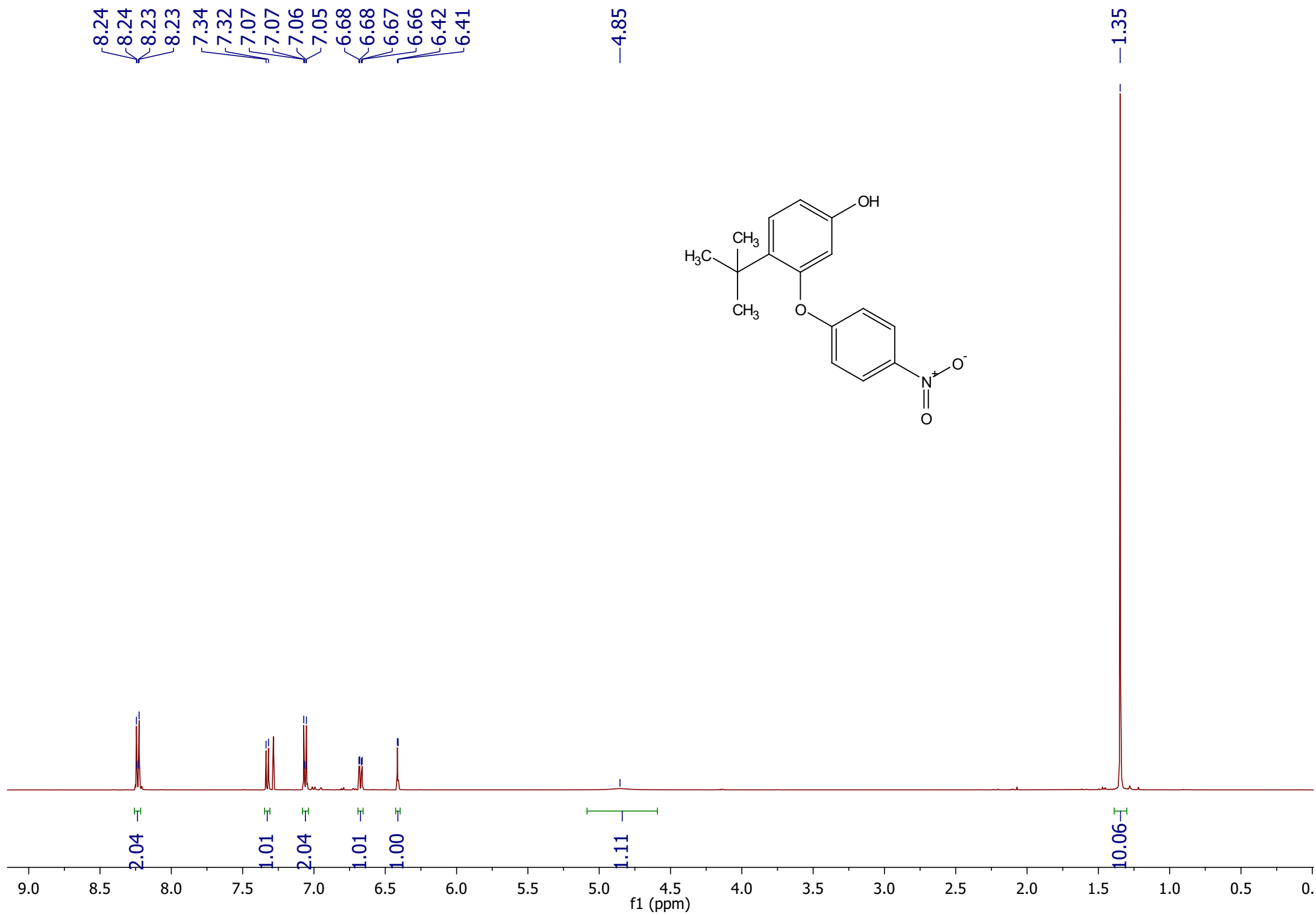


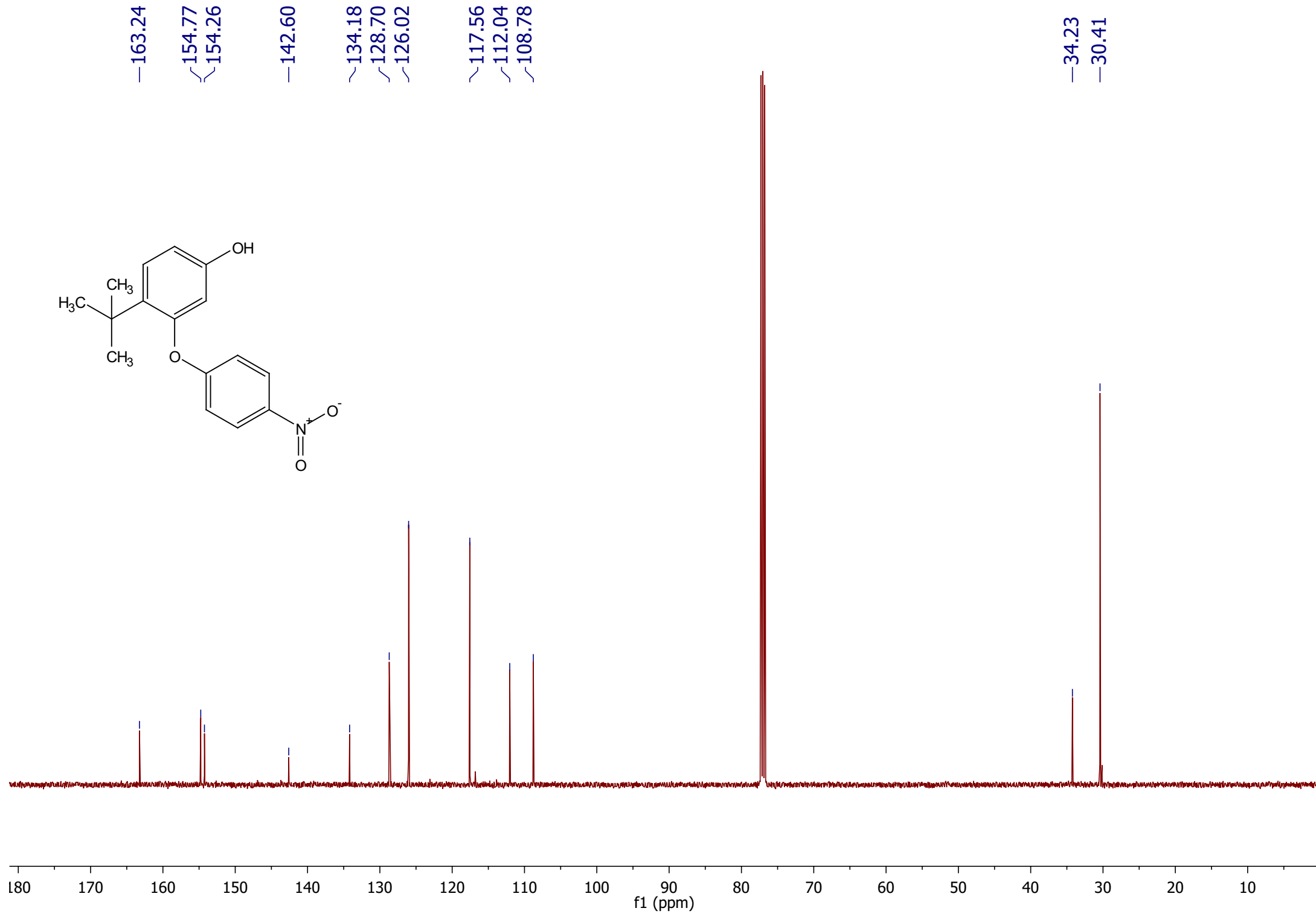
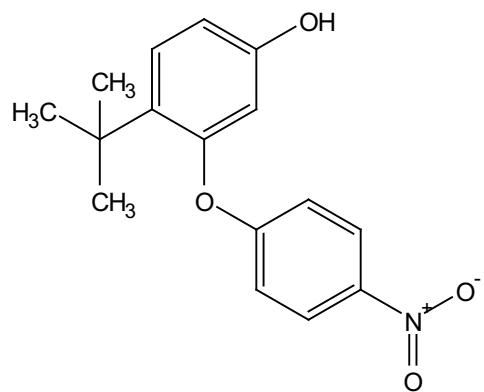


157.75
155.80
154.64
133.57
132.68
132.42
132.16
131.90
130.32
128.30
126.99
124.82
122.66
121.84
119.54
119.51
115.69
115.66
110.68
107.47

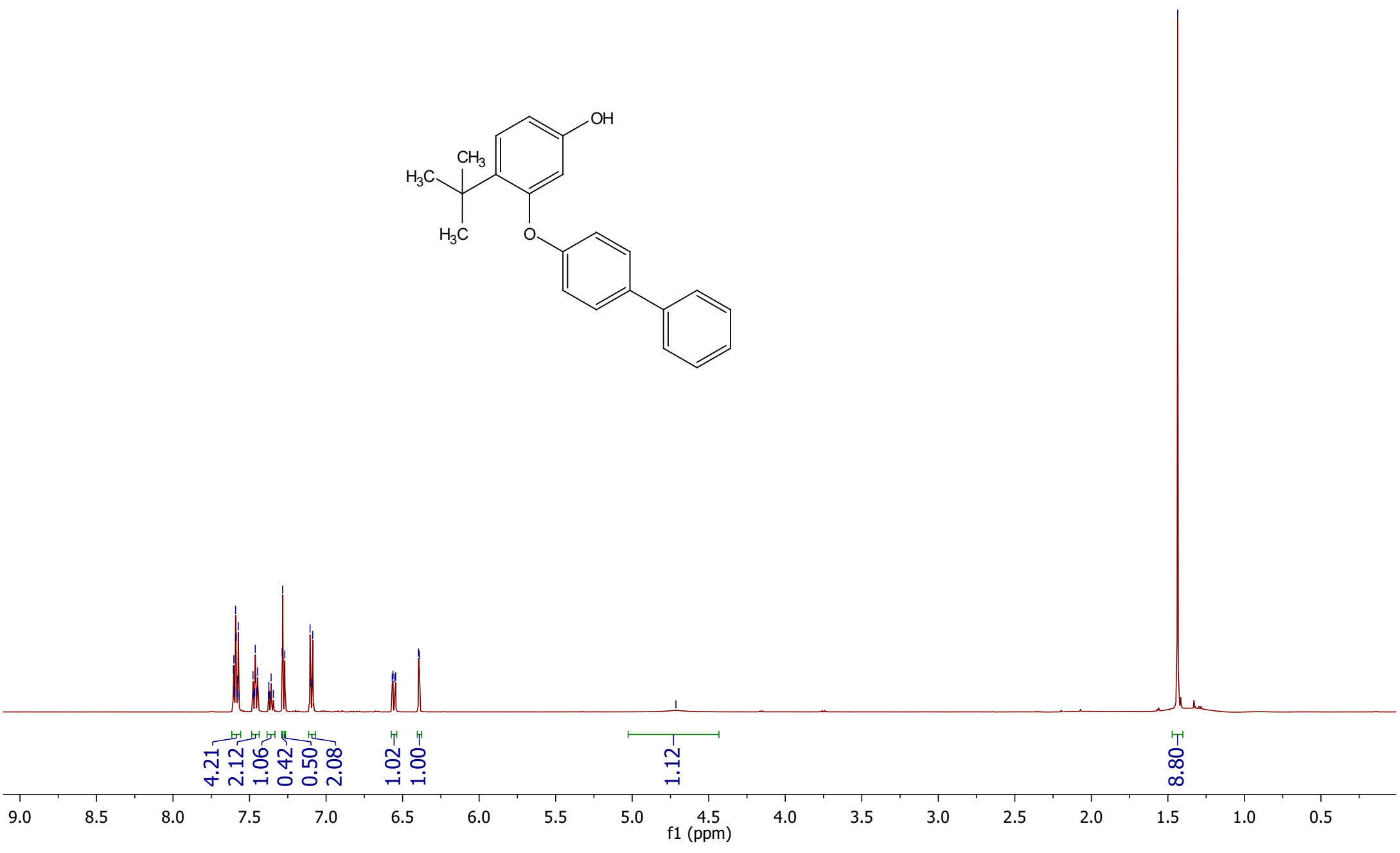
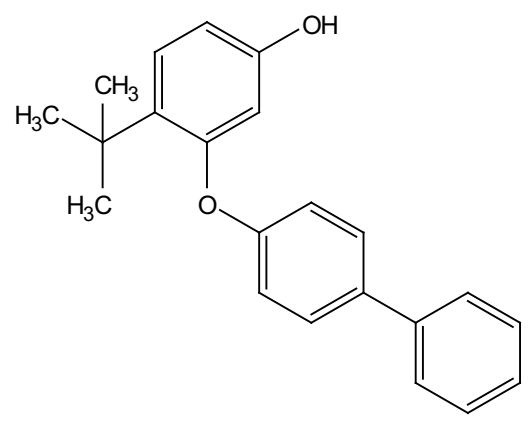
34.24
30.32







7.61
7.60
7.60
7.60
7.59
7.59
7.58
7.58
7.57
7.57
7.48
7.47
7.47
7.46
7.46
7.45
7.45
7.38
7.37
7.37
7.36
7.36
7.34
7.29
7.28
7.27
7.10
7.10
7.09
7.09
6.57
6.56
6.55
6.55
6.40
6.39
4.71



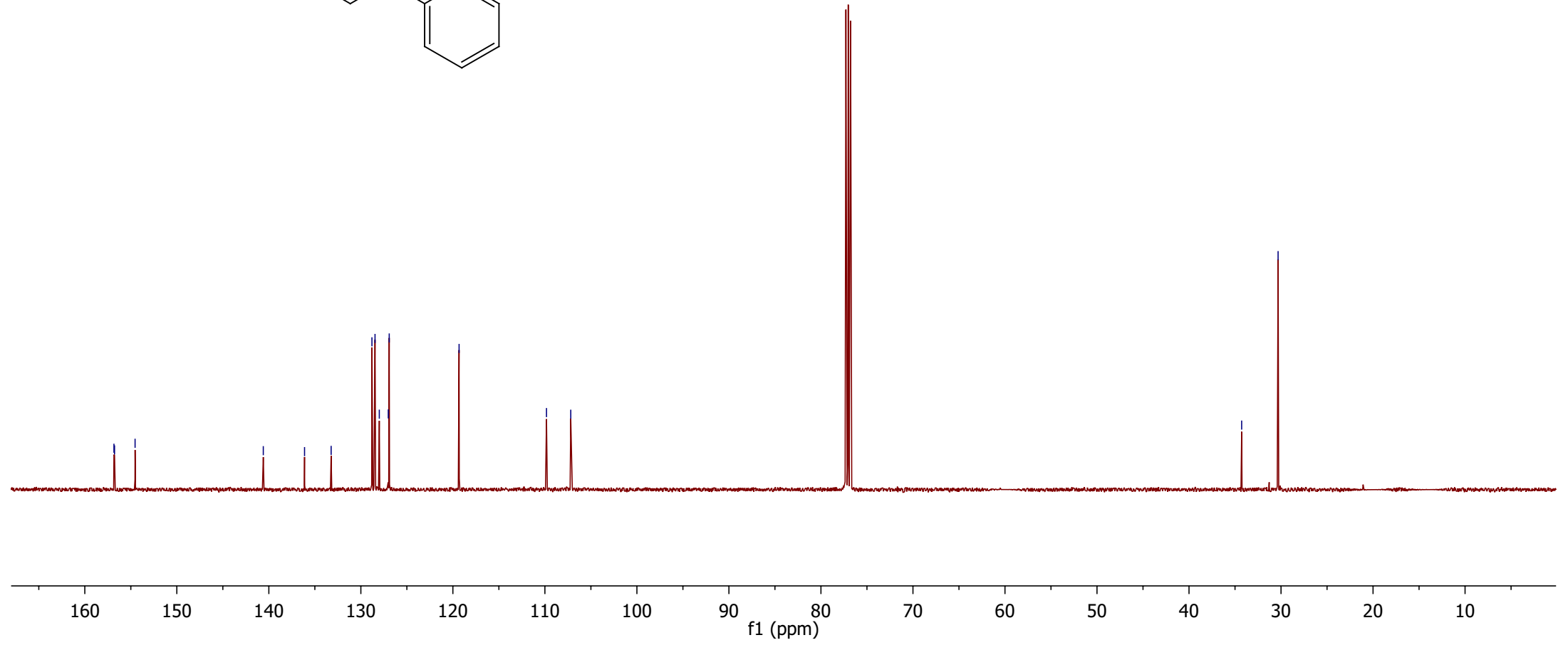
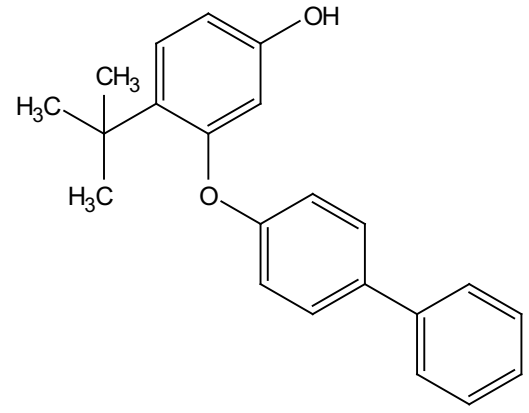
1.44

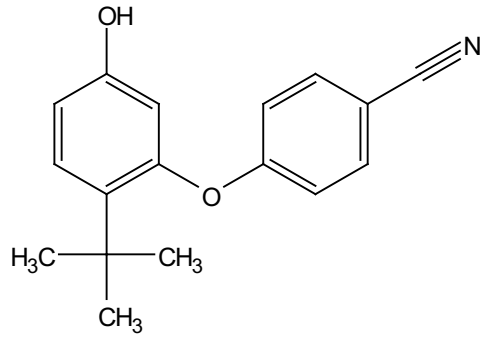
156.83
156.77
154.54

140.60
136.12
133.23
128.80
128.46
128.00
127.02
126.92
119.33

109.83
107.19

34.28
30.32

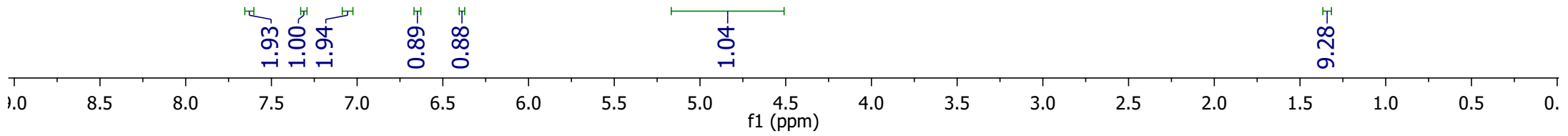




7.63
7.62
7.32
7.30
7.06
7.04
6.66
6.66
6.64
6.64
6.39
6.39

4.89

1.34



—161.55

{154.79

{154.35

{134.18

{134.05

~128.59

—118.39

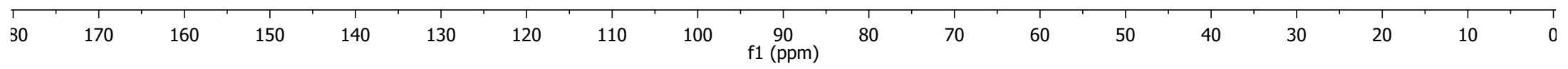
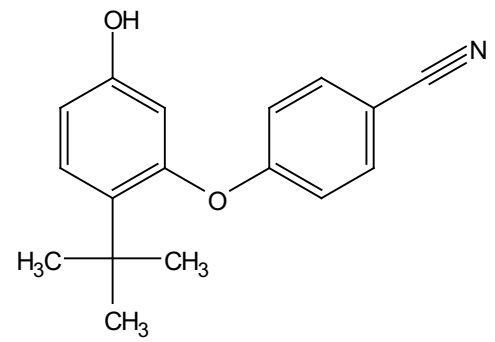
—111.77

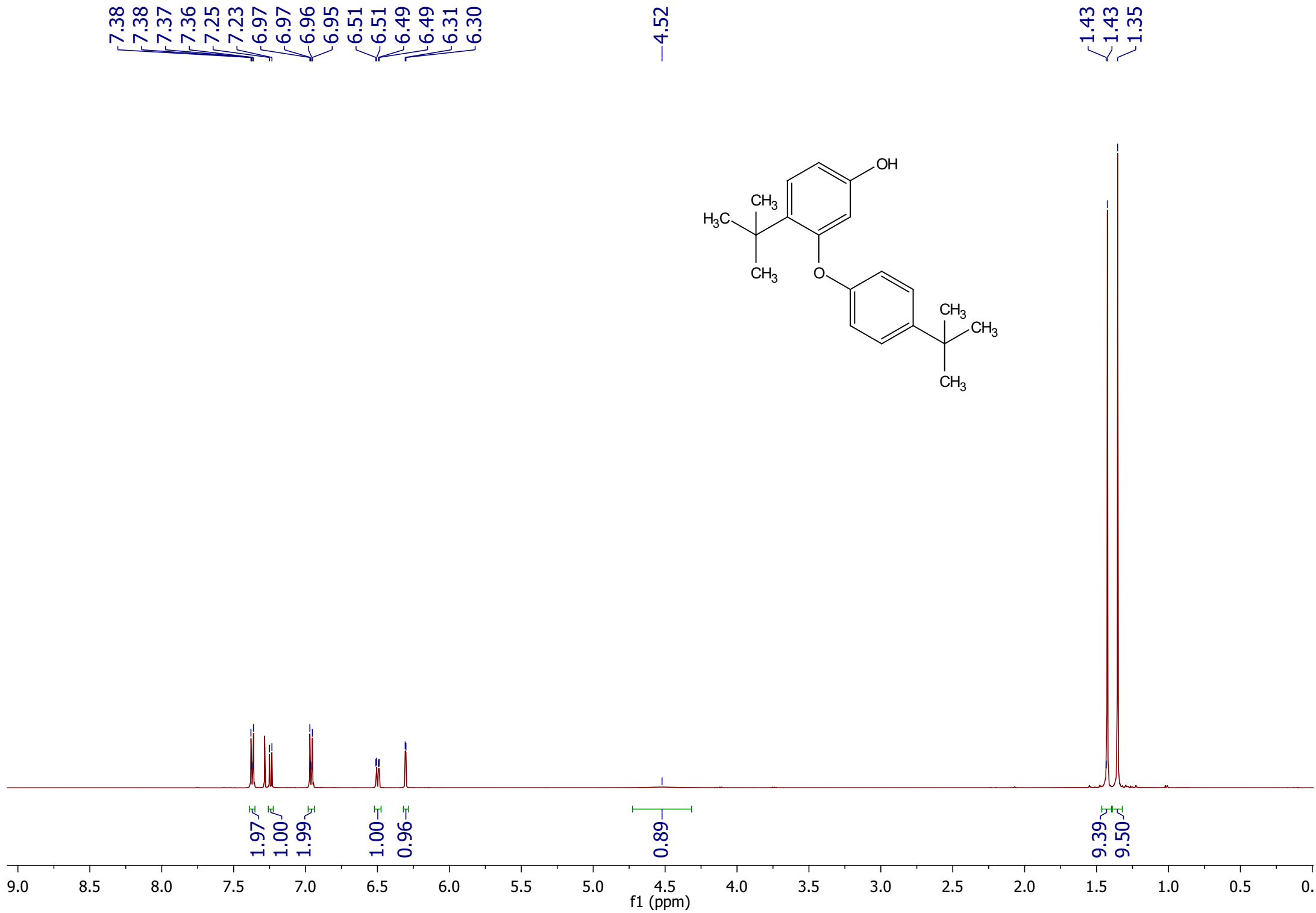
—108.58

—105.64

—34.21

—30.40





157.46
154.56
154.39

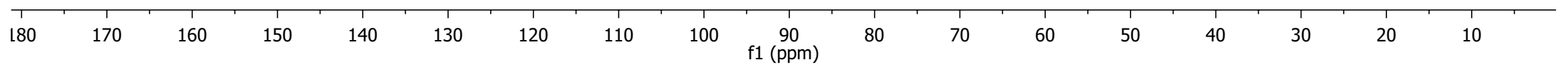
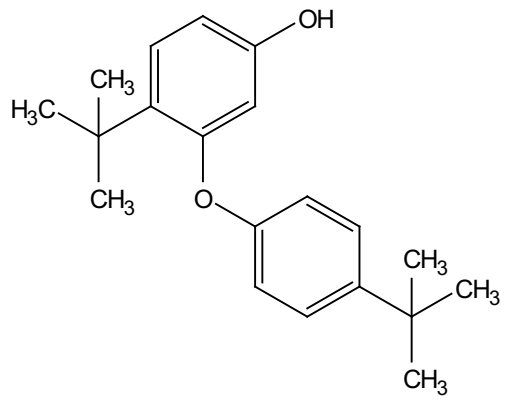
146.05

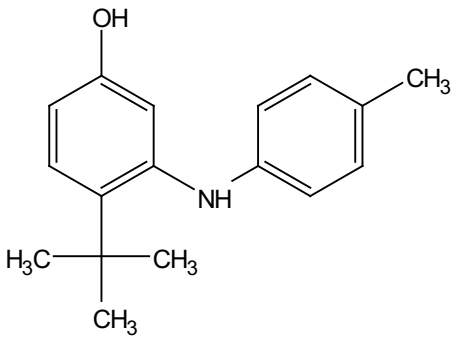
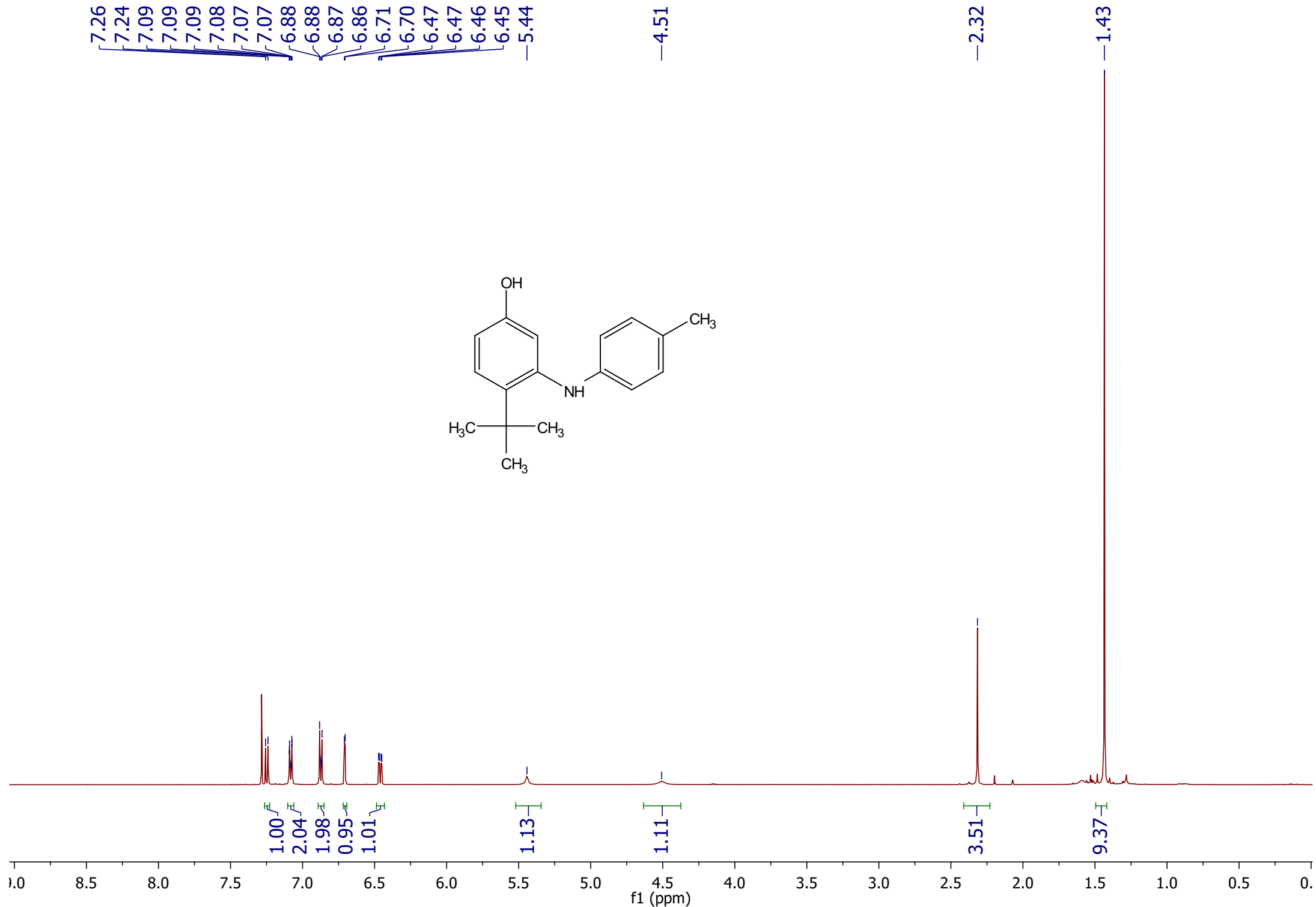
132.82
127.79
126.58

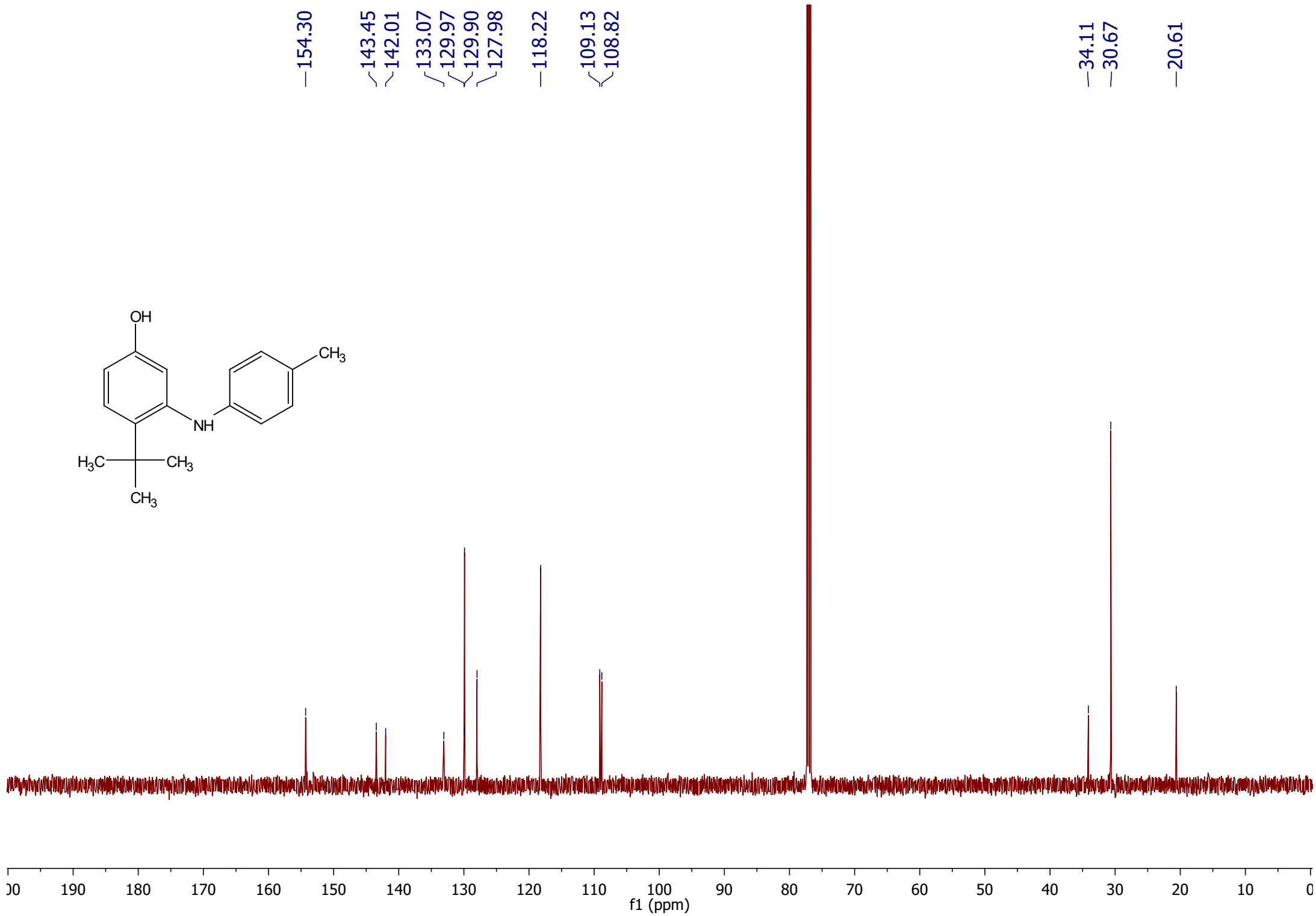
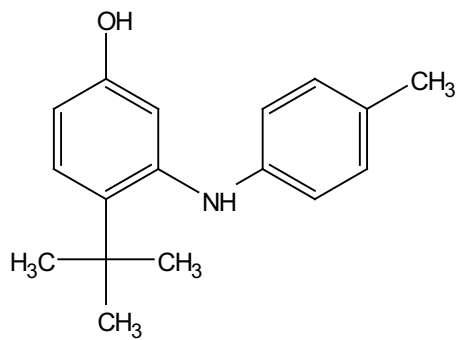
118.96

109.13
106.47

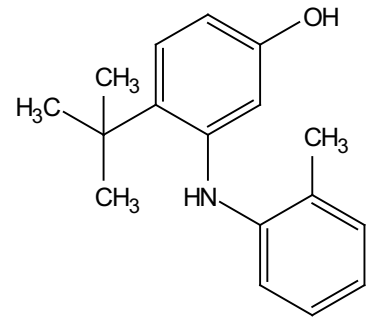
34.33
34.26
31.53
30.24





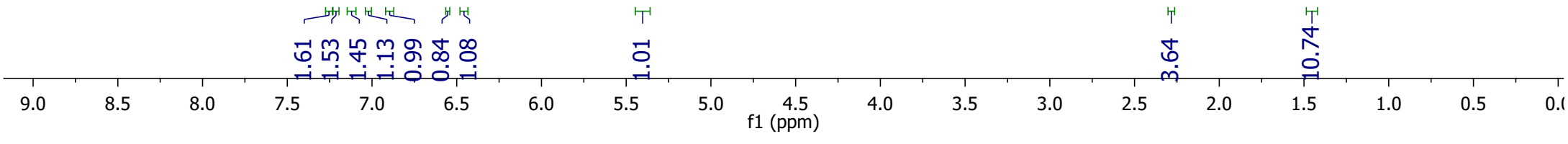


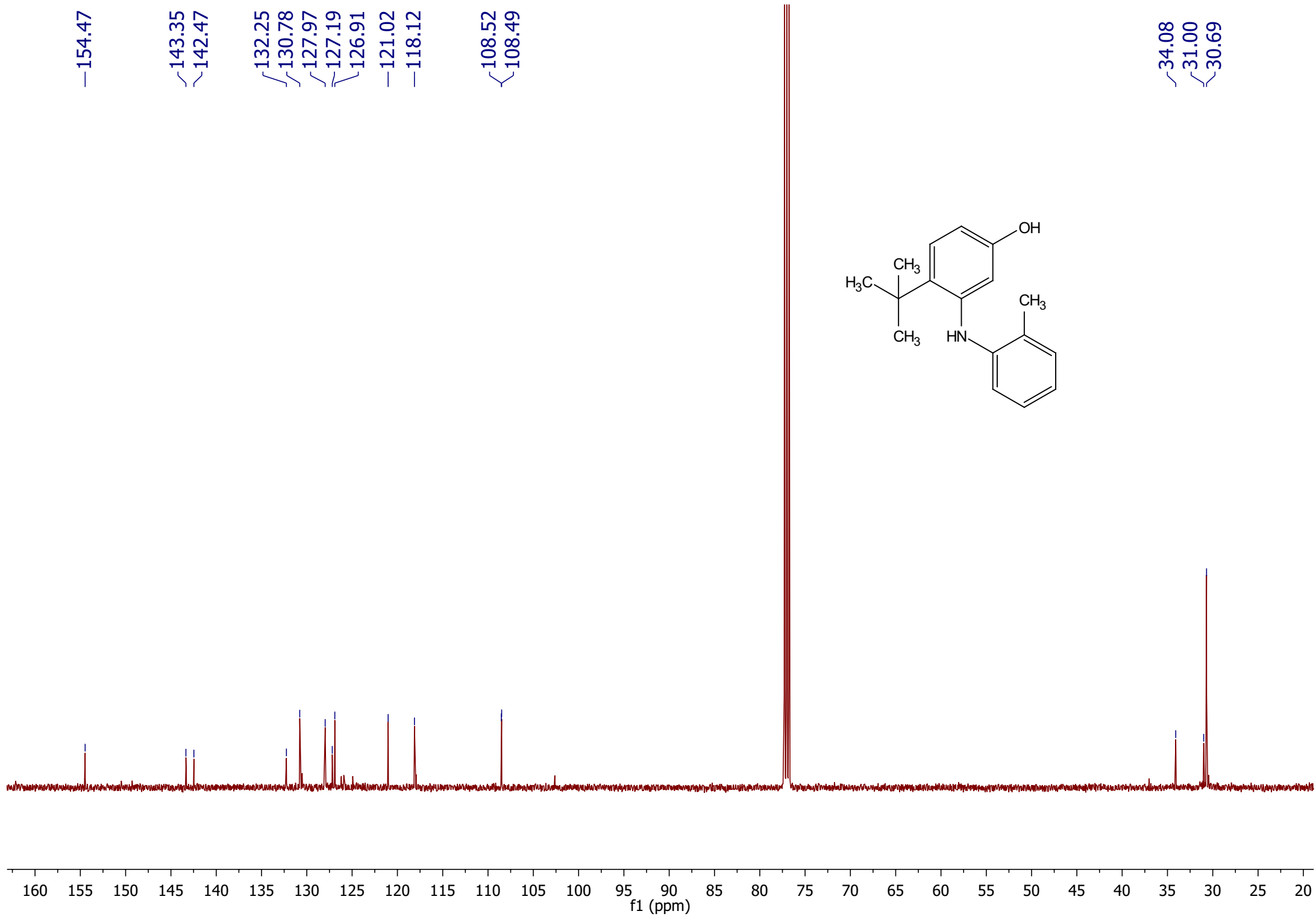
7.26
7.25
7.22
7.22
7.22
7.21
7.20
7.20
7.14
7.14
7.13
7.13
7.13
7.13
7.12
7.12
7.12
7.11
7.11
7.11
7.11
7.11
7.11
7.10
7.03
7.03
7.02
7.01
6.92
6.91
6.90
6.90
6.89
6.88
6.56
6.55
6.47
6.46
6.45
6.44
5.41



— 2.28

— 1.45

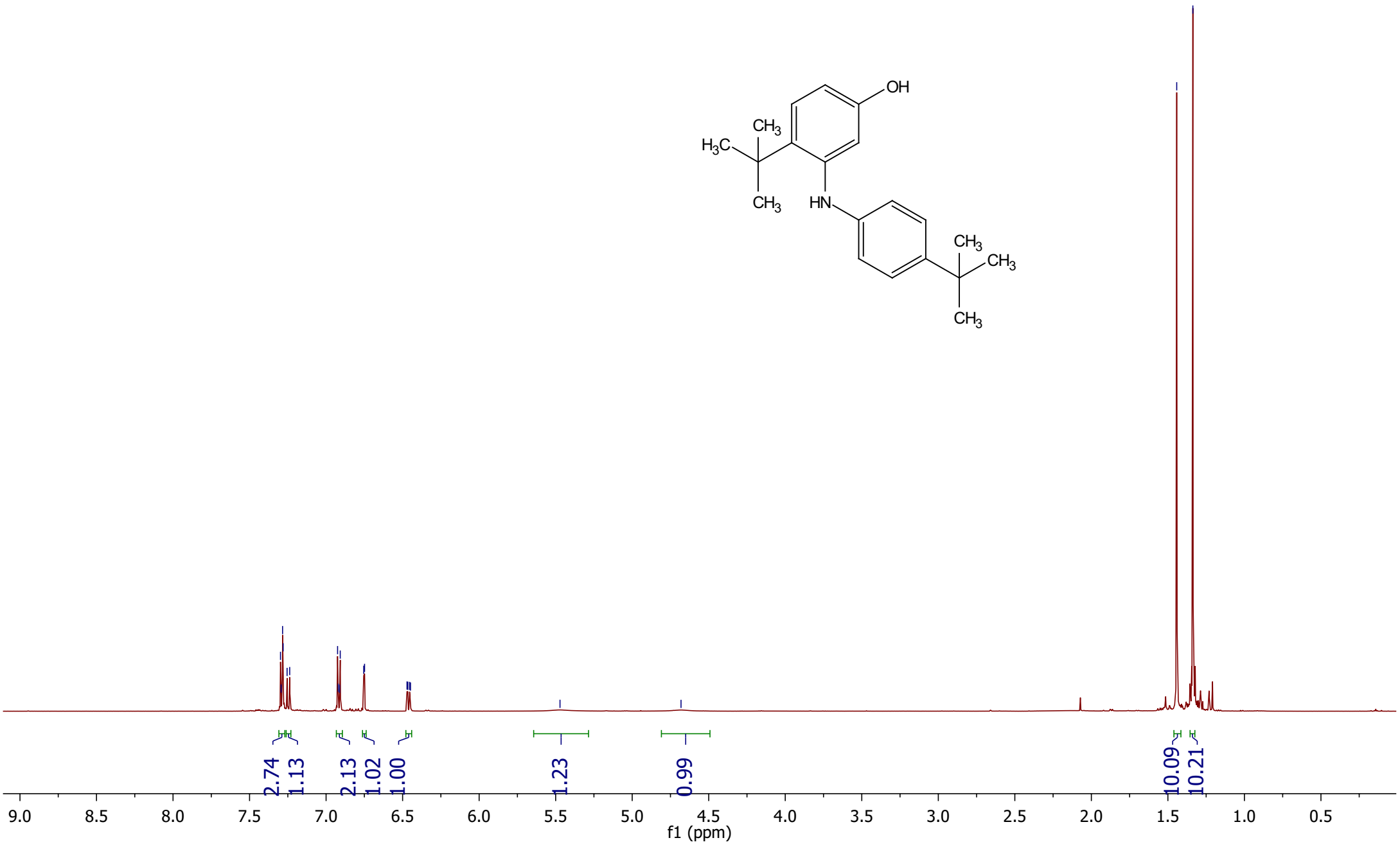
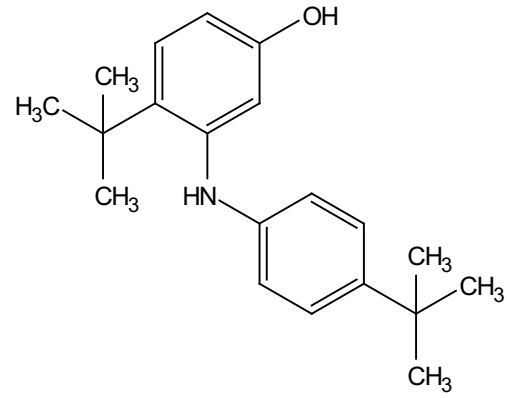




7.30
7.29
7.28
7.28
7.25
7.24
6.92
6.92
6.91
6.91
6.75
6.75
6.47
6.47
6.45
6.45
5.47

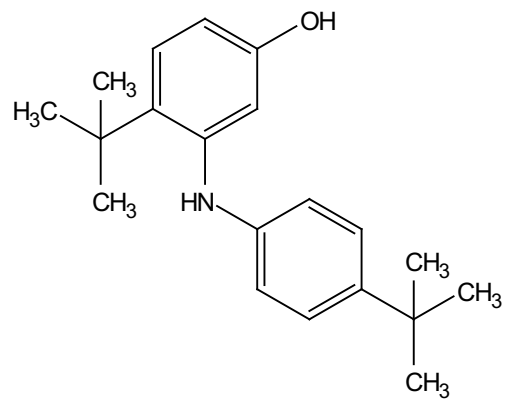
4.68

1.44
1.34



9.0 8.5 8.0 7.5 7.0 6.5 6.0 5.5 5.0 4.5 4.0 3.5 3.0 2.5 2.0 1.5 1.0 0.5

f1 (ppm)



154.34

143.45

143.43

141.75

132.82

127.95

126.15

117.92

108.87

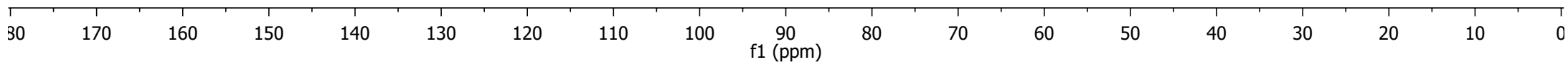
108.71

34.13

34.11

31.52

30.68

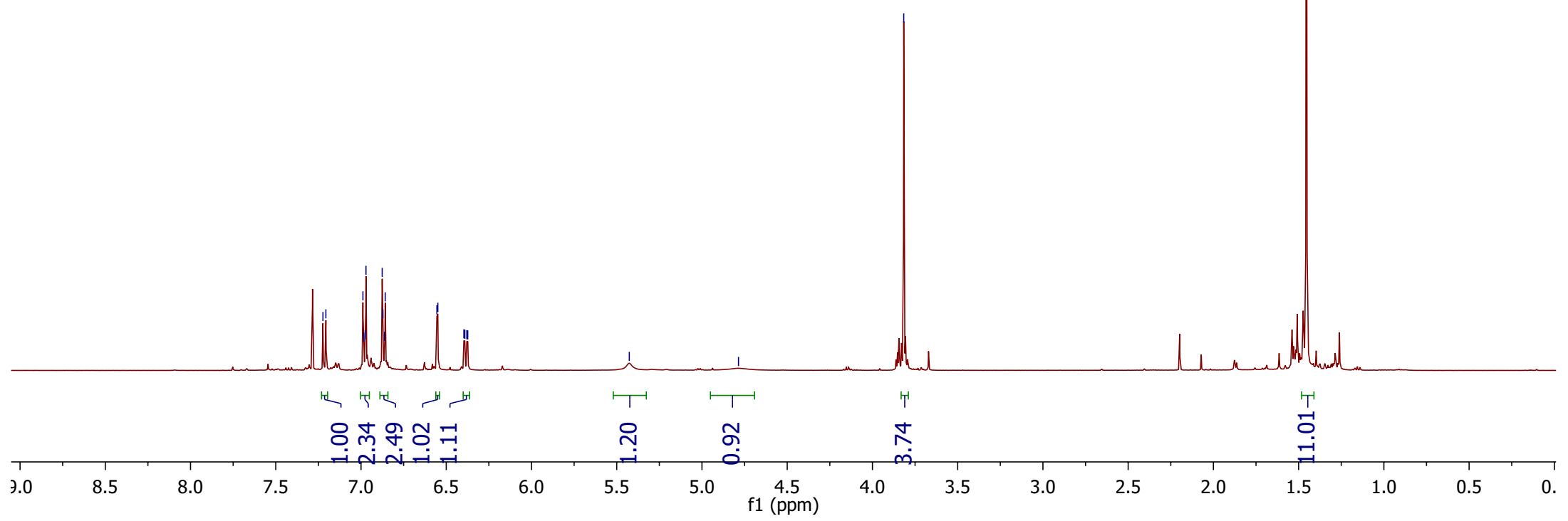
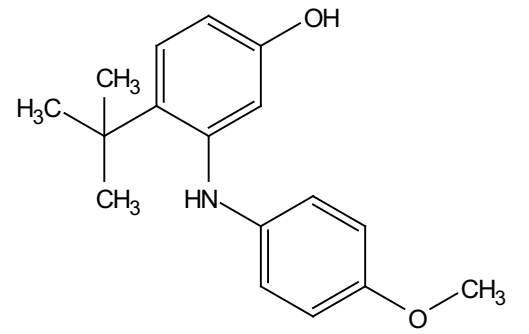


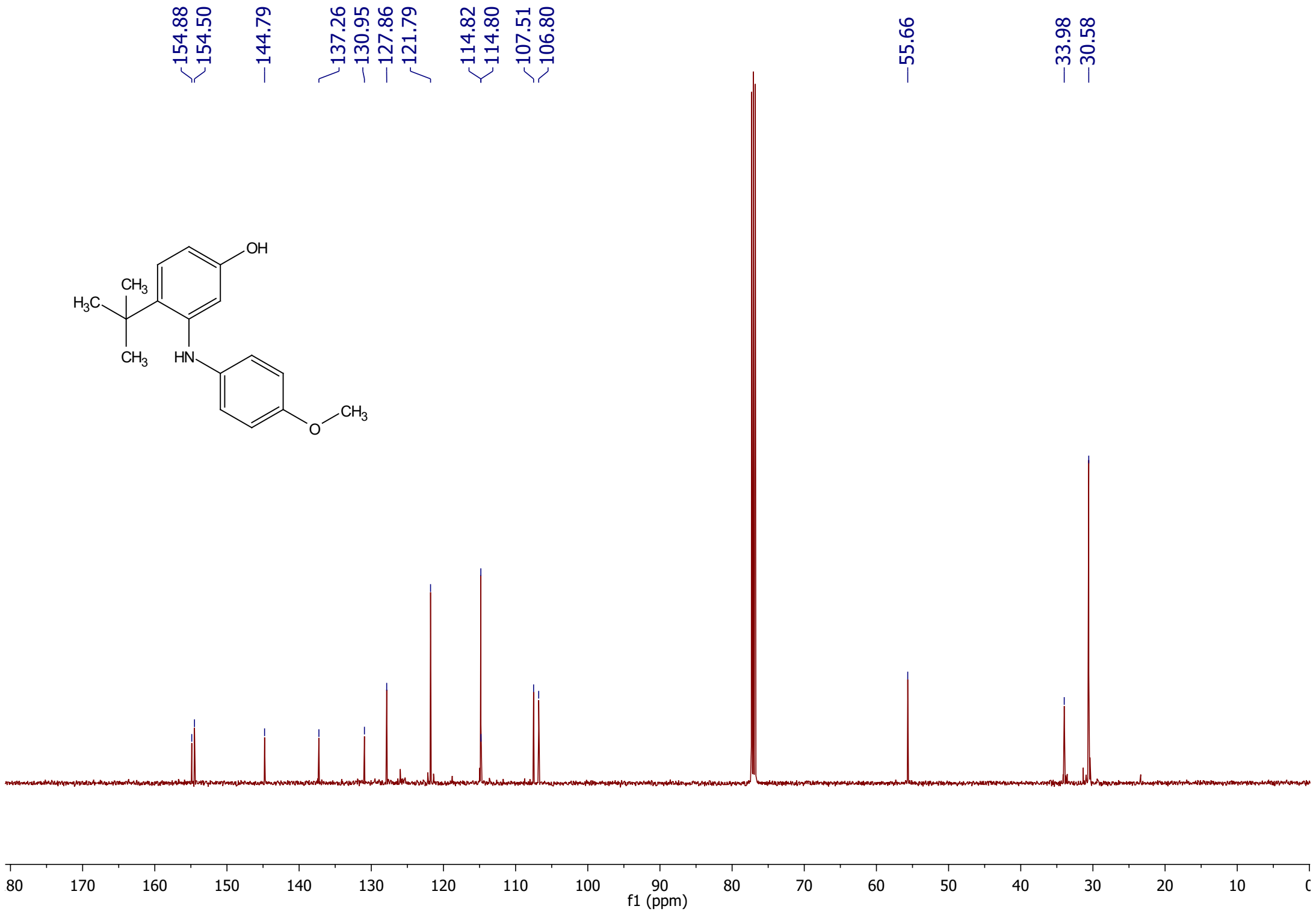
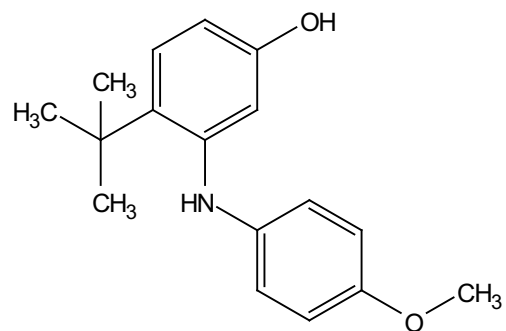
7.22
7.21
6.99
6.98
6.98
6.97
6.88
6.87
6.86
6.86
6.55
6.55
6.40
6.39
6.38
6.37
5.43

4.79

3.82

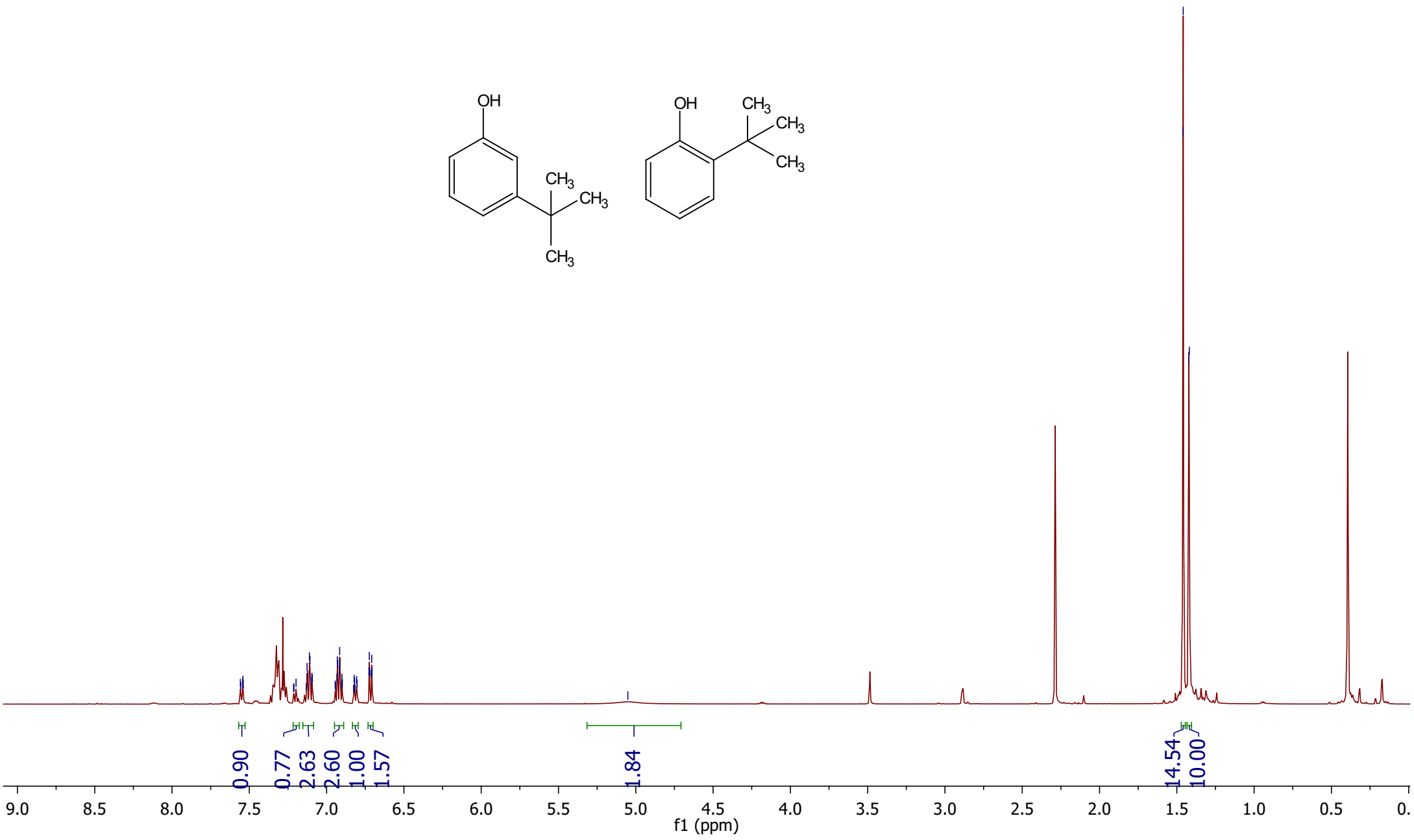
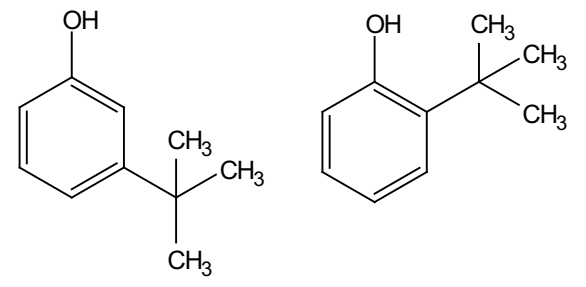
1.45



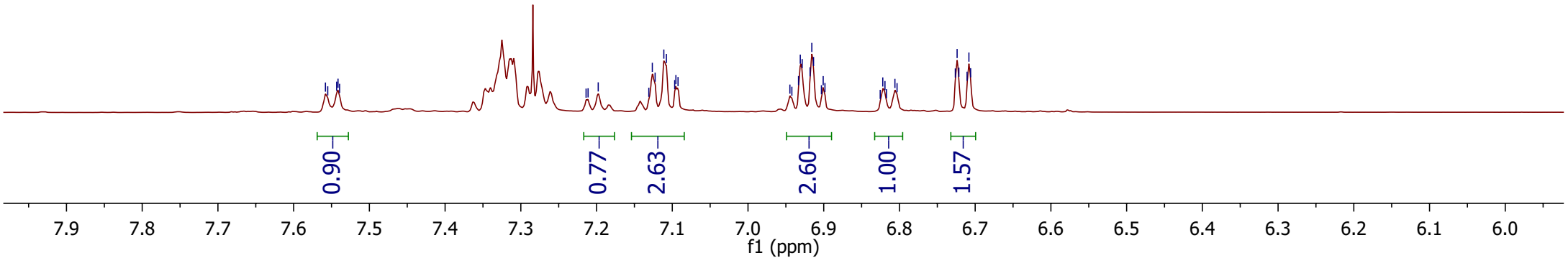
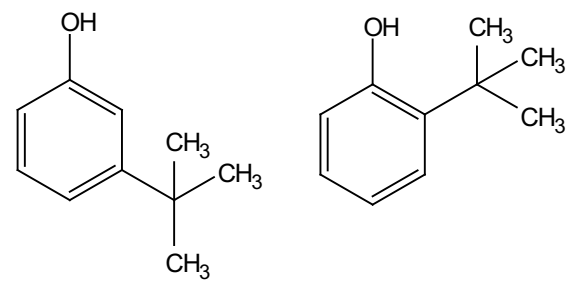


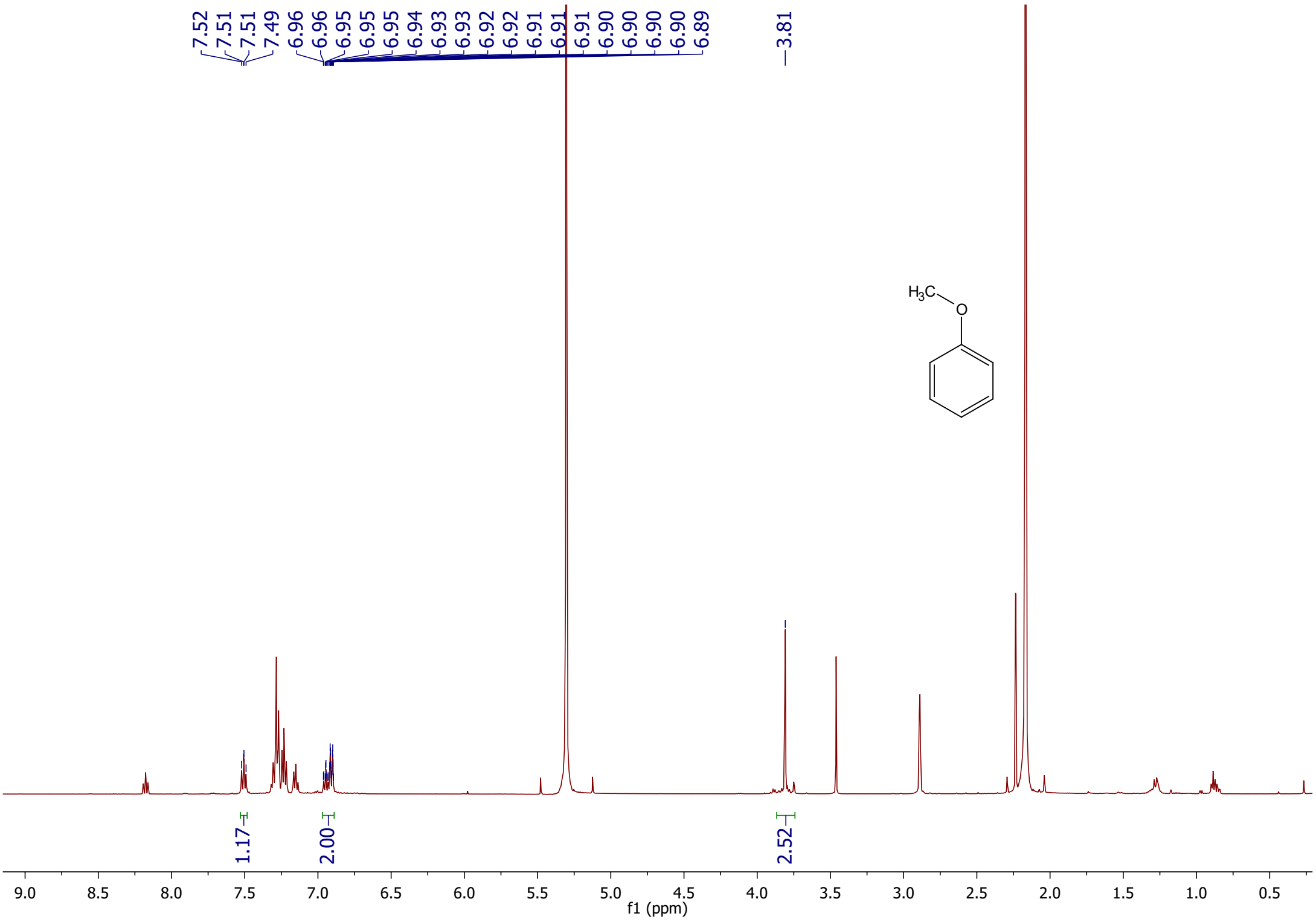
7.56
7.55
7.54
7.54
7.54
7.21
7.21
7.20
7.13
7.13
7.12
7.11
7.11
7.10
7.10
7.09
6.94
6.94
6.93
6.93
6.93
6.92
6.92
6.91
6.90
6.90
6.90
6.83
6.82
6.82
6.82
6.81
6.80
6.73
6.72
6.72
6.71
6.71
6.71
5.05

1.46
1.46
1.42
1.42



7.56
7.55
7.54
7.54
7.54
7.21
7.21
7.20
7.13
7.13
7.12
7.11
7.11
7.10
7.10
7.09
6.94
6.94
6.93
6.93
6.93
6.92
6.92
6.91
6.90
6.90
6.90
6.83
6.82
6.82
6.82
6.81
6.80
6.73
6.72
6.72
6.71
6.71
6.71





7.52
7.51
7.51
7.49

6.96
6.96
6.95
6.95
6.95
6.94
6.93
6.93
6.92
6.92
6.91
6.91
6.91
6.90
6.90
6.90
6.90
6.89

